Analysis of *Pax6* expression in the developing vertebrate head

Pei-Cheng David Lin, MSc

Submitted in satisfaction of the requirement for the degree of Ph.D. in the University of Edinburgh 1997

ABSTRACT

Pax6 is a member of the *Pax* gene family -- a family that encodes highly conserved and developmentally important transcription factors. Mutation of *Pax6* leads to *Small eye* (*Sey*) in the mouse and *aniridia* in the human. *Sey/Sey* mice are characterized by craniofacial abnormalities, including absence of eye and nasal derivatives, formation of supernumerary upper incisor teeth and a rod-like cartilaginous structure in the premaxilla, as well as defects in the developing brain. This thesis aims to investigate *Pax6* expression in the head region of normal and mutant vertebrate embryos in order to elucidate its role during development and understand the mutant phenotypes.

Pax6 expression in the mouse is investigated by *in situ* hybridization, with particular emphasis on the higher centres of the visual and olfactory nervous system -- areas that have not been previously investigated in detail. *Pax6* expression is detected along the visual pathway, in the neural retina, optic nerve, pretectum, superior colliculus, pulvinar, dorsal and ventral lateral geniculate nucleus and other neural nuclei that are implicated in visual connections. Within the olfactory nervous system, *Pax6* is expressed in the olfactory and vomeronasal epithelium, main and accessory olfactory bulb, anterior olfactory nucleus, precommisural hippocampus, piriform and endopiriform cortex, as well as olfactory and vomeronasal amygdaloid areas. The results demonstrate that *Pax6* is extensively expressed throughout the visual and olfactory pathways and strongly indicate that *Pax6* is involved in their development. It is also shown that *Pax6* expression is developmentally restricted during mouse embryogenesis. The restriction is implicated in neuroblast proliferation, migration, connection and axonogenesis.

Expression of *Pax6* in the chick has not been previously reported for stages later than Hamburger-Hamilton stage 14. This study confirms formerly reported data before stage 14 and establishes that *Pax6* is expressed in the olfactory epithelium, lens, corneal epithelium, and neural retina after stage 14. Furthermore, temporary *Pax6* expression is found in Hensen's node before stage 9. In the hindbrain, in addition to the formerly reported expression in all the rhombomeres, *Pax6* transcripts are also detected in cells flanking rhombomeres 3 and 5.

The distribution of *Pax6* transcripts in the head surface ectoderm appears to correspond to the previously reported areas that are capable of forming lens in culture. This suggests a crucial role for *Pax6* in lens differentiation, which is supported by absence of lens in the *Sey/Sey* mice. The correlation between *Pax6* expression and lens differentiation is investigated by culturing fragments of head surface ectoderm on millipore membranes. The fragments are then assessed for lens differentiation using an antibody against αB crystallin and the presence of *Pax6* transcripts is checked by *in situ* hybridization. The results indicate that lens can differentiate from non-*Pax6*-expressing fragments of head surface ectoderm, whilst *Pax6*-expressing fragments do not always give lens. Whenever lens differentiates in culture, however, *Pax6* is always expressed, suggesting that it is necessary for the process of lens differentiation.

The phenotype of *Sey/Sey* mice suggests that *Pax6* may play a role in tooth development and this possibility is preliminarily investigated in this study. The results demonstrate that *Pax6* is not expressed in the premaxilla, suggesting that the supernumerary teeth are not directly caused by *Pax6* mutation. To investigate whether the supernumerary teeth show normal development, the presence of two genes involved in tooth development, *Msx-1* and *Msx-2*, are examined. The results show that the patterns of *Msx-1* and *Msx-2* expression in the *Sey/Sey* premaxilla are normal, although the area exhibits formerly reported abnormalities and is developmentally retarded. This suggests that *Msx-1* and *Msx-2* are not directly regulated by *Pax6*. Possible mechanisms that may cause the abnormalities with presumptive involvement of *Pax6* regulation are discussed.

One possible regulator of *Pax6* is all-*trans*-retinoic acid (RA; a derivative of vitamin A). Maternal vitamin A deficiency causes a variety of abnormalities, including micropthalmia that is also seen in the *Sey/Sey* mice. In vitamin A-deficient quail embryos, the segmentation of rhombomeres 4 - 8, where *Pax6* is expressed, is disturbed. Furthermore, expression of some *Pax* genes, for example, *AmphiPax1* and *Pax2*, is affected by RA. This thesis investigates the effect of RA on *Pax6* expression during gastrulation. Six groups of chick embryos at stage 4 are treated *in vitro* with RA at concentrations from 1×10^{-8} M to 5×10^{-5} M. *Pax6* expression after culture for 30 hours is investigated by wholemount *in situ* hybridization. The results show dosage-dependent abnormalities in the head, heart, neural tube, and somites. *Pax6* remains expressed in all the abnormal embryos investigated after RA treatment, indicating that *Pax6* is not switched off by RA. In the head that is severely affected by RA treatment, most structures are condensed or distorted. In either cases, *Pax6* expression patterns are altered. The alteration appears to be resulted from the gross malformations following RA treatment, although direct effect of RA on *Pax6* expression can not be excluded.

DECLARATION

This thesis does not contain without acknowledgement any material previously submitted for a degree or diploma in any university, and except due reference is made, does not contain any material previously published or written by any another person.

Pei-Cheng David Lin

ACKNOWLEDGEMENT

My sincere and particular thank-you goes to Dr. Sarah E. Wedden for acting as my major supervisor during the course of this study. Without her guidance, encouragement, instruction, and very often tolerance, this thesis would nerver have been completed.

Special thanks to Professor Matthew H. Kaufman for his support and instruction in many aspects of this study. In particular, his teaching and help in mouse embryogenesis are most appreciated.

Many thanks are due to Dr. Robert E. Hill for providing training in molecular techniques and many enlightening discussions and instructions. I am particularly grateful for his encouragement at all stages of this study.

I am indebted to many friends in Edinburgh University and MRC Human Genetics Unit. Dr. Arthur Jurand kindly provided his advice and instruments for chick embryo culture. Many formal and informal helps have been provided by Drs. Duncan Davidson, Justin Grindley, Alistair MacKenzie, Jonathan Bard, Jamie Davis, Gordon Findlater, and David Price. Particular thanks are due to Drs. Gordon Findlater and David Price, who provide instructions in mapping expression areas in the mouse brain.

The work in this thesis was supported by a royal society research grant to Dr. Sarah E. Wedden and partly by research grants to Professor Matthew H. Kaufman. I am financially supported by Philip Norman Cuttner Bequest from the Faculty of Medicine, Edinburgh University.

Finally, I am most grateful to my wife -- Judy, and my son -- Herbert, for being with me in all aspects of my life.

CONTENTS PAGE

Chapter 1: Introduction

This thesis deals with the role of *Pax6* during vertebrate craniofacial development. Areas of investigation include the central nervous system (particularly the visual nervous system and the olfactory nervous system), the eye, and the teeth. The effect of retinoic acid on *Pax6* expression during early embryogenesis is also investigated. To investigate any topic with "gene" and "development" involved, one has to put these two terms both in conjunction and in contrast. In conjunction means that one can learn the role of genes during development by looking at their genotypes: normal expression (both at the RNA and the protein level), up-regulation, down-regulation, loss of function, ectopic function, function at the wrong time; but one also needs to look at the phenotypes: normal embryogenesis, hyperplasia, hypoplasia, aplasia, ectopic growth or teratogenesis, early maturation, growth retardation, and other non-morphological phenomena. In contrast means to compare normal development with the aftermaths of genetic deviations. Modern developmental biologists (or geneticists) like to refer to a study started with phenotypes as "genetics" and those started with genotypes as "reverse genetics", though the latter is becoming the more normal approach.

In the sense mentioned above, I put this introductory chapter in two parts. Part A is the "gene" side and part B is the "development" side. Part A (from section 1.1 to 1.6) introduces the background and current knowledge of *Pax6*, starting with the homeotic mutations and the homeobox genes, then going on to the *Pax* gene family --- their genomic organization, structures, and expression, and then to the mutations found in the *Pax* gene family, with concentrations on *Pax6 per se*. The common aspects of the *Pax* genes are summarized in section 1.6. In part B (from section 1.7 to 1.12), the development of vertebrate craniofacial areas to be investigated in this thesis, i.e. the central nervous system (particularly the visual nervous system and the olfactory nervous system), the lens, and the teeth, will be briefly described. This will provide the necessary background information for further discussions to be developed in the following chapters. After part A and part B, I will address the questions to be investigated in this thesis in section 1.13.

Part A: the "gene" side

1.1 Homeosis and homeobox genes

This thesis deals with *Pax6* which contains a paired-like homeodomain (a specific type of homeobox) and a paired domain. Section 1.1 will start with the definition of "homeosis", the identification of the homeotic mutants, the isolation of the homeobox genes, current understanding about these genes and the importance of homeobox genes in developmental biology. I will then introduce the paired box and the *Pax* genes.

1.1.1 Identification of the homeotic mutants and isolation of the homeobox genes

"Homeosis" was a term coined by William Bateson in order to describe "something has been changed into the likeness of something else" (Bateson, 1894). Twenty-one years later after Bateson introduced the term "homeosis", the first homeotic mutant -- *bithorax*, was established in the fruit fly (Bridges and Morgan, 1923). The second homeotic mutant, the *spineless-aristapedia*, was found in 1926 (Balkaschina,1929) and the third, *proboscipedia*, in 1931 (Bridges and Dobzhansky, 1933). After the development of recombinant DNA techniques in early 1980s, *bithorax* was found to belong to a complex gene cluster called BX-C and *proboscipedia* to another complex -- ANT-C. However, before that, E.B. Lewis had started some insightful genetic analyses and found that mutations in single genes can result in homeotic transformations. He therefore assumed that the mutations affected master regulating genes, which might then control consecutive gene activations and specify the plan of body formation (Lewis, 1978).

In early 1980s, W. Bender and colleagues became the first to isolate the genes in BX-C complex (Bender, *et al.*, 1983). They were followed by M.P. Scott and collaborators, who isolated first genes of the ANT-C complex (Scott, *et al.*, 1983; Gehring, 1987). Although quite a few genes that were responsible for the homeotic mutations had been isolated at that time, no one had a precise knowledge on how those genes worked to produce homeotic information during embryonic development. A crucial

finding came when W.J. Gehring and W.J. McGinnis found a DNA sequence that was conserved between one homeotic gene and another (McGinnis *et al*, 1984). The same conserved sequence was also independently found by M.P. Scott and A.J. Weiner in another laboratory (Scott and Weiner, 1984). The conserved sequence was named the "homeobox" which contained a 180-bp stretch coding for a homeodomain. Genes that contained the conserved sequence were hence called the homeobox-containing genes.

The finding of homeobox genes has been a huge impact in the field of developmental biology. In a very short period of time, dozens of homeobox-containing genes were identified, not only in fruit fly but also in a wild range of metazoans including vertebrates such as mammals and humans.

1.1.2 Current status of the homeobox genes

To date, the analyses of mouse and human homeobox genes are the most detailed in the vertebrates. Those genes most closely related to the *Drosophila* HOM-C (ANT-C and BX-C) complex are denoted the HOX complex in the vertebrate (reviewed by Krumlauf, 1994). By 1994, the vertebrate HOX complex had already been found to consist 38 genes that are organized into four different intra-chromosomal complexes (Hox-a, -b, -c, and -d); each intra-chromosomal complex is approximately 120 kb in length (Krumlauf , 1994). Even to date, the number of Hox genes being found is still increasing. The HOX genes, however, are only a subset of all the vertebrate homeobox-containing genes. For example, the homeobox-containing genes in the mouse has been divided into four families according to their sequence characteristics (Hill *et al.*, 1989). They are *Antp*-like (*Antennapedia*), *en*-like (*engrailed*), *paired*-like, and *Msh*-like (*muscle-segment*) (Hill *et al.*, 1989). All these families have homeoboxes similar to those in the *Drosophila*, but only the *Antp*-like genes are grouped into the HOX complex.

1.1.3 The importance of homeobox genes in developmental biology

The importance of homeobox genes in developmental biology is not revealed just by their large numbers. Extensive analyses have led to some striking findings in vertebrate embryos: (1) The expression patterns of Hox genes are spatially restricted according to their physical order along the chromosomes. This restriction can be found in most developing tissues, including the paraxial mesoderm, the neural tube, the neural crest, the limbs, the hindbrain segments, the surface ectoderm, the gut, the branchial arches, and the gonadal tissues (Dolle *et al.*, 1989; Dolle and Duboule, 1989; Graham *et al.*, 1989; Wilkinson *et al.*, 1989; Gaunt, 1991; Hunt and Krumlauf, 1991; Kessel and Gruss, 1991). This correlation between the physical order along chromosomes and patterns of expression is termed "spatial colinearity" (reviewed by Krumlauf, 1994). Typically, "spatial colinearity" is found in a way that the genes more at 3' end of each gene cluster are expressed more anteriorly in developing tissues, while those at more 5' end are activated more posteriorly. (2) There is also a "temporal colinearity" of Hox gene expression during embryogenesis (Krumlauf, 1994). The more 3' a gene is located in each cluster of Hox genes along the chromosome, the earlier the gene is activated (Munke *et al.*, 1986; Izpisua-Belmonte *et al.*, 1991). (3) The responding sensitivity to retinoic acid treatment in cell lines or embryos is also colinear with the organization of Hox genes, i.e. the extreme 3' end gene displays the highest sensitivity to retinoic acid and the extreme 5' end gene displays the lowest sensitivity (Simeone *et al.*, 1990, 1991; Papalopulu *et al.*, 1991; Dekker *et al.*, 1993; reviewed by Krumlauf, 1994). These colinear characteristics of Hox gene expression, along with information from gene knockouts (reviewed by Krumlauf, 1994) suggest that they are involved in establishing regional identities during vertebrate embryogenesis.

1.1.4 From the homeobox to the paired box

While the surprising structural-functional correlation of the Hox complexes were being discovered, the other homeobox-containing gene families, such as *paired*, *msh*, *engrailed*, and *Pit-Oct-Unc* (POU), were also under extensive investigation. For example, the *msh* is an ancient gene family, represented in animals ranging from coelenterates to mammals (reviewed by Davidson, 1995).

The paired-box, like the homeobox, was identified as a conserved motif in several *Drosophila* developmental genes. These genes in the *Drosophila* include *paired* (Frigerio *et al.*, 1986), *gooseberry-proximal, gooseberry-distal* (Baumgartner, *et al.*, 1987), *Pox meso*, and *Pox neuro* (Bopp *et al.*, 1991). These first *Drosophila* paired-box containg genes were used to isolate orthologous genes in other organisms such as nematodes, zebrafish, urodele, chicken, quail, mouse, rat, and man (Dressler *et al.*, 1988; Burri *et al.*, 1989; Quiring *et al.*, 1994; Ton *et al.*, 1991; Walther and Gruss, 1991; Li *et al.*, 1994; Turque *et al.*, 1994; Chisholm and Horvitz, 1995; Krauss *et al.*, 1991; Rio-Tsonis *et al.*, 1995). Thus, the vertebrate homologues were termed the *Pax* gene family.

1.2 Paired-box (*Pax*) gene family

1.2.1 Current members of the *Pax* gene family

In 1996, eight members of the *Pax* gene family have been isolated in the mouse (*Pax1* to *Pax8*) and nine members have been isolated in the human (*PAX-1* to *PAX-9*), along with other *Pax* genes found in other vertebrates. Among them, *Pax1, Pax2, Pax3,* and *Pax6* have been found to be involved in developmental abnormalities in the mouse, rat, and human (Balling *et al.*, 1988; Hill *et al.*, 1991; Ton *et al.*, 1991; Epstein *et al.*, 1991; Matsuo *et al.*, 1993; Keller *et al.*, 1994; Sanyanusin *et al.*, 1995).

Since the *Pax* gene family is best characterised in the mouse, I will introduce most of the information in the mouse. Information on *Pax* genes in other species will only be referred to if it is relevant to this thesis.

1.2.2 Genomic organization and structure of the *Pax* gene family

1.2.2.1 Genomic organization

Unlike the Hox genes, *Pax* genes are not arranged in physical clusters along chromosomes (Stapelton *et al.*, 1993; Pilz *et al.*, 1993; Walther *et al.*, 1991). The eight mouse *Pax* genes are located on five different chromosomes (chromosomes 1, 2, 4, 6 and 19) and the nine human *PAX* genes are located on eight different chromosomes (chromosomes 1, 2, 7, 9, 10, 11, 14, 20) (Stuart *et al.*, 1994; Chalepakis *et al.*, 1992; Hill and Hanson, 1992).

1.2.2.2 Structure

1.2.2.2.1 Gene structure

Vertebrate *Pax* genes contain three elements: a paired domain, a paired-specific homeodomain and a sequence encoding for an octapeptide (see figure 1.1 on the following page). They are arranged in a physical order as 5' -- paired box -- octapeptide -- paired-like homeodomain -- 3' (Hill and Hanson, 1992). The three elements (paired box, octapeptide, and paired-like homeodomain) vary from one member of the gene family to another so that, according to structure, the murine and human *Pax* genes can be grouped into four classes. The first class consists of *Pax1* and *Pax9*. They encode a paired domain and a conserved octapeptide sequence but lack a homeodomain. The second class consists of *Pax3* and *Pax7*. They have in addition to a paired domain, an octapeptide sequence and a full homeodomain. The third class is represented by *Pax2*, *Pax5* and *Pax8*. Each encodes a paired domain and an octapeptide, but only a partial homeodomain. *Pax4* and *Pax6* represent the fourth class. They encode a paired domain and a homeodomain but lack an octapeptide. This structure-based classification of the mouse and the human *Pax* genes has, to some extent, some implications of their expression patterns, particularly in the developing central nervous system (to be detailed in section 1.6.5) (Chalepakis *et al.*, 1993).

1.2.2.2.2 Messenger RNA

Pax genes encode mRNAs ranging from 3.0 to 5.0 kb in length, with the exception of *Pax5* whose mRNA is 9.5 - 10 kb long (Adams *et al.*, 1992; Chalepakis *et al.*, 1993; Chalepakis *et al.*, 1992). Each *Pax* gene probably has its alternative splice products, though so far only some *Pax* genes have been identified as having mRNA isoforms. For example, *Pax2* (Dressler and Douglass, 1992) and *Pax6* (Walther and Gruss, 1991) each have two isoforms of mRNA; *Pax8* has six splice products termed *Pax8a* to *Pax8f* (Kozmik *et al.*, 1993). These alternative splice products do not differ in DNA-binding ability but each isoform has its distinct transactivation ability (Stuart *et al.*, 1993).

Figure 1.1 The chromosomal location of the murine *Pax* and the human *PAX* genes (both denoted 'Pax'), their translated protein structures and names of established mutants. The eight mouse *Pax* genes are located on five different chromosomes (chromosomes 1, 2, 4, 6, 9), while the nine human *PAX* genes are located on eight different chromosomes (chromosomes 1, 2, 7, 9, 10, 11, 14, 20). The structure of Pax proteins is schematically represented, with the amino group (5' end on the DNA sequence) on the left and the carboxyl group (3' end on the DNA sequence) on the right. Pax proteins are generally arranged in a physical order as NH_2 - paired domain - homeodomain - COOH, with or without an octapeptide (OCT) insertion between the paired and the homeodomain. Although the paired domains are highly conserved, minor variations have been characterized. Thus, the paired domains are classified into four different types represented by blank (Pax-1), solid (Pax-2, Pax-5, and Pax-8), hatched (Pax-3, Pax-7), and dotted (Pax-4, Pax-6) boxes. The homeodomains also exhibit variations. The homeodomains within Pax-2, Pax-5, and Pax-8 are shorter as compared to those of Pax-3, Pax-4, Pax-6 and Pax-7. In particular, Pax-1 protein does not contain a homeodomain. Note that the whole structures of Pax-4 and Pax-7 have not been determined yet. Their amino and carboxyl ends are therefore not listed. Mouse Pax-3 and Pax-6 mutants have been established and regarded as human disease models. Mouse Pax-3 mutation leads to *Splotch* which is the counterpart of human *Waardenburg syndrome*. Pax-6 mutation in the mouse causes *Small eye*, a model for human *Aniridia*. Mutations of Pax-1 cause *Undulated* in the mouse, but no comparable human mutation has been established so far.

GENE	CHROMOSOMAL LOCATION MOUSE	HUMAN	STRUCTURE	MUTANT MOUSE	HUMAN
Pax-1	2	20p11		*Undulated*	
Pax-2	19	10q25	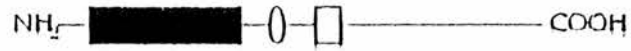		
Pax-3	1	2q35	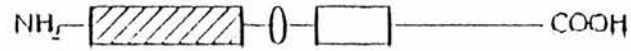	*Splotch*	*Waardenburg syndrome*
Pax-4	6	7	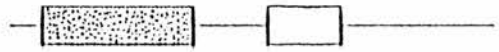		
Pax-5	4	9p13	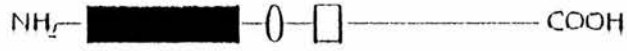		
Pax-6	2	11p13	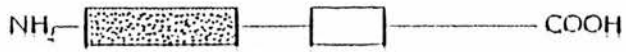	*Small eye*	*Aniridia*
Pax-7	4	1p36.2-p36.12	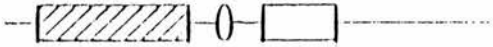		
Pax-8	2	2q12-q14	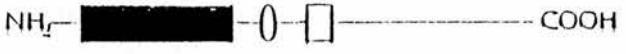		
Pax-9		14q12-q13			

Figure 1.1 The chromosomal location of the murine and human *Pax* genes, structure of the translated proteins and names of established mutants.

1.2.2.2.3 Pax protein

Pax proteins vary from 361 to 479 amino acids in length (Chalepakis *et al.*, 1992). The paired domain consists of a stretch of 128 amino acids and shows no obvious resemblance to other known DNA-binding motifs (Gruss and Walther, 1992). Pax proteins are assumed to act as nuclear transcription factors because they are present in the nucleus and they are able to bind DNA *in vitro* (Dressler and Douglas, 1992; Adama *et al.*, 1992; Chalepakis *et al.*, 1991; Chalepakis *et al.*, 1994; Zannini *et al.*, 1992).

Although only a few of the physiological targets of the Pax proteins have been identified, optimal binding sites have been selected from randomized DNA for the paired domains of *Drosophila* Prd protein and Pax2, Pax5, Pax6, and Pax8 proteins of mouse (Czerny *et al.*, 1993; Epstein *et al.*, 1994; Xu *et al.*, 1995). The Prd protein (encoded by *paired* gene) of the *Drosophila* is the most studied so far and thus provides an example of how Pax proteins interact with their target DNA sequences. Prd is shown to bind to the sequence in the *even-skipped* promotor fraction e5 (Triesman *et al* , 1989; Triesman *et al*, 1991). The target sequences bound by Prd protein include an ATTA motif which is recognized by the homeodomain, and further downstream sequences of the ATTA motif are presumably targeted by the paired domain (Triesman *et al.*, 1991). Furthermore, a pentanucleotide GTTCC has been identified as the DNA binding core motif recognized by the paired domain (Chalepakis *et al.*, 1991). A further analysis using Pax5 protein leads to the proposal of a DNA-paired domain interaction model in which the paired domain is composed of two subdomains (bipartite structure) that bind to the two sites in adjacent major grooves on the same side of the target DNA helix (Czerny *et al.*, 1993). This "bipartite structure" of the paired domain is clearly demonstrated by the crystal structure of *Drosophila* Prd protein in a paired domain-15 bp DNA complex (Xu *et al.*, 1995). The N-terminal domain of the bipartite structure consists of a turn which makes critical contacts in the minor groove, while a HTH (Helix-Turn-Helix) unit makes critical contacts in the major groove (Xu *et al.*, 1995). Analyses of crystal structures will provide a firm interpretation of the known Pax developmental mutations.

For Pax6, at least four variants (p46, p48, p43, and p33/32) have been detected in cellular extracts using specific antisera (reviewed by Cvekl and Joram, 1996). The presence of four Pax6 variants raises questions such as whether they possess equal transcriptional activity, whether all the four variants are present in developing cells *in vivo*, as well as whether they maintain relatively constant amounts during cellular differentiation. These questions are to be answered by further investigations in the future.

1.3 *Pax* gene expression and mutation - a general picture

Section 1.3 will briefly describe the areas of *Pax* gene expression and their mutations, except for *Pax4* which is not yet published, and *Pax6* which will be described in detail in section 1.4. Since *Pax* genes have been more commonly investigated in the mouse (except for *Pax9* that is only described in the chick), I will concentrate on information in the mouse, with data in human mutations if available. My intention here is to give a general picture of *Pax* gene expression and mutation in the vertebrate so that common aspects of the *Pax* genes may become explicit. For *Pax6 per se*, detailed expression profiles and mutations in all published reports available so far will be described in section 1.4 and section 1.5.

1.3.1 *Pax1*

Pax1 mutation leads to *undulated* in the mouse. Mouse *undulated* mutation is characterized by distortions to the vertebral column and sternum, fusion of the sternebrae, absence of intervertebral disks, reduction in the posterior part of the vertebrae, as well as fusions of the dorsal root ganglia, abnormalities of the pectoral girdle and reductions in the thymus and facial skeleton (Gruneberg, 1954; Deutsch *et al.*, 1988; Dietrich *et al.*, 1993; Koseki *et al.*, 1993; Timmons *et al.*, 1994; Wallin *et al.*, 1994; Dietrich and Gruss, 1995). It was originally identified by Wright (Wright , 1947) and described and designated "*un*" by Carter (Carter, 1947). Three alleles of the mouse *Pax1* mutants have been established so far: *un*, un^{ex}, and un^{x} (Balling *et al.*, 1988; 1992; Dietrich and Gruss, 1995). All three alleles display axial skeletal defects. Ectopic expression of *Pax1* transforms cells and lead them to oncogenesis (Maulbecker and Gruss, 1993).

Pax1 is expressed mainly in mesodermal tissues, notably during the formation of axial structures, the vertebral bodies, and the intervertebral disks (Deutsch *et al.*, 1988; Dietrich *et al.*, 1993; Wallin *et al.*, 1994; Dietrich and Gruss, 1995). *Pax1* is also expressed in extra-vertebral tissues such as in the connective tissues surrounding dorsal root ganglia, in the anterior forelimb, in the endoderm of the pharangeal pouches, and in the mandibular/maxillary processes (Deutsch *et al.*, 1988; Dietrich *et al.*, 1993; Timmons *et al.*, 1994; Wallin *et al.*, 1994; Dietrich and Gruss, 1995). *Pax1* is not expressed in the developing central nervous system, which is unusual among *Pax* genes (Deutsch *et al.*, 1988). The *chPax1* (chick *Pax1*) expression is similar to that of the mouse. It is expressed in the developing pectoral girdle, in cells of the ventral part of sclerotomes, in sclerotome cells of the perichordal tube, and later in sclerotome-derived cells in the intervertebral disks (Peters *et al.*, 1995).

The spectrum of mutant phenotypes, the expression data, and the transforming ability induced by ectopic expression suggest that *Pax1* could be important for regulating the proliferation of specific precursor cell populations. It may also play a role in regulating the early differentiation of affected structures, for example, by controlling the condensation of cells (Maulbecker and Gruss, 1993; Timmons *et al.*, 1994; Dietrich and Gruss, 1995).

1.3.2 *Pax2*

Pax2 is involved in kidney and eye development. This is from evidence of gene expression patterns (Dressler *et al.*, 1990; Nornes *et al.*, 1990), gene regulation studies (Rothenpieler and Dressler, 1993; Dressler *et al.*, 1993; Phelps and Dressler, 1993; Ryan *et al.*, 1995), together with analyses of phenotypes from mutations in the mouse (Keller *et al.*, 1994) and in the human (Sanyanusin *et al.*, 1995).

Pax2 is expressed during the differentiation of renal epithelium, being first in the induced mesenchyme and then in the same population of cells through transition and condensation stages (Dressler *et al.*, 1990; Dressler and Douglass, 1990). In more mature renal epithelium, *Pax2* is downregulated (Dressler and Douglass, 1990). In the developing eye, *Pax2* transcripts are first present in the distal part of the

optic vesicle before optic cup is formed. After optic cup formation, *Pax2* expression is restricted to the optic stalk and the ventral half to two-thirds of both inner and outer layers of the optic cup (Nornes *et al.*, 1990). *Pax2* is then expressed during optic nerve formation, in the region that forms the optic fissure, at the exit of the optic nerves from the eye, in the optic disk, optic stalk, and in cells along the vitreal border of the neuroblast layer of the central retina (Nornes *et al.*, 1990).

Phenotypes correlate well with expression data and with the roles of *Pax2* in kidney and eye development. In the mouse, dominant kidney and retina defects (*Krd*) have been described with a deletion including the entire *Pax2* sequences (Keller *et al.*, 1994). In the human, a frame-shift mutation is found in a family manifested with eye and kidney defects (Sanyanusin *et al.*, 1995).

1.3.3 *Pax3*

Pax3 seems to involve in the regulation of proliferation during neural tube development, as well as in neural crest migration and in the development of limb musculature. This is based on expression pattern (Goulding *et al.*, 1991; Bober *et al.*, 1994; Tsukamato *et al.*, 1994), mutant defects from mouse *Splotch* mutation (Epstein *et al.*, 1991, 1993; Goulding *et al.*, 1993; Vogan *et al.*, 1993), and human Waardenburgh syndrome (Tassabehji *et al.*, 1992; Baldwin *et al.*, 1992; Hoth *et al.*, 1993; reviewed by Farrar *et al.*, 1994).

Pax3 is expressed in the dorsal neural tube and in neural crest derivatives such as the dorsal root ganglia, as well as in some lateral parts of somites from which limb musculature is derived (Goulding *et al.*, 1991). In the mouse, homozygous *Splotch* animals exhibit neural tube defects, deficiencies in neural crest derivatives, and severely impaired development of limb musculature (Auerbach, 1954; Moase and Trasler, 1989, 1990; Franz, 1989, 1990, 1993; Franz *et al.*, 1993). In the human, *PAX3* mutation causes Waardenburg symdrome (WS). Waardenburg syndrome is a dominantly-inherited syndrome that displays variable phenotypes of deafness, pigmentary abnormalities such as a white forelock or heterochromic irises, and characteristic facial features (reviewed by Pantke and Cohen, 1971). According to the spectrum of defects, WS is clinically subdived into subtypes. WS type I and

type III are most likely to have resulted from mutations in *PAX3* (reviewed by Farrar *et al.*, 1994). WS type I patients typically have dystopia canthorum, in which the inner corner of the eye is displaced outwards and the bridge of the nose is unusually broad. WS type I patients also usually display pigmentation abnormalities and hearing defects, but rarely have neural tube defects similar to those found in the homozygous *Splotch* mutant mice (Pantke and Cohen, 1971; Narod *et al.*, 1988; Begleiter and Harris, 1992; Moline and Sandlin, 1993). WS type III patients have defects found in type I with additional limb abnormalities that are comparable to those found in the mouse *Splotch* mutants. Thus, patients of WS syndromes display phenotypes similar to those found in the mouse *Splotch*. This is consistent with the role of *Pax3* in the neural crest migration and in the development of limb musculature.

Pax3 is also involved in alveolar rhabdosarcoma, a tumour that is characteristically found in regions of striated muscle differentiation, suggesting a role for *Pax3* in controlling cellular proliferation (Barr *et al.*, 1993; Fredricks *et al.*, 1995).

1.3.4 *Pax5*

Pax5 has been demonstrated to involve in B cell differentiation and in the development of midbrain-hindbrain boundary by analyses of its expression patterns, loss-of-function phenotypes and gene regulation.

During hematopoiesis, *Pax5* encodes a B-cell specific transcription factor, BSAP (Adams *et al.*, 1992). BSAP is expressed in early B cell differentiation (Barberis *et al.*, 1990) and exhibits a role in the regulation of B cell proliferation (Wakatsuki *et al.*, 1994; reviewed by Dorshkind, 1994). The role of *Pax5* in B cell development is further demonstrated by Pax5 deficient mice in which early B cell differentiation is completely blocked (Urbanek *et al.*, 1995). *Pax5* is also expressed in the midbrain-hindbrain boundary, suggesting a role in the development of this region (Asano and Gruss, 1992). Further evidence from the homozygous *Pax5* mutant mice shows reduction in the posterior midbrain,

but without increased cell death or an imbalance in cell types, indicating that *Pax5* is important for proliferation of this region (Urbanek *et al.*, 1994).

1.3.5 *Pax7*

Pax7 is closely related to *Pax3* in structure, both at the DNA and at the amino acid sequence level (Jostes *et al.*, 1991; Goulding *et al.*, 1991). Their expression patterns and induction of expression are also similar. Both *Pax3* and *Pax7* are expressed in the dorsal nervous system and in the dermomyotome (Jostes *et al.*, 1991; Goulding *et al.*, 1991; Bober *et al.*, 1994). In the dermomyotome, both genes can be induced by contact with surface ectoderm and a diffusible signal from the dorsal neural tube (Fan *et al.*, 1994). *Pax7* is also involved in alveolar rhabdosarcoma, suggesting a role in controlling cellular proliferation (Davies *et al.*, 1994).

1.3.6 *Pax8*

Pax8 shares similarities in both structure and expression with *Pax2*, although some differences exist. Both genes are expressed in the developing kidney and in Wilms' tumours, although the dynamics of expression suggests that *Pax8* may be expressed slightly later than *Pax2* (Plachov *et al.*, 1990; Poleev *et al.*, 1992; Zannini *et al.*, 1992). Unlike *Pax2*, *Pax8* is not reported to be expressed in the developing eye (Plachov *et al.*, 1990). *Pax8* is also expressed in the thyroid where it appears to involve in the regulation of two target genes, *thyroglobulin* and *thyroperoxidase* (Zannini *et al.*, 1992).

1.3.7 *Pax9*

Pax9 expression has not been reported in the mouse; only chick *Pax9* (*chPax9*) expression is described (Peters *et al.*, 1995). Expression of *chPax9* is found in the epithelial cells of the embryonic and adult thymus and in cells of the developing intervertebral disks where it overlaps with the expression of

chPax1 (Peters *et al.*, 1995). Unlike *chPax1, chPax9* is not expressed in the perichordal sclerotome cells that will give rise to vertebral bodies. Transcripts of *chPax9* are also distributed in circumscribed areas of mesenchyme in the metatarsus as well as in endodermal derivatives, i.e. in the lining epithelium of the developing pharynx and of embryonic and adult esophagus (Peters *et al.*, 1995). No *Pax9* mutation has been described.

1.4 *Pax6* expression profiles

When this study was initiated, little was known about *Pax6* and its expression. The only publications concerning *Pax6* were only brief descriptions of patterns of expression in the mouse (Walther and Gruss, 1991), the human (Ton *et al.*, 1991), and the zebrafish (Krauss *et al.*, 1991; Puschel *et al.*, 1992). However, during the course of this study, much more information about *Pax6* has been published. For example, orthologous genes of *Pax6* have been isolated in other species and their expression profiles have been established. These orthologous genes were named either the same as their murine counterpart, for example, "*Pax6*" in the chick (Li *et al.*, 1994; Turque *et al.*, 1994), the urodele (Rio-Tsonis *et al.*, 1995), and in the nematode (Chisholm and Horvitz, 1995; Zhang and Emmons, 1995); or in other names such as *Pax-QNR* in the quail (Martin *et al.*, 1992; Carriere *et al.*, 1993; Turque *et al.*, 1994), *Pax[zf-a]* in the zebrafish (Krauss *et al.*, 1991; Puschel *et al.*, 1992) and *ey* in the *Drosophila* (Quirring *et al.*, 1994; Halder *et al.*, 1995). Section 1.4 will describe the expression profiles that have been published.

1.4.1 *Pax6* expression in the mouse/rat

In the mouse, *Pax6* is expressed in discrete regions of the brain, in the neural tube, in the developing eye, the pituitary, the pancreas, and the nasal epithelium (Walther and Gruss, 1991; Turque *et al.*, 1992; Goulding *et al.*, 1993; Matsuo *et al.*, 1993; Grindley *et al.*, 1995; Stoykova *et al.*, 1996). Details of *Pax6* expression in those areas are described in the following sub-sections (1.4.1.1 - 1.4.1.4).

1.4.1.1 In the developing brain

Pax6 expression is first detected in the presumptive telencephalon and rhombencephalon at day 8.0 p.c. (or alternatively denoted as E 8.0 p.c.) (Walther and Gruss, 1991; Grindley *et al.*, 1995); however, *Pax6* transcripts are not detectable in the presumptive met- and mesencephalon (Walther and Gruss, 1991). This overall distribution of *Pax6* expression in the developing brain is maintained, with the exception of the metencephalon where expression is detected from day 15.5 p.c. onwards (Walther and Gruss, 1991).

In the primitive telencephalon, high levels of expression are detected mainly at the ventricular zone in the lateral and dorsal neuroepithelium but not in the basal neuroepithelium. Some areas of expression have been specifically localized, including the ventricular zone, the epithalamus, the pineal gland, and the piriform cortex (Walther and Gruss, 1991; Grindley, 1996; Stoykova and Gruss, 1996). The olfactory bulbs also exhibit high levels of *Pax6* transcripts (Walther and Gruss, 1991).

From the telencephalon to the diencephalon, *Pax6* expression domain extends to a sharp caudal border at the posterior commissure (the boundary between diencephalon and mesencephalon). Expression in the ventral thalamus, the preoptic recess, and the supraoptic/paraventricular areas of the diencephalon can be specifically localized at day 10.5 p.c. to day 12.5 p.c. (Walther and Gruss, 1991; Grindley, 1996; Stoykova and Gruss, 1996). *Pax6* transcripts are not detected in the metencephalon until day 15.5 p.c. when expression can be detected in the external granular layer and in the cells distributed in the dorsal cerebellum. Transcripts of *Pax6* are also found in the pontine nuclei and the inferior olivary nuclei (Walther and Gruss, 1991).

Pax6 expression in the myelencephalon is basically the same as that in the spinal cord. Transcripts are most abundant in the ventricular zone at earlier stages and the expression is decreased later, as the ventricular zone becomes regressed (Walther and Gruss, 1991).

1.4.1.2 In the developing spinal cord

Pax6 transcripts are initially present in the developing spinal cord in a broad band of cells at day 8.5 p.c., being absent only from the most dorsal and ventral cells. As the spinal cord develops, *Pax6* expression is gradually restricted. At the beginning of day 9.0 p.c., *Pax6* expression in the dorsal part of the neural tube appears to be downregulated and *Pax6* transcripts are confined only in the ventral part, i.e. in the basal plate, although weaker signals can be detected in the alar plate (Walther and Gruss, 1991). Between day 11.5 p.c. to day 12.5 p.c., *Pax6* transcripts are only detectable in the ventricular zone and the ventral intermediate zone in the basal plate (Walther and Gruss, 1991). By day 13.5 p.c., *Pax6* transcripts are found further regressed, concordant with reduction of the ventricular zone. By day 15.5 p.c., further restriction has made *Pax6* transcripts only detectable within a subset of ependymal cells and in a subset of postmitotic cells (Walther and Gruss, 1991).

1.4.1.3 In the developing eye

The first transcripts of *Pax6* in the developing eye are detected in the optic pit at day 8.5 p.c. (Grindley *et al.*, 1995). Later, *Pax6* expression is found in the lens, the optic cup, and the optic stalk (Walther and Gruss, 1991; Matsuo *et al.*, 1993; Grindley *et al.*, 1995).

Pax6 expression is developmentally restricted in the developing eye. By day 9.5 p.c., *Pax6* transcripts are found in the optic vesicle, the optic stalk, and in a broad area of surface ectoderm, including the area where the furure lens will develop. Between day 10.0 p.c. and day 12.0 p.c., i.e. during the period when the optic cup and the lens are formed, *Pax6* is expressed in both the inner and the outer layers of optic cup, as well as in the lens and the overlying future cornea (Grindley *et al.*, 1995). By day 15.5 p.c.,

Pax6 transcripts are restricted to the rim of optic cup (Grindley *et al.*,, 1995). The broad area of *Pax6* expression in the surface ectoderm also becomes confined to the future corneal epithelium bordering at the conjunctiva (Grindley *et al.*, 1995).

1.4.1.4 In the developing pituitary, pancreas, and nasal epithelium

Pax6 expression is detected in the developing adenohypophysis (anterior pituitary) from day 11.5 p.c. (Walther and Gruss, 1991). Transcripts are detected within Rathke's pouch and its derivatives, the *pars intermedia* and *distalis,* but not in the infundibulum or the differentiating *pars neuralis* (Walther and Gruss, 1991). By day 15.5 p.c., *Pax6* expression is still detectable in the epithelium lining the lumen of Rathke's pouch and in the anterior lobe; the expression is reduced to just about background level by day 18.5 p.c.

In the nasal region, the earliest *Pax6* expression is found in the nasal placode by day 9.5 p.c. (Grindley *et al.*, 1995). *Pax6* transcripts remain in the placodal epithelium during the course of nasal pit formation and subsequently in the nasal epithelium (Walther and Gruss, 1991; Matsuo *et al.*, 1993; Grindley *et al.*, 1995).

Pax6 is also expressed in the developing pancreas in the mouse (Turque *et al.*, 1992).

1.4.2 *PAX6* expression in the human

PAX6 transcripts are expressed in the eyes, the brain, and the pancreas (Ton *et al.*, 1991). In the brain, the cerebellum and the pons have the highest level of expression, whilst the temporal lobe, midregions, medulla oblongata and choroid plexus have less expression (Ton *et al.*, 1991). *PAX6* transcripts are also detected in the olfactory bulb and in the intermediate brain layers (Ton *et al.*, 1991). In the human eye at 49 days of gestation, *PAX6* expression is found in the rim of the optic cup, the neural retina, the lens and the surface ectoderm that will give rise to cornea and conjunctiva, but no *PAX6* expression is found in the pigmented retinal epithelium (Ton *et al.*, 1991).

1.4.3 *Pax6* expression in the chick and *Pax-QNR* expression in the quail

1.4.3.1 *Pax6* expression in the chick

The first evident *Pax6* expression is detected at Hamburger-Hamilton stage 6 (Hamburger and Hamilton, 1951) during chick embryogenesis in a crescent-shaped band of prospective ectodermal cells near the anterior margin of the neural plate, but not in the neural plate itself (Li *et al.*, 1994). At stage 7^{+}, *Pax6* transcripts are concentrated in the cells lateral to the neural plate, i.e. the cells that will give rise to the facial, lens, and corneal ectoderm. The neural plate itself exhibits only trace amount of signals in contrast with those in the lateral cells. Thus, *Pax6* expression in the chick is initiated not in the neural tissues, but in the anterior ectodermal cells.

In the developing brain, a significant amount of *Pax6* transcripts appear at stage 8^{+} over the presumptive dorsal forebrain region. This distribution of *Pax6* expression in the presumptive forebrain is so quickly restricted that at stage 9 only the areas of optic outgrowths and the dorsal midline of diencephalon remain *Pax6*-expressing (Li *et al.*, 1994). By stage 11, *Pax6* expression is further restricted and found only in the roof of diencephalon and in the optic vesicle. *Pax6* is also expressed in the neuroepithelium of rhombomere 3 in the developing hindbrain, but not in the midbrain as shown in the published photographs by Li *et al.* (1994).

In the surface ectoderm of the head, the distribution of *Pax6* transcripts is restricted in accordance with that of the developing brain. At stage 8^+, a large area of surface ectoderm is *Pax6*-expressing. By stage 9, however, the *Pax6*-expressing territory in the head surface ectoderm is diminished and covers only the outgrowths of optic vesicles and the dorsal midline of diencephalon (Li *et al.*, 1994).

In the developing eye, *Pax6* is highly expressed in the optic placode and at later stages in the developing lens and its surrounding surface ectoderm where a part will give rise to the corneal epithelium. In the developing optic cup and optic stalk, *Pax6* transcripts are found in the neural retina and the optic nerve. In the nasal epithelium, however, whether *Pax6* expression is present is not yet determined (Li *et al.*, 1994).

In the trunk region, *Pax6* is expressed in the neural plate overlying each newly formed somite and in a cluster of endodermal cells of the stage 13 gut (Li *et al.*, 1994). Li *et al.* (1994) did not specify the cluster of endodermal cells in the midbody region as pancreatic cells.

1.4.3.2 *Pax-QNR* expression in the quail

The distribution of *Pax-QNR* transcripts during quail embryogenesis has been investigated using both Northern blot analysis and *in situ* hybridization and was reported to be comparable to that during chick embryogenesis (Martin *et al.*, 1992). In the developing quail brain, *Pax-QNR* is expressed in the forebrain area (particularly in components of the developing eyes) and the hindbrain area (particularly in the cerebellum), but not in the midbrain. In the developing eye, the lens and the neural retina are reported as highly expressing areas, whereas transcripts of *Pax-QNR* are not detected in the pigmented retinal epithelium (Martin *et al.*, 1992; Carriere *et al.*, 1993). In the neural retina, *Pax-QNR* transcripts are clearly shown in the ganglionic cell layer and in the ventral portion of the inner nuclear layer (Martin *et al.*, 1992). *Pax-QNR*-encoded proteins that contain only the homeodomain are also detected in the neural retina (Carriere *et al.*, 1993). *Pax-QNR* is also expressed in the developing pancreas (Turque *et al.*, 1994).

1.4.4 *Pax6* expression in the urodele

Pax6 expression during normal newt and axolotol eye development as well as during lens regeneration following lentectomy have been investigated (Del Rio-Tsonis *et al.*, 1995). *Pax6* transcripts are localized in the neural retina, the lens, and the corneal epithelium. Following lentectomy in the newt, *Pax6* transcripts are detected in all stages of lens regeneration in the growing lens, the retina, and the corneal epithelium (Del Rio-Tsonis *et al.*, 1995), whereas, in the axolotol which is not capable of regenerating lens, *Pax6* expression is decreased in the larval eye as the animal grows older (Del Rio-Tsonis *et al.*, 1995).

1.4.5 *Pax[zf-a]* expression in the zebrafish

Pax[zf-a], the *Pax6* homologue in the zebrafish, is expressed in the developing central nervous system, the eye, the olfactory bulb, and the pituitary (Krauss *et al.*, 1991; Puschel *et al.*, 1992). The expression is developmentally restricted in a way comparable to that in other vertebrates (Krauss *et al.*, 1991; Puschel *et al.*, 1992).

In the developing central nervous system, *Pax[zf-a]* expression begins in a strip of cells in the neuroectoderm, including the prospective diencephalon and a part of the telencephalon as well as the hindbrain and the ventral spinal cord extending from the level of the first rhombomere to the posterior end of the CNS (Puschel *et al.*, 1992). The anterior boundary of expression in the hindbrain lies between the met- and myelencephalon. The posterior boundary of expression in the diencephalon is detected at the border between the di- and mesencephalon. At later stages, expression in the brain becomes restricted to smaller groups of cells in the di- and telencephalon. *Pax[zf-a]* is also expressed in the olfactory bulb and in the pituitary (Puschel *et al.*, 1992).

In the eye, during the course of optic cup formation, *Pax[zf-a]* is expressed in the developing lens and the neural retina, but not in the optic stalk or the pigmented retinal epithelium. The expression in the

retina is first found in both the ganglion cell layer and the inner nuclear layer (Krauss *et al.*, 1991), but it becomes restricted to the ganglion cell layer at later stages (Puschel *et al.*, 1992).

1.4.6 *Pax6* expression in the nematode

The nematode *Caenorhabditis elegans Pax6* encodes at least two types of transcripts with two independent genetic functions. The first one is called *vab-3*. Transcripts of *vab-3*, like the other *Pax6* genes found in other species, contain a paired domain and a homeodomain (Chisholm and Horvitz, 1995). The second one is called *mab-18*. Transcripts of *mab-18* contain only the homeodomain and is expressed under the control from an internal promotor (between the paired domain and the homeodomain) (Zhang and Emmons, 1995. Transcripts of *vab-3* are found initially in precursors of the head hypodermal (epidermal-like) cells and neurons, and subsequently in the progeny of these cells (Chisholm and Horvitz, 1995). Transcripts of *mab-18* are located in the similar areas as those of *vab-3*, i.e. in the anterior hypodermal nuclei and head neurons (Zhang and Emmons, 1995; Chisholm and Horvitz, 1995).

1.4.7 Expression of *ey* in the *Drosophila*

The orthologous *Pax6* gene in the *Drosophila* is *ey*, which is established by homology of amino acid sequence and mutant phenotypes (Quiring *et al.*, 1994). The transcripts of *ey* are distributed in a bilaterally symmetrical pattern in the brain and in every segment of the ventral nervous system at the germ-band stage. *ey* is also expressed in the imaginal discs (primordia of eye) and in the salivary glands anterior to the brain (Quiring *et al.*, 1994). Later in embryogenesis, *ey* transcripts become confined to the brain and the primordia of the eye, while in the segmental ventral ganglions *ey* transcripts disappear (Quiring *et al.*, 1994).

1.5 *Pax6* mutations

1.5.1 *Pax6* mutations in the mouse and in the rat

Mutations in the *Pax6* gene result in *Small eye* (*Sey*) in the mouse (Hill *et al.*, 1991) and *rat Small eye* (*rSey*) in the rat (Matsuo *et al.*, 1993). These two species are very closely related and their mutations in the *Pax6* display very similar characteristics. They are therefore described together.

Small eye is an autosomal, semi-dominant, homozygous lethal mutation first found as a spontaneous mutation in Edinburgh in 1967 (Roberts, 1967), but without being described in detail until 1986 (Hogan *et al.*, 1986). To date, five murine *Small eye* alleles have been described: *Sey*, Sey^{neu}, Sey^{neu2}, Sey^{H}, and Sey^{Dey} (reviewed by Chalepakis *et al.*, 1993). Except for Sey^{neu2}, all *Small eye* alleles have been described in detail. Sequence analyses reveal that *Sey* is caused by a point mutation which introduces a stop codon between the paired and the homeodomain (Hill *et al.*, 1991). Sey^{neu} also displays a point mutation, leaving an unspliced intron and a premature translation termination signal at the downstream of the homeodomain. Both Sey^{H} and Sey^{Dey} contain a deletion in the *Pax6* locus (Chalepakis *et al.*, 1993).

In general, more severe phenotypes are found in the homozygous state, suggesting a gene-dosage effect. *Small eye* mutants in the homozygous state are generally 10 % smaller than their unaffected littermates (M.H. Kaufman, personal communication). Homozygous mutants do not survive and die either during early neonatal stage (for *Sey*) or at implantation (for Sey^{H}). The homozygous *Sey* mice die shortly after birth, probably because they do not develop nasal cavities and thus can not breathe (Hogan *et al.*, 1986). The homozygous Sey^{H} embryos die at implantation, presumably because the deletion also contains genes essential for early embryo survival (Glaser *et al.*, 1990).

The effect of *Sey* mutation was previously believed to be limited only to the growth and differentiation of the presumptive lens and nasal placodes (Hogan *et al.*, 1986). Homozygous *Sey/Sey* embryos can be distinguished as early as 10.5 days p.c. (Grindley, 1996). The optic cup grows, but the surface

ectoderm does not give rise to the lens and the nasal placode (Hogan *et al.*, 1986; Grindley *et al.*, 1995). As a result, the optic cup degenerates and all the other derivatives of the eye, including the cornea, do not develop (Grindley *et al.*, 1995).

More detailed analyses, however, led to discoveries of other affected areas. In the developing cerebral cortex in the forebrain at days 12.5 to 14.5 p.c., homozygous *Sey*^{neu} and *Sey* mice exhibit defects of neuronal migration and cortical plate reduction with heterotopic groups of cells found in the intermediate zone in the posterior and dorso-lateral telencephalon (Schmahl *et al.*, 1993; Grindley, 1996). The archicortex anlage fails to invaginate along the medial wall of the telencephalic vesicle (Stoykova *et al.*, 1996). In the developing diencephalon of the mutant brain (for *Sey/Sey*), the primordia of prosomere 3 (the very rostrodorsal part of the ventral thalamus) and prosomere 4 (eminentia thalami) grow in the wrong direction and the compartmentalization within the hypothalamus is distorted (Stoykova *et al.*, 1996). Further analyses at day 18.5 p.c. show underdevelopment of the internal capsule, corpus callosum, posterior commissure and the basal ganglia. The third and the lateral forebrain ventricles are connected through wide openings (instead of through the normally thin foramina Monro) (Stoykova *et al.*, 1996). The left and right sides of the diencephalon are not fused (Grindley, 1996; Stoykova *et al.*, 1996), probably as a result of dysgenesis in the diencephalon. The forebrain abnormalities are coincident with domains of *Pax6* expression and the boundaries between *Pax6*-expressing domains and those of other genes, for example *Dlx1*, are disturbed (Stoykova *et al.*, 1996).

In the developing maxilla, *Sey/Sey* embryos exhibit a shorter snout at day 14.5 p.c. as compared to that of their wildtype litermates (Hill *et al.*, 1991). The homozygous embryos also display a cartilaginous rod-like structure which protrudes forwards from the rostral part of the cranial base and extends to the tip of the shortened snout (Kaufman *et al.*, 1995). In addition to that rod-like structure, a high percentage (82 %) of the *Sey/Sey* embryos have one or two additional upper incisor teeth (Kaufman *et al.*, 1995). The *rat Small eye* (*rSey*) shows that *Pax6* mutation also impairs the migration of the midbrain neural crest cells in the homozygous state (Matsuo *et al.*, 1993).

In the heterozygous state, mice affected by *Sey* and Sey^{neu} can survive but display smaller eyes with defects in the lens and the cornea, although without obvious abnormalities within the nose and the teeth. In addition to the presence of smaller eyes, mice affected by Sey^{H} and Sey^{Dey} mutations also show growth retardation, small ears, white belly pots and eye coloboma in the heterozygous state (Chalepakis *et al.*, 1993).

The combination of these findings suggests extensive roles of *Pax6* during development, particularly in the craniofacial area.

1.5.2 *PAX6* mutations in the human

In the human, *PAX6* mutation leads to a variety of abnormalities associated with aniridia (*AN*) and *Peter's anomaly* (Ton *et al.*, 1991; Jordan *et al.*, 1992; Hanson and van Heyningen, 1995).

Aniridia is a panocular disorder with an incidence between 1 in 64,000 and 1 in 96,000 (Shaw, 1960). In the homozygous state, *PAX6* mutation may lead to death after birth (Hodgson and Saunders, 1980; Jordan *et al.*, 1992). In the heterozygous state, *AN* phenotypes are variable with anomalies of cataracts, lens dislocation, foveal dysplasia, optic nerve hypoplasia, and nystagmus. In particular, corneal vascularization and glaucoma are commonly found (Jordan *et al.*, 1992; Hanson and van Heyningen, 1995). The effects on vision are variable, in accordance with the anomalies. *Peter's anomaly* represents one of the wide spectrum of anterior segment malformations found in the patients affected by aniridia (Hanson and van Heyningen, 1995). *PAX6* mutations are therefore proposed to be associated with anterior segmentation in the human (Hanson and van Heyningen, 1995). The combination of these findings, like the findings in the mouse, also suggests extensive roles of *PAX6* during craniofacial development.

1.5.3 *Pax6* mutations in the nematode

Several nematode *C. elegans Pax6* mutants have been identified, including *vab-3* and *mab-18* mutants (Chisholm and Horvis, 1995; Zhang and Emmons, 1995). The abnormal phenotypes caused by loss-of-function defects in *vab-3* and *mab-18* include aberrant morphogenesis in the head region, transformation of hypodermal (epidermal-like) cell fates to those of posterior homologues, and abnormal specification of neurons (Chisholm and Horvis, 1995). In the tail region of the male animals, defects in gonadogenesis (for *vab-3*) and transformation of sense-organ identity (for *mab-18*) are found, i.e. the sense ray 6 is transformed into ray 4 (Chisholm and Horvitz, 1995; Zhang and Emmons, 1995). These mutant phenotypes are generally located in regions showing *Pax6* (both *vab-3* and *mab-18* transcripts) expression and support a general role of *Pax6* in defining cell fate during nematode embryogenesis.

1.5.4 The *eyeless* (*ey*) mutation in the *Drosophila*

The *eyeless* (*ey*) mutation of *Drosophila* was first reported in 1915 and since then was introduced as an artificially produced mutation characterized by partial or complete absence of compound eyes (Halder *et al.*, 1995). In addition to *ey* mutation, two spontaneous mutations, ey^2 and ey^R, were established afterwards among many others with mutated eye defects (Quiring *et al.*, 1994). However, the *ey* gene was not isolated until 1994 (Quiring *et al*, 1994), after *Pax6* in the mouse (Walther and Gruss, 1991) and *PAX6* in the human (Ton *et al.*, 1991) were isolated.

In addition to the obvious absence of eye formation, it is shown that *ey* expression is also disturbed in the mutants. In contrast to the normal embryos (see section 1.4.7), the ey^2 and ey^R mutant embryos show no *ey* expression in the anterior edge of the eye disk (Quiring *et al.*, 1995), supporting a role of *ey* in eye formation. More surprisingly, ectopic expression of the *ey* gene leads to ectopic eye formations on the wings, the legs, and the antennae (Halder *et al.*, 1995), indicating that *ey* may be a master gene in eye formation.

The finding of *ey* gene and its expression pattern in the normal and wildtype eye disks indicate a role of *ey* gene in the formation of the *Drosophila* eye.

1.6 Common aspects of the *Pax* genes

This section summarizes common aspects of the *Pax* genes. To support the common characteristics raised here, as many examples as possible are given. This will inevitably repeat many points that are already described in previous sections.

1.6.1 *Pax* genes are developmentally restricted

Pax genes are expressed at early stages of development, usually before the onset of an activity (differentiation, migration, or formation) in a cell population and become restricted as the embryo develops. *Pax1,* for example, is expressed during the formation of the vertebral bodies and intervertebral disks (Deutsch *et al.*, 1988; Dietrich *et al.*, 1993; Wallin *et al.*, 1994; Dietrich and Gruss, 1995). The expression is later downregulated as vertebral bodies begin to chondrify (Wallin *et al.*, 1994; Dietrich and Gruss, 1995). *Pax2* is first expressed in the mesenchyme and later is downregulated in more mature renal epithelium (Dressler *et al.*, 1990; Dressler and Douglas, 1990). *Pax3* is first expressed in the dorsal neural tube and in the neural crest derivatives. The expression of *Pax3* in the dorsal neural tube is later restricted to mitotic stem cell populations (Goulding *et al.*, 1991). *Pax6* expression is also developmentally restricted. *Pax6* expression in the head surface ectoderm is first detected in a broad domain, but later it is restricted to the areas of future cornea (Grindley *et al.*, 1995). Restriction of *Pax6* expression is also seen in the optic cup where *Pax6* transcripts can be detected only in the rim at later stages (Grindley *et* al., 1995). In the developing central nervous system, *Pax6*-expressing domains are reduced in older embryos (Walther and Gruss, 1991; Stoykova and Gruss, 1994; Stoykova *et al.*, 1996).

1.6.2 *Pax* genes are expressed in highly mitotic or immature cells

Pax genes are expressed in cells of highly mitotic activity and are often downregulated as cells differentiate, implicating involvement in cellular proliferation and oncogenesis (Read, 1995). *Pax1* is expressed in the mitotic scleratome and anterior limb mesenchyme and is later downregulated during chondrogenesis (Deutsch *et al.*, 1988; Timmons *et al.*, 1994). *Pax2* is expressed during the maturation of renal epithelium and is downregulated as the renal epithelium matures (Dressler *et al.*, 1990; Dressler and Douglas, 1990). In the developing CNS, *Pax2* expression correlates with the transition from predominantly mitotic to migratory behaviour of neuroblasts (Nornes *et al.*, 1990). *Pax3* is expressed in the myoblast stem cells in the developing limb (Bober *et al.*, 1994), as well as in the highly mitotic cells in the ventricular zone in the developing CNS where it is downregulated before neuroblast migration (Goulding *et al.*, 1991; Jostes, *et al.*, 1991). *Pax5* is expressed in early B cell proliferation (Barberis *et al.*, 1990) and is involved in the regulation of B cell proliferation (Wakatsuki *et al.*, 1994). *Pax6* expression in the telencephalon is seen within the mitotic ventricular zone (Walther and Gruss, 1991). *Pax7* expression in the CNS is also limited to mitotic stem cells in the ventricular zone and is downregulated before neuroblast migration (Jostes *et al.*, 1991).

Oncogenic potential has been reported for some *Pax* genes under *in vitro* (Maulbecker and Gruss, 1993) and *in vivo* conditions (Dressler and Douglas, 1992; Barr *et al.*, 1993; Poleev *et al.*, 1992 a, b). Overexpression of intact or truncated *Pax* genes (*Pax1, Pax2, Pax6* and *Pax8*) in fibroblasts leads to uncontrolled growth (Maulbecker and Gruss, 1993; reviewed by Stuart *et* al., 1993). Pax2 and Pax8 proteins have been detected in the Wilms' tumour (reviewed by Hastie, 1993), suggesting their involvements. *Pax3* and *Pax7* have also been implicated in the formation of alveolar rhabdosarcoma (Barr *et al.*, 1993; Davis *et al.*, 1994). *Pax5* may be involved in the progression of astrocytomas to glioblastoma (Stuart *et al.*, 1993).

1.6.3 Areas of *Pax* gene expression coincide well with sites of loss-of-function defects

Areas of *Pax* gene expressions are generally coincident with areas where loss-of-function defects are found during embryogenesis, which suggests functional necessity for *Pax* genes in their expression areas. For example, *Pax1* is expressed in mesodermal tissues during the formation of axial structures. Thus, *Pax1* mutation (*undulated*), leads to axial skeletal defects (Deutsch *et al.*, 1988; Balling *et al.*, 1988). *Pax2* is expressed during kidney and eye development. Defects in these two organs are found in the *Krd* mouse (Keller *et al.*, 1994) and in the family with *PAX2* mutation (Sanyanusin *et al.*, 1995). *Pax3* is expressed in the dorsal neural tube, neural crest derivatives, as well as in the tissues designated to form the limb musculature (Goulding *et al.*, 1991). Thus, homozygous *Splotch* mice show neural tube defects, deficiencies in neural crest derivatives, and severely impaired limb musculature (Moase and Trasler, 1989; 1990; Franz, 1989, 1990, 1993; Franz *et al.*, 1993). The coincidence is also seen in the human WS (Waardenburg syndrome) mutations. Neuralcristopathies such as pigmentary abnormalities, characteristic facial features, and deafness, as well as limb abnormalities are commonly seen in WS patients (Pantke and Cohen, 1971; Farrar *et al.*, 1994). *Pax6* is expressed in the eye, the nose, and the developing CNS. Thus, defects of *Sey* and *rSey* mutations are found in areas where *Pax6* is expressed (Hogan *et al.*, 1986, 1988; Matsuo *et al.*, 1993; Fujiwara *et al.*, 1994; Kaufman *et al.*, 1994; Grindley *et al.*, 1995; Stoykova *et al.*, 1996). Comparable coincidence is also seen in the *Aniridia* mutation in the human (Ton *et al.*, 1991; Jordan *et al.*, 1992; Hanson *et al.*, 1994a). Areas of functional necessity, as compared to loss-of-function phenotypes, are also seen in *Pax5*-expressing tissues (Adams *et al.*, 1990; Asano and Gruss, 1992; Urbanek *et al.*, 1994).

1.6.4 Regulatory signals of *Pax* genes from notochord and floor plate

Signals from notochord or floor plate appear to regulate *Pax* gene expression in various systems. *Pax1* expression in the scleratome depends on the presence of notochord, either for activation or maintenance (Koseki *et al.*, 1993; Brand-Saberi *et al.*, 1993). *Pax2* expression is also suggested to be regulated by notochord or floor plate, based on the presence of *Pax2*-expressing domains in the ectopic ventral basal plate found in the *Danforth's short tail* mice (Phelps and Dressler, 1993). In the developing spinal

chord, *Pax3* and *Pax6* expressing domains are altered in response to notochord grafts (Goulding *et al.*, 1993). Documented candidate signals that regulate *Pax* gene expression include *Sonic hedgehog* (*Shh*) (Echelard *el al.*, 1993; Roelink *et al.*, 1994; Johnson *et al.*, 1994; Macdonald *et al.*, 1995), NGF (Kioussi and Gruss, 1994), BDNF (Kioussi and Gruss, 1994), activin A (Yamada *et al.*, 1994; Pituello *et al.*, 1995) and bFGF (Yamada *et al.*, 1994). Most of them are signals that can be found in the notochord or the floor plate. The floor plate is also a site of retinoid synthesis (Wagner *et al.*, 1990; Chen *et al.*, 1992; Hogan *et al.*, 1992) and may have a regulatory role in *Pax* gene expression in a way similar to the regulation of many *Hox* genes (reviewed by Mavilio, 1993).

1.6.5 *Pax* genes in the developing CNS and in the adult brain

1.6.5.1 *Pax* genes in the developing central nervous system

All *Pax* genes (except for *Pax1*) are spatially and temporally expressed during the development of central nervous system (CNS) (Chalepakis *et al.*, 1992). Current data suggest that *Pax* genes are involved in the specification of cells along the anterior-posterior (A-P) and the dorsal-ventral (D-V) axis, in the developing brain and spinal cord (Chalepakis *et al.*, 1992; Stuart *et al.*, 1993; Puelles and Rubenstein, 1993).

The structure-based classification (introduced in section 1.2.2.2.1) of *Pax* genes have, to a certain extent, some implications on their expression patterns during CNS development as illustrated in figure 1.2 (Chalepakis *et al.*, 1992; Stuart *et al.*, 1993; Stoykova and Gruss, 1994).

Murine *Pax* genes (*Pax3*, *Pax6*, *Pax7*) that contain a paired-specific homeobox in addition to the paired box begin to express at day 8.0 - 8.5 p.c., i.e. before the onset of cellular differentiation in the developing central nervous system. The expression domains of these genes along the anterior-posterior axis are initially confined to the mitotically active cells of the ventricular neuroepithelium throughout the entire length of the prechordal (anterior) and the epichordal (posterior) subdivisions of the neural tube. By day 10.0 p.c., *Pax3* and *Pax7* expression domains retract to a rostral limit that appears to be at

the level of posterior commissure in the diencephalon (Goulding *et al.*, 1991; Jostes *et al.*, 1991). This area represents an anatomical landmark of an axon tract, which develops at the furrow between the diencephalon and the telencephalon. *Pax6* expression, comparable to that of *Pax3* and *Pax7*, also exhibits a caudal limit in the forebrain at day 10.5 p.c. (Walther and Gruss, 1991; Grindley, 1996).

Pax genes without a homeobox domain, i.e. *Pax2*, *Pax5* and *Pax8*, are first expressed in the neural tube between day 9.5 - 10.0 p.c. when CNS differentiation initiates (Chalepakis *et al.*, 1992; Stuart *et al.*, 1993; Stoykova and Gruss, 1994). *Pax2* and *Pax8* transcripts are confined within the epichordal part of the neural tube throughout the spinal cord, myelencephalon and pons, with a rostral limit of expression at the hindbrain-midbrain boundary (Stuart *et al.*, 1993). Areas of *Pax5* expression overlap with those of *Pax2* and *Pax8* throughout the spinal cord. *Pax5* exhibits an early (around day 9.5 p.c.) strong and specific expression at the hindbrain-midbrain boundary, extending into the posterior part of the mesencephalic tegmentum (Asano and Gruss, 1992).

Murine *Pax4* and *Pax9* expression in the developing CNS has not been reported.

1.6.5.2 *Pax* genes in the adult brain

Most murine *Pax* genes are expressed in discrete areas in the posterior regions of the adult brain (see figure 1.2 on the following page) (Stuart *et al.*, 1993). The expression patterns in the adult brain are similar to those of the midgestation brain, with the exception of *Pax6* which is expressed in the olfactory bulb that is formed during late gestation period (Walther and Gruss, 1991). In the adult brain, *Pax6* transcripts are also detected in the septum, in the lateral and septal nucleus, as well as in the nuclei of the diagonal band of Broca (Walther and Gruss, 1991). *Pax6* is also expressed in the zona inserta, endopeduncular nucleus, and reticular nucleus as well as the amygdala (Walther and Gruss, 1991).

In the adult midbrain, neurons in distinct nuclei express *Pax3*, *Pax5*, *Pax6*, and *Pax7* in accordance with that of midgestation stages (Stoykova and Gruss, 1994). *Pax6* transcripts are detected in a subset of neuronal cells in the dorsolateral part of the reticular substantia nigra and in the central gray matter

(Walther and Gruss, 1991). *Pax7* is expressed in the optic tectum, especially in the superficial, intermediate and deep layers of superior colliculus and in discrete nuclei of the tegmentum (Jostes *et al.*, 1991). *Pax5* is localized in the more caudolateral and the ventral parts of the central gray matter as well as in parts of the tegmentum. In the fovea isthmii, *Pax3*, *Pax7*, and *Pax6* are expressed in different nuclei. *Pax2* and *Pax8* are expressed in different nuclei of myelencephalon (Stuart *et al.*, 1993; Stoykova and Gruss, 1994).

Within the adult cerebellum, only three *Pax* genes are expressed. *Pax2* is expressed in two neuronal populations of the granular layer, i.e. the Golgi type II neurons and the granular neurons, but only in one type of the glial cells, the astrocyte. *Pax3* is expressed in Purkinje neurons, in the granule neurons, as well as in two types of the cerebellar glia -- the Bergmann glia and astrocytes. *Pax6* is expressed in granule neurons and astrocytes (Stuart *et al.*, 1993; Kioussi and Gruss, 1994).

Figure 1.2 Expression domains of *Pax* genes during early development of the mouse CNS (right) and in young adult mouse brain (left). A, B, and C indicate *Pax* gene expression in different areas of the brain at 8.5, 10.5, and 13.5 days p.c. D represents the expression of *Pax* genes on a transverse plane of the spinal cord at day 13.5 p.c. Abbreviations: 4V: 4th ventricle; AP: alar plate; BP: basal plate; Cb: cerebellum; Di: diencephalon; DT: dorsal thalamus; E: eye; ET: epithalamus; FP: floor plate; IZ: intermediate zone; Ms: mesencephalon; Mt: metencephalon; My: myelencephalon; NE: nasal epithelium; PN: pons; Pro: prosencephalon; PT: pretectum; Rh: rhombencephalon; RP: roof plate; Sc: spinal cord; SL: sulcus limitans; TCX: telencephalic cortex; TL: telencephalic vesicle; VT: ventral thalamus; VZ: ventricular zone (From Stuart *et al.*, 1994 with permission).

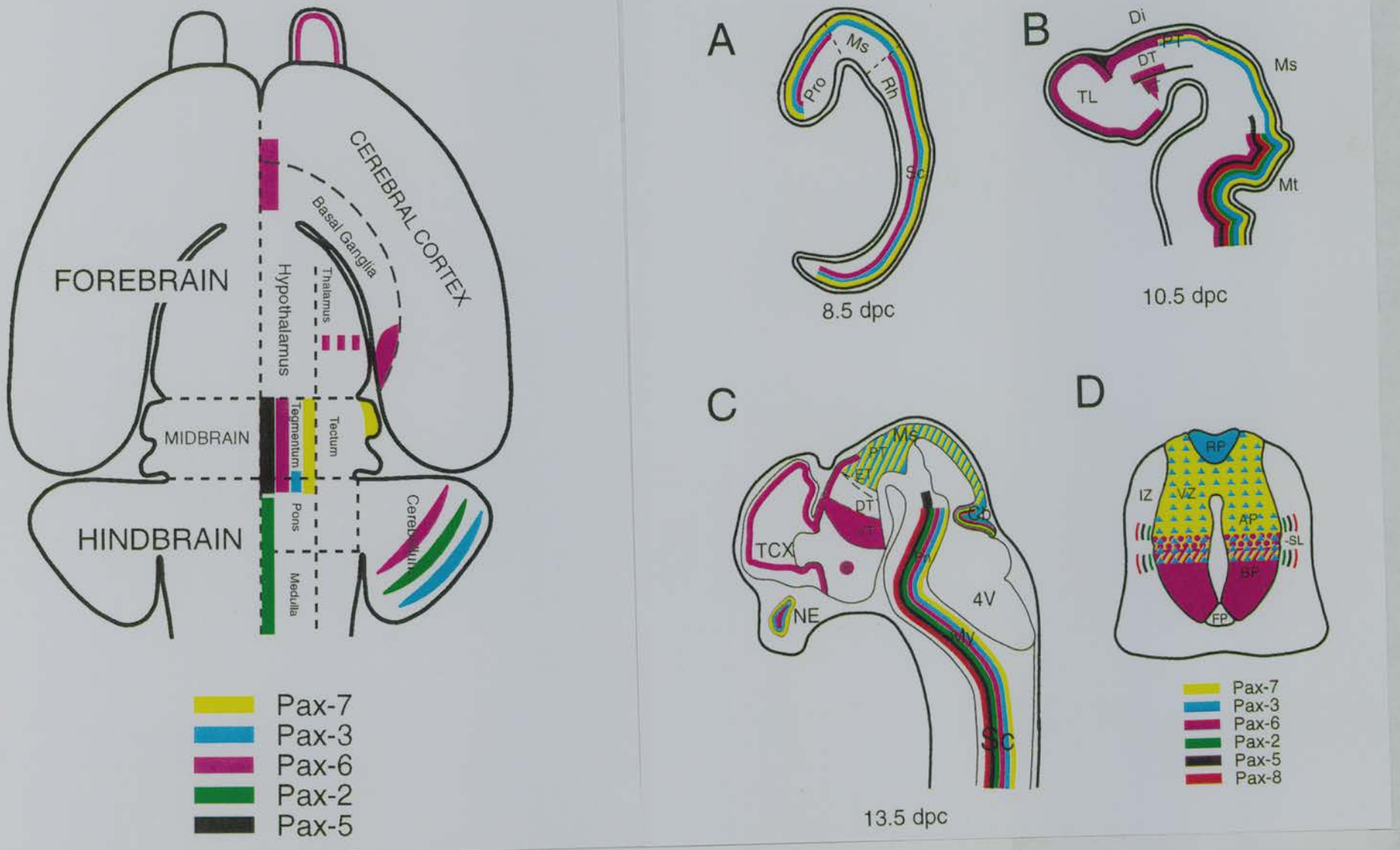

Figure 1.2 Expression domains of *Pax* genes during early development of the CNS (right) and in young adult mouse brain (left).

Part B: the "development" side

Part B will first give a general background on vertebrate craniofacial development with emphasis on the contribution of three primary germ layers to different parts of the head (section 1.7). It is then followed by common aspects of vertebrate CNS development (section 1.8) and the development of specific regions -- the visual nervous system (section 1.9), the olfactory nervous system (section 1.10), the eye (section 1.11) and the teeth (section 1.12). These regions are affected by *Pax6* mutation and are to be investigated in this study. The introduction here in part B aims to give a general background information for describing and discussing results in the present work. Therefore, it has to be brief on the general background and at the same time highly selective, concentrating on the craniofacial areas related to *Pax6* mutation and expression. Most of the background information is described regardless of temporal sequences.

1.7 Vertebrate craniofacial development -- general background

All vertebrate embryos develop following the same processes: fertilization, blastulation, gastrulation, neurulation, and then organogenesis. After fertilization, the fertlized egg becomes an early embryo and begins to divide until it becomes a mass of cells called a blastula. Following the formation of a blastula, the next stage of development concentrates on rearranging the embryonic cells into a body plan by polarizing them along three axes: the anteroposterior axis, the dorsoventral axis, and the left-right axis. This process of polarization is highlighted during gastrulation, when cells of the blastoderm are translocated to new positions in the embryo, producing three primary germ layers: ectoderm, mesoderm, and endoderm; all of them contribute to the genesis of craniofacial structures. During neurulation, the ectoderm will differentiate into three populations of cells: surface ectoderm, neural ectoderm and neural crest cells. The surface ectoderm contributes to the epidermis, hair, anterior pituitary gland, enamel of teeth, inner ear, and lens (Balinsky, 1981). The neural ectoderm will form the central nervous system, retina, pineal body, posterior pituitary (Purves and Lichman, 1985). The neural crest cells will contribute to cranial and sensory ganglia, pigment cells, branchial arch cartilages, a substantial part of the head mesenchyme (Le Douarin, 1981), most of the face (Hunt *et al.*, 1991), and some skeletal

elements within the head, including the nasal, lacrimal, zygomatic, maxillary, incisive, mandibular and squamous temporal elements (Noden, 1986).

A special feature of the ectodermal contribution to craniofacial development is the formation of placodes. Placodes are thickenings of the surface ectoderm and consist of the nasal placode, lens placode, otic placode, and smaller epibranchial and intermediate placode formations during vertebrate embryogenesis (Browder *et al.*, 1991). Some placodal cells, i.e. lens and otic cells, will detach from the surface ectoderm during development. Others, for example the nasal placodal cells, just invaginate and differentiate without detachment from the surface ectoderm.

The mesodermal derivatives contribute to most of the muscles and their innervating nerves in the head (Noden and Lahunta, 1985; Noden, 1983), as well as the frontal, parietal, petrous temporal, occipital, and most of the sphenoidal elements of the skull (Noden, 1986).

The endodermal derivatives contribute to the anterior pharyngeal pouches (Browder *et al.*, 1991). In the lower vertebrates, contact sites between the ectoderm and the endoderm in the pharyngeal pouches perforate to form gill slits. In the higher vertebrates, respiratory function of the gill is undertaken by the lungs. In the human, pharyngeal pouches will develop to contribute to the paired eustachian tubes and tympanic cavities of the ears and the tonsils (Moore, 1988).

1.8 Common aspects of the vertebrate CNS development

1.8.1 Macroscopic morphogenesis of the CNS

During gastrulation, embryonic cells are arranged into three primary germ layers through ingression of cells from the epiblast into the blastocoel. This displacement of cells leads to the formation of a long midline cleft, the primitive streak, while a thickening called the primitive knot (known as Hensen's node in the chick) develops at the anterior end of the primitive streak. Presumptive notochordal cells accumulate within the region of primitive knot.

When the primitive streak reaches its maximal length, the primitive knot appears to recede toward the posterior end and the presumptive notochordal cells, which are located in front of the retreating node, extend anteriorly to form the notochordal process. The majority of the length of the embryo takes shape as the notochordal process extends. During neurulation, the dorsal ectoderm covering the notochordal process becomes flattened and thickened to form the neural plate. Parts of the neural plate from each side of the embryo rise to form the neural folds that flank a central depression called the neural groove. The neural groove extends along the entire dorsal midline of the embryo. As the neural groove becomes deeper, the neural folds from each side of the embryo eventually meet and fuse, resulting in the formation of the neural tube -- the rudiment of CNS. The anterior portion of neural tube will become the brain and will be developed into distinct brain vesicles, while the posterior portion of the neural tube develops into a tube-like structure, the spinal cord.

The brain vesicles in the anterior portion of the neural tube will develop into, from the anterior to the posterior, the prosencephalon (forebrain), the mesencephalon (midbrain), and the rhombencephalon (hindbrain). These brain vesicles become more distinguishable as the cranial flexures between them form. The prosencephalon will rapidly subdivide into the anterior telencephalon (which gives rise to the cerebral cortex, basal ganglia and some other structures) and the posterior diencephalon (which gives rise to the thalamus and hypothalamus). The rhombencephalon is further partitioned into metencephalon (which gives rise to the cerebellum and the pons) and myelencephalon (which gives rise to the primordium of the medulla).

1.8.2 Microscopic histogenesis of the CNS

1.8.2.1 Three-zone pattern formation and its modifications

Histologically, the cells along the primitive neural tube (which includes both the brain and the spinal cord) are initially arranged in a layer of neuroectoderm. The neuroectodermal layer is also called the germinal epithelium (or the ventricular zone), since the neuroectodermal cells divide rapidly. Nuclei of

the dividing cells are predominantly located at the inner surface of the germinal epithelium and only when mitosis is completed, the nuclei migrate back toward the outer surface.

The highly mitotic activities in the germinal epithelium results in the formation of the second layer, the mantle layer (the intermediate zone). Cells within the mantle layer differentiate into both neurons and glia. The neurons in the mantle layer make connections among themselves and project axons away from the lumen. Thus, a third cell-poor layer -- the marginal zone is formed. Glial cells from the mantle layer eventually cover many of the axons in myelin sheaths, giving them a whitish appearance. The mantle zone where the neuronal cell bodies are located, is often called the "gray matter", while the axonal, marginal layer is often called the "white matter". Thus, at early stage of CNS development, three layers (or zones) are derived from a primary germinal layer. These layers are maintained throughout spinal cord development, but in many parts of the brain very complicated modifications occur. The modifications result from cell migration, differential growth, and selective cell death during axonogenesis. Modifications are particularly common in the cerebellum and the telencephalon (cerebrum) where the greatest structural deviation from the primitive neural tube occurs. Some neurons enter the white matter and differentiate into clusters of neurons known as nuclei. Many dividing neuronal precursor cells, the neuroblasts, migrate to the outer surface of the developing cerebellum and cerebrum to form a new germinal zone, the secondary germinative layer (or called the secondary germinative epithelium). Those secondary germinative layers that are close to the ventricle are known as "subventricular zones" and those farther away from the ventricle, usually in a submarginal position, are known as the "external germinal layers" or the "external granular layers" (Altman and Bayer, 1995). Typically, secondary germinal epithelia begin to expand in a given brain region after the primary neuroepithelium has started to shrink. Cell proliferation in the secondary germinal epithelia typically give rise to late-developed neurons with short axons, or microneurons known in many brain regions as granule cells (Altman and Bayer, 1995).

1.8.2.2 The alar plate and the basal plate formation

The division of developing CNS into a dorsal part (the alar plate) and a ventral part (the basal plate) along the dorsal-ventral axis is as important as the division of brain vesicles along the antero-posterior axis. In the spinal cord and the medulla, the basic three-zone pattern of ventricular (also called ependymal or primary germinal layer), mantle (intermediate), and marginal (pial) layers is maintained throughout development. The gray matter in the mantle zone gradually becomes a butterfly-shaped structure surrounded by white matter; both will be encased in connective tissues. As the neural tube develops, a longitudinal groove, the sulcus limitans, appears to divide the neural tube into dorsal and ventral halves (Arey, 1974). The dorsal half receives input from sensory neurons, whereas the ventral portion is involved in effecting various motor functions (Placzek *et al.*, 1991). This arrangement of sensory and motor neurons can be easily traced to the mesencephalon and the diencephalon (Altman and Bayer, 1995). In the mesencephalon, the alar plate is the source of neurons in the superior and inferior colliculus (which receive optic and auditory afferents, respectively), whereas the basal plate is the primordium of tegmentum (which is a major motor outflow region) (Altman and Bayer, 1981a, b, c). In the diencephalon, the alar plate is the source of neurons of the thalamic nuclei (which are relay stations in the somesthetic, auditory and visual pathways), while the basal plate is the primordium of the hypothalamus (which contains many of the efferent centers of the autonomic, endocrine, and other motor systems) (Altman and Bayer, 1979). However, the alar plate and basal plate are not tracible in the telencephalon. For example, the course of sulcus limitans is not tracible in the telencephalon.

1.8.2.3 Cerebral organization

The cerebral organization is established (see figure 1.3 on the following page) as a result of modifications on the three-layered primitive cerebrum through migration, differential growth, and selective cell death of neuroblasts. Neuroblasts may migrate from the mantle zone toward the outer surface to form a new zone of neurons -- the neocortex. The neortex will eventually stratify into six layers of cell bodies. These layers of the neocortex differ in their functional properties, the types of neurons found therein, and the set of connections that emerge. For example, neurons from layer 6 send

their major output to the thalamus, while neurons from layer 4 receive their major input from thethalamus (Rakic, 1974). Horizontally, the cerebral cortex is organized into more than 40 functional regions (Walsh and Cepko, 1988; 1992).

Figure 1.3 Diagrammatic representation of the formation of multiple layers in the cerebellum and cerebral cortex. The primitive neural tube contains three zones from which multiple cortical formations are differentiated at later stages of development, except in the spinal cord where the three layers are maintained. Abbreviations: CP: cortical plate; E: ependymal layer; EG: external granular layer; GL: granular layer; I: intermediate zone; L: lamina dissecans; M: marginal zone; P: Purkinje cell layer; S: subventricular zone; V: ventricular zone. (From Scott F. Gilbert (1994). *Developmental Biology, fourth edition, pp. 158*, Sinauer Associates Inc. Publishers)

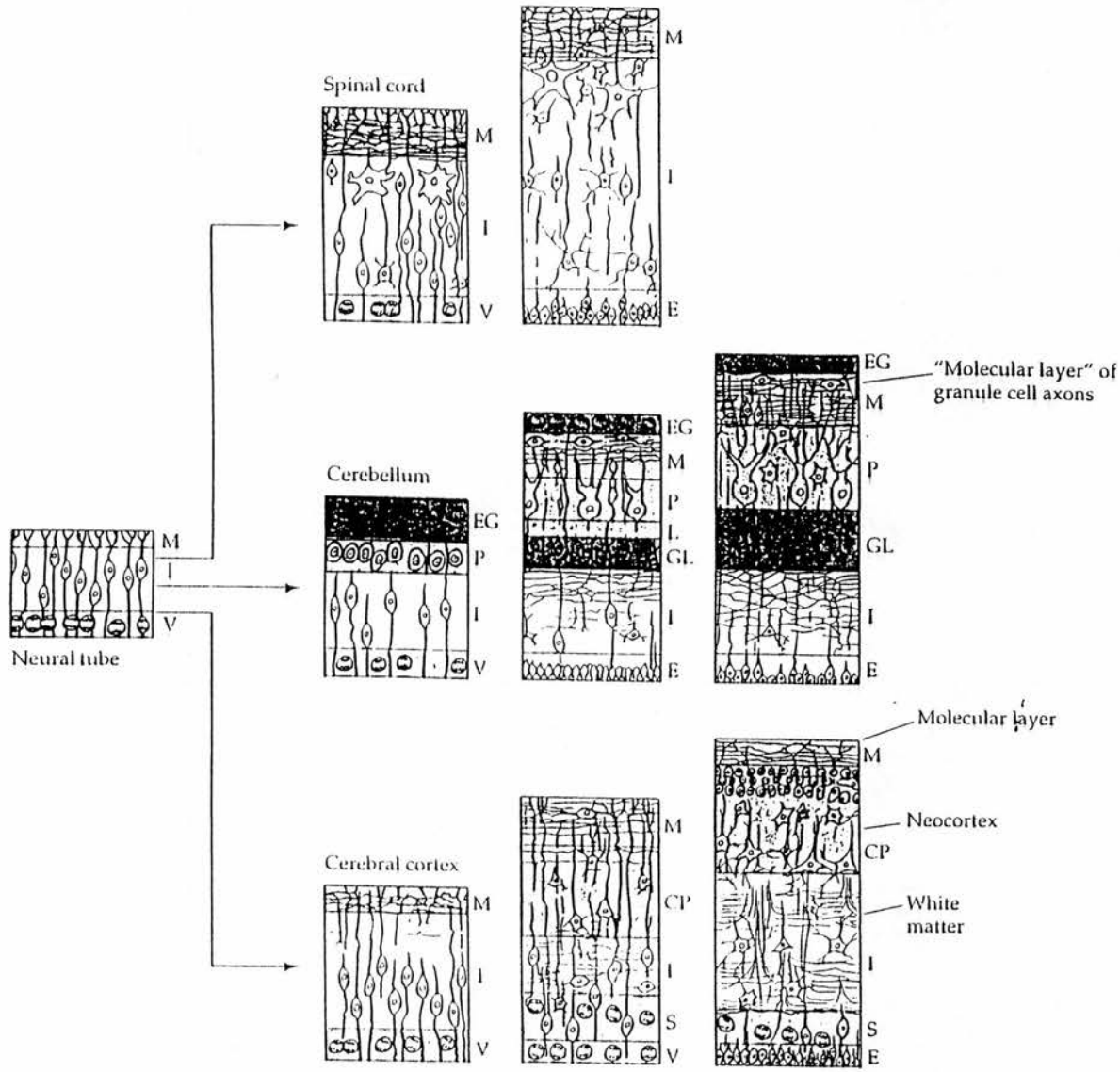

Figure 1.3 Diagrammatic representation of the formation of multiple layers in the cerebellum and cerebral cortex.

1.8.2.4 Cerebellar organization

The three-layered pattern is also modified in the cerebellum (see figure 1.3 on the preceding page). Neuroblasts proliferate at the secondary (external) germinal layer and form an inner and an outer compartment. The inner compartment contains postmitotic neuroblasts that constitute the precursors of the major neurons, the granular cells, in the cerebellar cortex (reviewed by Zilles and Wree, 1985). Some of the precursor cells migrate back into the cerebellar white matter to form a region of granular cell neurons, the internal granular layer. Meanwhile, the primary ventricular layer of the cerebellum generates a wide variety of neurons and glial cells, including the large Purkinje neurons. Purkinje neurons have an enormous dendritic apparatus and a slender axon that connects to the other cells in the deep cerebellar nuclei. Functionally, Purkinje neurons are the only output neurons of the cerebellar cortex.

1.8.3 Primary induction and regionalization

1.8.3.1 Primary induction

Experiments using amphibian embryos by Spemann and his colleagues (particularly Hilde Mangold) led to the discovery that the dorsal blastopore has an organiser activity that recruits surrounding cells to form the antero-posterior axis (reviewed by Spemann, 1938). Spemann referred to the dorsal blastopore lip cells as the "organiser" where dorsal mesoderm can provide directly or indirectly signals for the specification of neural tissues during gastrulation. In birds, Hensen's node acts as the dorsal blastopore lip. When a Hensen's node from young gastrula is transplanted into epiblasts of another young gastrula, it will induce the formation of a complete secondary axis (Waddington, 1933). Similar organizer activity is also found in the primitive node in the mouse (Storey *et al.*, 1992; Beddington, 1994).

Spemann's organiser used to be called the "primary organiser" because it is not sufficient to organise the entire embryo; instead, it initiates a series of sequential inductive events. But the concept of

primary organiser is gradually fading because of two main reasons: (1) there is evidence of multiple neural inductions (reviewed by Harland, 1994; Shawlot and Behringer, 1995). (2) regionalization of the nervous system occurs well before neurulation, at about the time when neural fates are being acquired (Quinlan *et al.*, 1995).

1.8.3.2 Forebrain and hindbrain regionalization

Regionalization is a necessary process following or during neural induction. Regionalization appears to occur well before the presence of obvious brain vesicles or even before the presence of neural plate (Quinlan *et al.*, 1995). Fate mapping studies in the mouse show that almost the entire precursor population of the neural tube is contained within the distal cap region of the epiblast, and there is already some regionalization within this population (Quinlan *et al.*, 1995). Mouse embryos start showing primary cranial flexures along the longitudinal axis well before the closure of neural tube (Jacobson and Tam, 1982). Early regionalization of the CNS is likely to involve in a mechanism similar to that in the process of neurulation. Concurrent changes in cell shape, such as the formation of wedged shaped cells and cell elongation, as well as influences from other tissues and extracellular matrix, are important for the shaping and bending of the neural plate during neurulation (Jacobson, 1981; Schoenwolf and Smith, 1990). Similar mechanisms may be involved in early regionalization of the CNS and in the formation of the cranial flexures and the brain vesicles.

Further regionalization of the developing brain vesicles leads to the formation of proneuromeres and neuromeres (reviewed by Berquist and Kallen, 1954; Vaage, 1969; Keyser, 1972). Based on neuromeric segmentation and expression patterns of the homeobox genes and other regulatory genes, seven rhombomeres (eight in the chick) in the hindbrain (rhombencephalon) and six prosomeres in the forebrain (telencephalon and diencephalon) are defined in the mouse (see figure 1.4 on the following page) (Lumsden and Keynes, 1989; Puelles and Rubenstein, 1993).

Figure 1.4 Forebrain and hindbrain regionalization based on neuromeric segmentation and patterns of expression of homeobox-containing genes and other regulatory genes. Six (P1 - P6) prosomeres are defined in the forebrain region, starting from the pretectum (p1) toward dorsal thalamus (P2), ventral thalamus (P3), mammillary area (P4), tuberal hypothalamus (P5), and terminating in retrochiasmatic area (p6). Seven rhombomeres (r1 - r7) are defined in the hindbrain region, starting with r1 in the boundary of the cerebellum and isthmus of mesencephalon and terminating with r7 that connects by its caudal end with the spinal cord (Based on the illustrations in Puelle and Rubenstein, 1993 and Stoykova *et al.*, 1996). Abbreviations: ACX: archicortex; AEP: anterior entopeduncular area; AH: anterior hypothalamus; Cb: cerebellum; CGE: caudal ganglionic eminence; DB: diagonal band (Broca); DT: dorsal thalamus; EMT: eminentia thalami; ET: epithalamus; HCC: hypothalamic cell cord; Is: isthmus of mesencephalon; LGE: lateral ganglionic eminence; M: mesencephalon; MA: mammillary area; MGE: medial ganglionic eminence; NCX: neocortex; OB: olfactory bulb; PEP: posterior entopeduncular area; POA: anterior preoptic area; POP: posterior preoptic area; PT: pretectum; RCH: retrochiasmatic area; SCH: suprachiasmatic area; SE: septum; SPV: supraoptic/paraventricular area; TU: tuberal hypothalamus; VT: ventral thalamus.

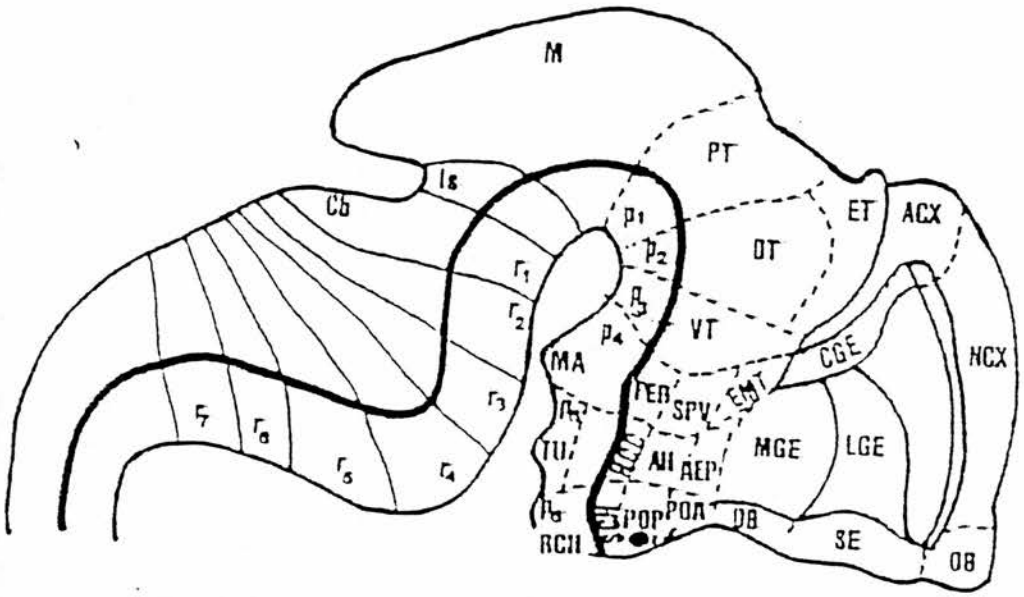
M
PT
Is
Cb
p1
p2
p3
p4
ET
ACX
OT
VT
r1
r2
r3
r4
r5
r6
r7
MA
CGE
NCX
PER
SPV
EMT
TU
AII
AEP
MGE
LGE
POP
POA
DB
SE
OB
RCH

Neuromeres are centres for proliferation, migration, compartmentation, and differentiation of the neuroblasts (Kallen, 1965; Layer and Alber, 1990; Fraser *et al.*, 1990; Fidger and Stern, 1993; Brigbauer and Fraser, 1994). Activities of proliferation and migration of neuroblasts are higher within the neuromeric domains than in their boundaries (reviewed by Bergquist and Kallen, 1954). Cells in the boundary regions are packed differently from those in the body of rhombomeres (Lumsden and Keynes, 1989; Figdor and Stern, 1993; Heyman *et al.*, 1993). Cells from neighbouring neuromeres mix little (Fraser *et al.*, 1990; Figdor and Stern, 1993), but those from two odd-numbered or two even-numbered neuromeres generally mix (Guthrie and Lumsden, 1991; Guthrie *et al.*, 1993). Furthermore, from the time the first neurons differentiate, the boundaries between rhombomeres become delineated by transversely oriented axons (Lumsden and Keynes, 1989; Keynes and Lumsden, 1990). Neurogenesis of the somatic motor system, reticular system and branchial neurons conforms to the rhombomeric pattern (Keynes and Lumsden, 1990). The neuromeric patterning of cell proliferation, migration, compartmentation, and differentiation can be correlated with segmental gene expression data therein (for example, see Kuratani, 1991), providing clues for the role of specific genes in those events.

1.8.4 Proliferation

Proliferation of neuroblasts occurs intially in the primary germinal epithelium and at later stages in the secondary germinal epithelium, which is governed by a strict timetable (Altman and Bayer, 1995). Most mammals cease producing neuroblasts in the CNS at some time after birth, as a result of gradually dissolution of the neuroepithelium and the rapid growth of the brain parenchyma. Neuronal cells are also reduced by cell death as they enter the phase of differentiation and pathfinding (reviewed by Cunningham, 1982; Cowan *et al.*, 1984; Oppenheim, 1991).

Based on the structural features of the developing rat brain, Altman and Bayer (1995) divide prenatal brain development into three stages: The initial stage spans from E11 to E14 and is characterised by rapid expansion of the primary germinal neuroepithelim. The differentiating brain regions with postmitotic neurons only become obvious in the caudal and ventral portion of the developing CNS by the end of the initial stage (E14). The intermediate stage covers period between E15 to E18. During

the intermediate stage, the germinal neuroepithelium remains prominent and expansion of the secondary germinal neuroepithelium adds to the increasing number of neuroblasts. Neuroblast proliferation is coupled with progressive enlargement of the brain parenchyma. As a result, by the end of the intermediate stage (E18), all major brain systems are identifiable. The third is the final stage that covers the period from E20 to E22. The final stage is characterised by gradual dissolution of the germinal neuroepithelium and rapid expansion of the brain parenchyma. Although neuroblast proliferation still continues in the secondary germinal neuroepithelium after birth, the major event in postnatal brain development is the accelerated differentiation of neurons and myelin fibers.

1.8.5 Migration and glial guidance

The three-layered structure of the developing CNS is formed as a result of the migration of neuroblasts produced in the primary and secondary germinal epithelia (Arey, 1974). Cells leaving the germinal layer generally lose their potential to divide and, during the same process, become differentiated into neurons and glial cells, depending on the environment they enter (Cajal, 1960; Miale and Sidman, 1961; Rakic and Goldman, 1982; Turner and Cepko, 1987). Upon leaving the germinal neuroepithelium, the young neurons either settle near the sites of proliferation or migrate to distant sites. Those settle near the germinal layer can permanently rest and differentiate into cranial nerve nuclei. Alternatively, young neurons may be displaced by new waves of later produced neurons leaving the germinal layer (Altman and Bayer, 1995). Those young neurons that migrate to distant sites take part in more drastic transformations. They can not only migrate in a relatively simple radially-directed process such as during the formation of the cerebral cortex, but also involve in long distance migration in various directions through dense brain tissue, over the surface of the brain, or in rare cases across the midline from one side to the other (O'Rouke *et* al., 1992; Walsh and Cepko, 1993; Tan and Breen, 1993; Lois and Alvarez-Buylla, 1994; Altman and Bayer, 1995).

Since migration is crucial for the spatial organization and thus obtaining proper functions of the developing CNS, it has to follow a strict timetable. The process of migration is not achieved merely by passive movement. Rather active positioning of young neurons through glial guidance constitues the

primary mechanism (Rakic, 1972; Hatten, 1990). A sunstantial amount of evidences suggest that throughout the cortex formation, neurons ride "the glial monorail" to their destinations (Rakic and Sidman, 1973; Rakic, 1975; Komuro and Rakic, 1992). Failure of glial guidance can lead to abnormalities in cortex organization, such as the absence of the granular neuron layer in the mouse *weaver* mutation (Goldowitz and Mullen, 1982; Hatten, 1990; Gao and Hatten, 1993).

1.8.6 Connection and pathfinding

Once the young neurons are following the tracts of migration and differentiation, neuronal connection and pathfinding take place to construct a functional and intergrated central nervous system. Axon growth cones navigate to their targets to make initial connections by two mechanisms: extratracellular matrix guidance and diffusible molecule guidance (reviewed by Hynes and Lander, 1992; Goodman and Shatz, 1993; Travis, 1994).

Extracelluar matrix may regulate axon growth by activities of specific adhesion and specific repulsion (Hynes and Lander, 1992). Laminin, for example, has axon-promoting activities. Axons of certain spinal neurons travel through the neuroepithelium over a transient laminin-coated surface that precisely marks the path of these axons (Letourneau *et al.*, 1988). There is also a good correlation between the elongation of retinal axons and the presence of laminin on the neuroepithelial cells and astrocytes in embryonic mouse brain (Cohen *et al.*, 1986, 1987; Liesi and Silver, 1988). Tenescin, for example, appears to have a repulsive function. It is only expressed at boundaries through which axons do not cross (Stenideler *et al.*, 1989).

An example for diffusible molecule guidance is the involvement of F-spondin in the growth of spinal commissural neurons toward the neural plate (Tessier-Lavigne *et al.*, 1988; Plazek *et al.*, 1990; Klar *et al.*, 1992). Another example is the expression of *netrin-1* and *netrin-2* in the developing floor plate and the spinal cord. Both act to promote initial ventral growth of commissural axons and to direct the growth cones ventral to the floor plate (Kennedy *et al.*, 1994; Serafini *et al.*, 1994). Molecule repulsion activity is also found for *netrin-1* (Colamario and Tesssier-Lavigne, 1995).

1.8.7 Cell death during axongenesis

In many parts of the vertebrate central nervous system, over half of neurons die during the normal course of development (reviewed by Cunningham, 1982; Cowan *et al.*, 1984; Oppenheim, 1991). The death of neurons seems to be due to inadequate supply of some critical survival factors such as NGF (nerve growth factor) (Levi-Montalcini and Booker, 1960), BDNF (brain-derived neurotrophic factor) (Oppenheim *et al.*, 1992), NT-3 (neurotrophin-3), NT-4/5 (neurotrophin-4/5), FGF-5 (fibroblast growth factor-5) (Hohn *et al.*, 1990; Maisonpiere *et al.*, 1990; Henderson *et al.*, 1993; Hughes *et al.*, 1993), GDNF (glial cell line-derived neurotrophic factor) (Lin *et al.*, 1993) and CNTF (ciliary neurotrophic factor) (Sendtner *et al.*, 1992). Some reports proposed that the neurotrophic factors, depolarilization and interactions with substrates all contribute to the determination of neuronal survival (Schmidt and Kater, 1993; Raff *et al.*, 1994).

1.9 Integration of the visual nervous system

The visual nervous system, particularly the mammalian visual nervous system, is generally regarded as a set of pathways working largely in parallel, i.e. separate classes of retinal ganglion cells send specific information through separate classes of relay cells within one particular visual nucleus (Stone, 1984). Thus, visual fields can be traced from the retina via optic nerve, chiasma, tract through dorsal and ventral lateral geniculate nuclei and superior colliculus, all the way to specific areas of the visual cortex (see figure 1.5 on page 49) (reviewed by Sefton and Drefer, 1985). This forms the retinogeniculocortical pathway that integrates the main parts of the visual nervous system. In addition to the nuclei of the retinogeniculocortical pathway, there have been suggestions of small retinal projections to the hypothalamus, including the inferior collicus, the anterodorsal and anteroventral thalamic nuclei, as well as the subthalamus (reviewed by Sefton and Drefer, 1985). But little is known about these additional pathways. From sections 1.9.1 to 1.9.9, I will therefore concentrate only on the nuclei and their afferent and efferent connections within the main parts of the visual pathways. In

section 1.9.9, a highly schematic diagram summarizing the major connections between the visual nuclei will be added to give a clear picture of the integration of the visual nervous system.

1.9.1 Retinal output through optic nerve, chiasma, and tract

Along the retinogeniculocortical pathway, the retina is the only site that provides efferent axons of ganglionic cells. The axons cross at the optic chiasma and thereafter are called the optic tracts. Although some axons branch at the chiasma to project into both optic tracts (Cunningham and Freeman, 1977), most axons project into the optic tract to the opposite side (Jeffery *et al.*, 1981). Within optic nerves and optic tracts, the relative positions of axons arising in different retinal quadrants are maintained (Yamadori, 1981), but the number of fibers in the optic tract exceeds that in the nerve (Sefton and Drefer, 1985). This excess presumably includes any branches of optic axons arising at the chiasma, as well as fibers that pass from one parabigeminal nucleus through the optic chiasma to contralateral visual nuclei (Stevenson and Lund, 1982; Watanabe and Kawana, 1979). Ganglion cells project to the superior colliculus (SC) (Linden and Perry, 1983), as well as the dorsal lateral geniculate nucleus (DLG) (Sefton, 1968). It is suggested that axons also branch to supply the ventral lateral geniculate nucleus (VLG) and pretectum (Giolli and Towns, 1980).

1.9.2 Dorsal lateral geniculate nucleus

The dorsal lateral geniculate (DLG) is a visual relay nucleus that occupies the dorsolateral part of the thalamus and relays information to the visual cortex. Apart from the retinal input (Hayhow *et al.*, 1962), afferents to the DLG arise in many sources: various layers of the occipital cortex (Montero and Guillery, 1968; Jacobson and Trojanowski, 1975), the visual Rt (visual thalamic reticular nucleus) (Ohara and Lieberman, 1981; Hale *et al.*, 1982), the superficial gray layer of the superior colliculus (Mason and Groos, 1981; Sefton and Martin, 1984), the optic tract nucleus and the olivary pretectal nucleus in the pretectal area (Mackey-Sim *et* al., 1983), the parabigeminal nucleus (Sefton and Martin, 1984), the dorsal terminal nucleus (Mackey-Sim *et al.*, 1983) and some other nuclei of the brain stem. Efferent projections from the DLG are restricted to the occipital cortex (Oc) and the visual thalamic reticular nucleus (visual Rt) (Matthews, 1973; Scheibel and Scheibel, 1966; Hale *et al.*, 1982).

1.9.3 Superior colliculus

In the rat, the superior colliculus (SC) or the optic tectum is the major target of the retinal ganglion cells (Linden and Perry, 1983). SC is organized in seven laminated layers: zonal, superficial gray, optic, intermediate gray and intermediate white, deep gray and deep white (Huber and Crosby, 1943). The superficial gray layer and upper optic layer are innervated by retinal axons. Cells in the innervated layers in turn project to deeper layers where neurons of other sensory systems are located (Harting *et al.*, 1973; Stein, 1981).

Connections of SC can be divided into those with the upper layers (zonal, superficial gray, and optic) and those with the deeper layers (below intermediate gray). Afferent axons to the upper layers include those from the retina (Cajal, 1911), different layers of occipital cortex (Huber and Crosby, 1943), parabigeminal nucleus (Sefton and Martin, 1984), pretectum (Huber and Crosby, 1943), and the magnocellular part of the ventral lateral geniculate nucleus (Brauer and Schober, 1982). Efferents from upper layers lead to deep layers of SC (Cajal, 1911), dorsal lateral geniculate nucleus (Perry, 1980; Rhoades and Fish, 1982), lateral posterior nucleus (Takahashi, 1985), ventral lateral geniculate nucleus

(Takahashi, 1985), parabigeminal nucleus (Sefton and Martin, 1984), and pretectum (Takahashi, 1985). Afferent axons to the deep layers include those from superficial gray and optic layers of SC (Cajal, 1911), retina (Beckstead and Frankfurter, 1983), occipital cortex (Takahashi, 1985), locus coerulus and substantia nigra (Pasquier and Tremazzini, 1979), spinal cord (Antonetty and Webster, 1952), magnocellular part of the ventral lateral nucleus (Brauer and Schober, 1982), and nucleus of posterior commisure (Pasquier and Tremazzini, 1979). Efferent axons from the deep layers lead to pontine nuclei (via tectopontine tract) (Petrovicky, 1975), lateral reticular regions in midbrain and pons (tectoreticular tract) (Petrovicky, 1975), medial reticular formation in brain stem (cruciate tectoreticular tract)(Petrovicky, 1975), medulla (Waldron and Gwyn, 1969), cervical spinal cord (Murray and Coulter, 1982), and hypothalamus (Fallon and Moore, 1979).

1.9.4 Lateral posterior nucleus (pulvinar)

The lateral posterior nucleus (LP) lies medial and caudal to the dorsal lateral geniculate (DLG) in the lateral thalamus (Paxinos and Watson, 1982). It receives projections from the SC and the occipital cortex and is considered to be the homologue of the pulvinar in the primates (Harting *et al.*, 1972) as well as the LP-pulvinar complex in cats (Berson and Graybiel, 1983; Updyke, 1983). Demonstrated afferent axons to the lateral posterior nucleus are from superior colliculus (Takahashi, 1985), pretectum (Schober, 1981), some layers of the occipital cortex (Takahashi, 1985), temporal cortex area 36 (Mason and Gross, 1981), and retina (Perry and Cowley, 1982). Efferent axons from the lateral posterior nucleus project to occipital layers and temporal cortical areas (Schober, 1981; Mason ans Groos, 1981).

1.9.5 Ventral lateral geniculate nucleus

The ventral lateral geniculate nucleus (VLG) extends deep to the DLG (dorsal lateral geniculate nucleus) and borders medially to the optic tract. Between DLG and VLG lies a small lamina, the intergeniculate leaflet (IGL) (Hickey and Spear, 1976). In many mammals, including the rat, two divisions can be recognized clearly within VLG (Niimi *et al.*, 1963). Only the external, lateral and magnocellular (VLGMC) divisions contain cells that respond to visual stimuli (Sumitomo *et al.*, 1979), receive a significant retinal input from both eyes (Hickney and Spear, 1976), and contain cells projecting to the superior colliculus (Brauer and Schober, 1982).

Afferent connections to VLG include those from retina, occipital cortex, superior colliculus, pretectum, dorsal raphe nucleus, perirubral reticular formation (Mackay-Sim, 1983), and locus coeruleus (Pasquier and Villar, 1982; Mackay-Sim *et al.*, 1983; Takahashi, 1985). Efferent connections from VLG lead to pretectum (including anterior pretectal nucleus, nucleus of the optic tract and olivary pretectal nucleus), superior colliculus (Perry, 1980; Brauer and Schober, 1982), pontine nuclei (Legg, 1979), and perirubral formation (Graybiel, 1975).

1.9.6 Pretectum

The pretectum is derived from the epithalamus and lies at the most rostral pole of the midbrain bordering the thalamus (Paxinos and Watson, 1985). Although often referred to as a single entity, the pretectum contains a number of distinct nuclear groups (Sefton and Dreher, 1985). The nuclei in the pretectum include nucleus of the optic tract (OT), olivary pretectal nucleus (OPT), anterior pretectal nucleus (APT), and posterior pretectal nucleus (PPT) (see figure 1.5 on the following page).

Afferent axons to the pretectum include those from the retina (Hayhow *et al.*, 1962; Hickey and Spear, 1976; Perry and Cowley, 1979), superior colliculus (Perry, 1980; Pasquier and Villar, 1982; Takahashi, 1985), ventral lateral geniculate (Mackay-Sim *et al.*, 1983) and the occipital cortex (Nauta and Bucher, 1954; Leong, 1980). Efferent axons from the pretectum lead to superior colliculus (Watanabe and

Kawana, 1979), dorsal and ventral lateral geniculate nuclei (Blanks *et al.*, 1982; Mackay-Sim *et al.*, 1983), lateral posterior thalamic nucleus (Schober, 1981), visual reticular thalamic nucleus (Hale *et al.*, 1982), laterodorsal thalamic nucleus (Robertson, 1983), optic tract nucleus (Terasawa *et al.*, 1979), lateral pons (Scalia and Arango, 1979), reticulotegmental nucleus of the pons (Terasawa *et al.*, 1979), and inferior olive (Robertson, 1983).

Figure 1.5 Diagrammatic representation of the visual pathways originating in the retina and terminating in the visual cortex. Each nucleus is depicted by a typical coronal section through it. On the left hand side of the diagram, visual nuclei are labelled. The shaded nuclei on the right hand side indicate those which have been reported to receive an input from visual cortical areas. Each projection is shown as a branch of a single fiber for simplicity, but this si not meant to imply that all nuclei are necessarily innervated by branches of retinocollicular axons. Note that the reticular thalamic nucleus (Rt) and the parabigeminal nucleus (PBg) do not receive a direct retinal input, but are reciprocally connected to the dorsal lateral geniculate nucleus (DLG) and the superior colliculus (SC) respectively. The dotted lines connecting the dorsal, lateral, and medial accessory nuclei (DT, LT, MT) indicate that they are not determined (Based on an illustration in Sefton and Dreher, 1985). Abbreviations: 17: area 17 of the visual cortex; 18: area 18 of the visual coetex; 18a, area 18a of the visual cortex; APT: anterior pretectal nucleus; DLG: dorsal lateral geniculate nucleus; DT: dorsal terminal nucleus of the accessory optic tract; iao: internal accessory optic tract; IGL: intergeniculate leaflet; InG: intermediate gray layer of the superior colliculus; LT: lateral terminal nucleus of the accessory optic tract; MT: medial terminal nucleus of the accessory optic tract; OPT: olivary pretectal nucleus; OS: optic nerve layer of the superior colliculus; OT: nucleus of the optic tract; ox: optic chiasma; PBg: parabigeminal nucleus; PPT: posterior pretectal nucleus; Rt: reticular thalamic nucleus; sao: superficial accessory optic tract; SC: superior colliculus; SGS: superficial gray layer of the superior colliculus; SCh: suprachiasmatic nucleus; VLGMC: ventral lateral geniculate nucleus, magnocellular part; VLGPC: ventral lateral geniculate nucleus, parvocellular part.

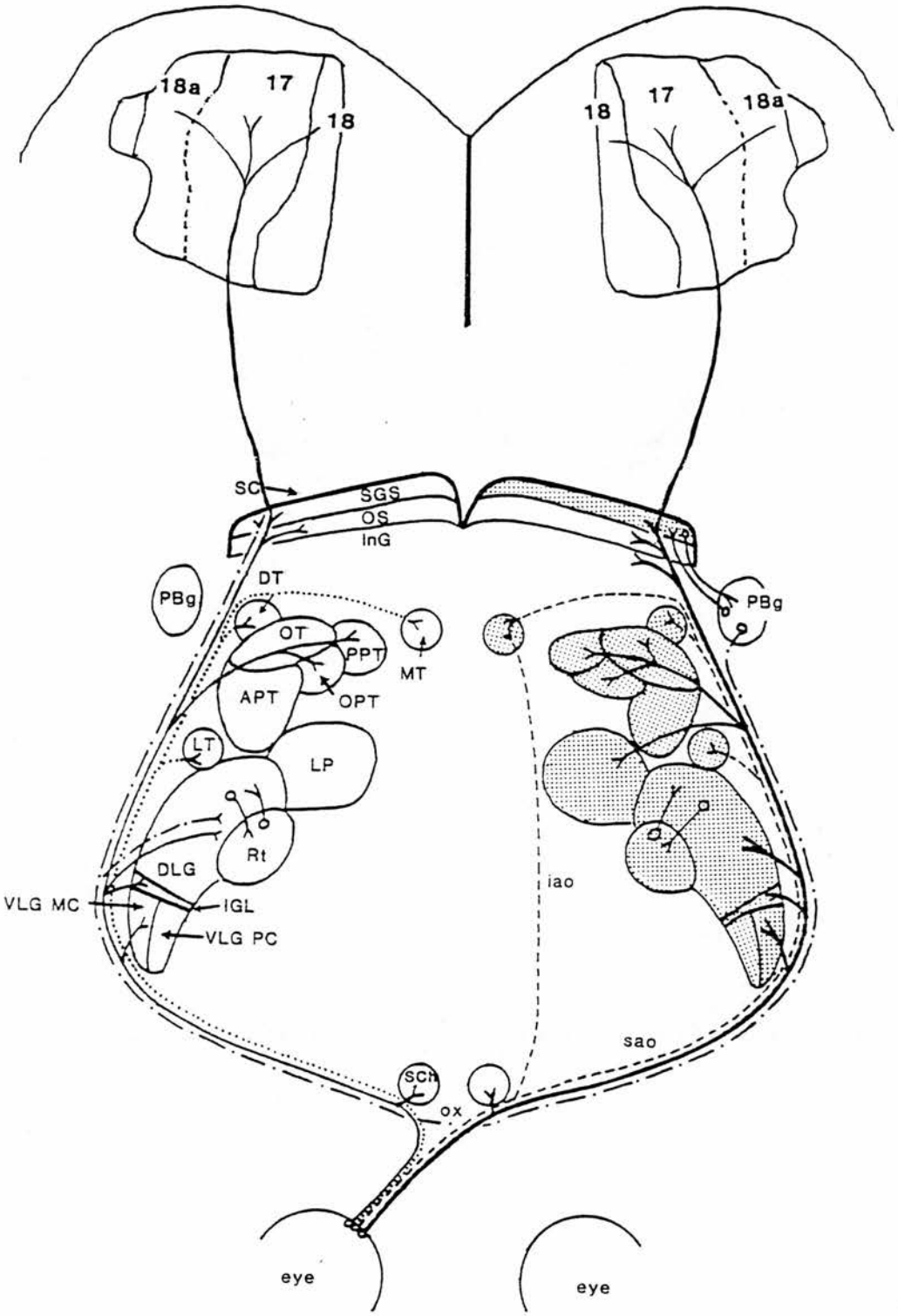

Figure 1.5 Diagrammatic representation of the visual pathways.

1.9.7 Accessory optic system

The accessory optic system include the dorsal terminal nuclei (DT), the lateral terminal nuclei (LT), and the medial terminal nuclei (MT) (Hayhow *et al.*, 1960). Two (superior and inferior) crossed accessory fasciculi leave the main optic tract behind the chiasm. The inferior fasciculus can be identified initially as a small separate bundle which lies medial to the main optic tract. Subsequently, its fibers intermingle with the median forebrain bundle as they run close to the base of the peduncle to innervate the medial terminal nucleus, the principle nucleus of the accessory optic system. The superior fasciculus terminates in two branches: one in the medial terminal nucleus; the other in the lateral terminal nucleus (Hayhow *et al.*, 1960).

Connections to the accessory optic system include those of retinal origin (Hayhow *et al.*, 1960) and of the ventral lateral geniculate nucleus (Mackay-Sim, 1983; Ribak and Peters, 1975) as well as the occipital cortex (Leong, 1980).

1.9.8 Visual cortex

The visual cortex in the rat is located in the occipital (Oc) region of the rat isocortex. The occipital region can be divided into three areas (Oc1, Oc2M, and Oc2L) on the basis of cytoarchitectural and myeloarchitectural methods (reviewed by Zilles and Wree, 1985). The Oc1 is the primary visual cortex and is partially surrounded at its rostromedial border by visual area Oc2M and at its rostrolateral border by visual area Oc2L. The visual cortex receives inputs from the retina via the dorsal lateral geniculate nucleus of the thalamus, as well as many extrageniculate thalamic nuclei including the pulvinar and lateral posterior complex (Price, 1991), the laterodorsal thalamic nucleus (Schober *et al.*, 1979), locus coeruleus (Morrison *et al.*, 1981), raphe nuclei (Lidov *et al.*, 1980), and temporal cortex 1 (Schober *et al.*, 1979). Between the right and the left hemispheres, the visual cortical areas are reciprocally interconnected by axons that run through the corpus callosum (Price, 1991).

Efferent axons from the occipital areas target to dorsal and ventral lateral geniculate nucleus (Nauta and Bucher, 1954; Sefton *et al.*, 1980), lateral posterior complex (Ribak, 1977; Schober *et al.*, 1976), superior colliculus (Sefton *et al.*, 1980), pontine nuclei (Ribak, 1977), reticular thalamic nucleus (Sefton *et al.*, 1980), and pretectal area (Nauta and Bucher, 1954; Ribak, 1977).

1.9.9 Summary of the visual pathways

Sections 1.9.1 to 1.9.8 describe the highly complicated pathways that connect and integrate components of the visual system. Garey *et al.* (1991) reviewed the organization of the visual thalamus in the laboratory rat, the domestic cat, and the macaque monkey and summarised their major visual nerve connections in a highly schematic diagram (see figure 1.6 on the following page). The diagram shows that the reticulogeniculostriate pathway and the pathway from the retina to extrastriate cortex via the superior colliculus and pretectum are the major (indicated by thick arrows) visual pathways. Other complicated minor pathways are also indicated. Thus, the diagram serves as a comprehensive map of the visual system at a glance.

Figure 1.6 A highly schematic diagram summarizing some of the connections between the visual nuclei as reviewed in the laboratory rat, domestic cat, and macaque monkey (After Garey *et al.*, 1991). The retinogeniculostriate pathway, and the pathway from the retina to extrastriate cortex via the superior colliculus and pretectum are indicated with thick arrows to highlight the main visual pathways. Abbreviations: CH: brainstem cholinergic nuclei; EX STR: extrastriate cortex; LGD: dorsal lateral geniculate nucleus; LGV PRE: ventral lateral geniculate nucleus/pregeniculate nucleus; PGB: parabigeminal nucleus; PG/RN: perigeniculate/reticular nucleus; PT: pretectum; PUL LP: pulvinar/lateral posterior complex; R LC: raphe nucleus and locus coeruleus; RET: retina; SC: superior colliculus; 17: area 17 of striate cortex (see following page for figure).

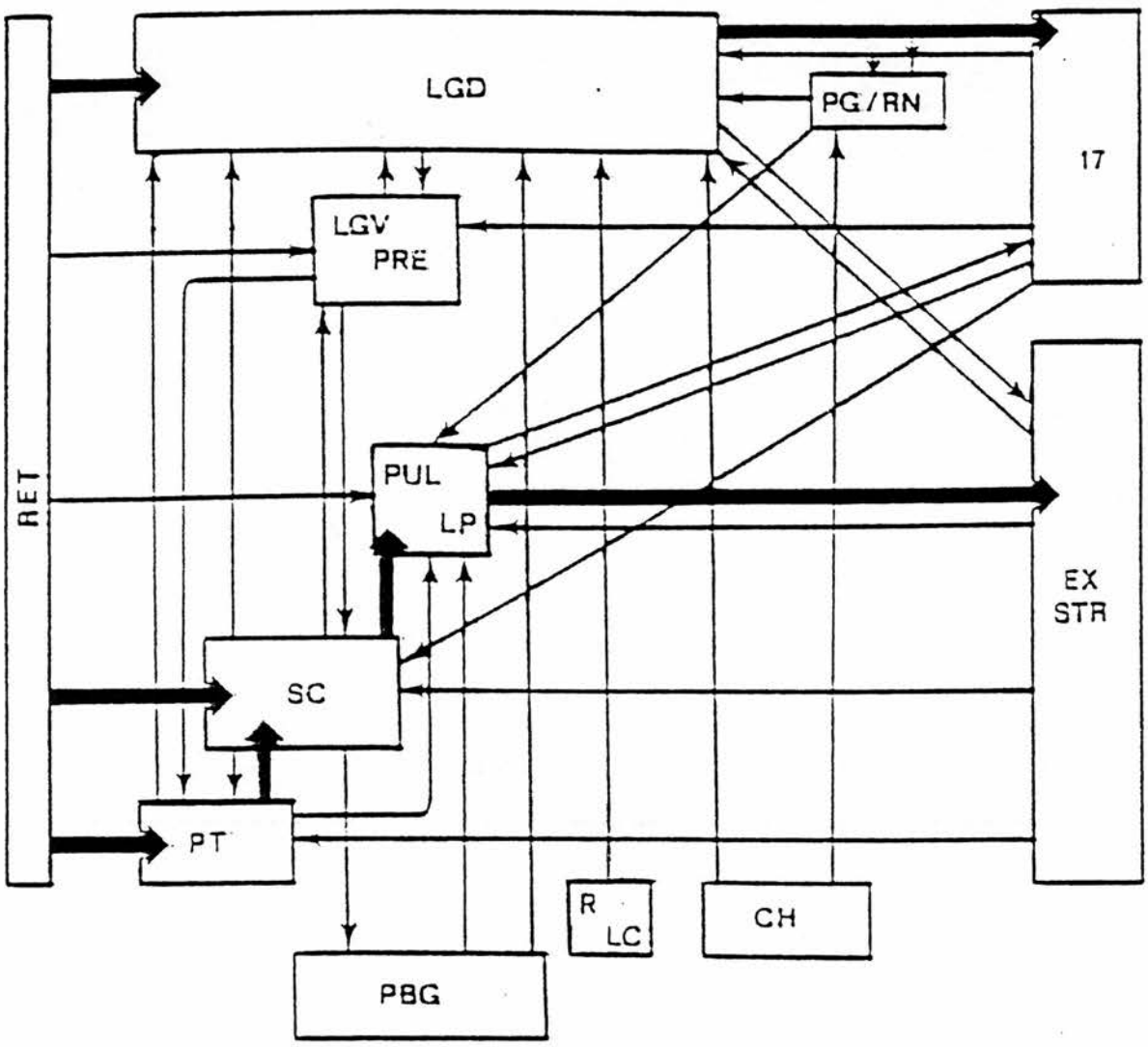

Figure 1.6 A highly schematic diagram summarizing visual connections in three species (see the preceding page for legend).

1.10 Integration of the olfactory nervous system

The olfactory nervous system, like the visual nervous system, covers a good variety of nuclei and pathways that can be traced from the external olfactory epithelium to the higher olfactory centers. The lateral olfactory tract and the lateral olfactory nucleus function in a comparable way as compared to the optic tract and the lateral geniculate nucleus in the visual nervous system. Components of the olfactory nervous system include the olfactory epithelium, the main olfactory bulb, the accessory olfactory bulb, the anterior olfactory nucleus, the precommissural hippocampus, the olfactory periallocortex, the endopiriform nucleus, the piriform cortex, the amygdalopiriform transition area, as well as the olfactory and vomeronasal amygdala (reviewed by Switzer *et al.*, 1985; Farman, 1992; Halasz, 1990). I will briefly describe, concentrating on afferent and efferent connections, each of these components from sections 1.10.1 to 1.10.9 (see figure 1.7 on the following page).

1.10.1 Main olfactory bulb

Most mammals have two chemosensory organs in the nasal cavity, the olfactory epithelium and the vomeronasal organ. The olfactory epithelium projects axons to the main olfactory bulb, while the vomeronasal organ projects axons to the accessory olfactory bulb (Farman, 1992). The olfactory epithelium covers the superior and the posterior regions of the nasal cavities and contains three cellular types: the olfactory receptor cells, the secretory or supporting cells, and the basal cells (Graziadei, 1971). The olfactory receptors are bipolar neurons. Each olfactory receptor emits a thin axon that joins others into small bundles. Bundles join together into fascicles that pass through the foramina of the sieve-like cribriform plate to form a fibrous outer layer of the main olfactory bulb and terminate in the glomeruli layer of the main olfactory bulb. The main olfactory bulb contains six well-defined layers, from the surface to the ependymal zone (the oblitered ventricular zone in the center of the bulb) (see figure 1.7 on the following page).

Figure 1.7 Histology of the main and accessory olfactory bulb (A,B,C) and diagrammatic representation of the major areas in the brain that contains olfactory connections (D) (A,B,C from Switzer *et al.*, 1985; D from Luskin and Price, 1983a). A. Low magnification of a Nissl preparation coronally sectioned through the main olfactory bulb (MOB). The outermost olfactory nerve layer (ON) engulfs the entire bulb and contains the incoming axons from the receptor cells in the olfactory epithelium. B. Another Nissl preparation sectioned caudally to A shows the caudomedial part of the main olfactory bulb (MOB), the accessory olfactory bulb (AOB), and the rostral part of the anterior olfactory nucleus (AO). C. A higher magnified portion of the main olfactory bulb (MOB) shows its layers in detail. D. A diagrammatic representation for the olfactory bulb and olfactory cortex transposed onto an unfolded map to show areas related to the olfactory connections. Abbreviations: A I_d: dorsal agranular insular cortex; A I_p: posterior agranular insular cortex; A L_v: ventral agranular insular cortex; AOB: accessory olfactory bulb; AOE: external part of anterior olfactory nucleus; AOL: lateral part of the anterior olfactory nucleus; AON: anterior olfactory nucleus; Co_o: anterior cortical nucleus of the amygdala; Co_p: posterior cortical nucleus of the amygdala; DLEA: dorsal part of the lateral entorhinal area; E: ependymal layer; EPI: external plexiform layer; g: glomerulus layer of the accessory olfactory bulb; GI: glomerular layer; GrA: granular cell layer; I Gr: internal granule cell layer; IL: infralimbic cortex; IPI: internal plexiform layer; LEA: lateral entorhinal area; lo: lateral olfactory tract; LOT: lateral olfactory tract; M.Tufted: sublayer of middle tufted cells; Me: medial nucleus of the amygdala; MOB: main olfactory bulb; Mtr: mitral cell layer; NLOT: nucleus of the lateral olfactory tract; O: output neurons of the accessory olfactory bulb (analogous to the mitral and tufted cells of the main olfactory bulb; OT: olfactory tubercle; Ot: optic tract; PAC: periamygdaloid cortex; PC: piriform cortex; Pr: perirhinal area; T T_d: dorsal tenia tecta; T T_v: ventral tenia tecta; VLEA: ventral part of the lateral entorhinal area; VMEA: ventromedial part of the lateral entorhinal area; Vn: vomeronasal nerve.

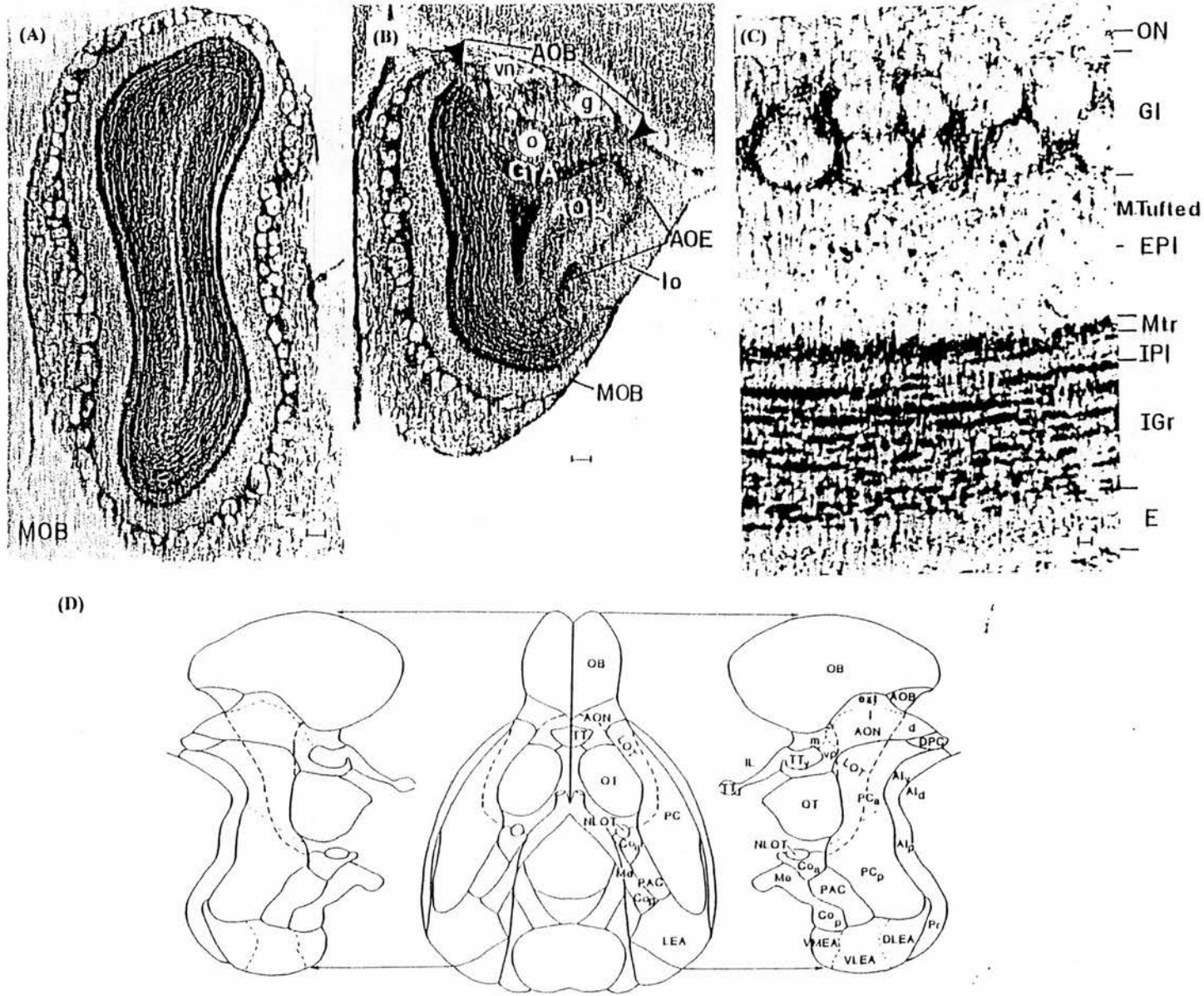

Figure 1.7 Histology of the main and accessory olfactory bulb (A,B,C) and diagrammatic representation of the major areas in the brain that contains olfactory connections (D).

Afferent axons to the main olfactory bulb include those from accessory olfactory bulb, piriform olfactory cortex, lateral, dorsal, and medial transition zone, nucleus of the vertical and horizontal limb of the diagonal band (Broca), nucleus of the lateral olfactory tract, taenia tecta, ventral pallidum, posterolateral cortical amygdaloid nucleus, anterior amygdaloid area, anterior pituitary, lateral hypothalamic area, zona incerta, locus coeruleus, dorsal raphe nucleus, median raphe nucleus and median septal nucleus (de Olmos *et al.*, 1978; Haberly and Price, 1978a, b; Luskin and Price, 1983; Macrides and Davis, 1983; Shipley and Adamek, 1984; Uemura-Sumi *et al.*, 1985). Efferent axons from the main olfactory bulb target to accessory olfactory lobe, piriform cortex, olfactory tubercle, anterior amygdaloid area, posterolateral cortical amygdaloid nucleus, rostral part of medial amygdaloid nucleus and entorhinal cortex (Heimer, 1968; Kosel *et al.*, 1981; Price, 1973; Scalia and Winans, 1975; White, 1965).

1.10.2 Accessory olfactory bulb

The receptors for the accessory olfactory bulb are distributed in the vomeronasal organ which is located in the rostral floor of nasal cavity (Estes, 1972). The vomeronasal nerve fibers penetrate the cribriform plate along with the olfactory nerve fibers and traverse, as a bundle, the medial surface of the main olfactory bulb in order to reach the accessory olfactory bulb. Input axons to the accessory olfactory bulb include the bed nucleus of the accessory nucleus tract, medial amygdaloid nucleus, posteromedial cortical amygdaloid nucleus, and ventral bed nucleus of the stria terminalis (medial part) (de Olmos *et al.*, 1978). Efferent axons lead to the bed nucleus of the accessory nucleus tract, medial amygdaloid nucleus, posteromedial cortical amygdaloid nucleus, and the posterodorsal bed nucleus of the stria terminalis (medial part) (Scalia and Winas, 1975).

1.10.3 Anterior olfactory nucleus

The anterior olfactory nucleus, which is first visible at the caudolateral border of the olfactory bulb, surrounds the anterior limb of anterior commissure and forms the main part of the olfactory peduncle. The caudal border of anterior olfactory nucleus is characterized by transitional areas (de Olmos *et al.*,

1978). The transitional areas separate it from anterior or frontal portions of the piriform cortex, frontal orbital cortex, and ventral precommissural hippocampus.

The anterior olfactory nucleus (AO) is closely related to the olfactory bulb. In particular, the centrifugal pathways from the anterior olfactory nucleus to the olfactory bulb are especially impressive (Switzer *et al.*, 1985). Apart from contributing to the centrifugal innervation of the main olfactory bulb, the AO participates in the formation of association systems of the primary olfactory (piriform) cortex, through which the AO is directly connected to the ventral precommissural hippocampus, the endopiriform nucleus, and particularly to the anterior part of the primary olfactory cortex. Anterior olfactory axons in the association system also branch to form a commissural projection to the anterior piriform cortex, the endopiriform nucleus and the AO on the opposite side (Haberly and Price, 1978b; Luskin and Price, 1983a). The AO also projects to the olfactory tubercle and the nucleus of the horizontal limb of the diagonal band (Broca), with the continum of projections contributing to the lateral preoptic and lateral hypothalamic areas (de Olmos *et al.*, 1978; Luskin and Price, 1983a). In addition, efferent projections to the bed nucleus of the stria terminalis, and to the nuclei gemini in the posterolateral part of hypothalamus have been reported in the rabbits (Broadwell, 1975).

Afferent connections of the AO include the main olfactory bulb, piriform cortex, transitional olfactory areas, lateral entorhinal area, as well as the complex composed of the ventral subiculum and CA1 division of the hippocampus, the horizontal and vertical nuclei of the diagonal band (Broca), the bed nucleus of stria terminalis, the nuclei comprising the olfactory amygdala, and the tuberomammillary hypothalamus (Conrad and Pfaff, 1976; de Olmos, 1972; de Olmos, 1978; Haberly and Price, 1978a; Kevetter and Winans, 1981b; Luskin and Price, 1983a).

1.10.4 Precommissural hippocampus

The precommissural hippocampus (taenia tecta) represents the rostral and ventral continuation of the supracommissural hippocampus (indusium griseum). Two divisions, the dorsal part and the ventral part, can be distinguished in the precommissural hippocampus. The ventral part is morphologically similar to the olfactory areas in the olfactory peduncle and contains extensive and reciprocal connections to the ipsilateral olfactory bulbs and several olfactory cortical areas (Haberly and Price, 1978a,b; Luskin and Price, 1983a). The dorsal part connections are less clear.

1.10.5 Olfactory periallocortex

Axons from the main olfactory bulb also project to the olfactory periallocortex -- the cortical areas outside the piriform cortex. In addition to the projections from the main olfactory bulb, afferent axons are from the posterior part of the piriform cortex, cortical amygdaloid nucleus, and entorhinal area (Haberly and Price, 1978a; Luskin and Price, 1983a). Other projections come from the ventrobasal thalamus, parabranchial nucleus (Saper, 1982; Shipley and Geinesman, 1984), as well as those mainly to the posterior insular cortex such as the mediodorsal nucleus of the thalamus and the basolateral amygdaloid body (Gerfen and Clavier, 1979; Saper, 1982). Efferent axons from the posterior insular cortex include the central amygdaloid nucleus, bed nucleus of stria terminalis, ventromedial and dorsomedial thalamus, and some brain stem structures, including the parabranchial complex and nucleus of the solitary tract (Saper, 1982; Shipley and Geinesman, 1984; reviewed by Switzer *et al.*, 1985).

1.10.6 Endopiriform nucleus

The endopiriform nucleus is situated immediately deep to the piriform cortex. It is continuous with the insular or dorsal claustrum in the dorsal direction, while ventrally it merges with the deepest portion of the ventromedial primary olfactory cortex and the deep parts of the amygdala. The endopiriform nucleus is one of the main recipients of subcortical projections from the piriform cortex and from other

recipients of the main olfactory bulb projection fibers (Luskin and Price, 1983a; Ottersen, 1982). The endopiriform nucleus is also a subcortical relay centre for fiber systems originating in periallocortical areas (Beckstead, 1979; Luskin and Price, 1983a). Most of the afferent pathways to the endopiriform nucleus are reciprocally projected. Efferently, the endopiriform nucleus projects to the mediodorsal thalamic nucleus, the ventral striatum, the lateral hypothalamus, and the tuberomammillary nucleus (Krettek and Price, 1977a, 1978a). Projections also lead to the 'vomeronasal amygdala' (Krevetter and Winans, 1981a) and the ventral subiculum, which are connected with the mediotuberal hypothalamus (Krettek and Price, 1978b).

1.10.7 Piriform cortex

The piriform cortex represents the major projection target of the main olfactory bulb and thus is the most extensive and important olfactory area in the brain for the integration and subsequent transmission of the incoming olfactory stimuli. Afferent axons to the piriform cortex include those from the main olfactory bulb, accessory olfactory bulb, ventral precommissural hippocampus, nucleus of the lateral olfactory tract, posterolateral cortical amygdaloid nucleus, anterior cortical amygdaloid nucleus, endopiriform nucleus, insular cortex, anterior amygdaloid area, sublenticular substantia innominata, nucleus of the horizontal and vertical limb of the diagonal band (Broca), midline thalamic nuclei, lateral hypothalamic area, lateral preoptic area, dorsal hypothalamic area, tuberomammillary nucleus, ventral tegmental area (Tsai), dorsal and medial raphe nucleus, and locus coeruleus (Haberly and Price, 1978a,b; Azmitia and Segal, 1978; Fallon and Moore, 1978; Lindvall and Bjorklund, 1983; Steinbusch, 1981). Efferent axons project to the main olfactory bulb, accessory olfactory bulb, taenia tecta, periallocortex, olfactory tubercle, endopiriform cortex, anterior amygdaloid area, nucleus of the lateral olfactory tract, anterior cortical amygdaloid nucleus, posterolateral cortical amygdaloid nucleus, posteromedial cortical amygdaloid nucleus, basolateral amygdaloid nucleus, basomedial amygdaloid nucleus, central amgdaloid nucelus, mediodorsal thalamic nucleus, and lateral hypothalamic area (Luskin and Price, 1983a,b; Heimer and Wilson, 1975; Millhouse and Heimer, 1984; Haberly and Price, 1978a; Krettek and Price, 1978a; Veening, 1978; Price and Slotnick, 1983; Young *et al.*, 1984) .

1.10.8 Amygdalopiriform transition area

The amygdalopiriform transition area is located deep to and in the external lip of the amygdaloid fissure. It receives projections from the piriform cortex, the ventral subiculum, and from some of the amygdaloid nuclei (Krettek and Price, 1977a, b; Luskin and Price, 1983a, b; Ottersen, 1982). Other afferent axons are from the insular periallocortex (Beckstead, 1979; Saper, 1982), the endopiriform nucleus, and the reuniens thalamic nucleus (Herkenham, 1978). Efferent projections lead to the caudomedial olfactory tubercle and accumbens nucleus, the subgenual periallocortex, basolateral and central amygdaloid nuclei, and the lateral portion of the bed nucleus of stria terminalis (reviewed by de Olmos *et al.*, 1985).

1.10.9 Olfactory and vomeronasal amygdala

The olfactory and vomeronasal amygdala were first named by Kevetter and Winas (1981a,b) to denote parts of the amygdaloid complex that receives direct projections from the main and accessory olfactory bulbs. Areas of the olfactory amygdala include the anterior amygdaloid area, nucleus of the lateral olfactory tract, anterior cortical amygdaloid nucleus and posterolateral amygdaloid nucleus. Vomeronasal amygdala includes the bed nucleus of the accessory olfactory tract, medial amygdaloid nucleus, posteromedial cortical amygdaloid nucleus, and the medial part of the bed nucleus of the stria terminalis.

Afferent and efferent axons are from the olfactory bulb and the primary olfactory (piriform) cortex, as well as some subcortical inputs from the telencephalon, the diencephalon, and the locus coerulus from the brain stem. These have been described in previous sections and will not be repeated here.

1.11 Development of the eye

1.11.1 Gross morphogenesis of the eye

The eye is derived from four sources of tissues: neuroectoderm of the forebrain, surface ectoderm of the head , neural crest, and head paraxial mesoderm. In the mouse, the first sign of optic placode formation can be seen at the 4-somite stage, i.e. at the time when the cephalic neural folds are first clearly recognizable (Kaufman, 1979; 1992). Shortly afterwards, an indentation in the central part of the optic placode, the optic pit, forms. This is followed by the fusion of the neural folds to form the forebrain vesicles at around days 8.5 - 9.0 p.c. in the mouse. During the fusion of the neural folds, the optic pits appear as an increasingly deepening pair of indentations of the neural ectoderm connected by a pair of shallow grooves, the optic sulci, in the region of future optic chiasma (Kaufman, 1992). As the neural folds fuse, the optic sulci evaginate to form hollow diverticula called optic vesicles. The optic vesicles (see figure 1.8a on the following page) are lateraly outgrowths from the caudal end of the prosencephalon. The primary optic vesicles form before the two lateral head neural folds fuse completely with each other, with little evidence of a previous dilation (O'Rahilly and Meyer, 1959; Pei and Rhodin, 1970). Following appearance of the optic vesicle is the formation of a constriction, the optic stalk, close to the midline of the prosencephalon. In the distal end of the primary optic vesicle, a further outgrowth gradually makes contact with the overlying surface ectoderm.

Shortly after the optic vesicle contacts the surface ectoderm, the surface ectoderm thickens and develops into the lens placode. The lens placode invaginates, pushing the optic vesicle toward the midline to form a two-layered pocket at each lateral end of the diencephalon (figure 1.8a). The invaginated lens placodes will detach from the overlying surface ectoderm and differentiate into the lens. The remaining ectoderm that covers the lens will become the outer layer of the future cornea. The cornea forms through an epithelium elongation (Bard *et al.*, 1988). A migration of neural crest cells from the margins of the optic cup contributes to the undersurface of the primary cornea stroma (Noden, 1978; Johnston *et al.*, 1979). The inpocketed optic vesicle later becomes a cup-shaped structure called the "optic cup". The optic cup is linked with the diencephalon through the optic stalk.

The optic cup is a double-layered structure: the inner layer (the layer facing toward the lens) is the neural retina, which is surrounded by the outer layer, the pigmented retinal epithelium. Cells of the pigmented retinal epithelium at the anterior ridge of the optic cup extend toward the lens and, together with retinal and neural crest derived cells, form the iris. Surrounding the optic cup are two outer coats -- the vascularized choroid and the connective-tissue sclera; both are derived from the neural crest (Johnston, 1979). Only the extrinsic ocular muscles are derived from the head paraxial mesoderm (Noden, 1983).

Figure 1.8a Diagrammatic representation of eye morphogenesis. A. At day 9 to 9.5 p.c., the lens placode forms as a thickened part of the surface ectoderm. The neuroectoderm in close proximity to the lens placode also becomes thickened. B. At day 9.5 to 10.0 p.c., the area of the lens placode has enlarged and the early optic cup forms. C. At day 10.5 p.c., two layers, the prospective neural retina and pigmented epithelium, of the optic cup become evident as the lens placode indents to form the lens pit. D. At day 11.5 p.c., the prospective cornea and the lens vesicle appear after the primitive lens is detached from the surface ectoderm. The lens vesicle will gradually diminish as the primary lens fibers elongate. E. At day 13.5 p.c., the lens comprises the anterior cuboidal epithelial cells and the posterior elongating fiber cells. The neural retina layer behind the lens begins to differentiate and the primitive cornea develops in front of the lens. (From Cvekl and Piatigorsky, 1996).

Figure 1.8b Differentiation of the lens. A. The lens epithelium shortly after detachment from the surface ectoderm with the hollow cavity of lens vesicle being enclosed. B. The lens vesicle is reduced as the primary fibers are enlongating. C. Two portions of the lens cells, the anterior and the posterior portion, are established. D. The posterior portion of the lens cells elongate and produce secondary lens fibers. E. The crystallin-synthesizing fibers continue to grow and eventually fill the space between the anterior and the posterior portion of the lens tissue. The anterior cells constitute a germinal epithelium (anterior lens capsule) which keeps dividing. The dividing cells move toward the equator of the vesicle (indicated by arrows), and as they pass through the equatorial region, they begin to elongate. (From Gilbert, 1994).

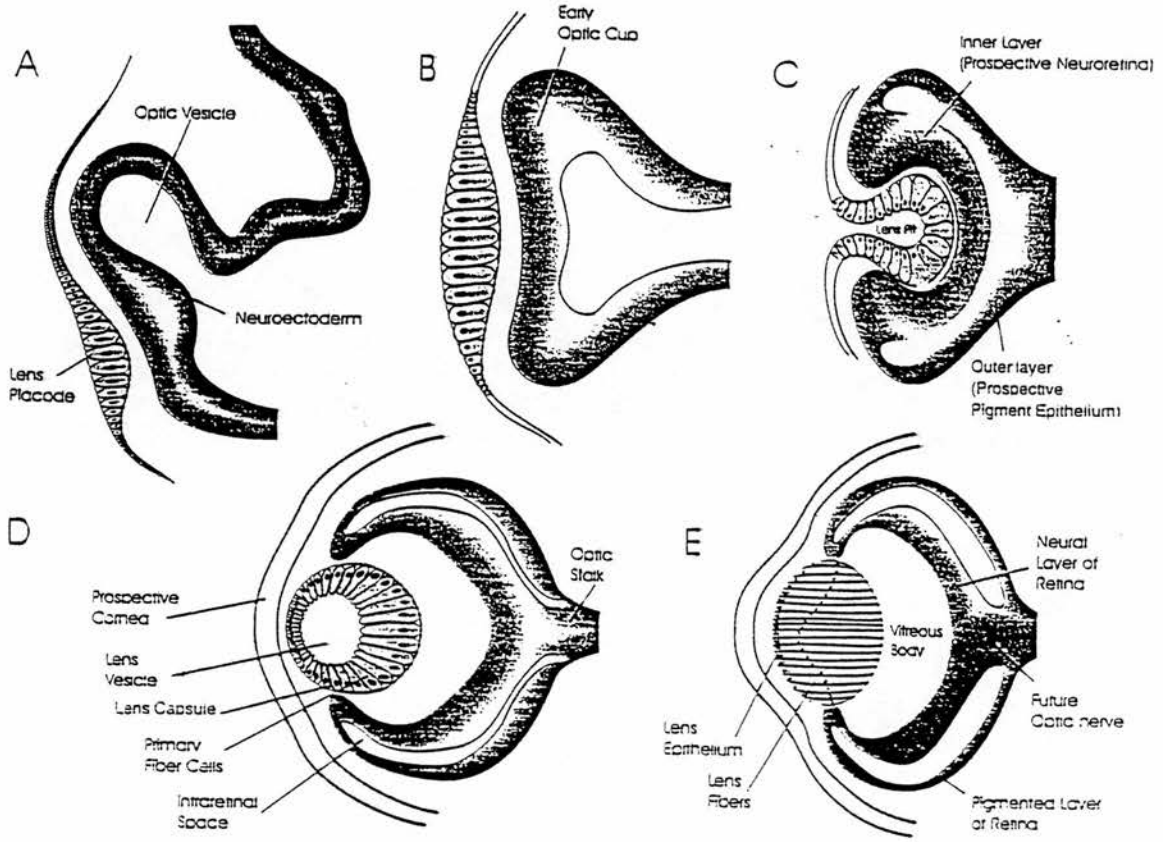

Figure 1.8a Diagrammatic representation of eye morphogenesis (from Cvekl and Piatigorsky, 1996).

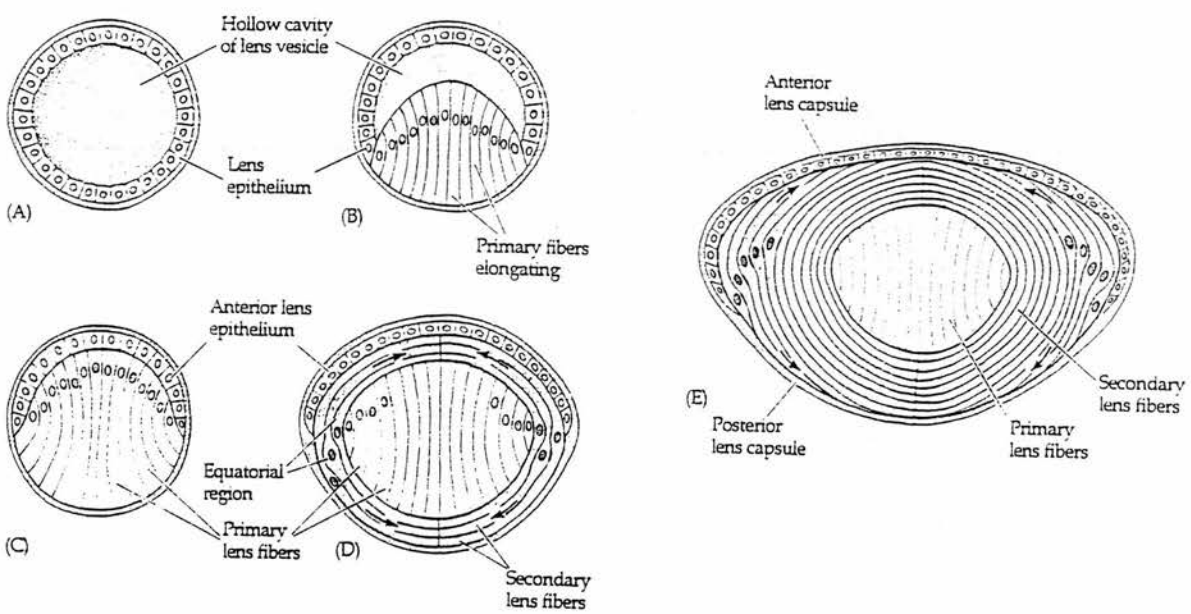

Figure 1.8b Diagrammatic representation of lens differentiation (from Gilbert, 1994).

1.11.2 Differentiation of the lens

As mentioned in section 1.11.1, during the course of neural tube formation, the optic vesicle (a protrusion of the lateral forebrain that gives rise to the optic stalk, pigmented epithelium, and neural retina) contacts the surface ectoderm. This ectoderm subsequently forms the lens and cornea. The optic vesicle then invaginates to form a multilayered optic cup where specific cells can process light stimuli into spatially organized images. For the correct focusing of light on the retina, correct curvature of the lens and the cornea is necessary. The differentiation of lens tissue into a transparent membrane capable of directing light onto the retina involves changes in the cell structure and shape as well as synthesis of lens-specific proteins, the crystallins. Crystallins are synthesized as cell shape changes occur, causing the lens vesicle to become the definitive lens (Wistow and Piatigorsky, 1988).

The lens tissue is first invaginated as a continuous but thickened part of the surface ectoderm. Then it detaches from the surface ectoderm and shapes into a ball-like structure, with the lens vesicle being enclosed (see figure 1.8b on the preceding page). Thus, two portions of the lens cells, the anterior and the posterior, are established. Cells in the posterior portion of the lens elongate and, under the influence of the neural retina (Piatigorsky, 1981; Wistow and Piatigorsky, 1988), produce the lens fibers. As the fibers continue to grow, crystallins are extensively synthesized such that they fill up the cell and cause the extrusion of the nucleus. The crystallin-synthesizing fibers continue to grow and eventually fill the space between the anterior and the posterior portion of the lens tissue.

The anterior cells constitute a germinal epithelium that keeps dividing. The newly-divided cells move toward the equator of the lens vesicle, and as they pass through the equatorial region, they begin to elongate. Thus, the lens contains three regions: an anterior zone of dividing epithelial cells, an equatorial zone of elongating cells, and a posterior and central zone of crystallin-containing fiber cells. This arrangement of lens cells persists throughout the lifetime of animals, since fibers are continuously being laid down.

1.11.3 Differentiation of the retina

Like the cerebral and the cerebellar organization, the neural retina develops into a multiple-layered structure containing different types of neuronal cells (see figure 1.9 on the following page). The layers include light-sensitive and colour-sensitive photoreceptor (rod and cone) cells, cell bodies of ganglions, and bipolar interneurons that transmit the electric stimulus from rod and cone cells to the ganglion cells. In addition, there are plenty of glial cells to maintain the integrity of the retina, as well as amacrine neurons and hirizontal neurons that transmit electrical stimuli horizontally.

To form and differentiate such a complicated but well-organized structure like the neural retina, precise temporal and spatial coordination is needed. As a derivative of the developing neural tube, the ventricular surface of retina is mitotically active. The ventricular zone initially includes the entire thickness of the retina, but once the inner plexiform layer has formed, the interkinetic migration becomes restricted to the region between the inner plexiform layer and the the outer limiting membrane. This region, where the interkinetic migration is confined, is termed the 'neuroblast' or "cytoblast layer" by Robinson *et al.* (1986). Nuclei of the dividing cells enter different phases of the cell cycle as they traverse the "cytoblast layer" (Robinson *et al.*, 1986). Thus, nuclei enter the M-phase and divide at the outer limiting membrane. After division, the daughter nuclei enter G_1-resting phase and migrate through the outer part of "cytoblast layer". The nuclei enter S-phase as they reach the inner part of the "cytoblast layer" and remain in this phase until they reached the inner plexiform layer. During S-phase, nuclei incorporate molecules they require for the replication of DNA. Nuclei enter G_2-resting phase during their return journey to the outer limiting membrane where they divide again (Sidman, 1961; Zavarzin and Stroeva, 1964; Denham, 1967; Robinson, 1986).

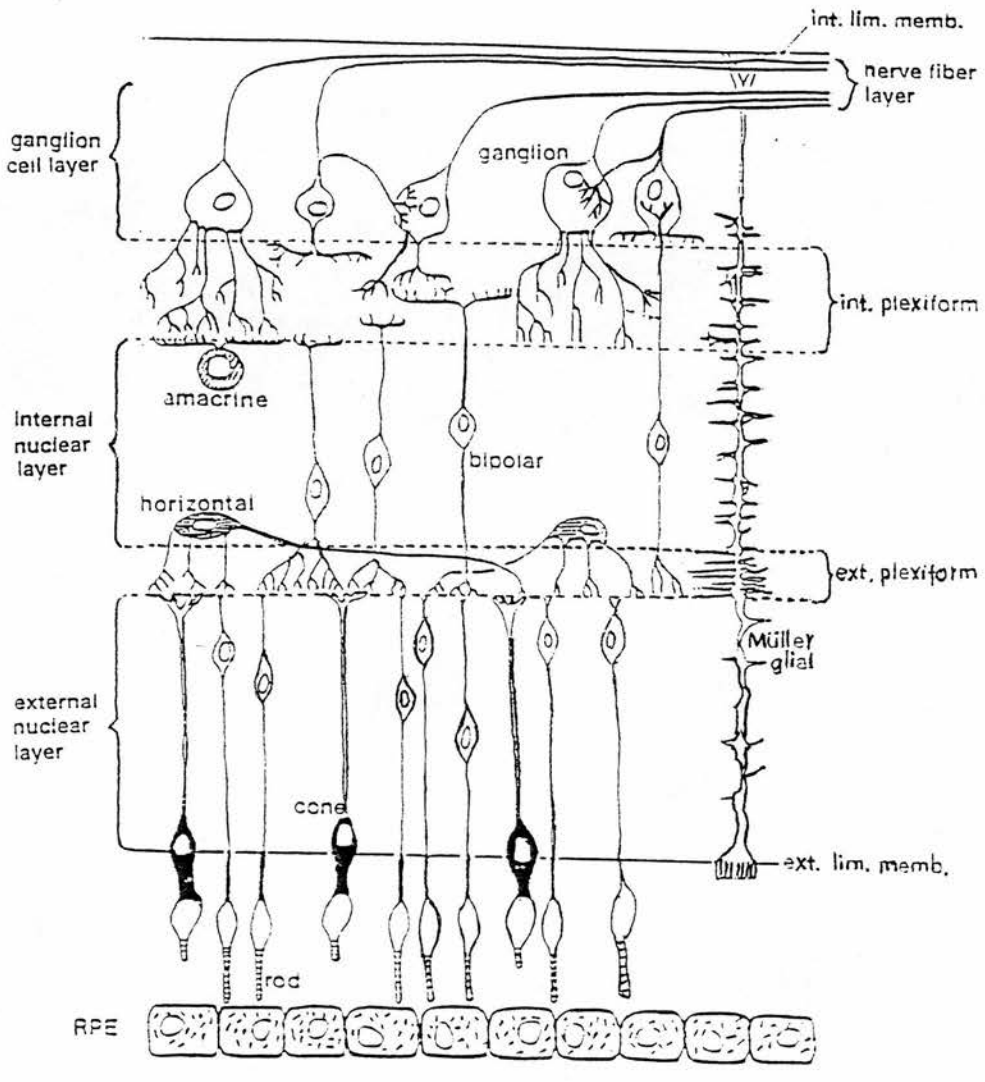

Figure 1.9 Laminar structure of the retina after differentiation from a single layer of neuroepithelium. The rod and cone photoreceptors in close proximity to the pigment layer project through the external limiting membrane (ext. lim. memb.) to make connection to the bipolar and horizontal cells in the inner nucler layer. The connection site is located within the external plexiform layer (ext. plexiform). The inter nuclear layer consists of horizontal, bipolar, and amacrine cells. Bipolar and amacrine cells connect to the dendrites of ganglion cells within the internal plexiform layer (int. plexiform). Axons of ganglion cells project together to form nerve fiber layer that eventually contribute to the optic stalk and exit the eye. Müller glia cells span between the internal limiting membrane and the outer limiting membrane (Based on an illustration in Kahle, 1986).

1.12 Development of the teeth

1.12.1 Histogenesis of the teeth

Early development of the teeth can be described in three stages according to morphogenesis: the bud stage, the cap stage, and the bell stage (Osborn, 1981; reviewed by Thesleff, 1994) (see figure 1.10 on page 82). In the mouse, the first sign of tooth development is the appearance of the dental lamina, a ridge of ectoderm overlying the developing bones of the upper and lower jaw, at E11.0. The dental lamina gives rise to two buds in the upper jaw and four buds in the lower jaw. These buds form the primordia of ectodermal components of the teeth (the bud stage). The deep surface of each bud invaginates to form a cap of ectoderm, the dental papilla, over the mesenchymal thickening (the cap stage). The cap consists of an outer layer of cells (the outer dental epithelium) and an inner layer (the inner dental epithelium). The mesenchymal cells of the dental papilla adjacent to the inner dental lamina then differentiate into odontoblasts that will later produce dentine. As the dentine layer thickens, the odontoblasts retreat into the dental papilla. The odontoblasts persist in producing predentine throughout life. The remaining cells of the dental papilla form the pulp of the teeth.

The epithelial cells of the outer dental lamina differentiate into the ameloblasts. The ameloblasts produce long enamel prisms to deposite over the dentine. The enamel is first laid down at the apex of the tooth, then spreads towards its neck. As the enamel thickens, the ameloblasts retreat and regress afterwards.

Root formation begins when the dental epithelial layers penetrate the underlying mesenchyme to form the epithelial root sheath. The odontoblasts of dental papilla lay down a layer of dentine continuous with that of the crown, narrowing the pulp chamber to a mere root canal containing blood vessels and nerves supplying the teeth. The mesenchymal cells in contact with root dentine produce a layer of cementum (specialized bone) and the peridontal ligaments that hold the tooth in place. During this process, the mandible and maxilla have grown to surround the tooth, forming medial and lateral alveolar plates joined by transverse septa between the teeth.

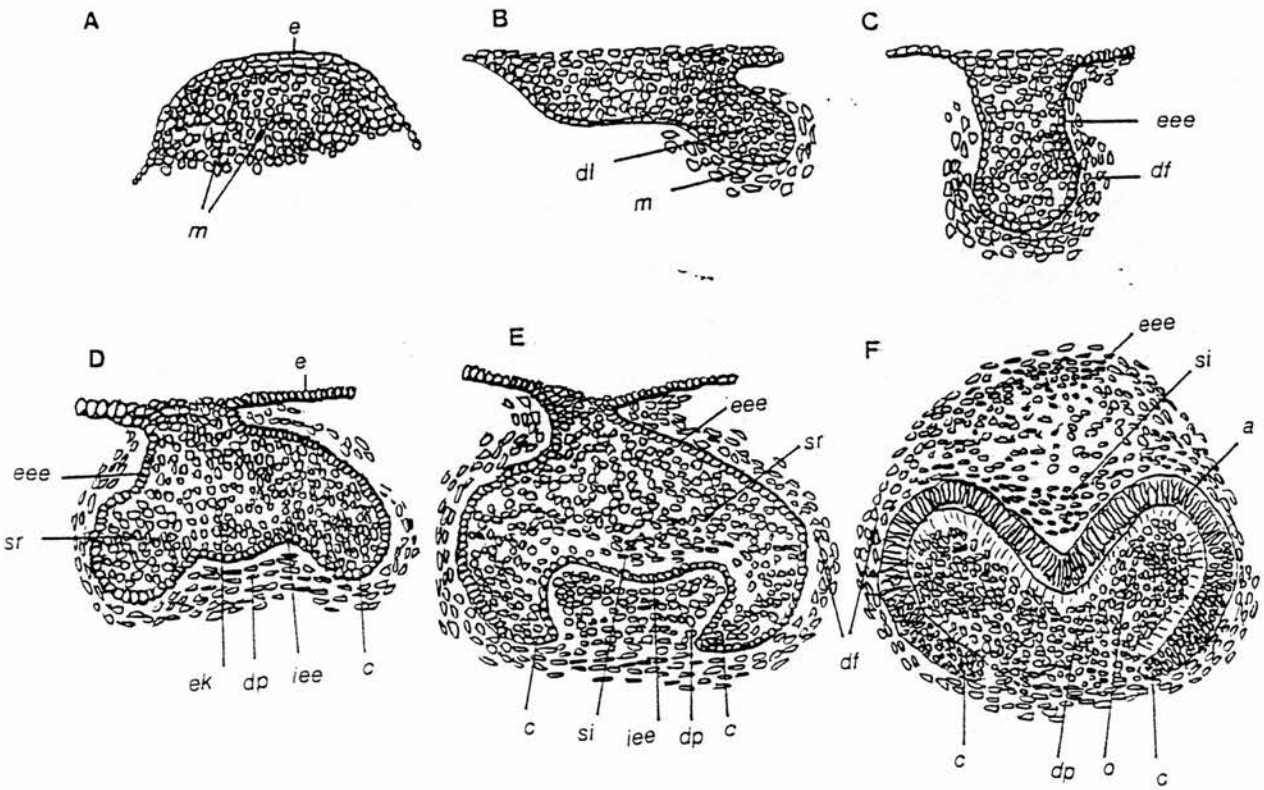

Figure 1.10 Diagrammatic representation of the formation of the lower first molar tooth at the times of (A) initiation, (B) dental lamina invagination, (C) bud, (D) cap, (E) early bell, (F) late bell stages of development. The development of incisors follows the same series of initiation, lamina invagination, bud, cap, and bell stages. Note that the site of tooth formation is largely located following the invagination of the dental lamina (dl). Abbreviations: a: ameloblasts; c: cervical loop; df: dental follicle; dpl: dental placode; dl: dental lamina; dp: dental papilla; e: jaw epithelium; eee: external enamel epithelium; ek: enamel knot; iee: internal enamel epithelium; m: mesenchyme; o: odontoblast; si: stratum intermedium; sr: stellate reticulum (Based on an illustration in Mackenzie *et al.*, 1991a).

1.12.2 Inducing events controling the initiation of odontogenesis

Various theories have been proposed to deduce the mechanism that determines number and shape of teeth during development. The notable theories include the 'regional field theory' (Butler, 1967), the 'prepattern gradient theory' (Valen, 1970), the 'source-sink theory' (Crick, 1970), the 'clone theory' (Osborn, 1973, 1978), and the 'innervation theory' (Pearson, 1977; Kollar and Lumsden, 1979; Lumsden, 1982). Lumsden (1979) grouped those theories into two broad categories: (1) theories share the requirement of an extrinsic signal generated by an external source to produce patterns in a homogeneous population and, (2) theories have the common notion that patterns are self-generated rather than organized from outside. However, none of the above mentioned theories have been strongly supported by experimental evidence. For example, the innervation theory suggested that initiating events of odontogenesis might involve a neural component. There are two facts underlying the idea of innervation theory: (1) the prospective dental nerves enter the jaw long before tooth formation, and (2) axons occur transiently at sites where odontogenesis will occur. Tooth initiation commences by a local thickening of the oral epithelium and by an underlying mesenchymal condensation, the dental lamina. After initiation, the subsequent development of tooth primordia runs more or less autonomously (Glasstone, 1967, 1973; Thesleff, 1976, 1977a, b; Thesleff and Hurmerinta, 1981). Therefore, if nervous elements are involved in the initiation of tooth formation, this should occur before or during the appearance of a dental lamina. However, after specific experiments with E 9.0 - E10.0 mouse mandibular arch fragments cultivated *in vitro* , with or without trigeminal ganglion explants, or grafted *in ocuo*, Lumsden and Buchanan (1986) concluded that tooth initiation does not involve a nervous component.

The current view of the initiation of odontogenesis tends to support that the oral epithelium provides neural crest-derived ectomesenchyme with competence to participate in tooth formation (Mina and Kollar, 1987; Thomas and Kollar, 1988, 1989; Kollar and Mina, 1991; Slavkin, 1991). These interactions are mediated by cell surface molecules, extracellular matrix molecules and soluble molecules (Kollar, 1981; Thesleff and Hurmerinta, 1981; Partanen *et al.*, 1985; Thesleff *et al.*, 1987). Thus, the local occurrence of growth factors such as epidermal growth factors and its receptors

(Partanen *et al.*, 1985; Partanen and Thesleff, 1987; Kronmiller *et al.*, 1991a, b), bone morphogenic proteins (Vainio *et al.*, 1993) and fibroblast growth factors (Vaahtokari *et al.*, 1996), or the local expression of transcription factors genes such as *Msx-1*, *Msx-2*, and *Egr-1* (Vainio *et al.*, 1993) have been implicated as candidate mechanisms in the initiation of odontogenesis.

1.13 Outline of this thesis

When this work was initiated, it was only known that *Pax6* is mutated in the *Small eye* mouse (Hill *et al.*, 1991) and that *Pax6* was important for the development of the eye, nose, and brain (Hogan *et al.*, 1986, 1988; Hill *et al.*, 1991). Very little was known about the other craniofacial areas affected by *Pax6* mutation, and what the possible roles of *Pax6* might be in those affected areas. *Pax6* was regarded as a putative transcription factor, but what gene(s) it might regulate or what gene(s) it might be regulated were unknown. *Pax6* expression in the mouse and in the human was reported (Walther and Gruss, 1991; Ton *et al.*, 1991), but without detailed description, particularly in the developing central nervous system. Furthermore, no clue of *Pax6* expression in other species was available.

This study began with an attempt to isolate chick *Pax6* by screening a cDNA library and by direct cloning via RT-PCR (Reverse Transcription - Polymerase Chain Reaction), using a mouse *Pax6* cDNA probe for identification. However, chick *Pax6* was isolated and sequenced (Li *et al*, 1994) in another laboratory before the goal was achieved. I therefore went on to study the expression pattern of *Pax6* during chick embryogenesis, in particular, during the later stages that had not been reported previously. This study also studied *Pax6* expression in the mouse, concentrating on the developing visual and olfactory nervous systems that had not been investigated in detail before (chapter 3). Once the expression pattern was established, further experiments was conducted to study the role of *Pax6* in lens differentiation (chapter 4), as well as the possible interaction of *Pax6* with two homeobox-containing genes, *Msx1* and *Msx2*, in the formation of supernumerary upper incisor teeth in the homozygous *Small eye* mutants (chapter 5). In chapter 6, the effect of all-*trans*-retinoic acid (RA) on *Pax6* expression during early chick embryogenesis is investigated. All details of materials and methods are described in chapter 2. A summary and some suggested future experiments are in chapter 7.

Chapter 2: Materials and Methods

All specifications concerning chemicals and solutions, i.e. full names for abbreviations used in this thesis, recipes, and preparations, are listed in the appendix. Linder's silver staining (chapter 3) was performed by Miss Corrine Arnott. A substantial amount of the *Msx1* and *Msx2* riboprobes used in this study (chapter 5) were synthesized by Dr. S. E. Wedden. Mouse embryos (chapters 3 and 5) were obtained under Professor M. H. Kaufman's license and were dissected, as the license allowed, by Professor M. H. Kaufman. Chick embryos were prepared for culture (chapter 6) with the assistance of Dr. Arthur Jurand.

2.1 *Small eye* mouse mutants

2.1.1 Source of the *Small eye* mouse mutants

The *Small eye* mutant mice were originally from stocks in the Department of Animal Genetics, Edinburgh University (Roberts, 1967) and were provided by Dr. R. Clayton, Department of Animal Genetics, to Professor M. H. Kaufman, Department of Anatomy (both at Edinburgh University).

2.1.2 *Small eye* mouse embryos

Homozygous (*Sey/Sey*) embryos were obtained by mating heterozygous males and females. The heterozygous (*Sey/+*) parents were selected on the basis of smaller eye size, in contrast to their wild type (+/+) littermates. The age of the embryos was judged according the vaginal plugs observed in their female parents. Twelve midday of the day on which a vaginal plug was observed was assumed to be day 0.5 p.c. (post coitus). Homozygous embryos were distinguished from their littermates by their absence of eyes and nasal cavities (Hogan *et al.*, 1986). Wildtype (+/+) littermates were used as controls for all experiments.

2.2 Chicken embryos

2.2.1 Source of chick embryos

Fertilized White Feather chick eggs were obtained from the Dryden-Mountmarle farm at Roslin Institute, Midlothian, Scotland.

2.2.2 Preparation of chick embryos at defined stages

Fertile eggs were incubated at 38.0° - 38.5° C in an incubator (McKay-and-Lynn, Edinburgh) in a humidified atmosphere. The eggs were placed and turned in the incubator during incubation so that the embryo in each egg could float freely to the top of the yolk in the shell. They were "windowed" after overnight incubation through the following standard procedure (Tickle, 1993):

The blunt end of each egg was swabbed with 70% alcohol and a hole was made into the air sac using a blunt pair of forceps. The uppermost part of each egg was then swabbed with 70% alcohol. The shell was punctured carefully with a coarse needle without piercing through the shell membrane. A small fragment of the shell was carefully picked away, leaving the shell membrane beneath it untouched. A fine needle was then used to make a hole in the shell membrane and the edge of the membrane was lifted carefully so that air could enter beneath it. This made the air free to escape from the air sac and the embryo would drop gradually. Once the embryo dropped, a piece of Sellotape was applied over the hole. It was then safer to enlarge the hole by cutting into the Sellotape together with the shell and the shell membrane with a pair of small scissors. Each embryo was then visible through the window and could be staged according to Hamburger-Hamilton system (Hamburger and Hamilton, 1951).

All embryos were "windowed" after overnight incubation, i.e. at stages 4 - 6. For embryos to be used at later stages, the "windowed" eggs were then reincubated until they had reached the required stages.

2.3 Histology for Haematoxylin-Eosin stain and Linder's silver stain

2.3.1 Preparation of microslides

Microslides for Haematoxylin-Eosin stain and Linder's silver stain were prepared by washing them in warm soapy water. They were then kept in 96% alcohol for storage. Shortly before use, the microslides were wiped using clean paper towels to remove alcohol on their surface and air-dried.

2.3.2 Preparation of tissue sections

For Haematoxylin-Eosin staining, chick or mouse tissues were dissected out of embryos. They were washed sufficiently in PBS (Phosphate-Buffered Saline) to get rid of blood clots or other unwanted tissues, and fixed in 10% formaldehyde in PBS or Bouin's solution for 4 - 24 hours depending on the size (Kaufman, 1992). After fixation, embryos were washed twice in PBS and then taken through a series of increased concentrations of alcohols, i.e. via 30 %, 50%, 75%, 96%, to twice in 100% alcohol. Large embryos or tissue samples were kept in each alcohol for not less than 2 hours. For smaller embryos or tissue fragments, the period of time in each alcohol was reduced, but was never less than 30 minutes. Once sufficiently dehydrated, the tissues were cleared in xylene and embedded in

paraplast wax (Sherwood Medical Co., St. Louis, USA; Product no. 8889-501007) by soaking in 60° C liquid paraplast in a vacuum chamber (Charles Hearson & Co. Ltd., London, England) for three times (at least 20 minutes each), and transferring them to freshly melted paraplast in cubic blocks. They were then allowed to cool down for sectioning.

Sections at 5 - 7 μm in thickness were cut on a Reichert-Jung 2050 microtome and placed on clean pre-washed slides. The slides were covered with a small volume of distilled water and pre-heated on a 40° C hot plate before the sections were placed to avoid folding of tissues. Once sections were flattened well on slides, the distilled water was removed and absorbed with tissue paper. Slides were completely dried in a 37° C oven and processed for Haematoxylin-Eosin stain or Linder's silver stain (see sections 2.3.3 - 2.3.4).

2.3.3 Haematoxylin-Eosin stain

The Haematoxylin-Eosin stain was performed according to the method described by Culling *et al.* (1985). Ehrlich's haematoxylin was used (recipe in appendix B-3). The procedures were:

1. Paraffin wax removed with xylene, two changes, 5 minutes each.

2. Slides treated with absolute alcohol, two changes, 1 minute each.

3. Washed in distilled water.

4. Stained in haematoxylin, 5 minutes.

5. Differentiated in acid alcohol until only nuclei remained blue.

6. Washed in distilled water.

7. Stained in 1% eosin for 3 minutes.

8. Washed in running tap water for 1 minute.

9. Quickly dehydrated in three changes of absolute alcohol, 10 seconds each.

10. Quickly cleared in two changes of xylene, 30 seconds each.

11. Mounted and covered by coverslips using DPX (BDH Laboratory Supplies, Prod. No. 36029, England).

2.3.4 Linder's silver stain

A variety of methods is available for staining non-myelated and myelated nerve fibres. Linder's silver method (Linder, 1978; recipe in appendix B-27) stains nerve fibers dark brown or black colour with good definition and was therefore the method of choice used to compare nerve fiber formation with the expression pattern of *Pax6* in the developing mouse brain (Chapter 3). Following silver impregnation, the tissues were counterstained with 1% Luxol fast blue which stained the myelinated nerve fibers blue. The following procedures were performed:

1. Paraffin was removed and sections were brought to distilled water as described in steps 1 - 3 in section 2.3.3.

2. Sections placed in diluted buffer (recipe in appendix B-27) at 60° C on a hot plate for 20 - 30 minutes.

3. Sections transfered directly to silver impregnating solution at 60° C on a hot plate and incubated for 10 - 30 minutes.

4. Sections washed by dipping in several changes of distilled water at room temperature for a total of 3 minutes.

5. Sections transferred into the physical developer working solution at room temperature.

6. Sections were stirred constantly in the physical developer working solution and the progress of development was monitored by washing with distilled water and examing under the microscope.

7. When results were optimal, the sections were counterstained in 1 % Luxol fast blue for 1 minute, washed in distilled water, dehydrated, cleared and mounted as described in steps 8 - 11 in section 2.3.3.

2.4 *In situ* hybridization for sections

All the protocols for *in situ* hybridization used in this thesis were based on *DNA Probes, second edition* by G. H. Keller and M.M. Manak, Stockton Press, New York, 1993.

2.4.0 General consideration

Before the *in situ* hybridization techniques were developed, temporal and spatial distribution of messenger RNAs of specific genes were studied by blotting and hybridization on membranes

(nitrocellulose or nylon). The messenger RNAs to be studied were extracted from developing tissues, further purified through oligo-dT columns, and run on agarose gels to separate them from each other according to their length. The separated RNA bands were then blotted on membranes and identified by hybridizing with radio-labelled probes. As the hybridization could be performed on membranes, similar procedures could be performed on tissue sections. Thus, *in situ* hybridization techniques were developed to save the efforts of extracting RNAs from tissues and, at the same time, to give better definition in localizing tissues where a gene is expressed. Therefore, general considerations that should be taken for the blotting and hybridization remain the same for *in situ* hybridization, either for sections or for wholemounts.

Considerations include: (1) Avoidance of any source of RNase contamination, as RNase can digest the messenger RNAs to be detected and the riboprobes. The net result of RNase contamination very often lead to complete loss of signals. Possible contamination was therefore prevented by using depc-treated distilled water (details in appendix) in riboprobe preparation and storage, as well as in any solution used before hybridization and in handling tissues. (2) Reduction of non-specific background signals. This was done by thorough pre-hybridizing and pre-blocking before the real hybridization and antibody binding were performed. (3) Optimization of hybridization by adjusting the stringency for each probe. The stringency of hybridization could be affected by the hybridizing temperature and the salt strength used in the hybridization mix. The stringency for any specific probe used can be optimized for best results (details in *Molecular Cloning, A Laboratory Manual,* 2nd edition by J. Sambrook, E. F. Fritsch, and T. Maniatis, Cold Spring Harbor Laboratory Press, 1989).

Particular consideration was taken in cutting sections, in that the sections are liable to be contaminated with RNase. Sterile surgical gloves were used whilst cutting all sections for *in situ* hybridization used in this thesis. Coughing and talking were avoided as much as possible when preparing sections.

The controls that should be used for *in situ* hybridization are always controversial. Some people argued that using only the sense probe for negative controls was not sufficient. Others suggested that positive controls from readily working probes of other genes should be included for each reaction. For DIG-labelled riboprobes, because antigen-antibody reaction is applied for colour detection, some people suggested that non-antibody controls were necessary. In the present work, only hybridization with sense probe was used for negative controls. The expressing cells, however, were critically checked against: (1) those non-expressing cells in the same piece of tissue from the same batch of reaction, and (2) those negative controls hybridized with the sense probe from the same batch of reaction. Results were regarded as genuine and acceptable only if the expressing cells were specified against their neighbouring cells and against their negative controls. Furthermore, *in situ* hybridization at any developmental stage investigated in this work was performed at least twice to confirm the result as 'genuine' and 'acceptable'. The same principle for controls was also applied for wholemount *in situ* hybridization described in section 2.5.

2.4.1 Preparation of microslides for *in situ* hybridization

For *in situ* hybridization on tissue sections, slides were coated with 3-aminopropyltrimethoxy-silane (TESPA) (Sigma Cat. No. A-1435, St. Louis, U.S.A.) according to the following procedures:

1. Slides were washed with warm soapy water and briefly dipped in 100% alcohol with 2% glacial acetic acid.

2. Slides were dried at room temperature, overnight.

3. Slides were dipped in acetone with 2% TESPA for 10 - 30 seconds.

4. Slides dipped into 100% acetone for 10 seconds.

5. Slides washed in diethylpyrocarbonate (depc)-treated distilled water (see appendix) for 10 seconds.

6. Slides air-dried at room temperature, overnight. Slides were then kept in their original boxes at 4 °C until use.

2.4.2 Preparation of tissue sections for *in situ* hybridization

2.4.2.1 Direct fixation

For mouse embryos younger than day 19 p.c. and for all chick embryos used in this study, direct fixation with 4 % para-formaldehyde was performed. Following dissection, embryos or tissues were promptly washed in cold PBS and fixed in cold (4° C), freshly prepared or defrosted 4 % paraformaldehyde in 1x PBS (Phosphate Buffered Saline). The PBS was prepared in depc-treated distilled water. Fixation was done at 4°C for at least 6 hours, but for no more than one week. Tissues were then washed, alcohol-treated, cleared, embedded, and sectioned as described in section 2.3. Sections were flattened on TESPA-coated slides (see 2.4.1). Particular care was taken to prevent any possible sources of RNase contamination by wearing gloves and using depc-treated water for placing sections on TESPA-coated slides. All solutions for *in situ* hybridization were made up in depc-treated distilled water. Slides were then dried in a 37° C oven as described in section 2.3.

2.4.2.2 Cardiac perfusion and fixation for the mouse brain

For mouse embryos older than day 19 p.c., cardiac perfusion with cold 4 % paraformaldehyde in PBS was performed to make sure that the brain could be immediately accessed by the fixative. The embryos was dissected out of the uteri and the thoracic cavity was opened to expose the heart. A no. 24 - 25 needle was carefully inserted into the left ventricle of the heart. The needle was connected to a syringe of 4 % paraformaldehyde in PBS so that the solution could be easily pushed into the circulatory system of the mouse. Approximately, 1 ml of 4 % paraformaldehyde in PBS was used to perfuse per gm of the mouse body weight. The sufficiency of perfusion was monitored by making a rupture in the liver to check the outflow of the fixative. Sufficient perfusion usually ended with rigid limbs that indicated the tissues were thoroughly fixed. Embryos that were not thoroughly fixed were discarded. The mouse heads were cut off after perfusion and put in cold 4 % paraformaldehyde in PBS at 4° C overnight for further fixation. They were then briefly washed in 30 % alcohol and put into 70 % alcohol for storage. The scalp and skull were carefully removed in 70 % alcohol to obtain the intact brain. The mouse brain was then processed for embedding and sectioning as described in section 2.3.2.

2.4.3 Sources of gene clones

All gene clones used in this thesis were provided by Dr. Robert E. Hill, MRC Human Genetics Unit, Edinburgh, and have been previously published (Walther and Gruss, 1991; MacKenzie et al., 1991; Mackenzie et al., 1992; Monaghan et al., 1991). The chick *Pax6* clone was originally provided by Dr. Peter Gruss, Max-Planck-Institut for Biophysical Chemistry, Gottingen.

2.4.4 Synthesis of riboprobes

The gene clones were received as inserts in plasmid vectors. They were grown in compatible host bacteria according to the following standard plasmid preparation procedures (Sambrook *et al.*, 1989):

2.4.4.1 Transformation and growth of plasmids

1. 40 ml aliquots of LB (Luria-Bertani)medium (recipe in appendix B-1) were added to sterile culture flasks.

2. One colony of bacteria was scraped from stock plate with a sterile loop.

3. The bacteria colony was transferred to medium and shaken off the loop. The flask was then kept shaking at 37° C for 5 - 6 hours or until cells grew to an O.D. (Optical Densitity) of 0.3 to 0.5 measured at 600 nm.

4. Bacterial cells were spun down at 2500 x *g* for 5 minutes at room temperature.

5. The supernatant was discarded. The pellet of cells was gently resuspended in 2 - 4 ml of 50 mM $CaCl_2$ and topped up to 20 ml with 50 mM solution of $CaCl_2$.

6. Bacterial cells were incubated on ice for 30 minutes to make them competent, i.e. ready for introducing plasmid.

7. Bacterial cells were centrifuged for 5 minutes at 2500 x *g* at 4° C and resuspended in 4 ml of ice cold 50 mM $CaCl_2$.

8. In a sterile tube, about 0.1 ug of plasmid vector DNA was added to the prepared competent cells and the cells were reincubated on ice for a further 30 minutes.

9. Cells were heat-shocked by transferring the tube to a water bath maintained at 42° C for 2 minutes.

10. 1 ml of LB medium containing ampicillin (50 µg/ml) was added to the tube and the cells were allowed to grow for 45 minutes at 37° C with vigorous shaking (300 cycles per minute on Lab Line Rotary Environ Shaker).

11. The cells were added to 500ml or 1.0 litre of Terrific Broth medium (prewarmed to 37° C; recipe in appendix) containing ampicillin (50µg/ml) and incubated for a further 12 - 16 hours at 37° C with vigorous shaking (300 cycles per minute) in order to achieve large-scale growth of the plasmid.

2.4.4.2 Large-scale preparation of plasmid DNA

1. After the large-scale growth of plasmid described in section 2.4.4.1 was achieved, the bacterial cells were harvested by centrifugation at 4000 rpm for 15 minutes at 4° C in a Sorvall GS3 rotor.

2. The bacterial pellet was resuspended in 100 ml STE buffer (recipe in appendix B-7) and recollected by centrifugation as described in step 1.

3. The bacterial pellet was resuspended in 10 ml of Solution I (recipe in appendix B-4).

4. A freshly prepared solution of lysozyme (10mg/ml in 10 mM Tris-Cl, PH 8.0) was added.

5. 20 ml of freshly prepared Solution II (recipe in appendix B-4) was added and the centrifuge bottle was gently inverted several times to thoroughly mix the bacterial cells within the solution. The bottle was kept at room temperature for 5 -10 minutes.

6. 15 ml of ice cold Solution III (recipe in appendix B-4) was added and the bottle was shaken several times to mix the contents. The bottle was stored on ice for 10 minutes. A flocculent white precipitate should form after 10 minutes.

7. The contents was centrifuged at 4000 rpm for 15 minutes at 4 ° C in a Sorvall GS3 rotor.

8. The supernatant was filtered through four layers of cheesecloth into a 250-ml centrifuge bottle. The filtered supernatant was added with isopropanol (60% of the supernatant volume) and the two mixed well together. The bottle was then stored at room temperature for 10 minutes.

9. The contents (the nucleic acids) were recovered by centrifugation at 5000 rpm for 15 minutes at room temperature in a Sorvall GS3 rotor.

10. The supernatant was decanted carefully. The pellet on the walls and the bottom of the bottle was rinsed with 70 % ethanol at room temperature.

11. The 70% ethanol was drained off and the bottle was placed inverted on paper towels to allow the final traces of ethanol to evaporate.

12. The pellet was disolved in 3 ml of TE (10 mM Tris-Cl, 10 mM EDTA, PH 8.0).

13. 3 g of solid Cesium Chloride was added to the 3 ml DNA solution (1 g per ml).

14. Ethidium bromide solution (10mg/ml in water) was added and mixed well in the prepared DNA/CsCl solution (0.8 ml of ethidium bromide solution per 10 ml DNA/CsCl solution).

15. The solution was centrifuged at 8000 rpm for 5 minutes at room temperature. A furry scum could be found floating on the top of the solution after centrifugation. A disposable syringe fitted with a large-gauge needle was used to transfer the clear, red solution under the furry scum to a Beckman Quick seal tube suitable for centrifugation in a Beckman Optima TL Ultracentrifuge. The tubes were balanced by filling the remainder of the tubes with light paraffin oil and sealed by Quick-Seal caps.

16. The density gradient (the sealed solution) was centrifuged at 60,000 for 24 hours at 20° C. Two bands of the DNA, located in the centre of the gradient, should be visible in ordinary light. The lower band should contain the closed circular plasmid DNA to be purified.

17. The lower band of closed circular plasmid DNA was collected by first inserting a needle into the top of the tube to allow air to enter, then removing the upper band in the centre of the gradient by another needle, and finally collecting the lower band in the centre with a third needle (18 gauge).

18. To the solution of the closed circular plasmid DNA, an equal volume of isoamyl alcohol was added. The two phases of the solution were mixed thoroughly by vortexing.

19. The mixture was centrifuged at 1500 rpm for 3 minutes at room temperature in an Eppendorf microcentrifuge.

20. The lower, aqueous phase was transferred to another clean tube. Another equal volume of isoamyl alcohol was added. The extraction (steps 18 - 20) was repeated 4 - 6 times until all the pink colour of the ethidium bromide disappeared from both the aqueous phase and the organic phase.

21. CsCl was removed by dialysis for 24 - 48 hours against several changes of TE (PH 8.0).

22. The OD_{260} of the final solution was measured and the concentration of the plasmid DNA was calculated. The plasmid DNA was stored in - 20° C in aliquots at a concentration of 1μg per μl.

2.4.4.3 Confirmation of prepared plasmids

The prepared plasmids were run on a 1.2 % agarose minigel (90 volts for 60 minutes in 1 x TAE buffer), together with the original plasmid DNA. Those prepared plasmids of the same running distance were heated in 92° C for 3 minutes and immediately dot-blotted on a Gene Screen Hybridization transfer membrane (Biotechnology System, Boston, cat. no. NEF-983). The membrane was then placed in oven for 2 hours at 80° C to bake DNA onto it and probed for confirmation with DIG-labelled RNA synthesized from the original gene clone according to standard procedures (Sambrook et al., 1989). The following procedures were taken through for probing:

1. The membrane (with plasmid DNA baked on it) was prehybridized with *in situ* hybridization mix for sections (recipe detailed in the appendix B-12). The membrane and the prehybridization mix solution were placed in a PVC transparent bag which was sealed with as few air bubbles as possible. The preparation was put in a 65° C water bath for at least 3 hours.

2. DIG-labelled RNA was added at 500 ng per ml in the prehybridization mix to hybridize at 55° C for at least 6 hours in a water bath.

3. After hybridization, the membrane was washed twice with 4x SSC in 50 % formamide at 65° C in a water bath for a total of 2 hours. The washes were done in a 50 ml Falcon tube with washing solutions covering the whole membrane.

4. The membrane and the washing solution was allowed to cool down to room temperature.

5. The washing solution was replaced twice by roughly the same volume of maleic acid buffer (0.1 M maleic acid, 0.15 M NaCl; pH 7.5). The membrane was in maleic acid buffer for 10 minutes each for a total of 20 minutes at room temperature.

6. The membrane was blocked by 1x blocking reagent (Boehringer-Mannheim, cat. no. 1096 176) for 10 minutes at room temperature.

7. The 1x blocking reagent was replaced by colour detection buffer (0.1 M Tris-HCl, 0.1 M NaCl, 50 mM $MgCl_2$; pH 9.5) with 9 µl NBT (Nitroblue Tetrazolium) solution (Boehringer Mannheim, cat. no. 1383 213) and 7 µl X-phosphate (Boehringer Mannheim, cat. no. 1383 221) in per ml of colour detection buffer.

8. Colour detection was carried out in the dark at room temperature for 15 - 30 minutes.

9. The presence of correctly prepared plasmids was judged by the appearance of black dots on the membrane against the background.

2.4.4.4 Linearization of plasmids

Once the purified plasmids were confirmed, plasmids were linearized with restriction enzymes cutting at specific restriction sites according to supplier's recommendation (see table 2.1) by the following procedures:

1. 10 μg of prepared plasmid DNA was removed from stock tubes to another Eppendorf tube. The tubes were put on ice before incubation at 37° C.

2. 2 μl of 10x reaction buffer for specific restriction enzyme (see table 2.1 on the following page) was added.

3. Specific restriction enzymes (see table 2.1 for details on the following page) were added to the tubes. The restriction enzymes were made at concentrations of 20 - 40 units in each linearization reaction.

4. The total reaction volume was topped up to 20 μl with distilled water and the solution mixed well.

5. After a short spin in an Eppendorf centrifuge, the tubes were incubated at 37° C for 60 - 90 minutes, except for Ptz 19 plasmid for *Msx 2* which was cut by BSS H II at 50° C for 90 - 120 minutes.

iboprobes to : synthesized	*plasmid name*	*Restriction enzymes*	*Buffer*	*Cutting sites*	*Reaction temperature (° C)*	*Reaction time*
ax6(mouse), nse	psm	Eco RI	H	G↓AATTC	37	1.5 hours
ax6(mouse), ntisense	psm	Bam HI	B	G↓GATCC	37	1.5 hours
ax6(chick), nse	pCh6	Eco RI	H	G↓AATTC	37	1.5 hours
ax6(chick), ntisense	pCh6	Bam HI	B	G↓GATCC	37	1.5 hours
'sx1(mouse), ntisense	ptz 19	Bss HII	A	G↓CGCGC	50	2.0 hours
'sx2(mouse), nse	ptz 18	Eco RI	H	G↓AATTC	37	1.5 hours
'sx2(mouse), ntisense	ptz 18	Bam HI	B	G↓GATCC	37	1.5 hours

Table 2.1 Linearilization of plasmids. The buffers used were SuRE/cut Buffers supplied by Boehringer Mannheim. All linearilizations were checked by running 1.5 - 2.0 % agarose gels stained with ethidium bromide and viewed under UV transillumination. Complete cuts were confirmed by the presence of single retarded bands as compared to those intact plasmids. For each restriction enzyme, the recognized sequence and the cutting site are listed. The arrows indicate the points where the phosphodiester linkages between two nucleotides were splitted.

2.4.4.5 Checking the linearization of plasmids

The linearised plasmids were run on 1.2 % agarose minigels (at 90 volts for 60 minutes) in 1x TAE buffer (Tris-acetate buffer; see appendix for recipe) against uncut circular plasmids to check the efficiency of cutting. Complete cuts were confirmed by single retarded bands. Those incomplete cuts displayed one retarded band with another band at the same running distance as that of the uncut controls. If incomplete cuts were found, more units of the same restriction enzymes were added to the reactions which were then reincubated for another 60 minutes. After that, the reincubated reactions were run on another 1.2 % agarose gel for a recheck. Only those complete cuts were used for the synthesis of riboprobes.

2.4.4.6 Synthesis of non-radioactive Digoxigenin-labelled riboprobes

Digoxigenin-labelled *in situ* probes were transcribed *in vitro* from those linearized plasmids using RNA labelling kit from Boehringer-Mannheim according to the manufacturer's protocol:

The following reagents were added to an Eppendorf tube:

depc -treated H_2O	13.5 µl
10x transcription buffer	2 µl
10x DIG RNA labelling mixture (Boehringer-Mannheim, cat. no. 1277 073)	2 µl
RNase inhibitor (40 units per µl) (Boehringer-Mannheim, cat. no. 799 017)	1 µl
linearized plasmid (0.5 -1.0 µg per µl)	1 µl

20 units of T_3 (Boehringer-Mannheim, cat. no. 1031 163) or T_7 (Boehringer-Mannheim, cat. no. 881 767) RNA polymerase was added to make a total reaction volume of 20 ul. The T_3 RNA polymerase was used for sense riboprobe synthesis and T_7 for anti-sense riboprobe synthesis.

All the reagents were mixed well, spun down briefly (15 seconds at 6000 rpm) in an Eppendorf microcentrifudge before incubation. The mixtures were incubated in 37°C for 1.5 hours. After incubation, 1µl (20 units per µl) of DNase I (Boehringer-Mannheim, cat. no. 104 132) was added for a further 10 minutes incubation. The RNA was then precipitated by adding 2.5 µl of 4 M Lithium Chloride and 75 µl of cold 100% ethanol. This was mixed well and kept in - 70°C for at least 2 hours. The precipitated synthesized DIG-labelled RNA probes were recovered by spinning again at 4° C, at 12000 rpm for 10 minutes. Normally, a small white pellet could be seen at the bottom of the Eppendorf tube. The supernatant was pipetted out. The pellet was then washed twice by pipetting in 75 µl of cold 75% ethanol and gentlly rolling the ethanol around the pellet. Pellets were dried in a vacuum chamber and diluted to a concentration around 100 ng/µl in depc-treated water.

2.4.4.7 Calibration and storage of synthesized riboprobes

The concentrations of synthesized riboprobes were calibrated by running, at serial dilutions, against standard RNAs with known concentrations provided by Boehringer-Mannheim on 1.2 % agarose gels (at 90 volts for 60 minutes in 1x TAE buffer) as described in section 2.4.4.1. The expected yield of synthesized riboprobes was 10 µg of labelled RNA out of 1 µg of the linearized DNA in each reaction. The synthesized riboprobes were then stored in a - 70° C freezer and thawed only immediately before use.

2.4.5 Prehybridization treatment

Fully-dried wax sections on microslides were placed back to back in a slide rack. A maximum of 20 slides were used at each run. The slides were taken through the following procedures:

1. Xylene I	10 minutes
2. Xylene II	10 minutes
3. Alcohols 100 % - 100% -95 % -85%- 70%-50%-30%	1 minute each
4. 2x SSPE (recipe in appendix)	5 minutes
5. Proteinase K (20 µg/ml in buffer)	5 minutes
6. 2x SSPE	30 seconds or a brief rinse
7. 4% cold paraformaldehyde in PBS at room temperature	15 minutes
8. 2x SSPE	5 minutes
9. 0.2 M HCl	15 minutes
10. 2x SSPE	5 minutes

11. Slides placed in 450 mls of 0.1 M TEA (Triethanolamine, Sigma cat. no. T-1377). While stirring, 3 ml of acetic anhydride was added slowly drop by drop for a total of 10 minutes.

12. Soaked in 2x SSPE for at least 5 minutes or until ready for hybridization.

2.4.6 Hybridization

Synthesized probes were thawed immediately before use. Probes were diluted at a concentration of approximately 100 ng in every 60 µl hybridization mix (recipe in appendix) in an Eppendorf tube. The hybridization mix, together with the added probes, were preheated at 80°C for 5 minutes in a multi-well metal heating block (MacKay-and-Lyn, Edinburgh). They were then quenched on ice for 3 minutes, spun briefly (3000 rpm in an Eppendorf microcentrifudge) and added to slides.

The slides were sitting in 2x SSPE as described in section 2.4.4. They were removed from 2x SSPE (using a pair of sterile forceps to avoid any source of RNase contamination) and placed onto a piece of clean paper towel. The slides were air-dried on the clean paper towel before adding probes. Hybridization mix (with probes added) was carefully spread on each slide, avoiding air bubbles. 60 µl of hybridization mix, i.e. at least 100 ng of probe was used for each slide. Slides were covered with coverslips (BDH no. 1, 22mm x 64 mm) straight out of box, ensuring all tissue sections covered with hybridization mix. Slides were then incubated at 50°C in a humidified chamber (humidified with 50% formamide in 1x salts solution) (see recipe in appendix) for overnight (or at least 7 hours).

2.4.7 Post-hybridization washes

After overnight incubation, slides were removed from the humidified chamber and placed back to back in a slide rack. Coverslips were removed from the slides by soaking in 2x SSC (Standard Saline Citrate; recipe in appendix B-8) at 50°C for at least 10 minutes. The slides were then taken through the following washes:

1. 2x SSC in 50% fromamide at 65°C	45 minutes
2. 4x SSPE at 50°C	5-8 minutes
3. Quickly rinsed in 4x SSPE at 50°C	30 seconds
4. 20 ug/ml RNase A in 4x SSPE in H2O	25 - 30 minutes
5. 50% formamide in 2x SSC at 65°C	45 minutes

6. Slides were then transferred to a 50° C, 2x SSC solution and let cool down in room temperature.

2.4.8 Binding anti-DIG-alkaline phosphatase conjugates to sections and colour detection

Before use, the anti-DIG-alkaline phosphatase conjugates were preabsorbed against chick serum to avoid any non-specific binding. Antibody conjugates were preabsorbed by adding at 1 in 5000 dilution in 1% blocking buffer (Boehringer-Mannheim, Catalogue no. 1096 176) in PBT with 2% chick serum. The preabsorption was carried out at 4°C overnight or at room temperature for at least 4 hours.

The slides were transferred from the 2x SSC solution and placed back-to-back in a glass container. This was to reduce the necessary volume of solutions and antibody to be used. The slides were taken through the following procedures:

1.Washed in PBT at room temperature	10 minutes
2. Soaked in 1 % blocking buffer in PBT	30 minutes
3. Incubated in preabsorbed antibody solution	over night, at 4° C
4. Slides were separated and washed in PBT with stirring	3X 20 minutes, at room temperature
5. Incubated in freshly prepared alkaline phosphatase buffer (alkaline phosphatase buffer also known as NTMT buffer)	5 minutes, at room temperature
6. Incubated in colour detection buffer at room temperature in dark	overnight

2.4.9 Mounting coverslips and photography

Slides were examined for positive blue/purple staining on the tissue sections after overnight incubation in the colour detection buffer. If colours were not satisfactory, slides were incubated again at room temperature for further 6 - 8 hours in the dark. Slides were then taken through the following procedures:

1. Incubated in 10 mM Tris-HCl (pH = 7.8), 10 mM EDTA at room temperature	5 minutes
2. Incubated in 1% pyronine B in water	10 minutes
3. 70 % alcohol	10 seconds
4. 90 % alcohol	10 seconds

5. 96 % alcohol	10 seconds
6. 100 % alcohol	10 seconds
7. 100 % alcohol	10 seconds
8. Xylene I	1 minutes
9. Xylene II	1 minutes

Coverslips were mounted with DPX. Slides were examined and photographed on a Wild Photo Makroscope M420 (Wild Heerbrugg, Switzerland). Kodak Gold 100 films were used for photography. Films were developed and printed by a commercial service.

2.4.10 Number of embryos used for *in situ* hybridization on tissue sections

Mouse embryos at gestation days from 10.0 to 19.0 and 1.0, 7.0, 20.0 postnatally were examined for *Pax6* expression in the head region (chapter 3). The number of embryos used at each gestation age is listed in table 2.2 on the following page. For *Msx1* and *Msx2* expression in the mouse maxillary process (chapter 5), the numbers of the homozygous *Small eye* embryos and their wildtype littermates at each gestation age are listed in table 2.3 on the following page. Chick embryos at some developmental stages (chapter 3) were also sectioned for studying *Pax6* expression (see table 2.4 on page 108). This study also investigated chick *Pax6* expression by *in situ* hybridization following tissue culture on millipore membranes (chapter 4). The number of tissues used is listed in table 2.5 in section 2.7.4.

age	9.5	10.0	11.0	12.0	13.0	14.0	15.0	16.0	17.0	18.0	19.0	P1.0	P7.0	P20
no.	4	4	3	3	3	2	3	3	4	4	2	4	4	3

Table 2.2 Mouse embryos used for studying *Pax6* expression in the head region. The numbers in the top row indicate days p.c., except for P1.0, P7.0, and P20 which indicate days after birth. Both transverse and coronal sections were used for the convenience of comparing with published atlases. Thus, expression at gestation days 9.5, 10, 11, and 12 p.c. were represented by coronal sections. Transverse sections were used for gestation days 13, 14, 15 p.c.. From day 16.0 p.c. onwards up to 21 days after birth, coronal sections were used. All embryonic sections were *in situ* hybridized with antisense DIG-labelled *Pax6* probe together with a number of controls hybridized with sense DIG-labelled probe at the same time. All sections were at 7.0 μm in thickness.

		D13	D14	D15	D16	D17
Msx1	+/+	4	5	4	4	4
Msx1	Sey/ Sey	4	4	5	4	5
Msx2	+/+	4	4	6	4	6
Msx2	Sey/ Sey	4	5	4	5	6

Table 2.3 Mouse embryos used for comparing *Msx-1* and *Msx-2* expression in the maxillary process between wildtypes and *Small eye* homozygotes. Transverse sections were *in situ* hybridized with antisense DIG-labelled *Msx-1* and *Msx-2* probes together with a number of controls hybridized with sense DIG-labelled probe at the same time. All sections were at 7.0 μm in thickness

stage	10	11	12	13	16	17	18	28
no.	3	4	4	6	5	3	3	2

Table 2.4 Number of chick embryos used for studying *Pax6* expression via *in situ* hybridization on tissue sections in the head region. The stages were judged according to Hamberger and Hamilton (1951). The number of chick embryos used for studying *Pax6* expression through wholemount *in situ* hybridization are listed in table 2.5 (in section 2.5.5).

2.5 *In situ* hybridization for wholemount embryos

2.5.0 General consideration

General consideration for avoiding RNase contamination, reducing non-specific background signals, and the optimization for hybridization conditions were the same as mentioned in section 2.4.0.

Particular considerations for wholemount *in situ* hybridizations were: (1) Proteinase K treatment was optimized according to the size of embryos. For chick embryos at stages 6 - 10, 7 minutes in proteinase K was sufficient. Overdigestion by proteinase K was not necessary and often caused damage to the embryos. (2) The duration and times of washing were increased. Wholemount embryos could easily trap non-hybridized riboprobes or non-binding antibodies in tissues, particularly in the closed neural tube. The duration and times of washing after hybridization and antibody binding were increased, if non-specific background signals were found to be too strong. (3) Wholemount embryos were very fragile after bleaching and proteinase K treatment. This was improved, to some extent, by increasing the refixation period from 20 minutes to 40 minutes. The washes and hybridization procedures were therefore performed with great care to avoid damage to the embryos.

2.5.1 Preparation of embryos for wholemount *in situ* hybridization

Embryos were dissected as quickly as possible in cold (preferably in 4°C) 1x PBS. They were quickly rinsed 2 - 3 times in fresh cold 1x PBS to get rid of blood and other unwanted membranes. For chick embryos at early developmental stages, 3 - 5 embryos were put in a 2.0 ml microtube (Sarstedt, Germany, catalogue no 72.694/026). No more than 3 tubes were run for wholemount *in situ* hybridization at the same time. Embryos were taken through the following procedures on a spiramix (Denley, U.K.):

1. Fixed in cold 4% paraformaldehyde at 4°C	4 hours to overnight
2. Washed in PBT at 4°C	5 minutes, twice
3. Washed in 25% -50%-75%-100% methanol in PBT at room temperature	5 minutes each
4. Rehydrated with 75%-50%-25%-0% methanol in PBT at room temperature	5 minutes each
5. Bleached with 6% hydrogen peroxide in PBT at room temperature	40-60 minutes

6. Washed in PBT three times — 5 minutes each

7. Treated with 10 ug/ml proteinase K (Sigma) in PBT at room temperature — 7 - 15 minutes

8 Washed with fresh 2 mg/ml glycine (Sigma, catalogue no. G-7126) in PBT at room temperature — 5 minutes

9. Washed twice with PBT at room temperature — 5 minutes each

10. Refixed with freshly- prepared 0.2 % glutaraldehyde with 4% paraformaldehyde in PBS, at room temperature — 20 - 40 minutes

11. Washed with PBT twice at room temperature — 5 minutes each

12. 1.0 ml of prehybridization mix (recipe in apppendix) was added to each tube. The solutions in the tube were gentlly, but thoroughly mixed manually.

13 Embryos were transferred to another 2 ml microtube containing 1 ml of prehybridization mix

14. Replaced with fresh 1 ml prehybridization mix, and incubated at 65°C in a water bath — at least 3 hours

2.5.2 Hybridization

After the embryos were pre-hybridized for at least 3 hours at 65° C. The pre-hybridization mix was drained off and replaced by fresh 1.0 ml (or at a volume to make sure embryos were completely covered) prehybridization mix. Around 0.2 - 1 μg DIG-labelled RNA probe was added in per ml of the replaced pre-hybridization mix. The tubes were then incubated at 55°C overnight.

2.5.3 Post-hybridization washes and antibody binding

All the procedures described in this section were performed in a same 2.0 ml microtube as used for section 2.5.2. All washes were performed on a spiramix (Denley, U.K.) at its pre-designed speed at room temperature, except for the washes in 37° C and 55° C which were performed in a waterbath (Grant, England). Wholemount embryos were taken through the following procedures:

1. Washed with 100%-75%-50%-25% prehybridization mix in 2x SSC at 55°C — 5 minutes each

2. Washed twice with 0.1% CHAPS (3-[(3-cholamidopropyl)dimethylammonio]-1-propanesulfonate) (Sigma, cat. no. C-3023) in 2x SSC at 55° C for 30 minutes.

3. Treated with 20 ug/ml RNase A (Sigma, cat no R-9009) in 2x SSC, with 0.1 % CHAPS at 37°C — 30 minutes

4. Washed twice in 2x SSC with 0.1% CHAPS at room temperature — 10 minutes each

5. Washed twice with 0.2 x SSC with 0.1% CHAPS at 55°C — 30 minutes each

6. Washed twice with PBS at room temperature — 10 minutes each

7. Washed with PBT at room temperature — 5 minutes

8. Embryos were pre-blocked by incubating in 10% sheep serum, 1% BSA (Bovine Serum Albumin; Sigma cat. no. A-9647) in PBT for at least 2-3 hours at room temperature

9. Whilst embryos were pre-blocked, anti-DIG antibody was pre-absorbed at 1 in 2000 dilution in PBT with 10% sheep serum, 1 % embryo powder, and 1% BSA at room temperature for 2 - 3 hours. After preabsorption, the antibody solution was briefly spun down to get rid of coarse debris of embryo powder (see appendix for preparation).

10.The pre-blocking solution was replaced with the pre-absorbed antibody solution and kept in 4° C overnight on a spiramix.

2.5.4 Post-antibody washes, colour detection, and photography

All the washes were performed on the same spiramix described in section 2.5.3. Embryos were taken through the following washes:

1. Washed 5 times in PBT with 0.1 % BSA, at room temperature	1 hour each
2. Washed with PBT at room temperature	30 minutes
3. Washed with NTMT (recipe in appendix) at room temperature	3 x 10 minutes
4. Incubated in colour detection buffer (recipe in appendix). (Kept at room temperature in dark.)	20 minutes

5. When colours were developed to the desired extent, the embryos were washed with NTMT at room temperature for 5 minutes. If colours were not satisfactory, embryos were kept in the colour detection buffer for 6-12 hours longer or until colours were considered appropriate.

6. Washed in PBT at room temperature	5 minutes
7. Fixed with 4% paraformaldehyde in PBS at 4°C	overnight

8. Photographed on a Wild Heerbrugg Photo Makroscope with Kodak Gold 100 films. The films were developed and printed comercially.

2.5.5 Embryos used for wholemount *in situ* hybridization

Only chick embryos were used for wholemount *in situ* hybridization. The numbers of embryos used for each stage investigated are listed in table 2.5.

stage	4	6	8	9	10	11	12	28
no.	4	7	10	12	12	10	6	2

Table 2.5 The number of chick embryos used for each stage investigated by wholemount *in situ* hybridization for *Pax6* expression.

2.6 Immunohistochemistry

2.6.1 Preparation of microslides for immunohistochemistry

TESPA-coated slides were used for immunohistochemistry. The same procedures as described in section 2.4.1 was taken for preparing TESPA-coated slides.

2.6.2 Preparation of tissues for immunohistochemistry

Tissues were prepared and sectioned in the same way as described in section 2.3. For tissues to be stained by immunohistochemistry after millipore culture, they were taken through, together with the millipore membranes, all the procedures described in section 2.3 and section 2.7.3.

2.6.3 Source of antibody

Chick anti-alpha B crystallin antibody was generously provided by Dr Paul Scotting, Department of Biochemistry, University of Nottingham.

2.6.4 Antibody binding and colour detection

Tissue sections were prepared following the same procedures for *in situ* hybridization. All washes described in this section were performed by gently pouring solutions over slides and sitting slides in a humidified chamber for a period of time as required.

Wax-embedded tissue sections were fully-dried in a 37°C oven and taken through the following procedures:

1. Sections dewaxed and rehydrated as described in section 2.3.

2. Incubated twice in PBS or TBS (Tris-Buffered-Saline, recipe in appendix) for 5 minutes each.

3. Incubated in 10% fetal calf serum (FCS) diluted in PBS or TBS for 10 minutes.

4. The 10 % FCS was drained off and any excess wiped off with a paper towel

5. Incubated in primary antibody (anti-alpha B crystallin) at 1 in 3000 dilution for 60 minutes at room temperature.

6. Primary antibody was washed off and sections given two PBS or TBS washes, for 5 minutes each.

7. Incubated in 10% FCS in PBS or TBS for 10 minutes.

8. The 10 % FCS was drained off and any excess was wiped off with a paper towel

9. Sections were incubated in biotinylated second antibody (anti-rabbit IgG 1:400 dilution) (Vector, cat no. C1-1000) at room temperature for 30 minutes.

10. The biotinylated second antibody was washed off and sections were washed twice in TBS for 5 minutes each.

11. Excess buffer was wiped off and sections were incubated in ABC complex (details in appendix) at room temperature for 30 minutes.

12. The ABC complex was washed off twice in TBS for 5 minutes each.

13. Colour was developed with freshly-made Vector Red mix (details in appendix) for up to 20 minutes at room temperature.

14. Sections were washed in running tap water.

15. Counterstained in 1% methyl green for 30-60 seconds.

16. Washed in tap water and dehydrated in 75%-90%-96%-100% alcohols.

17. Sections were cleared in xylene, mounted in DPX, viewed and photographed as described in section 2.3.

2.6.5 Number of tissues used for immunohistochemistry

The number of tissues used is listed in tables 4.1 and 4.2 in sections 4.2.2.2 - 4.2.2.3.

2.7 Chick tissue grafting and culture on millipore membranes

2.7.0 General consideration

All procedures described in section 2.7 were performed under laminar flow in a tissue culture room to avoid microbial contamination. Tissues were cultured with underlying mesenchyme and placed directly on millipore membranes (Whatman, cat. no. B431GN, pore size 0.45μm, 25 mm diameter) without trypsin treatment.

2.7.1 Grafting of tissues and isolation of ectodermal fragments

1. Whole chick embryos were incubated until suitable stages and were removed from eggs as described in section 2.2. They were then washed in PBS or medium 199 (Gibco BRL, Scotland, cat. no. 31153-018) containing 1% penicillin G (Sigma, cat. no. p3032) and 1% streptomycin (Sigma, cat. no. s-9137).

2. Pre-designated areas of tissues (see figure 4.7) were cut and isolated using a sharp Tungsten needle. The isolated tissues were then washed in medium 199 containing the same antibiotics.

3. The ectodermal layers were incubated for recovery in medium 199 with antibiotics for thirty minutes to two hours in a 37°C incubator (Vindon Scientific Ltd.) with 5% CO_2 in air and with saturated humidity.

2.7.2 Millipore culture of isolated tissues fragments

1. While the tissues were being recovered, a Falcon organ culture dish (60 x 15 mm style with centre well, cat. no. 3037) was prepared by adding M199 with antibiotics in the centre well.

2. A pore size 0.45μm millipore membrane (Whatman, cat no. B431 GN) was placed over the prepared medium in the centre well. The membrane was completely wet with medium underneath. The preparation was then placed in an incubator for optimizing the humidity and CO_2 concentration.

3. The recovered tissues were removed with a sterile pipette from the dishes and placed on the prepared millipore membranes.

4. The organ culture dishes were immediately put back into a 37° C incubator with saturated humidity and 5 % CO_2 in air.

5. Used medium was replaced by freshly balanced medium every day for 4 - 6 days.

2.7.3 Fixation and sectioning after culture

1. Tissues together with millipore membranes were removed from the culture medium and quickly washed in cold PBS.

2. Immediately after wash, tissues were fixed in cold 4% paraformaldehyde in PBS in a glass dish for at least 4-6 hours or overnight at 4 ° C.

3. After fixation, tissues with their underlying millipore membranes were dehydrated through 30%-50%-70%-90%-96%-100%-100% alcohols and finally cleared with xylene in the same way as described in section 2.3.

4. Tissues were processed with their attached millipore membranes through embedding, sectioning, developing on TESPA slides, *in situ* hybridization, and immunohistochemistry as described in previous sections.

2.7.4 Number of tissues grafted for millipore membrane culture, immunohistochemistry, and *in situ* hybridization

The number of tissues grafted for millipore membrane culture is listed together with the results of *in situ* hybridization and immunohistochemistry in table 4.1 and table 4.2 in sections 4.2.2.2. - 4.2.2.3.

2.8 Retinoic acid (RA) treatment on the developing chick embryos

2.8.0 General consideration

Retinoic acid is light-sensitive. It was therefore prepared and stored in a way to minimize light exposure by wrapping all containers with foil. Six concentrations of RA were used to treat chick embryos in six groups. The concentrations of RA and the number of chick embryos used in this study are listed together with the results in table 6.1.

2.8.1 RA treatment on the developing wholemount chick embryos

2.8.1.1 Preparation of wholemount chick embryo culture

1. A large glass dish was filled with autoclaved Pannet-Compton saline (New, 1955) with 0.1 % penicillin (Sigma, cat. no. p3032) and 0.1 % streptomycin (Sigma, cat. no. s-9137).

2. An incubated egg was opened at the blunt end at the desired stage of development. The thinner, water-like albumen (the liquid egg white) was collected in a small beaker for later use.

3. The other eggs at desired stages of development were windowed as described in section 2.2.2. The eggs were then drained of their albumen by tilting and sucking of the excess fluid with pipettes. Each egg yolk, together with the embryo, was carefully placed into the prepared Pannet-Compton saline in the large glass dish. While placing egg yolks, care was taken not to damage the vitelline membrane on the edge of the windowed egg shells. Each blastoderm, under the vitelline membrane, was kept facing upwards. If the blastoderm was facing downwards, the yolk was gently turned upside-down with a pair of blunt forceps.

4. A cut was made with scissors into the vitelline membrane enclosing the yolk just below its equator. Cutting was performed all the way around the circumference of the yolk.

5. With two pairs of fine forceps, the vitelline membrane, together with the early embryo, was carefully and completely peeled off from the yolk. The early embryo was kept facing upwards, with its dorsal side facing the bottom of the dish.

6. A sterile watch glass (25 mm in diameter) was placed in the saline. The embryo was removed with a pair of forceps to the centre of the watch glass. The dorsal side of the embryo was kept facing the bottom of the watch glass. After the embryo was removed and placed in the centre of the watch glass, a plastic ring (10 mm in diameter) was put over the embryo.

7. With fine forceps, the cut edges of the vitelline membrane was carefully folded over the edge of the ring, all the way around its circumference.

8. The whole preparation was removed carefully from the dish and out of the saline. The remaining saline inside and outside the plastic ring was removed as much as possible with a Pasteur pipette. Any remaining yolk around or over the embryo was washed off with Pannet-Compton saline.

2.8.1.2 Treatment with retinoic acid

1. Stock retinoic acid in DMSO (3mg/ml) was thawed from - 20° C to room temperature. Light exposure was avoided whenever possible.

2. Pannet-Compton saline with 10 % thinner egg albumen collected in step 2 was prepared by mixing them thoroughly (egg albumen to saline as 1: 9).

3. The already thawed stock retinoic acid solution was diluted to final desired concentrations (see table 2.6). The DMSO used for desolving retinoic acid was kept under 1% of the total volume. After the retinoic acid was added, the solution was wrapped in foil and gentlly mixed for 5 minutes.

4. A sterilized Pasteur pippet was used to slowly apply 10 drops of RA-added saline to each embryo.

5. Embryos were reincubated at 38° C in an atmosphere of 100 % humidity and allowed to develop until suitable stages for further analysis.

Chapter 3: *Pax6* expression during mouse embryogenesis

3.1 Introduction

3.1.1 Aims of this chapter

In this chapter, I have examined in detail the expression of *Pax6* in the mouse with the following aims: (1) to determine whether mouse *Pax6* is expressed along the pathways and in higher centres of the visual and the olfactory nervous system, (2) to compare areas of mouse *Pax6* expression with those of nerve fiber projection in the brain, (3) to investigate in detail mouse *Pax6* expression in areas that have not been reported before and to establish my own baseline data for further experiments. The rationale for the aims, except for aim (3) which is obvious, is to be described below (in sections 3.1.2 to 3.1.3). In the discussion, in addition to the aims, I will cover the implications of other *Pax6* functions as suggested by expression data and mutant phenotypes. Extensive comparisons of *Pax6* expression and mutant phenotypes across species will also be included in the discussion. The rationale for comparing across species is described in section 3.1.4. Experiments using *in situ* hybridization on both wholemount embryos and embryonic tissue sections were performed to obtain mouse *Pax6* expression data. Linder's silver impregnation method was used together with Luxol fast blue stain to detect areas of nerve fiber projection in the mouse brain.

3.1.2 Rationale for determining *Pax6* expression in the visual and olfactory nervous system

Pax6 is obviously involved in the normal development of the visual and the olfactory system in the mouse, based on the abnormal phenotypes and gene expression data that are described in chapter 1. This raises some immediate questions: Is the function of *Pax6* in the brain specifically involved in the integration of the visual and the olfactory pathways ? Can anything for *Pax6* function in relation to the eye and the nose be specified in the brain ? If *Pax6* is not exclusively engaged in the two systems, what are the other systems that *Pax6* is involved ?

Two initial approaches may be taken to support a role of *Pax6* in the integration of the visual and the olfactory systems. The first is to investigate *Pax6* expression in detail in the pathways and the axon relay centres of the two systems. During the course of this study, *Pax6* expression in the mouse has been extensively reported (Walther and Gruss, 1991; Stoykova and Gruss, 1994; Grindley *et al.*,1995; Quinn *et al.*,1996; Stoykova *et al.*,1996) but lack in determining the correlation of *Pax6* expression with the integration of the two systems. The second approach is to determine whether abnormalities can be found specifically within the two nervous systems in the homozygous and the heterozygous *Small eye* mutant mice. This approach, again, has not been taken so far. Aim (1) of this chapter is to take the first approach to investigate *Pax6* expression along the pathways and axon relay centres of the visual and olfactory nervous systems.

3.1.3 Rationale for comparing areas of *Pax6* expression with those of nerve fiber projection

Pax6 expression in the developing mouse brain is extensively investigated in this chapter. The sites of expression, including some nominated neuronal nuclei, are specified. The fact that *Pax6* transcripts are located in specified sites raises at least one question: Why is *Pax6* exclusively expressed in the specified sites (in other words, what is *Pax6* function in those sites) ? This question demands knowledge of distinctive activities that are only carried out in the *Pax6*-expressing areas in contrast to those non-expressing areas; thus it leads to a search for suitable techniques for a primitive demonstration of possible distinctive activities.

Neuronal migration sets up the foundation for connection and pathfinding, i.e. the process of nerve fiber projection (see chapter 1). Defects of neuronal migration was suggested in the Sey^{neu} mutants (Schmahl *et al.*, 1993). Furthermore, cerebellar primordium from mice homozygous for *Small eye* mutation, when cultured *in vitro*, fails to develop neuronal projections, while their wildtype controls exhibit extensive projections with abundant Pax6 proteins detected by immunohistochemistry (van Heningen, personal communication). Pax6 protein is also demonstrated as a binding protein for three different sites in the promotor region of the *L1* gene (Chalepakis *et al.*, 1994). *L1* encodes a cell surface glycoprotein that regulates vertebrate neuronal process outgrowth (Fisher *et* al., 1986; Trisler, 1991; Kadmon and Altevogt, 1997). One wonders whether *Pax6* is involved in neuronal projection that can not be found in other non-expression areas at the same gestation age ? Linder's silver impregnation (Linder, 1978) was described as an optimized method for the impregnation of myelinated as well as non-myelinated fibers, intradentina fibers, and various types of nerve end organs such as a motor end plate. Thus, the activities of nerve fibre projection can be shown. In conjunction with Luxol fast blue that gave a sensitive blue stain for myelinated nerves, Linder's method was suitable for the purpose and was therefore used.

3.1.4 Rationale for comparing expression data and mutant phenotypes across species

Mouse *Pax6* expression data obtained in this chapter will be used to compare with the published information in the same species as well as those in different species. Expression data will also be used to compare mutant phenotypes across species. These comparisons aim to shed new insights on the functions of *Pax6* for several obvious reasons: (1) The fact that a gene consistently expresses in specific areas of embryos through evolution implies a major function of that gene within those areas. (2) The existence of areas that exhibit abnormalities in mutated animals without expression of the normal gene in the wildtypes reflects an indirect role of that mutated gene in causing the abnormalities. (3) If a gene is extensively expressed in a specific area through evolution but without causing abnormalities when mutated, the possibility is that the function of that gene can be compensated by other genes. (4) The areas of expression for a gene may be expanded or reduced through evolution;

thus functional change or conservation of the same gene may be indicated by checking changes of expression areas.

Pax6, being a member of the *Pax* gene family, carries two conserved motifs --- the paired domain and the paired-specific homeodomain (details in chapter 1). The structural conservation in the DNA sequence among *Pax6* orthologues (*Pax6s* in different species) through evolution has been extrapolated to assume that the functions of *Pax6* have been conserved through evolution. However, only in some organs of a certain species experimental evidences are given (for examples, see Quiring *et al.*, 1994; Chisholm and Horvitz, 1995; Zhang and Emmons, 1995). There is still no general picture across all species on *Pax6* expression and mutant phenotypes being laid out and compared. In light of the above mentioned reasons, comparisons will be made in the discussion sections in this chapter.

3.2 Results

3.2.1 *Pax6* expression during mouse embryogenesis

Section 3.2.1 presents the results of mouse *Pax6* expression produced by *in situ* hybridization on tissue sections from day 9.5 p.c. up to 21 days after birth. The results are shown in figures 3.1 - 3.10 following the main text at the end of this chapter. Numeric labelling is used in the figures and all the keys are listed together to avoid repetition. My concentration here is on the mouse head, although *Pax6* expression may be found in the other regions.

To describe in a systematic way, the distribution of *Pax6* transcripts on transverse sections are presented from top of the head and serially downward to the cervical spinal cord. For coronal sections, expression is presented from the anterior to the posterior following the order of telencephalon, diencephalon, mesencephalon, rhombencephalon and spinal cord. After the spinal cord, *Pax6* expression in the eye and other areas are described. All the corresponding figures are presented in the same order.

To describe the sites of *Pax6* expression in the brain, many names of differentiation fields and specified neural nuclei have to be used. Differentiation fields are more roughly defined than neural nuclei. Therefore, terms of differentiation fields can be used with much more confidence than those of neural nuclei. However, when many terms of differentiation fields are used, much precision will be lost in the description. Thus, readers are reminded that using terms of specific nuclei does not mean that *Pax6* transcripts are present exactly in the three-dimensional structures of the specified sites. For example, *Pax6* transcripts may just occupy 1/5 space of a nucleus, or they may cover up a whole nucleus and their coverage is beyond its borders. In either case, the name of the nucleus is specified to describe *Pax6* expression. Readers are also reminded that neural nuclei are specifically located by extensive staining (for example Nissl or Golgi preparations) and neurophysiological experiments (for example

selective stimulation, ablation, or analysis of distribution of neurotransmitters) (Williams and Warwick, 1980). Thus, any neural nucleus described here represents an approximation.

3.2.1.1 Day 9.5 p.c.

At day 9.5 p.c. of mouse embryogenesis, when the proximal end of the optic stalk begins to narrow, *Pax6* expression is seen in the neuroepithelium of the entire telencephalic region and the neuroepithelium of the optic stalk that surrounds the optic recess (figure 3.1.a). The distal part of the optic stalk (no. 7 in figure 3.1.a), as it makes contact with the surface ectoderm (no. 6 in figure 3.1.a), appears to exhibit more intense expression than the proximal part. *Pax6* expression can also be detected in the germinal (ventricular) neuroepithelium of the cervical spinal cord (no. 4 in figure 3.1.a and no. 10 in figure 3.1.b), as well as in the neuroepithelium of the more posterior spinal cord in the trunk region (no. 3 in figures 3.1.a - b). The expression in the cervical spinal cord appears to concentrate in the middle part (for example see no. 4 in figure 3.1.a). Evidence of *Pax6* expression is also seen in the neuroepithelium of the dorsal diencephalon (thalamus, i.e. the neuroepithelium immediately ventral to the optic vesicle), but not in the ventral diencephalon (hypothalamus, i.e. no. 8 in figure 3.1.a) by day 9.5 p.c. In the head surface ectoderm, *Pax6*-expressing cells cover the area overlying the optic vesicle. There is no sign of *Pax6* expression in any region containing the precursors of cephalic neural crest cells, nor in the mesenchyme of the first and the second branchial arches (see no. 12 and no. 13 in figure 3.1.b).

3.2.1.2 Day 10.0 p.c.

At day 10.0 p.c., when the proximal end of the optic stalk is seen constricted, *Pax6* expression can be detected in the neuroepithelium of the whole telencephalon as well as in the whole optic stalk (see figure 3.1.c). At the junction of the proximal end of optic stalk and the ventral diencephalon (hypothalamus), a sharp boundary between expressing and non-expressing area is seen (see the boundary between no. 15 and the proximal end of the optic stalk in figure 3.1.c). *Pax6* transcripts are also clearly detected in the ventral half of pontine neuroepithelium (pontine neuroepithelium is labelled 'no. 16' in figure 3.1.c) as well as in the border between ventral pontine neuroepithelium and dorsal medullary neuroepithelium (no. 18 in figure 3.1.c). The expression clearly extends toward more ventral areas in the medullary neuroepithelium and appears to extend to the velum medullare (no. 17 in figure 3.1.c). In the head surface ectoderm, area of *Pax6* expression overlies the optic vesicle and extends ventrally to some extent (see no. 6 in figure 3.1.c).

3.2.1.3 Day 11.0 p.c.

At day 11.0 p.c., when the optic cup is formed (no. 27 in figure 3.2.a) and the lateral ganglionic eminence in the telencephalon becomes evident (see no. 34 in a higher magnified view in figure 3.2.c),

some interesting changes in *Pax6* expression are found. *Pax6* expression in the neuroepithelium of dorsal telencephalon remains; but in the ventral telencephalon most *Pax6* transcripts disappear (compare figure 3.1.c with 3.2.a), leaving just a slim strip of *Pax6*-expressing cells along the striatum of ventral telencephalon, i.e. from point A to point B as indicated in figure 3.2.c. Another change is seen in the rhombencephalon where *Pax6* expression in the ventral pons and the dorsal medulla oblongata is confined only within two 'comma-shape' areas, i.e. from point C (head of the 'comma') to point D (tail of the 'comma') as indicated in a higher magnified view in figure 3.2.d. The expression in the vellum medullare becomes minimal (compare figure 3.1.c with 3.2.a).

In the optic region, the optic stalk remains expressing *Pax6* (no. 19 in figure 3.2.a). The sharp boundary between the expressing and the non-expressing area in the thalamus remains clearly seen. The surface ectoderm overlying the lens and the optic cup also exhibits evidence of *Pax6* expression, but not as obvious as that at day 10.0 p.c. (compare figure 3.1.c with 3.2.a). In the optic cup, both the forming neural retina and the future pigmented retinal epithelium exhibit *Pax6* expression (nos. 27 - 28 in figure 3.2.a). *Pax6* transcripts are also detected in the pituitary primordium (no. 20 in figure 3.2.a), but not as obvious as that in the optic cup or other areas. The rim of the optic cup appears to exhibit more intense *Pax6* expression than the other portions (see the most distal parts of the optic cup in figure 3.2.a). There is also detectable *Pax6* expression in the nasal epithelium, though this is not as intense as that in the optic cup (see no. 33 in figure 3.2.b).

3.2.1.4 Day 12.0 p.c.

At day 12 p.c., the changes of *Pax6* expression formerly noted to have occured by day 11.0 p.c. in the ventral telencephalon become more apparent (compare 3.2.a with 3.3.a), as the pallidum of the ventral telencephalon becomes apparent (see nos. 42 and 45 in figures 3.3.a; b). The slim strip of *Pax6*-expressing cells located on each side of the ventral telencephalon becomes slimmer as the cells are traced from the ventral telencephalon through the junction of the striatum and the pallidum (no. 46 in figure 3.3.b) toward the differentiation field of the pallidum. Beyond the striatum, as they are traced, the two 'strips' of *Pax6*-expressing cells become reduced to 'threads' until they end in two aggregates of *Pax6*-expressing areas located lateral to the pallidal subventricular zone (see no. 45 in figure 3.3.b).

In the eye region, *Pax6* expression in the optic stalks is maintained (see no. 39 in figure 3.3.a), while the hypothalamic neuroepithelium (ventral diencephalon) remains absent of *Pax6* transcripts (see no. 49 in figure 3.3.a). *Pax6* is no longer expressed in the pigmented retinal epithelium by day 12.0 p.c. (see no. 28 in figures 3.3.b; c). In the rhombencephalon, the two 'comma-shape' areas of *Pax6* expression in the neuroepithelium of the pons and the medulla are still present, but these areas of expression become relatively smaller as compared to the increasing volume of the rest of the rhombencephalon (compare figure 3.3.a with 3.2.a). It is also noteworthy that no areas of the presumptive dental epithelium shows evidence of *Pax6* expression (not shown).

3.2.1.5 Day 13.0 p.c.

Pax6 expression at day 13.0 p.c. is shown by serial transverse sections in figures 3.4.a to 3.4.m. To look serially from top of the head, *Pax6* transcripts are first seen in the pretectal and anterior tectal neuroepithelium (nos. 56 and 57 in figure 3.4.b) as well as in the thalamic neuroepithelium (nos. 58 and 59 in figure 3.4.b). The tectal neuroepithelium does not appear to have *Pax6* expression (no. 55 in figure 3.4.a). In the anterior thalamic neuroepithelium (no. 59 in figure 3.4.a), *Pax6* transcripts are concentrated in the ependymal (germinal) layer, in contrast to those in the posterior thalamic neuroepithelium and in the pretectal neuroepithelium which are mostly in the intermediate or marginal layers (compare no. 59 with nos. 57 - 58 in figures 3.4.b; c). This difference of *Pax6* transcripts distribution becomes more obvious as the transverse planes go further down (see figures 3.4.d; e). In the dorsoanterior part of thalamus, i.e. the lamina terminalis, *Pax6* transcripts are seen within the neuroepithelial tissues stretching out from the midline (no. 54 in figure 3.4.a).

As the levels of the tranverse planes go further down, *Pax6* transcripts are found in the germinal layer of neocortical neuroepithelium in the telencephalon (no. 30 in figures 3.4.g; h). This *Pax6* expression is continuous within parts of the differentiation field of the amygdala (no. 29 in figure 3.4.h) and medial hippocampus and is further linked to the lateral part of the thalamus toward the epithalamus (see the arrow-indicated, continuous *Pax6*-expressing area that stretches from no. 30 toward no. 29 and links with the epithalamus in figure 3.4.h). No sign of *Pax6* expression is seen in the choroid plexus in the lateral ventricle (telencephalic ventricle) or in the fourth ventricle (nos. 69 and 72 in figures 3.4.g; h). In the neuroepithelium of thalamus, *Pax6*-expressing cells are found in the areas surrounding the sulcus limitans (the site marked with an asterisk in figures 3.4.f; g; h; also known as hypothalamic sulcus), i.e. in the areas posterior (figure 3.4.f), lateral (figure 3.4.g), and anterior (figure 3.4.h) to the sulcus limitans. The expression is continuous with the germinal layer of the anterior thalamic neuroepithelium (see figure 3.4.h). In the posterior hypothalamus that surrounds the hypothalamic recess, *Pax6* transcripts are not detected (for example no. 8 in figure 3.4.g).

Pax6 expression is also detected in the germinal neuroepithelium in the tegmentum (ventral mesencephalon) and in the rhombic lip where the cerebellar primordium is formed (nos. 64 and 68 in figure 3.4.h). In the tegmentum, two strips of *Pax6*-expressing cells are found in the anterior neuroepithelium where the future reticular formation is located (no. 73 in figure 3.4.h). In the pontine area, a patch of *Pax6*-expressing cells is found on each side of the superior central raphe nucleus (no. 75 in figure 3.4.i). There is also evidence of *Pax6* expression in the medulla oblongata (no. 71 in figure 3.4.h) where transcripts are confined within the medial ventricular zone. In the spinal cord, *Pax6* transcripts are detected in the medial ventricular zone and in the ventral root motor neurons (nos. 89 and 96 in figure 3.4.k).

In the eye region, *Pax6* expression is found in the lens, the optic cup, and the corneal epithelium (figures 3.4.l; m). Transcripts in the lens appear to be concentrated in the anterior germinal epithelium (see no. 103 in figure 3.4.m). In the optic cup, both the neural retina (no. 101 in figure 3.4.m) and the pigmented retinal epithelium (no. 28 in figure 3.4.m) contain *Pax6* transcripts. The rim of the optic cup (no. 98 in figure 3.4.m) remains the area of most intense expression than the posterior parts. In the corneal epithelium (no. 38 in figure 3.4.m), *Pax6* expression is seen limited within the upper and the lower conjunctivas (no. 37 represents upper conjunctiva in figure 3.4.m; see also figure 3.4.l for a clearer demarcation). In the nasal epithelium, a detectable level of *Pax6* expression is found (no. 33 in figure 3.4.l).

3.2.1.6 Day 14.0 p.c.

By day 14.0 p.c., *Pax6* expression is generally consistent with that seen at day 13.0 p.c., but some interesting changes are found (presented in figures 3.5.a to 3.5.p). In the posterior thalamic and pretectal neuroepithelium (see nos. 57 - 58 in figure 3.5.b), *Pax6*-expressing areas in the intermediate and marginal layers appear to expand as both neuroepithelial layers are enlarged (compare figure 3.4.c with figure 3.5.b). *Pax6* transcripts in the anterior thalamic neuroepithelium remain mainly within the germinal layer in contrast to those in the posterior thalamic neuroepithelium and in the pretectal neuroepithelium (see figures 3.5.b; c; d). But signs of expansion of *Pax6*-expressing area in the anterior thalamic neuroepithelium toward the intermediate and marginal zones are apparent. For example, the habenular and lateral habenular differentiation fields as well as the epithalamus (pineal gland) is seen exhibiting intense *Pax6* expression (see nos. 61 and 63 in figures 3.5.d; e, and compare with those in figure 3.4.e). Another change in the thalamus is that, although *Pax6* transcripts remain detected in the area surrounding the sulcus limitans and remain continuous with the anterior thalamic neuroepithelium (figures 3.5.f; g; h), the area of expression seems to expand in proportion to the enlargement of the thalamus. Furthermore, this expression area in the thalamus becomes restricted in the more ventral region where the internal capsule is formed (see no. 106 in figures 3.5.i; j). The posterior hypothalamus does not show evidence of *Pax6* expression, neither does the choroid plexus in the lateral ventricle and in the fourth ventricle (see figure 3.5.h). The pituitary primordium is clearly seen expressing *Pax6* (no. 20 in figures 3.5.l; m; n).

Pax6 transcripts are also detected in the germinal (ventricular) neuroepithelium of the telencephalon as well as the rhinencephalon where the future main olfactory bulb will be connected (see no. 113 in figure 3.5.o). In the amygdala (for example see no. 29 in figure 3.5.h), *Pax6*-expressing area is expanded covering the piriform and endopiriform differentiation fields and the future medial and lateral amygdaloid nuclei (compare figure 3.4.h with figures 3.5.h - l). In the tegmental neuroepithelium, *Pax6* expression remain in the posterior surface and in the area of reticular formation as found at day 13.0 p.c. (compare nos. 64 and 73 in figure 3.5.h with the corresponding areas in figure 3.4.h). In the pontine neuroepithelium, intense expression is found in the surface granular layer (see no. 104 in figure

3.5.h). *Pax6* expression in the cerebellar germinal layer becomes more obvious (see no. 108 in figure 3.5.j). The rhombic lip (a cerebellar primordium) remains intensively expressing *Pax6* (see no. 68 in figures 3.5.g; h). The rootlet of the vestibulocochlear (VIII) ganglion also exhibits intense *Pax6* expression (no. 82 in figure 3.5.j). In the medulla oblongata, *Pax6* expression is found in the medial and surface germinal layers and more intense transcripts are seen in the premedullary neuroepithelium (nos. 5, 71, 107 in figures 3.5.h; k). Further down to the spinal cord, *Pax6* expression is detected in the same areas as found at day 13.0 p.c., i.e. in the medial ventricular zone and the motor neuron cells in the ventral root (nos. 89 and 96 in figure 3.5.p).

In the eye region, *Pax6* expression remains in the lens, the optic cup, and the corneal epithelium (nos. 38, 98, 103 in figure 3.5.p). The confinement of *Pax6* transcripts within the anterior germinal epithelium in the lens becomes more obvious (compare no. 103 in figure 3.4.m with that in figure 3.5.p). Surprisingly, the optic stalk does not show *Pax6* expression, although trace amounts of *Pax6* transcripts in the optic chiasma are seen (nos. 39 and 114 in figure 3.5.0). In the nasal epithelium, *Pax6* expression is clearly seen (no. 33 in figure 3.5.p).

3.2.1.7 Day 15.0 p.c.

By day 15.0 p.c., areas of *Pax6* transcripts remain in the posterior thalamic neuroepithelium and in the pretectal neuroepithelium extending toward the tectum (nos. 56, 57 in figure 3.6.b). They are mainly in the intermediate or marginal layers (see figures 3.6.b; c). In the anterior thalamus, further expansion of *Pax6* expression in the habenular and lateral habenular differentiation fields is seen (see no. 63 in figure 3.6.g and its corresponding area in figures 3.6.f; h; i). Evidence of further expansion of *Pax6*-expressing areas in the anterior thalamus (including the epithalamic neuroepithelium) is also seen in the wall of the thalamic third ventricle (compare figure 3.6.c with figure 3.5.b). This expansion appears to stretch beyond the germinal layer and reach toward the intermediate or the marginal layers (see nos. 117 - 118 in figure 3.6.c). The pineal neuroepithelium remains exhibiting intense *Pax6* expression (no. 120 in figures 3.6.d; e). For the *Pax6*-expressing area in the thalamic neuroepithelium surrounding the sulcus limitans, several differentiating fields and nuclei can be specified by day 15.0 p.c. (see figures 3.6.i to 3.6.r): paraventricular nucleus (no. 129), supraoptic nucleus (no. 139), reticular nucleus (no. 134), zona incerta (no. 131), fields of Forel (no. 130), and dorsal lateral geniculate nucleus (no. 138). As the transverse plane is further down, this expression area is restricted, leaving a curb-shaped pattern of expression surrounding the internal capsule as formerly noted by day 14.0 p.c. (compare figure 3.6.p with figure 3.5.i). A magnified view of this intermediate thalamic differentiation area does show a substantial population of cells that connect the hippocampus (no. 137) are expressing *Pax6* (see figure 3.6.r).

In the amygdaloid neuroepithelium, the endopiriform and piriform differentiation fields remain expressing *Pax6*, as well as the area where the medial and the lateral amygdaloid nuclei are presumably located (for example see nos. 29, 166 in figure 3.6.s). Of particular interest in the telencephalic neuroepithelium is a hint of secondary germinal layer formation that can be seen, for example, no. 121 in figure 3.6.e. This presumptive secondary germinal neuroepithelium exhibits hints of *Pax6* expression. Another interesting finding in the mouse brain by day 15.0 p.c is the presence of concentrated *Pax6* transcripts in the thickening external germinal layer in the cerebellar primordium of the posterior pontine area (see nos. 122 - 123 in figures 3.6.f; g). This *Pax6* expression in the external germinal neuroepithelium even stretches to cover the anterior part of the medulla oblongata (for example see no. 127 in figure 3.6.j). In the anterior tegmentum, the midbrain reticular formation can be specified as a *Pax6*-expressing area (see no. 73 in figures 3.6.l; m; n). The pontine subventricular neuroepithelium is also highly concentrated with *Pax6* transcripts (no. 133 in figure 3.6.n). The primordium of cochlear/vestibular complex also expresses *Pax6* at a high level (no. 82 in figure 3.6.n). *Pax6* transcripts in the cervical spinal cord remain unchanged, i.e. in the medial germinal zone and in the ventral root motor neurons (see figure 3.6.s).

In the eye, the same *Pax6*-expressing pattern as that at day 14.0 p.c. is maintained (figure 3.6.t). In the lens, *Pax6* transcripts are concentrated within the anterior germinal epithelium (no. 103), whereas the

primary lens does not contain *Pax6* transcripts (no. 99). The pigmented retinal epithelium (no. 28) can be clearly seen without *Pax6* expression. The rim of the optic cup (no. 98) appears to have more intense *Pax6* transcripts than the other areas of the optic cup. *Pax6* expression also remains in the corneal epithelium (no. 38) and the expression is demarcated in the conjunctivas (no. 37).

3.2.1.8 Day 16.0 p.c.

By day 16.0 p.c., *Pax6* transcripts are detected in the neocortical (telencephalic) neuroepithelium (see no. 2 in figure 3.7.a) in conjunction with those in the neuroepithelium of subicular area (no. 50), hippocampal area (Ammon's horn) (no. 137), dentate gyrus (no. 145), and further with the differentiation fields of strionuclear area (no. 146), pallidum (no. 45), and amygdaloid area (no. 149 in figure 3.7.c). In the dorsal thalamus, the area of epithalamic neuroepithelium (where the pineal gland, the habenular and lateral habenular nucleus are differentiated) exhibits obvious *Pax6* expression (see no. 120 in figures 3.7.c and d). This expression is seen, if viewed more caudally, in the lateral posterior nucleus in the posterior thalamus (no. 157 in figure 3.7.h) and the anterior pretectal nucleus in the pretectum (no. 159 in figure 3.7.i). *Pax6* expression also appears in the areas of stria terminalis and stria medullaris in the anterior thalamus (nos. 143, 150 in figure 3.7.c). Transcripts of *Pax6* are also seen in the site of the lateral preoptic region in the anterior hypothalamus (no. 148 in figure 3.7.d). As the coronal sections are viewed further caudally (from the forehead further toward the occipital direction), *Pax6* expression in the intermediate thalamus is seen in a symmetrical branched pattern (see figures 3.7.d to h). The ventral branch joins with the dorsal branch in the Forelian neuroepithelium at the wall of hypothalamic third ventricle where the paraventricular nucleus (no. 129) can be specified (see figure 3.7.h). The dorsal branch stretches dorsolaterally (see figure 3.7.h), starting from the site of Forelian neuroepithelium and the paraventricular nucleus, to the area of zona incerta (no. 131) and the reticular nucleus (no. 134); the ventral branch stretches ventrolaterally toward the fields of Forel (no. 130) and the differentiation field of dorsolateral hypothalamus in close proximity to the piriform cortex (no. 77). In the hypothalamic area, patches of cells appear to exhibit *Pax6* expression (not specifically labelled; see figure 3.7.h).

Further caudally (toward the occipital direction), interesting patterns of *Pax6* expression in the intermediate and posterior thalamus are seen. The dorsal branch (paraventricular-zona incerta-reticular nucleus) becomes band-shaped and is present in the differentiation field of intermediate thalamus and ventrolateral geniculate nucleus (no. 160 in figure 3.7.i). Connections of *Pax6*-expressing cells between the dorsal and the ventral branch are apparent (see figure 3.7.j). This dorsal branch, i.e. the band-shaped expression area, will become segmented (figure 3.7.k) and forked (figure 3.7.l) as it is viewed more caudally in the tegmental area. The ventral (fields of Forel-dorsolateral thalamus) branch is also changed; it becomes a patch of cells in the subthalamic nucleus (no. 161 in figure 3.7.i) and, as viewed more caudally, is gradually diminished in the posterior and lateral hypothalamic differentiating fields (see figures 3.7.k; l). The posterior amygdaloid area where the basomedial amygdaloid nucleus

(no. 166) is located remains exhibiting *Pax6* expression as can be seen in figures 3.7.i to 3.7.n. The deep layers of the superior colliculus are also seen expressing *Pax6* (no. 168 in figure 3.7.o). The pituitary and the mammillary neuroepithelium are also *Pax6*-expressing areas (nos. 20, 169 in figure 3.7.p). Particularly intense expression can be located in areas of the lateral deep nucleus (no. 171), ventral tegmental nucleus (no. 172), magnocellular reticular nucleus (no. 175), cochlear nucleus (no. 176), and superior central raphe nucleus in the isthmus (no. 282) (see figures 3.7.p; q; s; t; u; w). The cerebellar primordium (no. 174 in figure 3.7.n) is also an area of intense *Pax6* expression. In the cervical spinal cord, *Pax6* expression remains in the ventral motor neurons (presumably the 7th layer of the spinal cord) (see no. 96 in figure 3.7.α). This expression is consistent through the whole span of cervical spinal cord (see figures 3.7.β; γ; δ; ε).

Pax6 transcripts remain in the main and the vomeronasal olfactory epithelium as well as in areas of the eye that are formerly seen by days 14.0 p.c. and 15.0 p.c. (see nos. 33, 91 in figures 3.7.b and c).

3.2.1.9 Day 17.0 p.c.

By day 17.0 p.c., *Pax6* transcripts remain in the areas formerly detected at earlier gestation days, with some minor changes. In the telencephalic region, *Pax6* expression remains in the neocortical neuroepithelium, spanning from the lateral neocortex to the hippocampal neuroepithelium close the midline (for example see figure 3.8.n) and is linked to the amygdaloid neuroepithelium in the more posterior region (see figures 3.8.r; s). There is also hints of *Pax6* expression in the outer layer of telencephalic neuroepithelium, although the level of expression is not as high as that in the neocortical neuroepithelium (for example, see figures 3.8.q; r). *Pax6* expression also appears in a patch of cells outside the brain. These presumably are neural cells (see no. 209 in figures 3.8.o and 3.8.p). The anterior thalamic neuroepithelium in the area of medial septum (no. 199 in figure 3.8.k), the pineal primordium (no. 120 in figure 3.8.s) and the thalamic neuroepithelium (figures 3.8.l to t) remain containing *Pax6* transcripts. Those previously noted areas in the thalamus, i.e. the paraventricular nucleus, fields of Forel, zona incerta, reticular nucleus, supraoptic nucleus and the differentiation fields of intermediate/lateral thalamus remain containing *Pax6* transcripts as formerly detected (see figure 3.8.o). The pituitary primordium also appears to express *Pax6,* although at a very low level (no. 20 in figures 3.8.q; r).

More caudally, *Pax6* expression is seen in the ventrobasal nucleus (no. 215 in figure 3.8.r), medial geniculate nucleus (no. 214 in figure 3.8.r), and the junction of medial geniculate nucleus and red nucleus (no. 219 in figure 3.8.t). In the pontine neuroepithelium, the cerebral peduncle (no. 216 in figure 3.8.t) and superior central raphe nucleus (no. 75) in the anterior pons (no. 217) constitute a symmetric 'tadpole' pattern of *Pax6*-expressing area (see figure 3.8.t). The cerebellar primordium, including the cochlear nucleus, exhibits apparent *Pax6* transcripts (no. 174 in figures 3.8.w; x). The areas of the reticular formation (nos. 73 and 225), the neuroepithelial cells in the wall of the fourth

ventricle (no. 22), the ventral tegmental nucleus (no. 172) and the lateral vestibular nucleus (no. 224) are also *Pax6*-expressing (figures 3.8.w; x; y). The choroid plexus in the fourth ventricle does not exhibit *Pax6* expression (see no. 69 in figure 3.8.z). In the medulla, *Pax6* transcripts are detected in the medullary reticular formation (no. 228 in figure 3.8.z; α).

In the olfactory epithelium and vomeronasal epithelium (olfactory epithelium in the Jacobson's organ), a low level of *Pax6* expression is detected (nos. 33 and 91 in figures 3.8.a to e). *Pax6* expression is also clearly detected in the tubules of serous gland (no. 194) and in the nasal glandular tissue in lateral wall of middle meatus (no. 195 in figure 3.8.c). In the main olfactory bulb (no. 196 in figure 3.8.d), *Pax6* transcripts are seen in the neuroepithelium and are connected, posteriorly, to those found in the lateral migratory stream (no. 200) and the endopiriform nucleus in the rhinencephalon (no. 111) (see figures 3.8.f to h). *Pax6* transcripts are also detected in the taenia tecta (see no. 283 in figures 3.8.f; h). These areas of *Pax6* expression in the rhinencephalon are linked posterolaterally with the amygdaloid neuroepithelium, particularly with the piriform cortex (no. 77 in figure 3.8.m).

In the eye (see figure 3.8.j), *Pax6*-expressing cells remain located in the anterior epithelium of the lens (no. 103), the neural retina that is differentiated into a multi-layered structure (nos. 201 - 205), as well as in the corneal epithelium (no. 38). In the pigmented retinal epithelium, however, no detectable *Pax6* transcript is found (no. 28 in figure 3.8.j). *Pax6* expression is also detected in the optic chiasma (no. 114 in figure 3.8.h) but not in the optic stalk (no. 39 in figure 3.8.j). Particularly interesting finding is in the differentiating neural retina where *Pax6* transcripts appear to distribute in various concentrations in different layers. The presumptive internal nuclear layer shows the most intense expression than other layers (no. 203 in figure 3.8.j).

3.2.1.10 Day 18.0 p.c.

By day 18.0 p.c., interesting changes of *Pax6* expression are found in the main olfactory bulb and in the telencephalic neuroepithelium, as well as in the thalamic neuroepithelium.

In the telencephalon (figures 3.9.i to t), the cingulate cortex and the neocortical neuroepithelium remain expressing *Pax6*, but the total area is reduced, i.e. the formerly thick layer of *Pax6*-expressing neuroepithelium is reduced to a thin layer (compare no. 2 in figures 3.7.b, 3.8.k, and 3.9.l). In the thalamic neuroepithelium, the dorsal (paraventricular-zona incerta-reticular) branch and the ventral (fields of Forel-dorsolateral hypothalamus) branch that are formerly noted at day 16.0 p.c. (in section 3.2.1.8) remain *Pax6*-expressing; but the total area seems to be slightly reduced as compared to that seen at day 16.0 p.c. (for example compare figure 3.6.h with figure 3.9.m). The differentiation fields of fornix (no. 234 in figure 3.9.i), medial septum (no. 199), diagonal band (both horizontal and vertical limb; see no. 235 in figure 3.9.h and no. 236 in figure 3.9.i) and lateral migratory stream (no. 200) all contain *Pax6* transcripts at identifiable level (see figure 3.9.i). Also, the lateral habenular nucleus (no.

245 in figure 3.9.q) and the dorsal periaqueductal gray (no. 247 in figure 3.9.t) are *Pax6*-expressing areas that can be specified. In the hypothalamus, *Pax6* transcripts are seen in the intermediate neuroepithelium (for example, see no. 237 in figure 3.9.k). The pituitary primordium remains expressing *Pax6* (no. 20 in figure 3.9.q; r). *Pax6* transcripts are even seen in the pituitary cells in the ossificating cartilage primordium of hypophyseal fossa of sphenoid bone, i.e. the sella turcica (no. 240 in figure 3.9.l; see also figure 3.9.m).

In the midbrain (see figures 3.9.o; p), *Pax6* transcripts are detected in the dorsal lateral geniculate nucleus, ventral lateral geniculate nucleus, and the junction of reticular nucleus and ventral lateral nucleus complex (no. 243). In the pontine area, the superior central raphe nucleus (no. 75), pontine reticular formation (no. 225), cerebral peduncle lateral to the trigerminal motor nucleus (no. 248), trigeminal motor nucleus (no. 249), as well as the facial motor nucleus (no. 252) can be specified as *Pax6*-expressing areas (see figures 3.9.s; t; u). The cerebral primordium lateral to the pontine area remain expressing *Pax6* at a high level (see no. 174 in figure 3.9.w).

In the olfactory bulb, the olfactory neuroepithelium and the anterior olfactory nucleus are clearly *Pax6*-expressing (nos. 231 and 232 in figure 3.9.d). *Pax6* transcripts are also found in the insular area of the rhinencephalic differentiation field that is in conncetion with the amygdaloid differentiation fields (for example see no. 200 in figure 3.9.g).

In the eye, *Pax6* transcripts are concentrated only in the ganglion cell layer and internal nucleus layer of the neural retina (nos. 203, 204 in figure 3.9.c) instead of being distributed in several other layers at day 17.0 p.c. (compare 3.9.c with 3.8.j). The pigmented retinal epithelium (no. 28) is seen completely devoid of its *Pax6* expression and the corneal epithelium (no. 38) contains only minimal *Pax6* transcripts (see figure 3.9.c).

3.2.1.11 After birth

Pax6 expression after birth is shown in figures 3.10.a to p. By day 1.0 after birth (see figure 3.10.a), in the olfactory bulb, *Pax6* expression is seen in the glomerular layer (no. 253), mitral cell layer (no. 255), and internal granular cell layer (no. 256). Ventral to the olfactory bulb is the rhinencephalon that exhibits *Pax6* transcripts in the frontal neocortex (no. 257 in figure 3.10.b). In the telencephalon, hints of *Pax6* expression remain seen in the neocortical neuroepithelium (see no. 2 in figure 3.10.d). The posterior hypothalamus (no. 259) and the cerebral peduncle (no. 216) also show hints of *Pax6* expression, as well as the fields of Forel (no. 130) and cortical plate (no. 258) (see figures 3.10.d; e). In the neural retina, convincing evidence for the confinement of *Pax6* transcripts within the ganglion cell layer (no. 204) and the internal nuclear layer (no. 203), as well as the absence of *Pax6* expression in the pigmented retinal epithelium (no. 28) is found (see figure 3.10.p).

By day 7.0 after birth, *Pax6* expression in the telencephalon and diencephalon is generally comparable to that seen at day 1.0 after birth (compare figures 3.10.d and 3.10.e with figure 3.10.f). However, in the thalamic area, *Pax6* transcripts can be specified in the area of the subthalamic nucleus (no. 161) and hints of expression are found in the hippocampal neuroepithelium (no. 137) (see figure 3.10.f). Particularly interesting changes regarding *Pax6* expression found by day 7.0 after birth are in the superior colliculus, the cerebellum, and the inferior olive. In the superior colliculus, *Pax6* transcripts are intensely concentrated in the surface layers of external germinal neuroepithelium (no. 222); this is not observed before birth (see figure 3.10.h). The cerebellum at this gestation age has been expanded to cover the lateral and ventrolateral part of the pons and *Pax6* transcripts are concentrated in the convoluted external granular (germinal) neuroepithelium (no. 229) (see figures 3.10.g; h). In the inferior olive, *Pax6* is also intensely expressed (nos. 263 and 264 in figure 3.10.i).

By day 21.0 after birth (see figures 3.10.j; k), in the olfactory bulb, *Pax6* transcripts are seen in the internal granular cell layer (no. 256) and glomerular layer (no. 253). The mitral cell layer (no. 255) as well as the external plexiform layer (no. 254) do not exhibit evidence of *Pax6* expression. In the telencephalon and diencephalon (see figures 3.10.m; n; o), *Pax6* transcripts are detected in the neocortical neuroepithelium (no. 2), cortical plate (no. 258), stria medullaris (no. 274), fimbria (no. 272), subicular area (no. 273), and the differentiation field of intermediate thalamus (no. 158). Particularly interesting is in the corpus callosum (no. 269) and in the deep layers of superior colliculus (no. 168) where *Pax6* transcripts are found along with the left-right neuronal projections (figure 3.10.o).

3.2.2 Nerve fiber projection as demonstrated by Linder's silver stain in the mouse brain

Linder's silver stain in conjunction with Luxol fast blue on the mouse brain is represented here only at day 15.0 p.c., although the same procedures have been performed on mouse heads at earlier gestation days. The reason is that not as much nerve fiber projection can be seen before day 14.0 p.c. and day 15.0 p.c. is more informative than that at day 14.0 p.c.

Seen on serial transverse sections, the mouse brain first shows apparent nerve fiber projections at the anterior pretectal (no. 56) and tectal region (no. 57) where *Pax6* is heavily expressed (compare figures 3.11.b and 3.11.c with figure 3.6.b). As the tranverse planes are lower, nerve fiber projections can be seen in the paraventricular nucleus (no. 129) and areas surrounding the lateral habenular nucleus (no. 277) (see figure 3.11.c). These are also *Pax6*-expressing areas (see figures 3.6.g and 3.6.n for a comparison). Nerve fiber projections are also found in the junction between tegmental formation and hypothalamus (no. 279 in figure 3.11.d) where *Pax6* transcripts are present (compare figures 3.6.d and figure 3.11.d) as well as in the cerebellar primordium (no. 174 in figure 3.11.e) whose *Pax6* expression is obvious (compare figure 3.11.e with 3.6.f). Furthermore, the correlations of *Pax6* expression with nerve fiber projection are found in the surface of medulla (no. 107; compare figure 3.6.j with 3.11.g), in the superior central raphe nucleus in the pons (no. 75; compare figure 3.11.k with 3.5.m), in the neural retina (no. 205 in figure 3.11.o; compare figure 3.6.t with figure 3.11.o), in the differentiation field of olfactory bulb (compare figure 3.11.n with figures 3.5.n; o) and in the optic chiasma (no. 114; compare figure 3.11.o with figure 3.5.o). In contrast to those with correlation, where there is no *Pax6* expression, for example in the choroid plexus (no. 72 in figure 3.4.h) and in the trigeminal ganglion (no. 21), there is no nerve fiber projection (compare figure 3.4.h with 3.11.e; also compare figure 3.11.n with figure 3.5.n).

However, there are almost equal number of exceptions to the correlation of *Pax6* expression with nerve fiber projection. In the internal capsule (no. 106; compare figure 3.11.f with figure 3.6.p) and the optic stalk (no. 39; compare figure 3.11.o with figure 3.5.o), nerve fiber projections are abundant without the presence of *Pax6* transcripts; while in the olfactory epithelium (no. 33; compare figure 3.5.p with figure 3.11.o), pineal primordium (no. 276; compare figure 3.11.b with figures 3.6.d; e) and the telencephalic neuroepithelium (compare figure 3.6.p with figure 3.11.f), *Pax6* is intensely expressed without the appearance of obvious nerve fibers. In the intermediate thalamic differentiation field, i.e. the areas presumably of the zone incerta, fields of Forel, reticular formation, and paraventricular nucleus, *Pax6* is extensively expressed, but nerve fibers are only seen in the paraventricular nucleus (no. 129; compare figure 3.6.n with figure 3.11.c). In the cerebellar primordium, a sharp boundary of expressing and non-expressing areas is seen between the tegmentum and the pons (for example, see figure 3.6.g), but nerve fiber projections appear to extend along the surface of tegmentum where no *Pax6* expression is found (compare figure 3.6.g with figure 3.11.e).

3.3 Discussion

3.3.1 *Pax6* in the visual nervous system

Pax6 is obviously involved in the development of visual nervous system as demonstrated by the distribution of its transcripts. If one colours, according to the presence of *Pax6* transcripts, the components reviewed and schematically represented by Garey *et al.* (1991) (see figure 1.6 and section 1.9.9), the involvement of *Pax6* in the visual nervous system is clearly shown (see figure 3.12 on next page).

In figure 3.12, almost every major component of the visual nervous system is coloured, except area 17 of the visual cortex and extrastriate cortex where *Pax6* expression is not determined; and the parabigeminal nucleus where *Pax6* is not expressed. The brainstem cholinergic nuclei (CH) can be represented by the area of zona incerta where the ventral tegmental ascending cholinergic pathway is located (Williams and Warwick, 1980). Thus, *Pax6* is not only involved in the development of eye but also in the higher centres of the visual nervous system. This is not surprising for two reasons: (1) Many orthologous *Pax6* genes in other species are consistently involved in nerves of sense organs, particularly in the optic nerve (Krauss *et al.*, 1991; Martin *et al.*, 1992; Carriere *et al.*, 1993; Turque *et al.*, 1994; Li *et al.*, 1994; Rio-Tsonis *et al.*, 1995; Hirsch and Harris, 1996). (2) The optic nerve, as one part of the visual nervous system is not formed when *Pax6* is not functional (Hogan *et al.*, 1986; 1988). This implies that other components of the visual nervous system may have *Pax6* involved in their development, if the whole system is evolved as an unit of a same origin.

Pax6 may also be involved in the connection of those components of the visual nervous system; but this is out of the limit of *in situ* hybridization experiments to demonstrate. However, some areas express *Pax6* in a way that suggests a role of *Pax6* in connecting visual pathways. For example, by day 21.0 after birth, *Pax6* transcripts are present in the corpus callosum and in the deep layers of superior colliculus along with left-right neuronal projections (see section 3.2.1.11). The corpus callosum is a place where the visual cortical areas of the right and left hemispheres are reciprocally interconnected by axons that run through it (Price, 1991). Similar contralateral connections exist in the superior colliculus (Fish *et al.*, 1982; Rhoades and Fish, 1982).

Mutant analysis on the *Sey/Sey* brain also supports a role of *Pax6* in the development of visual nervous system. For example, the area of zona incerta is absent from its normal position and the corpus callosum is severely underdeveloped in the *Sey/Sey* prenatal brain (Stoykova *et al.*, 1996). Also, the regions of zona incerta and ventral lateral geniculate body do not show their characteristic patterning for applied markers (*Pax6* and *Dlx 1*) and are severely underdeveloped, leaving an enlarged third ventricle (Stoykova *et al.*, 1996).

Figure 3.12 A schematic diagram of mouse *Pax6* expression in the visual nervous system. This diagram summarises connections of the main components within the visual nervous system as reviewed in the laboratory rat, domestic cat, and macaque monkey (from Garey *et al.*, 1991). The pink-coloured components are those where *Pax6* transcripts are detected. Thus, *Pax6* expression is detected in the neural retina (RET), dorsal lateral geniculate nucleus (LGD), ventral lateral geniculate nucleus/pregeniculate nucleus (LGV PRE), pulvinar/lateral posterior complex (PUL LP), superior colliculus (SC), pretectum (PT), raphe nucleus and locus coeruleus (R LC). Area 17 of the striate cortex (17), the extrastriate cortex (EX STR), and parabigeminal nucleus (PBG) do not appear to be *Pax6* expressing areas.

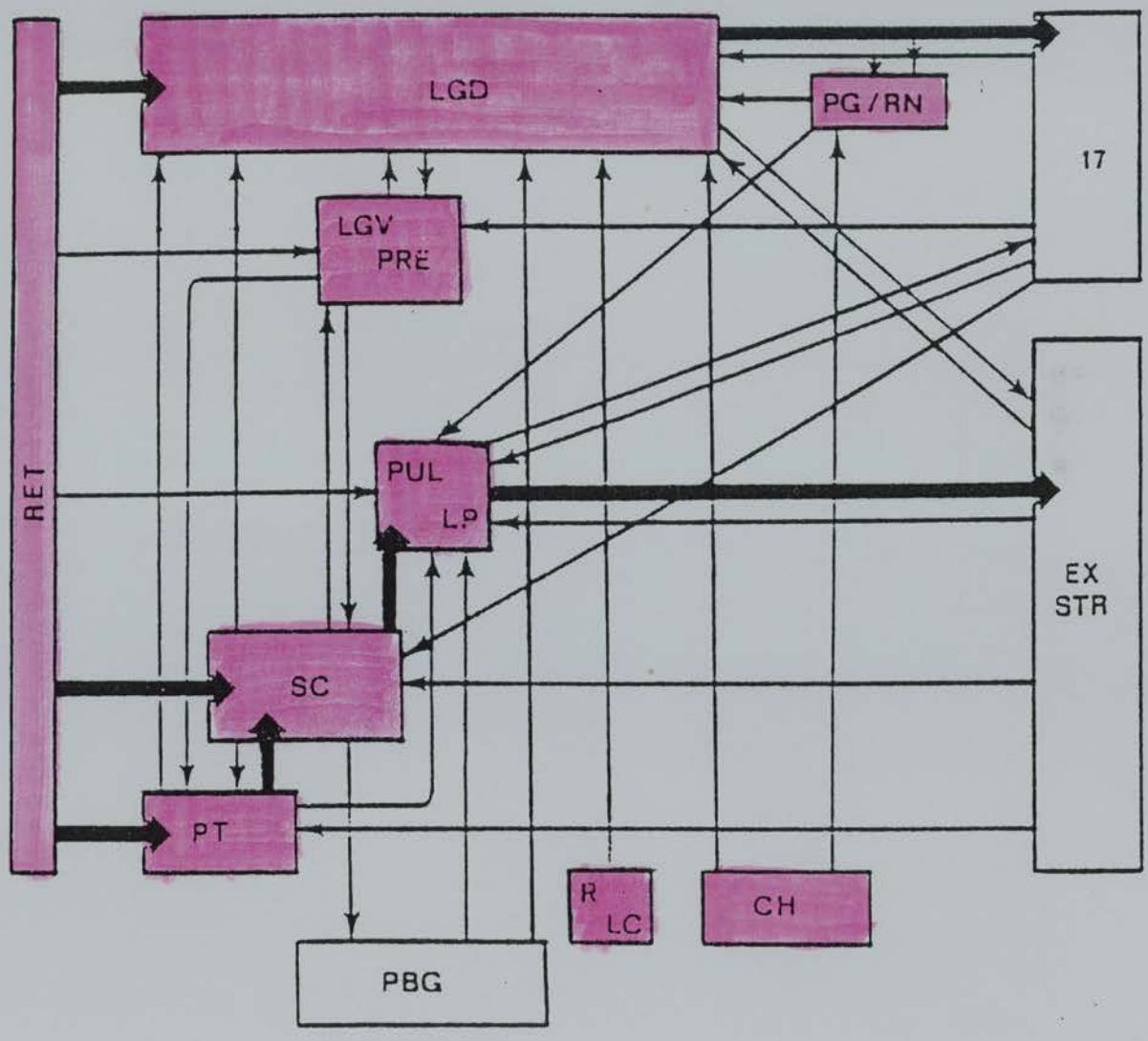
LGD
PG / RN
17
LGV
PRÉ
RET
PUL
L.P
EX
STR
SC
PT
R
LC
CH
PBG

The conclusion that *Pax6* is involved in the development of higher centres of visual nervous system implies that the variable effects of aniridia on vision (see section 1.5.2) may partly be due to abnormalities in the higher visual centres. Thus, to some patients, efforts trying to correct anomalies in the lens or the cornea may not be sufficient to improve their vision.

3.3.2 *Pax6* in the olfactory nervous system

Pax6 is also involved in the development of olfactory nervous system. This is based mainly on the presence of *Pax6* transcripts in most olfactory components. Externally, *Pax6* transcripts are present in the olfactory and vomeronasal epithelium. This expression is connected with that in the main and accessory olfactory bulb and further posteriorly with the expression of the anterior olfactory nucleus (AON) and precommissural hippocampus (taenia tecta). *Pax6* expression is also found in other olfactory components: piriform cortex and its promordium (lateral migratory stream), endopiriform cortex, olfactory periallocortex, and olfactory and vomeronasal amygdaloid areas (see section 1.10.9) such as the areas presumably of the anterior, lateral, and cortical amygdaloid nucleus. The extensive distribution of *Pax6* transcripts in the olfactory components allows a conclusion that *Pax6* is involved in the development of higher olfactory centres.

Pax6 may also be involved in the connection of olfactory pathways. For example, the connection of *Pax6* expression between hippocampal area and amygadaloid area is seen not only in the anterior region, i.e. the precommissural hippocampus (tenia tecta) with anterior amygdala. It is also seen at more caudal area; this is illustrated in figure 3.7.a. Interestingly, the habenular nucleus and lateral habenular nucleus are parts of this connection (see figure 3.7.a). The habenular nucleus is a station on some of the olfactory reflex pathways and is probably closely concerned with one of the sources of innervation of the pineal gland (Williams and Warwick, 1980); both the habenular nucleus and pineal gland exhibit intense *Pax6* expression. Furthermore, connections from amygdaloid nuclei to the habenular nucleus are supposed to project via the stria terminalis; and from hippocampal formation via the fornix (Williams and Warwick, 1980). Both the stria terminalis and the fornix exhibit *Pax6* expression. These observations suggest a role of *Pax6* in connecting olfactory centres.

Mutant analysis by Stoykova *et al.* (1996) also support a role of *Pax6* in the olfactory nervous system. For example, the amygdala differentiation field is underdeveloped and the restriction of *Pax6* and *Dlx1* expression in the amygdala is lost in the *Sey/Sey* brain (represented by figure 1 in Stoykova *et al.*, 1996).

3.3.3 *Pax6* in nerve fiber projection

The involvement of *Pax6* in nerve fiber projection is suggested by several lines of evidence as mentioned in section 3.1.3. However, *Pax6* expression seems not to correlate with nerve fiber projection, in that almost equal number of examples of non-correlation are found. But still, one can not exclude the possible involvement of *Pax6* in nerve fiber projection for the following reasons: (1) *Pax6* is a transcription factor that is encoded in the nucleus (Glaser *et al.*, 1995; Hanson *et al.*, 1995). *Pax6* signals represented by *in situ* hybridization are therefore located in the neuronal somata. Nerve fibers mainly represent axon projections that are extended to a distance away from the somata. Thus, lack of correlation between *Pax6* expression and sites of nerve fiber projection does not necessarily mean that *Pax6* is not involved. (2) The mouse brain nerve fiber projection is a process that starts from as early as E 8.5 (Easter *et al.*, 1993; Mastick and Easter, 1996) and continues even after birth (Edwards *et al.*, 1989). By day 15.0 p.c. (shown in this study), the sites where *Pax6* is expressed but without evident presence of nerve fibers may start their nerve fiber projection at later stages. (3) Both *in situ* hybridization and Linder's silver stain used in this study have their limits. The former may not be able to demonstrate tiny sites or lower level of expression. The latter reflects only established nerve fibers that are in detectable bundles under the optic microscope.

Mastick *et al.* (1997) reported that *Sey/Sey* embryos exhibited an axon pathfinding defect specific to the first longitudinal tract, i.e. tract of the posterior commisure (tpoc), in the prosencephalon. Although the tpoc axons in the mutants have normal initial projections, they make dramatic errors where they contact the neuron cell bodies, and fail to pioneer the first tract (Mastick *et al.*, 1997). The initial trajectory of tpoc is correlated well with the pattern of *Pax6* expression in the prosencephalon (p1 to p3 of prosomeres and in the optic vesicle region). Mastick *et al.* (1997) described in the same report that at least some of the posterior commisure (pc) neurons did not express *Pax6* by E 10.5, although the area of *Pax6* expression overlapped extensively with that of pc axon projections. By immunohistochemical analysis, 93 % (260 out of 279) of p1 cell bodies lacked nuclear labeling by E 10.5. However, the pc neurons project axons substantially at E 9.5 when nearly all p1 nuclei were labeled by the Pax-6 antibody (Easter *et al.*, 1993; Mastick *et al.*, 1996). Thus, current data support a role of *Pax6* in axon projection.

There are some presumptive pathways that *Pax6* may regulate axon projection. *Pax6* may regulate axonal projection by regulating neuronal process outgrowth through cell surface molecule like L1 (Mastick *et al.*, 1997). *Pax6* may also regulate other transcription factor genes like *Ets* (Plaza *et al.*, 1994), *Lim-1* and *Gsh-1* (Mastick *et al.*, 1997) or *Pax6* itself through autoregulation (Plaza *et al.*, 1993; Grindley *et al.*, 1995; Quinn *et al.*, 1996). The downsteram genes of *Ets, Lim-1, and Gsh-1* will be of interest in this aspect; particularly those involved in either extracellular matrix or diffusible molecule guidance during axon projection. *In vitro* studies showed that growth factors such as activin A, bFGF, NGF, BDNF could regulate *Pax6* expression (Yamada *et al.*, 1994; Kioussi and Gruss, 1994). In light

of the above mentioned data, I propose that for the integration of the visual and olfactory nervous system *Pax6* is first expressed in each axon relay centre under the regulation of growth factors. Once *Pax6* expression is established in the relay centres, point-to-point integration of the whole system is probably achieved by the downstream genes that are activated within the mass of cells where the axons are to pioneer. The activation of downstrean genes presumably depends on transient *Pax6* expression between each two points of axon relay centres. When the downstream genes are activated, they presumably exert a negative feedback effect so that *Pax6* expression will become downregulated or even disappeared; a phenomenon in agreement with the common theme of developmental restriction for *Pax6* (to be discussed in section 3.3.4).

Further experiments are necessary to demonstrate the proposed role of *Pax6* in nerve fiber projection. For example, one can have brains of the same gestational stage from *Sey/Sey* mouse run through Linder's silver stain and compare with their wildtype littermates. The double stain technique (DiI tracing of axons and immunohistochemistry) used by Mastick *et al.* (1997) can be used for correlation of axons with *Pax6* expression in other areas such as olfactory bulb, cerebellum, and spinal cord. The correlation together with mutant analyses and *in vitro* microexplant cultures will give more understanding on this topic.

3.3.4 Developmental restriction as a common theme for *Pax6* expression

Developmental restriction is defined here as a gene expresson that first appear in broader regions of embryos during earlier stages of development and later the expression is confined within smaller regions, i.e. become diminished, or the expression disappeared. Developmental restriction, by the definition, is a common theme for *Pax6* in most of its expression regions.

3.3.4.1 Examples of developmental restriction of *Pax6* expression

Examples for developmental restriction of *Pax6* are plenty in the mouse. As reported by Grindley *et al.* (1995), in the head surface ectoderm, *Pax6* expression first covers most of the head region but is gradually restricted to the area overlying the optic vesicle and finally to the presumptive corneal epithelium. Furthermore, in the pigmented neural epithelium at day 15.0 p.c., *Pax6* expression is only seen in the anterior region, i.e. near the rim of the optic cup (Grindley *et al.*, 1995), whereas *Pax6* transcripts are detected everywhere in the optic cup in earlier gestation days. In the neuroepithelium of spinal cord, *Pax6* first expresses in the whole ventricular layer but is gradually excluded from the dorsal and basal plate and is finally restricted to the medial ventricular zone (Walther and Gruss, 1991).

There are also plenty of examples that are not previously reported: (1) In the lens ectoderm, *Pax6* transcripts first appear in the entire lens placode but by day 13.0 p.c. it is already confined within the anterior germinal epithelium. (2) In the neural retina, *Pax6* expression is first seen evenly in all layers

but is gradually concentrated in several layers by day 16.0 p.c. and is further restricted to the inner nuclear layer and the ganglion cell layer by day 18.0 p.c. (3) In the telencephalic neuroepithelium, *Pax6* expression is developmentally restricted by two steps. The first step occurs between day 10.0 p.c. and day 11.0 p.c. during which the striatal and pallidal neuroepithelium become almost non-expressing. This restriction results in the 'strip' of *Pax6*-expressing cells along the lateral walls of the neuroepithelium. The second step is a gradual process that occurs from day 13.0 p.c. and afterwards when *Pax6* expression in the cerebral cortex is reduced from a thick zone to a thin layer. Some parts of the telencephalic neuroepithelium, for example the hippocampal and the dentate gyrus neuroepithelium, even become non-expressing. (4) In the pontine and medullary neuroepithelium, *Pax6* expression is also restricted to the 'comma-shape' area as the embryo develops. (5) By day 13.0 p.c., the optic stalk is seen no longer expressing *Pax6*, whereas intense expression is found at the same site at day 12.0 p.c.. (6) In the thalamic neuroepithelium, *Pax6*-expressing cells first cover a large proportion of the thalamus but the coverage area is gradually reduced to become a branched band.

There are also many examples of developmental restriction for *Pax6* in other species whose *Pax6* expression profiles are described in sections 1.4.2 to 1.4.7. These are not to be readdressed in avoidance of repetition.

3.3.4.2 Implication of stage-dependent functions by developmental restriction

Why is developmental restriction found ? The following two possible explanations may be made: (1) The expression is relatively diminished due to the increase of non-expressing areas as the embryo develops and becomes large, i.e. the net area and the original pattern of expression is not changed. This is not the case for two obvious reasons. Firstly, the pattern of *Pax6* expression is changed, for example, from a broad patch to branched lines in the thalamus. Secondly, some expressions even disappear, for example, the disappearance of *Pax6* expression can be found in the optic stalk, the posterior lens ectoderm and pigmented retinal epithelium. (2) The expression is developmentally restricted in correlation with stage-dependent gene functions. *Pax6* may function initially in broader domains as it is expressed and then, as the embryo grows, the function(s) being carried on by *Pax6* is either replaced by other gene(s) or become unnecessary. *Pax6* expression is therefore restricted accordingly. This is very likely the case for *Pax6* expression and function during embryogenesis and is to be discussed in the following sections.

3.3.4.3 *Pax6* functions in different areas as supported by developmental restriction

Pax genes are generally expressed in highly mitotic or immature cells (see section 1.6.2 for details). *Pax6* follows the general theme for all *Pax* genes by expressing in the ventricular layer of neuroepithelium in the developing brain and spinal cord, in the anterior germinal epithelium of the lens, and in the proliferative neural retina. All these *Pax6* expressions, as mentioned in the previous section, are developmentally restricted. In light of the stage-dependent nature of developmental restriction for *Pax6*, one wonders what sort of function(s) can be inferred when the stage-dependent developmental events are compared. This section is to specify these functions based on such comparisons.

3.3.4.3.1 *Pax6* is involved in proliferation during forebrain development

As introduced in section 1.8.2, the ventricular layer first covers the entire thickness of the neuroepithelium and is a layer of neuroblast proliferation. Following proliferation the main tasks during brain development are to form three-zone pattern and its modifications through migration, pathfinding, connection and in the meantime myelination. *Pax6* is expressed in the developing brain and should be involved in one or several such tasks. So what is *Pax6* doing during brain development ? As mentioned in section 1.8.4, Altman and Bayer (1995) divided prenatal brain development into three stages according to the structural features that indicate the distribution of germinal epithelium. The first stage (day 11.0 p.c. to day 14.0 p.c.) is characterized by rapid expansion of the primary germinal neuroepithelium. This first stage can be correlated well with the rapid expansion of *Pax6* expression in the ventricular layer during the same period. The second (intermediate) stage (from day 15.0 p.c. to day 18.0 p.c.) is characterized by the addition of secondary germinal epithelium and the maintenance of prominent primary germinal neuroepithelium. Looking at the present *Pax6* expression data in the developing brain, the addition of external granular germinal epithelium in the cerebellar primordium and pontine neuroepithelium and the secondary germinal epithelium in the telencephalic region during this period best fits the definition by Altman and Bayer. The third stage (from day 20.0 p.c. to day 22.0 p.c) which is characterized by the gradual dissolution of the germinal epithelium is also correlated with the rapid reduction of *Pax6*-expressing area in the developing brain, except the cerebellum. The correlation of areas of expression and its developmental restriction with developmental events supports a role of *Pax6* in the proliferation of neuroblast cells.

The involvement of *Pax6* in neuroblast proliferation is also supported by a study reported by Schmahl *et al.* (1993). It was reported that 100 % (11 out of 11 embryos examined) of homozygous (Sey^{neu} /Sey^{neu}) embryos exhibited reduced cell content in the cortical plate and hypocellularity in the intermediate zone. In contrast, the heterozygous littermates exhibited the same condition for only 12.5 % (11 out of 16 embryos examined) and none (0 out of 11 embryos examined) of the wildtype littermates exhibited the same abnormality (Schmahl *et al.*, 1993). The hypocellularity in the cortical plate and in the intermediate zone may be due to impairment of neuroblast proliferation or migration or

both. Warren and Price (1997) reported that diencephalic proliferative rates were abnormally low in mutants and the low proliferative rate lead to a depletion of the proliferative precursor pool. This resulted in a reduction in total diencephalic cell numbers in homozygous (*Sey/Sey*) mutants. Thus, normal expression of *Pax6* is required for the correct regulation of diencephalic precursor proliferation is concluded (Warren and Price, 1997). However, possible impairment of neuroblast migration in mutants can not be excluded for several reasons: (1) Regional differences in the diencephalic cell density that are normally found in the wildtypes as markers of prosomeric borders are lost in homozygous (*Sey/*Sey) mutants (Warren and Price, 1997). The markers of prosomeric borders are several transverse strips of low cell density that run dorsoventrally. The different cell density reflects regulation of the neuroblast distribution that is likely achieved through controlled migration. (2) Heterotopic groups of cells were found in the cerebral cortex of the homozygous mutant mice (Schmahl *et al.*, 1993; Grindley, 1996). Comparable heterotopic cell groups are also found in the cerebellum where neuroblast proliferation is also affected by *Pax6* mutation (van Heyningen, personal communication). These findings suggest that at least some neuroblasts have lost their normal distribution and are confined in groups. (3) *Sey/Sey* and +/+ cells are segregated into separate domains in the eyes of chimeras (Quinn *et al.*, 1996), suggesting that cell interactions and normal distribution of neuroblasts are altered.

3.3.4.3.2 *Pax6* is involved in proliferation, migration, and neuronal connection in the neural retina

Pax6 transcripts are initially distributed in the whole area of optic cup and is gradually restricted there. This restriction is observed in many species. In the mouse, only the ganglion cells layer and the internal nuclear layer exhibits *Pax6* transcripts by day 18.0 p.c. as the result of developmental restriction. The underlying developmental events can be correlated with the distribution of *Pax6* transcripts in several steps: (1) At earlier stages, the main tasks for the development of the optic cup are proliferation and migration. The primitive optic cup acts as a single layer of germinal epithelium like the ventricular layer in the brain or spinal cord. Active mitosis is undertaken in the entire optic cup for neuroblast proliferation (Sidman, 1961; Robinson *et al.*, 1986). Migration is carried out by interkinetic movement. During these earlier stages, *Pax6* expression is detected within the entire optic cup. (2) Following the activities of proliferation and migration, differentiation and stratification of the optic cup is initiated. This included the formation of the pigmented retinal epithelium and layers of cells, including the internal plexiform layer. Once the inner plexiform layer has formed, the interkinetic migration becomes restricted to the 'cytoblast' layer, i.e. the region between the inner plexiform layer and the the outer limiting membrane (Robinson *et al.*, 1986). Nuclei of the dividing cells enter different phases of the cell cycle as they traverse different parts of the cytoblast layer. Thus, nuclei enter the M-phase and divide at the outer limiting membrane. After division, the daughter nuclei enter G_1 -resting phase and migrate through the outer part of the cytoblast layer. The nuclei enter S-phase as they reach the inner part of the cytoblast layer and remain in this phase until they reached the internal plexiform layer.

During S-phase, nuclei incorporate molecules they require for the replication of DNA. Nuclei enter G_2-resting phase during their return journey to the outer limiting membrane where they divide again (Sidman, 1961; Zavarzin and Stroeva, 1964; Denham, 1967; Robinson, 1986). During this period, *Pax6* expression disappears in the pigmented retina epithelium and is characterised by stratified patterns between the external limiting membrane and the internal plexiform layer. (3) At later stages, the main event of proliferation is replaced by neuronal connection. A functional neural retina demands two neuronal connecting sites, the internal and the external plexifrom layers, in order to send the impulses stimulated by light from the rod and cone photoreceptors through the nerve fiber layer (see figure 1.9; Kahle, 1986) and via the optic stalk to the higer visual centres (see figure 1.5). Cell bodies that are involved in the two connecting sites are the amacrine, horizontal, and bipolar cells in the internal nuclear layer and the ganglion cells in the ganglion cell layer. Both the internal nuclear layer and the ganglion cell layer exhibit intense *Pax6* expression at later stages from day 18.0 p.c. afterwards.

The correlation between the distribution of *Pax6* transcripts and the developmental events in the optic cup, as described above, suggests that *Pax6* is involved in the proliferation, migration, and neuronal connection in the neural retina. The pigmented retinal epithelium, after being differentiated from the neuroectoderm, does not contain *Pax6* transcripts by day 15.5 p.c. (Grindley *et al.*, 1995). The distribution of *Pax6* transcripts is developmentally restricted in close correlation to developmental events. This close correlation is not unique in the neural retina. Similar close correlations are also found in other *Pax6*-expressing regions and the functions of *Pax6* are further supported by evidence from mutant analysis (for example, the reduced cell content and hypocellularity mentioned in 3.3.2.1) and other experiments (to be further discussed in other sections).

3.3.4.3.3 *Pax6* is involved in initiation and proliferation during lens development

During lens development, *Pax6* is first expressed in the lens placode before invagination (Walther and Gruss, 1991; Grindley *et al.*, 1995). Following invagination, *Pax6* transcripts are distributed in the whole primitive lens (see figures 3.6.a; 3.7.a; b) and by day 13.0 p.c. are restricted within the anterior germinal epithelium which is the only source of secondary lens fiber (see figure 1.8a; b). Based on the distribution of *Pax6* transcripts during lens development, two developmental events have the chance of direct *Pax6* involvement, initiation of lens development and proliferation of lens cells. The role in proliferation is supported by the confinement of *Pax6* transcripts in the anterior germinal epithelium. *Pax6* in the initiation of lens development is supported by the absence of lens formation in the homozygous (*Sey/Sey*) mouse mutants (Hogan *et al.*, 1986; 1988). Furthermore, the loss of lens regenerating capacity in older axolotl eyes is accompanied by the decline of *Pax6* expression (Del Rio-Tsonis *et al.*, 1995). This also suggests a role of *Pax6* in the initiation of lens development. This aspect of *Pax6* function will be investigated in chapter 4.

3.3.5 Developmental expansion of *Pax6* expression and its implications

Developmental expansion is defined here as (1) a gene expresson that first appear in smaller areas of embryos during earlier stages of development and later the expression is expanded into larger areas, or (2) a *de novo* gene expression that is detected within newly formed tissues, for example the olfactory bulb, as the embryo develops. Section 3.3.5 will list examples of developmental expansion for *Pax6* and discuss their implications.

3.3.5.1 Examples and common aspects of developmental expansion for *Pax6* expression

Developmental expansion, like developmental restriction, is common for *Pax6* expression during mouse embryogenesis. Examples are in the secondary germinal neuroepithelium in the cerebral cortex, cerebellar neuroepithelium, surface layer of superior colliculus, and in the olfactory bulb. There are two common aspects in these areas: (1) All of these areas are not initially formed during early brain development; but as the brain develops, they are formed in the due time. (2) All of these areas are highly proliferative.

3.3.5.2 *Pax6* function as implicated by developmental expansion

The common aspects of developmental expansion explicitly imply *Pax6* functions in those areas. *Pax6* is either involved in the initiation or in the proliferation of those areas of developmental expansion.

The region that represents the future olfactory bulb in the anterior rhinencephalon is identifiable only after day 13.0 p.c. (Kaufman, 1992) and at the same time *Pax6* transcripts are found in the olfactory epithelium (see figure 3.4.l). By day 14.0 p.c., *Pax6* expression is seen in the rhinencephalic neuroepithelium where the future olfactory bulb is projected (see figure 3.5.o). Mutant analyses show that the olfactory bulb and nasal cavities are not formed in the *Sey/Sey* mouse (Hogan *et al.*, 1986; 1988). During vertebrate nasal development, the formation and invagination of nasal placode (to form the nasal epithelium) from the head surface ectoderm is coordinated with the formation of olfactory bulbs from the head neuroectoderm (Farman, 1992; Halasz, 1990). Therefore it is possible that *Pax6* transcripts in the olfactory epithelium and in the site of future olfactory bulb projection may coordinate in the formation of olfactory bulb and nasal cavity.

In the Sey^{neu} mutation, although the homozygous embryos fail to develop nasal cavities, a substantial proportion (10/16; 62.5%) of heterozygous embryos exhibit enlarged nasal cavities (Schmahl *et al.*, 1993). In the nasal epithelium, an even higher proportion (13/16; 81.2%) of the heterozygous embryos exhibit increased diameter of germinative epithelium as compared to their wildtype controls (Schmahl *et al.*, 1993). These findings suggest that *Pax6* may be more involved in the formation of nasal epithelium than of the nasal cavity. Furthermore, a trend of increasing the diameter of germinative

epithelium was also found in the frontonasal forebrain, the dorsal forebrain, the diencephalon and the cerebellum both in the heterozygous and the homozygous embryos (Schmahl *et al.*, 1993); all these ares are *Pax6*-expressing. It may therefore be possible that the failure of sufficient presumptive olfactory neuronal migration at early stages of embryogenesis leads to the failure of nasal placode invagination in the homozygous embryos. This possibility is, of course, to be further supported by experimental evidence.

In the cerebellar primordium, *Pax6* transcripts are seen as early as day 13.0 p.c. in the thin structure of primary germinal layer. As the cerebellum is expanded, areas of *Pax6* expression is expanded accordingly. Furthermore, *Pax6* transcripts are located in the gray matter (for example, see figure 3.10.g) where the nuclei are undertaking active mitotic activities. *Pax6* is therefore implied in the proliferation of the cerebellum neuroepithelium. Developmental expansion is also seen in the presumptive secondary germinal epithelium in the cerebral cortex and in the superior colliculus; both undertake highly mitotic activities. This also suggests a role of *Pax6* in cellular proliferation.

3.3.6 Conservation and deviation of *Pax6* functions as supported by comparing data across species

As mentioned in sections 3.1.1 and 3.1.4, the expression profiles and mutant phenotypes of *Pax6* and its orthologous genes will be compared in order to shed new insights on *Pax6* functions. Here, I list all *Pax6* gene expression profiles published so far and my data obtained in this study in table 3.1 (see next page). Readers are reminded that the published information may not describe every organ listed here. Thus, those organs that are listed as information 'not available' in table 3.1 do not necessarily mean non-expression, simply that no information regarding these regions is available. In the following sections (3.3.7.1 - 3.3.7.5), I will discuss comparison across species in different organs.

Table 3.1 Comparison of the normal *Pax6* expression regions in various species. All reported data on the expression of *Pax6* and its orthologous genes are listed. The terms for describing areas of expression are used following exactly those appeared in the cited publications. Areas of expression across species are listed on the basis of structural and functional similarity, although some species may not have a specified area that has been generally described as an organ. For example, the *Drosophila* does not have a spinal cord or nose, while the nematode does not contain an eye. Their comparable areas, however, are listed for comparison. Note that the names of genes and their mutations may vary from one species to another and whether they represent the orthologous *Pax6* gene or not, in particular the *vab-3* and *mab-18* genetic loci in the nematode, are open to debate. The published information may not describe every area listed here. Many areas are therefore listed as 'not available'. This does not necessarily mean non-expression, simply that no information regarding these regions is available.

Table 3.1 Comparison of the normal *Pax6* expression regions in various species.

Species	Drosophila	nematode	zebrafish	Xenopus	urodele	quail	chick	mouse/rat	human
Name of gene	*ey*	*Pax-6*;containing genetic locus *vab-3* and *mab*-18	*pax[zf-a]*	*Pax-6*	*pax-6*	*pax-QNR*	*Pax-6*	*Pax-6*	*PAX-6*
Name of mutation	*eyeless*	*vab-3*; *mab-18*	not available	not available	not available	not available	not available	*Small eye*	*Aniridia*
eye	expressed;absent in a mutant (ey^2)	expressed in the head hypodermal cells which may parallel the expression of vertebrate *Pax-6* in the surface ectoderm of the presumptive lens placode	first expressed as the optic vesicle formed, and then found in the optic cup and optic stalk, and also in the lens and cornea	expressed in the lens ectoderm and become confined in the anterior lens at latter stages; expressed in the whole retina and become confined in the ganglion cell layer and inner nuclear layer	expressed in the neural retina, the lens, the cornea epithelium	expressed in the neural retina, but not in the pigmented epithelium	expressed in the cornea, the lens, the optic cup, the optic stalk	expressed in the cornea, the lens, the optic cup, and the optic stalk; expression in the pigmented epithelium is restricted at later stages	expressed in the eye; particularly intense signals found in the neural retina; no definite expression in the pigmented epithelium
nose	not available	expressed in a broad domain across the developing head, including many head neurons	expressed in the olfactory bulb	not available	not available	not available	expressed in the nasal epithelium	expressed in the nasal epithelium	expressed in the olfactory bulb
brain	expressed in a bilaterally symmetrical pattern	as described in the nose counterpart area	expressed in the forebrain and hindbrain	expressed in the forebrain and hindbrain	not available	expressed in the forebrain and hindbrain, but not in the midbrain	expressed in the forebrain and hindbrain, but not in the midbrain	expressed in the forebrain and hind brain, but not the midbrain	expressed in the cerebellum and pons (both are parts of hindbrain); not reported in the forebrain
spinal cord	expressed in every segment of the ventral nervous system	not available	expressed in the spinal cord, extending from the first rhombomere to the posterior end of CNS	expressed	not available	expressed	expressed in the spinal cord along with the tract of somite formation	expressed in the spinal cord	not available
other regions	expressed in the salivary glands	expressed in a peripheral sense organ	expressed in the pituitary gland	not available	not available	expressed in the pancreas	expressed in the pancreas	expressed in the pancreas and in the pituitary	expressed in the pancreas
References	Quiring et al., 1994; Halder et al., 1995.	Chisholm and Horvitz, 1995; Zhang and Emmons, 1995.	Krauss et al., 1991; Puschel et al., 1992.	Hirsch and Harris, 1996.	Rio-Tsonis et al., 1995.	Martin et al., 1992; Carriere et al., 1993; Turque et al., 1994.	Li et al., 1994; Turque et al., 1994; this study.	Walther and Gruss, 1991; Goulding et al., 1993; Grindley et al., 1995; Turque et al., 1994; this study.	Ton et al., 1991.

3.3.6.1 In the eye

In the eye, all the species listed in table 3.1 (see preceding page) exhibit *Pax6* expression. This conserved expression of *Pax6* in the eye across species does indicate that *Pax6* has a major role in eye formation and this role is already specified in early period of phylogenesis. The importance of *Pax6* in eye development is further supported by the absence of eye in loss-of-function mutations in the human (Ton *et al.*, 1991), the mouse (Hill *et al.*, 1991), and the *Drosophila* (Quiring *et al.*, 1994). Furthermore, in the *Drosophila* ey^2 mutation (another lack of eye mutation similar to the *ey* mutation), the *ey* gene expression was found absent, futher suggesting that *ey* gene is directly involved in the development of eye (Quiring *et al.*, 1994). Despite the different morphology and the mode of eye development in the *Drosophila* as compared to that in the vertebrates, the most important and the strongest evidence comes from the artificial production of ectopic eyes by targeted expression of the *ey* gene (the orthologous *Pax6* gene in *Drosophila*) on the wings, the legs, and the antennae (Halder *et al.*, 1995).

By comparing *Pax6* expression in the eye region across species, however, some minor differences are found. For example, one difference exists in the pigmented retinal epithelium. Chick *Pax6* is expressed persistently in the pigmented retinal epithelium even at later stages (stages 17 - 18) (data in chapter 4), whereas mouse *Pax6* expression appears at early stages but becomes absent by around day 15.5 p.c. (Grindley *et al.*, 1995) and similar developmental restriction is observed for *Xenopus Pax6* expression (Hirsch and Harris, 1996). In the quail (Martin *et al.*, 1992; Carriere *et al.*, 1993) and in the human (Ton *et al.*, 1991), however, *Pax6* expression in the pigmented retinal epithelium have not been reported. This variation of *Pax6* expression implies a transient or dispensable role of *Pax6* there, particularly when the pigmented retinal epithelium is differentiated. The possible transient role of *Pax6* in the pigmented retinal epithelium is supported by data from Martin *et al.* (1992). They reported that quail neuroretina can differentiate into pigment and lens cells *in vitro*. *Pax-QNR* transcripts are found in the neuroretina and in the lens, but not in the transformed pigmented retinal epithelium (Martin *et al.*, 1992). Another example of difference exists in the rim of the optic cup where in the chick, the mouse, and the human, *Pax6/PAX6* was found to be most intensely expressed, whereas in the zebrafish (Krauss *et al.*, 1991; Puschel *et al.*, 1992), the urodele (Rio-Tsonis *et al.*, 1995), and the quail (Martin *et al.*, 1992; Carriere *et al.*, 1993; Turque *et al.*, 1994), no similar observation was reported. It is possible that the difference in the rim of optic cup between species may be due to a trend of gain-of-function for *Pax6* through the evolution of higher vertebrates. This is supported by mutant phenotypes, for that in the human *AN* mutation, the iris in the rim of optic cup is absent (Ton *et al.*, 1991), whereas in the mouse there is no report regarding the absence of iris in the *Small eye* mutants. This difference in the mutant phenotypes between the mouse and the human implies that *Pax6* is more crucial in the iris of the human than in that of the mouse. This deviation of *Pax6* function is probably gained through evolution.

3.3.6.2 In the nose

In the nasal region, *Pax6* is expressed in the nasal epitheliumin the chick (data in chapter 4) and the mouse (Walther and Gruss, 1991; Grindley *et al.*, 1995). In the mouse, *Pax6* is also expressed in the higher olfactory centres (this study). In the zebrafish (Krauss *et al.*, 1991; Puschel *et al.*, 1992) and the human (Ton *et al.*, 1991), the olfactory bulb is found expressing *Pax6*. In the nematode, although no olfactory organ can be specified, many head neurons are expressing *Pax6* (Chisholm and Horvitz, 1995; Zhang and Emmons, 1995). This consistent involvement of *Pax6* in the olfactory system in different species suggests a conserved role of *Pax6* there through evolution.

3.3.6.3 In the brain

In the brain, *Pax6*-expressing domains exhibit interesting deviations across species. In the nematode, *Pax6* expression is observed in a broad domain across the developing head (see table 3.1). The broad expression domains in the brain appear to have narrowed through evolution. In the brain of *Drosophila*, *ey* gene expression was found in a bilaterally symmetrical pattern without segmentation; in the spinal cord of *Drosophila*, *ey* gene is expressed in every segment of the ventral nervous system (*Drosophila* has dorsal nervous system and ventral nervous system; both are a part of its central nervous system) (Quiring *et al.*, 1994; Halder *et al.*, 1995). Whereas, in the zebrafish, *pax[zf-a]*expression in the brain is confined within the forebrain and hindbrain and the transcripts in the midbrain are excluded (Krauss *et al.*, 1991; Puschel *et al.*, 1992). Comparable exclusion of *Pax6* expression in the midbrain persists in the *Xenopus*, the quail, the chick, and the mouse; but *Pax6* remain expressing in the forebrain (see table 3.1 and references therein). In the human, *PAX6* transcripts were not detected in the forebrain (Ton *et al.*, 1991), suggesting that a further restriction of regional functions in the forebrain could have happened through the evolution of higher mammals.

What does the restriction of *Pax6* expression in the brain through evolution imply ? Could the restriction through evolution in the brain imply a role of *Pax6* in the embryonic segmentation as suggested for many homeobox-containing genes (Holland, 1988; Gaunt *et al.*, 1988) ? Since no homeotic transformation was found in *Pax6* mutations across species, it seems not to be the case. Instead, the restriction of *Pax6* expression in the midbrain (as found in the fish, chick, and mouse) and the forebrain (as found in the human) through evolution may reflect the changing roles for this gene from in primitive species 'for specification of sense-organ identity' as described by Zhang and Emmons (1995) or for 'head-region specification' as described by Chisholm and Horvitz (1995) to later become involved in more specilized and localized functions such as the eye and nasal formation or even the migration of neuroblasts as suggested by Schmahl *et al.* (1993) or proliferation of neuroblasts as suggested in this study.

Another deviation of *Pax6* expression in the brain across species is found in the rhombomeres. In the zebrafish (Krauss *et al.*, 1991; Puschel *et al.*, 1992) and the mouse (Walther and Gruss, 1991; Stoykova *et al.*, 1996), *Pax6* expression extends from the first rhombomere (r1), whereas in the chick the most anterior presence of *Pax6* transcripts is in rhombomere 3 (r3) (Li *et al.*, 1994). This deviation may reflect the dynamic nature of *Pax6* expression in the spinal cord. It may also reflect that the identity of r3 in the chick probably corresponds, through evolution, to r1 in the mouse and the zebrafish.

3.3.6.4 In the spinal cord

Based on all available information in the vertebrates so far, *Pax6* is consistently expressed in the spinal cord (see table 3.1). In the *Drosophila, ey* is expressed in every segment of the ventral nervous system (Quiring *et al.*, 1994) that is presumably comparable to the spinal cord in the vertebrates. Particularly interesting is that in the chick *Pax6* expression in the spinal cord appears to be coordinated with somitogenesis and appears to be more intense in the areas flanked by somites (data in chapter 4); this is not observed in other species. The conservation of *Pax6* expression in the vertebrate spinal cord indicates that *Pax6* functions there.

3.3.6.5 In the pituitary and pancreas

As listed in table 3.1, *Pax6* expression is conserved in the pancreas in four species and in the pituitary in two species according to the information so far available. However, no abnormality in the pituitary or the pancreas have been reported as one part of *Pax6* mutant phenotypes. This does not necessarily indicate that *Pax6* has no function in the pituitary or pancreas, for that it is unlikely that a gene is persistently expressed in a specific site through evolution without any function there. In fact, in gene knock-out experiments in the mouse, many regions where a gene is intensely expressed do not appear to exhibit abnormalities. Several arguments have been advanced to explain the lack of a striking phenotype when so-called important genes have been disrupted (Ferguson, 1994). For example, the gene may function in the specific region in a redundant way and is easily compensated by other genes. Alternatively, maternal factors that pass across the placenta may compensate for the knock-out functions. Both can constitute parts of the reason why the pituitary and the pancreas is not apparently affected by *Pax6* mutation. The pituitary is one part of the hypothalamus-pituitary-gonadal axis that regulates neuroendocrine activities of reproduction. In the hypothalamus, the paraventricular nucleus and supraoptic nucleus constitute the major source of neurons that synthesize the neurohormones vasopressin and oxytocin and send axons to the posterior lobe of the pituitary, i.e. the neurohypophysis (Knobil *et al.*, 1988); both nuclei are *Pax6*-expressing. The paraventricular nucleus has a greater variety of connectivity and cell types than does the supraoptic nucleus and accordingly is also involved in control of anterior pituitary (Armstrong, 1985) where the gonadotropic hormones are released. The heterozygous (*Sey/+*) mice for *Pax6* mutation are generally poor in breeding performance than wildtypes (Douglas Scott, personal communication). Furthermore, *Pax6* mutation in the nematode

exhibits defects in gonadogenesis in the male tail and the identity of one pair of male-specific genital sensilla (a simple male reproductive sense organ) is transformed (Chisholm and Horvitz, 1995; Zhang and Emmons, 1995). It is therefore possible that *Pax6* mutation may affect directly the function of pituitary and indirectly affect reproductive performance.

3.3.6.6 In the salivary gland

In the *Drosophila*, *ey* expression is seen in the salivary gland, whereas in the same area no expression is found in other species, except in the mouse whose tubules of serous gland are clearly *Pax6*-expressing (see figure 3.8.c). However, information about *Pax6* expression in other species is not reported so far. This aspect of *Pax6* is worthy of further investigation.

3.3.6.7 Deviations of *Pax6* expression and mutant phenotypes found in the head neural crest cells and in the upper incisor teeth

In the rat homozygous for the *Small* eye mutation, failure of *Pax6* function leads to impairment of neural crest migration in the midbrain region, whereas *Pax6* transcripts are not detected in the neural crest cells in the wildtype rats (Matsuo *et al.*, 1994). Neither in the mouse nor in the chick, is *Pax6* ever reported being expressed in the neural crest cells. In the mouse homozygous for the *Small eye* mutation, a shorter snout is observed (Hill *et al.*, 1991) and a cartilaginous rod-like structure that projects from the rostral part of cranial base is found (Kaufman *et al.*, 1995). Most of the cells in the snout and rostral cranial base are contributed by neural crest cells (Le Douarin, 1981; Noden, 1986; see section 1.7). Thus, they are not *Pax6*-expressing. In the mouse homozygous for the *Small eye* mutation, supernumerary upper incisor teeth (usually one or two) is found in the premaxillae area (Kaufman *et al.*, 1995). The area of upper incisor teeth is not *Pax6*-expressing either. Then, why are abnormalities found there ?

Pax6 mutation must affect those areas in an indirect way or during very early stages of embryogenesis. In the mouse, the earliest presence of *Pax6* transcripts are found at day 8.0 p.c. in the presumptive forebrain and hindbrain (Walther and Gruss, 1991). By day 8.0 p.c., the head neural crest cells are still at premigratory stage (Serbedzija *et al.*, 1992). This gives the opportunity for *Pax6* transcripts to affect the premigratory neural crest cells. Osumi-Yamashita *et al.* (1994) reported that the lateral edge of the prosencephalon produced crest cells which migrated to the frontonasal mass. On the other hand, cells at the anterior neural ridge in the prosencephalon contributed mainly to the head epithelium including the nasal placode (Osumi-Yamashita *et al*, 1994). Both the lateral edge and the anterior neural ridge are *Pax6*-expressing areas at 8.0 days p.c. (Walther and Gruss, 1991). The frontonasal mass constitutes a high proportion of the total mass of the snout. It is therefore possible that the failure of *Pax6* function can deter the migration of neural crest cells from the lateral edge of the prosencephalon toward the frontonasal mass, in a way comparable to the impaired migration of crest cells in the midbrain found in

the *rSey/rSey* mouse. Thus, a shorter snout is found. Alternatively, the loss of *Pax6* function may detour neural crest cells toward the premaxillae area instead of the frontonasal mass. Thus, supernumerary upper incisor teeth are induced by the astrayed crest cells. One may also speculate that the failure of nasal placode formation in the *Sey/Sey* mouse is presumably caused to some extent by the failure of neural crest contribution from the anterior neural ridge of the prosencephalon.

Pax6 may not be directly involved in the contribution of neural crest cells in the affected areas where *Pax6* transcripts are not present in the wildtypes. In the premaxillae area, for example, no obvious tissue mass reduction comparable to that of the snout is reported. Therefore, it is possible that the formation of the supernumerary upper incisor teeth as well as the rod-like structure in the *Sey/Sey* mouse is not due to abnormal neural crest migration. Instead, *Pax6* may indirectly affect its downstream genes when it is mutated and leads to local abnormalities that are not necessarily located within its expression areas. This possibility will be further investigated in chapter 5.

3.3.7 *Pax6* expression in relation to neuromeric regionalization

Pax6 expression generally respects neuromeric regionalization in both the prosomeres and rhombomeres (Stoykova and Gruss, 1994). In the dorsal border of p1 (prosomere 1) and mesencephalon, transcripts of *Pax6* do not trespass the mesencephalic side (Stoykova and Gruss, 1994; Stoykova *et al.*, 1996; Mastick *et al*, 1997). In the ventral border of r1 and mesencephalon, *Pax6* transcripts do not trespass the mesencephalic side, either (Stoykova *et al.*, 1996). While *Pax6* expression in relation to neuromeric regionalization is considered, it should be noted that the earliest mouse *Pax6* transcripts in the brain are detected by day 8.0 p.c. (Walther and Gruss, 1991). The first immunoreactive neurons (using neuron-specific class III β-tubulin as a marker) appear at day 8.5 p.c. and the first axons appear at day 9.0 p.c. (Easter *et al.*, 1993). The prosomere formation is defined at around day 10.5 p.c. (Puelles and Rubenstein, 1993). *Pax6* has a potential involvement in all the events that occurs after its expression.

Neuromeres are centers for the proliferation, migration, compartmentation, and differentiation of neuroblasts (Kallen, 1965; Layer and Alber, 1990; Fraser *et al.*, 1990; Fidger and Stern, 1993; Brigbauer and Fraser, 1994). What are the possible roles that *Pax6* is likely to play in respect of neuromeric regionalization ? *Pax6* is involved in the correct regulation of diencephalic precursor proliferation (Warren and Price, 1997). *Pax6* is also likely involved in the proliferation of neocortical neuroepithelium, cerebellar neuroepithelium and the spinal cord ventricular layer, as suggested by expression patterns. However, in the diencephalon and spinal cord, the role of *Pax6* in proliferation seems more transient as compared to that in the telencephalon and cerebellum. This is implied by the fact that at later stages *Pax6* transcripts remain in the whole neocortical neuroepithelium and cerebellar primordium, whereas, in the ventricular layer along the longitudinal axis of the spinal cord, *Pax6* transcripts almost disappear by around day 16.0 p.c. as illustrated by figure 3.7.α. Instead, by day 16.0

p.c., *Pax6* expression in the spinal cord is concentrated in the intermediate and marginal zones where neuroblast proliferation has not occurred (see figure 3.7.ε). In the diencephalon, only discreet regions (the dorsal and ventral branches of expression areas illustrated in figure 3.7) are *Pax6*-expressing by day 16.0 p.c.. Furthermore, *Pax6*'s role in regulating proliferation is in agreement with the fact that after day 16.0 p.c. the volume of the diencephalon and of the spinal cord is not increased as much as that of the telencephalon and of the cerebellum.

Instead of being persistently involved in the proliferation of neuroblasts in the diencephalon, *Pax6* plays multiple roles in boundary formation, regional patterning, neuron specification and axon guidance; all the roles presumably are playing parts or as parts of the processes in the establishment of neuromeric identity and they are supported by mutant analyses (Stoykova and Gruss, 1996; Warren and Price, 1997; Mastick *et al.*, 1997). *Pax6* may distinguish the identity of p1 from mesencephalon by controlling expression of some markers such as *Lim-1*, *Gsh-1*, and *Pax6* itself in the caudal prosencephalon (Mastick *et al.*, 1997). When *Pax6* is not functional, expression of the three markers disappear and the p1/mesencephalon boundary is lost. The result is an anteriorization of the expression of *Dbx* (a mesencephalic marker) in the supposed p1 region (Mastick *et al.*, 1997). As no evidence of p1 deletion is found, the identity of p1 is apparently transformed to that of mesencephalon when *Pax6* is mutated. The involvement of *Pax6* in establishing p1 identity is probably not via building the border of expressing and non-expressing areas, as suggested by the sharp border between p1 and mesencephalon in wildtype brains. The strips of low cell density that correspond to p1/p2 and p2/p3 borders exist in wildtype brains (Warren and Price, 1997) and they are within the *Pax6*-expressing area without obvious downregulation (Mastick *et al.*, 1997). In the mutant mouse brain homozygous for *Sey* mutation, the strips of low cell density are lost together with the expression of *Lim-1,Gsh-1,* and *Pax6* itself in the p1 region, while the p1/p2 and p2/p3 boundaries remain expressing truncated *Pax6* transcripts (Warren and Price, 1997; Mastick *et al.*, 1997). Thus, unless the regulation of boundary formation for p1/mesencephalon differs from that of p1/p2 and p2/p3, border-building of *Pax6*-expressing and non-*Pax6*-expressing areas is unlikely to help establish p1 identity.

Interneuromeric cells are known to divide at a lower rate than those in neuromeres (Martinez *et al.*, 1992). *Pax6* could directly or indirectly inhibit proliferarion of interneuromeric cells to form the strips of low cell density observed by Warren and Price (1997). Alternatively, *Pax6* could direct formation of transversely oriented axons or glial cells like those observed in the rhombomeric boundaries (Lumsden and Keynes, 1989; Keynes and Lumsden, 1990). The axons or glial cells can exert a cell migration limitation that has been found in the p1/mesencephalon boundary in the chick (Figdor and Stern, 1993). This possibility is supported by the co-increase of vimentin (a marker for radial glial or glial precursors) and *Pax6* expression in the chick rhombomeric boundaries (Heyman *et al.*, 1995).

Pax6 could also be important for axonal projection by means of neuromeric regionalization. *Small eye* mutants exhibit errors in tpoc (tract of the postoptic commissure) axon pathfinding (Mastick *et al.*,

1997). The errors include axon projections that are too far into cerebral vesicle and far more axons that form loops, as well as the failure of tpoc caudal projection to project from p3 into p2 in contrast to that pass as far as p1/mesencephalon boundary in the wildtypes (Mastick *et al.*, 1997). All the errors may well have resulted from the failure of neuromeric regionalization that characterizes local identity at both the cellular and molecular levels in which *Pax6* is involved.

3.3.8 Conclusion: *Pax6* functions in a multiple, tissue-dependent and stage-dependent way during development

The expression and mutant phenotypes discussed in previous sections allows a conclusion that *Pax6* functions in a multiple, tissue-dependent and stage-dependent way during embryonic development. The first line and the most ancient *Pax6* function could be for the proliferation and specification of head regions, including the establishment of sense-organ identity in the developing CNS and in the head surface ectoderm. More specific and localized lines of functions for *Pax6* was developed through evolution. In the brain, neuroblast migration, axon projection and pathfinding has likely added to *Pax6* functions in higher animals. Likewise, the roles of *Pax6* in eye development have likely evolved from establishing an optic nerve forming bias to more specilizd functions such as lens and optic cup differentiation. These more localized and specilized functions of *Pax6* are reflected by the developmental restrictions observed in *Pax6*-expressing areas in different species. However, developmental restriction does not deviate *Pax6* function as a master visual or olfactory gene. The extensive presence of mouse *Pax6* transcripts in the higher visual and olfactory nervous systems as well as external and accessory apparatuses demonstrated clearly the conserved function of *Pax6* for the two systems.

Pax6 functions may also deviate in different tissues through evolution, as suggested by the not-so-conserved expression data in the pituitary, salivary gland and pancreas, although in the same species, *Pax6* could have slightly deviated functions in different tissues. For example, mouse *Pax6* is suspected to be more involved in the proliferation of neocortical neuroepithelium after day 16.0 p.c. as compared to that in the diencephalon. More obvious examples can be found in comparing *Pax6* function in the lens or cornea with that in the brain. *Pax6* functions may also differ according to developmental stages, as suggested by expression data in the retina and in the lens.

To carry out such multiple functions with a variety of tissue- and stage-dependence, *Pax6* must be posed in a complicated hierachy of gene activities with upstream and downstream genes that presumably are different according to tissues and gestational stages. Some genes in the hierachy are beginning to emerge. This is to be discussed further in chapter 5.

Keys for mouse *Pax6* expression

1. third ventricle
2. neocortical neuroepithelium
3. neuroepithelium in the trunk spinal cord
4. neuroepithelium in the cervical spinal cord
5. medullary neuroepithelium
6. surface ectoderm covering optic vesicle region
7. neuroepithelim enclosing optic vesicle
8. hypothalamic neuroepithelium
9. telencephalic neuroepithelium
10. neuroepithelium of middle cervical spinal cord
11. neuroepithelium of ventral cervical spinal cord
12. second branchial arch
13. mandibular component of first branchial arch
14. neuroepithelium forming optic cup
15. hypothalamic neuroepithelium in the ventral diencephalon
16. pontine neuroepithelium
17. velum medullare
18. border between ventral pontine neuroepithelium and dorsal medullary neuroepithelium
19. optic stalk formation
20. pituitary primordium
21. trigeminal (V) ganglion
22. fourth ventricle
23. neuroepithelium in the ventral medulla
24. neuroepithelium in the border of ventral pons and dorsal medulla
25. hypothalamic (ventral diencephalic) neuroepithelium
26. lens primordium
27. optic cup
28. pigmented retinal epithelium
29. amygdala (differentiation field)
30. neocortical neuroepithelium
31. ventricular layer of medullary neuroepithelium
32. otic vesicle
33. olfactory (nasal) epithelium
34. lateral ganglionic eminence
35. future piriform cortex
36. neuroepithelium in the ventral pons
37. conjunctiva
38. corneal epithelium
39. optic stalk [optic nerve (II)]
40. hypothalamic neuroepithelium in connection with optic stalk
41. pontine neuroepithelium
42. neuroepithelium of pallidum
43. cingulate cortex neuroepithelium
44. inferior sagittal dural venous sinus
45. pallidal neuroepithelium
46. neuroepithelium within the junction of striatum and pallidum
47. neural retina
48. optic recess
49. hypothalamic neuroepithelium
50. subicular neuroepithelium
51. striatum
52. roof of mesencephalon
53. mesencephalic vesicle
54. lamina terminalis
55. tectum
56. anterior tectal neuroepithelium
57. pretectum
58. posterior thalamus (intermediate/marginal zone)
59. anterior thalamus (ventricular zone)
60. aqueduct
61. pineal recess
62. floor of aqueduct
63. primitive habenulopeduncular tract formation
64. tegmentum
65. roof of ventral part of mesencephalon
66. lateral ventricle
67. roof of neopallial cortex
68. rhombic lip
69. choroid plexus in the fourth ventricle
70. posterior thalamus (ventricular zone)
71. medulla oblongata
72. choroid plexus in the lateral ventricle
73. midbrain reticular formation
74. motor neuron column in the medulla
75. superior central raphe nucleus (pontine)
76. infundibular recess
77. piriform cortex
78. frontal part of telencephalic vensicle
79. caudopallidal angle
80. ganglionic eminence
81. infundibulum (future pars nervosa)
82. vestibulocochlear ganglion (VIII)
83. medullary raphe
84. junction between fourth ventricle and central canal of spinal cord
85. extrinsic ocular muscle
86. first evidence of primitive eyelid
87. ventral telencephalic neuroepithelium
88. cervical spinal cord
89. medial ventricular zone of cervical spinal cord
90. primitive nasopharynx
91. vomeronasal organ (Jacobson's organ)
92. nasal cavity
93. primordium of first upper molar tooth
94. Meckle's cartilage
95. pinna of ear

96. motor neurons
97. upper cervical dorsal root ganglion
98. rim of optic cup
99. primary lens
100. proliferative zone of anterior germinal lens epithelium
101. future inner part of neural retina
102. tongue
103. anterior lens epithelium
104. external granular epithelium of pons
105. posterior neocortical neuroepithelium
106. internal capsule
107. surface of medulla oblongata
108. cerebellar primordium
109. anterolateral wall of thalamus
110. lateral piriform cortex
111. rhinencephalic neuroepithelium
112. ventricular neuroepithelium of rhinencephalon
113. rhinencephalic neuroepithelium (site of future olfactory bulb projection)
114. optic chiasma
115. saccule
116. glossopharyngeal (IX) ganglion
117. wall of third ventricle (ventricular zone)
118. wall of third ventricle (intermediate zone)
119. subcommisural organ
120. pineal primordium
121. presumptive external germinal layer of cerebrum
122. cerebellar primordium in junction with external granular layer of pons
123. external granular layer of cerebellar primordium
124. squamous part of occipital bone
125. cerebellar germinal trigone
126. hypothalamic differentiating field
127. anterior premedullar neuroepithelium
128. lateral recess of fourth ventricle
129. paraventricular nucleus
130. fields of Forel
131. zona incerta
132. intermediate thalamic neuroepithelium
133. pontine subventricular zone
134. reticular nucleus
135. central canal of anterior spinal cord
136. choroidal fissure
137. hippocampal neuroepithelium (Ammon's horn)
138. dorsal lateral geniculate nucleus
139. supraoptic nucleus
140. lateral hypothalamic differentiation field
141. bed nucleus of strial terminalis
142. medial forebrain bundle
143. stria medullaris
144. medial amygdala
145. dentate gyrus neuroepithelium
146. strionuclear neuroepithelium
147. nasal septum
148. lateral preoptic nucleus
149. lateral amygdaloid nucleus
150. stria terminalis
151. sign of external germinal layer formation
152. lateral preoptic region (anterior hypothalamus)
153. lateral thalamus (anterior)
154. oropharynx
155. third ventricle (thalamic and hypothalamic)
156. cartilage primordium of sphenoid bone enclosing optic chiasma
157. lateral posterior nucleus
158. intermediate thalamus (differentiation field)
159. anterior pretectal nucleus
160. ventral lateral geniculate nucleus
161. subthalamic nucleus
162. conjunctival sac
163. primordium of right upper molar tooth
164. midbrain differentiation field
165. junction between medial geniculate nucleus and ventral lateral geniculate nucleus
166. basomedial amygdaloid nucleus
167. red nucleus in tegmentum
168. superior colliculus (deep layer)
169. mammillary neuroepithelium
170. hypothalamus (posterior)
171. lateral deep nucleus (migration)
172. ventral tegmental nucleus (pontine)
173. aqueduct (tegmental and superior tectal)
174. cerebellar neuroepithelium
175. magnocellular reticular nucleus
176. cochlear nucleus (differentiation field)
177. pons
178. basiocciput
179. thymus (right lobe)
180. entrance into trachea
181. thyroid
182. entrance into esophagus
183. premedullary neuroepithelium
184. body of cervical vertebra
185. scapula
186. tranverse processes of cervical vertebra
187. lung
188. cervical vertebra
189. cervical dorsal root ganglion
190. ependymal layer
191. intermediate zone
192. marginal layer
193. primordium of incisor teeth
194. tubules of serous gland
195. nasal epithelial tissue

196. olfactory bulb
197. rhinencephalon (differentiation field)
198. primordium of lower molar tooth
199. medial septum
200. lateral migratory stream
201. external nuclear layer of retina
202. external plexiform layer of retina
203. internal nuclear layer of retina
204. ganglion cell layer of retina
205. nerve fiber layer of retina
206. anterior chamber
207. eyelid
208. internal surface of eyelid
209. nerve pathways outside of brain
210. junction between ventrolateral and dorsolateral nuclear complex
211. intermediate zone of lateral telencephalic neuroepithelium
212. epithalamic recess
213. amygdaloid fork of lateral ventricle
214. medial geniculate complex
215. ventrobasal nuclear complex
216. cerebral peduncle
217. anterior pons (differentiation field)
218. trigeminal boundary cap
219. junction between medial geniculate nucleus and red nucleus
220. superior olivary nucleus
221. superior tectal neuroepithelium
222. superior colliculus
223. aqueduct (superior tectal/tegmental)
224. lateral vestibular nucleus/ventral tegmental nucleus
225. pontine reticular formation
226. anterior pontine neuroepithelium
227. isthmus
228. medullary reticular formation
229. cerebellum
230. aqueduct (inferior tectal)
231. neuroepithelium of olfactory bulb
232. anterior olfactory nucleus
233. cartilage primordium of sphenoid bone
234. fornix
235. diagonal band (vertical limb)
236. diagonal band (horizontal limb)
237. intermediate hypothalamic neuroepithelium
238. endopiriform nucleus
239. lateral hypothalamus (differentiation field)
240. pituitary cells within sella turcica
241. trigeminal ganglion (V) in Meckel's cave
242. ossification within cartilage primordium of hypophyseal fossa (sella turcica) of sphenoid bone
243. junction of reticular nucleus and ventral lateral nuclear complex
244. hippocampal neuroepithelium near dentate gyrus
245. lateral habenular nucleus
246. aqueduct (pretectal)
247. dorsal periaqueductal gray
248. cerebral peduncle lateral to trigeminal motor nucleus
249. trigeminal motor nucleus
250. cerebral peduncle lateral to superior olivary nucleus
251. principle trigeminal nucleus
252. facial motor nucleus
253. glomerular layer of olfactory bulb
254. external plexiform layer of olfactory bulb
255. mitral cell layer
256. internal granular cell layer of olfactory bulb
257. frontal neocortex
258. cortical plate
259. posterior hypothalamus
260. CA1 field
261. third ventricle (hypothalamic)
262. Purkinje cell layer of cerebellum
263. germinal epithelium of inferior olive
264. inferior olive
265. internal plexiform layer of olfactory bulb
266. basal ganglia
267. insular cortex
268. third ventricle (thalamic)
269. corpus callosum
270. hippocampal commisure
271. striatum
272. fimbria
273. subicular area
274. stria medullaris leading to fimbria
275. optic tract
276. epithalamus (pineal primordium)
277. parahabenular nucleus
278. external surface of pons
279. junction between tegmental reticular formation and hypothalamus
280. aqueduct (tegmental/pontine)
281. internal plexiform layer of retina
282. superior central raphe nucleus (isthmus)
283. taenia tecta

Figure 3.1 Mouse *Pax6* expression represented by *in situ* hybridization on tissue sections. The planes of cutting are shown in the schematic diagram (on the right panel of this page). (a). A coronal section in the posterior head region at day 9.5 p.c. *Pax6* expression is seen in the neuroepithelium enclosing the optic vesicle (no. 7) and in the surface ectoderm covering the optic vesicle region (no. 6). *Pax6* transcripts are also detected in the neuroepithelium in the cervical spinal cord (no. 4) and in the trunk spinal cord (no. 3). (b). A coronal section in the anterior head region at day 9.5 p.c. *Pax6* expression is detected in the telencephalic neuroepithelium (no. 9) and the neuroepithelium in the middle cervical spinal cord (no. 10). No *Pax6* expression is found in the second branchial arch (no. 12) and the mandibular component of the first branchial arch (no. 13). (c). A transverse section in the head region at day 10.0 p.c. *Pax6* expression is seen in the neocortical neuroepithelium in the telencephalic region (no. 2), the primitive optic cup (no. 14), the surface ectoderm covering the optic vesicle region (no. 6), and the border between ventral pontine neuroepithelium and dorsal medullary neuroepithelium (no. 18). The expression appears to extend to the velum medullare (no. 17). Note that a sharp demarcation between expressing and non-expressing areas can be seen at the hypothalamic neuroepithelium in the ventral diencephalon (no. 15). All scale bars represent 0.1 mm.

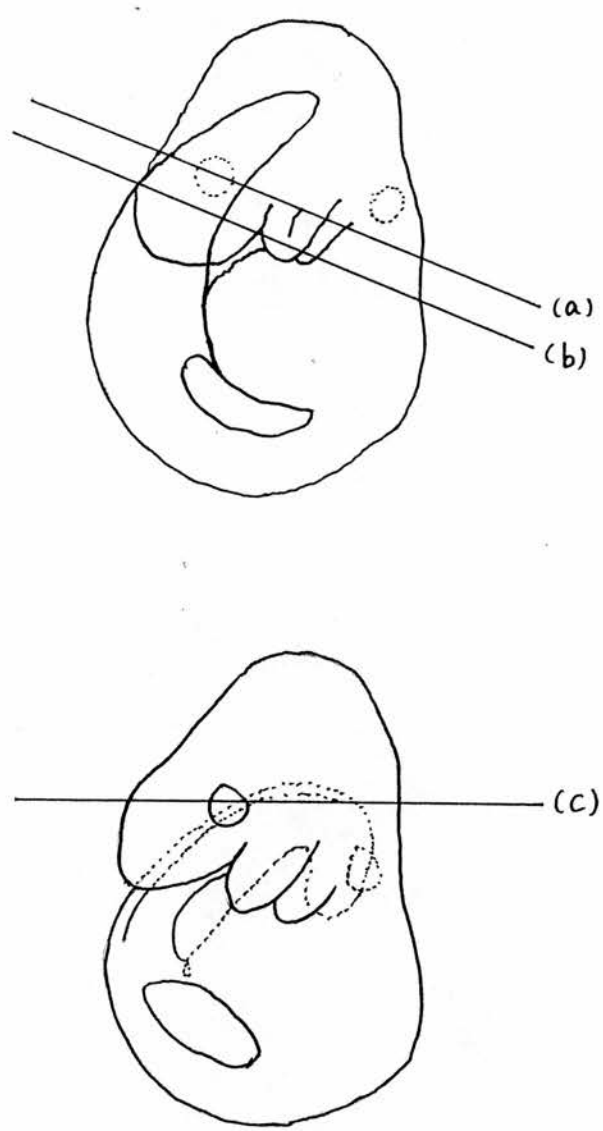

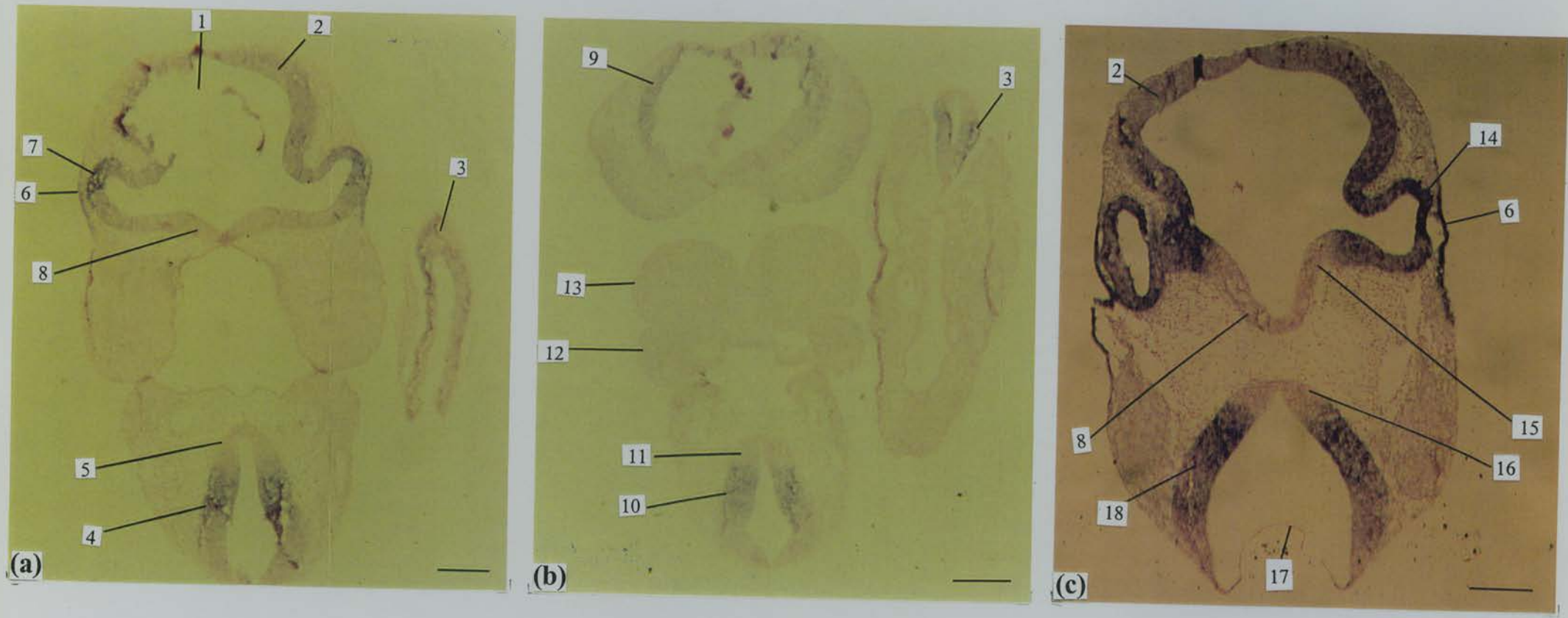
1
2
7
6
3
8
5
4
(a)
9
3
13
12
11
10
(b)
2
14
6
8
15
16
18
17
(c)

Figure 3.2 Mouse *Pax6* expression in the head region at day 11.0 p.c. represented by *in situ* hybridization on tissue sections. The planes of cutting are shown in the schematic diagram on the right panel of this page. (a) and (b) are transverse sections on different levels of the head region. (c) is a magnified view of the telencephalic region in (a). (d) is a magnified view of the pontine and the medullary region in (a). *Pax6* expression is seen in the neocortical neuroepithelium (no. 30), the optic stalk formation (no. 19), the differentiation field of the amygdala (no. 29), the pigmented retinal epithelium (no. 28), the optic cup (no. 27), the lens primordium (no. 26), the pituitary primordium (no. 20), the ventral medulla (no. 23), and in the neuroepithelium at the border of ventral pons and dorsal medulla (no. 24). *Pax6* transcripts are also seen in the olfactory epithelium (no. 33) and in the ventricular layer of the medullary neuroepithelium (no. 31). In the ventral telencephalon, a slim strip of *Pax6*-expressing cells can be traced toward the lateral ganglionic eminence (no. 34), i.e. from point A to point B as indicated in (c). In the rhombencephalon, symmetric 'comma-shape' areas of expression are seen, i.e. from point C (head of 'comma') to point D (tail of 'comma') as indicated in (d). All scale bars represent 0.1 mm in length.

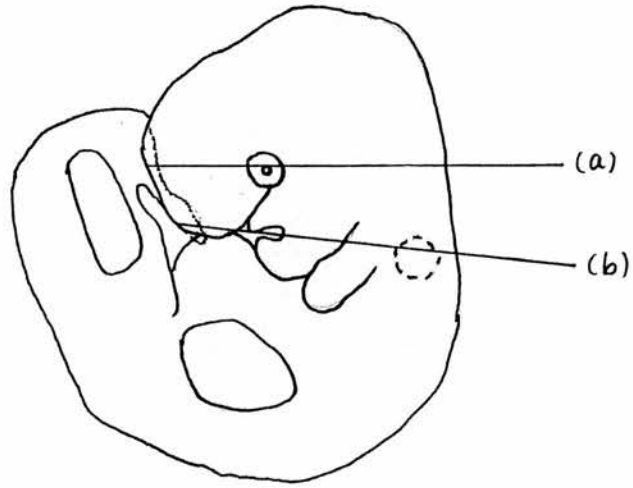

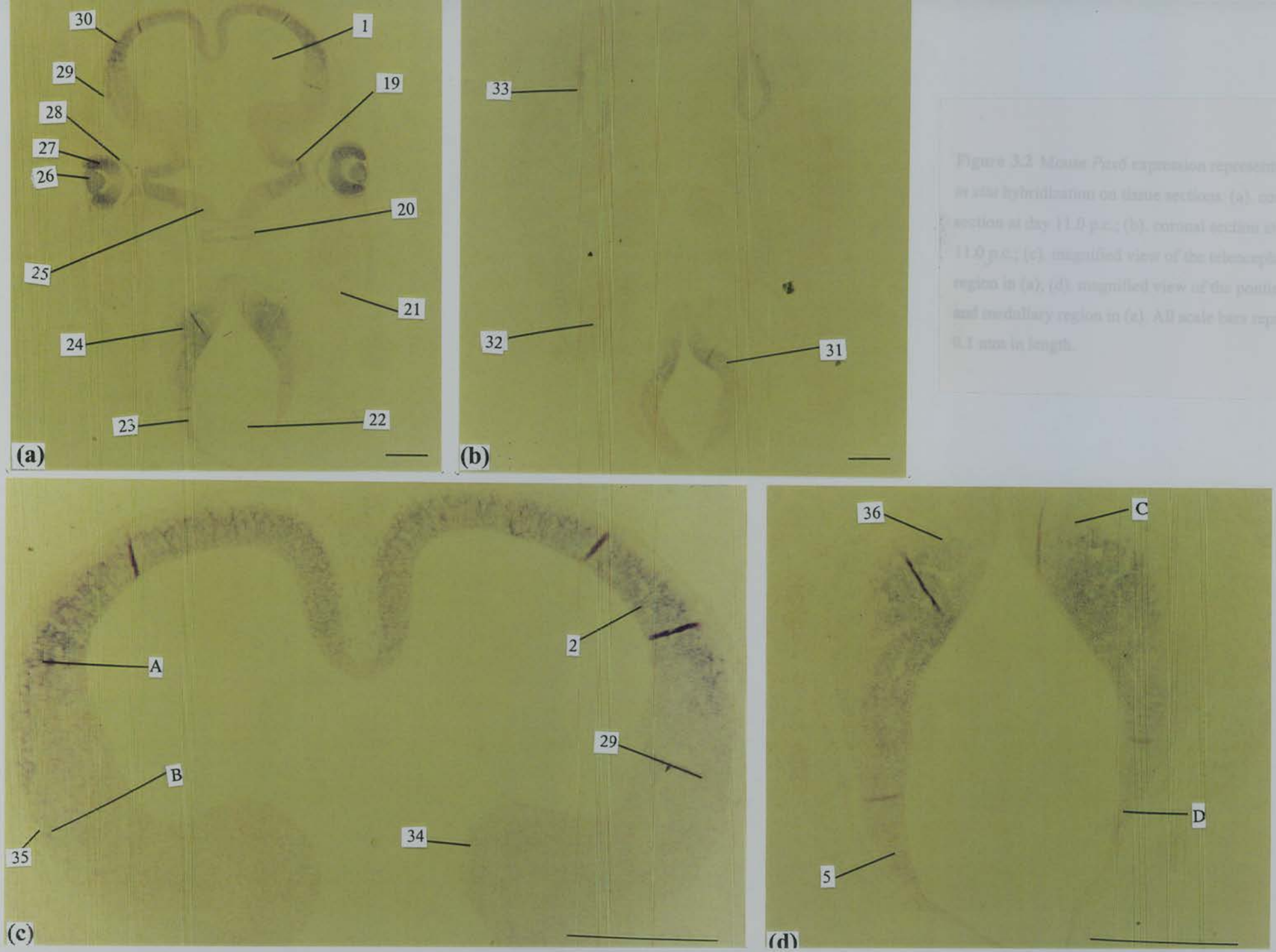
30
1
29
19
28
27
26
20
25
21
24
23
22
(a)
33
32
31
(b)
2
A
29
B
35
34
(c)
36
C
D
5
(d)

Figure 3.3 Mouse *Pax6* expression in the head region at day 12.0 p.c. represented by *in situ* hybridization on tissue sections. The plane of cutting is shown in the schematic diagram on the right panel of this page. (a) is a transverse section in the head region. (b) and (c) are magnified views to show the telencephalic region and the eye region. In the telencephalon, *Pax6* expression is seen in the neocortical (no. 2) neuroepithelium, cingulate cortex (no. 43), and in the subicular neuroepithelium (no. 50). *Pax6* transcripts can be traced through the junction of striatum and pallidum (no. 46) toward a site of the pallidal neuroepithelium where some *Pax6*-expressing cells are aggregated (no. 45). In the eye region, *Pax6* expression can be clearly seen in the neural retina (no. 47), pigmented retinal epithelium (no. 28), corneal epithelium (no. 38), the optic stalk (no. 39). A demarcation between expressing and non-expressing areas in the head surface ectoderm is seen in the conjunctiva (no. 37). In the hypothalamic neuroepithelium in conjunction with the optic stalk (no. 40), particularly around the optic recess (no. 48), *Pax6* transcripts are also detected. The pituitary primordium is also *Pax6*-expressing (no. 20). The medullary neuroepithelium (no. 5) also contains *Pax6* transcripts. Scale bars: in (a), 0.1 mm; in (b) and (c), 0.05 mm.

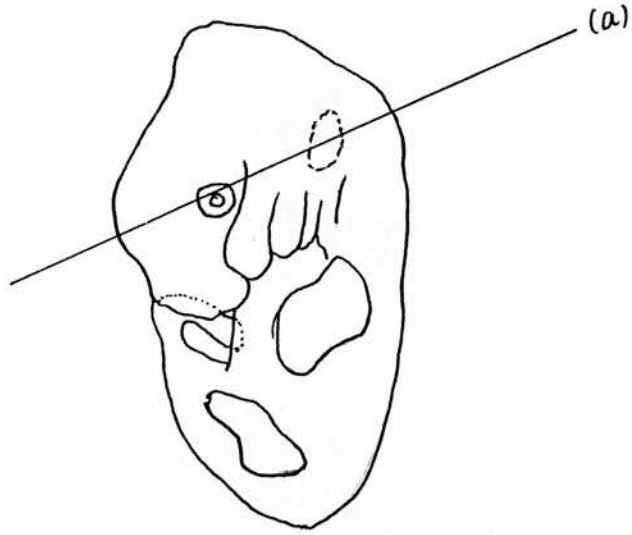

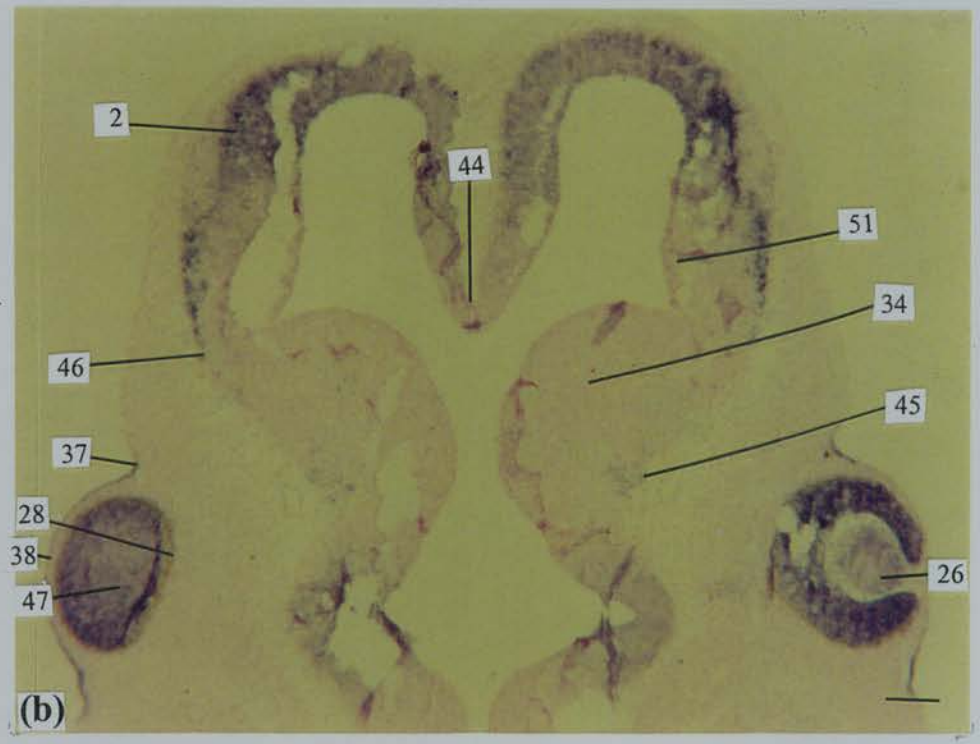

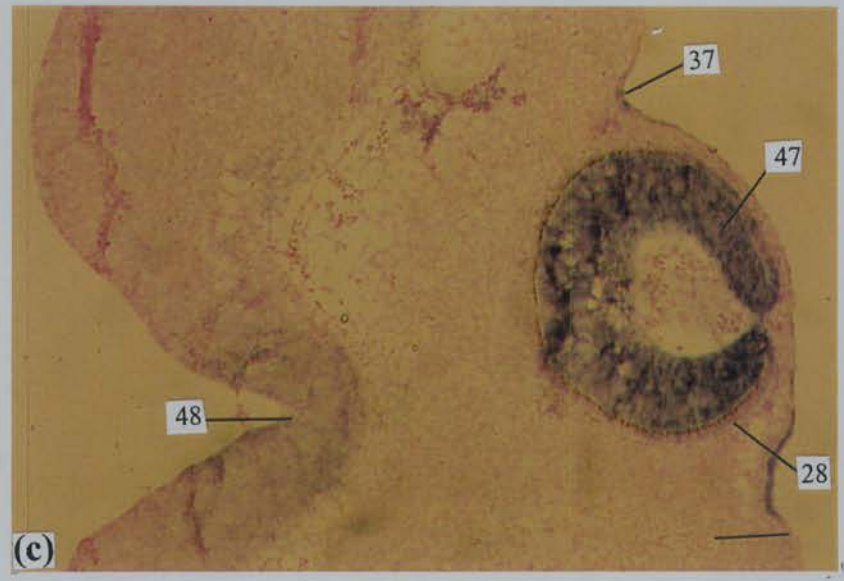

Figure 3.3 Mouse *Pax6* expression represented by in situ hybridization on tissue sections. (a): coronal section at day 12.0 p.c.; (b): magnified view of mesencephalic and diencephalic region of (a); (c): magnified view of the eye at day 12.0 p.c. Scale bars in length: a: 0.1 mm; b: 0.05 mm; c: 0.05 mm.

Figure 3.4 (a to h; to be continued on the following page) Mouse *Pax6* expression in the head region at day 13.0 p.c. represented by *in situ* hybridization on serial transverse tissue sections. The ventral side of each section points downwards. The planes of cutting are shown in a schematic diagram (on the right panel of this page). Sections from a to h are serial sections from top of the head. *Pax6* expression is detected in the lamina terminalis (no. 54 in a), anterior tectal neuroepithelium (no. 56 in b), pretectum (no. 57), posterior thalamus (no. 58), and anterior thalamus (no. 59) (see b and c). The pineal recess (no. 61), the primitive habenulopeduncular tract formation (no. 63), and the tegmentum (no. 64) are also *Pax6*-expressing (see d and e). As the levels of the transverse planes go further down, *Pax6* transcripts are seen in the roof of the neopallial cortex (no. 67 in f) and in the areas posterior (shown in f), lateral (in g), and anterior (in h) to the sulcus limitants (indicated by asterisks in f - h). *Pax6* expression in the neocortical neuroepithelium (no. 30 in h) is continuous within parts of the amygdala differentiation field (no. 29) and extends toward the epithalamus (indicated by arrows in h). In the midbrain and hindbrain regions, *Pax6* expression is detected in the tegmentum (no. 64 in f), the rhombic lip where the cerebellar primordium is formed (no. 68 in f), the midbrain reticular formation (no. 73 in h), and in the medulla oblongata (no. 71 in h). Note that *Pax6* expression is not seen in the choroid plexus (no. 69 in g and no. 72 in h). All scale bars represent 0.4 mm in length.

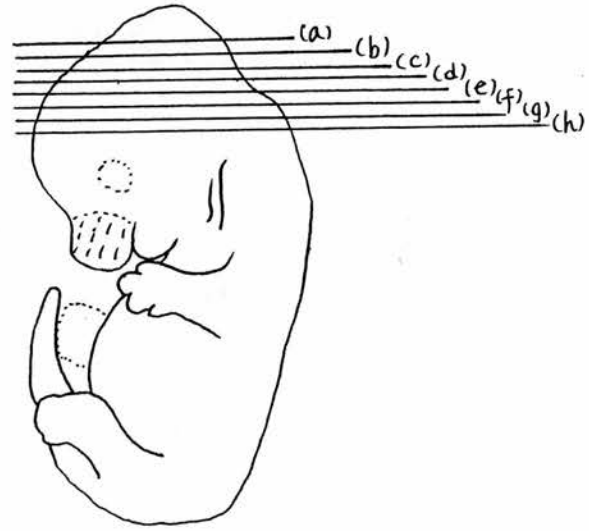

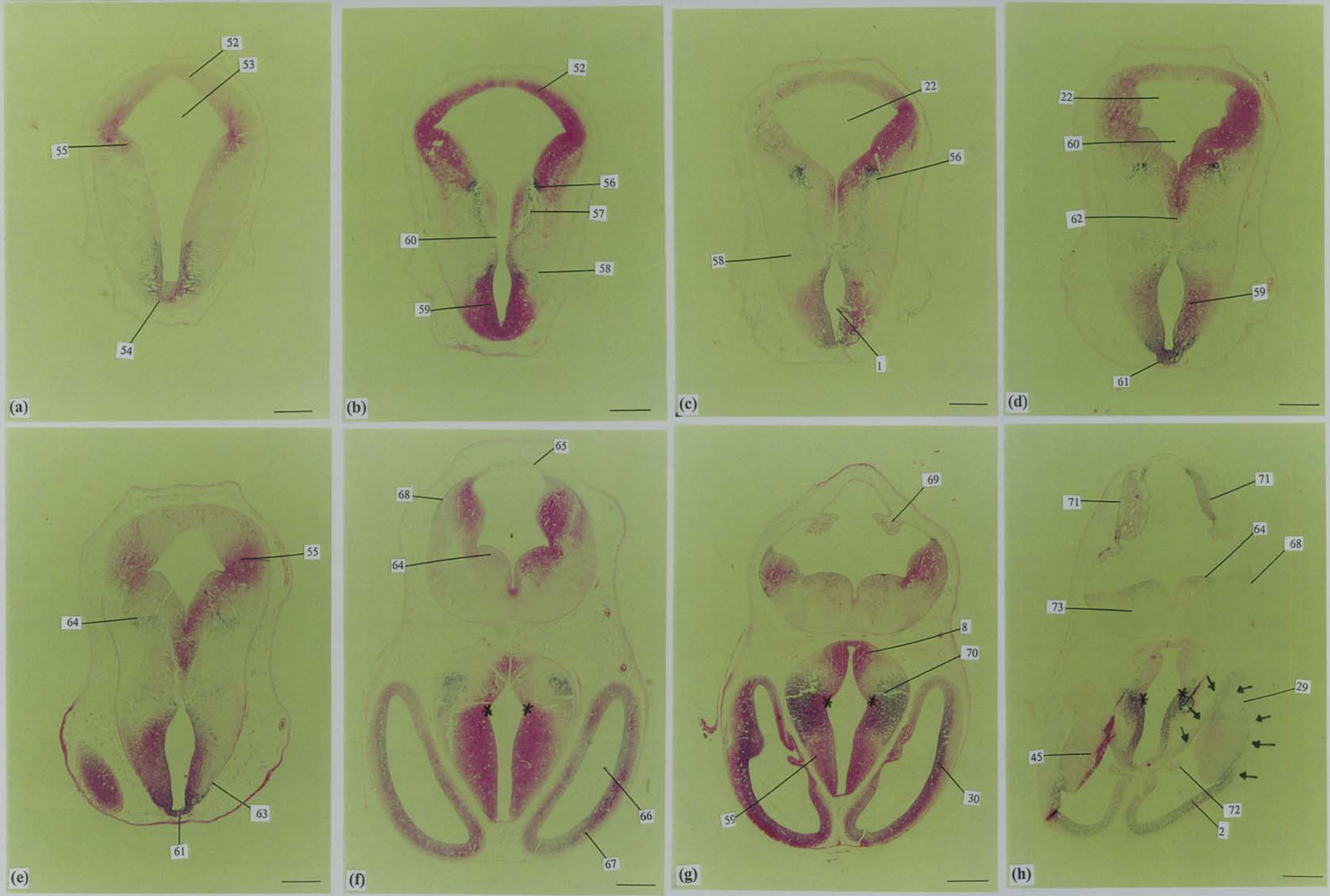
52
53
55
54
(a)
52
56
57
60
58
59
(b)
22
56
58
1
(c)
22
60
62
59
61
(d)
55
64
63
61
(e)
65
68
64
66
67
(f)
69
8
70
59
30
(g)
71
71
64
68
73
29
45
72
2
(h)

Figure 3.4 (i to m; continued) Mouse *Pax6* expression in the head region at day 13.0 p.c. In the telencephalon, *Pax6* expression is seen in the piriform cortex (no. 77 in i) and in the neocortical neurpepithelium including the site of caudopallidal angle (no. 79 in i) and the ventral telencephalic neuroepithelium (no. 87 in j). In the pontine area, *Pax6* expression is detected in the superior central raphe nucleus (no. 75 in i). *Pax6* transcripts are also seen in the motor neuron column in the medulla (no. 74 in i) and in the neuroepithelium surrounding the junction between the fourth ventricle and the central canal of the spinal cord (no. 84 in i). *Pax6* is also seen clearly in the olfactory epithelium (no. 33 in l). In the eye region, *Pax6* is expressed in the anterior lens epithelium (no. 103 in m), the proliferative zone of anterior germinal lens epithelium (no. 100 in m), the optc cup (no. 27 in l and nos. 28, 98, 101 in m), and the corneal epithelium (no. 38). Scale bars: in i - k, 0.4 mm; in l and m, 0.3 mm.

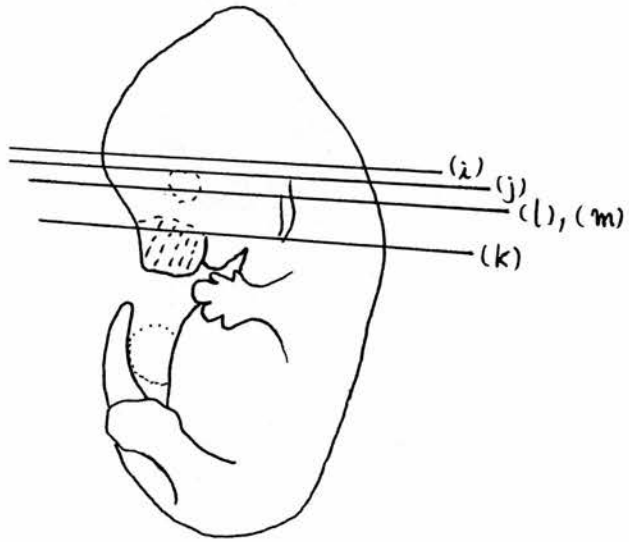

Figure 3.4 (day 13.0 p.c.; transverse sections; continued)

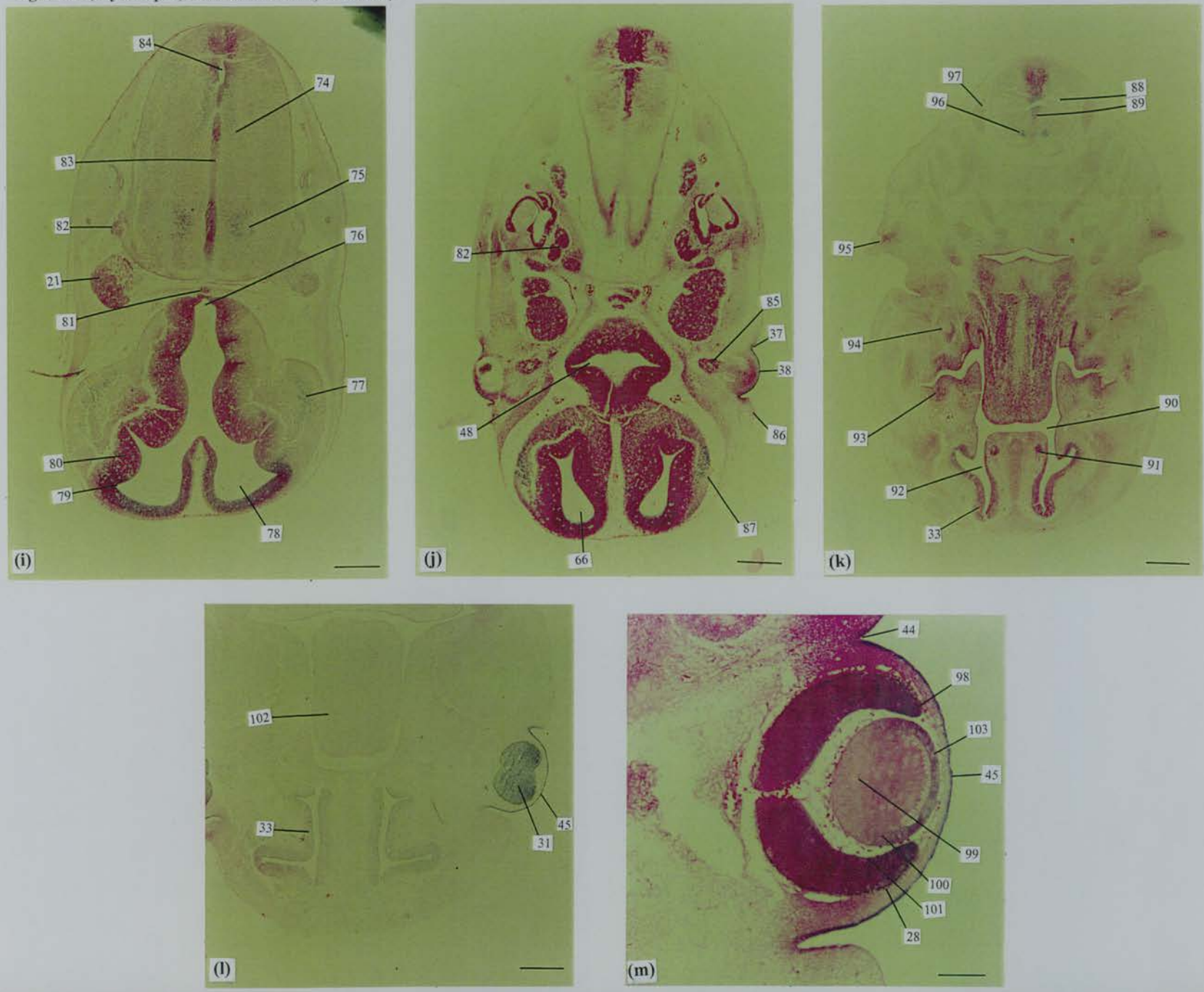

Figure 3.5 (a to h; to be continued on the following page) Mouse *Pax6* expression in the head region at day 14.0 p.c. represented by *in situ* hybridization on serial transverse tissue sections. The ventral side points downwards. The planes of cutting are shown in a schematic diagram (on the right panel of this page). In top of the head, *Pax6* expression is seen in the lamina terminalis (no. 54), anterior tectal neuroepithelium (no. 56), pretectum (no. 57), and posterior thalamus (no. 58) (in a and b). As the transverse plane is slightly lower, *Pax6* transcripts are seen in the pineal primordium (no. 120 in d), the primitive habenulopeduncular tract formation (no. 63 in d, e), and the tegmentum (no. 64 in d). In the telencephalon, *Pax6* expression is found in the whole neocortical neuroepithelium (no. 2 in e), including the posterior part (see no. 105 in h). *Pax6* expression is also detected in the thalamic neuroepithelium surrounding the sulcus limitans (indicated by asterisks in f, g, h) and in the amygdala differentiation field (no. 29 in h). In the midbrain and the hindbrain, *Pax6* transcripts are seen in the midbrain reticular formation (no. 73), the rhombic lip (no. 68), the tegmentum, (no. 64), the external granular epithelium of the pons (no. 104), and the medulla oblongata (no. 71). All scale bars represent 0.5 mm in length.

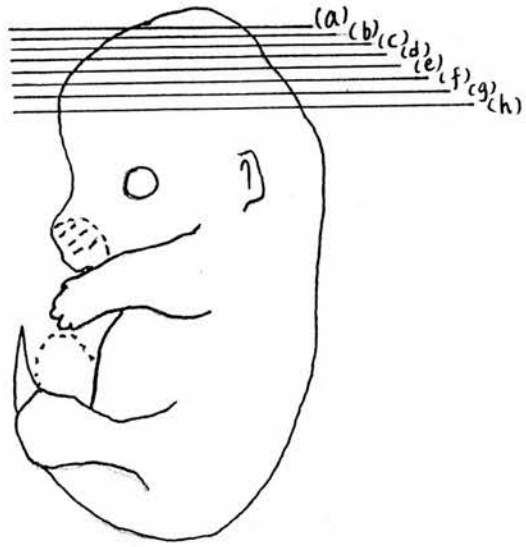

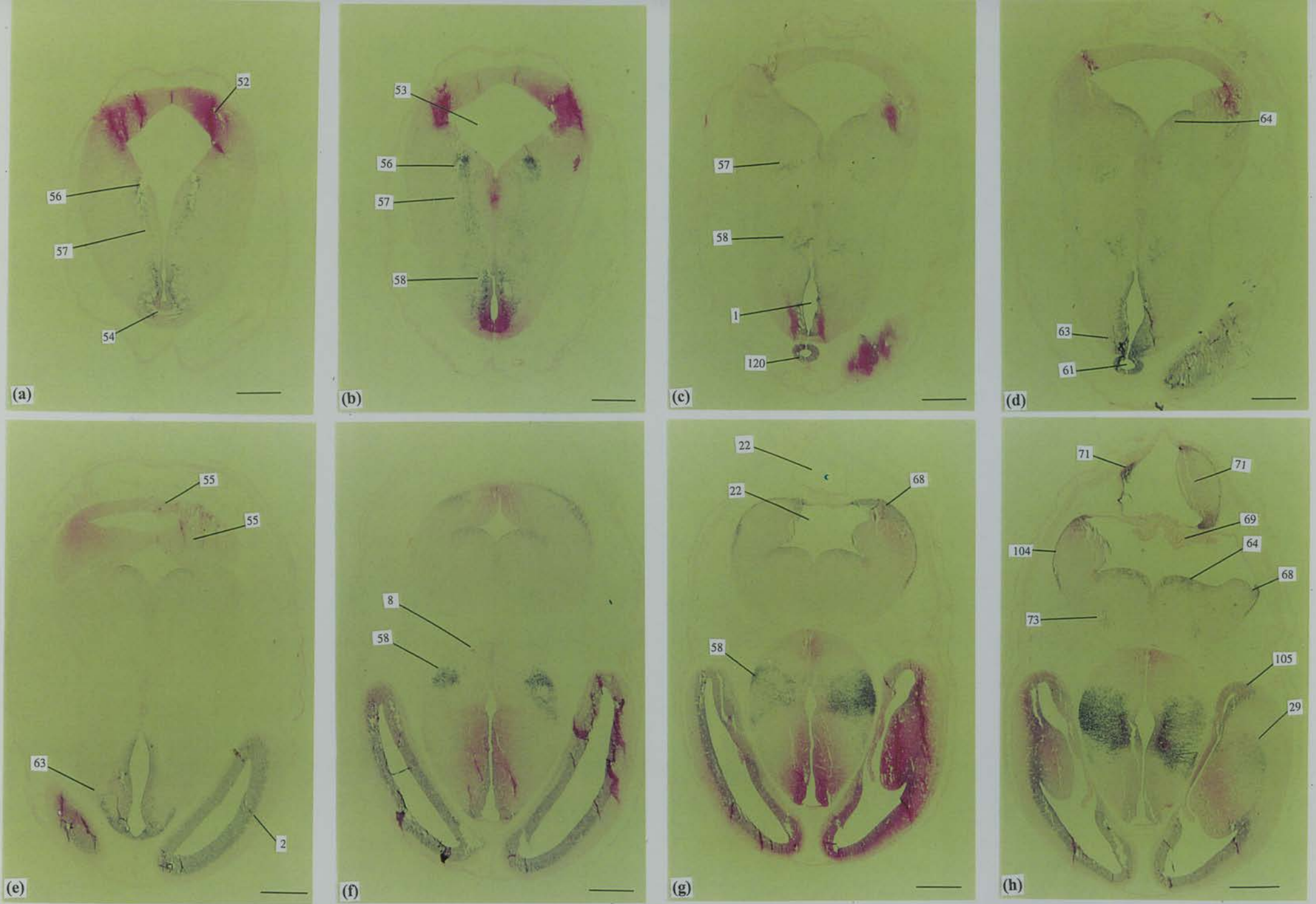
52
56
57
54
(a)
53
56
57
58
(b)
57
58
1
120
(c)
64
63
61
(d)
55
55
63
2
(e)
8
58
(f)
22
22
68
58
(g)
71
71
69
104
64
68
73
105
29
(h)

Figure 3.5 (i to p) Mouse *Pax6* expression in the head region at day 14.0 p.c. In the diencephalon, *Pax6* expression is seen in the floor of thalamus, including its anterolateral wall (no. 109 in j), but not in the internal capsule (no. 106) (in i, j). In the amygdala differentiation field, *Pax6* transcripts are found in the piriform (no. 77 in m) and the lateral piriform cortex (no. 110 in m). *Pax6* is also expressed in the rhinencephalon (nos. 111, 112 in n), in the rhinencephalic neuroepithelium where the future olfactory bulb projects (no. 113 in o), and in the pituitary primordium (no. 20 in l, m, n). In the midbrain, *Pax6* transcripts are detected in the vestibulocochlear ganglion (VIII) (no. 82), the tegmentum (no. 64), the pontine neuroepithelium (no. 41), and in the midbrain reticular formation (no. 73) (see j and k). In the hindbrain, *Pax6* is expressed in the cerebellar primordium (no. 108 in j), as well as in the medulla oblongata (no. 5 and no. 107 in k; no. 74 in l). In the spinal cord, *Pax6* transcripts are confined in the medial ventricular zone (no. 89) and in the motor neurons (no. 96) (in p). In the eye region, *Pax6* expression is detected in the optic chiasma (no. 114 in o), the corneal epithelium (no. 38 in p), the optic cup (particularly in the rim; see no. 98 in p), and the anterior lens epithelium (no. 103 in p). In the optic stalk, however, no *Pax6* expression is found (no. 39 in o). All scale bars represent 0.5 mm in length.

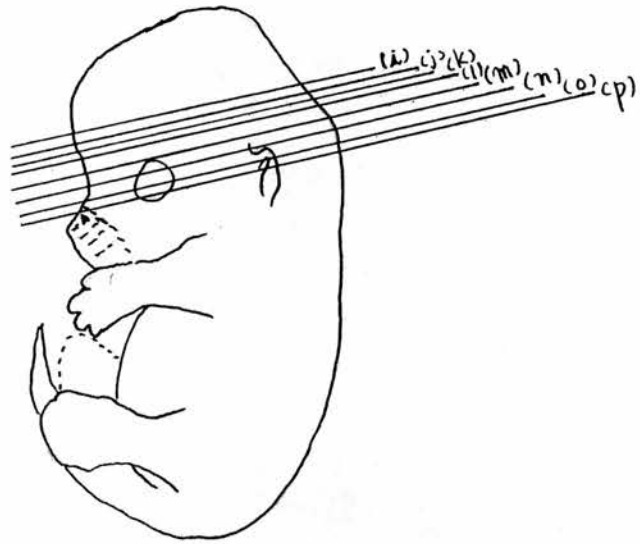

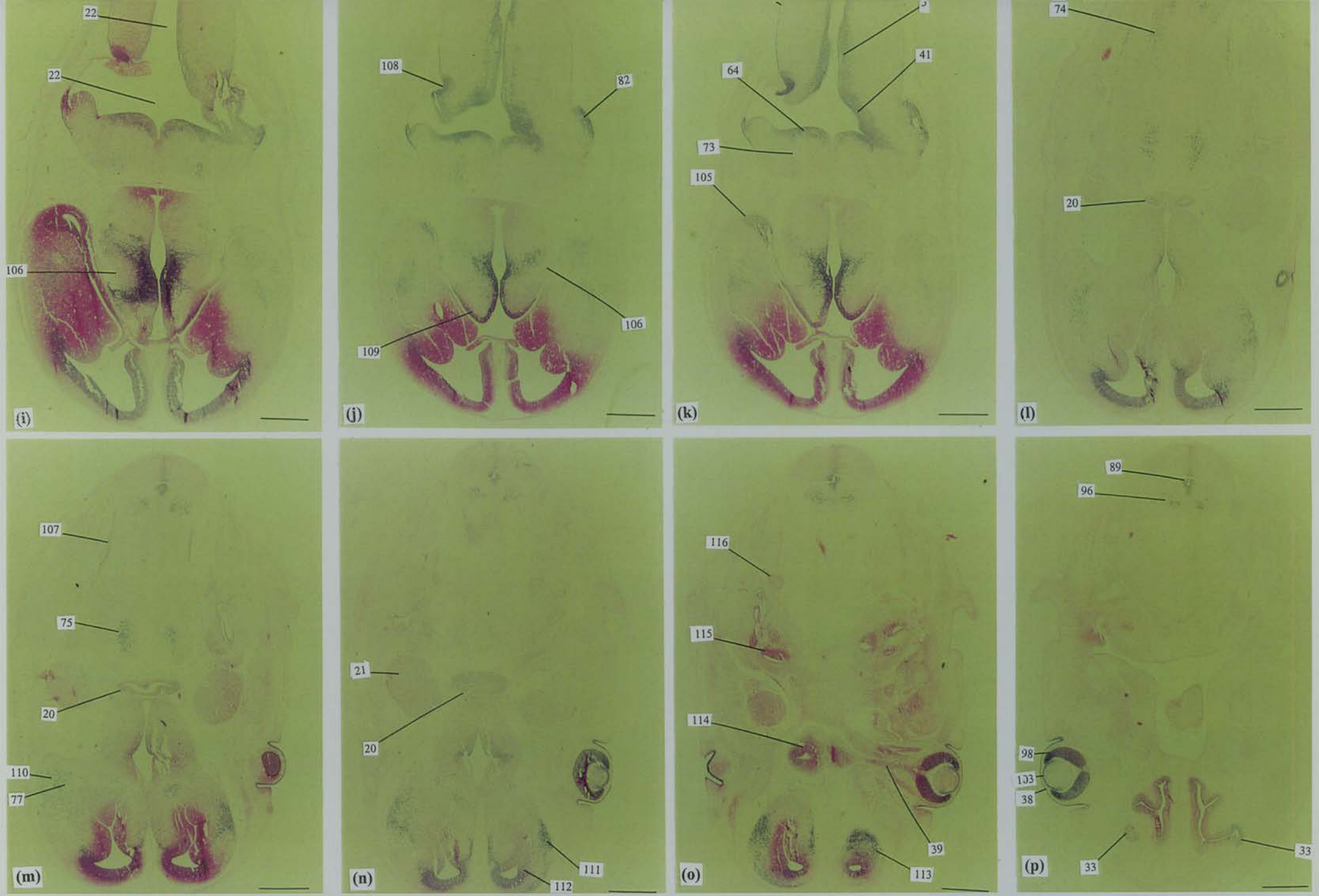
22
22
106
(i)
108
82
109
106
(j)
64
41
73
105
(k)
74
20
(l)
107
75
20
110
77
(m)
21
20
111
112
(n)
116
115
114
39
113
(o)
89
96
98
103
38
33
33
(p)

Figure 3.6 (a to h; to be continued on the following page) Mouse *Pax6* expression in the head region at day 15.0 p.c. represented by *in situ* hybridization on serial transverse sections. The ventral side points downwards. The planes of cutting are shown in a schematic diagram (on the right panel of this page). To view from top of the head, *Pax6* expression is first seen in the neuroepithelium surrounding the lamina terminalis (no. 54), the anterior tectum (no. 56), and the pretectum (no. 57) (see b), as well as in the neuroepithelium surrounding the third ventricle (no. 117 and no. 118 in c). On slightly lower transverse planes, *Pax6* transctipts are detected in the subcommissural organ (no. 119), the pineal primordium (no. 120), and in the telencephalic neuroepithelium (no. 9) (see c, d, e). In the telencephalon, *Pax6* expression is also seen in the presumptive external germinal layer (no. 121 in e) and in the primitive habenulopeduncular tract formation (no. 63 in g). In the midbrain, hints of *Pax6* expression appears in the junction between tegmental reticular formation and hypothalamus (no. 279 in d), the tegmentum (no. 64 in h), the cerebellar primordium in junction with external granular layer of pons (no. 122 in f, g), and in the external granular layer of cerebellar primordium (no. 123 in f). In the hindbrain, *Pax6* expression is detected in the medullary epithelium (no. 5 in h). All scale bras represent 0.5 mm in length.

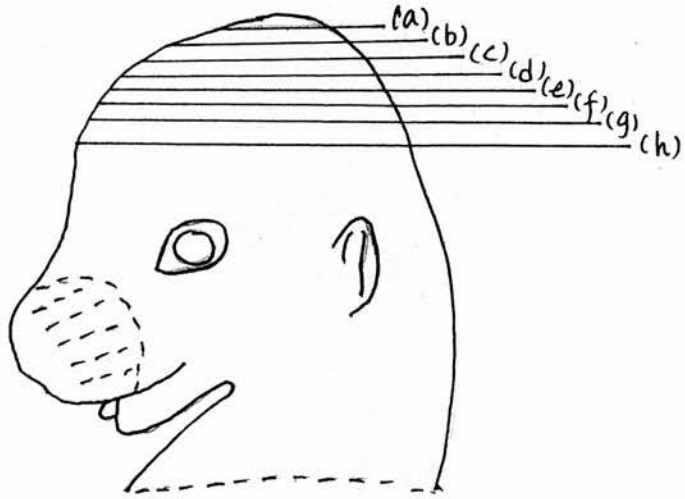

Figure 3.6 (day 15.0 p.c.; transverse sections)

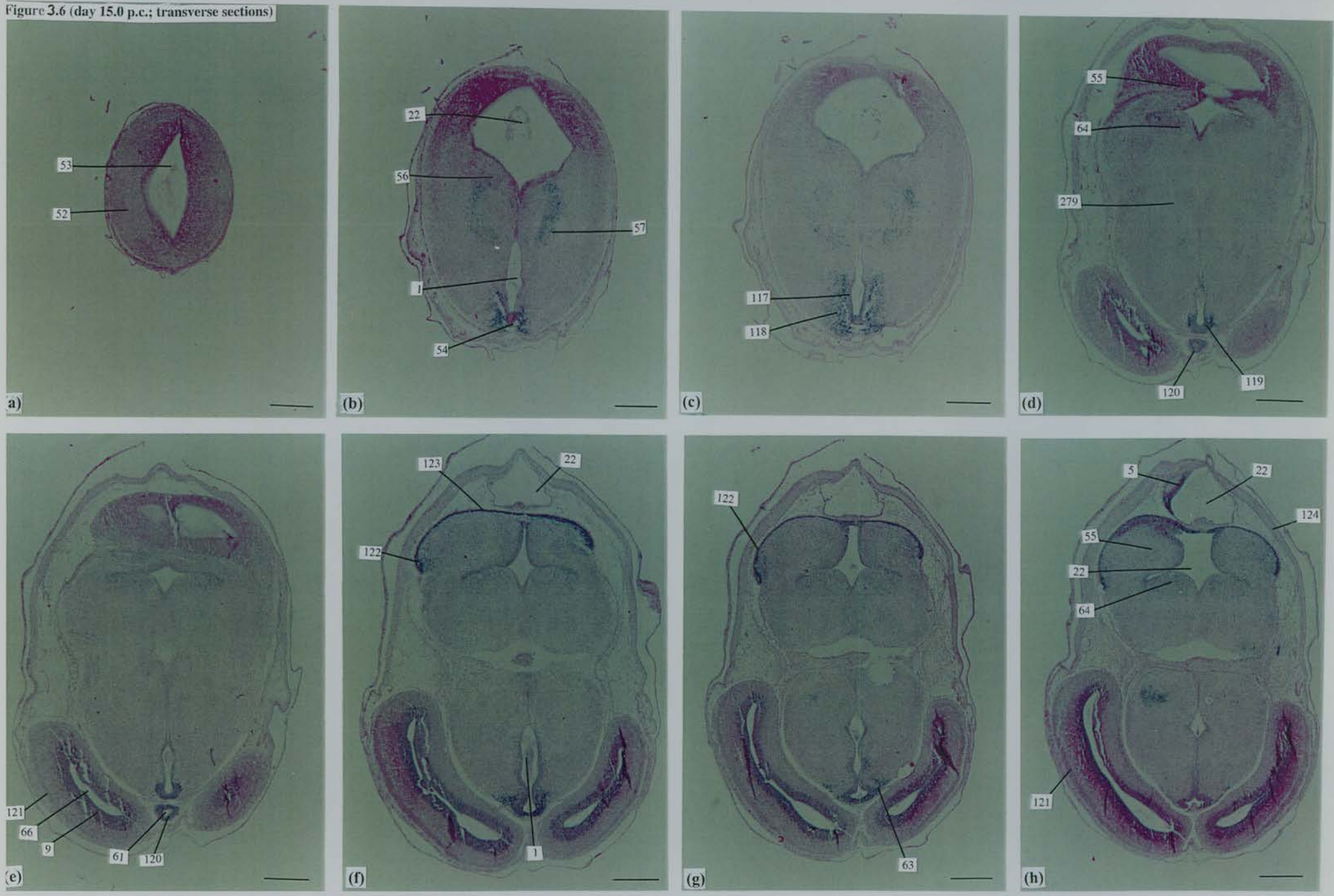

Figure 3.6 (i to p; to be continued on the following page) Mouse *Pax6* expression in the head region at day 15.0 p.c. represented by *in situ* hybridization on serial transverse sections. The ventral side points downwards. The planes of cutting are shown in a schematic diagram (on the right panel of this page). In the telencephalon, *Pax6* expression is seen in the telencephalic (neocortical) neuroepithelium (labelled in in 3.6.e to h). In the diencephalin, *Pax6* transcripts are seen in the hypothalamic differentiation fields (no. 126 in i, j) and in many sites that can be specified in the thalamic neuroepithelium, including paraventricular nucleus (no. 129), fields of Forel (no. 130), zona incerta (no. 131), intermediate thalamic neuroepithelium (no. 132), reticular nucleus (no. 134), and choroid fissure (no. 136) (see n - p). The internal capsule (no. 106 in o, p) in the thalamus does not express *Pax6,* leaving a pair of symmetrical curb-shaped areas of *Pax6* expression in the thalamus. In the midbrain, the tectum (no. 55 in j), the tegmentum (no. 64 in k), the pontine ventricular zone (no. 133 in n), and the midbrain reticular formation (no. 73 in l, m) are *Pax6*-expressing. Intense *Pax6* expression is also detected in the cerebellar primordium (no. 108 in i), the cerebellar germinal trigone (no. 125), the vestibulocochlear ganglion (VIII) in the midbrain-hindbrain junction. In the hindbrain, *Pax6* is expressed in the anterior premedullary neuroepithelium (no. 127 in j) and in the surface of medulla oblongata (no. 107 in p). All scale bars represented 0.5 mm in length.

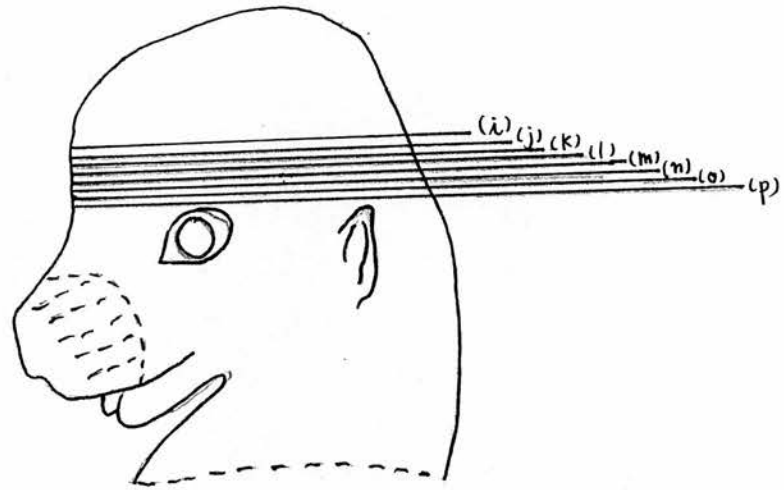

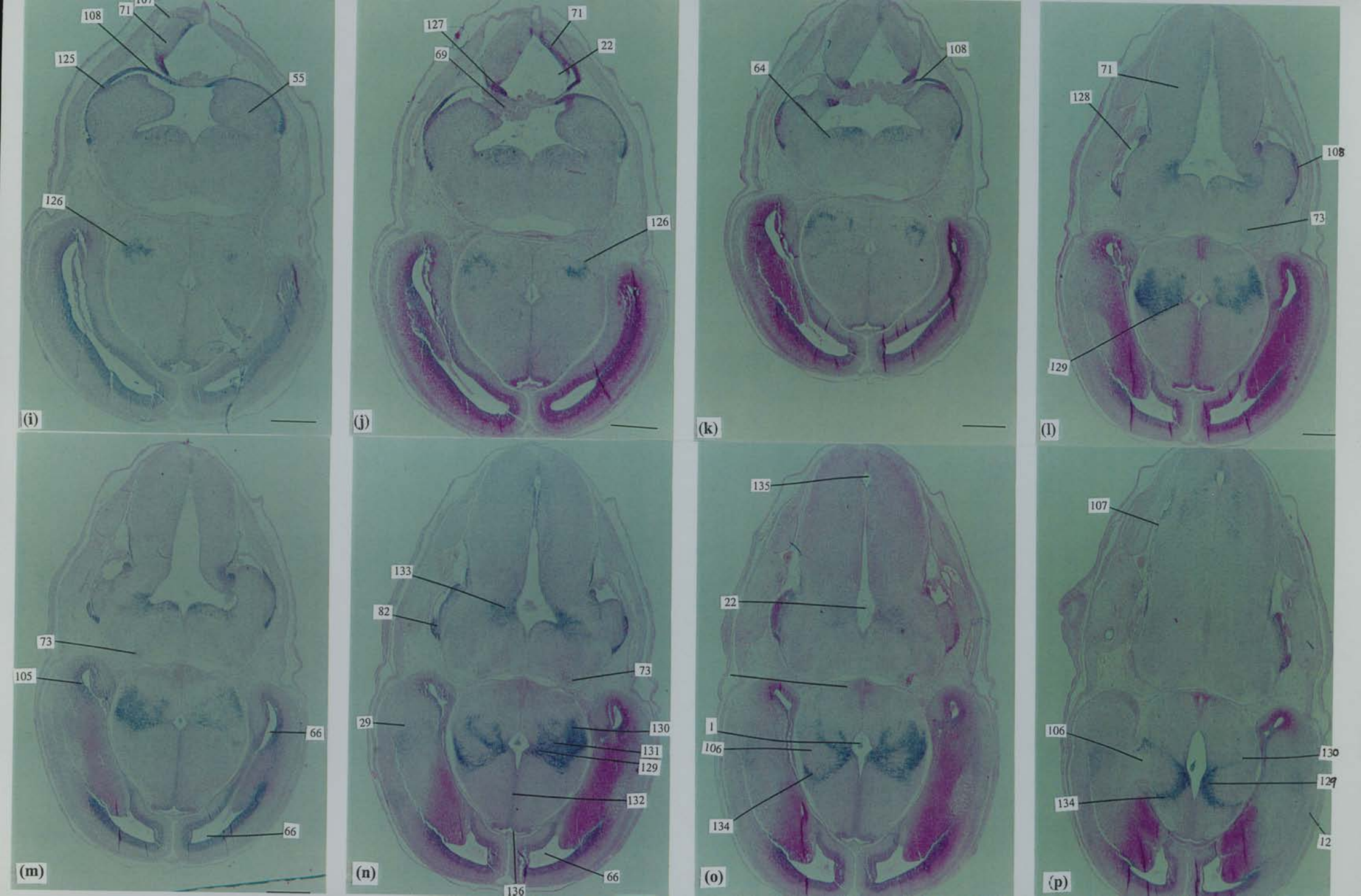
(i)
108
71
125
55
126
(j)
127
71
69
22
126
(k)
64
108
(l)
71
128
108
73
129
(m)
73
105
66
66
(n)
133
82
73
29
130
131
129
132
136
66
(o)
135
22
1
106
134
(p)
107
106
130
129
134
12

Figure 3.6 (q to t) Mouse *Pax6* expression in the head region at day 15.0 p.c. represented by *in situ* hybridization. The ventral side points downwards. The planes of cutting are shown in a schematic diagram (on the right panel of this page). q and s are serial transverse section continued from those in preceding pages. r is a magnified view on the squared area of intermediate thalamic differentiation field in q. t is a magnified view on the eye region. In the intermediate thalamic differentiation field, *Pax6* expression is seen in a pair of symmetric curb-shaped areas, including the paraventricular nucleus (no. 129), fields of Forel (no. 130), dorsal lateral geniculate nucleus (no. 138), reticular nucleus (no. 134), lateral hypothalamic neuroepithelium (no. 140), and supraoptic nucleus (no. 139). The *Pax6*-expressing cells in the reticular nucleus appear to be in conjunction with those in the hippocampal neuroepithelium (Ammon's horn; no. 137 in r). As the transverse plane is further lower (see s), *Pax6* expression is seen in the wall of third ventricle in the intermediate thalamic neuroepithelium (no. 132), bed nucleus of strial terminalis (no. 141), medial forebrain bundle (no. 142), stria medullaris (no. 143), and in the medial amygdala and the basomedial amygdaloid nucleus (no. 166). *Pax6* is also expressed in the surface of pontine area (no. 41) and in the superior central raphe nucleus (no. 75), as well as in the medula and cervical spinal cord (no. 71 and no. 88). In the eye region (see t), *Pax6* transcripts are detected in the corneal epithelium (no. 38), optic cup (particularly the rime, no. 98), anterior lens epithelium (no. 103). The pigmented retinal epithelium (no. 28), nerve fiber layer of retina (no. 205), and the connecting site of optic stalk (no. 39) are clearly seen without *Pax6* transcripts. Scale bars: in q and s, 0.5 mm; in r, 50 μm; in t, 125 μm.

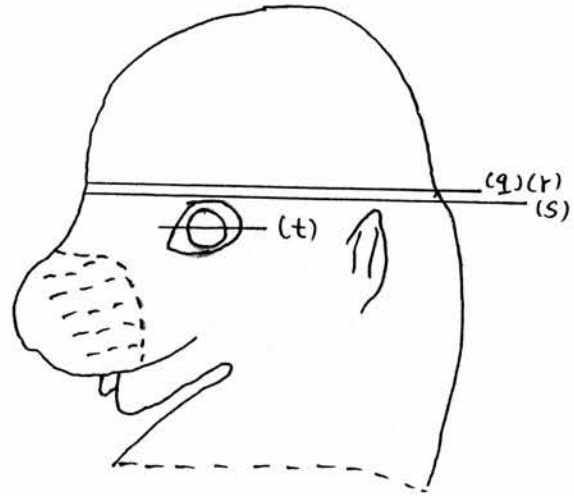

Figure 3.6 (day 15.0 p.c.; transverse sections; continued)

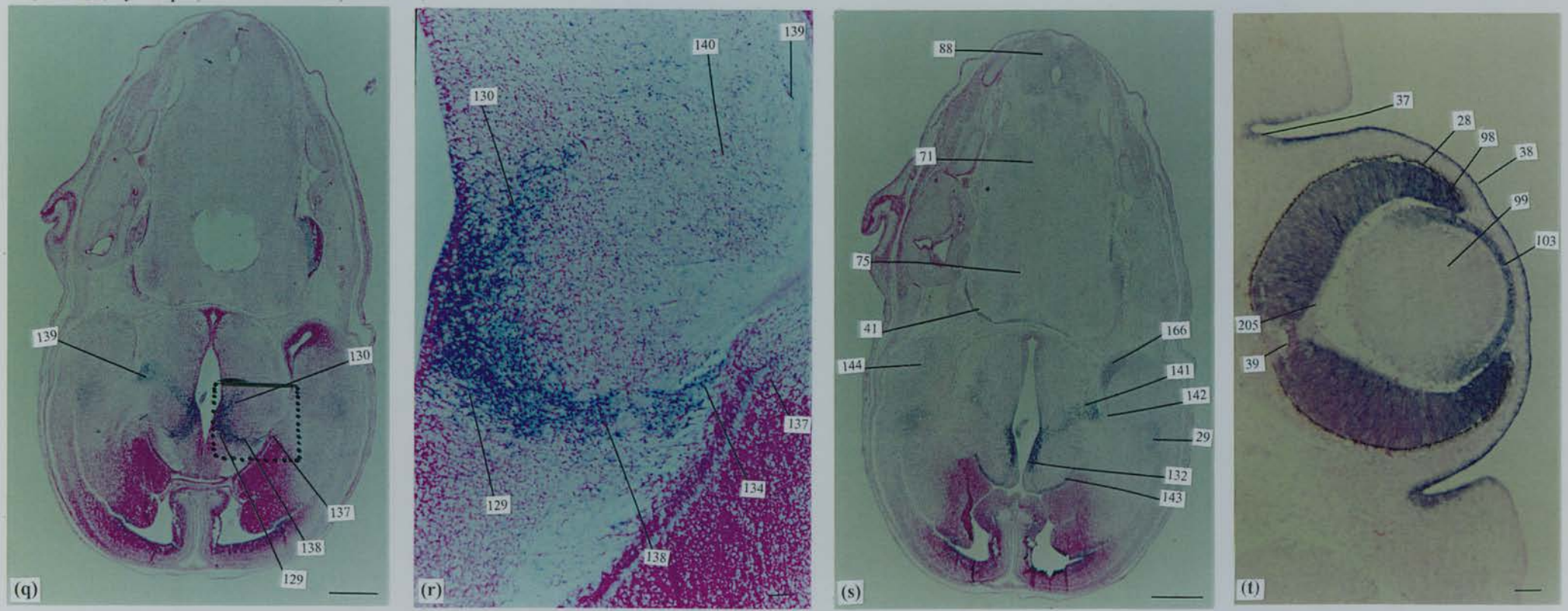

Figure 3.7 (a to h; to be continued on the following page) Mouse *Pax6* expression in the head region at day 16.0 p.c. represented by *in situ* hybridization on serial coronal sections. The ventral side points downwards. The planes of cutting are shown in a schematic diagram (on the right of this page). A continuous pattern of *Pax6* expression is seen (in a - c) from the neocortical neuroepithelium (no. 2) through the subicular area (no. 50), hippocampal area (Ammon's horn) (no. 137), dentate gyrus (no. 145), strionuclear area (no. 146), and the pallidum (no. 45) toward the amygdaloid area (no. 149 in c). In the dorsal thalamus, the area of epithalamic neuroepithelium (where the pineal gland, the habenular and lateral habenular nucleus are differentiated) exhibits obvious *Pax6* expression (no. 120 in c and d). This expression is seen, if viewed more caudally, in the lateral posterior nucleus in the posterior thalamus (no. 157 in h) and the anterior pretectal nucleus in the pretectum (no. 159 in i). *Pax6* expression also appears in the areas of stria terminalis and stria medullaris in the anterior thalamus (nos. 143, 150 in c), as well as in the site of the lateral preoptic region in the anterior hypothalamus (no. 148 in d). As the coronal sections are viewed further caudally, *Pax6* expression in the intermediate thalamus is seen in a symmetrical branched pattern (see d to h). The ventral branch joins with the dorsal branch in the Forelian neuroepithelium at the wall of hypothalamic third ventricle where the paraventricular nucleus (no. 129) can be specified (in h). The dorsal branch stretches dorsolaterally (see h), starting from the site of Forelian neuroepithelium and the paraventricular nucleus, to the area of zona incerta (no. 131) and the reticular nucleus (no. 134); the ventral branch stretches ventrolaterally toward the fields of Forel (no. 130) and the differentiation field of dorsolateral hypothalamus in close proximity to the piriform cortex (no. 77). In the hypothalamic area, patches of cells appear to exhibit *Pax6* expression (not specifically labelled; see h). *Pax6* is also expressed in the olfactory epithelium (no. 33 in b) and in the vomeronasal epithelium (no. 91 in b), as well as in the eye region (not labelled). All scale bars represent 0.5 mm in length.

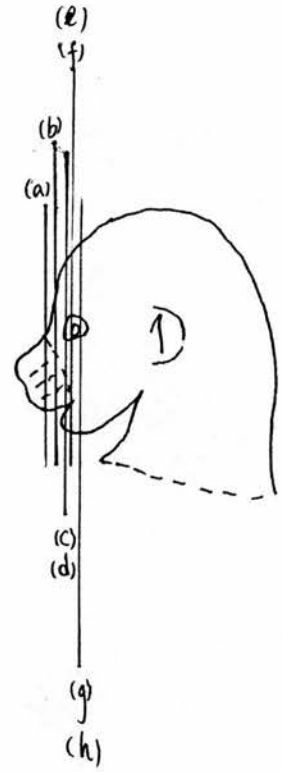

Figure 3.7 (day 16.0 p.c.; coronal sections)

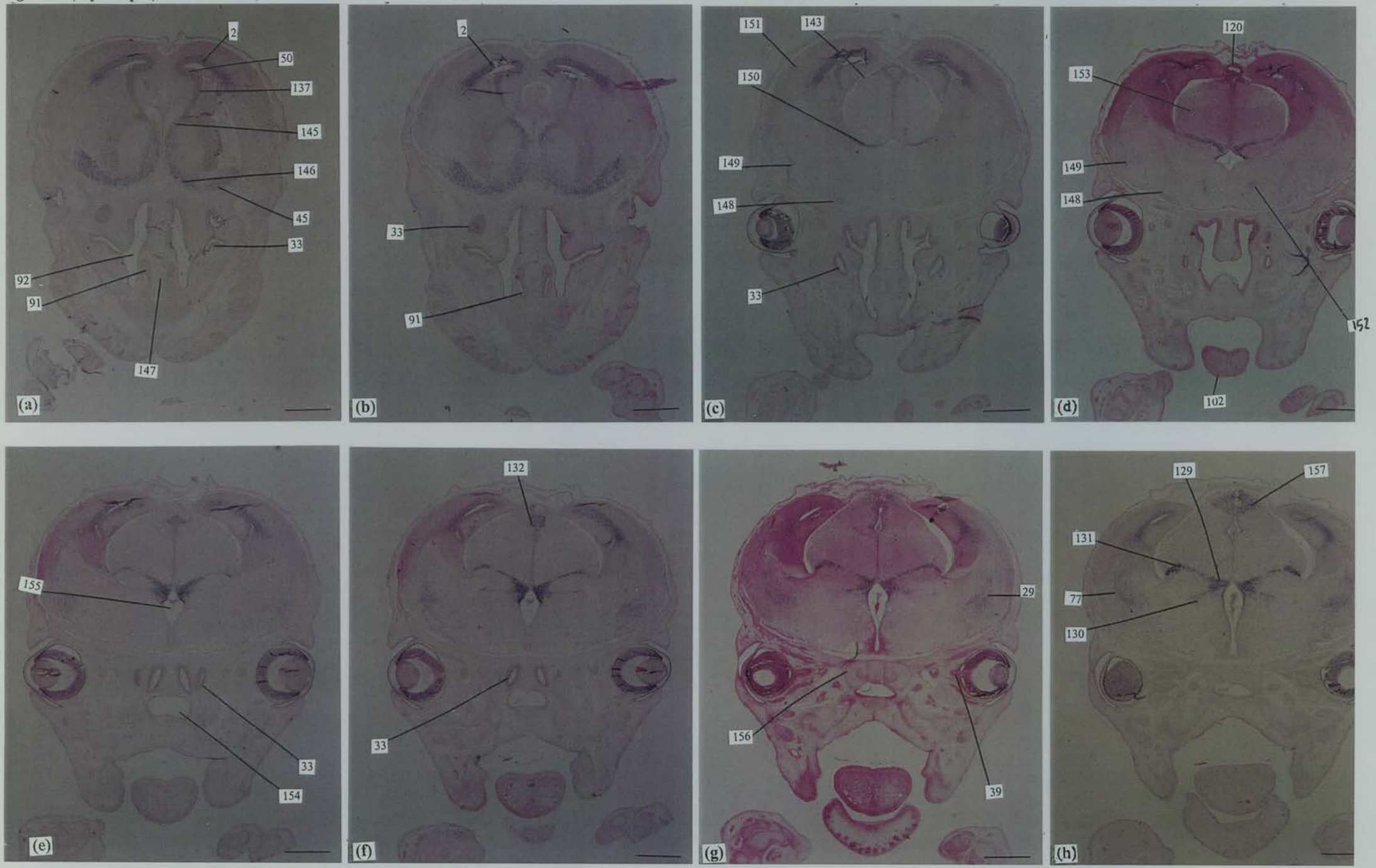

Figure 3.7 (i to p; to be continued on the following page) Mouse *Pax6* expression in the head region at day 16.0 p.c. represented by *in situ* hybridization on serial coronal sections. The ventral side points downwards. The planes of cutting are shown in a schematic diagram (on the right panel of this page). Interesting patterns of *Pax6* expression in the intermediate and posterior thalamus are seen. The dorsal branch (paraventricular-zona incerta-reticular nucleus; see the description on page 171) becomes band-shaped and is present in the differentiation field of intermediate thalamus and ventrolateral geniculate nucleus (no. 160 in i). Connections of *Pax6*-expressing cells between the dorsal and the ventral branch are apparent (in j). The dorsal branch, i.e. the band-shaped expression area, will become segmented (see k) and forked (see l) as it is viewed more caudally in the tegmental area. The ventral (fields of Forel-dorsolateral thalamus) branch is also changed; it becomes a patch of cells in the subthalamic nucleus (no. 161 in i) and, as viewed more caudally, is gradually diminished in the posterior and lateral hypothalamic differentiating fields (see l). The posterior amygdaloid area where the basomedial amygdaloid nucleus (no. 166) is located remains exhibiting *Pax6* expression as can be seen in figures 3.7.i to 3.7.n. The deep layers of the superior colliculus are also seen expressing *Pax6* (no. 168 in o). The pituitary and the mammillary neuroepithelium are also *Pax6*-expressing areas (nos. 20, 169 in p). All scale bars represent 0.5 mm in length.

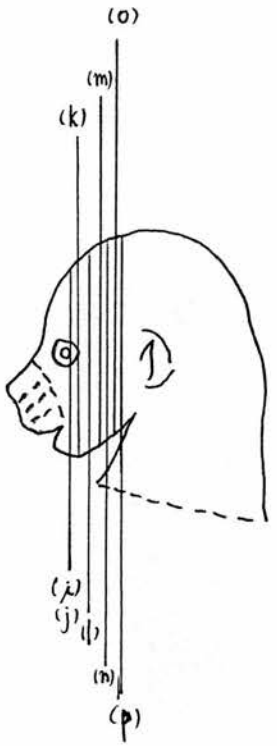

Figure 3.7 (day 16.0 p.c.; coronal sections; continued)

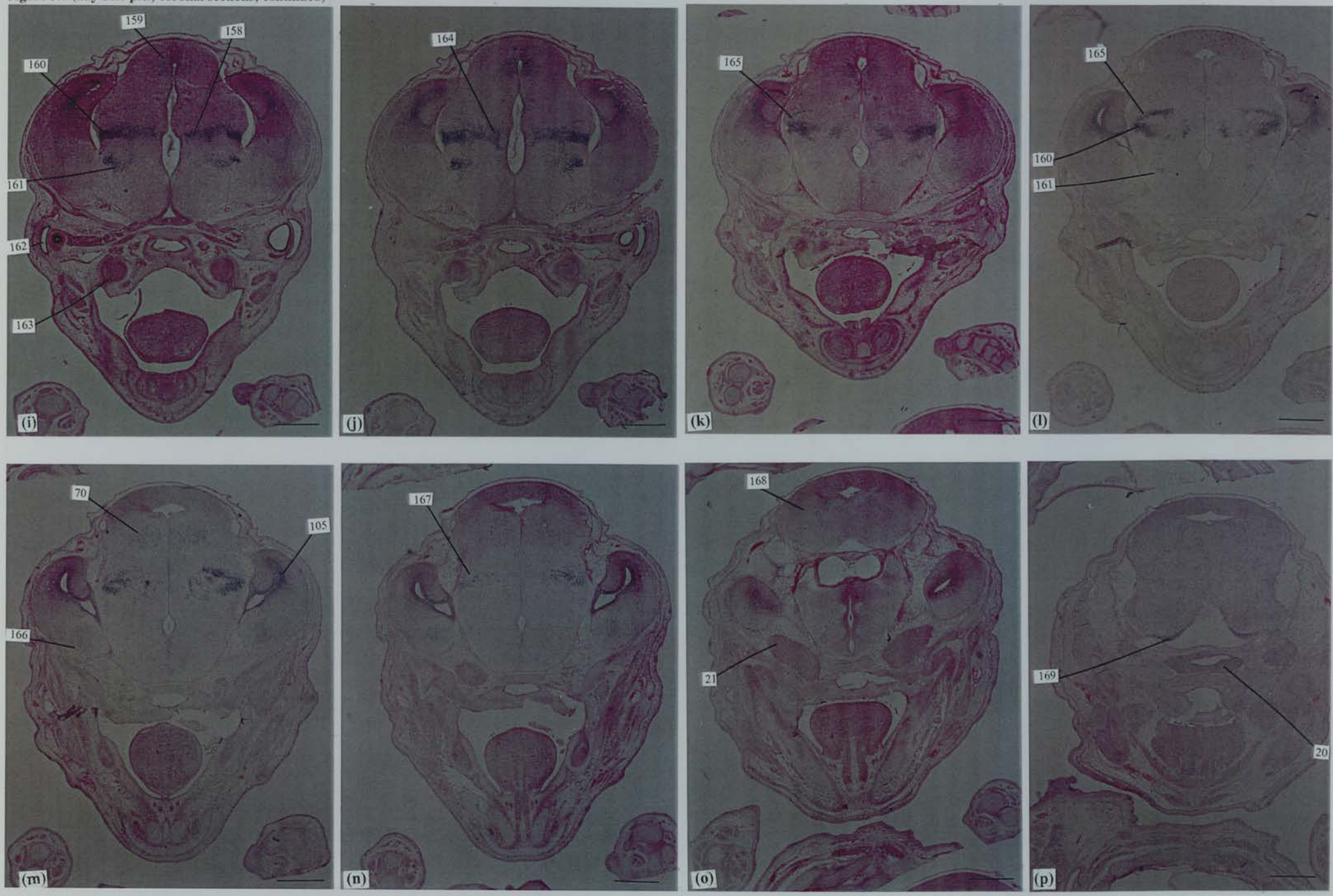

Figure 3.7 (q to x; to be continued on the following page) Mouse *Pax6* expression in the head region at day 16.0 p.c. represented by *in situ* hybridization on serial coronal sections (continued from preceding pages). The ventral side points downwards. The planes of cutting are shown in a schematic diagram (on the right panel of this page). The pituitary primordium is clearly *Pax6*-expressing (no. 20 in q, r). Particularly intense expression of *Pax6* can be located in the lateral deep nucleus (no. 171), the ventral tegmental nucleus (no. 172), the magnocellular reticular nucleus (no. 175), the cochlear nucleus (no. 176), and the superior central raphe nucleus in the isthmus (no. 282) (see p, q, s, t, u, w). *Pax6* transcripts are also located in the cerebellar primordium (no. 174 in u), the reticular nucleus (no. 134 in w), and in the tegmentum (no. 64 in w). All scale bars represent 0.5 mm in length.

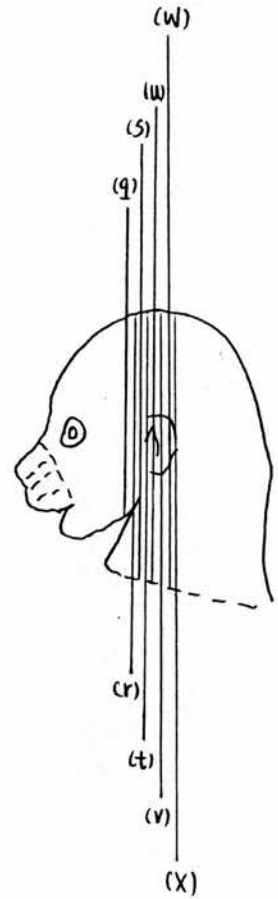

Figure 3.7 (day 16.0 p.c.; coronal sections; continued)

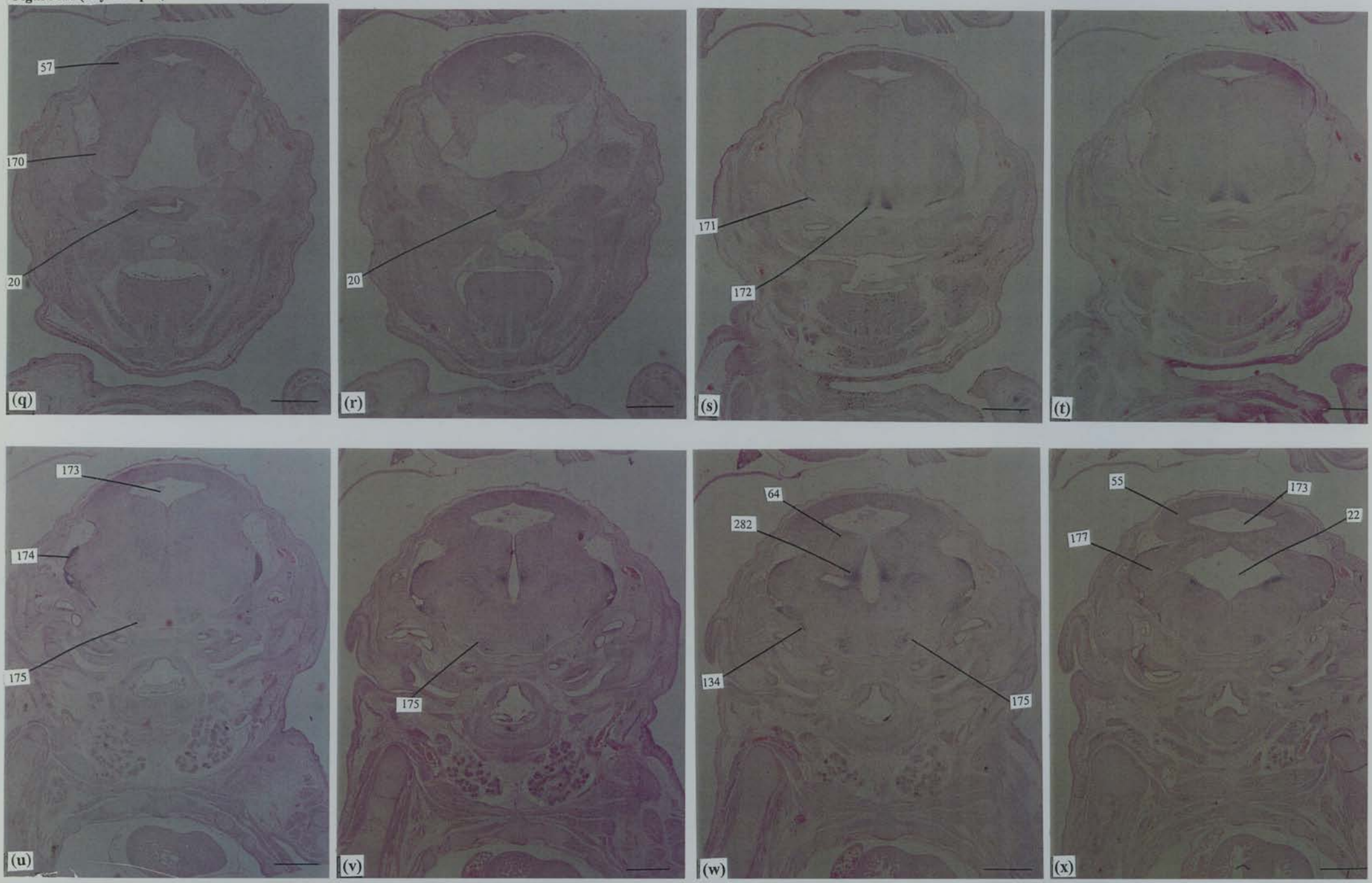

Figure 3.7 (y to ε) Mouse *Pax6* expression in the head region at day 16.0 p.c. represented by *in situ* hybridization on serial coronal sections. The ventral side points downwards. The planes of cutting are shown in a schematic diagram (on the right panel of this page). Sections in y, z, β, γ, and δ are serial sections that continuous from preceding pages. α is a magnified view on the spinal cord area shown in z. ε is a magnified view on the spinal cord shown in γ. *Pax6* expression is detected in the premedullary neuroepithelium (no. 183 in y) and the motor neurons of the cervical spinal cord (see no. 96 in z, α; also no. 74 in γ). Hints of *Pax6* expression can also be seen in the ventricular zone in the cervical spinal cord (no. 89 in α). In the more posterior spinal cord, *Pax6* transcripts are detected in the ependymal layer (no. 190) as well as in the intermediate zone (no. 191) and marginal zone (no. 192). Scale bars: in α and ε, 20 μm; all others, 0.5 mm.

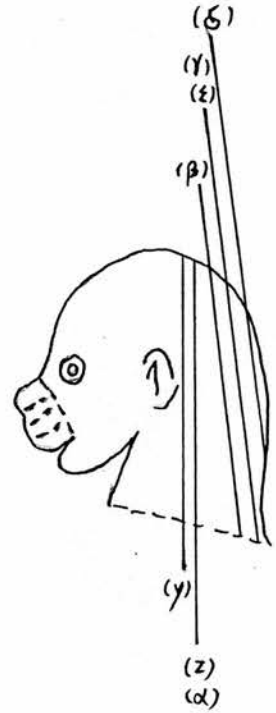

Figure 3.7 (day 16.0 p.c.; coronal sections; continued)

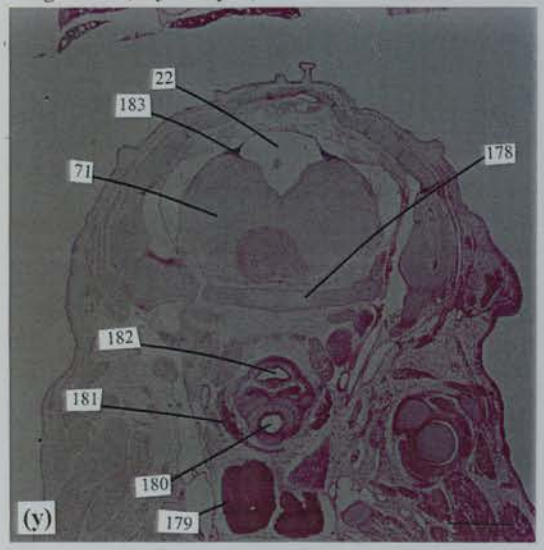

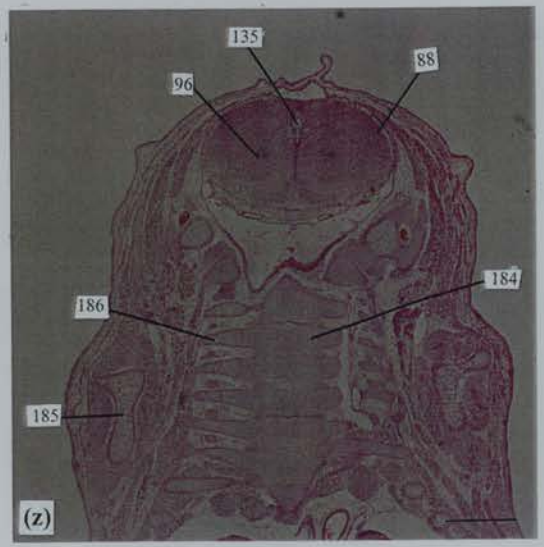

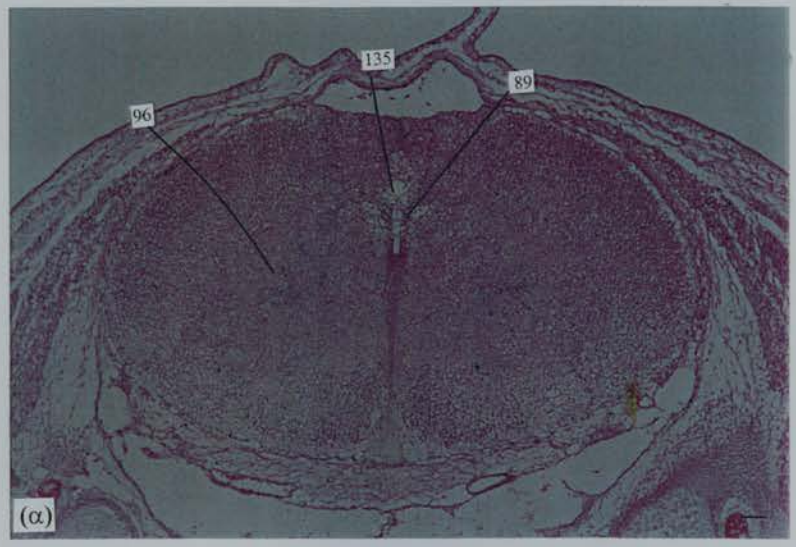

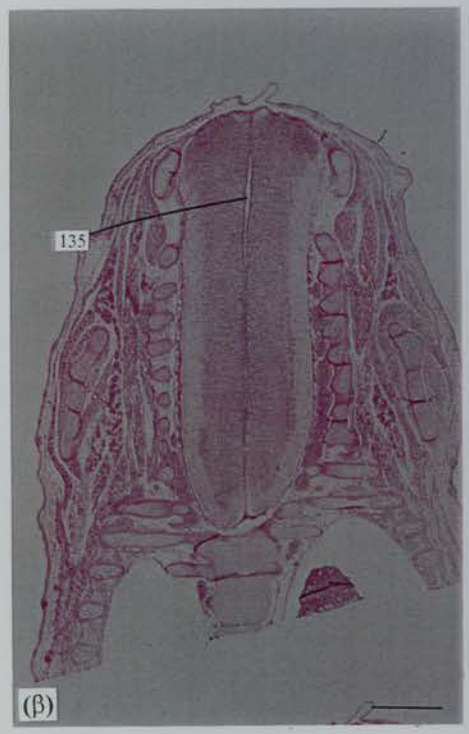

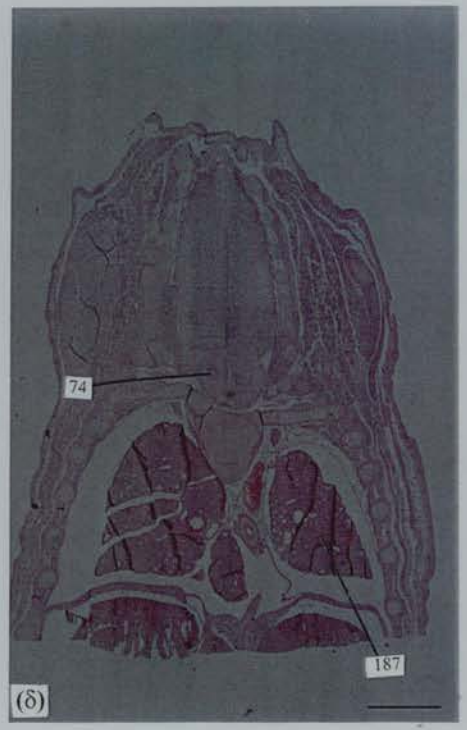

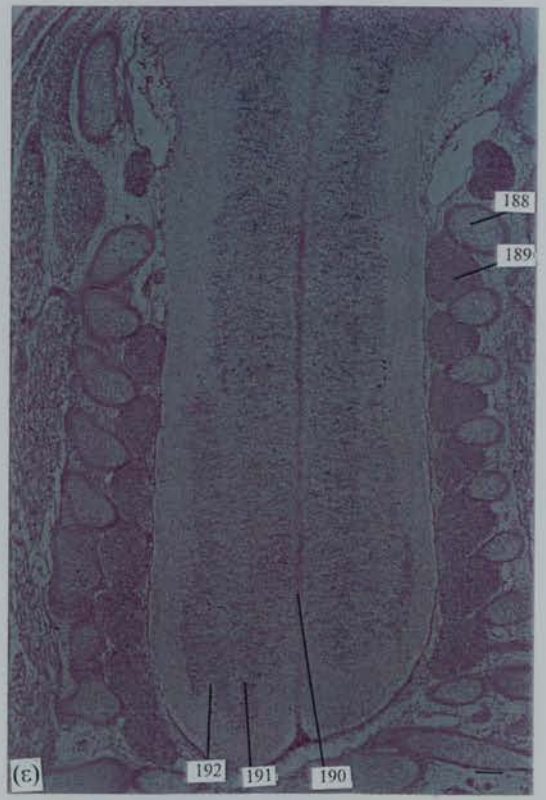

Figure 3.8 (a to h; to be continued on the following page) Mouse *Pax6* expression in the head region at day 17.0 p.c. represented by *in situ* hybridization on serial coronal sections. The ventral side points downwards. The planes of cutting are shown in a schematic diagram on the right panel of this page. In the olfactory epithelium (no. 33 in a, b, c, e) and vomeronasal epithelium (no. 91 in a), a low level of *Pax6* expression is detected. *Pax6* expression is also clearly detected in the tubules of serous gland (no. 194 in c) and in the nasal glandular tissue in lateral wall of middle meatus (no. 195 in c). In the main olfactory bulb (no. 196 in d), *Pax6* transcripts are seen and the distribution of *Pax6* transcripts appears to connect, posteriorly, to that found in the rhinencephalon (no. 197 in g) and in the piriform cortex (no. 77 in h), as well as in the lateral migratory stream (no. 200 in i; see the following page) and the endopiriform nucleus in the rhinencephalon (no. 111) (see f to h). *Pax6* transcripts are also detected in the taenia tecta (see no. 283 in f; h). All scale bars represent 0.5 mm in length.

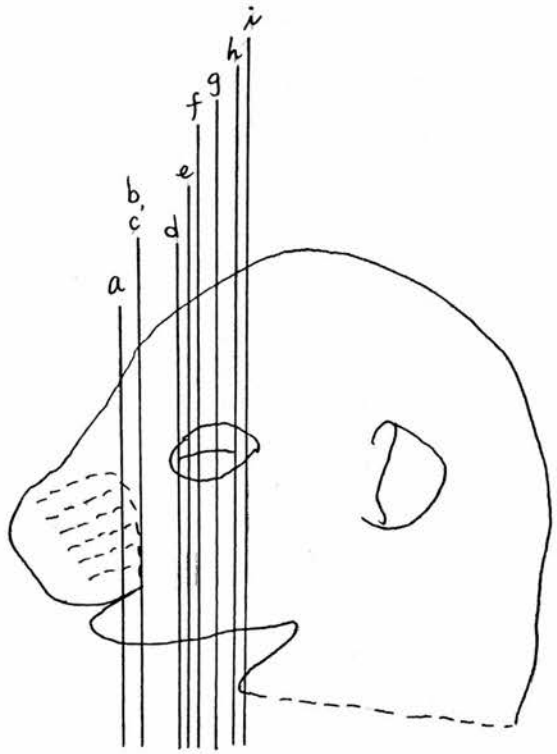

Figure 3.8 (day 17.0 p.c.; coronal sections)

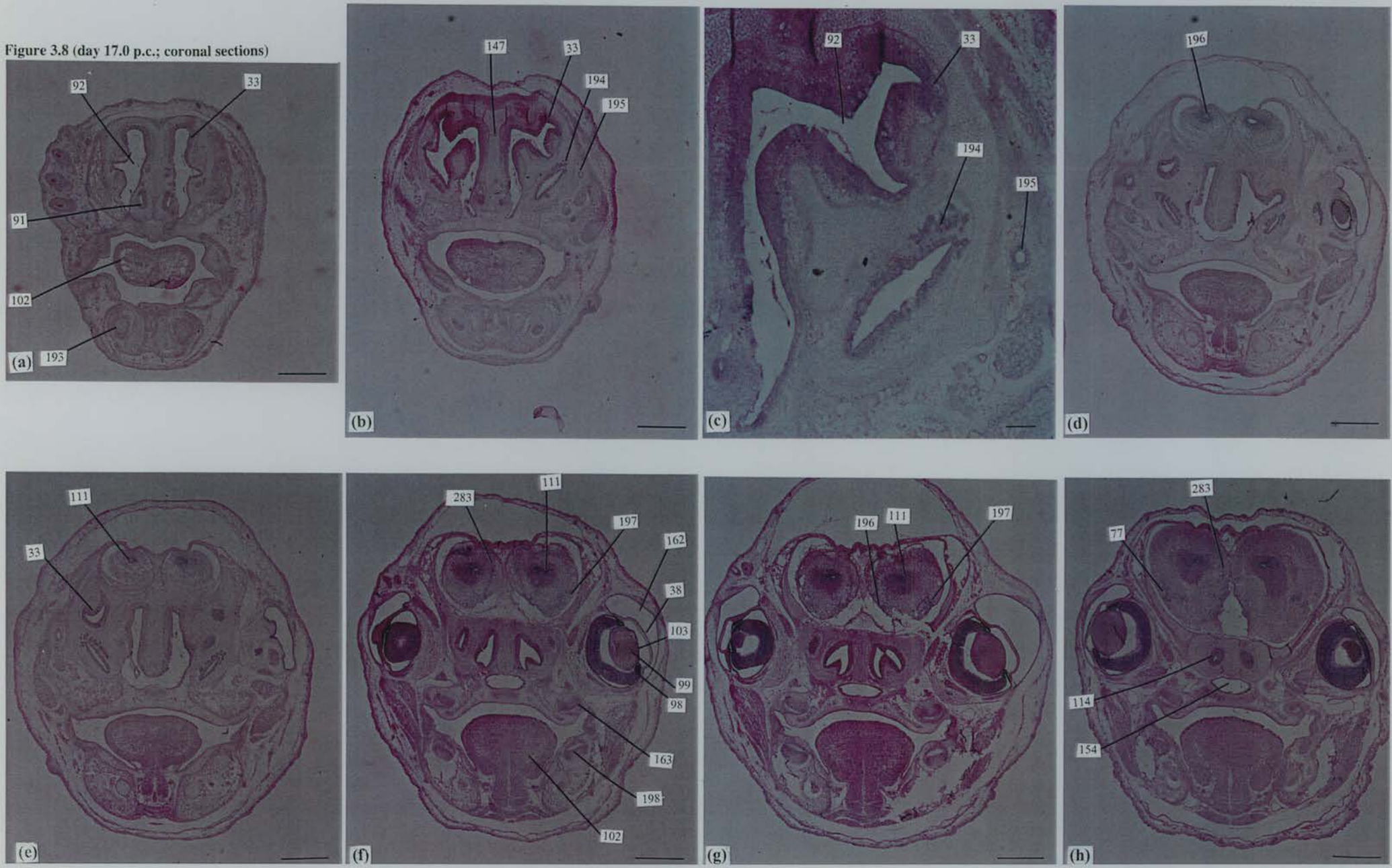

Figure 3.8 (i to p; to be continued on the following page) Mouse *Pax6* expression in the head region at day 17.0 p.c. represented by *in situ* hybridization on serial coronal sections. The ventral side points downwards. The planes of cutting are shown in a schematic diagram on the right panel of this page. In the telencephalic region, *Pax6* expression is seen in the neocortical neuroepithelium (no. 2) and in the medial septum (no. 199), as well as in the lateral migratory stream in the amygdala (no. 200) (in i). In the eye (see j), *Pax6*-expressing cells remain located in the anterior epithelium of the lens (no. 103), the neural retina that is differentiated into a multi-layered structure (nos. 201 - 205), as well as in the corneal epithelium (no. 38). In the pigmented retinal epithelium, however, no detectable *Pax6* transcript is found (no. 28 in j). *Pax6* expression is also detected in the optic chiasma (no. 114 in h) but not in the optic stalk (no. 39 in j). Particularly interesting finding is in the differentiating neural retina where *Pax6* transcripts appear to distribute in various concentrations in different layers. The presumptive internal nuclear layer shows the most intense expression than other layers (no. 203 in j). *Pax6* expression also appears in a patch of cells, presumably neural cells, outside the brain (see no. 209 in o, p). The anterior thalamic neuroepithelium in the area of medial septum (no. 199 in k), the pineal primordium (no. 120 in s) and the thalamic neuroepithelium (in l to t) remain containing *Pax6* transcripts. Those previously noted areas of expression, i.e. the paraventricular nucleus (no. 129), fields of Forel (no. 130), zona incerta (no. 131), reticular nucleus (no. 134), and the differentiation fields of lateral hypothalamus (no. 140) remain containing *Pax6* transcripts as formerly detected (in o). All scale bars represent 0.5 mm in length.

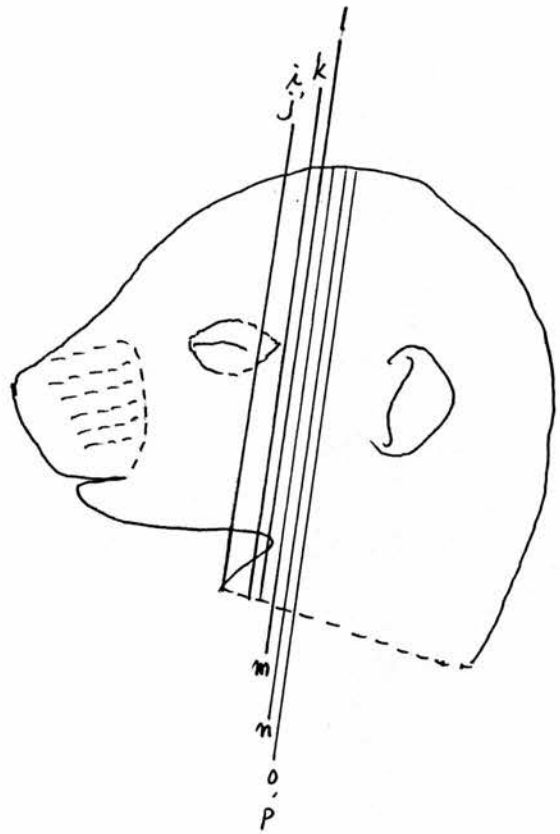

Figure 3.8 (day 17.0 p.c.; coronal sections; continued)

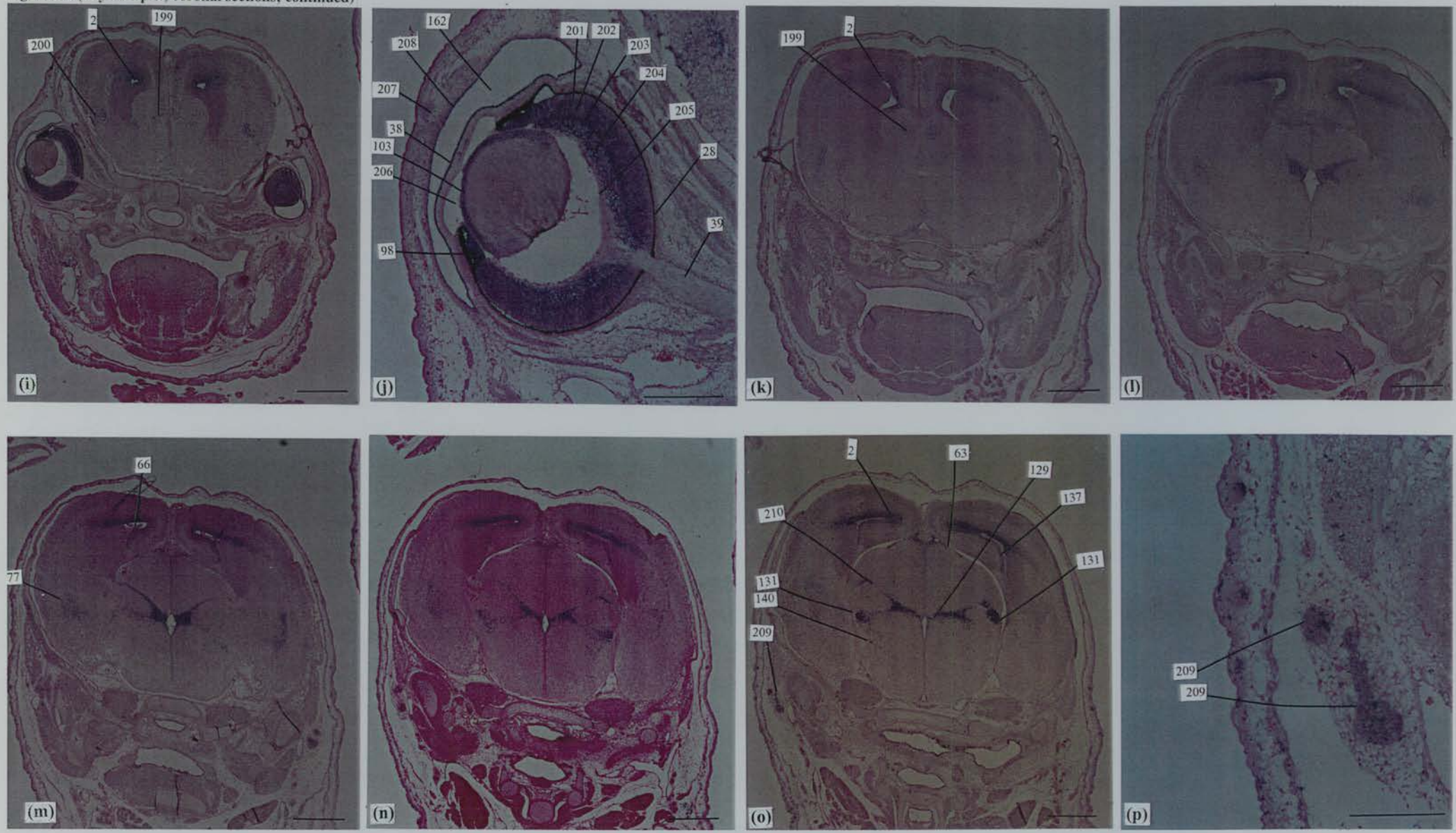

Figure 3.8 (q to x; to be continued on the following page) Mouse *Pax6* expression in the head region at day 17.0 p.c. represented by *in situ* hybridization on serial coronal sections. The ventral side points downwards. The planes of cutting are shown in a schematic diagram on the right panel of this page. In the telencephalic region, *Pax6* expression is seen in the neocortical neuroepithelium (no. 2 in q) and the expression appears to extend to the intermediate zone of the lateral telencephalic neuroepithelium (no. 211 in q). The expression also extends to the neuroepithelium surrounding the amygdaloid fork (no. 213 in r, s). There are also hints of *Pax6* expression in the outer layer of telencephalic neuroepithelium, although the level of expression is not as high as that in the neocortical neuroepithelium (not labelled; see q, r). *Pax6* expression is also seen in the medial septum (no. 199 in k) and in the pineal primordium (no. 120 in s). *Pax6* expression in the anterior thalamic neuroepithelium (in l to o) appears to link with that in the intermediate and posterior thalamic neuroepithelium where the lateral posterior nucleus (no. 157 in r), the medial geniculate complex (no. 214 in r), the ventrobasal nuclear complex (no. 215 in r), and the junction between medial geniculate nucleus and red nucleus (no. 219) are all *Pax6*-expressing. The pituitary primordium also appears to express *Pax6,* although at a very low level (no. 20 in q, r). In the pontine neuroepithelium, the cerebral peduncle (no. 216 in figure t) and superior central raphe nucleus (no. 75) in the anterior pons (no. 217) constitute a symmetric 'tadpole' pattern of *Pax6*-expressing area (see t). The cerebellar primordium, including the cochlear nucleus, exhibits apparent *Pax6* transcripts (no. 174 and no. 176 in w; x). The areas of the reticular formation (nos. 73 and 225), the neuroepithelial cells in the wall of the fourth ventricle (no. 22), the ventral tegmental nucleus (no. 172) and the lateral vestibular nucleus (no. 224) are also *Pax6*-expressing (figures 3.8.w; x). All scale bars represent 0.5 mm in length.

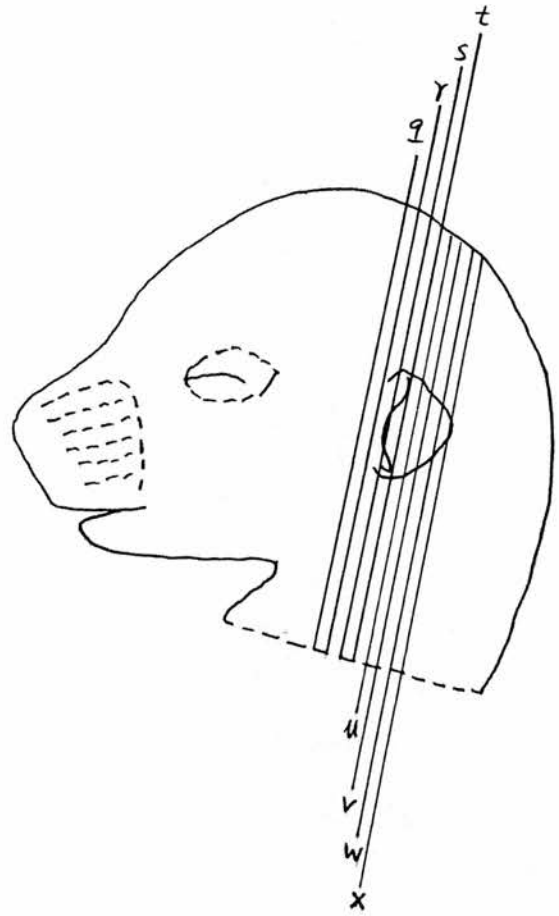

Figure 3.8 (day 17.0 p.c.; coronal sections; continued)

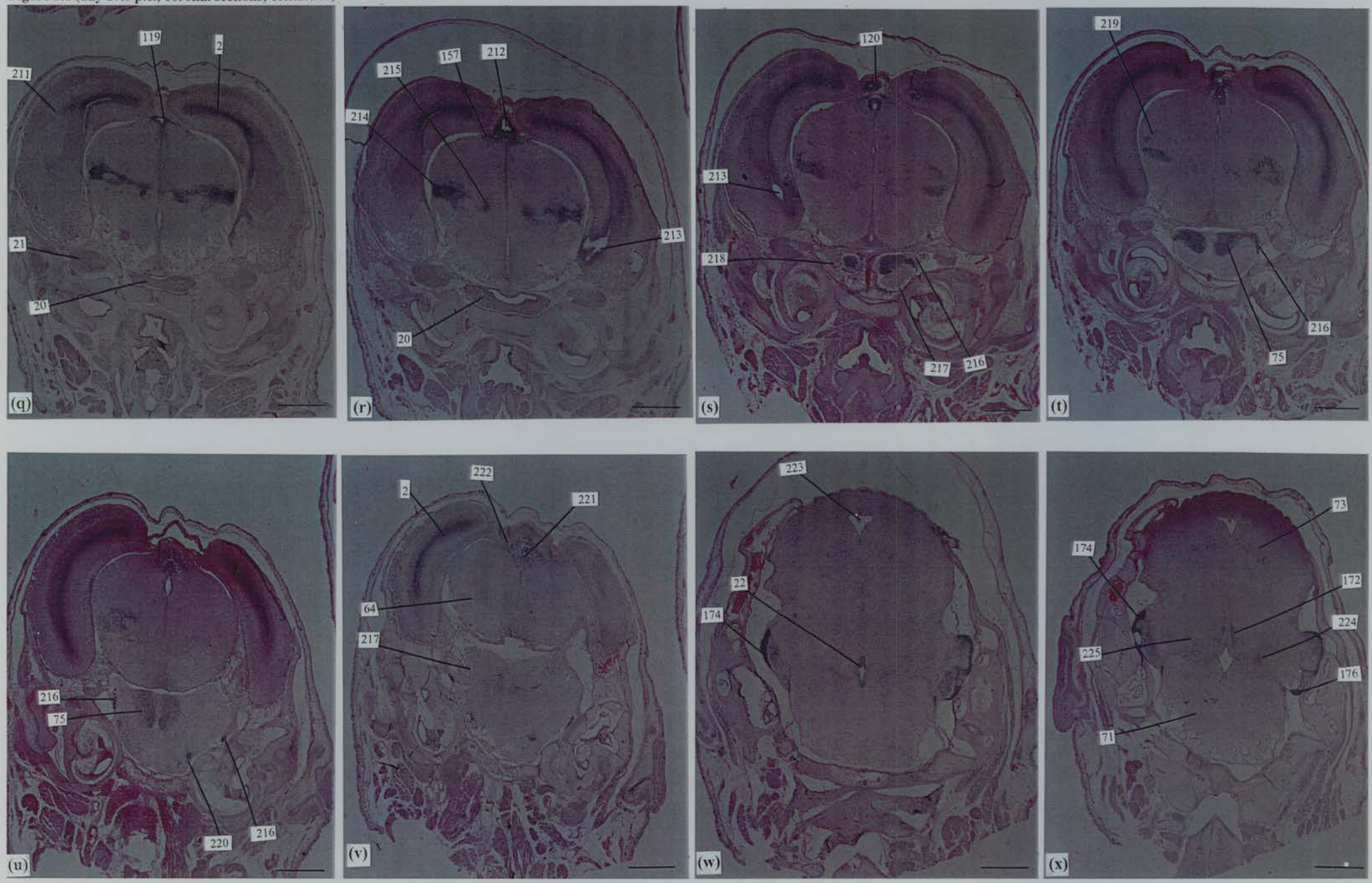

Figure 3.8 (y to α) Mouse *Pax6* expression in the head region at day 17.0 p.c. represented by *in situ* hybridization on serial coronal sections that are continous from those in preceding pages. The ventral side points downwards. The planes of cutting are shown in a schematic diagram on the right panel of this page. *Pax6* expression in the junction of the pontine and medullary neuroepithelium can be seen in the midbrain reticular formation (no. 73), the pontine ventral tegmental nucleus (no. 172), the cerebellar primordium (no. 174), the cerebellar germinal trigone (no. 125), the cochlear nucleus (no. 176), and in the anterior pontine neuroepithelium (no. 226) (in y - α). The choroid plexus in the fourth ventricle does not exhibit *Pax6* expression (no. 69 in z). In the medulla, *Pax6* transcripts are detected in the medullary reticular formation (no. 228 in z; α) and in the premedullary neuroepithelium (no. 183 in α). All scale bars represent 0.5 mm in length.

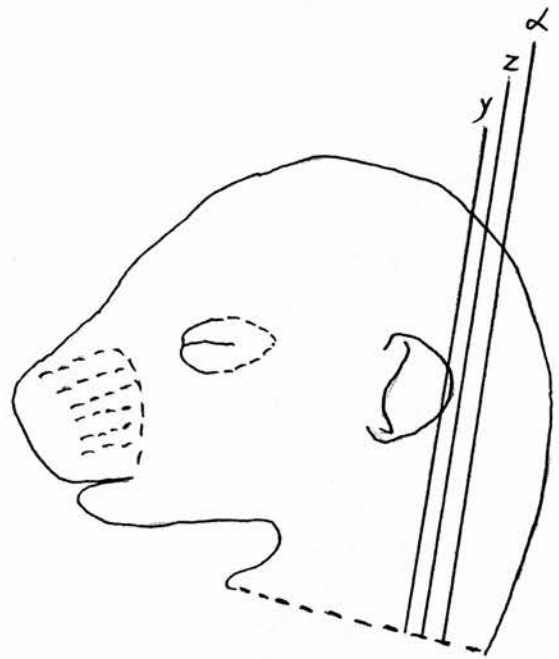

Figure 3.8 (day 17.0 p.c.; coronal sections; continued)

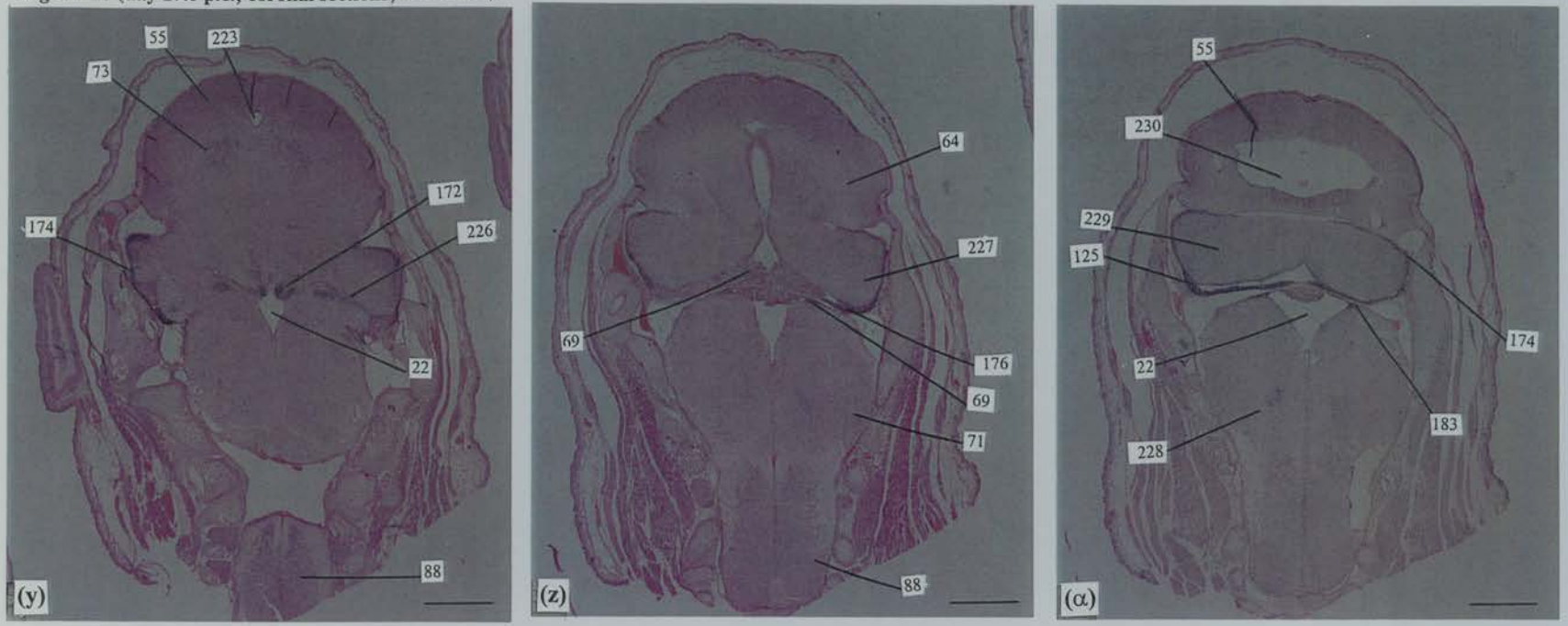

Figure 3.9 (a to h; to be continued on the following page) Mouse *Pax6* expression in the head region at day 18.0 p.c. represented by *in situ* hybridization on serial coronal sections (except for the magnified view on the eye region in c). The ventral side points downwards. The planes of cutting are shown in a schematic diagram on the right panel of this page. In the olfactory bulb, the olfactory neuroepithelium and the anterior olfactory nucleus are clearly *Pax6*-expressing (nos. 231 and 232 in d). *Pax6* transcripts are also found in the insular area of the rhinencephalic differentiation field that is in conncetion with the amygdaloid differentiation fields (no. 200 in g). In the eye, *Pax6* transcripts are concentrated only in the ganglion cell layer and internal nucleus layer of the neural retina (nos. 203, 204 in c). The pigmented retinal epithelium (no. 28) is seen completely devoid of its *Pax6* expression and the corneal epithelium (no. 38) contains only minimal *Pax6* transcripts (see c). In the telencephalon (see g, h), *Pax6* transcripts are detected in the neocortical neuroepithelium (no. 2), the medial septum (no. 199), the lateral migratory stream (no. 200), the diagonal band (no. 235), and in the fornix (no. 234). Scale bars: in c, 250 μm; all the others, 1 mm.

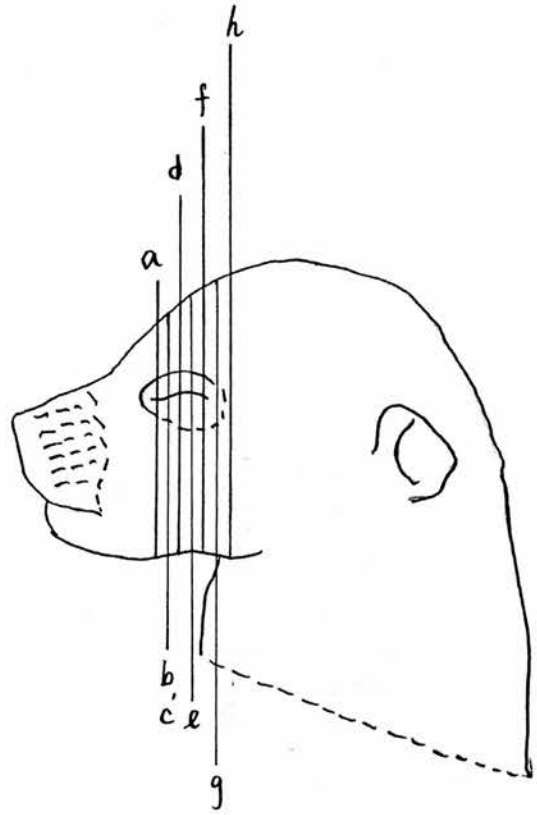

Figure 3.9 (day 18.0 p.c.; coronal sections)

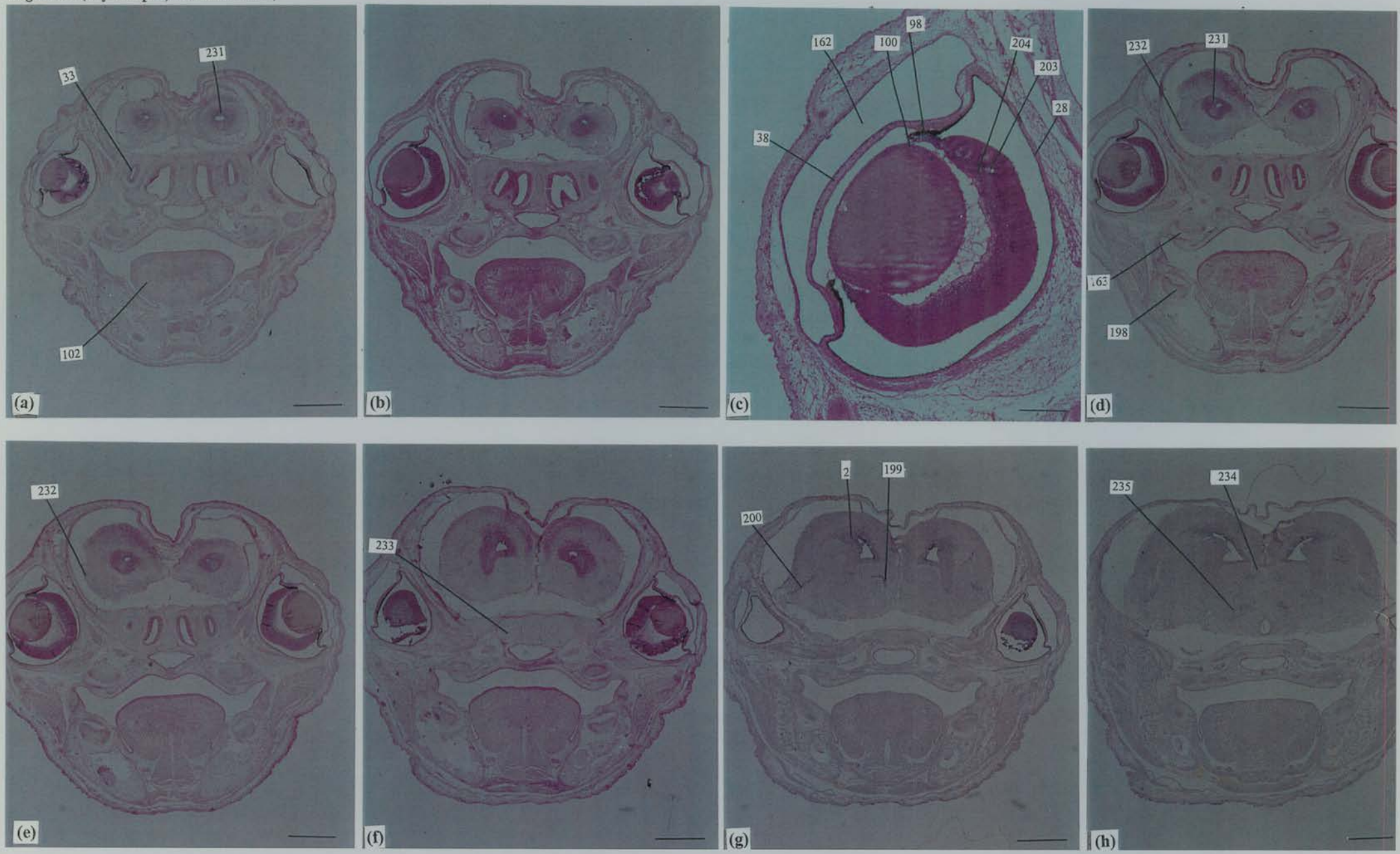

Figure 3.9 (i to p; to be continued on the following page) Mouse *Pax6* expression in the head region at day 18.0 p.c. represented by *in situ* hybridization on serial coronal sections. The ventral side points downwards. The planes of cutting are shown in a schematic diagram on the right panel of this page. In the telencephalon, the cingulate cortex and the neocortical neuroepithelium remain expressing *Pax6*, but the total area is reduced, i.e. the formerly thick layer of *Pax6*-expressing neuroepithelium is reduced to a thin layer (compare no. 2 in figures 3.7.b, 3.8.k, and 3.9.l). In the thalamic neuroepithelium, the dorsal (paraventricular-zona incerta-reticular) branch and the ventral (fields of Forel-dorsolateral hypothalamus) branch that are formerly noted at day 16.0 p.c. (in section 3.2.1.8) remain *Pax6*-expressing; but the total area seems to be slightly reduced as compared to that seen at day 16.0 p.c. (compare figure 3.6.h with figure 3.9.m). The differentiation fields of fornix (no. 234 in 3.9.i), medial septum (no. 199), diagonal band (both horizontal and vertical limb; see no. 235 in 3.9.h and no. 236 in 3.9.i) and lateral migratory stream (no. 200) all contain *Pax6* transcripts at identifiable level (see 3.9.i). In the hypothalamus, *Pax6* transcripts are seen in the intermediate neuroepithelium (see no. 237 in 3.9.k). *Pax6* transcripts are even seen in the pituitary cells in the ossificating cartilage primordium of hypophyseal fossa of sphenoid bone, i.e. the sella turcica (no. 240 in 3.9.l; see also 3.9.m). In the midbrain (see 3.9.o, p), *Pax6* transcripts are detected in the dorsal lateral geniculate nucleus, ventral lateral geniculate nucleus, and the junction of reticular nucleus and ventral lateral nucleus complex (no. 243). All scale bars represent 1 mm in length.

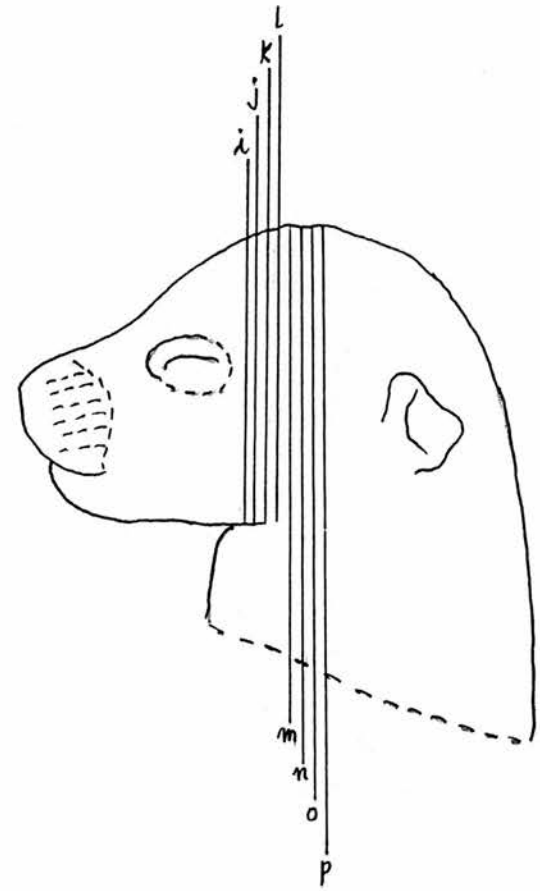

Figure 3.9 (day 18.0 p.c.; coronal sections; continued)

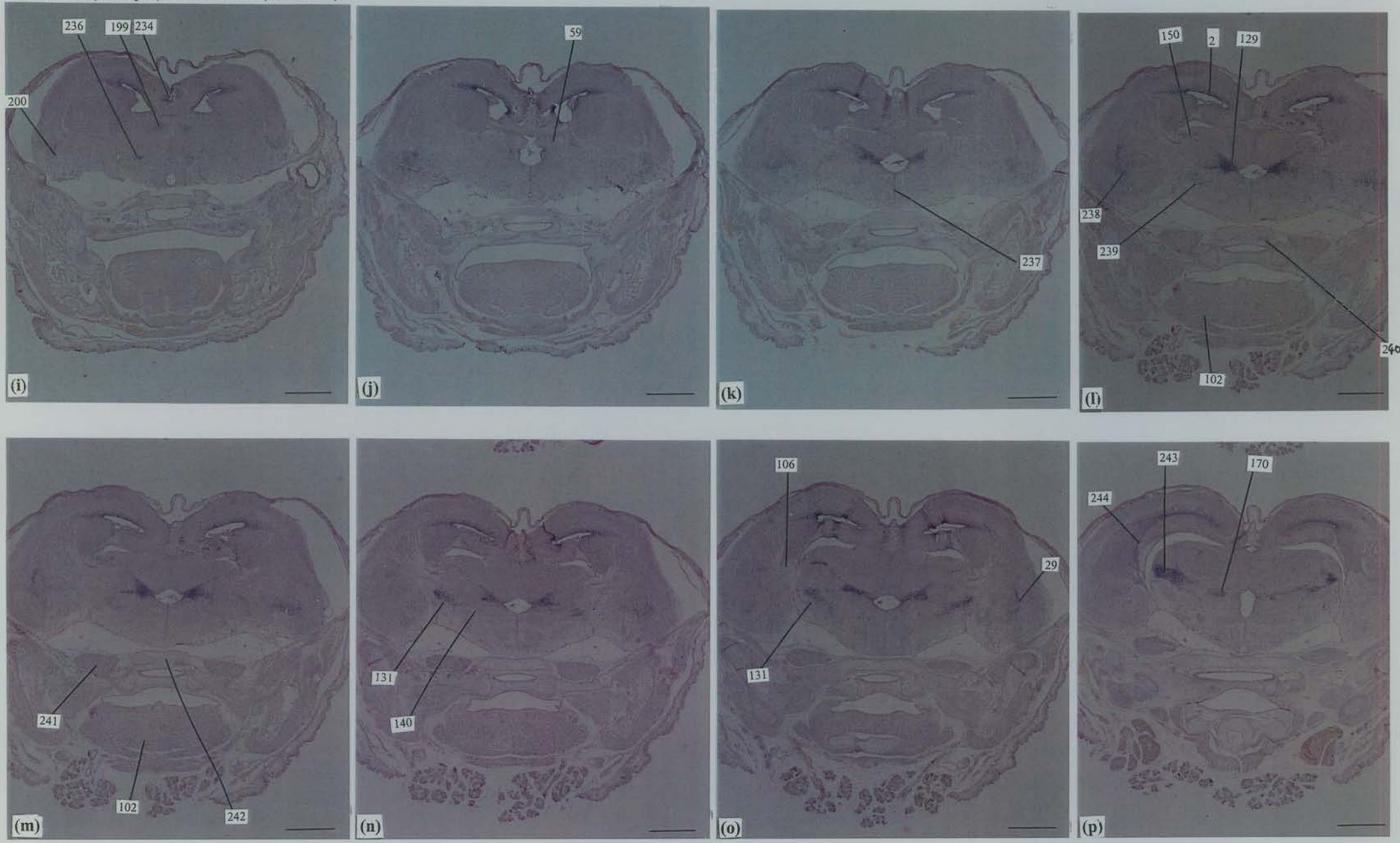

Figure 3.9 (q to w) Mouse *Pax6* expression in the head region at day 18.0 p.c. represented by *in situ* hybridization on serial coronal sections. The ventral side points downwards. The planes of cutting are shown in a schematic diagram on the right panel of this page. *Pax6* expression is seen in the lateral habenular nucleus (no. 245 in 3.9.q) and the dorsal periaqueductal gray (no. 247 in 3.9.t). In the telencephalic neuroepithelium, in addition to that in the neocortical neuroepithelium (no. 2 in q), *Pax6* expression is also seen in the intermediate zone (no. 191 in q). The pituitary primordium remains expressing *Pax6* (no. 20 in q, r). In the pontine area, the superior central raphe nucleus (no. 75), pontine reticular formation (no. 225), cerebral peduncle lateral to the trigerminal motor nucleus (no. 248), trigeminal motor nucleus (no. 249), as well as the cerebral peduncle lateral to the superior olivary nucleus (no. 250), the principle trigeminal nucleus (no. 251), and the facial motor nucleus (no. 252) can be specified as *Pax6*-expressing areas (in s, t, u). The cerebral primordium lateral to the pontine area remain expressing *Pax6* at a high level (see no. 174 in w). All scale bars represent 1 mm in length.

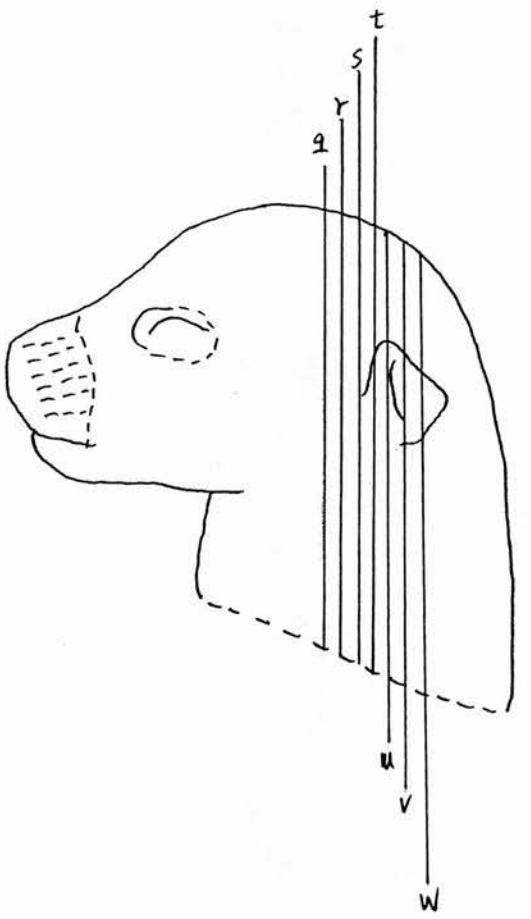

Figure 3.9 (day 18.0 p.c.; coronal sections; continued)

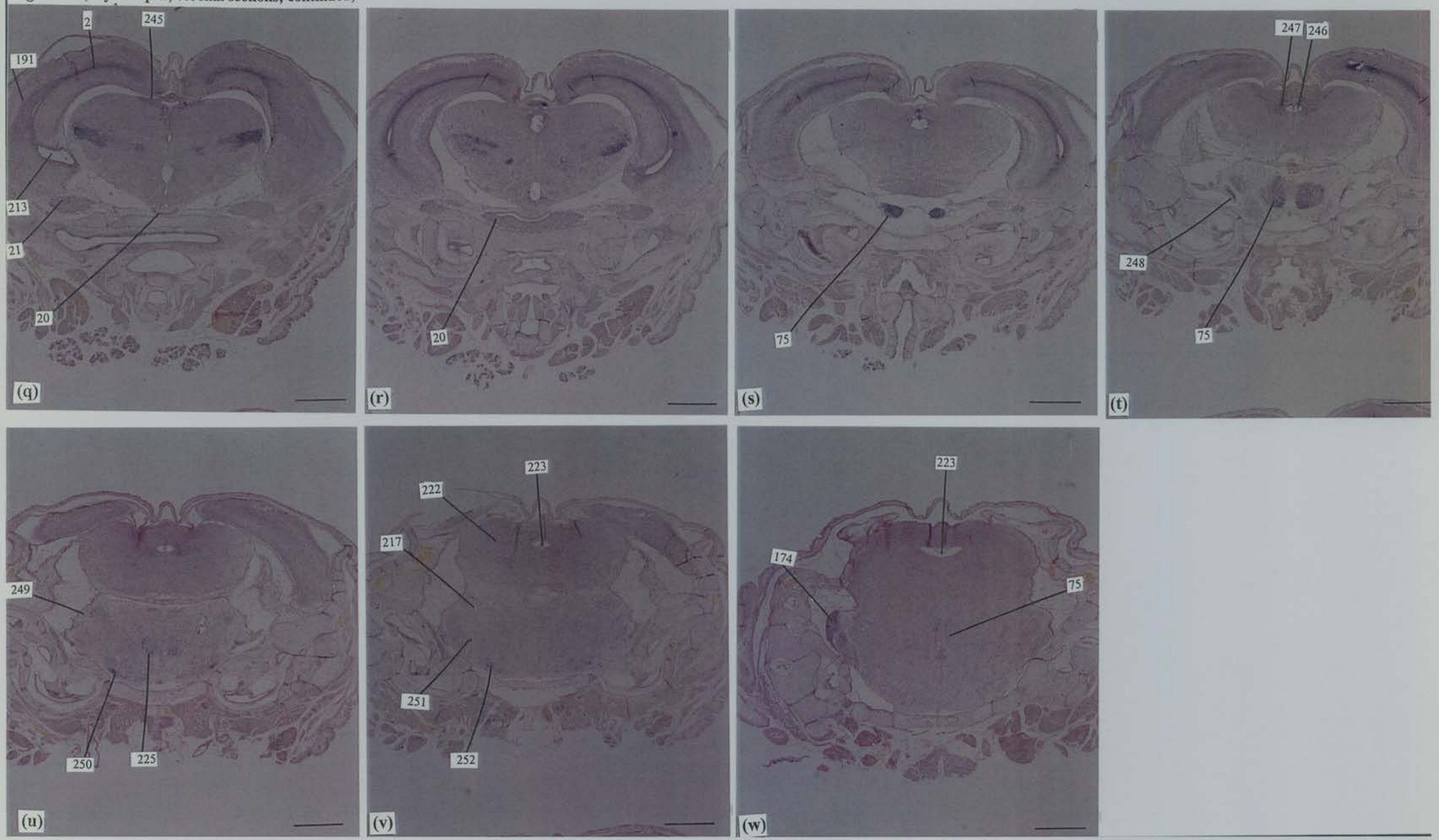

Figure 3.10 (a to h; to be continued on the following page) Mouse *Pax6* expression in the brain after birth represented by *in situ* hybridization on coronal sections.. The ventral side points downwards. The planes of cutting are shown below in a schematic diagram. Tissues in a to e are at day 1.0 after birth. Those tissues in f to h are at day 7.0 after birth. At day 1.0 after birth (see a), in the olfactory bulb, *Pax6* expression is seen in the glomerular layer (no. 253), mitral cell layer (no. 255), and internal granular cell layer (no. 256). Ventral to the olfactory bulb is the rhinencephalon that exhibits *Pax6* transcripts in the frontal neocortex (no. 257 in b). In the telencephalon, hints of *Pax6* expression remain seen in the neocortical neuroepithelium (no. 2 in d). The posterior hypothalamus (no. 259) and the cerebral peduncle (no. 216) also show hints of *Pax6* expression, as well as the fields of Forel (no. 130) and cortical plate (no. 258) (see d; e). At day 7.0 after birth, *Pax6* expression in the telencephalon and diencephalon is generally comparable to that seen at day 1.0 after birth (compare 3.10.d, e with 3.10.f). However, in the thalamic area, *Pax6* transcripts can be specified in the area of the subthalamic nucleus (no. 161) and hints of expression are found in the hippocampal neuroepithelium (no. 137) (see 3.10.f). Particularly interesting changes regarding *Pax6* expression found by day 7.0 after birth are in the superior colliculus, the cerebellum, and the inferior olive. In the superior colliculus, *Pax6* transcripts are intensely concentrated in the surface layers of external germinal neuroepithelium (no. 222); this is not observed before birth (see 3.10.h). The cerebellum at this gestation age has been expanded to cover the lateral and ventrolateral part of the pons and *Pax6* transcripts are concentrated in the convoluted external granular (germinal) neuroepithelium (no. 229 in g; h). Scale bars: in a to e, 5 mm; in f - h, 6 mm.

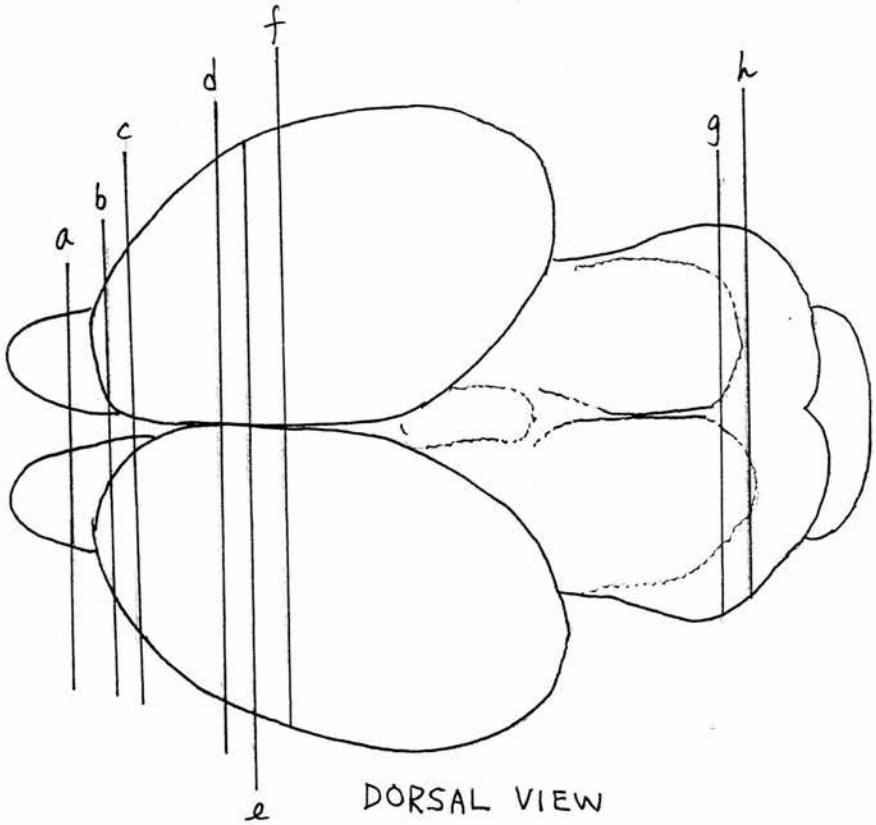

Figure 3.10 (postnatal; coronal sections)

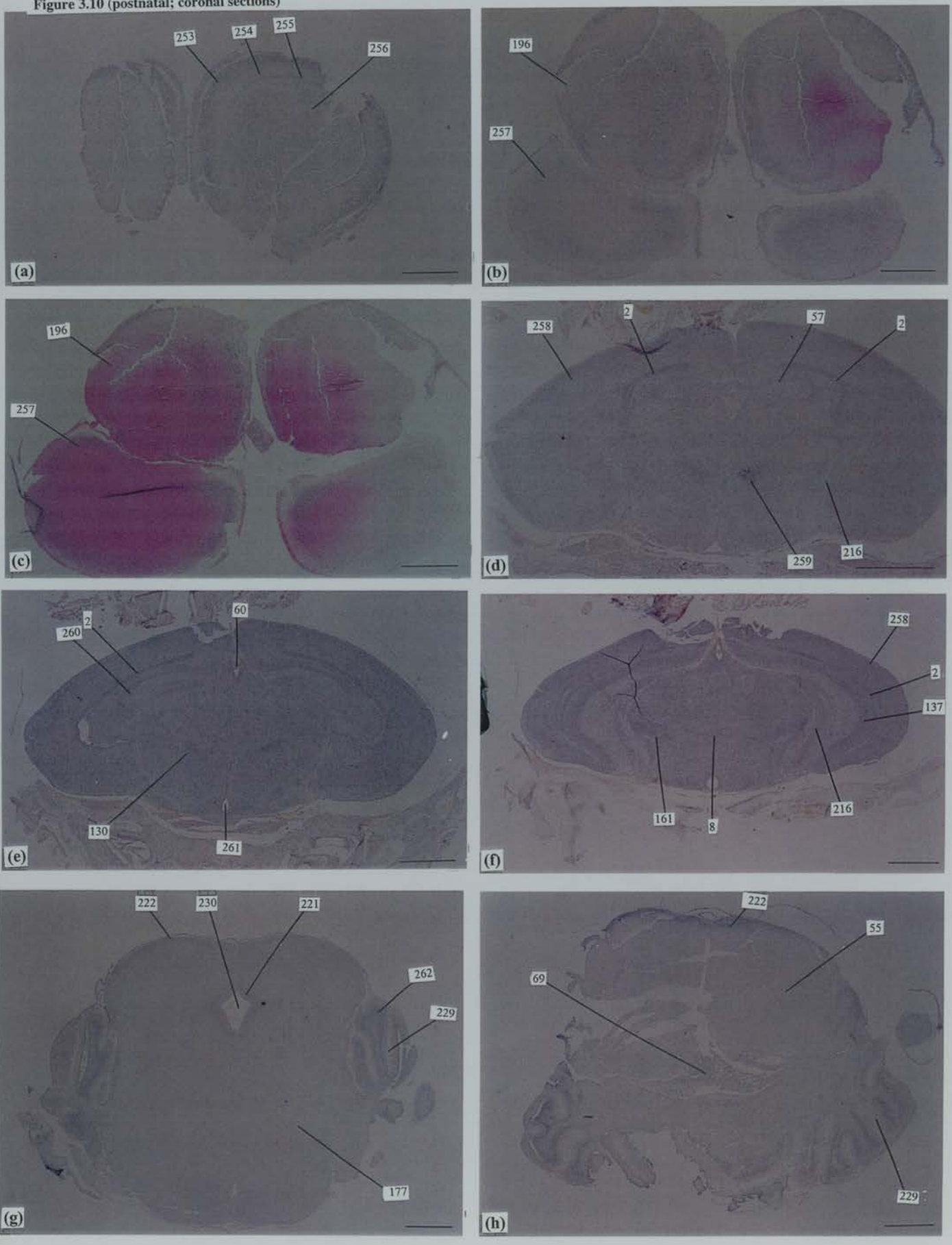

Figure 3.10 (i to p) Mouse *Pax6* expression in the brain after birth represented by *in situ* hybridization on coronal sections.. The ventral side points downwards. The planes of cutting are shown in a schematic diagram below. The tissue in i is at day 1.0 after birth. Those tissues in j to o are at day 21.0 after birth. k is a magnified view of the olfactory bulb shown in j. p is a magnified view on the proximal end of the optic cup. In the neural retina at day 1.0 after birth, convincing evidence for the confinement of *Pax6* transcripts within the ganglion cell layer (no. 204) and the internal nuclear layer (no. 203), as well as the absence of *Pax6* expression in the pigmented retinal epithelium (no. 28) is found (see 3.10.p). In the inferior olive at day 7.0 after birth, *Pax6* is also intensely expressed (nos. 263 and 264 in 3.10.i). At day 21.0 after birth (see 3.10.j, k), in the olfactory bulb, *Pax6* transcripts are seen in the internal granular cell layer (no. 256) and glomerular layer (no. 253). The mitral cell layer (no. 255) as well as the external plexiform layer (no. 254) do not exhibit evidence of *Pax6* expression. In the telencephalon and diencephalon (see 3.10.m, n, o), *Pax6* transcripts are detected in the neocortical neuroepithelium (no. 2), cortical plate (no. 258), stria medullaris (no. 274), fimbria (no. 272), subicular area (no. 273), and the differentiation field of intermediate thalamus (no. 158). Particularly interesting is in the corpus callosum (no. 269) and in the deep layers of superior colliculus (no. 168) where *Pax6* transcripts are found along with the left-right neuronal projections (see 3.10.o). Scale bars: in i, 6 mm; in j, l, m, n, o, 10 mm; in k, 250 μm; in p, 200 μm.

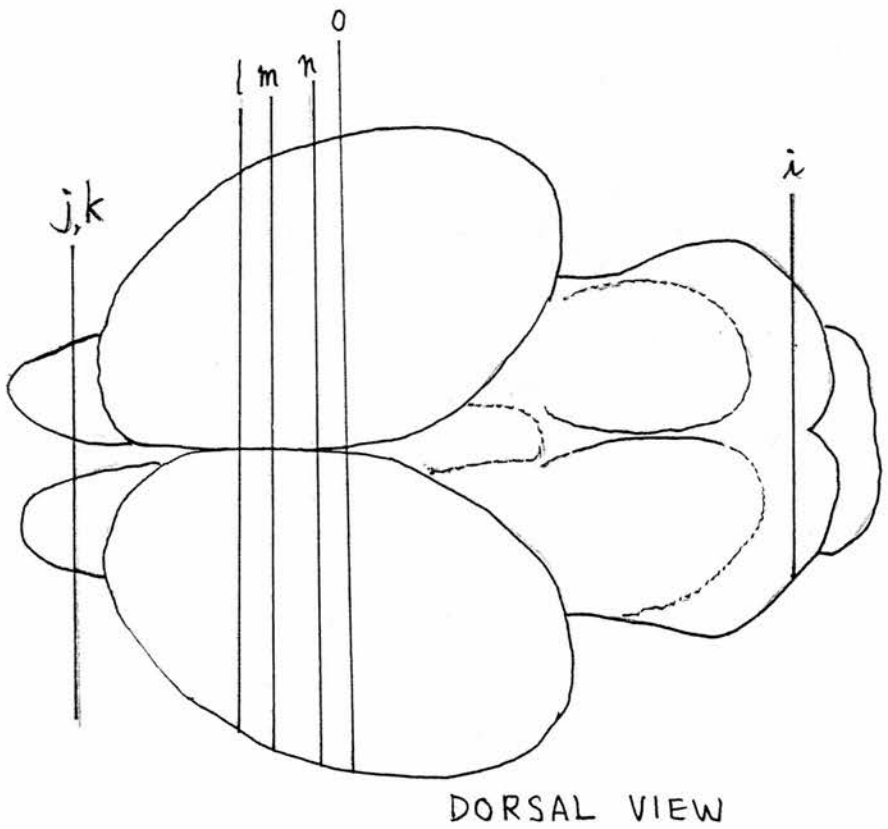

gure 3.10 (postnatal; coronal sections; continued)

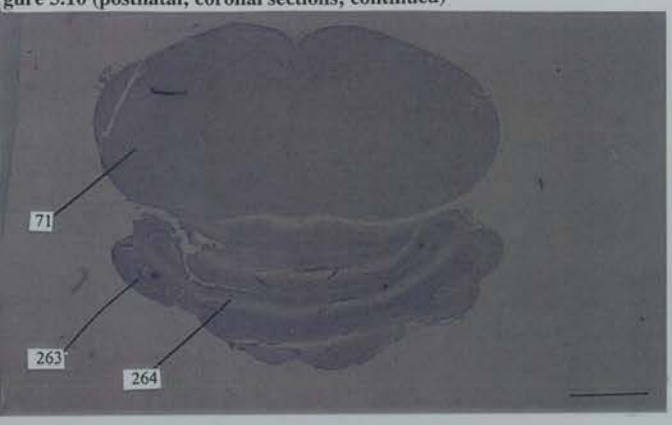

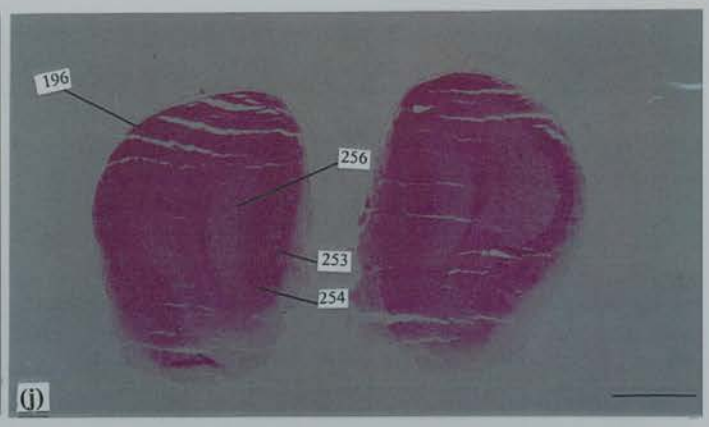

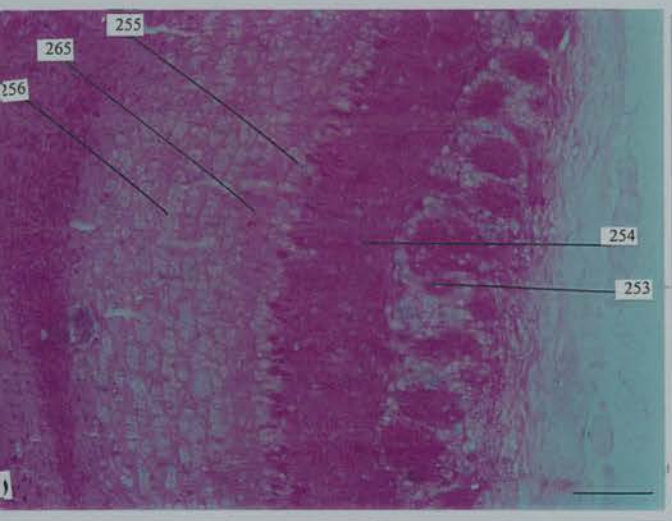

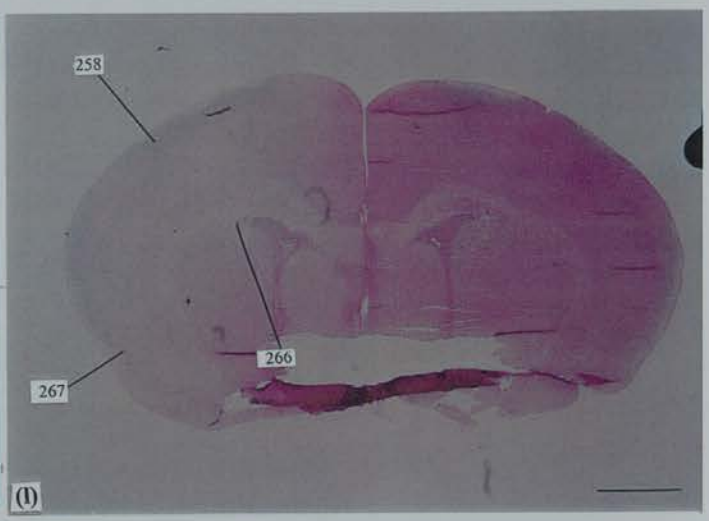

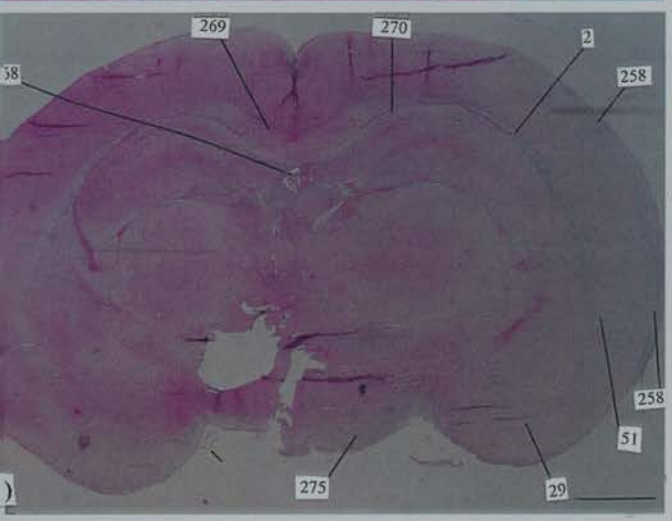

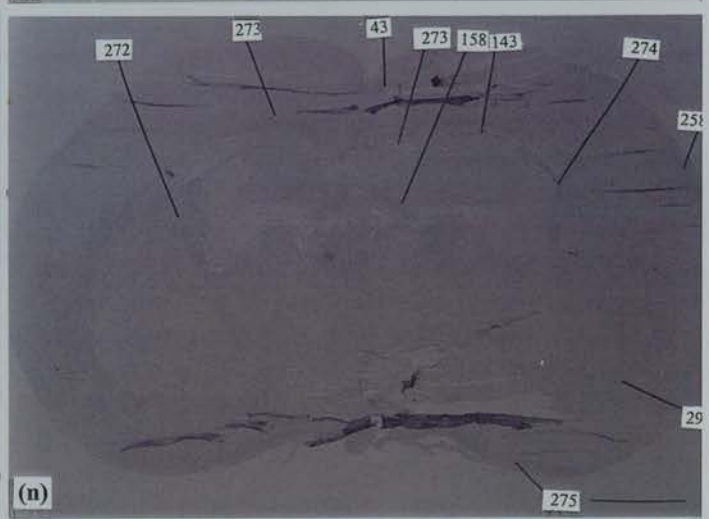

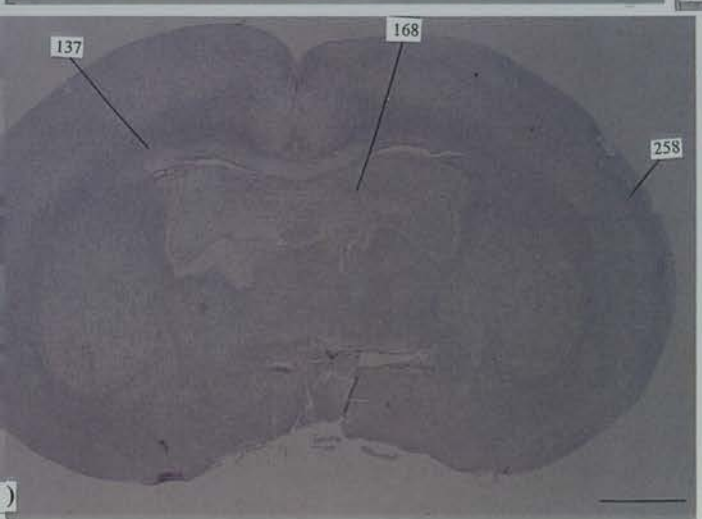

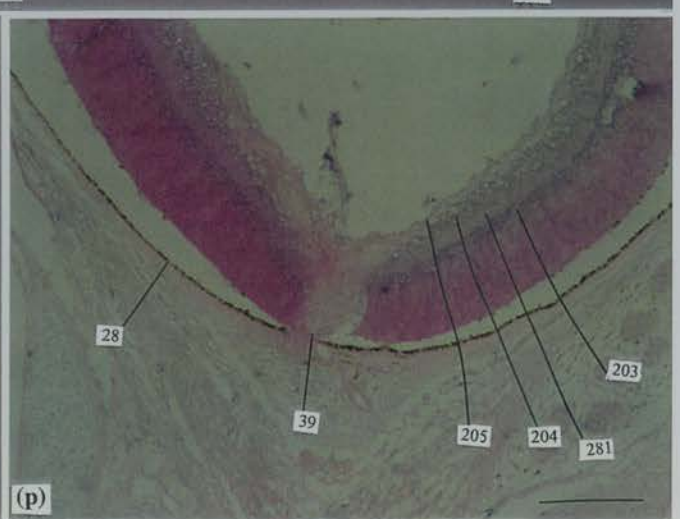

Figure 3.11 (a to h; to be continued on the following page) Nerve fiber projections in the mouse head region at day 15.0 p.c. represented by serial transverse sections that have been processed through Linder's silver impregnation with Luxol fast blue stain. The axons are in brown colour and the myelin in dark green colour. The brain shows apparent nerve fiber projections at the anterior pretectal (no. 56 in c) and tectal region (no. 57 in b) where *Pax6* is heavily expressed (compare figures 3.11.b and 3.11.c with 3.6.b). As the tranverse planes are lower, nerve fiber projections can be seen in the paraventricular nucleus (no. 129) and areas surrounding the lateral habenular nucleus (no. 277) (see 3.11.c). As the transverse planes go lower, nerve fiber projections are found in the junction between tegmental formation and hypothalamus (no. 279 in 3.11.d) where *Pax6* transcripts are present (compare figures 3.6.d with 3.11.d), as well as in the cerebellar primordium (no. 174 in 3.11.d, e) and the midbrain reticular formation (n0. 73 in e) whose *Pax6* expression is obvious (compare figure 3.11.e with 3.6.f). However, apparent nerve fibers are found in the internal capsule where *Pax6* is not expressed (no. 106 in f). Nerve fibers can also be seen in the medulla (no. 71 in h) and the surface of medulla (no. 107); both are *Pax6*-expressing. All scale bars represent 0.5 mm.

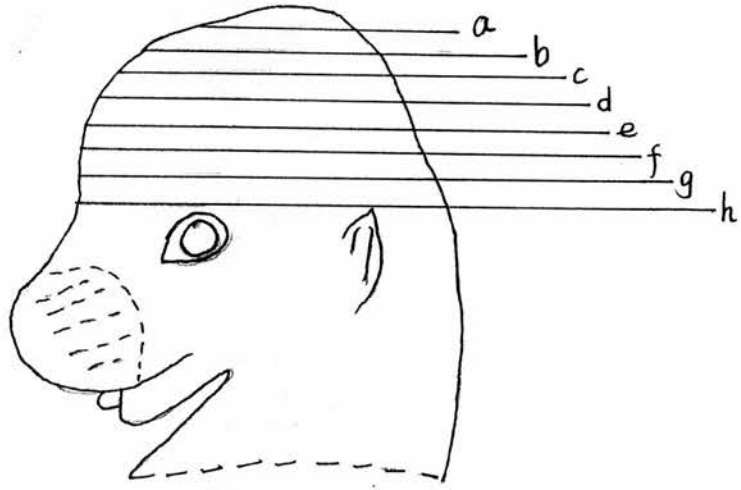

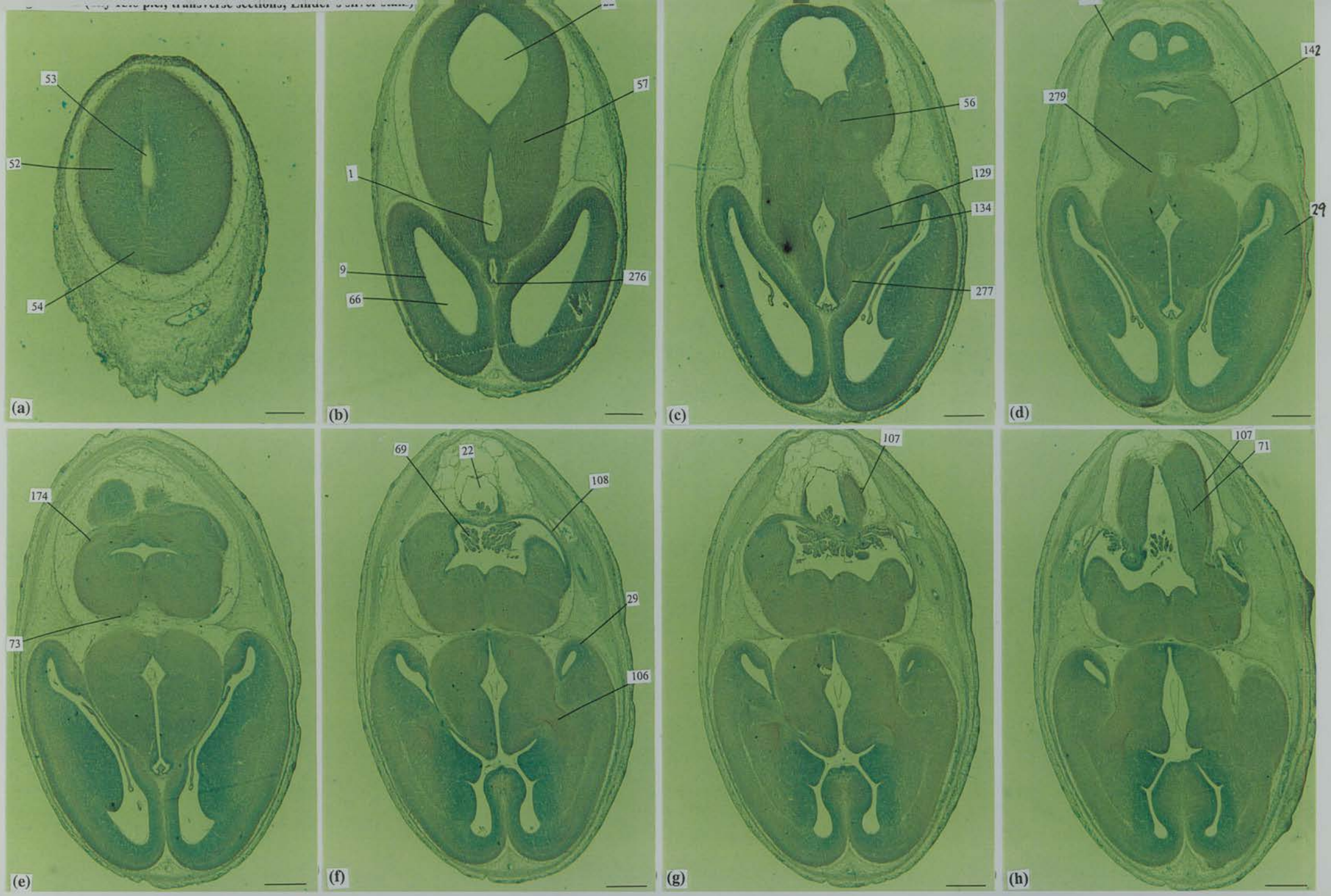
53
52
54
(a)
57
1
9
276
66
(b)
56
129
134
277
(c)
142
279
29
(d)
174
73
(e)
69
22
108
29
106
(f)
107
(g)
107
71
(h)

Figure 3.11 (i to p) Nerve fiber projections in the mouse head region at day 15.0 p.c. represented by serial transverse sections that have been processed through Linder's silver impregnation with Luxol fast blue stain. The axons are in brown colour and the myelin in dark green colour. Nerve fiber projections are seen in the cerebellar primordium (no. 108 in i), the surface of medulla oblongata (no. 107 in i), and in the superior central raphe nucleus in the pontine area (no. 75 in k). Apparent nerve fiber projections are also found in the cerebellar primordium (108 in i and m). In the pituitary primordium, however, no apparent nerve fiber projection is found (no. 20 in o), although *Pax6* is expressed there. In the *Pax6*-expressing optic chiasma (no. 114 in o) and the neural retina (no. 205 in o), nerve fiber projections are detected. The optic stalk also contains nerve fiber projections, although *Pax6* is not expressed there after day 14.0 p.c. (see figure 3.5.o). All scale bars represent 0.5 mm in length.

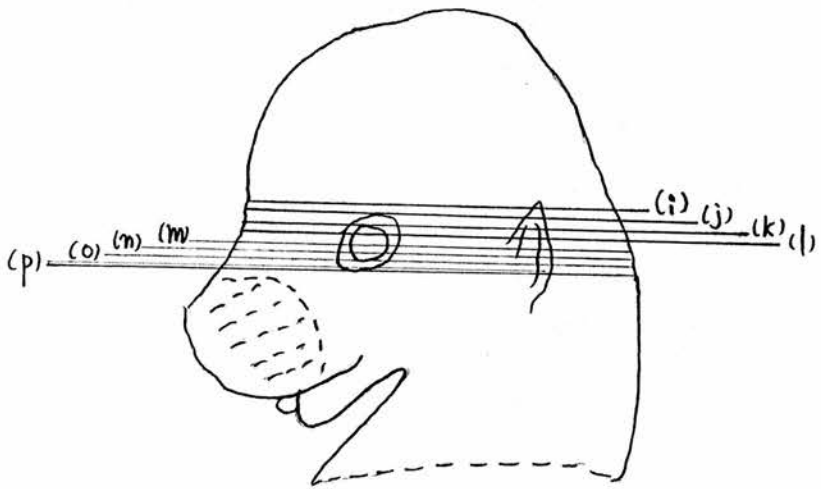

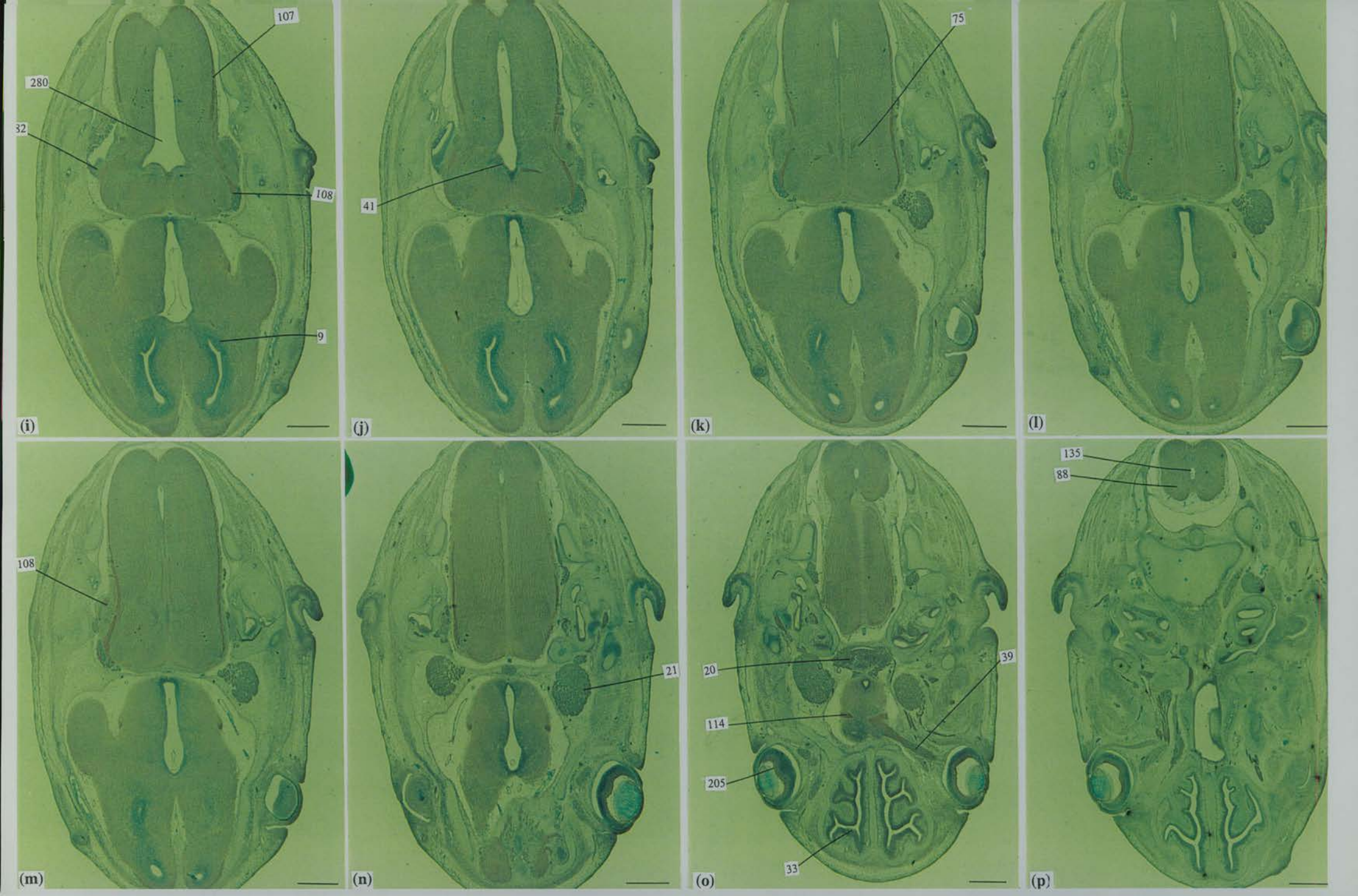
107
280
32
108
9
(i)
41
(j)
75
(k)
(l)
108
(m)
21
(n)
20
114
205
39
33
(o)
135
88
(p)

Chapter 4: *Pax6* expression during chick embryogenesis and its correlation with lens differentiation

4.1 Introduction

4.1.1 Aims of this chapter

Aims of this chapter are (1) to investigate *Pax6* expression during chick embryogenesis, particularly at stages relevant to eye formation and (2) to investigate whether *Pax6* expression correlates with lens differentiation in the chick head surface ectoderm. *In situ* hybridization on wholemount embryos and tissue sections was used to obtain the expression data. For the correlation of *Pax6* expression with lens differentiation, specified areas of chick head surface ectoderm were cultured *in vitro* and αB crystallin as a marker for lens differentiation was detected by immunohistochemistry (Scotting *et al.*, 1991). All technical details are described in chapter 2 (sections 2.6 - 2.7).

4.1.2 Rationale for determining chick *Pax6* expression at later stages of development

During the course of this study, *Pax6* expression in the chick was reported by Li *et al.* (1994), Heyman *et al.* (1995), Simon *et al.* (1995) and Buxton *et al.* (1997). The latter three reports only looked at *Pax6* expression in the rhombomeres. The expression data reported by Li *et al.*, however, did not go beyond stage 14. Li *et al.*, therefore, did not describe whether *Pax6* is expressed in the optic cup, lens, optic stalk, and corneal epithelium. Furthermore, whether *Pax6* is expressed in the olfactory epithelium was not determined and the precise pattern of *Pax6* expression in the definite fore-, mid-, or hindbrain was not described. The lack of chick *Pax6* expression data in these areas makes it difficult to use chick as a model animal. Thus, the first aim of this chapter is to investigate chick *Pax6* expression in the tissues and at the stages that have not been previously reported, with particular emphasis on the expression of *Pax6* during eye formation.

4.1.3 Rationale for correlating chick *Pax6* expression with lens differentiation

When this study was initiated, several lines of evidence suggested that *Pax6* is involved in lens differentiation. For example, *Pax6* mutation causes absence of lens as a part of the failure of eye formation in the mouse (Hogan *et al.*, 1986; 1988). The absence of lens in the *Sey/Sey* mice does not result from degeneration or developmental retardation of lens or lentoid cells, but rather from the lack of lens placodes (Grindley, 1996). It was also found that *Pax6* expression in the normal mouse head surface ectoderm is first in a broad domain and is downregulated and specifically maintained in the developing lens placode at later stages (Grindley *et al*, 1995). Furthermore, *Pax6*-expressing tissues such as the pineal gland, embryonic retina, iris, and the anterior pigmented retinal epithelium (Walther and Gruss, 1991; Grindley *et al.*, 1995) are capable of being transdifferentiated into lens (reviewed by

Okada, 1991). *Pax6* expression could therefore be a prerequisite for establishing a lens-forming bias in those tissues.

The distribution of lens differentiation capacity in the chick head surface ectoderm during early stages of development had been investigated by Barabanov and Fedtsova (1982). It was demonstrated that, in addition to presumptive lens ectoderm, the lateral head ectoderm and stomodeal ectoderm of stages 10 - 11 (S10 - S11) chick embryos could differentiate into lens when cultured without adjacent mesenchyme (Barabanov and Fedtsova, 1982). Chick head surface ectoderm at earlier stages (S4 - 5, S6 and S8) also exhibited lens forming capacity in broad domains that were not necessarily located within the presumptive lens ectoderm. Comparison of the distribution of lens differentiation capacity in the chick head surface ectoderm reported by Barabanov and Fedtsova (1982) with the distribution of *Pax6* transcripts reported by Li *et al.* (1994) shows striking similarity, supporting the idea that *Pax6* may establish a lens forming bias. For example at stage 6, the area marked A in Barabanov and Fedtsova's report (see figure 4.6), which exhibits high lens-forming capacity, corresponds to a high level of *Pax6* expression. This is in contrast to adjacent areas (marked B) with a low level of *Pax6* expression and low lens-forming capacity. Furthermore, Barabanov and Fedtsova (1982) reported restriction of lens-forming capacity in the surface ectoderm adjacent to the mesencephalon in which Li *et al.* (1994) demonstrated downregulation of *Pax6* expression.

However, there is one point that devalues Barabanov and Fedtsova's data (1982) in supporting the involvement of *Pax6* in lens differentiation -- no controls were used in their study. Surface ectoderm outside the presumably broad lens-forming domain, for example from more caudal region such as the rhombencephalon or trunk region, could have been used as negative controls to exclude the possible lens-inductive effect from unknown factors in the culture medium. Particularly, the medium used by Barabanov and Fedtsova (1982) contained 10 % fetal calf serum and 10 % embryonic extract from 9-day chick embryos (although without eyes). Transcriptional stimulation of δ1-crystallin is found in growth factors such as insulin and insulin-like growth factor I (IGF-I) (Beebe *et al.*, 1987; Alemant *et al.*, 1990; Hyatt and Beebe, 1992); both are commonly present in fetal calf serum and in embryonic tissues (McAvoy and Chamberlain, 1990). Thus, the lens-forming capacity observed by Barabanov and Fedtsova in some areas of head surface ectoderm could possibly be conferred by the stimulatory effects of growth factors rather than by innate factors.

The above mentioned data prompt me to investigate the correlation of *Pax6* expression and lens differentiation. If *Pax6* expression is switched off during culture and lens tissues are still obtained after culture, it is less likely that *Pax6* functions in the process of lens differentiation. *Pax6* may be switched on in those tissues where *Pax6* transcripts are not present in the beginning of culture. Determination of whether lens is differentiated in those tissues will better define the role of *Pax6* during the process of lens differentiation.

In light of the above mentioned reasons, a precise correlation of *Pax6* expression and lens differentiation is performed in this study.

4.2 Results

4.2.1 *Pax6* expression during chick embryogenesis

4.2.1.1 Stage 6^+

No *Pax6* expression is found at stages earlier than stage 6 (i.e. stage 4). The earliest appearance of *Pax6* expression in the chick is seen at stage 6^+ in the anterior margin of the neural plate and in the neural ridge in the anterior part of the embryo (see figure 4.1.a, no. 6). The neural plate itself (no. 1), however, does not appear to exhibit *Pax6* expression. There is also evidence of expression in the posterior 1/3 of the developing embryo at stage 6^+. The surrounding cells of Hensen's node (no. 3) appear to show higher level of expression than the others within the posterior region. This expression in the posterior 1/3 of the developing embryo and in the cells surrounding Hensen's node is never detected in the controls (not shown).

4.2.1.2 Stage 8

At stage 8, intense *Pax6* expression is detected in the neural folds, particularly in the neural ridge (no. 5 in figure 4.1.b), in the prospective cephalic region (see figure 4.1.b). The expression is less intense in the cephalic neural plate (no. 1) which is located lateral to the cephalic neural folds. In the trunk region, *Pax6* transcripts are detected in the developing neural folds adjacent to the sites of somite formation (see the first pair of somites, i.e. no. 8 in b). This expression diminishes in the portion immediately caudal to the last pair of somites seen at this stage of development. Evidence of *Pax6* expression is also found in the area surrounding Hensen's node (no. 3 in b).

4.2.1.3 Stage 9

At stage 9 (7 - 8 pairs of somites), *Pax6* is expressed in two lateral cephalic regions in the rostral half of the cephalic region (see no. 10 in figure 4.1.c). There are sharp boundaries between the expressing and non-expressing regions. In the wall of the anterior neuropore (no. 9), no obvious presence of *Pax6* transcripts is found.

In the trunk region, *Pax6* transcripts are detected in the neural fold as noted at stage 8. This expression extends rostrally to the cephalic region and caudally to a region just beyond the last defined pair of somites that are present at this stage of development. The somites and the intersomitic grooves do not show any *Pax6* expression. In the trunk neural folds where *Pax6* transcripts are detected, the

expression appears to be more intense in the segments that are not flanked by somites. In the site of Hensen's node (no. 3), *Pax6* transcripts are only minimally detectable.

4.2.1.4 Stage 10

At stage 10 (9-10 pairs of somites), *Pax6* expression in the cephalic region is found in the two lateral bulges of presumptive optic vesicles (see figure 4.1.e, no. 10). This expression in the cephalic region is similar to that formerly noted at stage 9 (compare figure 4.1.e with figure 4.1.d), and the sharp lines of demarcation between the caudal and the rostral as well as between the lateral and the midline cephalic regions are maintained. In particular, as viewed externally in wholemount preparations, *Pax6* is absent from the wall of anterior neuropore (no. 9) and from the cephalic midline region (nos. 11 and 12). To confirm the lack of expression in the two regions, *in situ* hybridization on coronal sections was performed. The results (see figure 4.2.a) show apparent absence of *Pax6* transcripts in both the surface ectoderm and the neuroectoderm that surround the anterior neuropore. In the midline cephalic neuroepithelium (see the intense stain surrounding the future third ventricle, i.e. no. 16 in figure 4.2.a), however, *Pax6* transcripts are detected.

In the trunk region, *Pax6* expression within the developing neural folds extends more caudally in association with the formation of additional somites. The more intense expression in the neural fold segments that are not flanked by somites, i.e. the intersomitic trunk neuroepithelium (no. 14 in figure 4.1.e) becomes more obvious (see figure 4.1.e; compare no. 14 with no. 15). In Hensen's node (no. 3 in figure 4.1.e), however, no evidence of *Pax6* expression is seen by stage 10.

4.2.1.5 Stages 11 - 12

At stage 11, when the optic vesicles are clearly present and bulge laterally into the optic recesses (no. 30 in figure 4.2.b) in the presumptive forebrain, *Pax6* expression is detected in loop-shaped structures that constitute the surface ectoderm (no. 24) and the neuroectoderm (no. 25) of the primitive optic primordium (see figure 4.2.b). In the neuroepithelium of the presumptive mesencephalon (no. 29) and anterior rhombencephalon (no. 28), no evidence of *Pax6* expression is found, nor are *Pax6* transcripts present in the neuroepithelium that surrounds the closing anterior neuropore (no. 22 in figure 4.2.b). In the more caudal rhombencephalic region, however, hints of *Pax6* expression are found in the neuroepithelium and in the cells flanking rhombomere 3 (r3) and rhombomere 5 (r5) at stage 11 (see arrows in figure 4.5.a). By stage 12, *Pax6* expression in those cells becomes more evident (see figure 4.5.b). In the head surface ectoderm, the part surrounding the closing anterior neuropore shows no expression, while the two lateral regions overlying the optic vesicles as well as regions overlying the presumptive mesencephalon and rhombencephalon show intense expression (see figure 4.2.b). In the trunk region, *Pax6* expression within the neural folds extends more caudally as more somites are formed (data not shown).

4.2.1.6 Stage 13

At stage 13, *Pax6* continues to be expressed in the loop-shaped structures that constitute the primitive optic stalks (see figures 4.2.c, d). *Pax6* transcripts are clearly present in the telencephalic neuroepithelium (no. 40 in figure 4.2.d) and at the most anterior end of the presumptive prosencephalic neuroepithelium, i.e. at the site of the now closed anterior neuropore (see figure 4.2.d). This is confirmed in transverse sections in figure 4.3.a, although only few *Pax6*-expressing cells are seen and the level of expression is not as intense as that in the lateral surface ectoderm. *Pax6* is also expressed in the neuroepithelium of the presumptive prosencephalon (see figures 4.2.c; d), but not in the presumptive mesencephalon (see figure 4.3.b).

Pax6-expressing cells are present around the entire area of head surface ectoderm at the same level of transverse plane as the optic vesicle (see figure 4.2.c). In contrast, in the region close to the anterior neuropore, only the lateral parts of the head surface ectoderm display evidence of *Pax6* expression (see no. 43 in figure 4.3.a). The same *Pax6* expression in the lateral head surface ectoderm is also detected in the presumptive mesencephalic region (see no. 46 in figure 4.3.b).

Pax6 transcripts are clearly seen in the neuroepithelium of the anterior (no. 38) and the posterior (no. 39) spinal cord in the trunk region, as demonstrated in figure 4.2.d.

4.2.1.7 Stage 16

By stage 16, when the epithelium of the lens placode has invaginated and the optic cup has differentiated into an inner neural retina (no. 48) and an outer pigmented neural epithelium (no. 49), *Pax6* expression is detected in the differentiating lens (no. 52) and the surface ectoderm overlying it (no. 50) (see figure 4.3.c). *Pax6* transcripts are also present in the neural (no. 48) and pigmented layer (no. 49) of the optic cup, the neuroepithelium of the rostral part of the prosencephalon (no. 58), as well as in the anterior medulla (no. 53) in the rhombencephalon which is in close proximity to the otic vesicles (no. 55) (see figure 4.3.c). In the optic cup, higher levels of expression are seen in the rim (no. 57). This is particularly obvious for the neural retina. The hypothalamic neuroepithelium and the otic vesicles do not exhibit *Pax6* expression. In the head surface ectoderm, *Pax6* expression covers a broad area overlying the eye and extends both dorsally and ventrally.

4.2.1.8 Stages 17 - 18

By stages 17 - 18, *Pax6* expression in the anterior part of the head neuroepithelium (no. 64) (now the neocortical neuroepithelium in the anterior forebrain) is still apparent (see figure 4.4.a). *Pax6* expression remains in the optic cup and the optic stalk (no. 59), although the expression is not as obvious as that at stage 16. Transcripts of *Pax6* are also detected in the head surface ectoderm

overlying the presumptive eye region, particularly the corneal epithelium (no. 60) (figure 4.4.a), as well as in the ventral pontine neuroepithelium and the dorsal part of medullary neuroepithelium (no. 62 and no. 71 in figure 4.4.a). Efforts have been made to detect *Pax6* transcripts in the olfactory epithelium, but only by stage 17 is definite *Pax6* expression seen (see figure 4.4.b, no. 66).

4.2.1.9 Stage 28

By stage 28, *Pax6* expression appears to be detectable within the surface ectoderm covering the eye region as shown in the whole mount preparation illustrated in figure 4.4.c.

4.2.2 Correlation of *Pax6* expression with lens differentiation *in vitro*

To investigate correlation of *Pax6* expression with lens differentiation, small tissue fragments from designated areas of chick head surface ectoderm (with their underlying mesenchymes) at stages 8 and 11 were cultured *in vitro*. The areas of head surface ectoderm were designated according to *Pax6* expression pattern reported by Li *et al.* (1994), as shown in figure 4.7.

Following culture, the presence of *Pax6* transcripts and αB crystallin were analysed (technical details in sections 2.6 - 2.7 in chapter 2).

4.2.2.1 Morphological varieties of cultured surface ectoderm and definition of lens differentiation

At the onset of this study, it was observed that lens or lens-like cellular differentiation exhibited a variety of morphological forms after culture. For example, with a simple eosin staining, some cultured tissues from different areas of the surface ectoderm exhibited a typical lens shape that appeared to contain primary lens fibers (figure 4.8.a). Others just showed bubble-like lentoid bodies combined with fibre-like structures (figure 4.8.b). More commonly, they were simply fibre-like (figure 4.8.c) or bubble-like structures (figure 4.8.d). The formation of these morphological variations was irrespective of the origin of cultured tissues, i.e. all designated areas were capable of forming each type of morphology mentioned above. To examine whether a specific morphology could be readily regarded as 'positive in lens differentiation', an antibody against αB crystallin was used. The results showed that no specific morphology could be readily correlated with the presence of αB crystallin. Thus, the cultured surface ectoderm was defined 'positive in lens differentiation' only on the basis of αB crystallin expression, i.e. irrespective of their morphology. Two examples are shown in figure 4.9 (a and c; with their respective *Pax6* expression pattern in b and d).

4.2.2.2 Head surface ectoderm cultured from stage 8

Table 4.1 shows the expression of αB crystallin and *Pax6* in different areas of stage 8 chick head surface ectoderm following 4 - 6 days of culture on millipore membranes.

area	total no. of cultures performed and analysed	no. of surface ectoderm with presumptive *Pax6* expression before culture	αB crystallin expression after culture	*Pax6* expression after culture	αB crystallin expression combined with *Pax6* expression after culture
AA	8	8	3	3	3
AP	7	7	2	2	2
B	12	12	8	8	8
C	10	0	0	0	0

Table 4.1 Correlation of *Pax6* expression and lens differentiation in stage 8 chick head surface ectoderm. All tissues were grafted with underlying mesenchyme and cultured on millipore membranes for at least 4 days. The area codes were according to those illustrated in figure 4.7. All the *Pax6*-expressing tissues were also expressing αB crystallin. Whenever αB crystallin was absent after culture, *Pax6* expression was also absent.

4.2.2.3 Head surface ectoderm cultured from stage 11

Table 4.2 shows the expression of αB crystallin and *Pax6* in different areas of stage 11 chick head surface ectoderm following 4 - 6 days of culture on millipore membranes.

area	total no. of cultures performed and analysed	no. of surface ectoderm with presumptive *Pax6* expression before culture	αB crystallin expression after culture	*Pax6* expression after culture	αB crystallin expression combined with *Pax6* expression after culture
a	6	6	6	6	6
b	6	6	3	3	3
c (dorsal)	5	0	0	0	0
c (ventral)	6	0	3	3	3
d	4	0	0	0	0
e	4	0	0	0	0

Table 4.2 Correlation of *Pax6* expression and lens differentiation in stage 11 chick head surface ectoderm. All tissues were grafted with underlying mesenchyme and cultured on millipore membranes for at least 4 days. The area codes were according to those illustrated in figure 4.7. All the *Pax6*-expressing tissues were also expressing αB crystallin. Whenever αB crystallin was absent after culture, *Pax6* expression was also absent.

4.3 Discussion

4.3.1 Establishment of *Pax6* expression in the olfactory epithelium, the eye region, the brain and the head surface ectoderm after stage 14

Results of this study confirm the data previously reported by Li *et al.* (1994) on chick *Pax6* expression before stage 14. Furthermore, transient *Pax6* expression in the Hensen's node is found at stages 6^{+} - 9, which is not previously reported. After stage 14, *Pax6* expression in the eye region, the brain and the head surface ectoderm is established by this study. Particularly, this study demonstrates the presence of *Pax6* transcripts in the olfactory epithelium, which was not determined by Li *et al.* (1994).

Chick *Pax6* expression data after stage 14 is consistent with what has been found in many other species as discussed in chapter 3. The data also supports involvement of *Pax6* during the development of olfactory and visual nervous system. For example, in the developing eye, extensive *Pax6* expression in the optic cup, optic vesicle, cornea and lens after stage 14 is found. The rim of the optic cup exhibits the most intense expression, which is similar to the situation in the mouse. In the developing brain, *Pax6* transcripts are detected in the presumptive telencephalic and thalamic neuroepithelium, but not in the hypothalamic area. Again, this is comparable to the expression patterns in the mouse.

Pax6 expression during chick embryogenesis also exhibits developmental restriction that has been defined and discussed for mouse expression in chapter 3 (see section 3.3.4). In the brain, for example, the most obvious developmental restriction occurs between stage 8 to 9. By stage 8, the neural plate and the neural ridge in the presumptive head exhibit *Pax6* expression throughout the whole region, whereas by stage 9 only the anterior half of the presumptive head expresses *Pax6*, and the expression in not found in the midline (compare figure 4.1.b with 4.1.c). Another example of developmental restriction is found in the head surface ectoderm. At stages 17 - 18, *Pax6* transcripts are still detected in a broad domain. By stage 28, however, *Pax6* transcripts are distributed only in the head surface ectoderm covering the eye (compare figure 4.4.a with 4.4.c). Although the precise timing of this developmental restriction is not clear, it must occur between the two stages. The implications of the developmental restrictions observed in the chick are likely to be similar to those in cellular proliferation, migration, and differentiation as have been discussed in chapter 3 for the mouse. My particular interest is in the relevance of this restriction to lens differentiation and this is further discussed in section 4.3.7.

4.3.2 The different first appearance of *Pax6* expression between the chick and the mouse

Li *et al.* (1994) reported that the first appearance of chick *Pax6* transcripts appeared earlier than stage 6 and they described 'a scattered population of weakly *Pax6*-positive cells at the anterior end of the embryo, near the prechordal plate', although they also mentioned that stage 6 embryos are 'the earliest

to exhibit definite expression of *Pax6*'. In this study, the earliest *Pax6* expression was observed at stage 6 in the same region as described by Li *et al.* (1994). My result has confirmed that stage 6 is the first stage when definite *Pax6* expression can be observed in the chick.

The first expression of *Pax6* in the chick in the non-neural ectodermal cells is surprisingly different from the data in the mouse whose earliest detectable *Pax6* expression is seen in the neuroepithelium of the presumptive forebrain and hindbrain by day 8.0 p.c. (Walther and Gruss, 1991). This difference of earliest site of *Pax6* expression may be due to the different mode of embryogenesis between the chick and the mouse. Alternatively, mouse *Pax6* may be first expressed in the non-neural ectodermal cells that have not been described in previous reports.

Both the mouse and the chick embryo start to develop by cell divisions (mitosis) from a single fertilized cell. Following cell divisions, the total number of cells is multiplied and differentiation of lineages of cells become possible. In the chick, early cell divisions after fertilization lead to the formation of the epiblast, the hypoblast, with the blastocoelic cavity located between the epiblastic and the hypoblastic layers of cells (Stern, 1990). By this arrangement, the early embryonic cells migrate from the margins of the blastocoel to become extra-embryonic derivatives which are approximately equivalent to the trophectodermal cells in the mouse. However, in the mouse, the first cell divisions lead to the formation of the inner cells mass (ICM), the trophectoderm, and the blastocyst (blastocoelic) cavity (Kaufman, 1992). The blastocoelic cavity is surrounded by the trophectodermal cells which are approximately equivalent to those in the margins of the blastocoel in the chick. As the embryo develops, cells migrate rostrally from the primitive knot. In the chick, those cells that are located in the anterior margin of blastocoel migrate forward during embryogenesis in the anterior direction (Spratt, 1946; Stern, 1990). This migration results in a crescent-shaped band of cells in the anterior margin of the head neural plate, though the cells do not form the neural plate itself (Spratt, 1946). This crescent-shaped band of cells described by Spratt (1946) corresponds well to the site where *Pax6* expression was first observed at stage 6 (Li *et al.*, 1994). In the *Xenopus,* the first detectable embryonic *Pax6* expression is reported to be located in a similar crescent-shaped area in the anterior part of the embryo (Hirsch and Harris, 1997), suggesting that the specific site of earliest expression may be common in vertebrates.

In the mouse, similar to that in the chick, cell migration of trophectodermal cells in the anterior margin of the blastocoelic cavity is observed (Tam and Beddington, 1992). The first appearance of *Pax6* expression may therefore be in the trophectodermal cells, i.e. in the extra-embryonic derivatives of the ICM adjoining the anterior amniotic fold by days 7.5 - 8.0 p.c. This area of extra-embryonic derivatives was not described in the previous reports and remains to be investigated.

4.3.3 Implications of *Pax6* expression in the Hensen's node

Evidence of *Pax6* expression in the chick Hensen's node between stage 6 $^{+}$ to stage 9 was observed in this study, which was not previously reported. After stage 9, *Pax6* expression in the Hensen's node was minimal as the signals were not significantly different from the background, reflecting the transient nature of *Pax6* expression in this site.

The transient expression of *Pax6* in the Hensen's node has interesting implications. Hensen's node is the site where most hypoblastic cells start to migrate anteriorly (Stern, 1990). The migrating cells leave Hensen's node in an elongated array that gives rise to midline structures including the notochord, the floor plate, the midline endoderm and the medial part of somites (Hogan *et al.*, 1992). The period of hypoblastic cell migration in the chick overlaps with the period when *Pax6* transcripts are present in the Hensen's node. Hensen's node is also an organising centre governing the formation of the anterior-posterior axis in the chick embryo (Chen *et al.*, 1992). Furthermore, retinoic acid (RA), a presumptive morphogen, is enriched in Hensen's node and is developmentally regulated in the early chick embryo (Hogan *et al.*, 1992). Thus, it was suggested that endogenous retinoids may establish a concentration gradient from Hensen's node and play a role in establishing the primary anterior-posterior axis in the vertebrate (Chen *et al.*, 1992). One may therefore speculate that chick *Pax6* could possibly be implicated in the migration of the hypoblastic cells, as well as in the establishment of anterior-posterior axis under the regulation of RA during early chick embryogenesis. This possible involvement of *Pax6* in embryonic cell migration is supported by the abnormal cell sorting (Quinn *et al.*, 1996), as well as by the presence of heterotopic groups of cells found in the cerebral cortex in the *Sey/Sey* mice (Schmahl *et al.*, 1993; Grindley, 1996). The abnormal cell sorting is suggested to result from changes of adhesion molecules or cell surface molecules (Quinn *et al.*, 1996); both kinds of molecules are involved in cell migration. Possible involvement of *Pax6* in the establishment of primary anterior-posterior axis is supported by the loss of anterior-posterior identity of prosomeres in the *Sey/Sey* mouse (Warren and Price, 1997). The loss indicates that at least some parts of the anterior-posterior axis is disturbed.

4.3.4 Chick *Pax6* expression in the hindbrain suggests roles in establishing rhombomeric identity, axonogenesis and neuronal cell migration

In the rhombencephalon, as reported by Li *et al.* (1994), *Pax6* transcripts could be detected in the rhombomere 3 (r3) at stage 9. By stage 11, *Pax6* transcripts can be seen in r3 and r5 (illustrated in figure 2.F of Li *et al.*, 1994). In this study, however, no similar expression was found at stage 9 (see figure 4.1.c) and by stage 11 *Pax6* expression is seen in the entire rhombencephalic neuroepithelium (figure 4.5.a). In addition, the *Pax6*-expressing cell populations flanking the neuroepithelium of r3 and r5 were not described by Li *et al.* (1994). The differences between the present data and that of Li *et al.* (1994) likely result from the dynamic nature of *Pax6* expression in the chick hindbrain, which is suggested by other reports. For example, Heyman *et al.* (1995) reported that, although chick *Pax6* is

expressed in specific rhombomeres at stage 11, the transverse rhombomere specific stripes disappear and dorsal-ventral differences become more apparent at about stage 16. From stages 16 - 24, chick *Pax6* is preferentially expressed in rhombomere boundaries and in longitudinal stripes in the basal plate (Heyman *et al.*, 1995). Simon *et al.* (1995) reported that, at stage 15, *Pax6* expression in the alar plate of r3 and r5 weakens, while in the r2, r4 and r6 *Pax6* expression disappears altogether. Buxton *et al.* (1997) reported that, at stage 14, r2, r4, and r6 (and more caudally) show *Pax6* expression in the lateral and ventral neural tube, whereas expression in r3 and r5 extends more dorsally. Thus, significant changes of *Pax6* expression occur between stages 11 - 15, reflecting the dynamic nature of *Pax6* expression in the hindbrain.

There are several functions that can be suggested by *Pax6* expression in the rhombomeres. Firstly, the fact that *Pax6* is expressed specifically in non-neuroectodermal cells in r3 and r5, as observed at stage 11, suggests a role of *Pax6* in establishing r3 and r5 identities, in that cells from neighbouring neuromeres do not mix, while cells from two odd-numbered or two even-numbered neuromeres generally mix (Fraser *et al.*, 1990; Guthrie and Lumsden, 1991; Figdor and Stern, 1993; Guthrie *et al.*, 1993). Secondly, the preference of *Pax6* expression in the rhombomere boundaries (Heyman *et al.*, 1995) suggests that *Pax6* may be involved in axonogenesis. Rhombomere boundaries become delineated by transversely oriented axons from the time the first neurons differentiated (Lumsden and Keynes, 1989; Keynes and Lumsden, 1990). Thirdly, *Pax6* is reported to be co-expressed and co-increased with vimentin, a marker for radial glial and glial precursors (Heyman *et al.*, 1995). This suggests a role of *Pax6* in neuronal cell migration and is supported by the observation in this study that *Pax6* transcripts are not confined only within the neural tube but are also found in the cell populations flanking both r3 and r5.

4.3.5 Chick *Pax6* expression in the trunk neuroectoderm suggests a role in trunk neurogenesis

Results from this study on chick *Pax6* expression in the trunk neuroectoderm generally confirm the data formerly reported by Li *et al.* (1994). In addition, there are two new findings that are not previously described by Li *et al.* (1994). Firstly, more intense *Pax6* expression is found in segments of the trunk neuroectoderm that is flanked by intersomitic grooves in contrast to those flanked by somites. Secondly, *Pax6* expression appears to correlate with somitogenesis, in that both are gradually extended in the caudal direction.

The preference of *Pax6* expression in areas that are flanked by intersomitic grooves, i.e. the boundaries of somites, is comparable to *Pax6* expression in the hindbrain where transcripts are preferentially expressed in the rhombomeric boundaries (Heyman *et al.*, 1995). Thus, similar to the suggested roles in the hindbrain, *Pax6* is also possibly involved in neuronal cell migration and axonogenesis in the trunk region.

The correlation of *Pax6* expression with somitogenesis is of particular interest in the relevance to trunk neurogenesis. The segmented disposition of spinal nerves is consequent on the formation of somites (Lehman, 1927; Detwiler, 1934) as well as the subdivision of the paraxially repeated mesodermal units into anterior (A) and posterior (P) halves. The anterior and posterior halves are distinguished by the migration of crest cells that set up the basis of sensory neuron development in the trunk region (Rickmann *et al.*, 1985; Teillet *et al.*, 1987). The crest cell migration and differentiation are speculated to be regulated by *Pax6* for two reasons: (1) Midbrain crest migration has been found to be impaired in the *rat Sey* mutants (Matsuo *et al.*, 1993). Although no morphological malformation have been reported in the *Sey/Sey* mice so far, subtle abnormalities in the trunk crest cell migration may exist. Possible involvement of *Pax6* in the trunk neural crest cell migration can not be excluded. (2) The crest cell populations contain full range of developmental potentials. For example, forebrain crest (which normally does not produce neural derivatives) gives rise to dorsal root ganglion when transposed to the trunk level (Le Duarin *et al.*, 1986). Thus, the specific environment into which (or through which) the crest cells migrate is important in the determination of their fates. NGF and BDNF are factors that provide the environmental cues for trunk neurogenesis (Davies, 1987; Hofer and Barde, 1988) and both can regulate *Pax6* expression *in vitro* (Kioussi and Gruss, 1994).

4.3.6 Involvement of *Pax6* in lens determination and differentiation

4.3.6.1 Chick *Pax6* expression correlates with lens determination and differentiation *in vivo*

Li *et al.* (1994) reported that chick *Pax6* is regionally expressed in the head surface ectoderm during the same period and in the corresponding location where early lens determination takes place in *Xenopus* (Henry and Grainger, 1990). Furthermore, the domain of *Pax6* expression remains present during further development of the head ectoderm and is gradually divided into bilateraly patchces of *Pax6*-positive ectoderm that define the population of cells from which the lens is derived (Li *et al.*, 1994). Results of this study confirm the data previously reported by Li *et al.* (1994). This study further demonstrates that at later stages (S16 - S18) *Pax6* expression in the head surface ectoderm remains present and the expression is gradually restricted to the eye region before stage 28. Thus, *Pax6* is expressed in the head surface ectoderm in a gradually restricted way similar to that in the mouse (Grindley *et al.*, 1995). Furthermore, this study demonstrates that *Pax6* is expressed in the primitive lens at stage 16 in the chick. This suggests that *Pax6* is involved in lens determination and differentiation (Li *et al.*, 1994; Grindley *et al.*, 1995; Cvekl and Piatigorsky, 1996).

4.3.6.2 *Pax6* expression persists with the determination of lens formation *in vitro*

Results of this study show that lens determination is correlated with *Pax6* expression under *in vitro* conditions. At stage 8, 8 out of 12 fragments of surface ectoderm from the presumptive lens-forming area (coded 'B' in figure 4.7) go into lens differentiation, whilst at stage 11 all fragments (6 out of 6)

from the presumptive lens-forming area (coded 'a' in figure 4.7) give lens (see data in tables 4.1 - 2). Thus, the data reflect a gradual determination of lens formation in the presumptive lens-forming surface ectoderm when cultured *in vitro*. *Pax6* is expressed persistently with this gradual determination before (shown by Li *et al.*, 1994) and after culture (shown in table 4.1), suggesting its involvement in lens determination.

4.3.6.3 *Pax6* expression is necessary for lens differentiation *in vitro*

Results in this study show that whenever lens differentiate in culture, *Pax6* is always expressed, irrespective of whether it is expressed in the fragments before culture or not (see tables 4.1; 4.2). This suggests that *Pax6* expression is necessary during the process of lens differentiation. This necessity, during the course of this study, is demonstrated through investigations on the expression of αA, αB, and δ1 crystallins by a combination of DNA binding studies, immunological identification of proteins forming protein-DNA gel-shift complexes, loss of function after site-specific mutagenesis of the Pax6 protein binding sites in transfected lens cells, and gain of function in co-transfection experiments using fibroblasts (reviewed by Cvekl and Piatigorsky, 1996). Multiple Pax6 binding sites are implicated. For example, mouse αB crystallin is presumably controlled by multiple regulatory elements with four Pax6 binding sites (Gopal-Srivastava *et al.*, 1995; Cvekl and Piatigorsky, 1996).

Results in this study also indicate that lens can differentiate from non-*Pax6*-expressing head surface ectoderm, whilst *Pax6*-expressing surface ectoderm does not always give rise to a lens (see tables 4.1 and 4.2). For example, some fragments from non-*Pax6*-expressing area c (ventral) of stage 11 embryos differentiate into lens, while some from the *Pax6*-expressing area b do not. This is not contradictory to the necessity for *Pax6* during the process of lens differentiation. *Pax6* may be switched on or off during the course of *in vitro* culture, which is demonstrated in this study.

The switch-on or switch-off of *Pax6* expression in the cultured tissues is consistent with the picture of multiple regulatory elements that control crystallin expression (Gopal-Srivastava *et al.*, 1995; Cvekl and Piatigorsky, 1996). Some members of the multiple regulatory elements, for example activin A, are diffusible factors that do not co-exist with *Pax6* transcripts (Cvekl and Piatorsky, 1996). In stead, they can be synthesized by surrounding non-*Pax6*-expressing cells. Grafting out and culturing specific areas of surface ectoderm from an intact head implies that the effect of diffusible factors can be lost, which leads to the failure of crystallin expression. Lens differentiation, therefore, does not occur in those *Pax6*-expressing tissue fragments under *in vitro* condition. Thus, the *Pax6* autoregulatory loops of self-stimulation (Plaza *et al.*, 1993; Grindley *et al.*, 1995; Cvekl and Piatigorsky, 1996) fail, leading to the switch-off of *Pax6* expression.

Alternatively, *Pax6* can be switched on due to grafting and culturing under *in vitro* condition. Macdonald *et al.* (1995) and Ekker *et al.* (1995) suggested that *Shh* (*Sonic hedgehog*) or closely related

signalling molecules emanating from ventral midline of the neural tube in the forebrain may inhibit *Pax6* expression in the zebrafish. Their suggestion may explain why *Pax6* is switched on in some of the cultured surface ectoderm (for example, area c in stage 11 embryos), in that the inhibitory effect from the ventral midline of the neural tube is removed when the surface ectoderm is grafted.

4.3.7 *Pax6* is crucial in both the lens ectoderm and the optic vesicle

Despite extensive efforts, the whole picture of detailed molecular events in the processes of lens differentiation is still unknown (Saha *et al.*, 1992; Grainger, 1992; Cvekl and Piatigorsky, 1996; Li *et al.*, 1997). Although *Pax6* can be involved in lens determination and differentiation as supported by the results in this study and by many other published data, it is only one of many transcription factors that are implicated in lens development. *Pax6* mutation in the homozygous state, however, does not only lead to the failure of lens differentiation; it also leads to the absence of all the other structures of the eye. It is therefore interesting to take my discussion further on the reason why other structures of the eye are absent due to a single *Pax6* gene mutation.

To form a functional vertebrate eye, coordinated development of the neuroectoderm, surface ectoderm, neural crest and paraxial mesoderm has be be achieved (introduced in section 1.11.1). Single or combined defects in these components will lead to different degrees of abnormalities in the eye. *Sey* mutation leads to the most severe phenotype, since no eye derivative is formed. Analyses of *Sey/Sey* phenotypes reveal that the optic vesicles are abnormally broad and fail to constrict proximally (Grindley *et al.*, 1995). The abnormal optic vesicles eventually become distorted and degenerate (Hogan *et al.*, 1986; 1988). The lens placode, however, is not even formed (Hogan *et al.*, 1988), which is confirmed by morphological criteria and by using a lens-specific marker (Grindley *et al.*, 1995). The phenotypes raise some possibilities for elucidating the absence of lens placode in the *Sey/Sey* mice: (1) The lens-enhancing property of the optic vesicle (reviewed by Grainger, 1992) may be maintained, while primary lens induction in the presumptive lens ectoderm fails. (2) Both the lens-enhancing property in the optic vesicle and primary lens induction in the presumptive lens ectoderm are faulty. (3) The optic vesicle does not maintain its lens-enhancing property, while primary lens induction occurs in the presumptive lens ectoderm without apparent placode formation.

The possibilities described above prompt tissue recombination studies. Fujiwara *et al.* (1994) cultured optic vesicles combined with presumptive lens ectoderm from *rSey/rSey* mice and their littermates. They found that the failure of lens forming capacity in the presumptive lens ectoderm of day 10.0 p.c. r*Sey/rSey* rat could not be reversed by culturing with normal (+/+ or *rSey/+*) optic vesicles, whilst the presumptive lens ectoderm of normal rat could differentiate into lens even cultured with optic vesicles from the *rSey/rSey* mice. Their data indicates that, at least at day 10.0 p.c., lens differentiation in the presumptive lens ectoderm is autonomous, i.e. independent of effects from optic vesicles.

If *Pax6* is involved in the autonomy of lens differentiation in the presumptive lens ectoderm, it has to be expressed there irrespective of the presence of optic vesicles. This is demonstrated by the data published by Li *et al.* (1994). Li *et al.* (1994) performed neural plate ablation that resulted in the absence of the optic vesicle in chick embryos. *Pax6*, however, remained expressed in the presumptive lens ectoderm in lack of optic vesicles. The autonomy of lens differentiation in the presumptive lens ectoderm is also supported by the *in vitro* lens differentiation studies by Barabonov and Fedtsova (1982) and in this study. Head surface ectoderm can differentiate into *Pax6*-expressing lens under *in vitro* culture conditions which obviously does not involve optic vesicles. Furthermore, Quinn *et al.* (1996) produced chimeric mouse embryos composed of wildtype and *Sey* mutant cells. They found that mutant cells were excluded from the lens epithelium in the chimeric embryos with lens sizes comparable to the wildtypes. When high proportions of mutant cells were found in the chimeric embryos, the lenses were either reduced in their sizes or completely absent (Quinn *et al.*,1996). These lines of evidence indicate that *Pax6* is autonomously crucial in the lens ectoderm during the process of lens differentiation.

The lens has been proposed as an 'organizer' during eye development (Beebe and Dhawan, 1997). For example, targetted ablation of lens cells by transgenic hybrids of crystallin and diphtheria (a cytotoxic protein) leads to abnormal phenotypes including size reduction in the sclera, cornea and ciliary epithelium and the formation of a highly convoluted retina that extensively fills the vitreous chamber (Breitman *et al.*, 1989; Kaur *et al.*, 1989; Harrington *et al.*, 1991; Klein *et al.*, 1992; Key *et al.*, 1992). The absence of lens formation in the *Sey/Sey* mice, therefore, leads to the loss of 'organizer' activity and probably contributes to the absence of many other eye structures.

Although the *Sey* mutation does not eradicate optic vesicle formation (Hogan *et al.*, 1986, 1988; Grindley *et al.*, 1995), *Pax6* is also crucial in the optic vesicle. This is not only supported by expression data and mutant phenotypes, but also by evidence from chimaeric mouse embryos that exhibit severely affected morphology in the optic cup (Quinn *et al.*, 1996).

Keys for chick *Pax6* expression

1. neural plate
2. border between neural plate and neural ridge
3. Hensen's node
4. first somite formation
5. neural ridge
6. anterior margin of the neural plate (head fold)
7. migrating pre-cardiac cells
8. first somite
9. anterior neuropore (unfused)
10. lateral cephalic region
11. midline of the dorsal encephalic region
12. midline of the ventral encephalic region
13. heart tube
14. intersomitic neuroepithelium
15. neuroepithelium medial to somite
16. future third ventricle
17. telencephalic neuroepithelium
18. mesencephalic vesicle
19. mesencephalic neuroepithelium
20. surface ectoderm
21. neuroepithelium near the anterior neuropore
22. closing anterior neuropore
23. third ventricle
24. surface ectoderm covering optic vesicle
25. neuroepithelium enclosing optic vesicle
26. mesencephalic vesicle
27. fourth ventricle
28. rhombencephalic neuroepithelium
29. mesencephalic neuroepithelium
30. optic recess
31. third ventricle
32. optic vesicle
33. anterior dorsal aorta
34. surface ectoderm covering optic vesicle
35. neuroepithelium enclosing optic vesicle
36. optic cup
37. somites
38. spinal neuroepithelium (anterior)
39. spinal neuroepithelium (posterior)
40. telencephalic neuroepithelium
41. anterior neuropore
42. neuroepithelium surrounding anterior neuropore
43. lateral surface ectoderm near the anterior neuropore
44. mesencephalic neuroepithelium
45. mesencephalic vesicle
46. lateral surface ectoderm in the mesencephalic region
47. third ventricle
48. pigmented retinal epithelium
49. neural retina
50. corneal epithelium
51. lens vesicle
52. lens
53. neuroepithelium in the anterior medulla
54. fourth ventricle
55. otic vesicle
56. hypothalamic neuroepithelium
57. rim of optic cup
58. neocortical (telencephalic) neuroepithelium
59. forming optic stalk
60. corneal epithelium
61. fourth ventricle
62. medullary neuroepithelium
63. hypothalamic neuroepithelium
64. neocortical (telencephalic) neuroepithelium
65. third ventricle
66. nasal (olfactory) epithelium
67. olfactory cavity
68. mandibular component of first branchial arch
69. rhombencephalic (pontine) neuroepithelium
70. cornea
71. pontine neuroepithelium

Figure 4.1 Chick *Pax6* expression represented by wholemount *in situ* hybridization. (a). stage 6^+ (dorsal view): The earliest appearance of *Pax6* expression in the chick is seen at stage 6^+ in the anterior margin of the neural plate and in the neural ridge in the anterior part of the embryo (no. 6). The neural plate itself (no. 1), however, does not appear to exhibit *Pax6* expression. There is also evidence of expression in the posterior 1/3 of the developing embryo at stage 6^+. The surrounding cells of Hensen's node (no. 3) appear to show higher level of expression than the others within the posterior region. (b). stage 8 (dorsal view): At stage 8, intense *Pax6* expression is detected in the neural folds, particularly in the neural ridge (no. 5) within the prospective cephalic region. The expression is less intense in the cephalic neural plate (no. 1) which is located lateral to the cephalic neural folds. In the trunk region, *Pax6* transcripts are detected in the developing neural folds adjacent to the sites of somite formation (see the first pair of somites, i.e. no. 8). This expression diminishes in the portion immediately caudal to the last pair of somites seen at this stage of development. Evidence of *Pax6* expression is also found in the area surrounding Hensen's node (no. 3). (c). stage 9 (dorsal view): At stage 9 (7 - 8 pairs of somites), *Pax6* is expressed in two lateral cephalic regions in the rostral half of the cephalic region (see no. 10). There are sharp boundaries between the expressing and non-expressing regions. In the wall of the anterior neuropore (no. 9), no obvious presence of *Pax6* transcripts is found. In the trunk region, *Pax6* transcripts are detected in the neural fold as noted at stage 8. This expression extends rostrally to the cephalic region and caudally to a region just beyond the last defined pair of somites that are present at this stage of development. The somites and the intersomitic grooves do not show any *Pax6* expression. In the trunk neural folds where *Pax6* transcripts are detected, the expression appears to be more intense in the segments that are not flanked by somites. In the site of Hensen's node (no. 3), *Pax6* transcripts are only minimally detectable. (d). and (e). stage 10 (ventral view): At stage 10 (9-10 pairs of somites), *Pax6* expression in the cephalic region is found in the two lateral bulges of presumptive optic vesicles (no. 10). This expression in the cephalic region is similar to that formerly noted at stage 9 (compare figure 4.1.e with figure 4.1.d), and the sharp lines of demarcation between the caudal and the rostral as well as between the lateral and the midline cephalic regions are maintained. In particular, as viewed externally in wholemount preparations, *Pax6* is absent from the wall of anterior neuropore (no. 9) and from the cephalic midline region (nos. 11 and 12). In the trunk region, *Pax6* expression within the developing neural folds extends more caudally in association with the formation of additional somites. The more intense expression in the neural fold segments that are not flanked by somites, i.e. the intersomitic trunk neuroepithelium (no. 14) becomes more obvious (compare no. 14 with no. 15 in 4.1.e). In Hensen's node (no. 3 in figure 4.1.e), however, no evidence of *Pax6* expression is seen by stage 10. All scale bars represent 0.1 mm in length. Keys for all numeric labelling of chick *Pax6* expression are listed in page 216.

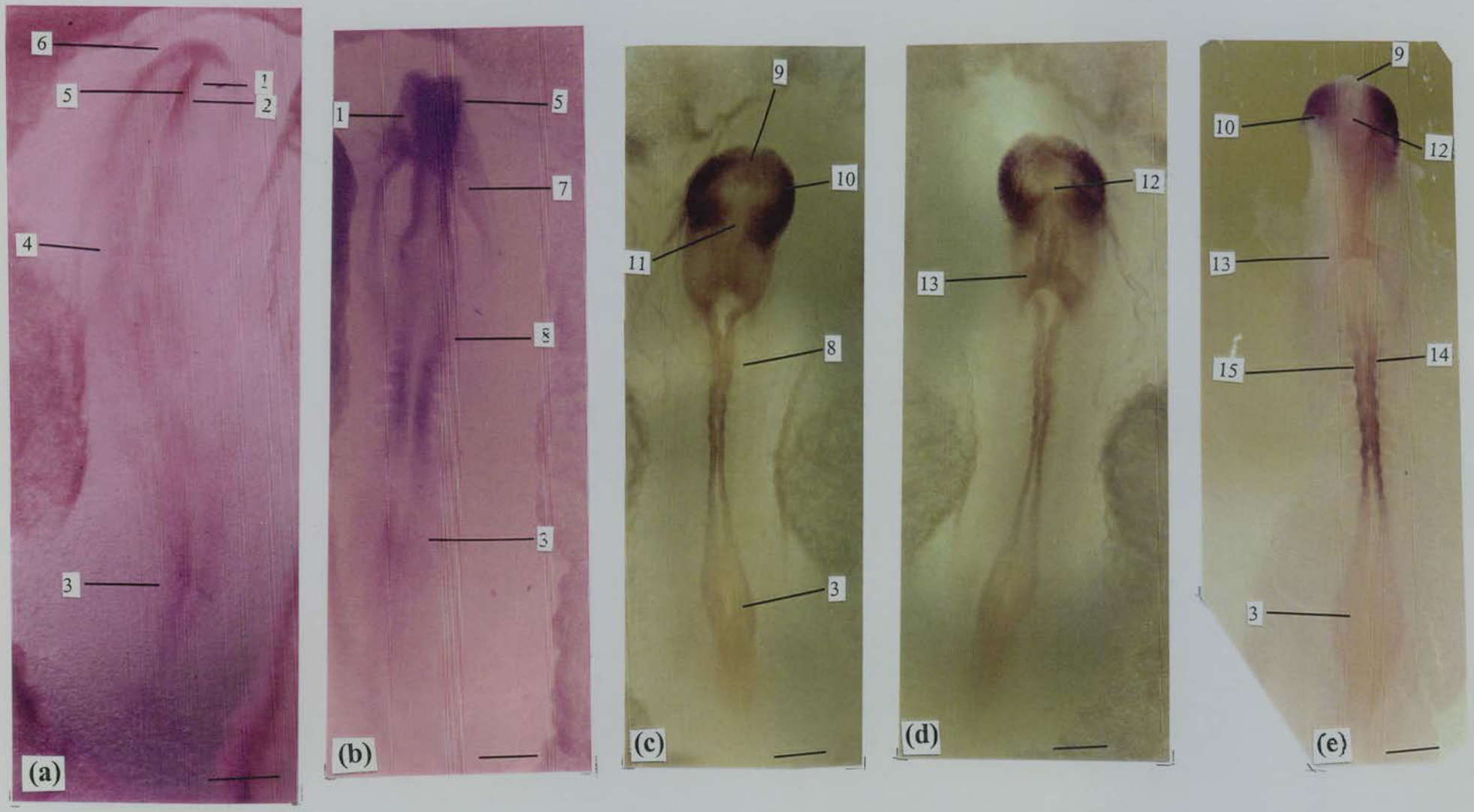
6
1
5
2
4
3
(a)
1
5
7
8
3
(b)
9
10
11
8
3
(c)
12
13
(d)
9
10
12
13
15
14
3
(e)

Figure 4.2 Chick *Pax6* expression represented by *in situ* hybridization on tissue sections. The planes of sectioning are shown in a schematic diagram on the right panel of this page. (a). Stage 10 (coronal section): *Pax6* transcripts are absent in both the surface ectoderm and the neuroectoderm that surround the anterior neuropore. In the midline cephalic neuroepithelium that constitutes the wall of the third ventricle (see the intense stain surrounding the future third ventricle, i.e. no. 16), however, *Pax6* transcripts are detected. (b). Stage 11 (coronal section): At stage 11, *Pax6* expression is detected in the loop-shaped structures that constitute the surface ectoderm (no. 24) and the neuroectoderm (no. 25) of the primitive optic primordium. In the neuroepithelium of the presumptive mesencephalon (no. 29) and anterior rhombencephalon (no. 28), no evidence of *Pax6* expression is found, nor are *Pax6* transcripts present in the neuroepithelium that surrounds the closing anterior neuropore (no. 22). In the head surface ectoderm, the part surrounding the closing anterior neuropore shows no expression, while the two lateral regions overlying the optic vesicles as well as regions overlying the presumptive mesencephalon and rhombencephalon show intense expression. (c). and (d): Stage 13 (transverse section in (c); coronal section in (d)): At stage 13, *Pax6* continues to be expressed in the loop-shaped structures that constitute the primitive optic stalks. *Pax6* transcripts are clearly present in the telencephalic neuroepithelium (no. 40) and at the most anterior end of the presumptive prosencephalic neuroepithelium, i.e. at the site of the now closed anterior neuropore. *Pax6*-expressing cells are present around the entire area of head surface ectoderm at the same level of transverse plane as the optic vesicle. *Pax6* transcripts are clearly seen in the neuroepithelium of the anterior (no. 38) and the posterior (no. 39) spinal cord in the trunk region. All scale bars represent 0.1 mm in length.

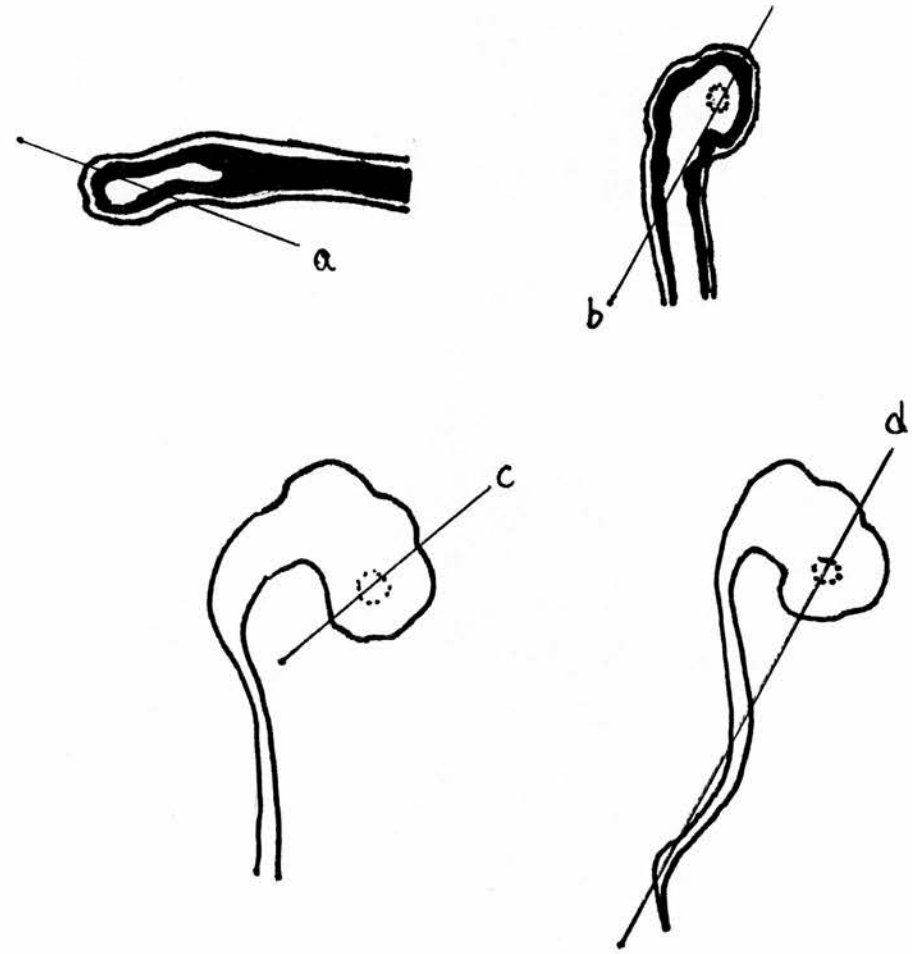

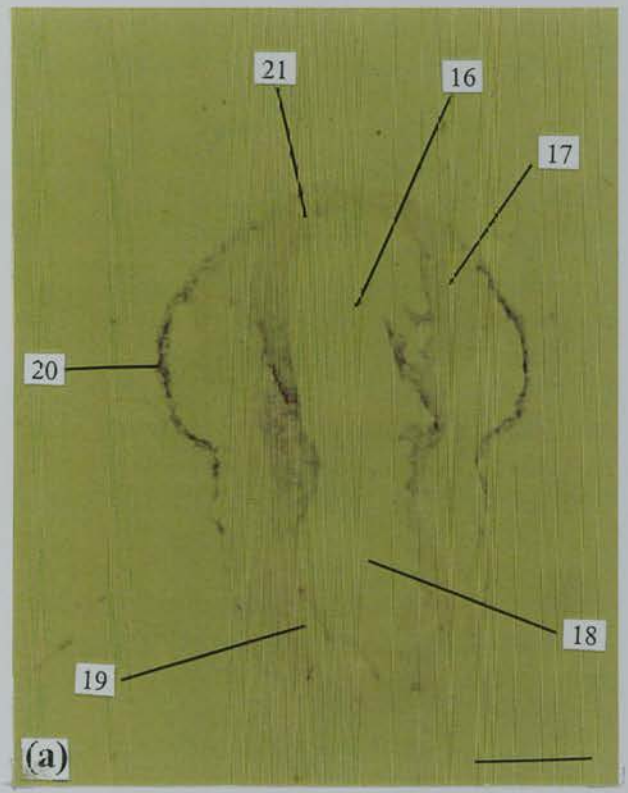

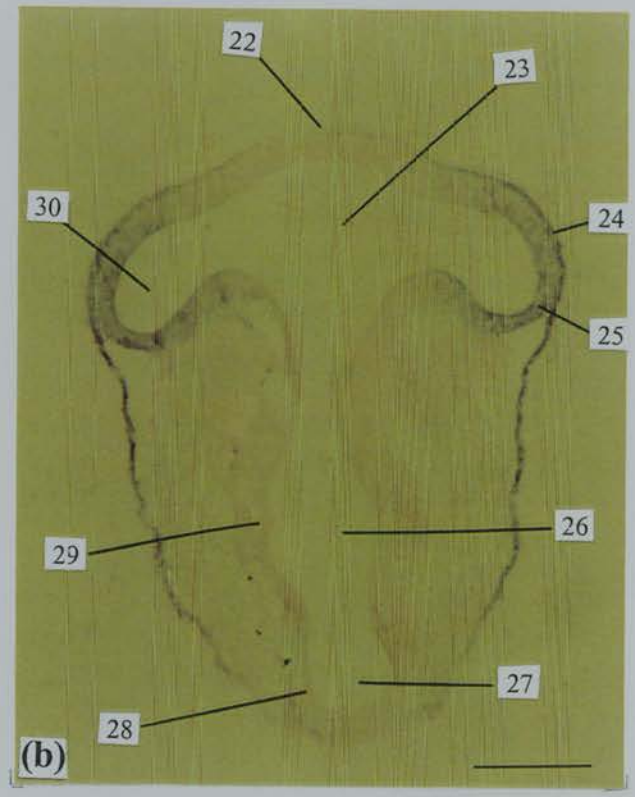

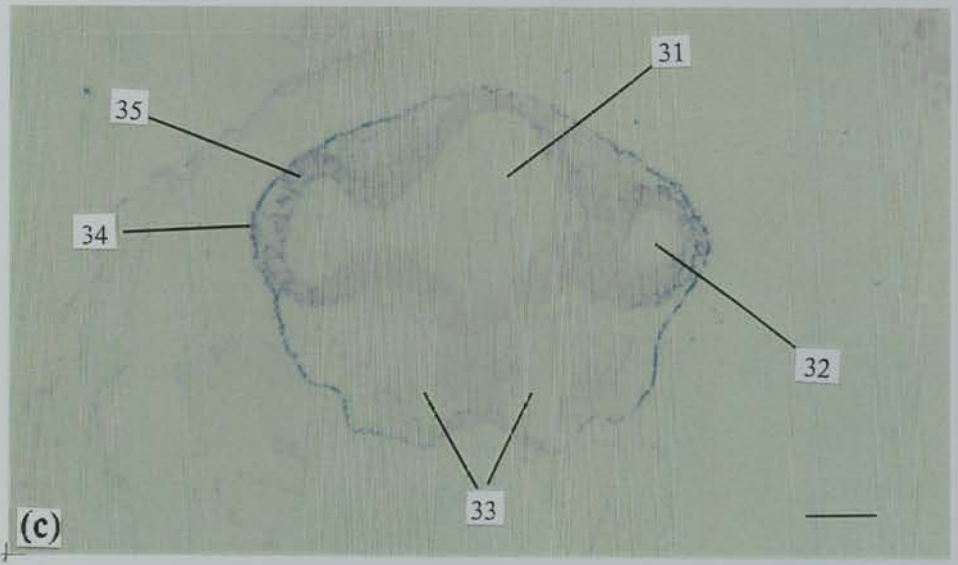

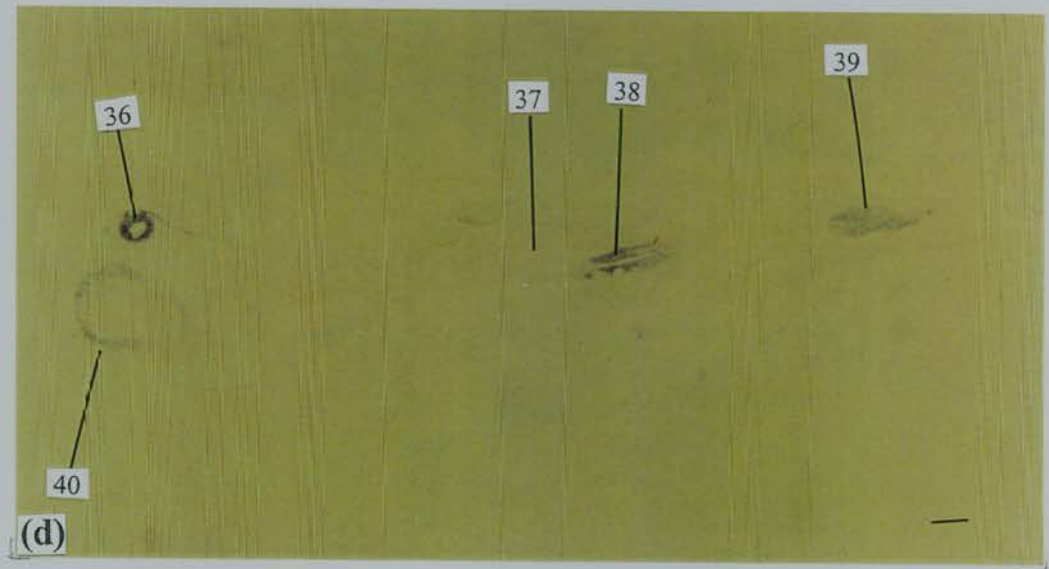

Figure 4.2 Chick *Pax6* expression as demonstrated by *in situ* hybridization on tissue sections. (a). stage 10 (coronal section); (b). stage 11 (coronal section); (c). stage 13 (transverse section); (d). stage 13 (coronal section). All scale bars represent 0.1 mm in length.

Figure 4.3 Chick *Pax6* expression represented by *in situ* hybridization on tissue sections, with the ventral side pointing downwards. The planes of sectioning are shown in a schematic diagram on the right panel of this page. (a) is a transverse section on top of the head at stage 13. (b) ia a transverse section on the mesencephalon at stage13 (the same embryo as in (a)). (c) is a coronal section at stage 16. In (a): The lateral parts of the head surface ectoderm in the region close to the anterior neuropore display intense *Pax6* expression (see no. 43). In (b): *Pax6* transcripts are detected in the lateral surface ectoderm (no. 46). In (c): At stage 16, when the epithelium of the lens placode has invaginated and the optic cup has differentiated into an inner neural retina (no. 48) and an outer pigmented neural epithelium (no. 49), *Pax6* expression is detected in the differentiating lens (no. 52) and the surface ectoderm overlying it (no. 50). *Pax6* transcripts are also present in the neural (no. 48) and pigmented layer (no. 49) of the optic cup, the neuroepithelium of the rostral part of the prosencephalon (no. 58), as well as in the anterior medulla (no. 53) in the rhombencephalon which is in close proximity to the otic vesicles (no. 55). In the optic cup, higher levels of expression are seen in the rim (no. 57). This is particularly obvious for the neural retina. The hypothalamic neuroepithelium and the otic vesicles do not exhibit *Pax6* expression. In the head surface ectoderm, *Pax6* expression covers a broad area overlying the eye and extends both dorsally and ventrally. All scale bars represent 0.1 mm in length.

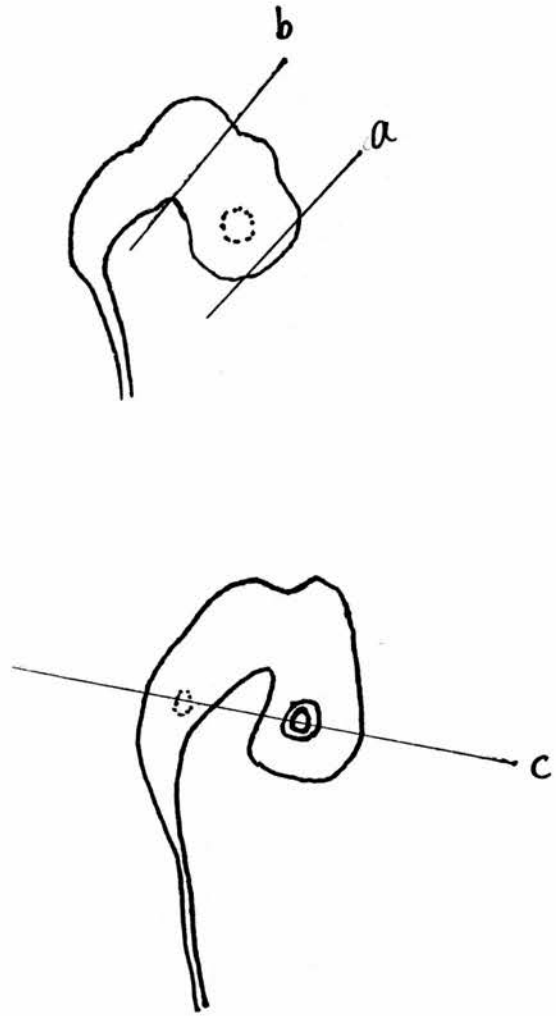

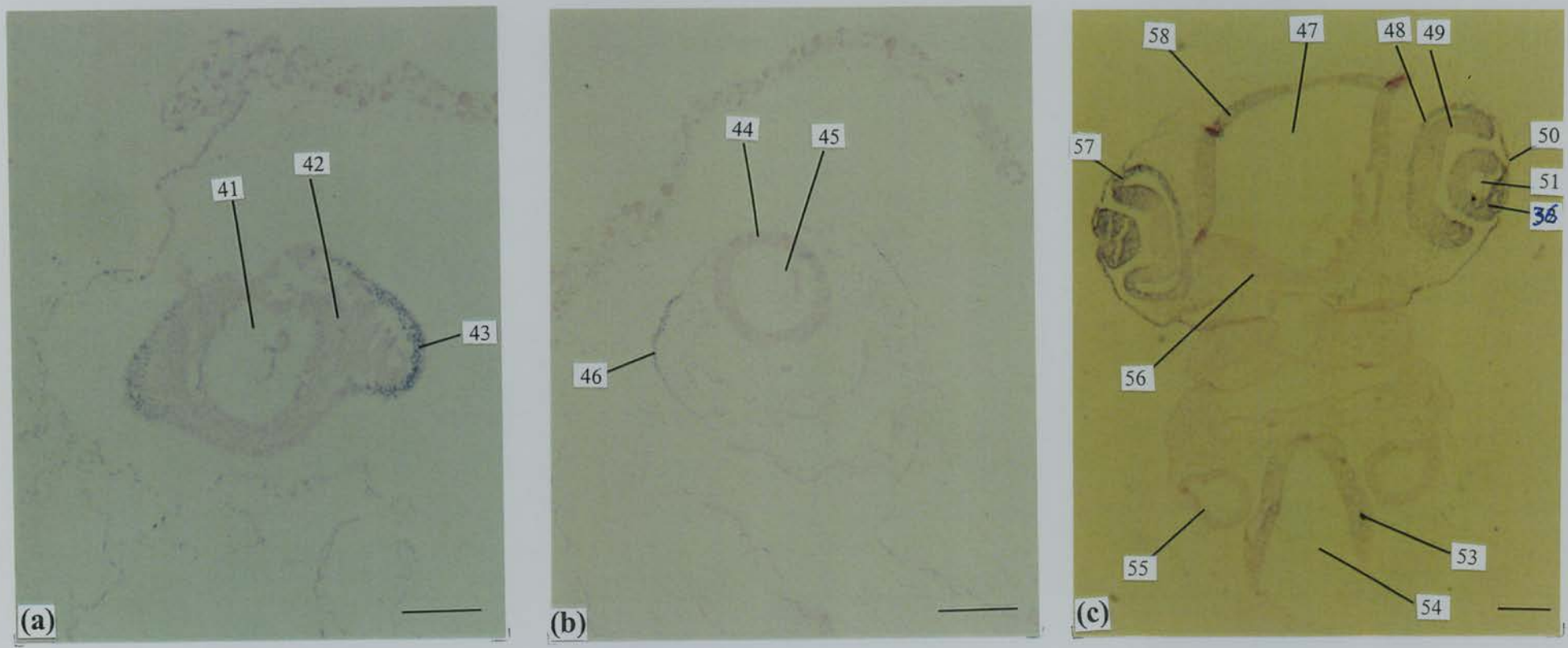

Figure 4.3 Chick *Pax6* expression as demonstrated by *in situ* hybridization on tissue sections. (a). transverse section on top of the head at stage 13; (b). transverse section on the mesencephalon at stage 13 (the same embryo as a.); (c). coronal section at stage 16. All scale bars represent 0.1 mm in length.

Figure 4.4 Chick *Pax6* expression represented by *in situ* hybridization on tissue sections and a wholemount embryo. The planes of sectioning in (a) and (b) are shown in a schematic diagram on the right panel of this page. (a) is a coronal section at stage 17 - 18. By stages 17 - 18, *Pax6* expression in the anterior part of the head neuroepithelium (no. 64) (now the neocortical neuroepithelium in the anterior forebrain) is still apparent. *Pax6* expression remains in the optic cup and the optic stalk (no. 59), although the expression is not as obvious as that at stage 16. Transcripts of *Pax6* are also detected in the head surface ectoderm overlying the presumptive eye region, particularly the corneal epithelium (no. 60), as well as in the ventral pontine neuroepithelium and the dorsal part of medullary neuroepithelium (no. 62 and no. 71). (b) is a coronal section at day 17 showing that *Pax6* is expressed in the olfactory epithelium (no. 66). (c) is a preparation of wholemount *in situ* hybridization on the head region at stage 28. *Pax6* expression appears to be detectable within the surface ectoderm covering the eye region. Scale bars: in (a) and (b), 0.1 mm; in (c), 15 mm.

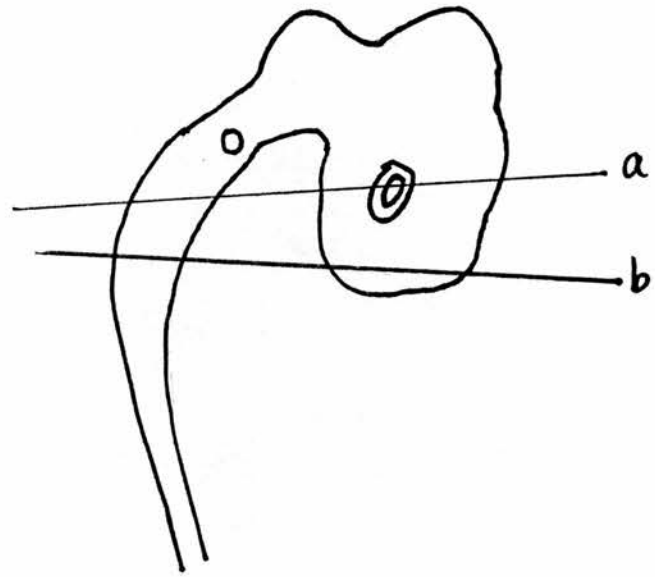

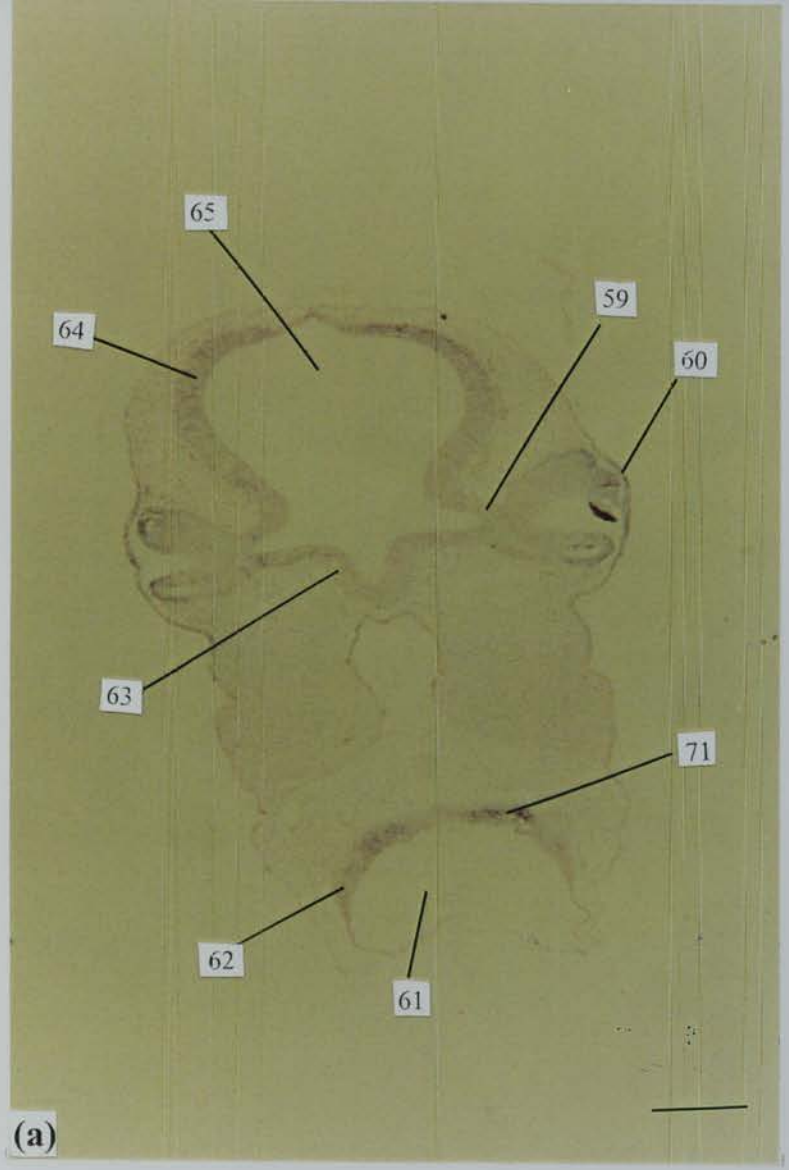

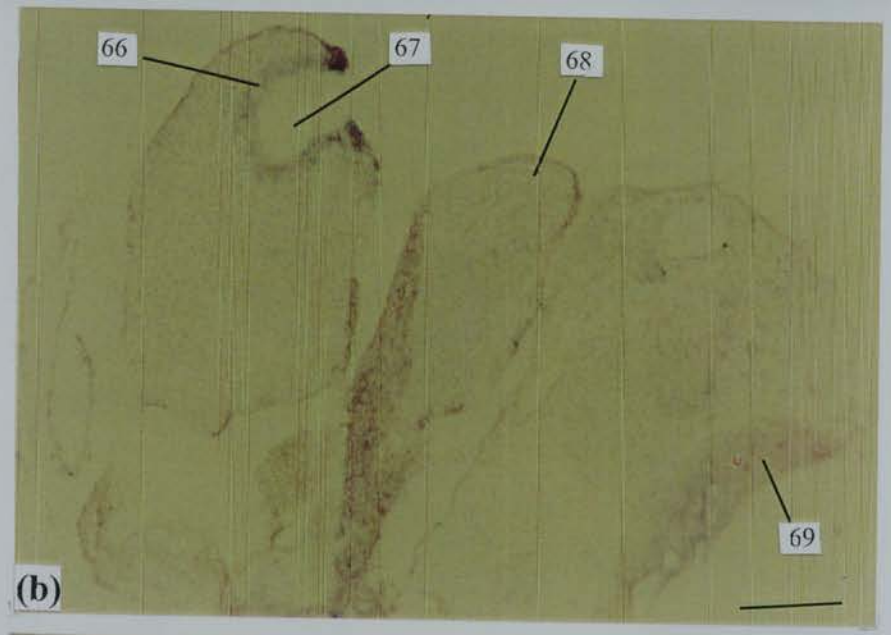

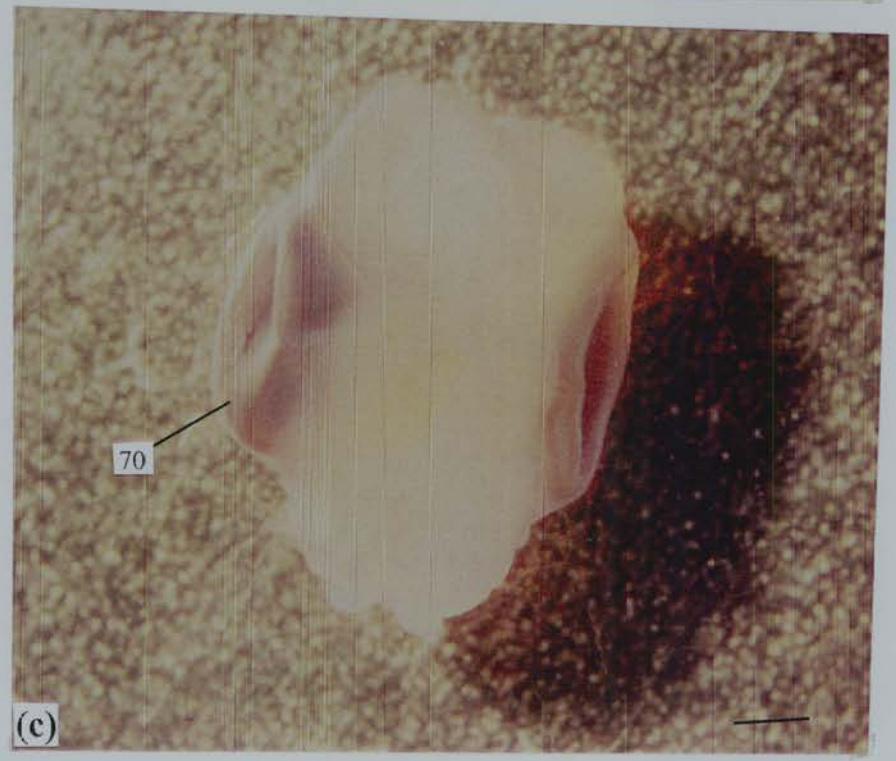

Figure 4.4 Chick *Pax6* expression as demonstrated by *in situ* hybridization on tissue sections and a wholemount embryo. (a). stage 17 - 18 (coronal section); (b). stage 17 (coronal section showing the olfactory epithelium); (c). wholemount on the head at stage 28. Scale bars in length: a. 0.1mm; b. 0.1 mm; c. 15 mm.

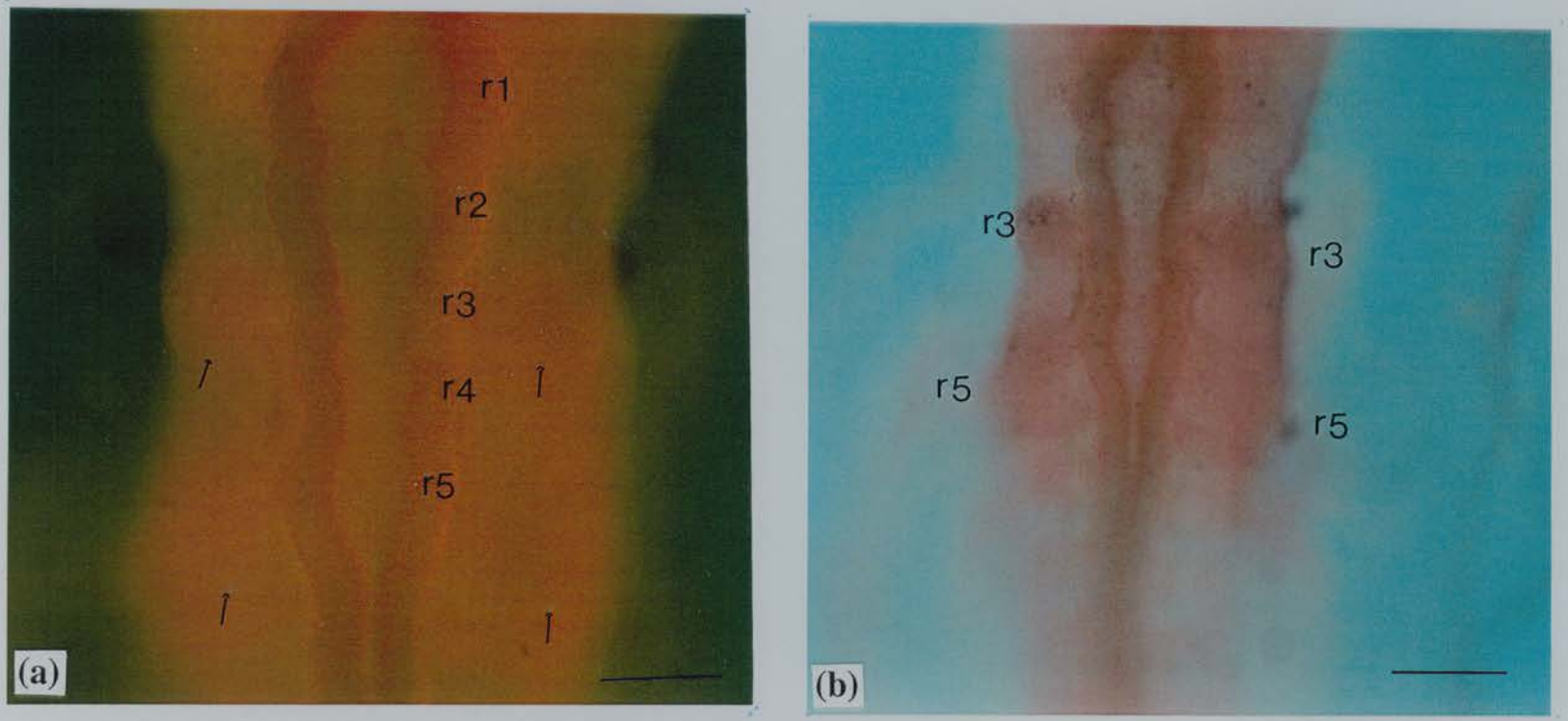

Figure 4.5 Chick *Pax6* expression in the hindbrain as demonstrated by *in situ* hybridization on stages 11 - 12 wholemount embryos. (a) a stage 11 wholemount embryo shows *Pax6* expression in the rhombomere area. Note that some hints (arrows) of *Pax6* expression can be found in the cells flanking the neuroepithelium of rhombomere 3 (r3) and rhombomere 5 (r5); (b) *Pax6* expression at stage 12. The expression in the cells flanking neuroepithelium of r3 and r5 becomes more evident than that at stage 11. Scale bars (approximately): a, 250 mm; b, 160 mm.

Figure 4.6 A comparison of areas of chick head surface ectoderm cultured by Barabanov and Fedtsova (1982) for lens differentiation *in vitro* with the patterns of *Pax6* expression in the corresponding areas reported by Li *et al.* (1994). Embryos in (a), (c), and (e) (on the left) indicate the areas grafted for culture by Barabanov and Fedtsova (1982). Those in (b), (d), and (f) show the areas of *Pax6* expression. Note that the stages investigated by Li *et al* (1994) do not exactly correspond to those by Barabanov and Fedtsova (1982). For each coded area in (a), (c), and (e) (on the left), following *in vitro* culture, the number of explants containing lens cells out of the total number is listed as X/Y (from Barabanov and Fedtsova, 1982). X represents the number of explants containing lens cells. Y represents total number of explants that have been cultured. Abbreviations: hn, Hensen's node; s1, first somite. Scale bars: a, 0.5 mm; b, 0.4 mm; c, 2 mm; d, 4mm; e, 2 mm; f, 4 mm. (figures are from Barabanov and Fedtsova (1982) and Li *et al.* (1994) with permission)

Barabanov and Fedtsova (1982)

Li *et al.* (1994)

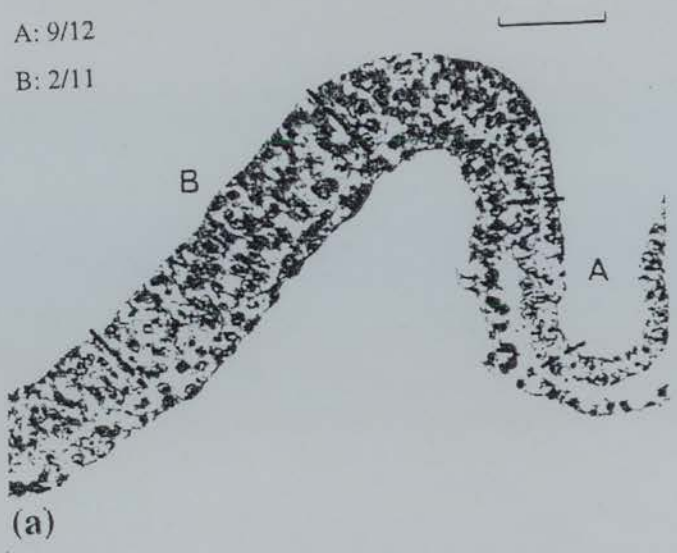

Stage 6 (longitudinal section)

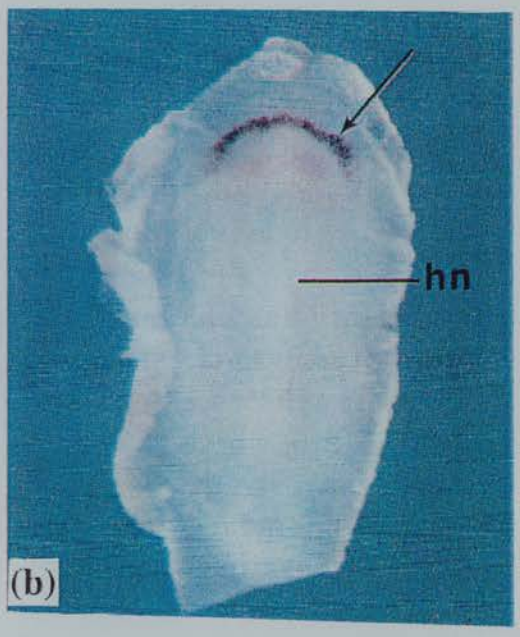

Stage 6 (dorsal view)

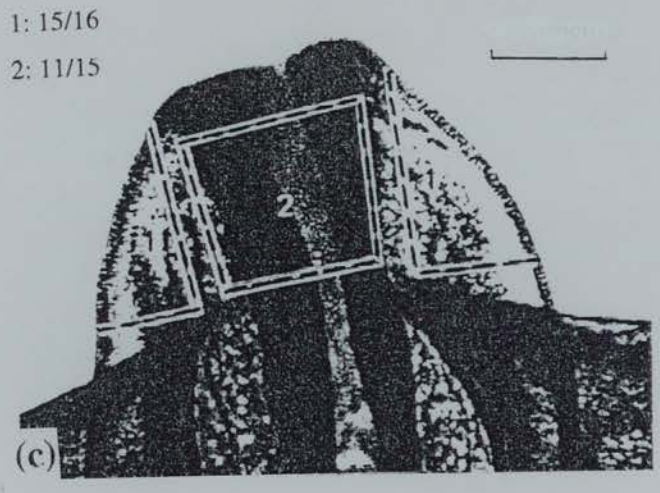

Stage 8 (dorsal view)

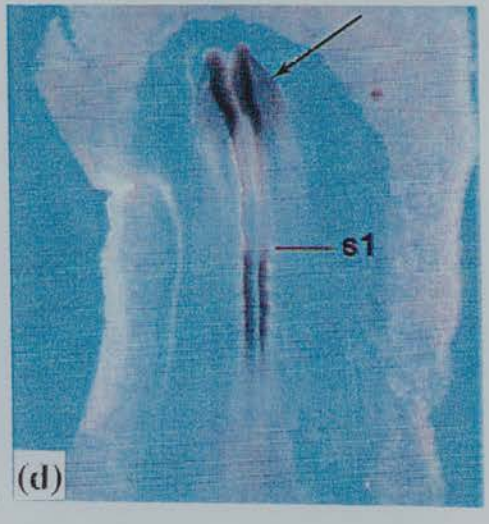

Stage 8^{+} (dorsal view)

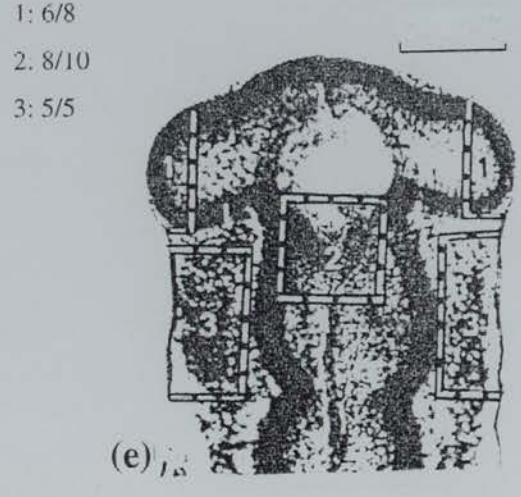

Stage 10 (ventral view)

Stage 11 (dorsal view)

Figure 4.7 Fragments of chick head surface ectoderm that were grafted and cultured in this study. All fragments are grafted under the dorsal view. For the coded area 'c' at stage 11, both dorsal and ventral surface ectoderm are used. It was noted that, in grafting different areas of the surface ectoderm, no apparent line of demarcation could be seen in the intact chick embryos. A consistency in grafting areas of surface ectoderm was therefore demanded, to ensure that the lines of demarcation could be used for distinguishing *Pax6*-expressing and non-*Pax6*-expressing areas. This was tested initially by measuring the length and width of each grafted area in relation to the whole head. The grafted areas were analysed to determine whether they were consistent with the pattern of *Pax6* expression. Chick embryos at the same developmental stage, however, could vary in their size, which lead to inconsistent demarcation. Furthermore, grafting by measurement could take such a long time that the tissues would not survive during the subsequent culture. Later, a consistency in grafting was achieved by dividing the head region in three parts of the same length -- rostral, intermediate, and caudal, according to morphological features that were distinguishable under a dissection microscope. The stage 8 heads were cut into thirds, spanning from the rostral end to the first pair of somites. Thus, the rostral part had areas AA, AP, and B, whilst C was in the intermediate part and the caudal part was not grafted. The stage 11 heads were also cut into three parts. They spanned from the rostral end to rhombomere 3 (r3). Thus, the area 'a' belonged to the rostral part. Areas 'b' and 'c' were in the intermediate part, whilst areas 'd' and 'e' were grafted from the caudal part. All tissue fragments were grafted in avoidance of borderlines to ensure that they were within the designated areas. Five batches of grafts obtained by dividing the head region into three parts were analysed by wholemount *in situ* hybridization. All of them were consistent with the pattern of *Pax6* expression. The tissues used for culture in this study were therefore obtained by first dividing the developing chick head region into three parts as described above. Abbreviations: r3, rhombomere 3; s1, the first somite. Scale bars: 500 μm. (figures are from Li *et al.* (1994) with permission)

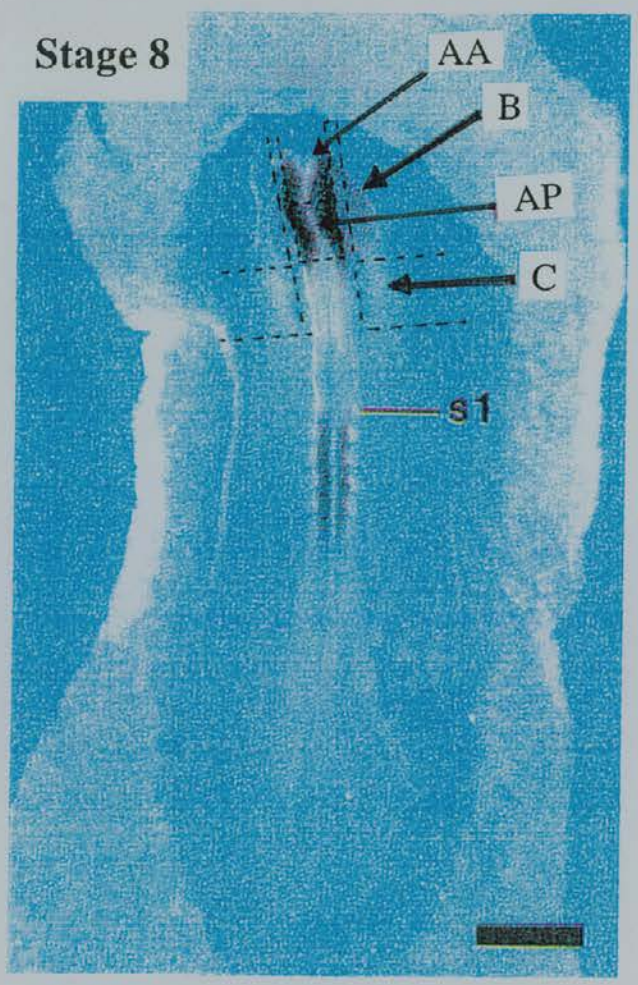
Stage 8
AA
B
AP
C
s1

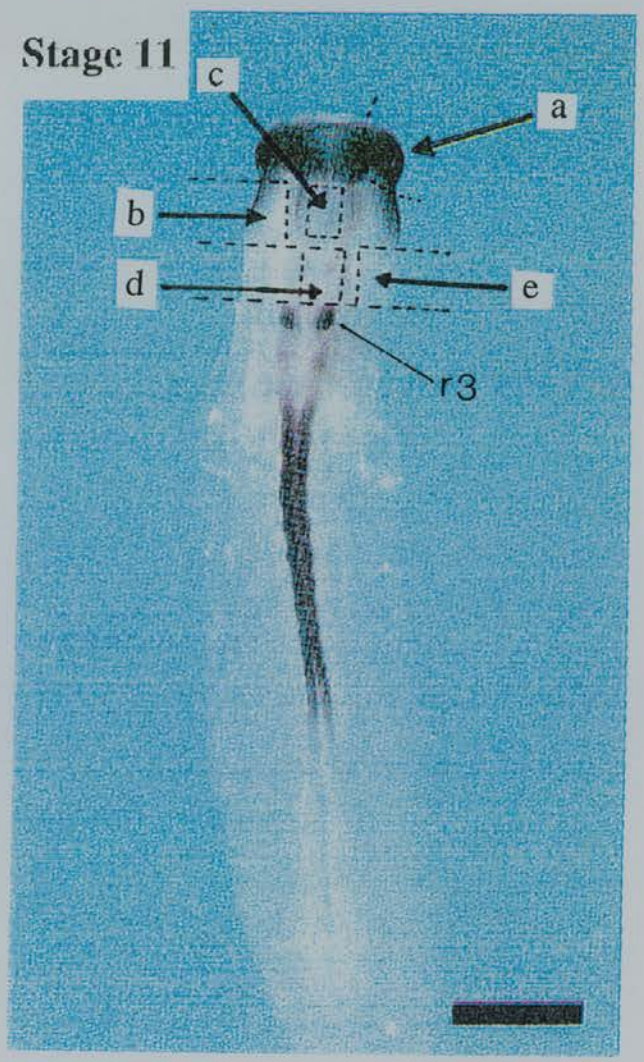
Stage 11
c
a
b
d
e
r3

Figure 4.8 Morphology of the fragments of head surface ectoderm following *in vitro* culture on millipore membranes for 4 -6 days. A variety of morphological forms were observed after culture. With a simple eosin staining, some cultured tissues from different areas of the surface ectoderm exhibited a typical lens shape that appeared to contain primary lens fibers (in a). Others just showed bubble-like lentoid bodies combined with fibre-like structures (in b). More commonly, they were simply fibre-like (in c) or bubble-like structures (in d). The formation of these morphological variations was irrespective of the origin of cultured tissues, i.e. all designated areas were capable of forming each type of morphology mentioned above. Abbreviations: f, lens-like fiber; l, lens; lb, lentoid body; m, millipore membrane. All scale bars represent 500 μm in length.

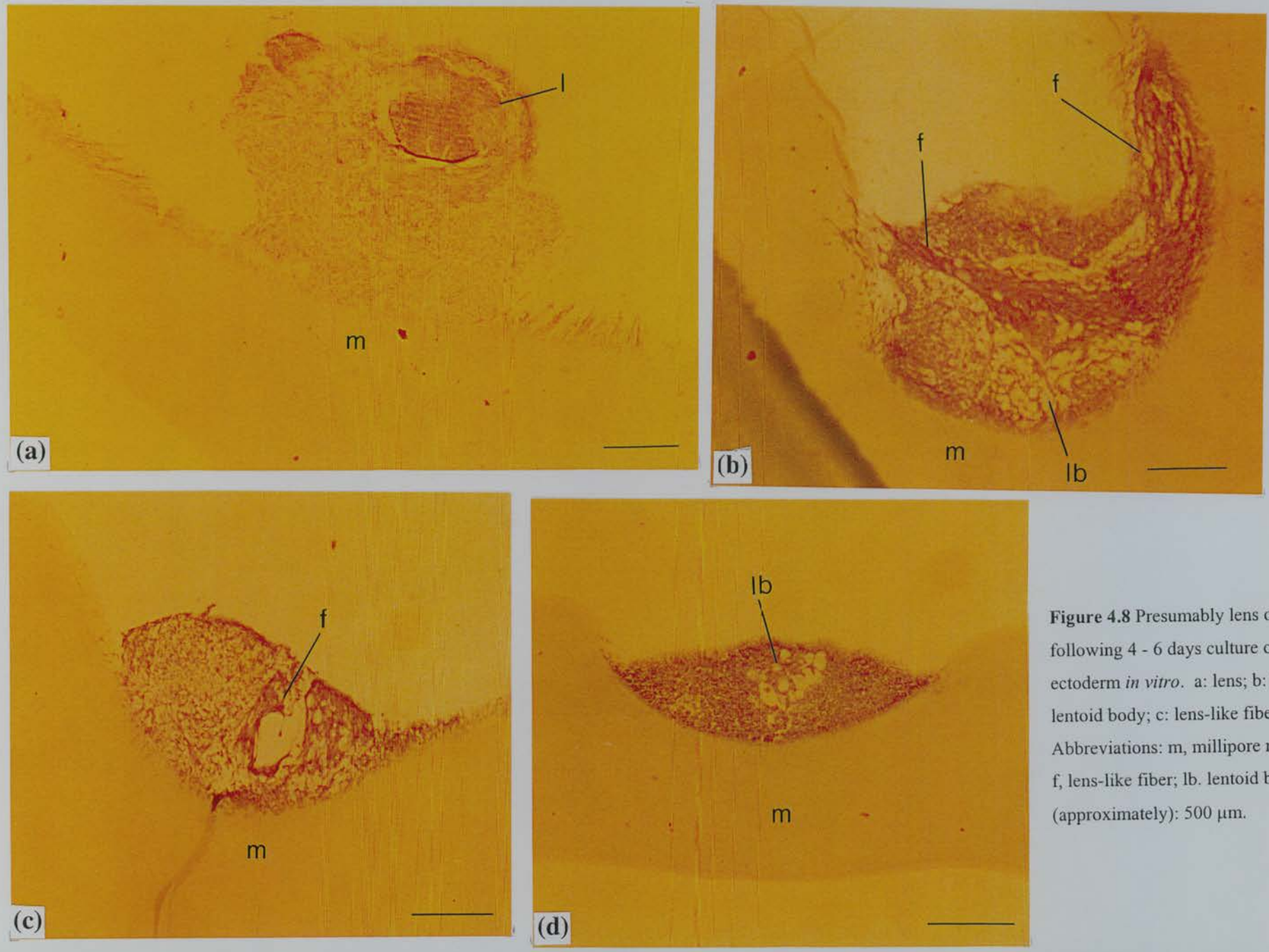

Figure 4.8 Presumably lens or lens-like tissues following 4 - 6 days culture of chick head surface ectoderm *in vitro*. a: lens; b: lens-like fibers with lentoid body; c: lens-like fibers; d: lentoid body. Abbreviations: m, millipore membrane; l, lens; f, lens-like fiber; lb. lentoid body. All scale bars (approximately): 500 μm.

Figure 4.9 Two examples of *Pax6* expression in correlation with αB crystallin expression in fragments of chick head surface ectoderm following 4 - 6 days culture on millipore membrane. The tissues were fixed, embedded, sectioned, and run through *in situ* hybridization and immunohistochemistry together without detachment from the millipore membranes. The red colour on the left (in a and c) indicates αB crystallin expression. The blue colour on the right (in b and d) indicates *Pax6* expression. Cells in a and b are from one fragment; those in c and d are from another fragment. m: millipore membrane. All scale bars represent 500 μm in length.

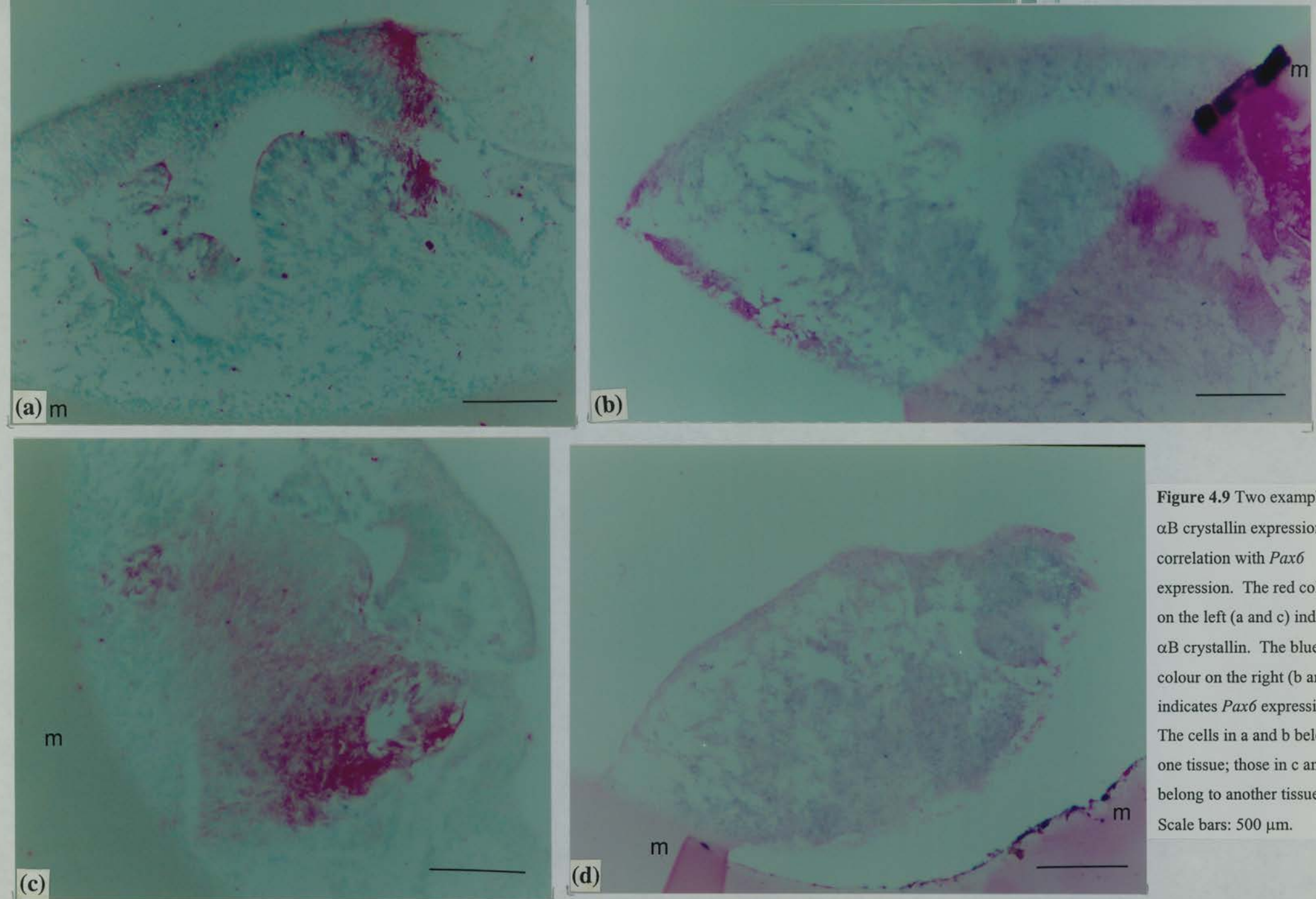

Figure 4.9 Two examples of αB crystallin expression in correlation with *Pax6* expression. The red colour on the left (a and c) indicates αB crystallin. The blue colour on the right (b and d) indicates *Pax6* expression. The cells in a and b belong to one tissue; those in c and d belong to another tissue. Scale bars: 500 μm.

Chapter 5: Comparison of *Msx-1* and *Msx-2* expression in the premaxilla between *Sey/Sey* mice and wildtypes

5.1 Introduction

The phenotype of the *Sey/Sey* mice is not limited to a lack of eyes and nasal derivatives. They also have shorter snouts (Hill *et al.*, 1991) and, perhaps more surprisingly, possess supernumerary upper incisor teeth and a cartilaginous rod-like structure (Kaufman *et al.*, 1995). These extra structures are unexpected in the sense that *Pax6* is not reported to be expressed in the developing premaxilla and I found no evidence of expression during my investigations in chapter 3. The aim of this chapter is to investigate the formation of the supernumerary upper incisor teeth in more details, and in particular examine the expression of *Msx-1* and *Msx-2* in order to give some explanations for the abnormalities in the *Sey/Sey* premaxillary region.

Msx-1 and *Msx-2* are genes implicated in tooth formation (Mackenzie *et al.*, 1991a, 1991b, 1992; Jowett *et al.*, 1993; Satokata and Maas, 1994) and have been shown to be expressed in the premaxilla, in the primitive teeth, and in some parts of nasal derivatives (Robert *et al.*, 1989; Hill *et al.*, 1989; Mackenzie *et al.*, 1991a, 1991b, 1992). It is therefore of interest to find out whether patterns of *Msx-1* and *Msx-2* expression are altered in the mice homozygous for the *Sey* mutation. There is also some evidence that *Msx-1* may be a target for *Pax6* (Grindley *et al.*, 1995). This is suggested by the altered expression pattern of an *Msx-1* transgene in the *Sey/Sey* mice. The lack of a functional Pax6 protein may therefore have an affect on *Msx* genes, which may be reflected in tooth development. In this preliminary study, I investigated *Msx-1* and *Msx-2* expression using non-radioactive *in situ* hybridization, in the premaxilla of the *Sey/Sey* mice and their wildtype littermates.

5.2 Results

The expression of *Msx-1* and *Msx-2* during normal tooth development in wildtype mice has been previously reported (Robert *et al.*, 1989; Hill *et al.*, 1989; Mackenzie *et al.*, 1991a, 1991b, 1992; Jowett *et al.*, 1994). I have documented it here for comparison with the expression in the *Sey/Sey* mice. Efforts have been made to process wildtype and *Sey/Sey* tissue sections through *in situ* hybridization at the same time and under the same conditions, to ensure that the comparisons are not biased on methodological variations.

5.2.1 Observation of phenotypes and expression of *Msx-1* and *Msx-2* in the *Sey/Sey* and wildtype embryos on sagittal sections at day 13.0 p.c.

Figure 5.1 shows the expression of *Msx-1* and *Msx-2* on sagittal sections at day 13.0 p.c. The wildtype embryos at the same stage of development are generally larger than the *Sey/Sey* embryos and the latter have a shorter and smaller snout (compare figure 5.1.a with 5.1.b). The formation of the nasal cavity has invariably failed in the *Sey/Sey* embryos (for example, see figure 5.1.b).

Msx-1 is expressed in the mesenchyme of the lateral nasal, maxillary and mandibular processes in the wildtype embryos, but the expression does not extend to the surface, oral, or nasal epithelium (see figures 5.1.a; c). In the *Sey/Sey* embryos, *Msx-1* is expressed in the areas, which despite differences in morphology, roughly correspond to those of their wildtype littermates (compare figure 5.1.a with 5.1.b; figure 5.1.c with 5.1.d). For example, the lateral nasal process is located rostral to the maxillary process, forming the roof of the external naris (arrow in figure 5.1.a) in the wildtype embryos as seen on sagittal sections. The corresponding area of the lateral nasal process, despite the fact that there are no nostrils, should therefore be located rostral to the maxillary process in the *Sey/Sey* mice (see figure 5.1.b).

The level of *Msx-1* expression appears to be higher in the *Sey/Sey* embryos than that in their wildtype littermates and this higher level of expression appears throughout the embryo, including the limb bud (compare figures 5.1.a; c with 5.1.b; d). One exception to this is in the mesenchymal capsule that surrounds the anterior prosencephalon, where more intense *Msx-1* expression is seen in the wildtypes than in their *Sey/Sey* littermates (compare the arrow-indicated areas in figures 5.1.c; d). This may be explained by the fact that the section shown in figure 5.1.d is more lateral than that in 5.1.c.

Msx-2, like *Msx-1,* is expressed in both the *Sey/Sey* embryos and their littermates, but at a lower level (see figures 5.1.e; f). Hints of *Msx-2* expression can be found in the lateral nasal, maxillary and mandibular processes, as well as in the mesenchymal capsule and its covering surface ectoderm (see arrows in figures 5.1.e, f) that surrounds the rhombencephalon. *Msx-2* expression is also found in the limb bud at a similar level to that in the maxillary process.

It is impossible to make comparisons on the level of *Msx-2* expression between the *Sey/Sey* embryos and their wildtype littermates.

5.2.2 Observation of phenotypes and expression of *Msx-1* in the *Sey/Sey* and wildtype premaxilla on transverse sections at days 14 - 17 p.c.

Msx-1 expression in the developing maxillary process at days 14 - 17 p.c. is shown by transverse sections in figure 5.2. It is noted that the *Sey/Sey* embryos are behind in development by at least 24 hours as compared to their wildtype littermates. It may therefore be of interest to compare the *Sey/Sey* embryos with their wildtype littermates that are 24 hours younger.

5.2.2.1 Day 14 p.c.

In the wildtype embryos, *Msx-1* is expressed in the nasal derivatives including the nasal capsule and the nasal septum, as well as in the mesenchymal cells and surface ectoderm that surround them; but it is

excluded from the nasal epithelium that flanks the nasal septum (see figure 5.2.a). *Msx-1* is also expressed in the mesenchymal cells that disperse in the region between the nasal derivatives and the dental lamina and their surrounding areas. There are, however, symmetrical zones which do not express *Msx-1* but are located within the mesenchymal condensations of the presumptive dental papilla (arrows in figure 5.2.a). The thickening dental lamina, which forms the future enamel organ, does not contain any *Msx-1* transcripts (figure 5.2.a).

In the *Sey/Sey* maxillary process, no nasal derivatives are seen (see figure 5.2.b). The *Sey/Sey* maxillary process shows more torsions in its external contour in contrast to that in the wildtype embryos. A clump of non-*Msx-1*-expressing cells that presumably constitutes the rod-like cartilaginous structure (see figure 5.2.b) is seen amid the mesenchyme where *Msx-1* is expressed. The mesenchymal expression of *Msx-1* appears to be at a higher level than that in the wildtype embryos (compare figure 5.2.a with 5.2.b). The presumptive more intense *Msx-1* expression in the *Sey/Sey* embryos does not seem to be due to a higher cell density in this region, in that no apparent compaction of cells is seen under higher magnification (not shown). The development of upper incisors is retarded in the *Sey/Sey* maxilla in that the dental lamina is still not formed in contrast to the thickening of the dental papilla in the wildtypes (compare figure 5.2.a with 5.2.b).

5.2.2.2 Day 15 p.c.

At day 15 p.c., the distribution of *Msx-1* transcripts in the wildtype maxillary process is comparable to that found at day 14 p.c. (figure 5.2.c). *Msx-1* expression is seen in the nasal septum, the anterior and lateral nasal capsule, as well as in the mesenchymal cells that surround the nasal derivatives and disperse within the maxillary process. *Msx-1* is also expressed in the mesenchymal cells between the primitive enamel organs and the mesenchymal condensations. Transcripts of *Msx-1* remain absent in the nasal epithelium flanking the nasal septum, in the condensed mesenchyme of the presumptive dental papilla, as well as in the future enamel organs. All the non-*Msx-1*-expressing areas are located in left-right symmetrical pairs that are separated by *Msx-1*-expressing cells in the middle. This is particularly interesting in the presumptive incisor region where the separation by *Msx-1*-expressing cells is not obvious at day 14 p.c., but it becomes evident at day 15 p.c. as the primitive enamel organs are formed.

In the maxillary process of the *Sey/Sey* embryos, *Msx-1* is expressed in the mesenchymal cells that surround the rod-like structure and the presumptive dental derivatives. Transcripts of *Msx-1* are also found in the mesenchymal cells between the primitive enamel organs and their surrounding mesenchymal condensations (see figure 5.2.d), which is comparable to that in the wildtype embryos (compare figure 5.2.c with 5.2.d). The primitive enamel organs of upper incisors, as illustrated in figure 5.2.d, are surrounded by a single large condensation of mesenchyme which forms the future dental papilla. The single dental papilla, in contrast to that in the wildtypes, is not evidently separated by *Msx-1*-expressing cells (compare figure 5.2.c with 5.2.d).

The *Sey/Sey* maxilla also appears to form more torsions in its internal contour (the oral epithelium) as compared to the wildtype maxilla (compare figure 5.2.c with 5.2.d; see also arrows in 5.2.f). One of the internal torsion appears to form an epithelial thickening similar to presumptive dental lamina (arrow in figure 5.2.d) that is significantly retarded as compared to the other incisors.

The cells that constitute the presumptive rod-like cartilaginous structure appear to be *Msx-1*-expressing in figure 5.2.d. This expression, however, is not found in any other *Sey/Sey* preparations at the same stage of development.

5.2.2.3 Day 16 p.c.

At day 16 p.c., *Msx-1* expression in the wildtype maxilla is detected in the dental papilla that is previously non-expressing (see figure 5.2.e). In the mesenchymal cells, particularly those surrounding the lateral side of the dental derivatives, the previously observed high level of expression is decreased. Minimal expression of *Msx-1* also appears to be present in the nasal capsule and the nasal septum. There are also signs of *Msx-1* expression in the whisker follicles (see figure 5.2.e).

In the *Sey/Sey* maxilla, *Msx-1* is also expressed in the dental papilla (see figure 5.2.f). Of the specific example illustrated in figure 5.2.f, the presumptive upper incisors are arranged in two groups that are separated by *Msx-1*-expressing cells. The one with two presumptive dental papillas (on the right) is surrounded by a single enamel organ. Transcripts of *Msx-1* are also seen in the whisker follicles and the mesenchymal cells between the enamel organs. The cells within the rod-like structure remain non-*Msx-1*-expressing.

5.2.2.4 Day 17 p.c.

At day 17 p.c., *Msx-1* expression in the wildtype maxilla follows the same theme as observed at day 16 p.c. Transcripts of *Msx-1* are found in the nasal septum and the lateral nasal capsule (see figure 5.2.g). The nasal epithelium remains non-*Msx-1*-expressing. The cartilage primordium of the sphenoid bone is clearly seen without *Msx-1* transcripts by day 17 p.c. In the incisors, *Msx-1* is expressed in the dental papilla, while the enamel organ is non-expressing. The expression appears to be more intense in the demarcation between the dental papilla and its enclosing enamel organ. Transcripts of *Msx-1* are also found in the presumptive dental follicles that flank the medial side of the upper incisors. In the mesenchymal cells surrounding the lateral side of the upper incisors, *Msx-1* expression is reduced, which is comparable to that observed at day 16 p.c. The mesenchymal cells between the incisors, however, remain expressing *Msx-1* at a level comparable to that in the dental papilla. Between the dental follicle and the medial mesenchyme, a non-expressing zone is found in each side of the maxilla

(see arrows in figure 5.2.g). In the wildtype whisker follicles, *Msx-1* expression is maintained at day 17 p.c.

In the *Sey/Sey* maxillary process at day 17 p.c., *Msx-1* is expresed in the dental papilla, as well as in the whisker follicles and in the medial mesenchymal cells (see figure 5.2.h). The rod-like structure does not express *Msx-1*. The pattern of *Msx-1* expression in the dental papilla seems similar in the wildtype and the *Sey/Sey* embryos. The *Sey/Sey* dental papilla, however, is reduced in size. The non-expressing zones between the dental follicle and the medial mesenchyme are significantly reduced in the *Sey/Sey* embryos as compared to those in the wildtypes (compare arrow-indicated areas in figure 5.2.g and 5.2.h).

5.2.3 Expression of *Msx-2* in the *Sey/Sey* and wildtype premaxilla on transverse sections at days 13 - 15 p.c.

Msx-2 expression in the wildtype and *Sey/Sey* maxillary processes at days 13 - 15 is shown by transverse sections in figure 5.3.

At day 13 p.c., hints of *Msx-2* expression in the wildtype maxilla are detected along the oral epithelium, particularly in the site where the dental epithelium is presumably located (see figure 5.3.a). Signs of *Msx-2* expression are also found in the nasal epithelium in the wildtype embryos. In the *Sey/Sey* embryos at day 13 p.c., no apparent *Msx-2* expression is found in the maxilla, while localized *Msx-2* expression is seen in the mandible (figure 5.3.b).

At day 14 p.c., *Msx-2* expression is clearly seen along the oral epithelium in the wildtype maxilla (see figure 5.3.c). In particular, the sites of dental lamina exhibit more intense expression. *Msx-2* expression is also seen around the entrance of the nasal cavity, in the surface ectoderm covering the nasal derivatives, and in the nasal septum. Transcripts of *Msx-2* are also detected in the whisker follicles in the wildtype maxillary process. In the *Sey/Sey* maxillary process, hints of *Msx-2* expression is seen in the dental laminas and in other specified areas where presumably the dental epithelia are localized (see figure 5.3.d; in this specific example, two torsions of presumptive dental epithelium are found).

At day 15 p.c., *Msx-2* expression is detected notably in the dental papilla in the wildtype maxilla (figure 5.3.e). Signs of *Msx-2* expression also appear in the anterior nasal capsule and in the oral epithelium. In the *Sey/Sey* maxilla, *Msx-2* transcripts are detected in the thickening dental lamina and in the site where the dental epithelium is presumably located (see figure 5.3.f). The expression in the dental primordia appears to be continuous with that in the oral epithelium. More than three upper incisor primordia are commonly found in the *Sey/Sey* maxilla. In the specific example shown in figure 5.3.f,

four dental laminas with a torsion in the oral epithelium are found. *Msx-2* is also expressed in the whisker follicles in the *Sey/Sey* maxillary process, as shown in figure 5.3.f.

5.3 Discussion

5.3.1 Mutant phenotypes in the *Sey/Sey* mice and *Msx-1*, *Msx-2* expression in the wildtype embryos

This study confirms all the abnormalities that have been previously reported in the *Sey/Sey* premaxilla. Results in this study on *Msx-1* and *Msx-2* expression in the wildtype maxilla also confirm previously reported data by MacKenzie *et al.* (1991a, 1991b, 1992) and Jowett *et al.* (1993) in that: (1) *Msx-1* is expressed in the papillary and follicular mesenchyme (for example see 'df' and 'dp' in figure 5.2.g) and is excluded from the dental epithelium (for example see the 'eg' that is differentiated from dental epithelium in figure 5.2.g). (2) *Msx-2* is expressed initially in the dental epithelium (or called dental lamina when it becomes thickened; see 'de' and 'dl' in figures 5.3.a; c) and later is expressed in the mesenchyme of the dental papilla (see 'dp' in figure 5.3.e).

In addition to the confirmation of previously reported data, this study shows that *Msx-1* is not expressed in the condensing mesenchyme that constitutes the future dental papilla of the upper incisor. This exclusion of *Msx-1* expression can obviously be seen between day 14 and 15 p.c. By day 17 p.c., a symmetrical non-*Msx-1*-expressing zone can be seen between the dental follicle and the medial mesenchyme, which has never been reported before.

5.3.2 *Msx-1* expression in the *Sey/Sey* maxilla

Although *in situ* hybridization does not give differential expression on a quantitative basis, results of this study suggest that *Msx-1* expression is increased and that the increase seems to occur in most areas of expression in the *Sey/Sey* embryos. For *Msx-2* expression, results of this study do not allow a direct comparison between wildtype and *Sey/Sey* embryos based on *in situ* hybridization. It would therefore be interesting to investigate, for example, by quantitative Northern transfers or quantitative *in situ* RT-PCR (Reverse Transcriptase - Polymerase Chain Reaction) to determine this issue.

Increase of *Msx-1* expression may imply that it is involved in the formation of supernumerary upper incisors in the *Sey/Sey* mice, as *Msx-1* is suggested to involve in the initiation of tooth development (MacKenzie *et al.*, 1991a, 1991b, 1992). Mina and Kollar (1987) reported that the mesenchyme beneath pre-patterned regions of the oral epithelium, during the process of condensation, becomes capable of inducing tooth formation when cultured in combination with oral epithelium and non-oral epithelium. This property of mesenchyme to induce odontogenesis has been suggested to be due to the presence of *Msx-1* transcripts. *Msx-1*, as a putative transcription factor, may play a role in regulating

the expression of other genes in the mesenchyme or in the epithelium during tooth formation (Jowett *et al.*, 1993). One can, however, argue against that the formation of supernumerary upper incisors involves an increase of *Msx-1*. *Msx-1* expression also appears to increase in the mandibular process (as seen in figure 5.1.b), but no formation of supernumerary lower incisors has ever been reported.

Increase of *Msx-1* expression can also imply that *Pax6* may directly or indirectly have an inhibitory effect on *Msx*-1 expression. This is particularly supported by *Msx-1* expression in the maxillary process, in that areas of *Msx-1* expression do not overlap with those of *Pax6* expression. In the wildtype maxillary process, the nasal cavity and *Pax6*-expressing nasal epithelium obviously take up some space that can be filled with *Msx-1*-expressing mesenchyme, indicating that at least an indirect effect exists.

5.3.3 Origin of the rod-like cartilaginous structure

Kaufman *et al.* (1995) reported that, in addition to the supernumerary upper incisors, the *Sey/Sey* mice also exhibit a median cartilaginous rod-like structure in the premaxilla and that the exact derivation of the rod-like structure is unclear. This study shows that *Msx-1* is not expressed in the rod-like structure (see figures 5.2.b;f;h), indicating that the rod-like structure is derived from cells without the presence of *Msx-1* transcripts. In the wildtype premaxilla, *Msx-1* is not expressed in three areas: the future dental papilla (the condensed mesenchyme), the primitive enamel organ (the thickening dental epithelium) and the nasal epithelium flanking the nasal septum (see figures 5.2.a; c). Thus, the rod-like structure in the *Sey/Sey* mice is likely derived from one or more than one of the three non-*Msx-1*-expressing areas (compare figure 5.2.a with 5.2.b). Another possibility is that it is derived from tissues where *Msx-1* is initially expressed, but the expression is later turned off as the cells change their characteristics. The third possibility is that the rod-like structure is derived from an aberrant, ectopic outgrowth of non-*Msx-1*-expressing structure from outside of the maxillary process.

The rod-like structure, however, is most likely to have originated from outside of the maxillary process for the following reasons: (1) It is differentiated into cartilaginous cells in contrast to the other candidates. (2) It co-exists with the other non-*Msx-1*-expressing areas and, in some cases, shows obvious detachment from them (for example, see figures 5.2.d). (3) The non-*Msx-1*-expressing cells within the mesenchymal condensation of future dental papilla will eventually be transfromed into *Msx-1*-expressing cells. This is not seen in the rod-like structure. (4) The enamel organ, be it from wildtype or *Sey/Sey* embryos, will have *Msx-1*-expressing cells of dental papilla wrapped inside it (see figures 5.2.g; f). This, again, is not seen in the rod-like structure. (5) Most importantly, the rod-like cartilaginous structure is continuous with the base of the skull (Kaufman *et al.*, 1995) where *Msx-1* expression has never been documented.

5.3.4 Non-synchronized formation of upper incisor primordia in the *Sey/Sey* maxilla

Results in this study show that torsions of the oral epithelium (presumably secondary dental epithelia), which are never found in the wildtypes, appear in the *Sey/Sey* maxilla after the primary dental epithelia are invaginated to form the presumptive enamel organs (for example, see figure 5.2 f). The identity of some of the torsions of the oral epithelium are confirmed by the presence of *Msx-2* transcripts as exemplified in figures 5.3.d and 5.3.f. Thus, the supernumerary upper incisors are developed in a non-synchronous way, in that some of the dental epithelia have already been differentiated into the primitive enamel organs, while others are still torsions of the oral epithelium.

The presence of secondary dental epithelia in the *Sey/Sey* maxilla indicates that the epithelial-mesenchymal interaction is maintained after the primary dental epithelia are invaginated. *Pax6* mutation therefore either lifts the presumptive inhibition of primary epithelial-mesenchyme interaction or cause a *de novo* secondary induction. In either case, it is interesting to see that the maintained primary induction or the secondary induction are potentially capable of producing more than two upper incisors, as suggested by figure 5.2.f. It is also interesting to see that a condensed or condensing mesenchyme always accompanies a dental lamina (as seen in figure5.2.f) in close proximity, suggesting that the condensation is necessary for induction.

The non-synchronous nature reflects that *Pax6* mutation does not only affect the number of upper incisors but also the temporal determination of those upper incisors.

5.3.5 Symmetrical vs asymmetrical distribution of supernumerary upper incisors

Results of this study indicate that the supernumerary upper incisors are formed either symmetrically or asymmetrically in the *Sey/Sey* maxilla. This could result from the disturbance of left-right symmetry or the formation of odd numbers of incisors that will eventually be distributed unequally to each side of the maxilla. The disturbance of left-right symmetry is less likely for the following reasons: (1) In the *Sey/Sey* maxilla, no other obvious asymmetry in the other tissues, for example the hair follicles, is observed in this study. The possibility of a local effect on symmetry may be excluded. (2) No disturbance of left-right symmetry is reported in the other areas of the *Sey/Sey* mice. (3) In the *Sey/Sey* maxilla, the cartilaginous rod-like structure is always located in the median plane, suggesting that a sense of left-right identity is maintained. (4) In rare cases of *Sey/Sey* maxilla that form 5 primitive upper incisors, a left-right balance is commonly maintained (see figure 5.3.f for example).

5.3.6 Non-corresponding number of dental papilla formation in relation to the enamel organ

Results of this study show that encapsulement of two dental papillas by a single large enamel organ is common in the *Sey/Sey* maxilla (for example, see figures 5.2.d; f; h). The enamel organ itself, however, is invariably surrounded by a single dental follicle. The fact that the formation of the enamel organ and

the dental papilla does not correspond may be due to fusion of neighbouring enamel organs during odontogenesis. Alternatively, it may result from dividing a single mesenchyme condensation into two separate dental papillas. Analyses of *Sey/Sey* embryos at day 14 p.c. readily reveal that the dental placodes (which will form enamel organs) can outnumber mesenchyme condensations and the former are usually linked in their epithelial surface before invagination, suggesting that fusion of neighbouring enamel organ is more likely the case. For example, in figure 5.2.d, three invaginated dental placodes are surrounded by two mesenchyme condensations. Thus, results in this study indicate that the previously reported supernumerary upper incisors in the *Sey/Sey* maxilla (Kaufman *et al.*, 1995) were counted by the number of dental papillas, not by the number of enamel organs.

In the wildtype embryos, the formation of a dental placode is always on a one-to-one basis with the condensation of dental papilla mesenchyme. This reflects a precise mechanism that controls the number of teeth in either the maxilla or the mandible. Obviously, the *Sey/Sey* maxilla does not follow the one-to-one basis so that the number of upper incisors is increased. The increase is probably mediated by the capability of inducing two or more dental placodes by a single condensation of dental papilla. The *Sey/Sey* mandible, however, has so far not been reported to exhibit supernumerary lower incisors or other apparent abnormalities, suggesting that the formation of supernumerary upper incisors is caused by a local interference rather than general effects on odontogenesis.

5.3.7 Formation of a shorter snout in the *Sey/Sey* maxilla

Hill *et al.* (1991) reported that the *Sey/Sey* mice exhibit shorter than normal snouts as compared to their wildtype littermates. This was also observed in this study. The mouse snout is composed mostly of the neural crest cells that form the mesenchymal and skeletal elements in the maxillary process (Le Douarin, 1982; Noden, 1986), with relatively few epithelial cells contributing to the nasal and surface epithelium. The shorter snout in the *Sey/Sey* mice, therefore, may be caused by the following two mechanisms that can determine the final numer of neural crest cells in that region:

The first possible mechanism is that it may be caused by abnormally excessive apoptosis following the accumulation of neural crest cells that are initially comparable in cell numbers to those in the wildtypes. Apoptosis is involved in the development of many embryonic regions, including the maxillary process. During odontogenesis, apoptosis is implicated in the removal of the enamel knots, disruption of dental lamina and reduction of dental epithelium during enamel formation (Vaahtokari *et al.*, 1996). Marazzi *et al.* (1997) reported that *Msx*-2, whose expression is seen in the maxilla (MacKenzie *et al.*, 1992; Jowett *et al.*, 1993), is involved in the BMP4-mediated programmed cell death pathway. Furthermore, *Msx-2* has been implicated in programmed cell death of neural crest cells during development (Graham *et al.*, 1993; 1994). The possible involvement of apotosis in causing the shorter snout in the *Sey/Sey* mice therefore remains an open question.

The second possibility is that the shorter snout may result from deficit of the neural crest, either via insufficient migration or mitosis. Matsuo *et al.* (1993) reported that anterior midbrain neural crest cells in rats homozygous for the *rSey* mutation migrated only to the presumptive eye region and did not reach the nasal rudiments. Their data suggest that *Pax6* mutation can impair midbrain neural crest migration toward the maxillary process. The maxillary neural crest cells are reported to be mainly from the midbrain (Tam and Morris-Kay, 1986; Serbedzija *et al.*, 1992; Osumi-Yamashita *et al.*, 1994), strongly supporting that the shorter snout is caused by shortage of crest cells. Interestingly, however, the midbrain is not a region of *Pax6* expression during the period of neural crest migration and *Pax6* has never been reported to be expressed in the migrating neural crest cells (Walther and Gruss, 1991; Stoykova and Gruss, 1994; Grindley *et al.*, 1995; Stoykova *et al.*, 1996; Warren and Price, 1997; Mastick *et al.*,1997). How can *Pax6* mutation affects neural crest migration or mitosis ? In the mouse, the earliest presence of *Pax6* transcripts is found at day 8.0 p.c. in the presumptive forebrain and hindbrain (Walther and Gruss, 1991). By day 8.0 p.c., the head neural crest cells are still at premigratory stage (Serbedzija *et al.*, 1992). This gives an opportunity for *Pax6* transcripts to affect the premigratory neural crest cells. Osumi-Yamashita *et al.* (1994) reported that the lateral edge of the prosencephalon produced crest cells which migrated to the frontonasal mass. On the other hand, cells at the anterior neural ridge in the prosencephalon contributed mainly to the head epithelium including the nasal placode (Tam and Morris-Kay, 1986; Serbedzija *et al.*, 1992; Osumi-Yamashita *et al.*, 1994). Both the lateral edge and the anterior neural ridge are *Pax6*-expressing areas at 8.0 days p.c. (Walther and Gruss, 1991). The frontonasal mass constitutes a high proportion of the total mass of the snout. It is therefore possible that the failure of *Pax6* function can deter the migration of neural crest cells from the lateral edge of the prosencephalon toward the frontonasal mass, in a way comparable to the impaired migration of crest cells in the midbrain found in the *rSey/rSey* mouse. Thus, a shorter snout is found.

5.3.8 Abnormalities in the *Sey/Sey* maxilla may be caused by the failure of nasal derivative formation

In section 5.3.7, two explanations for the formation of a shorter snout in the *Sey/Sey* maxillary process are discussed, with particular interest in the determination of the number of neural crest cells. The two explanations may not be exclusive and may overlap to some extent. Whatever is the case, one can develop the question further by asking why does excessive apoptosis and/or impaired migration (or mitosis) of the neural crest cells occur ?

Extensive reports have been published on the absence of nasal derivatives in the *Sey/Sey* embryos (Hogan *et al.*, 1986, 1988; Hill *et al.*, 1991; Kaufman *et al.*, 1995; Grindley *et al.*, 1995). The failure of nasal derivative formation is characterized by the absence of nasal placode formation. Furthermore, *Pax6* expression is turned off in the nasal region of *Sey/Sey* embryos (Grindley *et al.*, 1995). Nasal

derivatives are therefore never present in any primitive form in the *Sey/Sey* embryos. This means that any possible local effect from nasal derivatives on the maxilla can not occur in the *Sey/Sey* embryos.

The nasal placode is a source of hormone-producing cell populations which migrate to the medial basal forebrain (Schwanzel-Fukuda and Pfaff, 1990) and probably induce the formation of the olfactory bulb (Gong and Shipley, 1995). The hormone-producing cell populations, during migration, have an opportunity to interact with the maxillary mesenchyme, which may play a role in the normal development of the maxillary process. The nasal region may be a source of developmentally important diffusible molecules such as growth factors. A possible example is FGF8 that is expressed in the nasal placode (Crossley and Martin, 1995). Lack of such a source in the nasal region means that factors to attract or direct neural crest cell migration is lost. Alternatively, the nature of the maxillary mesenchyme may be altered in the absence of diffusible molecules from the nasal region, which results in supernumerary mesenchymal condensations in the *Sey/Sey* maxilla.. The nasal derivatives may also contribute to the boundary formation in the base of the skull by diffusible inhibitory factors. When the inhibitory effects fail in the *Sey/Sey* maxilla, overgrowth of the skull leads to the formation of the rod-like structure.

5.3.9 Summary -- the whole picture of abnormalities in the *Sey/Sey* maxilla and possible involvement of *Msx-1* and *Msx-2*

In this study, as well as in previous reports, abnormal phenotypes in the maxillary process are found in the *Sey/Sey* mice. The abnormal phenotypes can be caused by localized effects in the maxilla, as well as be associated with malformations in the eye and the brain.

Pax6 is unlikely to be involved directly in the process of odontogenesis, in that it is not expressed in any tooth primordium, nor in the mesenchymal or epithelial tissues. The fact that the lower incisors or molars are not affected in the *Sey/Sey* mice also supports that *Pax6* does not possess a direct role during odontogenesis. Instead, the formation of supernumerary upper incisors in the *Sey/Sey* mice appears to be associated with localized effects -- the failure of nasal formation and the formation of the rod-like cartilaginous structure (discussed in section 5.3.3), as well as the impaired contribution of midbrain neural crest cells that normally constitute the major source of the maxillary mesenchyme. Failure of nasal formation and the presence of the rod-like cartilaginous structure in the *Sey/Sey* mice indicate that the normal compartmentation in the maxillary process is disturbed, which may lead to the disturbance of local identity in the mesenchyme. As the local identity in the mesenchyme is disturbed, the number of dental papilla no longer corresponds to that of the enamel organ (see section 5.3.6).

The abnormalities in the *Sey/Sey* maxilla may also be associated with the defects in the eye or the brain. Lack of eye formation means that the neural crest cells from the prosencephalon can migrate more freely before they reach the frontal nasal mass. The disturbance of p1/mesencephalon boundary and the

absence of regional cell density in the diencephalon (Warren and Price, 1997; Mastick *et al.*, 1997) implies that the normal contribution of the neural crest cells from these regions can be affected.

Little is known about the molecular activities underlying the normal morphogenesis of the maxilla and less is understood during odontogenesis. Efforts made in this study to interpret the malformation in the *Sey/Sey* maxilla on a molecular basis, therefore, has to be preliminary. The presumably upregulation of *Msx-1* suggests that it is involved. The involvement, however, has to be indirectly implicated for the following reasons: (1) Areas of expression between *Msx-1* and *Pax6* are not overlapped extensively, and (2) No gel shift assay showing that Pax6 protein can affect the electrophoretic motility of *Msx-1* transcripts has been reported so far. (3) The effect of *Pax6* mutation on upper incisor formation differs from that of the eye and the nose. Formation of the eye and nose is completely blocked, indicating that the sequential events and gene activities involved therein have never happened. The formation of upper incisors (including the activities of both *Msx-1* and *Msx-2*), is allowed to proceed although in an abnormal way.

If *Msx-1* and *Msx-2* are unlikely to be the direct targets of *Pax6,* one has to wonder why *Pax6* mutation may lead to upregulation of both genes ? Vainio *et al.* (1993) reported that bone morphogenetic protein 4 (BMP-4), a member of the transforming growth factor β superfamily, is expressed in the presumptive dental epithelium at the initiation of tooth development. Subsequently, the epithelial BMP-4 signalling can induce its own mesenchymal expression, as well as the expression of *Msx-1, Msx-2,* and *Egr-1* (Vainio *et al.*,1993). BMP-2 can also stimulate *Msx-1* and *Msx-2* expression *in vitro* (reviewed by Thesleff *et al.*, 1995). *Msx-2,* in particular, has been further demonstrated as a downstream gene of *BMP*-4 and is implicated in the *BMP-4*-mediated programmed cell death pathway (Marazzi *et al.*, 1997). It is therefore likely that *BMP-2* and *BMP-4* are upregulated in the *Sey/Sey* mice and their overexpression is responsible for the formation of the rod-like cartilaginous structure. Abnormalities in the *Sey/Sey* mice are also found in the skull (Kaufman, personal communication), supporting the possible involvement of the two BMP proteins.

Figure 5.1 *Msx-1* and *Msx-2* expression in the +/+ and *Sey/Sey* embryos sagitally sectioned at day 13 p.c. (see the schematic diagram below). The left panels (a, c, e) represent *Msx-1* expression in the wildtypes. The panels on the right (b, d, f) represent *Msx-1* expression in the *Sey/Sey* mice. All the embryonic tissues are processed under the same condition through *in situ* hybridization (detailed in chapter 2). a and b show the maxillary process under higher magnification. Note that the *Sey/Sey* embryos are reduced in size, without nasal cavity, and with shorter snouts, as compared to their wildtype littermates. *Msx-1* is expressed in the mesenchyme of lateral nasal, maxillary, and mandibular process (in a), as well as in the mesenchymal capsule that surrounds the anterior prosencephalon and in the limb bud (in c). In the *Sey/Sey* embryos, although no nasal derivatives are formed, *Msx-1* appears to be expressed in the corresponding regions as compared to those in the wildtypes (in b). *Msx-2* expression is less obvious, but still can be seen in the lateral nasal, maxillary, mandibular process, as well as in the limb bud and in the mesenchymal capsule surrounding the rhombencephalon (in e). *Msx-2* expression in the *Sey/Sey* embryo also corresponds to that in the wildtypes (in f). Note that *Msx-1* expression appears to increase in the *Sey/Sey* embryos. Abbreviations: lb, limb bud; ln, lateral nasal process; mes, mesencephalon; mn, mandibular process; mx, maxillary process; nc, nasal cavity; nep, nasal epithelium; pro, prosencephalon; r, residual lumen of Rathke's pouch; rho, rhombencephalon. Scale bars: a - b, 750 μm; c - f, 500 μm.

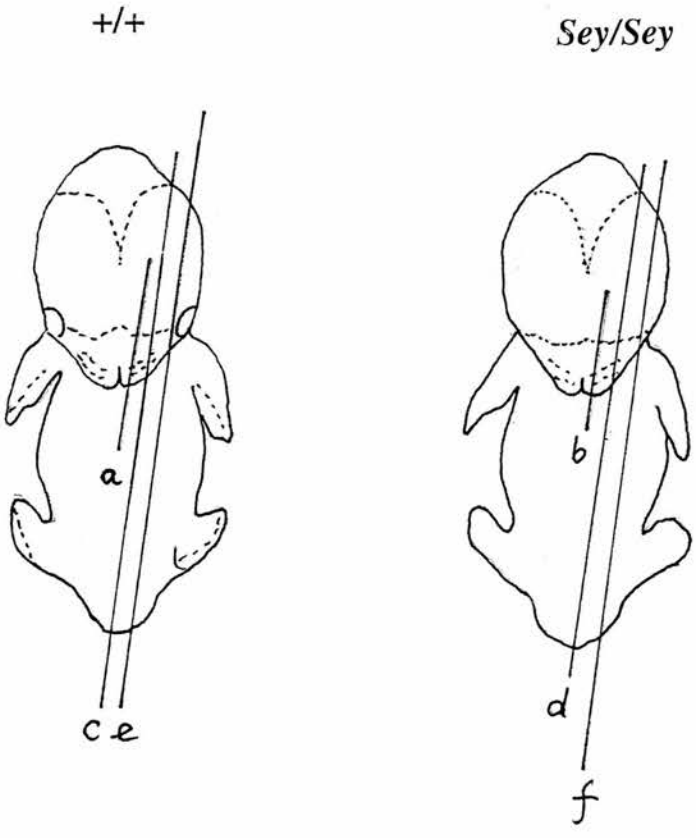

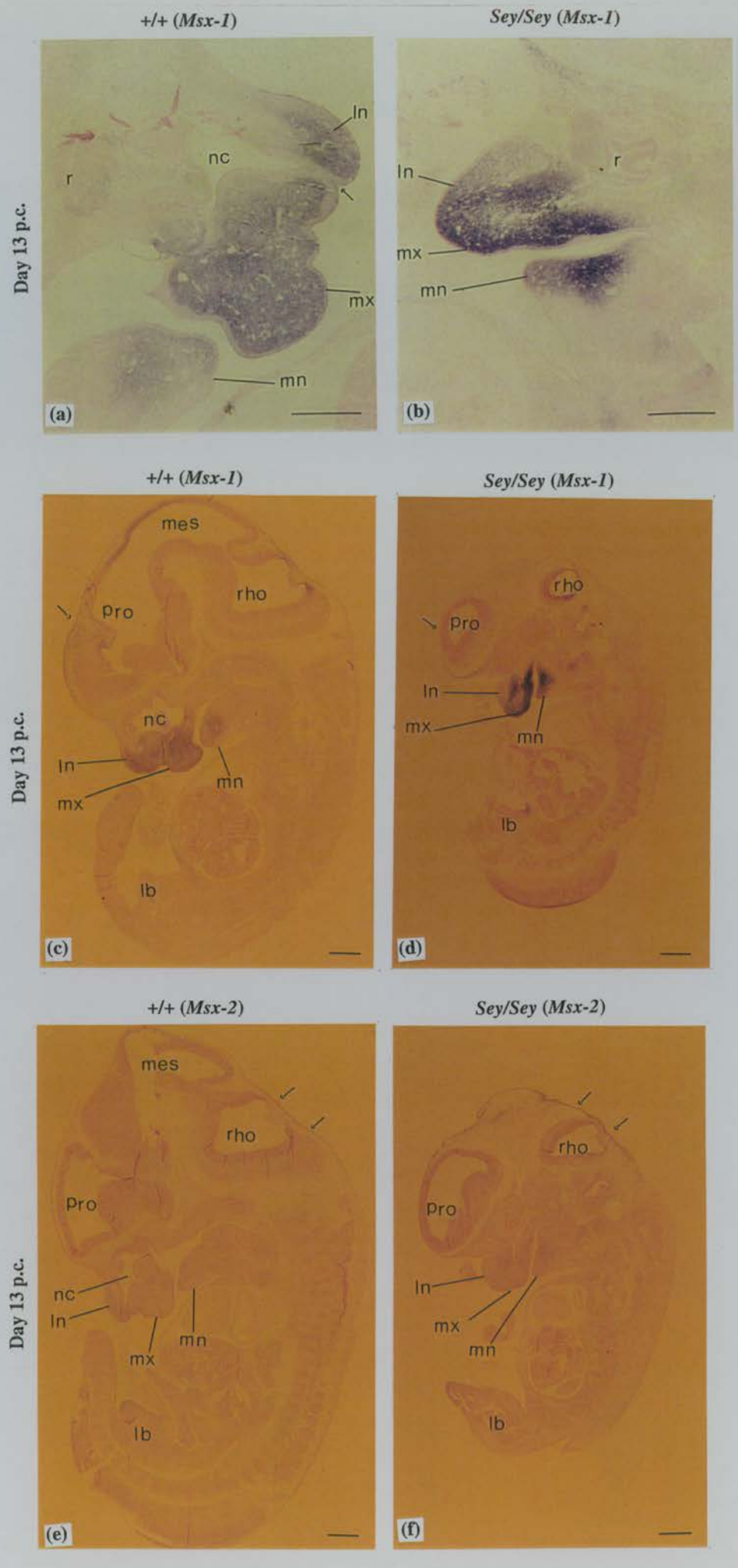
+/+ (Msx-1)
Sey/Sey (Msx-1)
Day 13 p.c.
ln
nc
r
mx
mn
(a)
(b)
mes
rho
pro
lb
(c)
(d)
+/+ (Msx-2)
Sey/Sey (Msx-2)
(e)
(f)

Figure 5.2 *Msx-1* expression in the +/+ and *Sey/Sey* maxillary processes transversly sectioned at days 14, 15, 16 and 17 p.c. (see the schematic diagram below). The left panels (a, c, e, and g) represent *Msx-1* expression in the wildtype maxilla. The right panels (b, d, f, and h) represent *Msx-1* expression in the *Sey/Sey* maxilla. All the embryonic tissues are processed under the same condition through *in situ* hybridization (detailed in chapter 2). In the wildtype embryo, *Msx-1* expression is seen in the nasal septum, in the anterior and lateral nasal capsule, and in the mesenchymes that disperse within the maxilla (in a, c). *Msx-1* expression is excluded from the nasal epithelium, the mesenchymal condensation that forms the future dental papilla, and the dental lamina (in a, c). Later at day 16 and 17 p.c., *Msx-1* expression is seen in the dental papilla and the dental follicle (in e, g). In the *Sey/Sey* maxilla, *Msx-1* is expressed in the mesenchyme, but is excluded from the rod-like structure (in b). Later at day 16 and 17 p.c., *Msx-1* is expressed in the dental papilla in a pattern comparable to that in the wildtypes (compare g with h). Note that *Msx-1* is expressed in the whisker follicles in the wildtype and *Sey/Sey* maxillary processes. Note also that the *Sey/Sey* maxillas have more torsions along the oral epithelium as compared to the wildtypes. Abbreviations: anc, anterior nasal capsule; cm, condensed mesenchyme; cps, cartilaginous primordium of the sphenoid bone; df, dental follicle; dl, dental lamina; dp, dental papilla; eg, enamel organ; i, incisor; lnc, lateral nasal capsule; m, mesenchyme; nep, nasal epithelium; ns, nasal septum; r, rod-like structure; t, tongue; wf, whisker follicle. Scale bars: 500 μm.

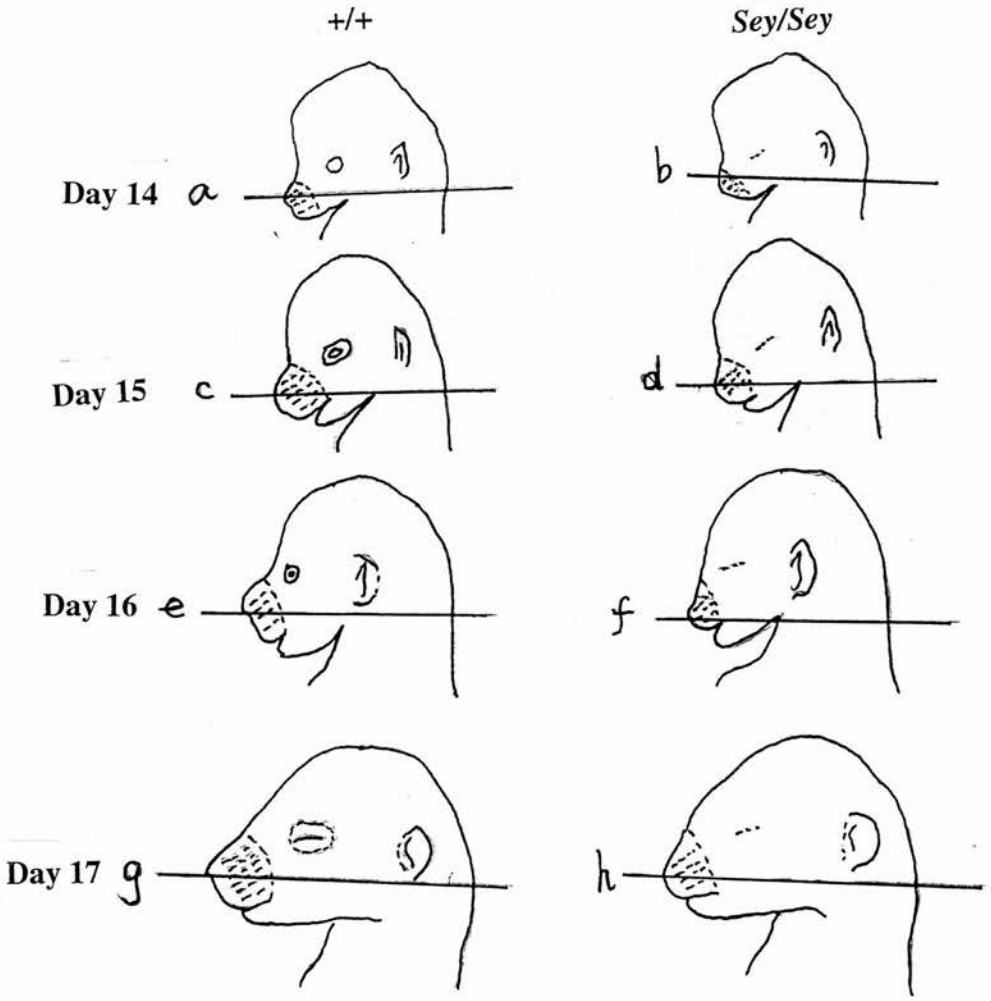

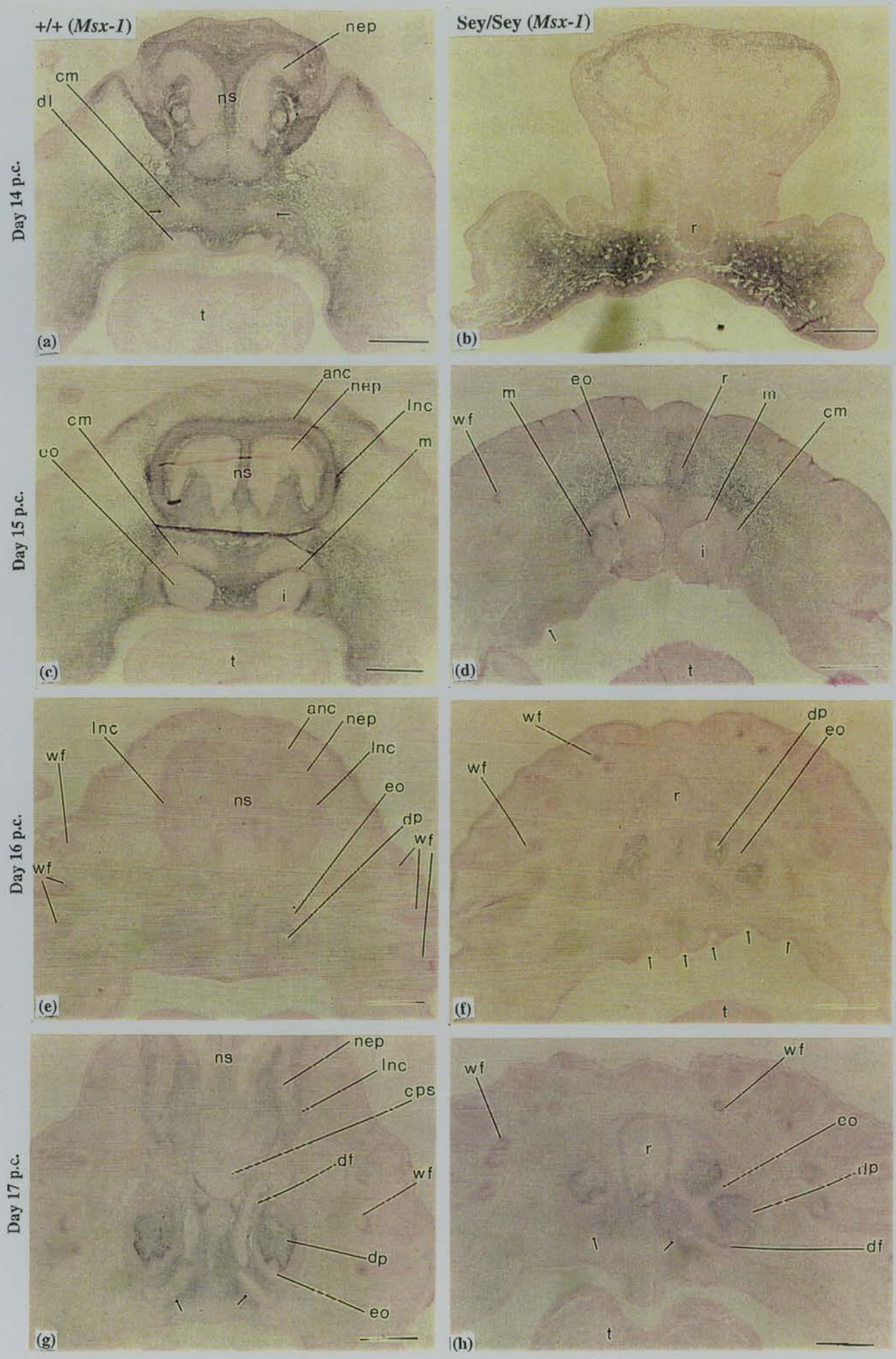

Figure 5.2 *Msx-1* expression in the +/+ and *Sey/Sey* embryos at days 14, 15, 16 and 17 p.c. (see preceding page for legend).

Figure 5.3 *Msx-2* expression in the +/+ and *Sey/Sey* maxillary processes on transverse sections at days 13, 14 and 15 p.c. (see the schematic diagram below). The left panels (a, c, e) represent *Msx-2* expression in the wildtypes. The panels on the right (b, d, f) represent *Msx-2* expression in the *Sey/Sey* mice. All the embryonic tissues are processed under the same condition through *in situ* hybridization (detailed in chapter 2). In the wildtype maxilla, *Msx-2* expression is already located in the dental epithelium along the line of oral epithelium by day 13 p.c. (in a). This is in contrast to that in the *Sey/Sey* embryo whose *Msx-2* expression can only be seen in the mandibular process (in b). *Msx-2* expression in the wildtypes is more clearly seen when the dental epithelium is further developed into the dental lamina (in c), and by day 15 p.c., the expression is seen in the dental papilla (in e). In the *Sey/Sey* maxilla, however, *Msx-2* expression remains in the dental laminas, indicating that the embryo is retarded in development. Note that *Msx-2* is expressed in the nasal derivatives in the wildtypes. *Msx-2* is also expressed in the whisker follicles, in both the wildtype and *Sey/Sey* embryos. Abbreviations: anc, anterior nasal capsule; cm, condensed mesenchyme; cps, cartilaginous primordium of the sphenoid bone; df, dental follicle; dl, dental lamina; dp, dental papilla; eg, enamel organ; i, incisor; lnc, lateral nasal capsule; m, mesenchyme; nep, nasal epithelium; ns, nasal septum; r, rod-like structure; t, tongue; wf, whisker follicle. Scale bars: 500 μm.

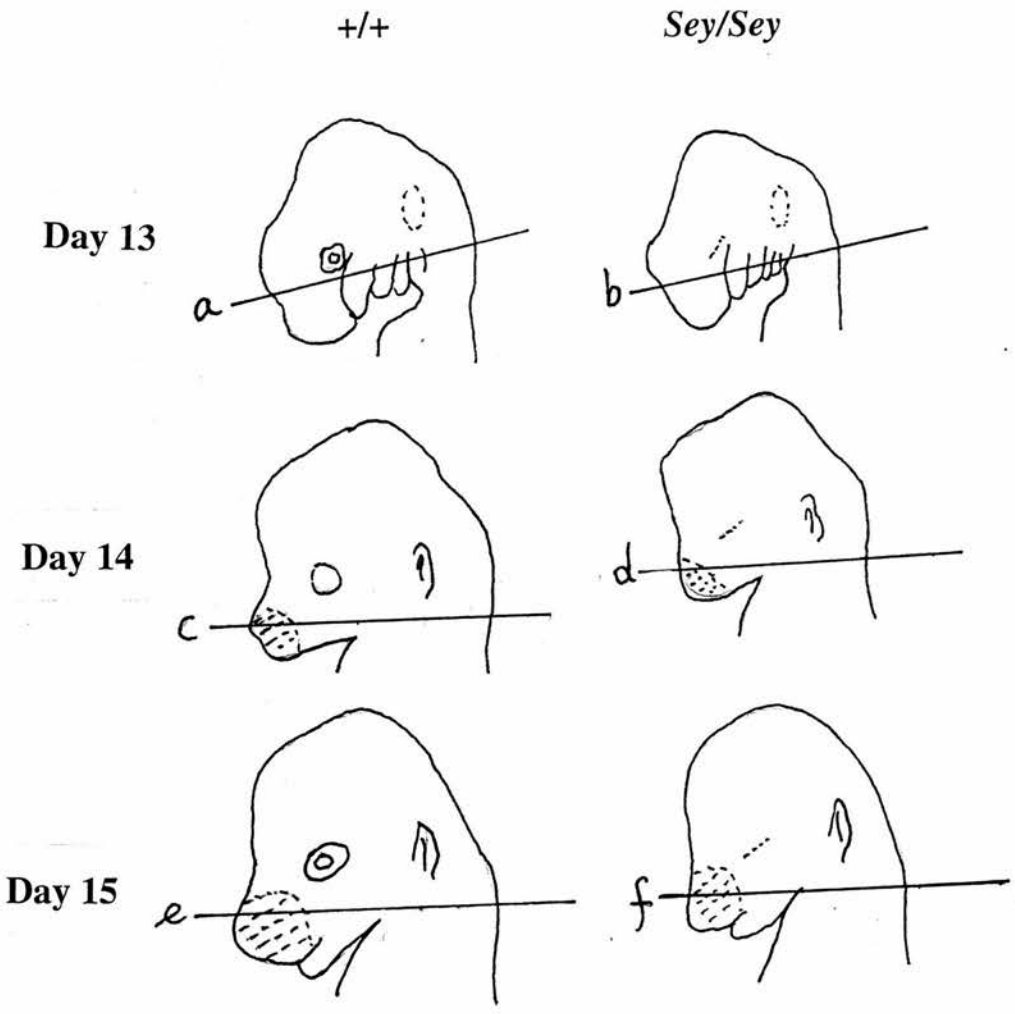

Figure 5.3 *Msx-2* expression in the +/+ and *Sey/Sey* embryos at days 13, 14 and 15 p.c. (see preceding page for legend).

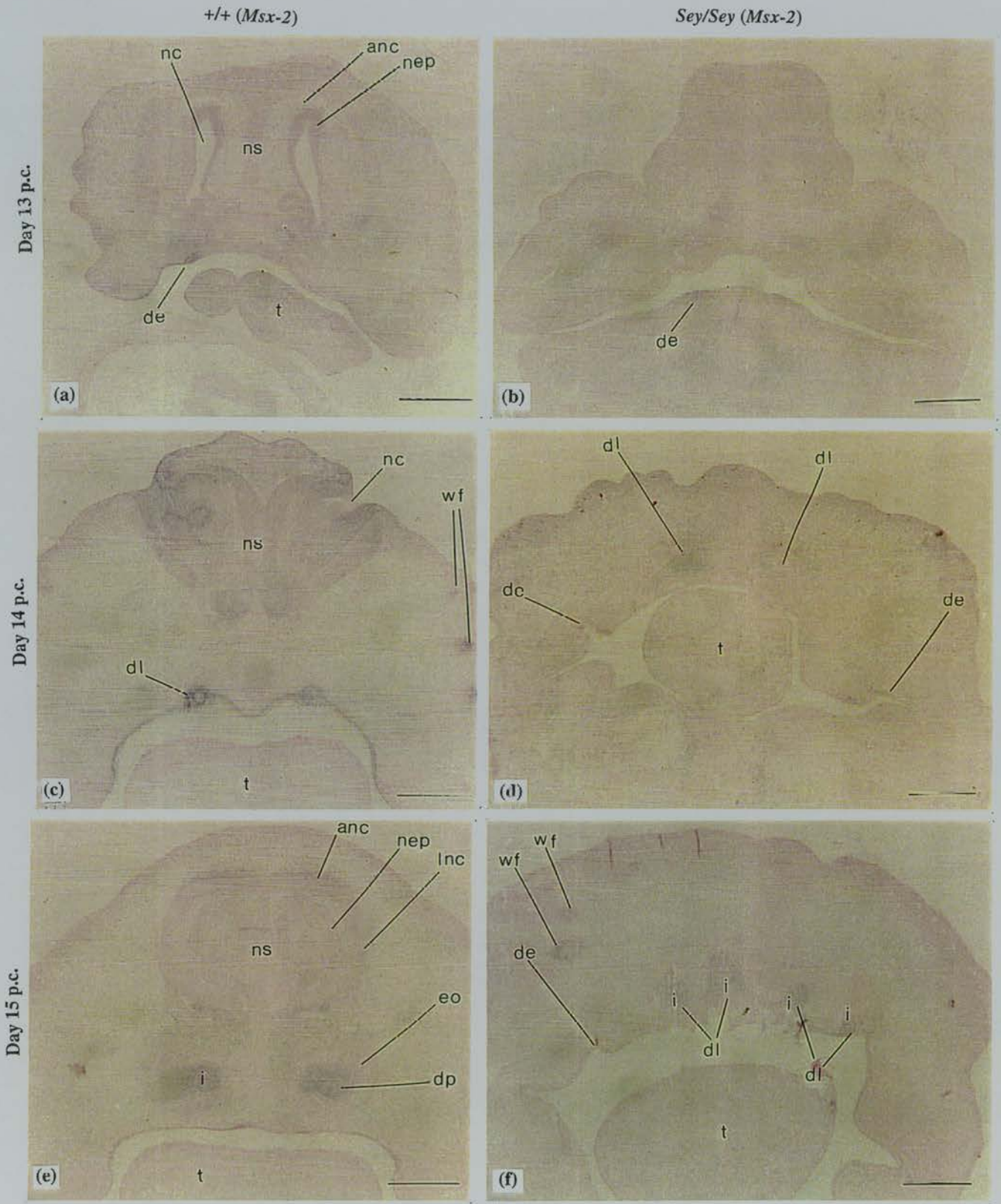

Chapter 6: The effect of retinoic acid (RA) on *Pax6* expression following *in vitro* treatment on gastrulating chick embryos

6.1 Introduction

6.1.1 Aim of this chapter

The aim of this chapter is to investigate the effect of all-*trans*-retinoic acid (RA) on *Pax6* expression following its treatment on the gastrulating chick embryos. Chick embryos at Hamburger-Hamilton stage 4 were treated *in vitro* with RA at concentrations ranging from 1×10^{-8} M to 5×10^{-5} M. Following RA treatment, the embryos were examined and *Pax6* expression was investigated by *in situ* hybridization on wholemounts. All the technical details are described in chapter 2 (section 2.8, pages 110 - 111).

6.1.2 Rationale for investigating the effect of RA on *Pax6* expression

Several lines of experimental data suggest that RA might regulate *Pax6* expression: (1) Deficiency of maternal vitamin A (the metabolic precursor of RA) causes a variety of abnormalities, including micropthalmia, that are also seen in the *Sey/+* mice (Hale, 1937; Wilson *et al.*, 1953; Sporn *et al.*, 1994; Blomhoff, 1994; Chambon, 1994). Micropthalmia can be prevented by supplementing the maternal vitamin-A deficient diet with RA (Howell *et al.*, 1964; Blomhoff, 1994). (2) Many *Pax-6*-expressing areas overlap with sites where endogenous RA is present. For example, both *Pax6* transcripts (see chapter 4) and endogenous RA (Hogan *et al.*, 1992; Chen *et al.*, 1992) are present in Hensen's node and both are implicated in the development of eye and brain. (3) *Pax6* expression falls into the areas where high or low doses of RA (or its precursor) can cause abnormalities. In vitamin A-deficient quail embryos, for example, the segmentation of rhombomeres 4 - 8 (where *Pax6* is expressed) is disrupted (Maden *et al.*, 1996). (4) Expression of some other *Pax* genes, for example *AmphiPax1* (Holland and Holland, 1996) and *Pax2* (Zhang *et al.*,1996), is affected by RA. In light of the above mentioned experimental data, the effect of RA treatment on *Pax6* expression in the early chick embryo is investigated.

6.2 Results

The results are shown in table 6.1 and in figures 6.1 - 6.8 at the end of this chapter. The effects of RA treatment on early chick embryos are mainly in the developing head, heart, and neural plate, with some malformations in the developing somites (see table 6.1). Malformations are examined both macroscopically and microscopically.

6.2.1 Macroscopic effect of RA treatment

6.2.1.1 Effect on the head development

RA treatment on the gastrulating chick embryos causes a variety of abnormalities in the rostral region of the embryos, including (1) condensed ''heads'' that are shorter than untreated controls (see figure 6.1.A; B), (2) formation of multiple bubble-like structures that are presumably derived from head neuroectoderm (for examples, see figures 6.1.C, D, E; 6.6.a, c and 6.7.a), (3) complete absence of head formation (see figure 6.3.c), and (4) formation of strip structures (see figures 6.8.a, b, c) that are presumably resulted from hyperplasia of the neuroectoderm. These abnormalities are due to the effect of RA treatment, as no comparable malformations are commonly found in the controls (see table 6.1).

Specific effects on the fore-, mid-, or hindbrain were not distinguishable in most cases, since most of the head abnormalities occurred before the gross morphological subdivisions on the brain were distinguishable (for example, see figures 6.1.B, C, D, E). The abnormalities were therefore counted together without distinguishing which specific part (or parts) of the brain was affected. In a few cases, however, specific effects on the fore-, mid- and hindbrain were seen. In figure 6.2.B, for example, the RA-treated embryo exhibited a smaller, underdeveloped forebrain as compared to the control (figure 6.2.A), whilst its midbrain and hindbrain were not formed.

6.2.1.2 Effect on heart development

RA treatment lead to the enlargement and bifurcation of hearts, as well as the absence of heart formation in a substantial amount of embryos (see table 6.1). Typically, the heart enlargement or bifurcation were accompanied by the condensed malformation as illustrated in figure 6.1.A. In most of the cases when multiple, bubble-like structures were found, no heart was formed. Interestingly, in 3 cases (1 in group III and 2 in group IV) when no head was formed, the embryos maintained a beating heart without enlargement or bifurcation.

6.2.1.3 Effect on neural plate development

The neural plates following RA treatment exhibited zigzag malformation (see figure 6.3.A), as well as abnormally short or retarded formations (figure 6.3.B). In 3 specific cases (1 in group I and 2 in group II), complete loss of one side of the neural plate (or neural tube) together with the absence of somatogenesis on the same side were found (see figure 6.3.C).

6.2.1.4 Effect on somite development

RA-treated embryos exhibited somites of smaller size (see figure 6.2.B), as well as bilateral (for example, see figures 6.3.B, C; 6.1.D, E) or unilateral (see figure 6.3.C) absence of somitogenesis.

6.2.2 Dosage-dependent, differential effect of RA treatment in different regions

RA treatment caused dosage-dependent, differential effect in different regions. As the concentrations of RA were increased, the percentage of abnormalities in the head region became higher (see Table 6.1). Head abnormalities constituted 3 out of 22 cases of abnormal embryos following RA treatment in Group I, but increased to 11 out of 13 cases in Group VI. The increase of head abnormalities was mainly due to more formation of 'multiple bubble-like structures' which amounted to 62 % (8/13) of the abnormal embryos in the experimental Group VI, whereas none was found in Group I and II. The percentage of condensed 'heads' increased from 14 % (3/22) in Group I to 58 % (14/24) in Group III.

The percentage of heart abnormalities did not change as much as compared to those in the head. Heart abnormalities ranged from 16/22 (Group I) to 20/24 (Group III), and to 13/13 in Group VI.

The percentage of neural tube abnormalities decreased as the concentrations of RA were increased. A total of 18 % (Group I) - 58 % (Group II and Group III) decreased to 8 % (Group VI) - 9 % (Group V).

6.2.3 Microscopic effect of RA treatment

A total of 24 embryos out of all treated abnormal embryos (7, 3, 3, 5, 4, and 2 embryos from Groups I to VI respectively) were sectioned and stained for histological analyses. Results are described below.

6.2.3.1 Hyperplastic effect on the neuroectoderm and suppresive effect on the mesoderm

Hyperplasia was found in the neuroectoderm of most (18/24) of the embryos sectioned for histological analyses. The hyperplastic effect was seen in the head as well as the trunk region (see figures 6.4.B, D). Gross morphological malformations were commonly accompanied by hyperplasia in the neuroectoderm, but this is not always the case. In figure 6.2.B, for example, the head neuroectoderm exhibited underdevelopment instead of hyperplasia.

The effect of RA treatment on the mesodermal cells was suppressive in all (24/24) embryos that were sectioned for histological analyses. The numbers of mesodermal cells were reduced in the RA-treated embryos as compared to those in the controls. The reduction occurred in the head region (see figure 6.4), as well as in the trunk region (see figure 6.5).

6.2.3.2 Enlargement of the dorsal aorta and dispersion of the somitic cells

Among the 24 embryos that were sectioned and analysed, a primitive vascular system was seen in 16 of them. Enlargement of the dorsal aorta was seen in all (16/16) the analysed embryos that developed a primitive vascular system (see figures 6.2 B; 6.5.B). In some embryos, the dorsal aortas were so enlarged that they took up the space where the surrounding mesodermal derivatives should be (see figure 6.5.B).

Somitogenesis was also affected by RA treatment. Somitic cells were dispersed, leaving a non-aggregated somitic formation with a cavity in the centre (see figure 6.5.D). Somitic abnormalities were often concurrent with disturbance of neural tube closure (not shown).

6.2.4 *Pax6* expression following RA treatment

At least 4 embryos from each RA-treated experimental group were used to study *Pax6* expression following RA treatment. The results are summarised in the following sections.

6.2.4.1 *Pax6* expression is maintained after RA treatment

In all RA-treated embryos that were investigated by wholemount *in situ* hybridization, *Pax6* expression was maintained and the level of expression appeared roughly equivalent to that in the controls. This maintenance of *Pax6* expression was unaffected by different concentrations of RA treatment. In the head region, *Pax6* expression is seen in the neuroectoderm, although it is less obvious in the surface ectoderm (see figures 6.6.b, d). *Pax6* transcripts are also detected in the trunk region in the presumptive neuroectoderm, although the morphology can be very abnormal (see figures 6.8.a, c).

6.2.4.2 *Pax6* is expressed in the multiple bubble-like structures in the RA-treated embryos

Pax6 expression is found in the multiple bubble-like structures, presumably within the cephalic region in the RA-treated embryos (see figures 6.6; 6.7). The bubble-like structures exhibit double (for example, see figures 6.6.a, b), triple (see figures 6.6.c, d; 6.7.a, b), as well as more complicated (figure 6.7.d) or simplified (figure 6.7.c) circular formations. *Pax6* appears to be expressed in all the varieties of the bubble-like structures.

6.2.4.3 *Pax6* is expressed in the strip structures in the RA-treated embryos

Pax6 is also expressed in the strip structures that are found in the RA-treated embryos (see figures 6.8.a, b). The strips of *Pax6* expression are continuous with the more caudal areas of *Pax6* expression in the trunk region.

6.2.4.4 *Pax6* expression in the trunk neural plate

Pax6 expression is detected in the trunk region of the RA-treated embryos. Expression is located in the the neural plate, when it exists (see figure 6.8.a). Malformations in the trunk neural plates, for example the zigzag structures, do not affect *Pax6* expression (see figures 6.8.c, d).

6.3 Discussion

This study investigates the effect of RA treatment on wholemount chick embryos during their gastrulation *in vitro*, in order to determine whether *Pax6* expression can be regulated by RA. Results show that a variety of abnormalities can be induced by RA treatment during gastrulation, which has not been previously reported and has many implications in the roles of RA during chick embryogenesis. Since the effect of RA on *Pax6* is the main goal for this study, this discussion concentrates on the data that are related to *Pax6* regulation or function. Other data will be referred only when necessary.

6.3.1 Concentrations of RA used in this study as compared to endogenous RA sources

The concentration of endogenous RA in the limb bud of stage 21 chick embryos has been reported to be between 1.9 - 4.9 x 10^{-8} M (Thaller and Eichele, 1987). In another report, with a different assay method, RA concentration was reported to be 2.1 x 10^{-9} M in limb buds at stage 23-24, and 1.3 - 1.5 x 10^{-9} M in Hensen's nodes at stage 4 -6 (Chen and Solursh, 1992). As all the embryos used in our study were treated with RA at stage 4, the concentrations for all six experimental groups were higher than those of endogenous sources when compared to that of stage 4 -6 Hensen's node. The concentrations of RA used in this study were, however, lower than or similar to those previously used under *in vitro* systems by other authors (Dhouailly and Hardy, 1978; Osmond *et al.*, 1991; Chuong *et al.*, 1992; Dersch and Zile, 1993). They were therefore regarded as suitable for the purpose of this study.

6.3.2 *Pax6* expression supports the neuroectodermal origin of the multiple, bubble-like structures

Multiple, bubble-like structures in the presumptive cephalic region were found in the RA-treated embryos. The multiple, bubble-like structures are likely derived from surface ectoderm or neuroectoderm, since the two tissues constitute most of the early cephalic region and are the only tissues visible on wholemount preparations. There are, however, two points that favour the neuroectodermal origin: (1) The structures are continuous with the neural plate in the trunk region (see figures 6.1.C - E), suggesting that they are derived from neuroectoderm. (2) In many cases, *Pax6* is expressed in the bubble-like structures in a way similar to that observed in the neuroectoderm of the controls. In figure 6.6.d, for example, the circular structures '1' and '3' are *Pax6*-expressing and located bilaterally in

relation to the midline, resembling by their morphology and position the optic vesicles in the normal embryos.

6.3.3 Strip structures in the RA-treated head are rhombomeric units as suggested by *Pax6* expression

Strip structures that are presumably derived from head neuroectoderm are found in the RA-treated embryos in this study. *Pax6* is expressed in all of the strip structures, which are continuous with *Pax6*-expressing areas in the more caudal part of the brain, as well as in the trunk neural plate (figures 6.8.a; b). Thus, the pattern of *Pax6* expression indicates that the strip structures are derivatives of the head neuroectoderm. *Pax6* expression also suggests that they are rhombomeric units, in that only r3 and r5 in the developing chick brain exhibit strip pattern of expression (see figure 4.5.b).

The strip structures could be derived from anteriorization of the whole rhombencephalon with repetitive formation of r3 or r5 or both, whilst the area of forebrain is reduced. RA induced anteriorization of the expression of genes or gene families has been reported in a wide range of tissues and the developing nervous system seems to be a primary target for RA-induced teratology (Leonard *et al.*, 1995). In particular, the hindbrain is most susceptible to the effects of exogenous RA (Holder and Hill, 1991; Morris-Kay *et al.*, 1991; Marshall *et al.*,1992; Kessel, 1993). The anteriorization involves respecification of a *Hox* code, which then leads to respecification of regional identity (Krumlauf, 1993). Once the regional identity is respecified, cell fate may be changed with a concurrent loss of the forebrain, which has been demonstrated in the *Xenopus* (Agarwal and Sato, 1993). Higher doses of RA lead to progressively more severe truncations in the *Xenopus* brain (Agarwal and Sato, 1993).

Results in this study demonstrate that RA can also induce anteriorization of *Pax6* expression as a concurrent event with the anteriorization of rhombomeric units.

6.3.5 Effect of RA on *Pax6* expression -- direct or indirect ?

Although various malformations were observed in a certain proportion in the RA-treated experimental groups (see table 6.1), *Pax6* expression is maintained in all embryos analysed by wholemount *in situ* hybridization. Even in the highly twisted zigzag structures of the trunk neural plate or in the bubble-like malformations of the cephalic region, *Pax6* expression can still be detected. The maintenance of *Pax6* expression suggests that *Pax6* is unlikely to be a direct target of RA, neither is it likely to be involved in the RA regulatory pathways.

One needs to be cautious, however, because *Pax6* may be upregulated or downregulated in a way that is beyond the limits of *in situ* hybridization, i.e. *Pax6* expression may have been modified in a subtle way

that can not be detected by *in situ* hybridization. Minor upregulation, downrgulation, expansion, reduction, or displacement of *Pax6* expression are still possible.

The regulation of RA activities is complicated. For a long time an operational explanation for the action of RA remained elusive. RA regulation involves retinoid receptors (RAR_s and RXR_s) and retinoid binding proteins ($CRABP_s$ and $CRBP_s$) (reviewed by Underhill *et al.*, 1995). Factors that influence retinoid receptor activity include ligand availability, receptor dimerization, inhibitors of receptor function, factors that promote retinoid receptor-mediated transcativation, post-translational modification of the receptors, as well as configuration and sequence of the DNA binding site (Underhill *et al.*, 1995). These factors may at a certain level (or levels) affect *Pax6* expression, either directly or indirectly.

RA has been reported to be involved in the regulation of *Sonic hedgehog* (*Shh*) (Riddle *et al.*, 1993; Chang *et al.*, 1994), members of the transfoming growth factor β (TGF-β) family such as TGF-β1, TGF-β2 (Mahmood *et al.*, 1992), BMP-2, BMP-4 (Rogers *et al.*, 1992; Francis *et al.*, 1994), and members of *Hox* genes (Krumlauf, 1993; Mavillo, 1993; Langston and Gudas, 1994), as well as cellular and neural adhesion molecules (Husmann *et al.*, 1989; Jonk *et al.*, 1994). These RA-regulated genes, growth factors, or extracellular matrix will certainly interact with *Pax6* function, at least in the context of local histogenesis or organogenesis. *Shh*, for example, has been suggested to either directly or indirectly inhibit the expression of *Pax6*, while the optic stalks are partitioned with the retinal tissues (Macdonald *et al.*, 1995). Thus, a possible indirect regulation of RA on *Pax6* expression can not be excluded.

Table 6.1 The effect of all-*trans*-retinoic acid (RA) on early chick embryogenesis. Six groups (Group I - Group VI) of chick embryos were treated with RA by culturing from stage 4 (Hamburger and Hamilton, 1951) for 30 hours under the effect of RA. The concentrations of RA range from 1×10^{-8} M to 5×10^{-5} M in Pannet-Compton saline (New, 1955). The controls were prepared and cultured in the same way, except that no RA was added in the Pannet-Compton saline. Abnormalities induced by RA were counted individually regardless of whether they were formed in one embryo or in different embryos. Heads with apparent duplicate bubble shapes were defined as 'multiple heads'. This abnormality was easy to distinguish from those which were due to early necrosis. Embryos which were already dead at the start of culture did not have any sign of the head process or other organ formation. Heads of shorter than normal length were defined as 'condensed heads', irrespective of whether fore-, mid-, or hindbrain, or branchial arches were affected. Embryos apparently without head formation were classified as 'no head'. Hearts with apparently larger than normal size were defined as 'enlarged'. Those with two separate hearts or with one heart but only partially fused were defined as 'bifurcation'. Embryos apparently without heart were classified as 'no heart'. Embryos with zigzag-shape neural ridges were classified as 'zigzag'. All other abnormalities in the neural tube were listed together as 'other neural tube defects'.

Table 6.1 The effect of All-*trans*-retinoic acid on early chick embryogenesis.

Concentration of retinoic acid		Head			Heart			Neural plate		Somites	Other defects[c]	Total abnormalities[d]	Abnormal embryos after treatment	Normal embryos after treatment	Dead at start of culture	Total embryos used
		multiple head	condensed head[a]	no head	enlarged	bifurcation	no heart	zigzag	others[b]							
Group I	$1x\ 10^{-8}$M	0	3 (14%)[e]	0	8 (36%)	4 (18%)	4 (18%)	2 (9%)	2 (9%)	0	1 (5%)	24	22	28	7	57
	control	0	0	0	0	0	0	0	1	0	0	1	1	12	1	14
Group II	$2x10^{-8}$ M	0	17 (45%)	3 (8%)	9 (24%)	12 (32%)	5 (13%)	8 (21%)	14 (37%)	8 (21%)	5 (13%)	81	38	25	11	74
	control	0	1	0	0	0	0	0	2	0	1	4	3	11	4	18
Group III	$5x10^{-8}$ M	2 (8%)	14 (58%)	3 (13%)	6 (25%)	10 (42%)	4 (17%)	7 (29%)	7 (29%)	4 (17%)	3 (13%)	60	24	5	6	35
	control	0	0	0	0	0	0	0	0	0	0	0	0	10	2	12
Group IV	$2x\ 10^{-6}$ M	6 (33%)	8 (44%)	4 (22%)	4 (22%)	5 (28%)	8 (44%)	7 (39%)	2 (11%)	7 (39%)	2 (11%)	53	18	3	2	23
	control	0	0	0	0	0	0	1	1	0	0	2	1	6	3	10
Group V	$5x\ 10^{-6}$ M	6 (55%)	4 (36%)	0	1 (9%)	2 (18%)	6 (55%)	1 (9%)	0	1 (9%)	0	21	11	1	0	12
	control	0	0	0	0	0	0	0	0	0	0	0	0	4	0	4
Group VI	$5x10^{-5}$ M	8 (62%)	2 (15%)	1 (8%)	1 (8%)	0	12 (92%)	1 (8%)	0	0	0	25	13	0	5	18
	control	0	0	0	0	0	0	0	0	0	0	0	0	8	2	10

a. Condensed head represents deletions in parts of the developing brain, which result in shorter and/or condensed head formation.

b. Others include shorter and retarded, particularly in the caudal region.

c. Other defects are those not listed in this table. Defects like left-right asymmetry, twisted trunk in the caudal region, deficit of vasculature systems are listed in this column.

d. Total abnormalities are counted and added up from all the abnormal embryos.

e. The percentages represent particular abnormalities out of total abnormalities from abnormal embryos after treatment.

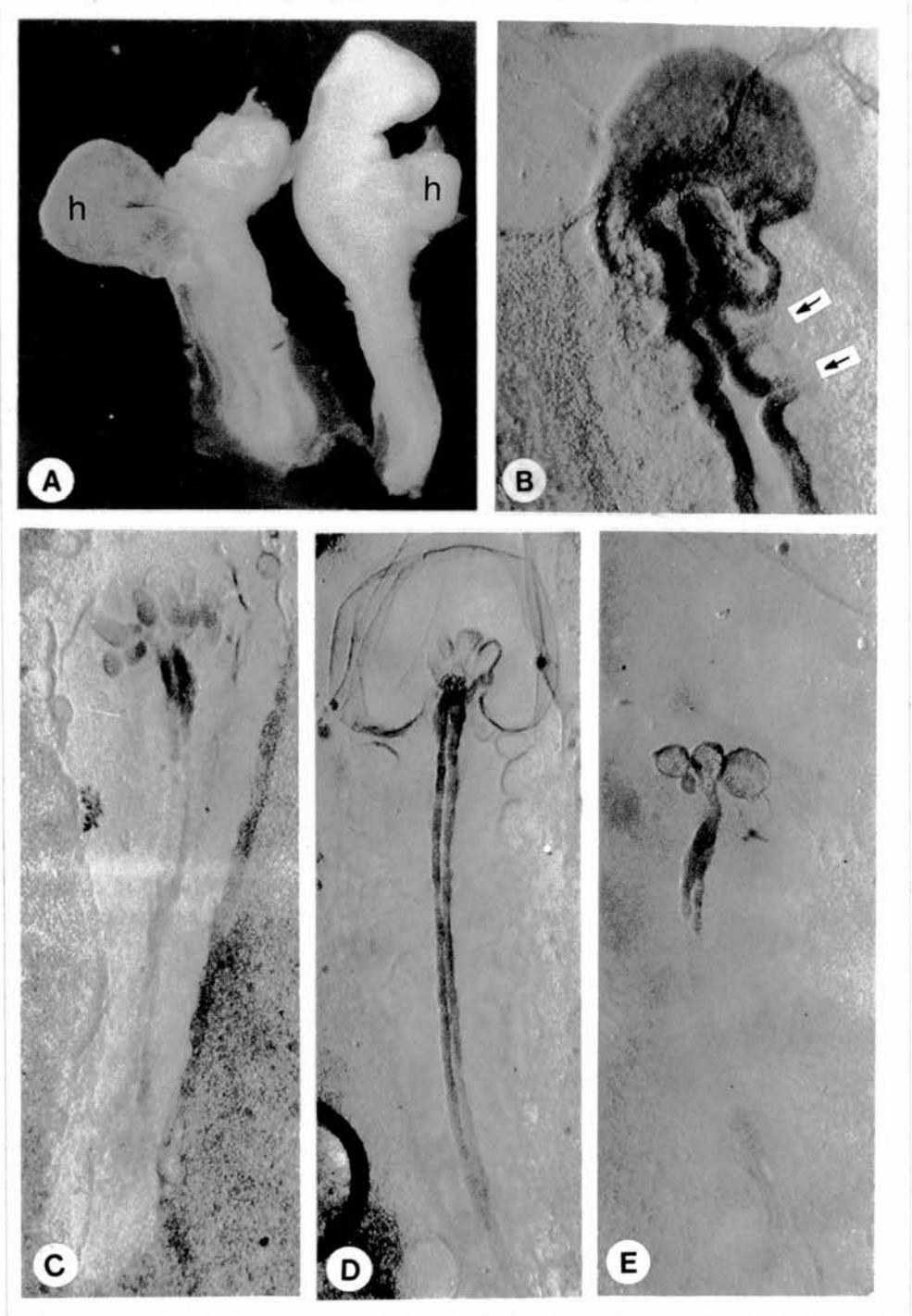

Figure 6.1 Wholemount preparations of the RA treated embryos showing the main effects of RA on the head and on the heart. (A) At 2 x 10^{-8} M, some treated chick embryos are able to develop to stages 12 - 13 (left), showing typical abnormalities of head condensation and heart enlargement as compared to the control (right). The neural tube of the treated embryo is noticeably shorter than the control. (B) A condensed head abnormality. The embryo is retarded at stage 8^{+} as compared to the controls which are at stages 11 - 12. Note that the neuroectoderm is hyperplastic and the 'zigzag' is formed (arrows). (C - E) Various multiple, bubble-like structures at rostral end of the RA-treated embryos. The bubble-like structures are continuous with the neural plate, indicating that they are derivatives of the neuroectoderm. In (A), the slit in the trunk region of the RA-treated embryo (left) is an artefact. Magnifications: A, X *25;* B - E, X *60.* Abbreviation: h, heart.

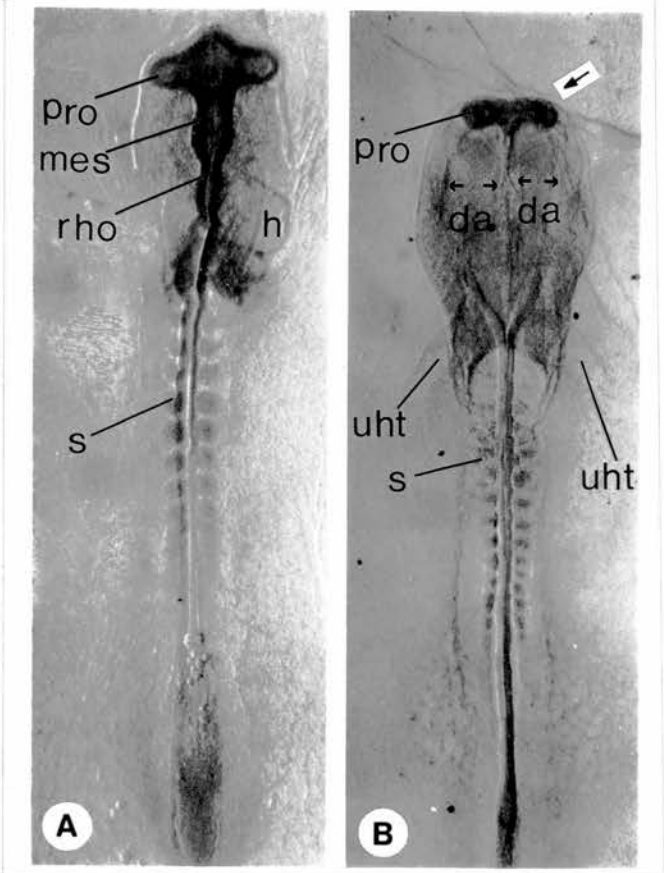

Figure 6.2 Macroscopic effects of RA treatment at concentration 2 x 10^{-8} M on the head, the heart, and the somites. The treated embryo (B) develop to a comparable stage as the control (A), but without the midbrain and the hindbrain (arrow). Other abnormalities included retardation of heart formation, enlargement of the dorsal aorta, and formation of smaller somites. Abbreviations: h, heart; s, somite; da, dorsal aorta; uht, unfused heart tube; pro, mes, and rho, same as in figure 5.1. Magnifications: A - B, X *40*.

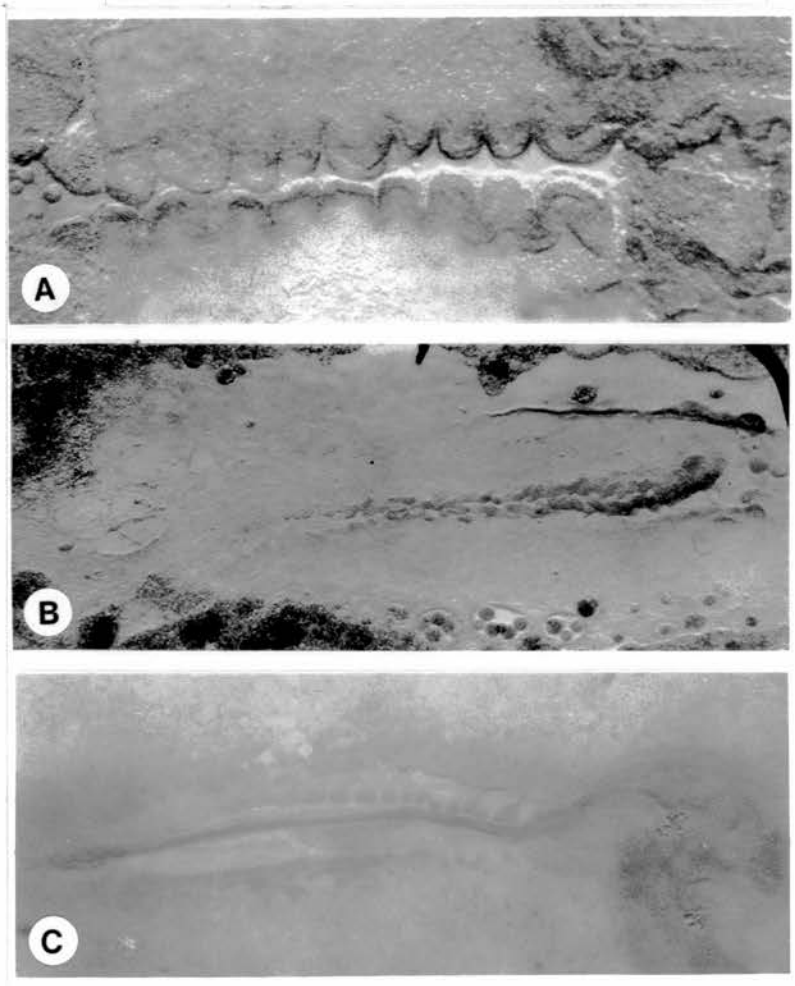

Figure 6.3 Various neural tube abnormalities found in wholemount embryos following RA treatment (concentrations: A, 5 X 10^{-6} M; B and C, 5 X 10^{-5} M). (A) the 'zigzag' shape of neural tube. (B) clumps of neuroectodermal tissues without indication of the somitic tissue aggregations. (C) complete loss of one row of somites in one side of the the neural tube. Note also lack of head formation in (B) and (C). Magnifications: A - C X *60*.

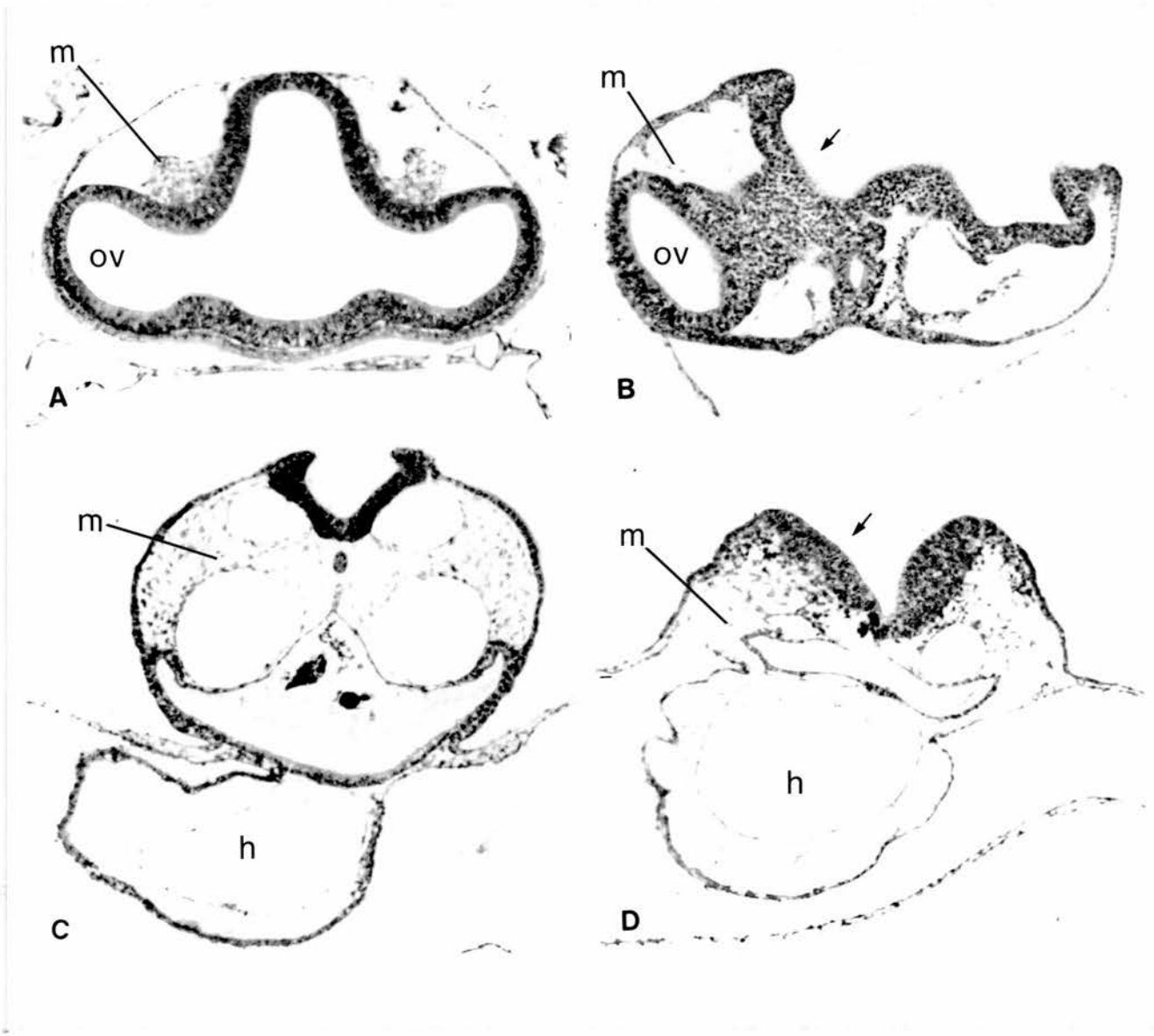

Figure 6.4 Transverse sections showing the hyperplastic effect on the neuroectoderm and suppresive effect on the mesodermal cells following RA treatment at 1 X 10^{-8} M (B and D). A and C are control embryos. The arrows indicate the more thickened neuroectoderm in the head and in the trunk regions of the RA-treated embryos, as compared to the controls. Note in B and D that few mesodermal cells could be found in the treated embryos. Abbreviations: m, mesodermal cells; ov, optic vesicle; h, heart. Magnifications: A - D, X *120*.

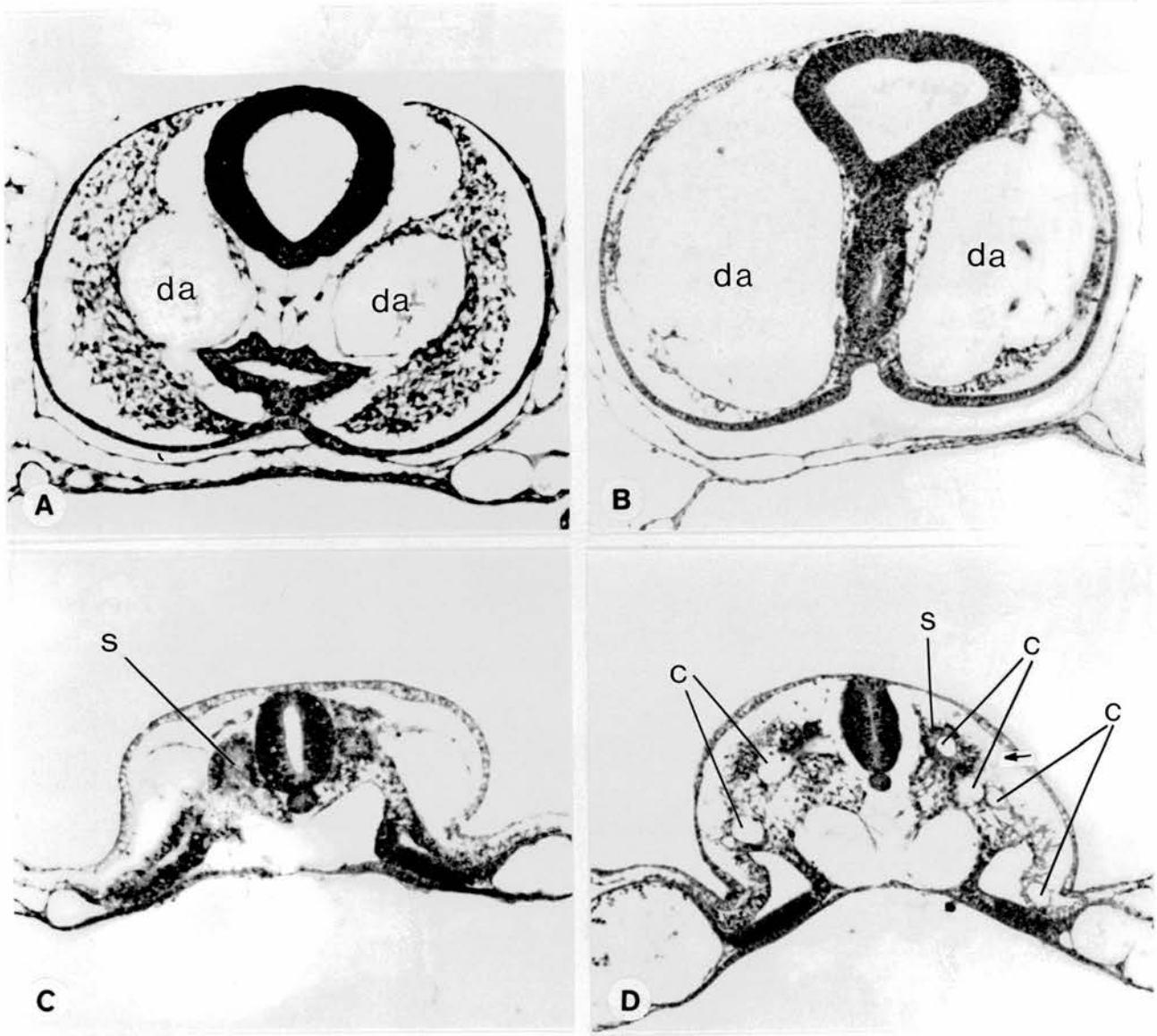

Figure 6.5 Transverse sections showing enlargement of the diameters of the dorsal aortas in the head region following RA treatment at 1 X 10^{-8} M (A, C, controls; B, D, RA-treated embryos). In B, note that the dorsal aortas are enlarged as compared to the controls. In D, note that the somitic cells were dispersed, surrounding cavities (arrow and ''c''-marked areas) in the trunk region of the embryo following the same treatment as for B, in contrast to the aggregated somitic cells in the control embryo in C. Abbreviations: da, dorsal aorta; c, cavity; s, somite. Magnifications: A - D, X *120*.

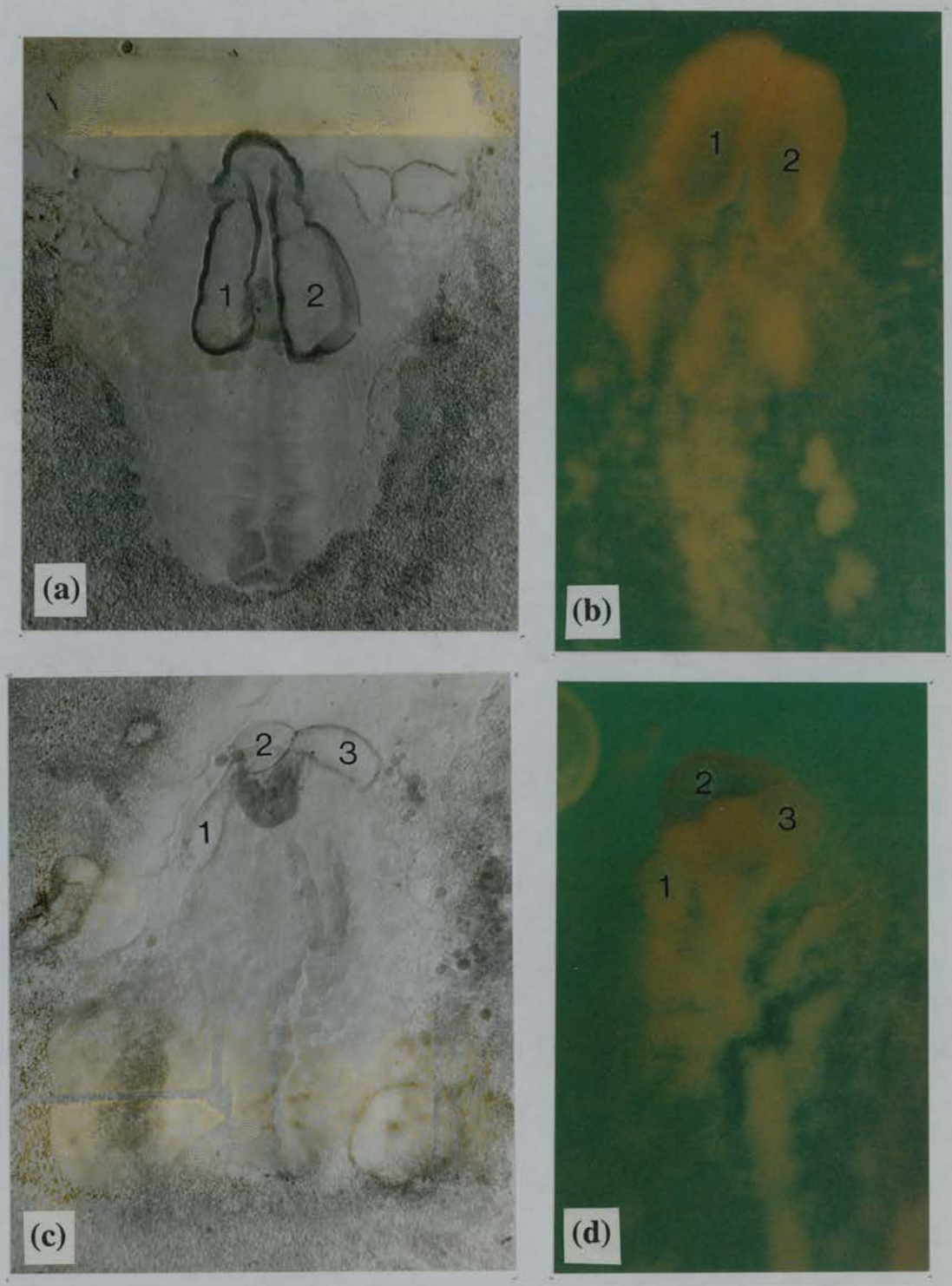

Figure 6.6 Examples of RA-treated embryos showing abnormalities and *Pax6* expression. (a) and (c) are wholemount preparations without staining; (b) and (d) are preparations of wholemount *in situ* hybridization with chick *Pax6* riboprobe. (a) An embryo treated by RA at 2 x 10^{-6} M. Note that the presumptive head neuroectoderm is hyperplastic and forms two circular, bubble-like structures. Different degrees of zigzag malformations can be seen in the trunk neural plate. (b) Another embryo exhibiting similar abnormalities to those in (a). *Pax6* expression can be seen in the circular, bubble-like structures. (c) An embryo treated by RA at 5 x 10^{-6} M shows hyperplasia in the presumptive cephalic and trunk neuroectoderm. Three circular, bubble-like structures are formed in the cephalic region. (d) Another embryo showing similar abnormalities to those in (c). *Pax6* expression is detected in the three circular, bubble-like structures. Note that the two lateral bubbles (1 and 3) are morphologically comparable to optic vesicles. (Magnification: a - c, *X 60* approximately).

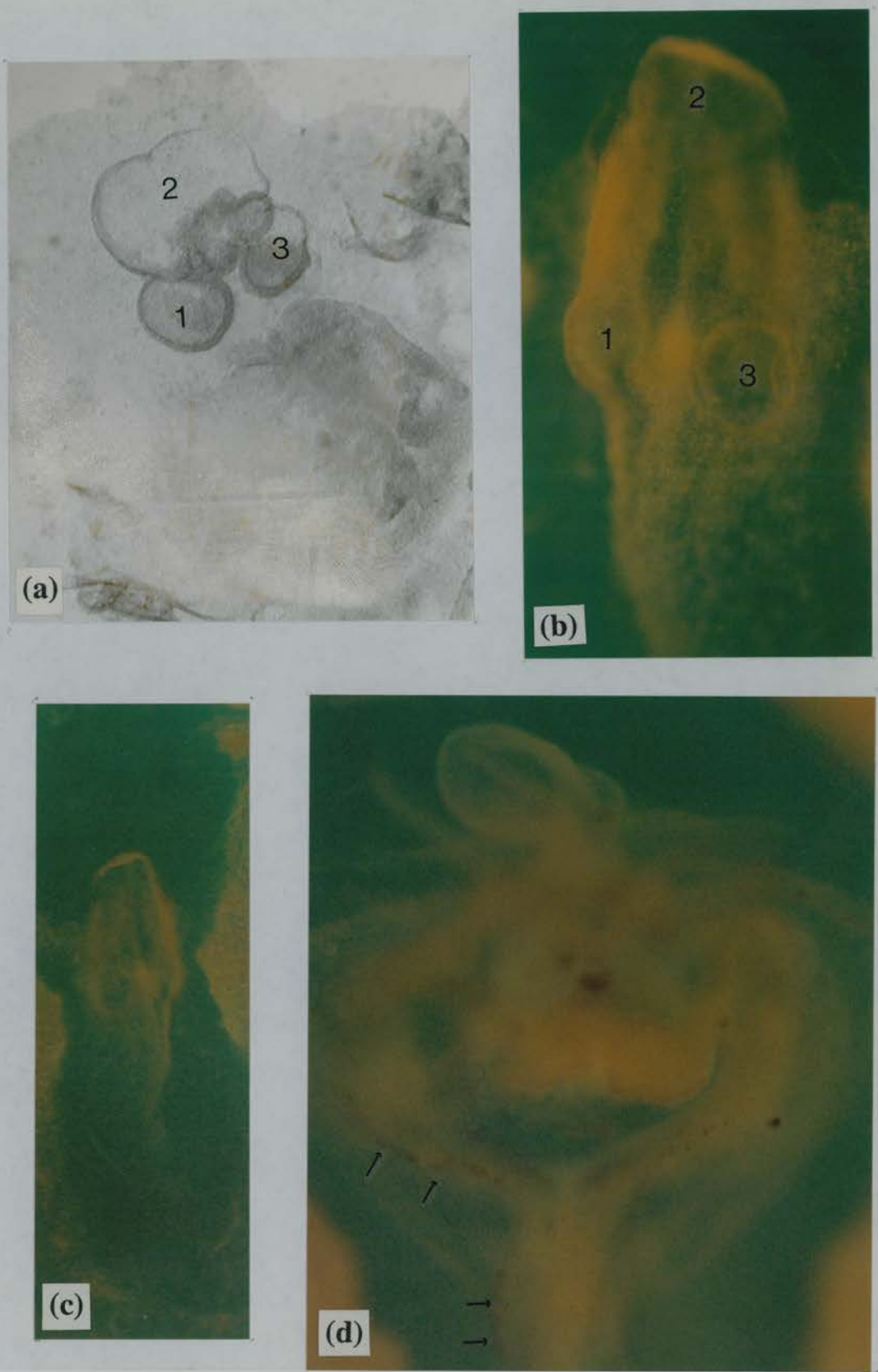

Figure 6.7 Examples of RA-treated embryos showing abnormalities and *Pax6* expression. (a) is a wholemount preparation without staining; (b), (c), and (d) are preparations of wholemount *in situ* hybridization with chick *Pax6* riboprobe. (a) Three circular, bubble-like structures are formed in an embryo treated with RA at 5 x 10^{-6} M. Note that hyperplasia in the presumptive neuroectoderm can be been in the cephalic and trunk region. (b) Another embryo exhibiting similar abnormalities to those in (a). *Pax6* expression can be seen in the circular, bubble-like structures, particularly in 1 and 3. (c) An embryo treated by RA at 5 x 10^{-5} M. *Pax6* transcripts are detected along the presumptive head neuroectoderm. Note that little or no trunk neural plate is developed. (d) Another embryo treated by RA at 5 x 10^{-5} M. The embryo exhibits a condensed malformation enclosed by a single circular structure, with a bubble-like formation attached rostrally. *Pax6* expression is seen in the lateral margins of the circular structure and the expression is continuous caudally. (Magnifications: a and b, *X 60*; c, *X 40*; d, *X 80* approximately).

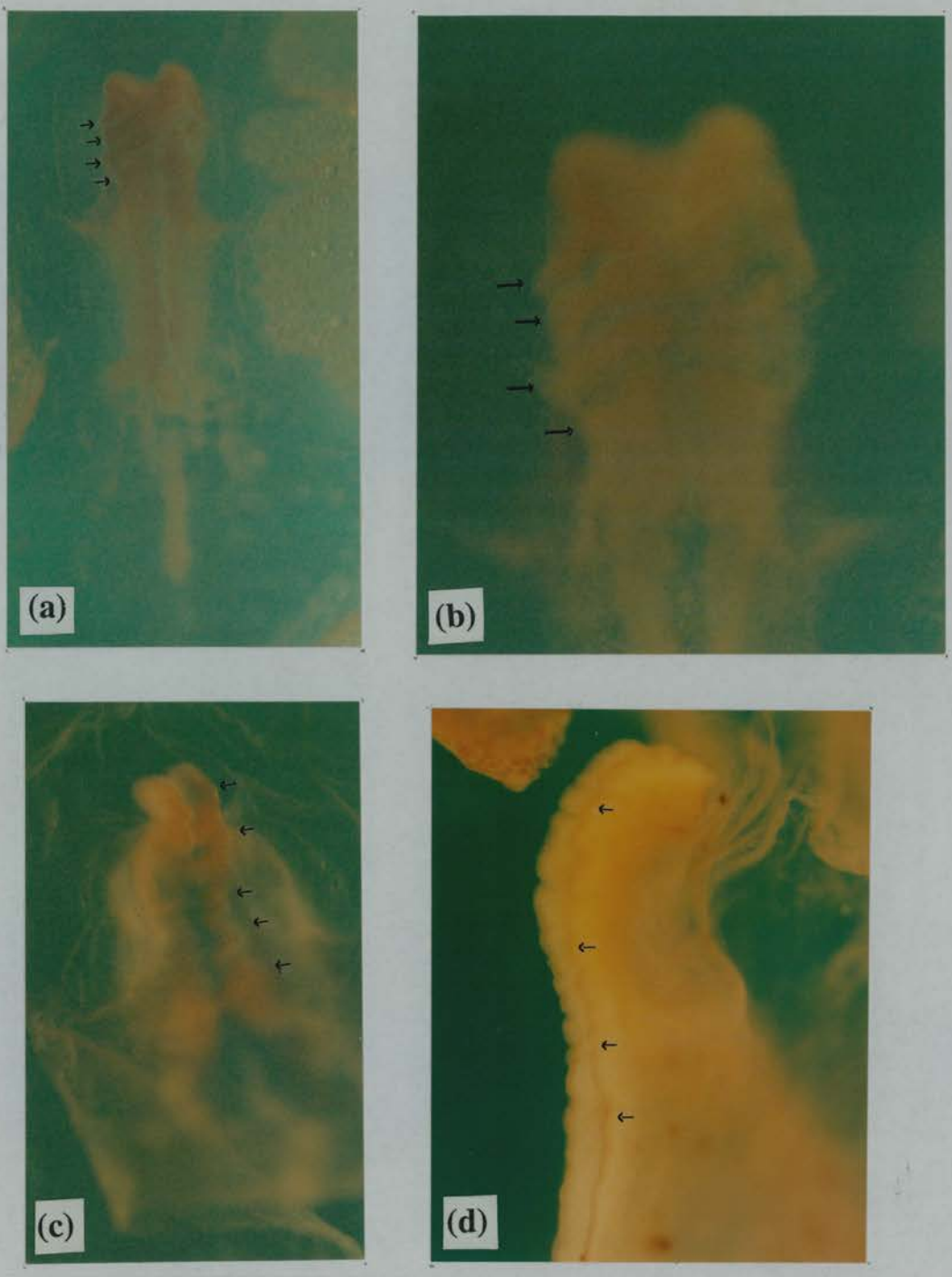

Figure 6.8 Examples of RA-treated embryos showing abnormalities and *Pax6* expression. (a) - (d) are preparations of wholemount *in situ* hybridization with chick *Pax6* riboprobe. (a) An embryo treated with RA at 5 x 10^{-6} M showing strips (see arrows) of *Pax6*-expressing structures in the cephalic region. Note that *Pax6* expression in the cephalic region is continuous with that in the zigzag neural plate in the trunk region. (b) The same embryo as in (a) viewed under higher magnification. The strips are clearly seen (arrows). (c) Another embryo treated by RA at 5 x 10^{-6} M. The embryo is developmentally retarded. *Pax6* expression is maintained throughout the presumptive head and trunk neuroectoderm (see arrows). (d) Another example of RA-treated (2 x 10^{-6} M) embryo. The embryo does not exhibit apparent fore-, mid-, or hindbrain divisions. Instead, it shows continuous zigzag malformation along the anterior-posterior axis of the neural plate. *Pax6* expression is seen within the dorsal neural plate (arrows). (magnifications: a and c, *X 60*; b, *X 180*; d, *X 120* approximately).

Chapter 7: General discussion

This chapter aims (1) to give an overall review of this study, which will be more comprehensive than the abstract, and (2) to describe some future experiments.

7.1 Summary of this study

In the beginning of this study, the overall plan was to start with establishing *Pax6* expression in the mouse, as well as in the chick. The data of *Pax6* expression would then be used as a baseline information for further investigation. However, reports about *Pax6* expression in the mouse had been published extensively before and during the course of this study (Walther and Gruss, 1991; Goulding *et al.*, 1993; Turque *et al.*, 1994; Stoykova and Gruss, 1994; Grindley *et al.*, 1995; Stoykova *et al.*, 1996; Quinn *et al.*, 1996; Warren and Price, 1997; Mastick *et al.*, 1997). *Pax6* expression in the chick had also been published extensively (Li *et al.*, 1994; Turque *et al.*, 1994; Heyman *et al.*, 1995; Simon *et al.*, 1995; Buxton *et al.*, 1997). Despite intensive interest and attention from so many developmental biologists in recent years, *Pax6* has been such a versatile and important gene during vertebrate development that it allowed me to exploit further on gene expression patterns.

Results of this study demonstrated that *Pax6* was expressed in higher centres of the visual and the olfactory nervous systems in the mouse. This was shown by the identification of many *Pax6*-expressing neural nuclei in the developing brain that has not been previously analysed in detail. *Pax6* expression was detected, along the visual pathway, in the neural retina, optic nerve, pretectum, superior colliculus, pulvinar, dorsal and ventral lateral geniculate nucleus and other nuclei that had been implicated in visual connections. Within the olfactory nervous system, transcripts of *Pax6* were found in the olfactory and vomeronasal epithelium, main and accessory olfactory bulb, anterior olfactory nucleus, precommisural hippocampus, piriform and endopiriform cortex, as well as olfactory and vomeronasal amygdaloid areas.

This study also showed that developmental restriction has been a common theme for *Pax6* expression in the mouse, giving many examples that were not formerly described. The examples of developmental restriction included *Pax6* expression in the lens ectoderm, neural retina, telencephalic neuroepithelium, pontine and medullary neuroepithelium, optic stalk, and thalamic neuroepithelium. Furthermore, developmental expansion of mouse *Pax6* expression was shown in the cerebral cortex, cerebellar neuroepithelium, surface layer of superior colliculus, and in the olfactory bulb. Both developmental restriction and expansion were correlated with normal developmental events, as well as previously published mutant phenotypes found in the *Sey/Sey* or *Sey/+* mice. Thus, *Pax6* was implicated in the proliferation and migration of forebrain neuroblasts, as well as in the neuromeric regionalization. In the neural retina, in addition to proliferation and migration, *Pax6* was further implicated in the process of

axonal initiation and connection. *Pax6* was also implicated in the process of lens initiation and lens cell proliferation.

Expression data and mutant phenotypes in different species were compared in an effort to shed new insights on the functions of *Pax6*. The species for comparision included *Drosophila,* nematode, zebrafish, *Xenopus,* urodele, quail, chick, mouse/rat, and human. *Pax6* has been well documented across species as a crucial gene in eye development. In the pigmented neural retina and rim of the optic cup, however, changes were found in *Pax6* expression and mutant phenotypes across species, suggesting that the function of *Pax6* might have been altered evolution within both tissues. In the developing brain, *Pax6* expression domains appeared to be narrowed through evolution. Thus, it was suggested that the roles of *Pax6* had been changed from 'for specification of sense-organ identity' (Zhang and Emmons, 1995) or 'for head-region specification' (Chisholm and Horvitz, 1995) in primitive species to become involved in more specialized and localized functions in higher mammals. In the spinal cord, *Pax6* has been consistently expressed across species. In the pituitary, pancreas, and salivary gland, *Pax6* expression maintained a certain degree of conservation through evolution. Areas of *Pax6* expression, therefore, had been generally maintained across species in concordance with the conservation of paired domain DNA sequence through evolution. There were, however, two deviations of *Pax6* expression in comparison with the *Sey/Sey* mutant phenotypes. Abnormalities were found in the *Sey/Sey* maxillary process, which involved the head neural crest cells and the upper incisor teeth; both were confirmed without *Pax6* transcripts in this study. The deviations reflected a complicated hierarchy of gene activities between *Pax6* and the other genes, as well as the interactions between *Pax6*-expressing and non-*Pax6*-expressing cells.

Pax6 expression in the chick was also investigated, with particular interest in the eye and the olfactory epithelium after Hamburger-Hamilton stage 14, which had not previously been reported. Results of this study confirmed previuosly reported data and, in addition, established that chick *Pax6* was expressed in the olfactory epithelium, the eye region, the brain, and the head surface ectoderm after Hamburger-Hamilton stage 14. Furthermore, a transient chick *Pax6* expression in Hensen's node before stage 9 and the presence of *Pax6* transcripts in cell populations flanking rhombomeres 3 and 5 were found. *Pax6* was speculated to be involved in the migration of hypoblasts that played a part in establishing anterior-posterior axis during early embryogenesis. *Pax6* was also implicated in rhombomeric and trunk neurogenesis.

Chick *Pax6* expression has been described to correlate with lens determination and differentiation *in vivo*, in reference to data found in the *Xenopus* (Li *et al.*, 1994). This study investigated directly whether chick *Pax6* expression was correlated with lens differentiation, by culturing *Pax6*-expressing and non-*Pax6*-expressing head surface ectoderm *in vitro*. It was shown that the lens can differentiate from non-*Pax6*-expressing head surface ectoderm, while *Pax6*-expressing head surface ectoderm did

not always give rise to a lens. When lens differentiated in culture, *Pax6* was always expressed. The results indicated that *Pax6* expression was necessary for lens differentiation *in vitro*.

In light of the deviation between *Pax6* expression and mutant phenotypes found in the *Sey/Sey* maxillary process, a preliminary investigation on the formation of supernumerary upper incisor teeth was conducted. In particular, the expression of *Msx-1* and *Msx-2* were examined in order to give some explanations for the abnormalities. The results showed that both *Msx-1* and *Msx-2* were expressed in the *Sey/Sey* maxillary process. Patterns of *Msx-1* and *Msx-2* expression did not differ between the *Sey/Sey* and the wildtype mice, although areas of expression were increased in the *Sey/Sey* embryo as the number of upper incisors was increased. Furthermore, the level of *Msx-1* expression appeared to increase ubiquitously in the *Sey/Sey* mice. Results of this study also showed some details of the *Sey/Sey* mutant phenotypes that had not previously been reported. This included the non-synchronized formation of upper incisor primordia and the non-corresponding number of dental papilla in relation to the enamel organ. *Msx-1* expression pattern supported the view that the rod-like cartilaginous structure in the *Sey/Sey* mice has been derived as a protrusion from the base of the skull.

Finally, the effects of all-*trans*-retinoic acid (RA) on *Pax6* expression in gastrulating chick embryos were investigated, using an *in vitro* system. Macroscopic effects of RA treatment were shown by abnormalities in the head, heart, neural tube, and somites. Microscopically, RA treatment had a hyperplastic effect on the neuroectoderm and a suppresive effect on the mesoderm. RA treatment also caused enlargement of the dorsal aorta and dispersion of the somitic cells. Results of *in situ* hybridization on wholemount embryos showed that *Pax6* expression was not switched off following RA treatment, although the morphology of RA-treated embryos could be very abnormal. While the results indicates that *Pax6* expression was less likely under the direct regulation by RA, the possibility of an indirect regulation could not be excluded.

7.2 Future experiments

As introduced on page 1 of this thesis, any topic involved with "gene" and "development" can be approached starting with either phenotypes (genetics) or genotypes (reverse genetics). For convenience, I will address future experiments in terms of these two categories. The nature of any scientific research is always the same -- more questions are produced while in the process of solving a single question. *Pax6*, being such a versatile and crucial gene during development, is liable to produce more questions out of the scope of this study. I will therefore propose only a limited number of future experiments that are either revelant to this study or interesting to me. Some of them have been described in previous chapters, but they can be properly put in this chapter for a general discussion.

7.2.1 Starting with "phenotypes"

Many mutant phenotypes of the *Sey/Sey* or *Sey/+* mice have been described before and during the course of this study, such as those in the eye and nose (Hogan *et al.*, 1986; 1988), in the maxillary process (Hill *et al.*, 1991; Kaufman *et al.*, 1995), and in the brain (Schmahl *et al.*, 1993; Warren and Price, 1997; Mastick *et al.*, 1997). These previously reported phenotypes emphasize mostly on gross morphogenesis. Phenotypes in morphology, however, should not be limited by the level of magnification or by the technique of staining. For example, efforts have been made to locate axon projections by Linder's silver staining in the wildtype mice in order to compare with normal *Pax6* expression patterns. The same analyses should be performed in the *Sey/Sey* and *Sey/+* embryos to add to more mutant "phenotypes". Since this study shows that *Pax6* is expressed along the visual and the olfactory pathways in the wildtype mice, Golgi or Nissl preparations may reveal differential distribution of revelant neural nuclei in the *Sey/Sey* mice. Another example is to use double stain technique (tracing axons with DiI stain and using an anti-Pax6 antibody for immunochemical stain), which has been performed by Mastick *et al.* (1997) for correlating *Pax6* expression with local axonogenesis. Furthermore, differential morphogenesis between the *Sey/Sey* mice and their littermates may be extended to cellular or subcellular levels.

In addition to changes in morphology, there are plenty of other "phenotypes" that can be explored. For example, neurophysiological functions such as alteration in transduction of electric pulse or in thresholds for action potential may change in the *Sey/Sey* visual or olfactory pathways. Chimeric mouse studies, as demonstrated by Quinn *et al.* (1996), offer a good approach to see the effect of different proportions of *Sey/Sey* cells on the development of local tissues. Since current data concentrate mainly on the prosencephalon, researchers interested in cellular proliferation may find chimeric mouse studies useful in demonstrating *Pax6* functions in the formation of olfactory bulbs, which contain intensvie *Pax6* expression and do not exist in the *Sey/Sey* mice.

7.2.2 Starting with "genotypes"

Reports revelant to *Pax6* "genotypes" have also been published extensively before and during the course of this study. Most commonly, orthologous genes of *Pax6* in other species are cloned and characterized by their DNA sequence and patterns of expression (see table 3.1 for examples). Ectopic *Pax6* expression causes ectopic formation of optic structures, which demonstrates that *Pax6* is a crucial gene for eye formation (Halder *et al.*, 1995). Overexpression of *Pax6* leads to oncogenesis, suggesting that *Pax6* is involved in cellular proliferation (Maulbecker and Gruss, 1993). These are examples of starting with "genotypes", as described on page 1 of this thesis.

My interests are in the regulation of *Pax6* expression. Although this study shows that *Pax6* expression is not switched off following RA treatment, an indirect effect of RA on *Pax6* expression can not be

excluded. This is due to the limitation of *in situ* hybridization used in this study, and probably is also due to the complicated regulation of *Pax6* expression. *Pax6* has been implicated in a hierarchy of genes, including *Shh* (Macdonald *et al.*, 1995), *Ets* (Plaza *et al.*, 1994), *Lim-1*, and *Gsh-1* (Mastick *et al.*, 1997). In vitro studies shows that growth factors such as activin A, bFGF, NGF, and BDNF can regulate *Pax6* expression (Yamada *et al.*, 1994; Kioussi and Gruss, 1994). Some of these genes or growth factors may be regulated by RA. For example, *Pax6* expression may be altered through regulation of *Shh* by RA, according to data published by Riddle *et al.* (1993) and Macdonald *et al.* (1995).

The effect of RA on *Pax6* expression may be investigated using a microexplant culture system. The system has been successfully applied in culturing brain tissues with specific antibodies to detect axons or glial cells, in an effort to differentiate the role of *Pax6* in axonogenesis or gliagenesis (Veronica van Heyningen, personal communication). The system may be modified by adding RA, growth factors, cell adhesion molecules, extracellular matrix, and transcripts of genes in different combinations to study the complicated hierarchy that regulates *Pax6* expression. For example, the *Sey/Sey* maxillary process provides interesting prospects in elucidating the interactions among *Pax6, Msx-1, Msx-2, BMP-2, BMP-4, Egr-1* and their downstream genes. Investigations in the interactions will be greatly facilitated by the *in vitro* system.

REFERENCES

Adams, B., Dorfler, P., Aguzzi, A., Kozmik, Z., Urbanek, P., Maurer-Fogy, I. and Busslinger, M. (1992). *Pax-5* encodes the transcription factor BSAP and is expressed in B lymphocytes, the developing CNS, and adult testis. *Genes Dev.* 6, 1589-1607.

Agarwal, V. R. and Sato, S. M. (1993). Retinoic acid affects central nervous system development of *Xenopus* by changing cell fate. *Mechanisms of Development* 44, 167-173.

Alemany, J., Borras, T. and De Pablo, F. (1990). Transcriptional stimulation of the δ1-crystallin gene by insulin-like growth factor I and insulin requires DNA *cis* elements in chick. *Proc. Natl. Sci. U S A* 87, 3353-3357.

Alexander, L. E. (1947). An experimental study of the role of optic cup and overlying ectoderm in lens formation in the chick embryo. *J. Exp. Zool.* 75, 41-73.

Altman, J. and Bayer, S. A. (1979). Development of the diencephalon in the rat. VI. Re-evaluation of the embryonic development of the thalamus on the basis of thymidine-radiographic datings. *J. Comp. Neurol.* 188, 501-524.

Altman, J. and Bayer, S. A. (1981a). Time of origin of neurons of the rat inferior colliculus and the relations between cytogenesis and tonotopic order in the auditory pathway. *Exp. Brain Res.* 42, 411-423.

Altman, J. and Bayer, S. A. (1981b). Time of origin of neurons of rat superior colliculus in relation to other components of the visual and visuomotor pathways. *Exp. Brain Res.* 42, 424-434.

Altman, J. and Bayer, S. A. (1981c). Development of the brain stem in the rat. V. Thymidine-radiographic study of the time of origin of neurons in the midbrain tegmentum. *J. Comp. Neurol.* 198, 677-716.

Altman, J. and Bayer, S. A. (1988). Development of the rat thalamus: I. Mosaic organization of the thalamic neuroepithelium. *J Comp. Neurol.* 275, 346 -377.

Altman, J. and Bayer, S. A. (1995). *Atlas of prenatal rat brain development.* CRC Press.

Altmann, C. R., Chow, R. L., Lang, R. A. Hemmati-Brivanlou, A. (1997). Lens induction by *Pax-6* in *Xenopus laevis. Developmental Biology* 185, 119-123.

Antonetty, C. M. and Webster, K. E. (1975). The organisation of the spinotectal projection: Experimental atudy in the rat. *J. Comp. Neurol.* 153, 449-466.

Arey, L. B. (1974). *Developmental anatomy:A textbook and laboratory manual of embryology.* W. B. Saunders, Philadelphia and London.

Asano, M. and Gruss, P. (1992). *Pax-5* is expressed at the midbrain-hindbrain boundary during mouse development. *Mech. Dev.* 39, 29-39.

Auerbach, R. (1954). Analysis of the developmental effects of a lethal mutation in the house mouse. *J. Exp. Zool.* 127, 305-329.

Azmitia, E.C. and Segal, M. (1978). An auto radiographic analysis of the differential ascending projections of the dorsal and medium raphe nuclei in the rat. *J. Comp. Neurol.* 179, 641-668.

Baldwin, C. T., Hoth, C. F. and Desplan, C. (1992). An exonic mutation in the *HuP2* paired domain gene causes Waardenburgh's sysdrome. *Nature* 355, 637 - 638.

Balinsky, B. I. (1981). *An Introduction to Embryology* (5th ed). Saunders College Publishing, Philadelphia.

Balkaschina, E. I. (1929). *Wilhelm Roux' Arch. Entwicklungsmech. Ori.* 115, 448-463.

Balling, R., Deutsch, U. and Gruss, P. (1988). *Undulated*, a mutation affecting the development of the mouse skeleton, has a point mutation in the paired box of *Pax1*. *Cell* 55, 531-535.

Balling, R., Lau, C. F., Dietrich, S., Wallin, J. and Gruss, P. (1992). Development of the skeletal system. *Ciba Foundation Symposium* 165, 132-140.

Barabanov, V. M. and Fedtsova, N. G. (1982). The distribution of lens differentiation capacity in the head ectoderm of chick embryos. *Differentiation* 21, 183-190.

Barberis, A., Widenhorn, K., Vitelli, L. and Busslinger, M. (1990). A novel B-cell lineage specific transcription factor present at early but not late stages of differentiation. *Genes Dev.* 4, 849-859.

Bard, J. B. L., Bansal, M. K. and Ross, A. S. A. (1988). The Extracellular Matrix of the Developing Cornea: Diversity, Deposition, and Function. *Development* 103 (*Suppl*), 195-205.

Barr, F.G., Galili, N., Holick, J., Biegel, J.A., Rovera, G. and Emmaunuel, B. S. (1993). Rearrangement of the *PAX3* paired box gene in the pediatric solid tumor alveolar rhabdomyosarcoma. *Nature Genet.* 3, 113-117.

Bateson, W. (1894). *Materials for the Study of Variation Treated with Especial Rregard to Discontinuity in the Origin of Species*, Macmillan.

Baumgartner, S., Bopp, D., Burri, M. and Noll, M. (1987). Structure of two genes at the *gooseberry* locus related to the *paired* gene and their spatial expression during embryogenesis. *Genes Dev.* 1, 1247-1267.

Beachy, P. A. (1995). Patterning activities of vertebrate *hedgehog* proteins in the developing eye and brain. *Current Biology* 5, 944-955.

Beckstead, R. M. (1979). An autoradiographic examination of cortico-cortical and suncortical projections of the mediodorsal projection (prefrontal) cortex in the rat. *J. Comp. Neurol.* 184, 43-62.

Beckstead, R. M. and Frankfurt, A. (1983). A direct projection from the retina to the intermediate gray layer of the superior colliculus demonstrated by anterograde transport of horseradish peroxidase in monkey, cat, and rat. *Exp. Brain Res.* 52, 261-268.

Beddington, R. S. P. (1994). Induction of s second neural axis by the mouse node. *Development* 120, 613-620.

Beebe D. C. and Dhawan, R. R. (1997). The lens is the 'organizer' of the eye. In *Society of Developmental Biology Meeting Abstracts* B5 *Developmental Biology*, 186, 311.

Beebe, D. C., Silver, M. H., Belcher, K. S., Van Wyk J. J., Svoboda, M. E. and Zelenka, P. S. (1987). Lentropin, a protein that controls lens fiber formation is related functionally and immunologically to insulin-like growth factors. *Proc. Natl. Sci. U S A* 84, 2327-2330.

Begleiter, M.L. and Harris, D.J. (1992). Waardenburg syndrome and meningocele. *Am. J. Hum. Genet.* 44, 541.

Bender, W., Akam, M. E., Karch, F., Beachy, P. A., Peifer, M., Spierer, P., Lewis, E. B. and Hogness, D. S. (1983). Molecular genetics of the bithorax complex in *Drosophila melanogaster*. *Science*, 221, 23-29.

Berquist, H. and Källén, B. (1954). Notes on the early histogenesis and morphogenesis of the central nervous system in vertebrates. *J. Comp. Neurol.* 100, 627-659.

Berson, D. M. and Graybiel, A. M. (1983). Organization of the striate-recipient zone of the cat's lateralis posterior-pulvinar complex and its relations with the geniculate system. *Neurosci.* 9, 337-372.

Birgbauer, E. and Fraser, S. E. (1994). Violation of cell lineage restriction compartments in the chick hindbrain. *Development* 120, 1347-1356.

Blanks, R. H. I., Giolli, R. A. and Pham, S. V. (1982). Projection of the medial terminal nucleus of the accessory optic system upon pretectal nuclei in the pigmented rat. *Exp. Brain Res.* 48, 228-237.

Blomhoff, R. B. (1994). Vitamin A in health and diseases. R. Blomhoff ed. (Marcel Dekker Inc.: New York).

Bober, E., Franz, T., Arnold, H. H., Gruss, P. and Tremblay, P. (1994). *Pax-3* is required for the development of limb muscles: a possible role for the migration of dermomyotomal muscle progenitor cells. *Development* 120, 603-12.

Boncinelli, E., Simeone, A., Acampora, D., and Mavilio, F. (1991). *HOX* gene activation by retinoic acid. *Trends Genet.* 7: 329-334.

Bopp, D., Burri, M., Baumgarter, S., Frigeiro, G. and Noll, M. (1986). Conservation of a large protein domain in the segmentation gene *paired* and in functional related genes of *Drosophila. Cell* 47, 1033-1040.

Bopp, D., Janet, E., Baumgartner, S., Burri, M. and Noll, M. (1991). Isolation of two tissue-specific *Drosophila* paired box genes, *Pox meso* and *Pox neuro. EMBO J.* 8, 3447-3457.

Brand-Saberi, B., Ebensperger, C., Wilting, J., Balling, R. and Christ, B. (1993). The ventralizing effect of the notochord on somite differentiation. *Anat. Embryol.* 188, 239-245.

Brauer, K. and Schober, W. (1982). Identification of geniculo-tectal relay neurons in the rat's ventral lateral geniculate necleus. *Exp. Brain Res.* 45, 84-88.

Breitman, M. L., Bryce, D. M., Giddens, E., Clapoff, S., Goring, D., Tsui, L. -C., Klintworth, G. K. and Bernstein, A. (1989). Analysis of lens cell fate and eye morphogenesis in transgenic mice ablated for cells of the lens lineage. *Development* 106, 457-463.

Bridges, C. B. and Dobzhansky, T. (1933). *Wilhelm Roux' Arch Entwicklungsmech Org.* 127, 575-590.

Bridges, C. B. and Morgan, T. H. (1923). *The third chromosome group of mutant characters of Drosophila melanogaster.* Carnegie Instuitution of Washington.

Broadwell, R. D. (1975). Olfactory relationships of the telencephalon and diencephalon in the rabbit. II. An autoradiographic and horseradish peroxidase study of the efferent connections of the anterior olfacxtory nucleus. *J. Comp. Neurol.* 164, 389-409.

Browder, L. W., Ericson, C. A., and Jeffery, W. R. (1991). *Developmental Biology 3rd ed.* Saunders College Publishing.

Burri, M., Tromvoukis, Y., Bopp, D., Frigerio, G. and Noll, M. (1989). Conservation of the paired domain in metazoans and its structure in three isolated human genes. *EMBO J.* 8, 1183-1190.

Buxton, P., Hunt, P., Ferretti, P. and Thorogood, P. (1997). A role for midline closure in the reestablishment of dorsoventral pattern following dorsal hindbrain ablation. *Developmental Biology* 183, 150-165.

Cajal, S. R. y. (1911). *Histologie du systeme nerveux. Vol. II.* Malonie, Paris.

Cajal, S. R. y. (1960). *Studies on vertebrate neurogenesis* (L. Guth trans.), C.C. Thomas, Springfiled, Illinois.

Carriere, C., Plaza, S., Martin, P., Quatannens, B., Bailly, M., Stehelin, D. and Saule, S. (1993). Characterization of quail Pax-6 (Pax-QNR) proteins expressed in the neuroretina. *Mol. Cell. Biol.* 13, 7257-7266.

Carter, T. C. (1947). A new linkage in the house mouse: *undulated* and *agouti. Heredity* 1, 367-372.

Chalepakis, G., Fritsch, R., Fickenscher, H., Deutsch, U., Goulding, M. and Gruss, P. (1991). The molecular basis of the *undulated/Pax1* mutation. *Cell* 66, 873-884.

Chalepakis, G., Fritsch, R., Fickenscher, H., Deutsch, U., Goulding, M., and Gruss, P. (1992). *Pax* genes, mutants and molecular function. *J Cell Sci.* 16 (*suppl.*) 61 -67.

Chalepakis, G., Goulding, M., Read, A., Strachan, T. and Gruss, P. (1994). The molecular basis of *splotch* and *Waardenburg Pax3* mutations. Proc. *Natl. Acad. Sci. USA* 125, 417-42.

Chalepakis, G., Stoykova, A., Wijnholds, J., Tremblay, P. and Gruss, P. (1993). *Pax*: Gene regulators in the developing nervous system. *J. Neurobiol.* 24, 1367-1384.

Chalepakis, G., Tremblay, P. and Gruss, P. (1992). *Pax* genes, mutants, and molecular function. *J. Cell Sci.* 16, 61-67.

Chalepakis, G., Wijnholds, J. and Gruss, P. (1994). *Pax3*-DNA interaction: flexibility in the DNA binding and induction of DNA conformational changes by paired domains. *Nucl. Acids Res.* 22, 3131-3137.

Chalepakis, G., Wijnholds, J., Giese, P., Schachner, M. and Gruss, P. (1994). Characterization of *Pax-6* and *Hoxa-1* binding to the promotor region of the neural cell adhesion molecule L1. *DNA Cell Biol.* 13, 891-900.

Chambon, P. (1994). The retinoid signaling pathway: molecular and genetic analysis. *Semin. Cell Biol.* 5, 115-125.

Chang, D. T., Lopez, A., von Kessler, D. P., Chiang, C., Simandl, B. K., Zhao, R., Seldin, M. F., Fallon, J. F. and Beachy, P. A. (1994). Products, genetic linkage and limb patterning activity of a murine *hedgehog* gene. *Development* 120, 3339-3353.

Chen, Y. P. and Solurch, M. (1992). The determination of myogenic and cartilage cells in the early chick embryo and the modifying effect of retinoic acid. *Roux' Arch. Dev. Biol.* 200:162-171.

Chen, Y. P., Huang, L., Russo, A. F. and Solursh, M. (1992). Retinoic acid is enriched in Hensen's node and is developmentally regulated in the early chicken embryo. *Proc. Natl. Acad. Sci. U.S.A.* 89: 10056-10059.

Chisholm, A. and Horvitz, H. R. (1995). Patterning of the *Caenorhabditis elegans* head region by the *Pax-6* family member *vab-3*. *Nature* 377, 52-55.

Chung. C. -M., Ting, S. A., Widelitz, R. B. and Lee, Y.-S. (1992). Mechanism of skin morphogenesis. II Retinoic acid modulates axis orientation and phenotypes of skin appendages. *Development* 115: 839-852.

Cohen, J., Burne, J. F., McKinlay, C. and Winter, J. (1987). The role of laminin and the laminin/fibronectin receptor complex in the outgrowth of retinal ganglial cell axons. *Dev. Biol.* 122, 407-418.

Cohen, J., Burne, J. F., Winter, J. and Bartlett, P. (1986). Retinal ganglial cells lose responsiveness to lamina with maturation. *Nature* 322, 465-467.

Colamarino, S. A. and Tessier-Lavigne, M. (1995). The axonal chemoattractant netrin-1 is also a chemorepellant for trochlear motor axons. *Cell* 81, 621-629.

Conrad, L.C. A. and Pfaff, D.W. (1976). Efferents from medial basal forebrain and hypothalamus in the rat. I. An autoradiographic study of the medial preoptic area. *J. Comp. Neurol.* 169, 185-220.

Crossley, P. H. and Martin, G. R. (1995). The mouse Fgf8 gene encodes a family of polypeptides and is expressed in regions that direct outgrowth and patterning of the developing embryo. *Development* 121, 439-451.

Cunningham, T. and Freeman, J. (1971). Bilateral ganglion cell branches in the normal rat: A demonstration with electrophysiological collision and cobalt tracing methods. *J. Comp. Neurol.* 172, 165-176.

Cvekl, A. and Piatigorsky, J. (1996). Lens development and crystallin gene expression: many roles for *Pax-6. BioEssays* 18, 621-630.

Cvekl, A., Sax, C. M., Bresnick, E. H. and Piatigorsky, J. (1994). A complex array of positive and negative elements regulates the chick αA-crystallin gene: involvement of *Pax-6*, USF, CREB, and/or CREM, and AP-1 proteins. *Mol. Cell. Biol.* 14, 7363-7376.

Cvekl, A., Sax, C. M., Li, X., McDermott, J. B. and Piatogorsky, J. (1995). *Pax-6* and lens-specific transcription for the chicken δ1-crystallin gene. *Proc. Natl. Acad. Sci.* 92, 4681-4685.

Czerny, T., Schnaffer, G. and Busslinger, M. (1993). DNA sequence recognition by Pax proteins: Bipartite structure of the paired domain and its binding site. *Genes Dev.* 7, 2048-2061.

Davidson, D. (1995). The function and evoliution of *Msx* genes: pointers and paradoxes. *Trends Genet.* 11, 405-411.

Davies, A. M. (1987). Molecular and cellular aspects of patterning sensory neurone connections in the vertebrate nervous system. *Development* 101, 185-208.

Davis, A. and Cowell, J. K. (1994). Mutations in the *PAX6* gene in patients with hereditary *aniridia. Hum. Mol. Genet.* 2, 2093-2097.

Davis, R. J., D'Cruz, C. M., Lovell, M. A., Biegel, J. A. and Barr, F. G. (1994). Fusion of PAX7 to FKHR by the variant t(1:13)(p36;q14) translocation in alveolar rhabdosarcoma. *Cancer Res.* 54, 2869-2872.

De Olmos, J. S. (1972). The amygdaloid projection field in the rat as studied with the cupric-silver method. *In*: *The Neurobiology of the Amygdala* (ed. Eleftheriou, E. B.), pp. 145-204. Plenum Press, New York.

De Olmos, J. S., Hardy, H. and Heimer, L. (1978). The afferent connections of the main and accessory olfactory formations in the rat: An experimental HRP-study. *J. Comp. Neurol.* 181, 213-244.

De Olmos, J., Alheid, G. F. and Beltramino C.A. (1985). Amygdala. *In :The Rat Nervous System Vol 1 Forebrain and Midbrain* (ed. Paxinos, G.), Academic Press.

Dekker, E. -J., Pannese, M., Houlzager, F., Boncielli, E., and Durston, A. (1993). Colinearity in the *Xenopus laevis Hox-2* complex. *Mech. Dev.* 40, 3-12.

Denham, S. (1967). A cell proliferation study of the neural retina in the two-day rat. *J. Embryol. Exp. Morphol.* 18, 53-66.

Dersch, H. and Zile, M. H. (1993). Induction of normal cardiovascular development in the vitamin A-deprived quail embryo by natural retinoids. *Dev. Biol.*160: 424-433.

Detwiler, S. R. (1934). An experimental study of spinal nerve segmentation in *Amblystoma* with reference to the plurisegmental contribution to the branchial plexus. *J. Exp. Zool.* 67, 395-441.

Deutsch, U. and Gruss, P. (1991). Murine paired domain proteins as regulatory factors of embryonic development. *Seminar Dev. Biol.* 2, 413-424.

Deutsch, U., Dressler, G. R. and Gruss, P. (1988). *Pax1*, a member of a paired box homologous murine gene family, is expressed in segmented structures during development. *Cell* 53, 617-625.

Dhouailly, D. and Hardy, M. H. (1978). Retinoic acid causes the development of feathers in the scale-forming integument of the chick embryo. *Wilhelm Roux' Arch* 185, 195-200.

Dietrich, S., and Gruss, P. (1995). *Undulated* phenotypes suggest a role of *Pax-1* for the development of vertebral and extravertebral structures. *Dev. Biol.* 167, 529-548.

Dietrich, S., Schubert, F. R. and Gruss, P. (1993). Altered *Pax* gene expression in murine notochord mutants: the notochord is required to initiate and maintain ventral identity in the somite. *Mech. Dev.* 44, 189-207.

Dolle, P. and Chambon, P. (1994). Genetic analysis of RXR_{α} developmental function: convergence of RXR and RAR signaling pathways in heart and eye morphogenesis. *Cell* 78, 987-1003.

Dolle, P. and Duboule, D. (1989). Two gene members of the murine *HOX5* complex show regional and cell-type specific expression in developing limbs and gonads. *EMBO J.* 8, 1507-1515.

Dolle, P., Izpisua-Belmonte, J.C., Falkenstein, H., Renucci, A. and Duboule, D. (1989). Coordinate expression of the murine *Hox-5* complex homeobox-containing genes during limb pattern formation. *Nature* 342, 767-772.

Dorshkind, K. (1994). Transcriptional control points during lymphopoesis. *Cell* 79, 751-753.

Dressler, G. R. and Douglass, E. C. (1992). *Pax-2* is a DNA-binding protein expressed in embryonic kidney and Wilms' tumor. *Proc. Natl. Acad. Sci. USA* 89, 1179-1183.

Dressler, G. R., Deustch, U., Chowdhury, K., Norres, H.O. and Gruss, P. (1990). *Pax-2*, a new murine paired box-containing gene and its expression in the developing excretory system. *Development* 108, 787-795.

Dressler, G. R., Deutsch, U., Balling, R., Simon, D., Guenet, J. -L. and Gruss, P. (1988). Murine genes with homology to *Drosophila* segmentation genes. *Development* 104 (*Suppl.*), 181-186.

Dressler, G. R., Wilkinson, J. E., Rothenpieler, U. W., Patterson, L. T., Williams-Simons, L. and Westphal, H. (1993). Deregulation of *Pax-2* expression in transgenic mice generates severe kidney abnormalities. *Nature* 362, 65-67.

Drysdale, T. A. and Crawford, M. J. (1994). Effects of localized application of retinoic acid on Xenopus laevis development. *Dev. Biol.* 162: 394-401.

Dupin, E. and Le Douarin, N. M. (1995). Retinoic acid promotes the differentiation of adrenergic cells and melanocytes in quail neural crest cultures. *Dev. Biol.* 168: 529-548.

Durston, A. J., Timmermans, J. P. M., Hage, W. J., Hendriks, H. F. J., De Vires, N. J., Heiceveld, M. and Nieuwkoop, P. D. (1989). Retinoic acid causes an anteroposterior transformation in the developing central nervous system. *Nature* 340, 140-144.

Easter, S. S. Jr., Ross, L. S. and Frankfurter, A. (1993). Initial tract formation in the mouse brain. *J. Neurosci.* 13, 285-299.

Eates, R. D. (1972). The role of the vomeronasal organ in mammalian reproduction. *Mammalia* 36, 315-341.

Echelard, Y., Epstein, D. J., St-Jacques, B., Shen, L., Mohler, J., McMahon, J. A. and McMahon, A. P. (1993). Sonic hedgehog, a member of a family of putative signaling molecules, is implicated in the regulation of CNS polarity. *Cell* 75, 1417-1430.

Edwards, M. A., Crandall, J. E., Wood, J. N., Tanaka, H. and Yamamoto, M. (1989). Early axonal differentiation in mouse CNS delineated by an antibody recognizing extracted neurofilaments. *Developmental Brain Research* 49, 185-204.

Ekker, S. C., Ungar, A. R., Greenstein, P., von Kessler, D. P., Porter, J. A., Moon, R. T., Epstein, D. J., Vekemans, M. and Gros, P. (1991). *Splotch* (Sp^{2H}), a mutation affecting development of the mouse neural tube, shows a deletion within the paired homeodomain of *Pax-3*. *Cell* 67,767-774.

Epstein, D.J., Vogan, K. J., Trasler, D. G. and Gros, P. (1993). A mutation within intron 3 of the *Pax3* gene produces aberrantly spliced mRNA transcripts in the *splotch* (*Sp*) mouse mutant. *Proc. Natl. Sci. USA*. 90, 523-526.

Epstein, J. A., Glaser, T., Cai, J., Jepeal, L., Walton, D. S. and Maas, R. L. (1994). Two independent and interactive DNA-binding subdomains of the *Pax-6* paired domain are regulated by alternative splicing. *Genes Dev.* 8: 2022-2034.

Epstein, J.A., Cai, J., Glaser, T., Jepeal, L. and Maas, R. L. (1994a). Identification od a Pax paired domain recognition sequence and evidence fro DNA-dependent conformational changes. *J. Biol. Chem.* 269, 8355-8361.

Fallon, J. H. and Moore, R. Y. (1979). Superior colliculus efferents to the hypothalamus. *Neurosci. Lett.* 14, 265-270.

Fallon, J.H. and Moore, R.Y. (1978). Catecholamine innervation of basa forebrain. III. Olfactory bulb, anterior olfactory nuclei, olfactory tubercle and piriform cortex. *J. Comp. Neurol.* 180, 533-544.

Fan, C. M. and Tessier-Lavigne, M. (1994). Patterning of mammalian somites by surface ectoderm and notochord: evidence for scleratome induction by a hedgehog homolog. *Cell* 79, 1175-1186.

Farman, A.I. *TheCell Biology of Olfaction.* Cambridge University Press, Cambridge, 1992.

Farrer, L. A., Arnos, K. S., Asher, J. H. Jr., Baldwin, C. T., Diehl, S. R., Friedman, T. B., Greenberg, J., Grundfast, K. M., Hoth, C., Lawani, A. K., Landa, B., Leverton, K., Milunsky, A., Morell, R., Nance, W. E., Newton, V., Ramesar, R., Rao, V. S., Reynolds, J. E., San Agustin, T. B., Wilcox, E. R., Winship, I. and Read, A. P. (1994). Locus heterogeneity for Waardenburg syndrome is predictive of clinical subtypes. *Am. J. Hum. Genet.* 55, 728-737.

Fidger, M. C. and Stern, C. D. (1993). Segmental organization of embryonic diencephalon. *Nature* 363, 630-634.

Fish, S., Goodman, D., Kuo, D., Polcer, J. and Rhoades, R. (1982). The intercollicular pathway in the golden hamster: An anatomical study. *J. Comp. Neurol.* 204, 6 -20.

Fisher, G., Kunemund, V. and Schachner, M. (1986). Neurite outgrowth patterns in cerebellar microexplant cultures are effected by antibodies to the cell surface glycoprotein L1. *J. Neurosci.* 6, 605-612.

Francis, P. H., Richardson, M. K., Brickell, P. M. and Tickle, C. (1994). Bone morphogenetic proteins and a signalling pathway that controls patterning in the developing chick limb. *Development* 120, 209-218.

Franz T and Besecke A. (1991). The development of the eye in homozygotes of the mouse mutant extra-toes. *Anat Embryol* 184: 355-361.

Franz, T. (1989). Persistent truncus arteriosus in the *Splotch* mutant mouse. *Anat. Embryol.* 180, 457-464.

Franz, T. (1990). Defective ensheathment of motoric nerves in the *Splotch* mutant mouse. *Acta. Anat.* 138, 246-253.

Franz, T. (1992). Neural tube defects without neural crest defects in *Splotch* mice. *Teratology* 46, 599-604.

Franz, T. (1993). The *Splotch* (Sp^{1H}) and *Splotch-delayed* (Sp^{d}) alleles: differential phenotypic effects on neural crest and limb musculature. *Anat-Embryol-Berl.* 187, 371-377.

Franz, T., Kothary, R., Surani, M. A., Halata, Z. and Grim , M. (1993). The *Splotch* mutation interferes with muscle development in the limbs. *Anat-Embryol-Berl.* 187, 153-160.

Fraser, S., Keynes, R. and Lumsden, A. (1990). Segmentation in the chick embryo hindbrain is defined by cell lineage restrictions. *Nature* 344, 431-435.

Fredricks, W. J., Galili, N., Mukhopadhyay, S., Rovera, G., Bennicelli, J., Barr, F. G.and Rauscher, F. J. 3rd (1995). The PAX3-FKHR fusion protein created by the t(2;13) translocation in alveolar rhabdomyosarcomas is a more potent transcriptional activator than PAX3. *Mol. Cell Biol.* 15, 1522-1535.

Frigerio, G., Burri, M., Bopp, D., Baumgartner, S., and Noll, M. (1986). Structure of the segmentation gene paired and *Drosophila* PRD gene set as part of a gene network. *Cell* 47, 735-746.

Fujiwara, M., Uchida, T., Osumi-Yamashita, N. and Eto, K. (1994). *Uchida rat* (*rSey*): a new mutant with craniofacial abnormalities resembling those of the mouse *Sey* mutant. *Differentiation* 57: 31-38.

Gao, W.-Q. and Hatten, M. E. (1993). Neuronal differentiation rescued by implantation of *Weaver* granule cell precursors into wild-type cerebral cortex. *Science* 260, 367-369.

Garey, L. J., Dreher B. D., and Robinson, S. R. (1991). *TheOrganization of theVisual System. In*: Dreher B. and Ribinson S.R. (ed.), *Neuroanatomy of the Visual Pathways and their Development,* Macmillan Press.

Gaunt, S. J and Singh, P. B. (1990). Homeogene expression patterns and chromosomal imprinting. *Trends Genet.* 6: 208-212.

Gaunt, S. J. (1991). Expression patterns of mouse *Hox* genes: clues to an understanding of developmental and evolutionary strategies. *Bioessays* 13, 505-513.

Gaunt, S. J., Sharpe, P. T. and Wedeen, C. J. (1988). Spatially restricted domains of homeo-gene transcripts in mouse embryos: relation to a segmented body plan. *Development* 104 *Suppl.* 169-180.

Gehring, W. J. (1987). Homeoboxes in the study of development. *Science* 236, 1245-1252.

Gendron-Maguire M, Mallo, M., Zhang, M. and Gridley, T. (1993). *Hoxa-2* mutant mice exhibit homeotic transformation of skeletal elements derived from cranial neural crest. *Cell* 75: 1317-1331.

Gerfen C. R. and Clavier, R. M. (1979). Neural inputs to the prefrontal agranular insular cortex in the rat: Horseradish peroxidase study. *Brain Res. Bull.* 4, 347-353.

Giolli, R. A. and Towns, L. C. (1980). A review of axon collateralization in the mammalian visual system. *Brain Behav. Evol.* 17, 364-390.

Glaser, T., Lane, J. and Houseman, D. (1990). A mouse model for the aniridia-Wilms tumor deletion syndrome. *Science* 250, 823-827.

Goldowitz, D. and Mullen, R. J. (1982). Granule cell as a site of gene action in the *weaver* mouse cerebellum: Evidence from heterozygous mutant chimera. *J. Neurosci.* 2, 1474-1485.

Gong, Q. and Shipley, M. T. (1995). Evidence that pioneer olfactory axons regulate telencephalon cell cycle kinetics to induce formation of the olfactory bulb. *Neuron* 14, 91-101.

Goodman, C. S. and Shatz, C. J. (1993). Developmental mechanisms that generate precise patterns of neuronal connectivity. *Cell* 72, 77-98.

Gopal-Srivastava, R., Haynes, J. I. II, and Piatigorsky, J. (1995). Regulation of the murine αB-crystallin/small heat shock protein gene in cardiac muscle. *Mol. Cell. Biol.* 15, 7081-7090.

Goulding, M D., Lumsten, A. and Gruss, P. (1993a). Signals from the notochord and floor plate regulate the region-specific expression of two Pax genes in the developing spinal cord. *Development* 117, 1001-1016.

Goulding, M. D., Chalepakis, G., Deutsch, U., Erselius, J. and Gruss, P. (1991). *Pax-3* , a novel murine DNA-binding protein expressed during early neurogenesis. *EMBO J.* 10, 1135-1147.

Goulding, M. D., Sterrer, S., Fleming, J., Balling, R., Nadeau, J., Moore, K. J., Brown, S. D., Steel, K. P. and Gruss, P. (1993b). Analysis of the *Pax3* gene in the mouse mutant *Splotch*. *Genomics* 17, 355-363.

Graham, A., Francis-West, P., Brickell, P. and Lumsden, A. (1994). The signalling molecule BMP4 mediate apoptosis in the rhomb-encephalic neural crest. *Nature* 372, 684-686.

Graham, A., Heyman, I. and Lumsden, A. (1993). Even-numbered rhombomeres control the apoptotic elimination of neural crest cells from odd-numbered rhombomeres in the chick hindbrain. *Development* 119, 233-245.

Graham, A., Papalopulu, N., and Krumlauf, R. (1989). The murine and *Drosophila* homeobox clusters have common features of organization and expression. *Cell* 57, 367-378.

Grainger, R. M. (1992). Embryonic lens induction: shedding light on vertebrate tissue determination. *Trends Genet.* 8, 349-355.

Grainger, R. M., Henry, J. J., Saha, M. S. and Servetnick, M. (1992). Recent progress on the mechanisms of embryonic lens formation. *Eye* 6: 117-122.

Graybiel, A. M. (1974). Visuo-cerebellar and cerebello-visual connections involving the ventral lateral geniculate nucleus. *Exp. Brain Res.* 20, 303-306.

Graziadei, P. P. C. (1971). *The Olfactory Mucosa of Vertebrates. In* (ed.Beidler, M.) *Handbook of Sensory Physiology Vol. IV, pp.* 27-58. Springer-Verlag, New York.

Grindley, J. C. (1996). *The Pax6 Gene in Development of the Eye, Nose, and Brain.* Ph.D. thesis, Edinburgh University.

Grindley, J. C., Davidson, D. and Hill, R. E. (1995). The role of *Pax-6* in eye and nasal development. *Development* 121, 1433-1442.

Gruneberg, H. (1954). Genetical studies on the skeleton of the mouse XII. The development of *undulated*. *J. Genet.* 54, 43-62.

Gruneburg, H. (1950). Genetical studies on the skeleton of the mouse. II. Undulated and its modifiers. *J Genet.* 50, 142-173.

Gruss, P. and Walther, C. (1992). *Pax* in development. Cell 69, 719-722.

Guthrie, S. (1992). Lineage in the cerebral cortex: when is a clone not a clone ? *Trends Neurosci.* 115, 273-275.

Guthrie, S. and Lumsden, A. (1991). Formation and regeneration of rhombomere boundaries in the developing chick hindbrain. *Development* 112, 221-230.

Guthrie, S., Prince, V. and Lumsden, A. (1993). Selective dispersal of avian rhombomere cells in orthotopic and heterotopic grafts. *Development* 118, 527-538.

Haberly, L. B. and Price, J. L. (1978a). Association and commisural fiber systems of the olfactory cortex of the rat. I. Systems originating in the piriform cortex and adjacent areas. *J. Comp. Neurol.* 178, 711-740.
Haberly, L. B. and Price, J. L. (1978b). Association and commisural fiber systems of the olfactory cortex of the rat. I. Systems originating the olfactory peduncle. . *J. Comp. Neurol.* 178, 781-808.

Halasz, N.. (1990). *The Vertebrate Olfactory System.* Academiai Kiado, Badapest0.

Halder, G., Callaerts, P. and Gehring, W. J. (1995). Induction of ectopic eyes by targeted expression of the *eyeless* gene in *Drosophila*. *Science* 267, 1788-1792.

Hale, P., Sefton, A. J., Bauer, L. A. and Cottee, L. J. (1982). Interrelations of the rat's thalamic reticular and dorsal lateral geniculate nuclei. *Exp. Brain Res.* 45, 217-229.

Hamburger, V. and Hamilton, H. L. (1951). A Series of Normal Stages in the Development of the Chick Embryos. *J. Morphol.* 88, 49-92.

Hanson, I. and van Heyningen, V. (1995). *Pax6*: more than meets the eye. *Trends Genet.* 11, 268-272.

Hanson, I. M., Fletcher, J. M., Jordan, T., Brown, A., Taylor, D., Adams, R. J., Punnett, H. and van Heyningen, V. (1994a). Mutations at the *PAX6* locus are found in heterogeneous anterior segment malformations including *Peters' anomaly*. *Nature Genet.* 6, 168-173.

Hanson, I. M., Jordan, T. and van Heyningen, V. (1994b). 'Aniridia'. *In 'Molecular genetics of inherited eye disorders'* (A. F. Wright and B. Jay, eds.), pp445-467. Harwood Academic Publishers, Chur, Switzerland.

Hanson, I. M., Seawright, A., Hardman, K., Hodgson, S., Zaletayev, D., Fekete, G. and van Heyningen, V. (1993). *PAX6* mutations in aniridia. *Hum. Mol. Genet.* 2, 915-920.

Harland, R. M. (1994). Neural induction in *Xenopus*. *Curr. Opin. Gen. Dev.* 4, 543-549.

Harrington, L., Klintworth, G. K., Secor, T. E. and Breitman, M. L. (1991). Developmental analysis of ocular morphogenesis in αA-crystallin/diphtheria toxin transgenic mice undergoing ablation of the lens. *Developmental biology* 148, 508-516.

Hart, R. C., Winn, K. J. and Unger, E. R. (1992). Avian model for 13-*cis*-retinoic acid embryopathy: morphological characterisation of ventricular septal defects. *Teratology* 46, 533-539.

Harting, J. K., Hall, W. C., Diamond, I. T. and Martin, G. F. (1972). Evolution of the pulvinar. *Brain Behav. Evol.* 6, 424-452.

Harting, J. K., Hall, W. C., Diamond, I. T. and Martin, G. F. (1973). Anterograde degeneration study of the superior colliculus in *Tupaia glis*: Evidence for a subdivision between superficial and deep layers. *J. Comp. Neurol.* 148, 361-386.

Hastie, N. D. (1993). Wilm's tumor gene and function. *Curr. Opin. Genet. Dev.* 3, 408-13.

Hatten, M. E. (1990). Riding the glial monorail: A common mechanism for glial-guided neuronal migration in different regions of the mammalian brain. *Trends Neurosci.* 13, 179-184.

Hayhow, W. R., Sefton, A., and Webb, C. (1962). Promary optic centres of the rat in relation to the terminal distribution of the crossed and uncrossed optic nerve fibers. *J. Comp. Neurol.* 118, 295-322.

Hayhow, W. R., Webb, C., and Jervie, A. (1960). The accessory optic fiber system in the rat. *J. Comp. Neurol.* 115, 187-216.

Heimer, L. (1968). Synaptic distribution of centripetal and centrifugal nerve fibers in the olfactory system of the rat. An experimental anatomical study. *J. Anat.* 103, 413-432.

Heimer, L. and Wilson, R. D. (1975). The subcortical projections of the allocortex:Similarities in the neural associations of the hippocampus, the piriform cortex, and the neocortex. In M. Santini (ed.), Golgi centiennial symposium: Perspectives in neurobiology, pp. 177-193. Raven Press, New York.

Henderson, C. E., Camu, W., Mettling, C., Gouin, A., Pouisen, K., Karihaloo, M., Rullamas, J., Evans, T., McMahon, S. B., Armanini, M. P., Berkemeier, L., Philips, H. S. and Rosenthal, A. (1993). Neurotrophins promote motor neuron survival and are present in embryonic limb bud. *Nature* 363, 266-270.

Hewitt, J. E., Clark, L. N., Ivens, A. and Williamson, R. (1991). Structure and sequence of the human homeobox gene *Hox7*. *Genomics* 11, 670-678.

Heyman, I., Faissner, A. and Lumsden, A. (1995). Cellular and molecular specializations of rhombomere boundaries. *Dev. Dynam.* 204, 301-315.

Heyman, I., Kent, A. and Lumsden, A. (1993). Cellular morphology and extracellular space at rhombomere boundaries in the chick embryo hindbrain. *Dev. Dyn.* 198, 241-53.

Hickey, T. L. and Spear, P. D. (1976). Retinogeniculate projections in hooded and albino rats: An autoradiographic study. *Exp. Brain Res.* 24, 523-529.

Hill, R E., Jones, P. F., Rees, A. R., Sime, C. M., Justice, M. J., Copeland, N. G., Jenkins, N. A., Graham, E. and Davidson, D. R. (1989). A new family of mouse homeo box-containing genes: molecular structure, chromosomal location and developmental expression of *Hox-7.1*. *Genes Dev.* 3, 26-37.

Hill, R. E. and Hanson, I. M. (1992). Molecular genetics of the *Pax* gene family. *Curr. Opin.Cell Biol.* 4, 967-972.

Hill, R. E. and van Heyningen, V. (1992). Mouse mutations and human disorders are paired. *Trands Genet.* 8, 119-120.

Hill, R. E., Favor, J., Hogan, B. L. M., Ton, C. C. T., Saunders, G. F., Hanson, I. M., Prosser, J., Jordon, T., Hastie, N. D. and van Heyningen, V. (1991). Mouse *Small eye* results from mutations in a paired-like homeobox-containing gene. *Nature* 354, 522-525.

Hill, R. E., Jones, P. F., Rees, A. R., Sime, C. M., Justice, M. J., Copeland, N. G., Jenkins, N. A., Graham, E. and Davidson, D. R. (1989). A new family of mouse homeobox containing genes:

molecular structure, chromosomal location and developmental expression of *Hox 7.1. Genes and Dev* 3, 26-37.

Hirsch, N. and Harris, W. A. (1997). *Xenopus Pax-6* and retinal development. *J. Neurobiol.* 32, 45-61.

Hodgson, S. V. and Saunders, K. E. (1980). A probable case of the homozygous condition of the aniridia gene. *J. Med. Genet.* 6, 478-480.

Hofer, M. M. and Barde, Y. A. (1988). Brain derived neutrophic factor prevents neuronal death *in vivo*. *Nature* 331, 261-262.

Hogan, B. L. M., Hirst, E. A., Horsburgh, G. and Hetherington, C. M. (1988). *Small eye* (*Sey*): a mouse model for the genetic analysis of craniofacial abnormalities. *Development* 103 (*Suppl.*), 115-119.

Hogan, B. L. M., Horsburgh, G., Cohen, J., Hetherington, C. M., Fisher, G. and Lyon, M. F. (1986). *Small eye* (*Sey*): a homozygous lethal mutation on chromosome 2 which affects the differentiation of both lens and nasal placodes in the mouse. *J. Embryol. Exp. Morphol.* 97, 95-100.

Hogan, B. L. M., Thaller, C. and Eichele, G. (1992). Evidence that Hensen's node is a site of retinoic acid synthesis. *Nature* 359: 237-241.

Hohn, A., Leibrock, J., Bailey, K. and Barde, Y. -A. (1990). Identification and characterization of a novel member of the nerve growth factor/brain-derived neurotrophic factor family. *Nature* 344, 339-341.

Holder, N.. and Hill, J. (1991). Retinoic acid modifies development of the midbrain-hindbrain border and affects cranial ganglion formation in zebrafish embryos. *Development* 113: 1159-1170.

Holland, L. Z. and Holland, N. D. (1996). Expression of *AmphiHox-1* and *AmphiPax-1* in amphioxus embryos treated with retinoic acid: insights into evolution and patterning of chordate nerve cord and pharynx. *Development* 122, 1829-1838.

Holland, P. W. H. (1991). Cloning and evolutionary analysis of msh like homeobox genes from mouse, zebrafish, and ascidian. *Gene* 98, 253-257.

Hornbruch, A. and Wolpert, L. (1986). Positional signaling by Hensen's node when grafted to the chick limb bud. *J. Embryol. Exp. Morphol.* 94, 257-265.

Hoth, C. F., Milunsky, A., Lipsky, N., Sheffer, R., Clarren, S. K. and Baldwin, C. T. (1993). Mutations in the paired domain of the human *PAX3* gene cause *Klien-Waardenburg Syndrome* (*WS-III*) as well as *Waardenburg syndrome type I* (*WS-I*). *Am. J. Hum. Genet.* 52, 455-462.

Huber, G. C. and Crosby, E. C. (1943). A comparison of the mammalian and reptilian tecta. *J. Comp. Neurol.* 78, 133-169.

Hughes, R. A., Sendtner, M., Goldfarb, M., Linholm, D. and Thoenen, H. (1993). Evidence that fibroblast growth factor 5 is a major muscle-derived survival factor for cultured spinal motoneurons. *Neuron* 10, 369-377.

Hunt, P. and Krumlauf, R. (1991). Deciphering the Hox code: clues to patterning branchial regions of the head. *Cell* 66, 1075-1078.

Hunt, P. and Krumlauf, R. (1991). Hox genes coming to a head. *Curr. Biol.* 1, 304-306.

Hunt, P., Gulisano, M., Cook, M., Sham, M., Faiella, A., Wilkinson, D., Boncielli, E. and Krumlauf, R. (1991). A distinct Hox code for the branchial region of the head. *Nature* 353, 25-34.

Hunt, P., Wilkinson, D. and Krumlauf, R. (1991). Patterning of vertebrate head: murine Hox 2 genes mark distinct subpopulations of premigratory and migrating cranial crest. *Development* 112, 43-50.

Husmann, M., Gorgen, I., Weisgerber, C., and Bitter-Suermann, D. (1989). Up-regulation of embryonic NCAM in an EC cell line by retinoic acid. *De. Biol.* 136, 194-200.

Hyatt, G. A. and Beebe, D. C. (1992). Regulation of lens cell growth and polarity by an embryo-specific growth factor and by inhibitors of lens cell proliferation and differentiation. *Development*

Hynes, R. O. and Lander, A. D. (1992). Contact and adhesive specificities in the associations, migrations and targeting of cells and axons. *Cell* 68, 303-322.

Izpisua-Belmonte, J., Falkenstein, H., Dolle, P., Renucci, A. and Duboule, D. (1991). Murine genes related to the *Drosophila AbdB* homeotic gene are sequentially expressed during development of the posterior part of the body. *EMBO J.* 10, 2279-2289.

Jabs, E. W. et al (1993). A mutation in the homeodomain of the human MSX2 in a family effected with autosomal dominant craniosynostosis. *Cell* 75, 443-450.

Jacobson, A. G. (1966). Inductive processes in embryonic development. *Science* 152: 25-34.

Jacobson, A. G. (1981). Morphogenesis of the neural plate and tube. *In ''Morphogenesis and Pattern Formation''*, (T.G. Connelly, L. L. Brinkley and B. M. Carlson, Eds.) *pp.* 233-263. Raven Press. New York.

Jacobson, A. G. and Tam, P.P. L. (1982). Cephalic neurulation in the mouse embryo analysed by SEM and morphometry. *Anat. Rec.* 203, 375-396.

Jacobson, M. (1991). *Developmental Neurobiology*, 2nd ed. Plenum, New York.

Jacobson, S. and Trojanowski, J. Q. (1974). The cells of origin of the corpus callosum in rat, cat, and rhesus monkey. *Brain Res.* 74, 149-155.

Jeffery, G., Cowley, A and Kuypers, H. (1981). Bifurcating retinal ganglion cell axons in the rat, demonstrated by retrograde double labelling. *Exp. Brain Res.* 44, 34-40.

Johnson, R. L., Laufer, E., Riddle, R. D. and Tabin, C. (1994). Ectopic expression of sonic hedgehog alters dorso-ventral patterning of somites. *Cell* 79, 1165-1173.

Johnston, M. C. (1979). Origins of avian ocular and periocular tissues. *Exp Eye Res.* 29, 27-43.

Jonk, L. J., De Jonge, M. E. J., Vervarrt, J. M. A., Wissink, S. and Kruijer, W. (1994). Isolation and developmental expression of retinoic-acid-induced genes. *Dev. Biol.* 161, 604-614.

Jordan, T., Hanson, I. M., Zaletayev, D., Hodgson, S., Prosser, J., Seawright, A., Hastie, N. and van Heyningen, V. (1992). The human *PAX6* gene is mutated in two patients with aniridia. *Nature Genet.* 1, 328-332.

Jostes, B., Walther, C. and Gruss, P. (1991). The murine paired box gene, *Pax7*, is expressed specifically during the development of the nervous and muscular system. *Mech. Dev.* 33, 27-38.

Jowett, A. K., Vainio, S., Ferguson, M. W. J., Sharpe, P. T. and Thesleff, I. (1993). Epithelial-mesenchymal interactions are required for *Msx-1* and *Msx-2* gene expression in the developing murine molar teeth. *Development* 117, 461-470.

Källén, B. (1965). *Early morphogenesis and pattern formation in the central nervous system. In ''Organogenesis''* (R. L. Dehaan and H. Ursprung, Eds.), *pp* 107-128. Holt, Rinehart and Winston, New York.

Kadmon, G. and Altevogt, P. (1997). The cell adhesion molecule L1: species and cell-type-dependent multiple binding mechanisms. *Differentiation* 61: 143-150.

Karkinen-Jääskeläinen, M. (1978). Permissive and directive interactions in the lens induction. *J. Embryol. Exp. Mprphol.* 44, 167-179.

Kaufman, M. H. (1979). Cephalic neurulation and optic vesicle formation in the early mouse. *Am. J. Anat.* 155, 425 -444.

Kaufman, M. H. (1992). *The Atlas of Mouse Development.* Acadamic Press.

Kaufman, M. H., Chang, H.-H., Shaw, J. (1995). Craniofacial abnormalities in homozygous Small eye (*Sey/Sey*) embryos and newborn mice. *J. Anat.* 186, 607-617.

Kaur, S., Key, B., Stock, J., McNeish, J. D., Akeson, R. and Potter, S. S. (1989). Targeted ablation of α-crystallin-synthesizing cells produces lens-deficient eyes in transgenic mice. *Development* 105, 613-619.

Keller, R., Shih, J. and Sater, A. (1992). The cellular basis of the convergence and extension of the *Xenopus* neural plate. *Dev. Dyn.* 193, 199-217.

Keller, S. A., Jones, J. M., Boyle, A., Barrow, L. L., Killen, P. D., Green, D. G., Kapousta, N. V., Hichcock, P. F., Swank, R. T. and Meiser, M. H. (1994). Kidney and retinal (*Krd),* a transgene induced mutation with a deletion of mouse chromosome 19 that includes the *Pax2* locus. *Genomics* 23, 309-320.

Kennedy, T. E., Serafini, T., de La Tore, J. R. and Tessier-Lavigne, M. (1994). Netrins are diffusible chemotropic factors for commisular axons in the embryonic spinal cord. *Cell* 788, 425-435.

Kessel, M. (1993). Reversal of axonal pathways from rhombomere3 correlates with extra Hox expression domains. *Neuron,* 10, 379-393.

Kessel, M. and Gruss, P. (1991). Homeotic transformations of murine prevertebrae and concommitant alteration of Hox codes induced by retinoic acid. *Cell* 67, 89-104.

Kevetter G. A. and Winas S. S. (1981a). Connections of the corticomedial amygdala in the golden hamster. I. Efferents of the ''vomeronasal amygdala''. *J. Comp. Neurol.* 197, 81-89.

Kevetter G. A. and Winas S. S. (1981b). Connections of the corticomedial amygdala in the golden hamster. II. Efferents of the ''olfactory amygdala''. *J. Comp. Neurol.* 197, 99-111.

Key, B., Liu, L., Potter, S. S., Kaur, S. and Akeson, R. (1992). Lens structures exist transiently in development of transgenic mice carrying an α-crystallin-diphtheria toxin hybrid gene. *Exp. Eye Res.* 55, 357-367.

Keynes, R. and lumsden, A. (1990). Segmentation and the origin of regional diversity in the vertebrate central nervous system. *Neuron* 4, 1-9.

Keyser, A. (1972). The development of the diencephalon of the Chinese hamster. An investigation of the validity of the criteria of subdivision of the brain. *Acta Anat.* 83, (*Suppl.* 59) 1-17.

Kioussi, C. and Gruss, P. (1994). Differential induction of *Pax* genes by NGF and BDNF in cerebellar primary cultures. *J. Cell Biol.* 125, 417-425.

Kitamoto, T., Momoi, M. and Momoi, T. (1989). Expression of cellular retinoic acid binding protein II (chick-CRABP II) in the chick embryo. *Biochem. Biophy. Res. Commu.* 164: 531-536.

Klar, A., Baldassare, M. and Jessel, T. M. (1992). F-spondin: A gene expressed at high levels in the floor plate encodes a secreted protein that promotes neural cell adhesion and neurite extension. *Cell* 69, 95-110.

Klein, K. L., Klintworth, G. K., Bernstein, A. and Breitman, M. L. (1992). Embryology and morphology of microphthalmia in transgenic mice expressing a γ F-crystallin/diphtheria toxin A hybrid gene. *Laboratory Investigation* 67, 31-41.

Kollar, E. J. and Baird, G. R. (1969). The influence of the dental papilla on the development of tooth shape in embryonic mouse tooth germs. *J. Embryol. Exp. Morph.* 21, 131-148.

Komuro, H. and Rakic, P. (1992). Selective role of N-type calcium channels in neuronal migration. *Science* 157, 806-809.

Konyukhov, B. V. and Sazhina, M. G. (1971). Genetic control over the duration of G_1 phase. *Experentia*, 27, 970-971.

Koseki, H., Wallin, J., Wilting, J., Mizutani, Y., Kispert, A., Ebensperger, C., Herrman, B. G., Christ, C. and Balling, R. (1993). A role for *Pax-1* as a mediator of notochordal signals during the dorsoventral specification of vertebrae. *Development* 119, 649-660.

Kosel, K. C., Van Hoesen, G. and West, J. R. (1981). Olfactory bulb projections to the parahippocampal area of the rat. *J. Comp. Neurol.* 198, 467-482.

Kozmik, Z., Kurzbauer, R., Dorfler, P. and Busslinger, M. (1993). Alternative splicing of *Pax-8* gene transcripts is developmentally regulated and generates isoforms with different transactivation properties. *Mol. Cell Biol.* 13, 6024-6035.

Krauss, S., Johansen, T., Korzh, V., Moens, U., Ericson, J. U. and Fjose, A. (1991). Zebrafish *pax[zf-a]*: a paired box-containing gene expressed in the neural tube. *EMBO J.* 10, 3609-3619.

Krettek J. E. and Price J. L. (1977a). Projections from the amygdaloid complex to the cerebral cortex and thalamus in the rat and cat. *J. Comp Neurol.* 178, 255-280.

Krettek J. E. and Price J. L. (1977b). Projections from the amygdaloid complex and adjacent olfactory structures to the entorhinal cortex and to the suniculum in the rat and cat. *J. Comp. Neurol.* 172, 723-752.

Krettek J. E. and Price J. L. (1978a). Amygaloid projections to subcortical structures within the basal forebrain and brainstem in the rat and cat. *J. Comp. Neurol.* 178, 225-254.

Krettek J. E. and Price J. L. (1978b). A description of the amygdaloid complex in the rat and cat with observations on intra-amygdaloid axonal connections. *J. Comp. Neurol.* 178, 255-280.

Krumlauf, R. (1993). Hox genes and pattern formation in the branchial region of the vertebrate head. *Trends Genet.* 9, 106-112.

Krumlauf, R. (1994). Hox genes in vertebrate development. *Cell* 78, 191-201.

Kuhlenbeck, H. (1973). *The CentralNervous System of Vertebrates. Vol. 3, part II. Overall Morphologic Pattern.* S. Karger, Basel.

Kuratani, S. C. (1991). Alternate expression of the HNK-1 epitope in rhombomeres of the chick embryo. *Dev. Biol.* 144, 215-219.

Langston, A. W. and Gudas, L J. (1994). Retinoic acid and homeobox gene regulation. *Curr. Opin. Genet. Dev.* 4, 550-555.

Layer, P. G. and Albert, R. (1990). Patterning of chick brain vesicles as revealed by peanut agglutinin and chilinesterases. *Development* 109, 613-624.

Le Douarin, N. (1982). *The Neural Crest.* Cambridge University Press, Cambridge.

Legg, C. R. (1979). An autoradiographic study of the efferent projections of the ventral lateral geniculate nucleus of the hooded rat. *Brain Res.* 170, 349-352.

Lehman, F. (1927). Further studies on the morphogenetic role of somites in the development of the nervous system of amphibians. The differentiation and arrangement of the spinal ganglia in *Pleurodeles waltilii. J. Exp. Zool.* 49, 93-131.

Leonard, L., Horton, C, Maden, M. and Pizzey, J. A. (1995). Anteriorization of CRABP-I expression by retinoic acid in the developing mouse central nervous system and its relationship to teratogenesis. *Dev. Biol.* 168, 514-528.

Leong, S. K. (1980). Plasticity and interaction after ablations of visual or somatosensory motor cortex or retina in neonatal rats. *J. Neurol. Sci.* 45, 87-102.

Letourneau, P., Madsen, A. M., Palm, S. M. and Furcht, L. T. (1988). Immunoreactivity for laminin in the developing ventral longitudinal pathway of the brain. *Dev. Biol.* 125, 135-144.

Levi-Montalcini, R. and Booker, B. (1960). Destruction of the sympathetic ganglia in mammals by an antiserum to the nerve growth factor protein. *Proc. Natl. Acad. Sci. USA* 46, 384-390.

Lewis, E. B. (1978). A gene complex controlling segmentation in *Drosophila. Nature (Lond.),* 276, 565-570.

Li, H -S, Yang, J -M, Jacobson, R. D., Pasko, D. and Sundin, O. (1994). *Pax-6* is first expressed in a region of ectoderm anterior to the early neural plate: implications for stepwise determination of the lens. *Dev. Biol.* 162, 181-194.

Li, H. -S., Tierney, C., Wen, L., Wu, J. Y. and Rao, Y. (1997). A single morphogenetic field gives rise to two retina primordia under the influence of the prechordal plate. *Development* 124, 603-615.

Lidov, H. G. W., Grzanna, R., and Molliver, E. M. (1980). The serotonin innervationof the cerebral cortex in the rat - an immunohistochemical analysis. *Neurosci.* 5, 207-227.

Liesi, P. and Silver, J. (1988). Is astrocyte laminin involved in axon guidance in the mammalian CNS ? *Dev. Biol.* 130, 744-785.

Lin, L.-F. H., Doherty, D. H., Lile, J. D., Bektesh, S. and Collins, F. (1993). GDNF: A glial cell-line derived neurotrophic factor for midbrain dopaminergic neurons. *Science* 260, 1130-1132.

Linden, R. and Perry, V. H. (1983b). Retrograde and antero-transneuronal degeneration in the parabigeminal nucleus following tectal lesions in developing rats. *J. Comp. Neurol.* 218, 208-281.

Linden, R. and Perry, V.H. (1983a). Massive retinotectal projection in rats. *Brain Res.* 272, 145-149.

Lindvall, O. and Bjorklund, A. (1983). *Dopamine- and norepinephrine-containing neuron systems: Their anatomy in the rat brain.* In P.C. Emson (ed.) *Chemical neuroanatomy, pp.* 229-255. Raven Press, New York.

Lois, C. and Alvarez-Buylla, A. (1994). Long-distance neuronal migration in the adult mammalian brain. *Science* 264, 1145-1148.

Lumsden, A. and Keynes, R. (1989). Segmental patterns of neural development in the chick hindbrain. *Nature* 337, 635-647.

Luskin M. B. and Price J. L. (1983a). The topographic organization of associational fibers of the olfactory system in the rat, including centrifugal fibers to the olfactory bulb. *J. Comp. Neurol.* 216, 264-291.

Luskin, M. B. and Price, J. L. (1983b). The laminar distribution of intracortical fibers originating in the olfactory bulb of the adult hamster. *J. Comp. Neurol.* 216, 292-302.

Maas, R. (1996). Keeping an eye on eye development. *Nature Genetics* 12, 346-347.

Macdonald, R., Barth K. A., Xu, Q., Holder, N., Mikkola, I. and Wilson, S. W. (1995). Midline signalling is required for *Pax* gene regulation of the eyes. *Development* 121, 3267-3278.

Macdonald, R., Xu, Q., Barth, K. A., Mikkola, I., Holder, N., Fjose, A., Krauss, S. and Wilson, S. W. (1994). Regulatory gene expression boundaties demark at the sites of neuronal differentiation in the embryonic zebrafish forebrain. *Neuron* 13, 1039, 1053.

Mackay-Sim, A., Sefton, A. J. and Martin, P. R. (1983). Subcortical projections to lateral geniculate and thalamic reticular nuclei in hooded rat. *J. Comp. Neurol.* 213, 24-35.

MacKenzie, A., Leeming, G. L., Jowett, A. K., Ferguson, M. W. J. and Sharpe, P. T. (1991a). The homeobox gene *Hox-7.1* has specific regional and temporal expression patterns during early murine craniofacial embryogenesis, especially tooth development *in vivo* and *in vitro*. *Development* 111, 269-285.

MacKenzie, A., Ferguson, M. W. J. and Sharpe, P. T. (1991b). Hox-7 expression during murine craniofacial development. *Development* 113, 601-611.

MacKenzie, A., Ferguson, M. W. J. and Sharpe, P. T. (1992). Expression patterns of the homeobox gene, *Hox8*, in the mouse embryo suggest a role in specifying tooth development and shape. *Development* 115, 403-420.

Macrides, F. and Davis, B. J. (1983). The olfactory bulb. In P. C. Emson (ed.), *Chemical Neuroanatomy, pp.* 391-426. Raven Press, New York.

Maden, M. (1994a). Distribution of cellular retinoic acid-binding proteins I and II in the chick embryo and their relationship to teratogenesis. *Teratology* 50: 294-301.

Maden, M. (1994b). Vitamin A in embryonic development. *Nutritional Rev.* 52 (2): S3-S12.

Maden, M. and Holder, N.(1991). The involvement of retinoic acid in the development of the vertebrate central nervous system. *Development* (*Suppl.*) 2: 87-94.

Mahmood, R., Flanders, K. C. and Morris-Kay, G. M. (1992). Interactions between retinoids and TGF β_s in mouse morphogenesis. *Development* 115, 67-74.

Maisonpiere, P. C., Belluscio, L., Squinto, S., Ip, N. Y., Furth, M. E., Lindsay, R. M. and Yancopoulos, G. D. (1990). Neurotrophin-3: A neurotrophic factor related to NGF and BDNF. *Science* 247-1446-1451.

Marazzi, G., Wang, Y. and Sassoon, D. (1997). Msx2 is a transcriptional regulator in the BMP4-mediated programmed cell death pathway. *Developmental Biology* 186, 127-138.

Marshall, H., Nonchev, S., Sham, M. H., Muchmore, I., Lumsden, A. and Krumlauf, R. (1992). Retinoic acid alters hindbrain Hox code and induces transformation of rhombomeres 2/3 into 4/5 identity. *Nature* 360, 737-741.

Martin, P., Carriere, C., Dozier, C., Quatannens, B., Mirabel, M. -A., Vandenbunder, B., Stehelin, D. and Saule S. (1992). Characterization of a paired box- and homeobox-containing quail gene (Pax-QNR) expressed in the neuroretina. *Oncogene* 7: 1721-1728.

Martinez, G. S., Geijo, E., Sanchez-Vives, M. V., Puelles, E. and Gallego, R. (1992). Reduced junctional permeability at interrhombomeric boundaries. *Development* 116, 1069-1076.

Mason, R. and Groos, G. A. (1981). Cortico-recipient and tecto-recipient visual zones in the rat's lateral posterior (pulvinar) nucleus: An anatomical study. *Neurosci. Lett.* 25, 107-112.

Mastick, G. S. and Easter, S. S. Jr. (1996). Initial organization of neurons and tracts in embryonic mouse fore- and midbrain. *Dev. Biol.* 173, 79-94.

Mastick, G. S., Davis, N. M., Andrews, G. L. and Eastes, S. S. (1997). *Pax-6* functions in boundary formation and axon guidance in the embryonic mouse forebrain. *Development* 124, 1985-1997.

Matsuo, T., Osumi-Yamashita, N., Noji, S., Ohuchi, H., Koyama, E., Myokai, F., Matsuo, N., Taniguchi, S., Doi, H., Iseki, S., Nimomiya, Y., Fujiwara, M., Watanabe, T. and Eto, K. (1993). A mutation in the *Pax-6* gene in the *rat Small eye* is associated with impaired migration of midbrain crest cells. *Nature Genetics* 3, 299-304.

Matthews, M.A. (1973). Death of the central neuron: An electron microscopic study of thalamic retrograde degeneration following cortical ablation. *J. Neurocytol.* 2, 265-288.

Maulbecker, C. C. and Gruss, P. (1993). The oncogenic potential of *Pax* genes. *EMBO J.* 12, 2361-2367.

Mavillo, F. (1993). Regulation of vertebrate homeobox-containing genes by morphogens. *Eur. J. Biochem.* 212, 273-288.

McAvoy, J. W. and Chamberlain, C. G. (1990). Growth factors in the eye. *Prog. Growth Factor Res* 2, 29-43.

McCaffery, P., Posch, K. C., Napoli, J. L., Gudas, P. and Drager, U. C. (1993). Changing patterns of the retinoic acid system in the developing retina. *Dev. Biol.* 158: 390-399.

McGinnis, W. and Krumlauf, R. (1984). Homeobox genes and axial patterning. *Cell* 68, 283-302.

Meer-de Jong, R., Dickinson, M. E., Woychik, R. P., Stubbs, L., Hetherington, C. and Hogan, B. L. M. (1990). Location of the gene involving the small eye mutation on mouse chromosome 2 suggests homology with human *aniridia 2* (*AN2*). *Genomics* 7: 270-275.

Millhouse, O.E. and Heimer, L. (1984). Cell configurations in the olfactory tubercle of the rat. *J. Comp. Neurol.* 228, 571-597.

Mina, M. and Kola, E. J. (1987). The induction of odontogenesis in non-dental mesenchyme combined with early murine mandibular arch epithelium. *Arch. Oral. Biol.* 32, 123-127.

Moase, C. E. and Trasler, D. G. (1989). Spinal ganglia reduction in the *Splotch-delayed* mouse neural tube defect mutant. *Teratology* 40, 67-75.

Moase, C. E. and Trasler, D. G. (1990). Delayed neural crest emigration from *Sp* and Sp^{d} mouse neural tube explants. *Teratology* 42, 171-182.

Moase, C. E. and Trasler, D. G. (1993). N-CAM alterations in splotch neural tube defect mouse embryos. *Development* 113, 1049-1058.

Moline, M. L. and Sandlin, C. (1993). Waardenburg syndrome and meningomyelocele. *Am. J. Hum. Genet.* 47, 126.

Montero, V. M. and Guillery, R. W. (1968). Degeneration in the dorsal lateral geniculate nucleus of the rat following interruption of the retinal or cortical connections. *J. Comp. Neurol.* 134, 211-242.

Moore, K. L. (1988). *The Developing Human: Clinically Oriented Embryology. 4th ed.* W B Saunders Company.

Morris-Kay, G. M. (1993). Retinoic acid and craniofacial development: molecules and morphogenesis. *BioEssays* 15: 9-15.

Morris-Kay, G. M., Murphy, P., Hill, R. E. and Davidson, D. R. (1991). Effects of retinoic acid excess on expression of Hox 2.9 and Krox-20 and of morphological segmentation in the hindbrain of mouse embryos. *EMBO J.* 10, 2985-2995.

Morrison, J. H., Molliver, M. E., Grzanna, R. and Coyle, J. T. (1981). The intra-cortical trajectory of the coeruleo-cortical projection in the rat: A tangentially organized cortical afferent. *Neurosci.* 6, 139-158.

Mudhar, H. S., Pollock, R. A., Wang, C., Stiles, C. D. and Richardson, W. D. (1993). PDGF and its receptors in the developing rodent retina and optic nerve. *Development* 118: 539-552.

Munke, M., Cox, D. R., Jackson I. J., Hogan, B. L. M. and Francke, U. (1986). The murine *Hox-2* cluster of homeo box containing genes maps distal on chromosome 11 near the tail-short (*Ts*) locus. *Cytogenet. Cell Genet.* 42, 236-240.

Murray, E. A. and Coulter, J. D. (1982). Organization of tectospinal neurons in the cat and rat superior colliculus. *Brain Res.* 243, 201-214.

Muto, K., Nojis, S., Nohno, T., Koyama, E., Myokai, F., Hishijima, K., Saito, T. and Taniguchi, S. (1991). Involvement of retinoic acid and its receptor β in differentiation of motoneurons in chick spinal cord. *Neuroscience Lett.* 129: 39-42.

Narod, S. A., Siegel-Bartelt, J. and Hoffman, H. J. (1988). Cerebellar infarction in a patient with *Waardenburg sysdrome. Am. J. Hum. Genet.* 31, 903-907.

Nauta, W. J. H. and Bucher, V. M. (1954). Efferent connections of the striate cortex in the albino rat. *J. Comp. Neurol.* 100, 257-285.

Nelson, L. B., Spaeth, G. L., Nowinski, T. S., Margo, C. E. and Jackson, L. (1984). *Aniridia.* A review. *Surv.Opthalmol.* 28, 621-642.

New, D. A. T.(1955). A new technique for the cultivation of the chick embryo in vitro. *J. Embryol. Exp. Morphol.* 3: 326-331.

Niimi, K., Kaneseki, T. and Takimoto, T. (1963). The comparative anatomy of ventral nucleus of the lateral geniculate body in mammals. *J. Comp. Neurol.* 121, 313-323.

Noden, D. M. (1978). The control of the avian cephalic neural crest cytodifferentiation. *Dev. Biol.* 67, 296-312.

Noden, D. M. (1983). Origin and patterning of avian cephalic and cervical muscles and associated connective Tissue. *Am J Anat.* 168, 257-276.

Noden, D. M. (1983). The role of the neural crest in patterning of avian cranial skeletal, connective, and muscle tissues. *Dev. Biol.* 96, 144-165.

Noden, D. M. (1986). Origins and patterning of craniofacial mesenchyme tissues. *J. Craniofacial Genet. Dev. Biol. 2 (Suppl.)*,15- 31.

Noden, D. M. and de Lahunta, A. (1985). *The Embryology of Domestic Animals: Developmental Mechanisms and Malformations.* Williams & Wilkins Co. Blatimore.

Noll, M. (1993). Evolution and role of *Pax* genes. *Curr. Opin. Genet. Dev.* 3, 595-605.

Nomura, K. (1982). Differentiation of lens and pigment cells in cultures of brain cells of chick embryos. *Differentiation* 22, 179-184.

Nornes, H. O., Dressler, G. L., Knapik, E. W., Deutsch, U. and Gruss, P. (1990). Spatially and temporally restrcited expression of *Pax-2* during murine neurogenesis. *Development* 109, 797-809.
O'Rahilly, R. (1966). *Contributions to Embryology* 38, 1-42.

O'Rouke, N. A., Dailey, M. E., Smith, S. J. and McConnel, S. K. (1992). Diverse migratory pathways in the developing cerebral cortex. *Science* 258, 299-302.

O'Rahilly, B and Meyer, D. B. (1959). The early development of the eye in the chick. *Acta. Anat.* 36, 20-58.

Ohara, P. T. and Lieberman, A. R. (1981). Thalamic reticular nucleus: Anatomical evidence that cortical-reticular axons establish monosynaptic contact with reticulo-geniculate projection cells. *Brain Res.* 207, 153-156.

Okada, T. S. (1991). *Transdifferentiation: Flexibility in Cell Differentiation.* Oxford University Press, Oxford.

Oppenheim, R. W., Qin-Wei, Y., Prevette, D. and Yan, Q. (1992). Brain-derived neurotrophic growth factor rescues developing avian motoneurons from cell death. *Nature* 360, 755-757.

Osmond, M. K., Butler, A. J., Voon, F. C. T. and Bellairs, R. (1991). The effects of retinoic acid on heart formation in the early chick embryo. *Development* 113: 1405-1417.

Ottersen, O. P. (1982). Connections of the amygdala in the rat. IV. Corticoamygdaloid and intra-amygdaloid connections as studied with axonal transport of HRP. *J. Comp. Neurol.* 205, 30-48.

Pannet, C. A. and Compton, A. (1924). The cultivation of tissues in saline embryonic juice. *Lance*t 1: 381-384.

Pantke, O. A. and Cohen, M. M. Jr. (1971). The Waardenburg sysdrome. *Birth Defects: Original Article Series Vol. VII* (7) 147-152.

Papalopulu, N., Lovell-Badge, R., and Krumlauf, R. (1991). The expression of murine *Hox-2* genes is dependent on the differentiation pathway and displays collinear sensitivity to retinoic acid in F9 cells and *Xenopus* embryos. *Nucl. Acids Res.* 19, 5497-5506.

Pasquier, D. A. and Tremazzini, J. H. (1979). Afferent connections of the hypothalamic retrochiasmatic area in the rat. *Brain Res. Bull.* 4, 765-771.

Pasquier, J. G. and Villar, M. J. (1982). Subcortical projections to the lateral geniculate body in the rat. *Exp. Brain Res.* 48, 409-419.

Patten, B. M. (1971). *Early Embryology of the Chick, 5th ed.* McGraw-Hill Book Co. New York.

Paxinos, G. and Watson, C. (1982). *The Rat Brain in Stereotaxic Coordinates.* Academic Press, Sydney.

Pei, F. Y. and Rhodin, J. A. G. (1970). The prenatal development of the mouse eye. *Anat. Rec.* 168, 105-126.

Pelletier, J., Bruening, W., Li, F. P., Haber, D. A., Glaser, T. and Housman, D. E. (1991). *WTI* mutations contribute to abnormal genital system development and hereditary Wilm's tumor. *Nature* 353, 431-434.

Perry, V. H. (1980). A tectocortical visual pathway in the rat. *Neurosci.* 5, 915-927.

Perry, V. H. and Cowley, A. (1979). Changes in the retino-fugal pathways following cortical and tectal lesions in neonatal and adult rats. *Exp. Brain Res.* 35, 97-108.

Peters, H., Doll, U., and Niessing, J. (1995). Differential expression of the chicken *Pax-1* and *Pax-9* gene: *in situ* hybridization and immunochemical analysis. *Dev. Dyn.* 203: 1-16.

Peters, K. G., Werner, S., Chen, G., and Williams, L. T. (1992). Two FGF receptor genes are differentially expressed in epithelial and mesenchyme tissues during limb formation and organogenesis in the mouse. *Development* 114, 233-243.

Petrovicky, P. (1975). Projections from the tectum mesencephali to the brain stem structures in the rat. I. The superior colliculus. *Morphologica* 41-48.

Phelps, D. E. and Dressler, G. R. (1993). Aberrant expression of *Pax-2* in *Danforth's short tail* (*Sd*) mice. *Dev. Biol.* 157, 251-258.

Pilz, A. J., Povey, S., Gruss, P. and Abbott, C. M. (1993). Mapping of the human homologues of the murine paired-box-containing genes. *Mammalian Genome* 4: 78-82.

Pituello, F., Yamada, G. and Gruss, P. (1995). Activin A inhibits *Pax-6* expression and perturbs cell differentiation in the developing spinal cord *in vitro*. *Proc. Natl. Acad. Sci.USA* 92, 6952-6956.

Plachov, D., Chowdhury, K., Walther, C., Simon, D., Guenet, J. -L. and Gruss, P. (1990). *Pax8,* a murine paired box gene expressed in the developing excretory system and thyroid gland. *Development* 110, 643-651.

Placzek, M., Jessel, T. M. and Dodd, J. (1993). Induction of floor plate differentiation by contact-dependent homeogenetic signals. *Development* 117, 205-218.

Placzek, M., Tessier-Lavinge, M., Yamada, T., Jessell, T. and Dodd, J. (1990). Mesodermal control of neural cell identity: Floor plate induction by notochord. *Science* 250, 985-988.

Placzek, M., Yamada, T., Tessier-Lavinge, M., Jessel, T. and Dodd, J. (1991). Control of dorsoventral pattern in vertebrate neural development: induction and polarizing properties of the floor plate. *Development* (*Suppl.*) 2, 105-122.

Plaza, S., Grevin, D., MacLeod, K., Stehelin, D. and Saule, S. (1994). Pax-QNR/Pax-6, a paired- and homeobox-containing protein, recognizes Ets binding sites and can alter the transactivation properties of Ets transcription factors. *Gene Expression* 4, 44-52.

Poleev, A., Fickenscher, H., Mundlos, S., Winterpacht, A. and Zabel, B. (1992). *PAX8*, a human paired box gene: isolation and expression in developing thyroid, kidney, and Wilms' tumor. *Development* 116, 611-623.

Price, D. J. (1991). The development of visual cortical afferents. In: (Cronly-Dillon J. R. ed.) *Development and Plasticity of the Visual System, pp.* 337-345.

Price, J. L. (1973). An autographic study of complementary laminar patterns of termination of afferent fibers to the olfactory cortex. *J. Comp. Neurol.* 150, 87-108.

Price, J. L. and Slotnick, B. M. (1983). Dual olfactory representation in the rat thalamus: An anatomical and electrophysical study. *J. Comp. Neurol.* 215, 63-77.

Pritchard, D. J. and Clayton, R. M. (1974). Abnormal lens capsule carbohydrate associated with the dominant gene "Small-eye" in the mouse. *Exp Eye Res* 19, 335-340.

Pueles, L. and Rubenstein, J. L. R. (1993). Expression patterns of homeobox and other putative regulatory genes in the embryonic mouse forebrain suggests a neuromeric organization. *Trends Neurosci* 16, 472-479.

Purves, D. and Lichtman, J. W. (1985). *Principles of Neural Development.* Sinauer Associates, Sunderland MA.

Puschel, A. W., Gruss, P. and Westerfield, M. (1992). Sequence and expression pattern of *Pax-6* are highly conserved between zebrafish and mouse. *Development* 114, 643-651.

Quinlan, G. A., Williams, E. A., Tan, S.-S. and Tam, P. P. L. (1995). Neuroectodermal fate of epiblast cells in the distal region of the mouse egg cylinder: implication for body plan organization during early embryogenesis. *Development* 121, 87-98.

Quinn, J. C., West, J. D. and Hill, R. E. (1996). Multiple functions for *Pax6* in mouse eye and nasal development. *Genes & Development* 10, 435-446.

Quiring, R., Walldorf, U., Kloter, U. and Gehring, W. J. (1994). Homology of the eyeless gene of *Drosophila* to the small eye gene in mice and *Aniridia* in humans. *Science* 265, 785-789.

Raff, M., Barres, B. A., Burne, J. F., Coles, H. S., Ishizaki, Y. and Jacobson, M. D. (1993). Programmed cell death and the control of cell survival: Lessons from the nervous system. *Science* 262, 695-700.

Ragsdale, C. W. and Brockes, J. P. (1991). Retinoids and their targets in vertebrate development. *Curr. Opin. Cell Biol.* 3:928-934.

Rakic, P. (1972). Mode of cell migration to superficial layers of fetal monkey neocortex. *J. Comp. Neurol.* 145, 61-84.

Rakic, P. (1974). Neurons in rhesus visual cortex: Systematic relation between time of origin and eventual deposition. *Science* 183, 425-427.

Rakic, P. (1975). Cell migration and neuronal ectopias in the brain. *In* (D. Bergsma ed.) *Morphogenesis and Malformations of Face and Brain. Birth Defect Original Article Series II* 7, 95-129.

Rakic, P. and Goldman, P.S. (1982). Development and modifiability of the cerebral cortex. *Neurosci. Rev.* 20, 429-611.

Rakic. P. and Sidman, R. L. (1973). Organization of cerebellar cortex secondary to deficit of granule cells in *weaver* mutant mice. *J. Comp. Neurol.* 152, 133-162.

Read, A. P. (1995). *Pax* genes- paired feet in three camps. *Nature Genet.* 9, 333-334.

Rhodes, R. W. and Fish, S. E. (1982). Altered organization of intercollicular pathway in bilaterally enucleated hamsters. *Dev. Brain Res.* 4, 356-360.

Ribak, C. E. (1977). A note on the laminar organization of rat visual cortical projections. *Exp. Brain Res.* 27, 413-418.

Ribak, C.E. and Peters, A. (1975). An autoradiographic study of the projections from the lateral geniculate body of the rat. *Brain Res.* 92, 341-368.

Rickman, M., Fawcett, J. W. and Keynes, R. J. (1985). The migration of neural crest cells and the growth of motor axons through the rostral half of the chick somite. *J. Embryol. Exp. Morphol.* 90, 437-455.

Riddle, R. D., Johnson, R. L., Laufer, E., and Tabin, C. (1993). *Sonic hedgehog* mediates the polarizing activity of the ZPA. *Cell* 75, 1401-1416.

Rio-Tsonis K. D.., Washabaugh, C. H. and Rsonis, P. A. (1995). Expression of *Pax-6* during urodele eye development and lens regeneration. *Proc. Natl. Acad. Sci. U.S.A.* 92, 5092-5096.

Robert, B., Sassoon, D., Jacq, B., Gehring, W. and Buckingham, M. (1989). *Hox-7*, a mouse homeobox gene with a novel pattern of expression during embryogenesis. *EMBO J.* 8, 91-100.

Roberts, R. C. (1967). *Small eye*- a new dominant mutation in the mouse. *Genet. Res. Camb.* 9, 121-122.

Robertson , R. T. (1983). Efferents of the pretectal complex: Separate populations of neurons project to lateral thalamus and to inferior olive. *Brain Res.* 258, 91-95.

Robinson, S. R., Chaffee, S. and Galton, V. (1986). Nuclear movement during the cell cycle in the kitten retina. *Naurosci. Lett. (Suppl.)* 23, S27.

Roelink, H., Augsburger, A., Heemskerk, J., Korzh, V., Norlin, S., Ruiz, I., Altaba, A., Tanabe, Y., Placzek, M., Edlung, T., Jessel, T. and Dodd, J. (1994). Floor plate and motor neuron induction by vhh, a vertebrate homolog of hedgehog expressed by notochord. *Cell* 76, 761-775.

Rogers, M. B., Rosen, V., Wozney, J. M. and Gudas, L. J. (1992). Bone morphogenetic proteins-2 and -4 are involved in the retinoic acid-induced differentiation of embryonal carcinoma cells. *Mol. Biol. Cell* 3, 189-196.

Rothenpieler, U. W. and Dressler, G. R. (1993). *Pax-2* is required for mesenchyme-to-epithelium conversion during kidney development. *Development* 119, 711-720.

Rowe, A., Eager, N. S. G. and Brickell, P. M. (1991). A member of the RXR nuclear receptor family is expressed in neural crest-derived cells of the developing chick peripheral nervous system. *Development* 111, 771-778.

Rowe, A., Richman, J. M. and Brickell, P. M. (1992). Development of the spatial pattern of retinoic acid receptor-β transcripts in embryonic chick facial primordia. *Development* 114, 805-813.

Rubenstein, L. R. and Puelles, L. (1993). Expression patterns of homeobox and other putative regulatory genes in the embryonic mouse fore brain suggest a neuromeric organization. *Trends Neuro. Sci.* 16, 472-479.

Ruizi i Altaba, A. and Jessel, T. M. (1991). Retinoic acid modifies the pattern of cell differentiation in the central nervous system of neurula stage *Xenopus* embryos. *Development* 112, 945-958.

Russel, W. L. (1947). *Splotch*, a new mutation in the house mouse *Mus musculus*. *Genetics* 32, 107.

Ryan, G., Steel-Perkins, V., Morris, J. F., Rauscher, F. J. III and Dreessler, G. R. (1995). Repression of *Pax-2* by *WTI* during normal kidney development. *Development* 121, 867-875.

Saha, M. S., Spann, C. L. and Grainger, R. M. (1989). Embryonic lens induction: more than meets the optic vesicle. *Cell Different. Dev.* 28, 153-172.

Sanyanusin, P., Schimmenti, L. A., McNoe, L. A., Ward, T. A., Pierpoint, M. E. M., Sullivan, M. J., Dobyns, W. B. and Eccles, M. R. (1995). Mutation of the *PAX2* gene in a family with optic nerve colobomas, renal anomalies and vesicoureral reflux. *Nature Genet.* 9, 358-364.

Saper C. B. (1982). Convergence of autonomic and limbic connections in the insular cortex of the rat. *J. Comp. Neurol.* 210, 163-173.

Satokata, I. and Maas, R. (1994). *Msx-1* deficient mice exhibit cleft papate and abnormalities of craniofacial and tooth development. *Nature Genetics* 6, 348-356.

Sax, C. M. and Piatigorsky, J. (1994). Expression of the α-crystallin/small heat shock protein/molecular chaperone genes in the lens and other tissues. *Adv. Enzymol. Relat. Areas Mol. Biol.* 69, 155-201.

Scalia, F. and Arango, V. (1979). Topographic organization of the projections of the retina to pretectal region in the rat. *J. Comp. Neurol.* 186, 271-292.

Scalia, F. and Winas, S. S. (1975). The differential projections of the olfactory bulb and accessory olfactory bulb in mammals. *J. Comp. Neurol.* 161, 31-56.

Scheibel, M. E. and Scheibel, A. B. (1966). The organization of the nucleus reticularis thalami: A Golgi study. *Brain Res.* 1, 43-62.

Schmahl, W., Knoedlseder, M., Favor, J. and Davidson, D. (1993). Defects in neuronal migration and the pathogenesis of cortical malformations are associated with *Small eye* (*Sey*) in the mouse, a point mutation at the *Pax-6* locus. *Acta Neuropathol.* 86, 126-135.

Schmidt, M. and Kater, S. B. (1993). Fibroblast growth factors, depolarization, and substrate interact in a combinatorial way to promote neuronal survival. *Dev. Biol.* 158, 228-237.

Schober, W. (1981). Efferente und afferente Verbindungen des Nucleus lateralis posterior thalami (''Pulvinar'') der Albinoratten. *Z. mikrosk. -anat. Forsch.* 95, 827-844.

Schoenwolf, G. C. and Smith, J. L. (1990). Mechanisms of neurulation: traditional viewpoint and recent advances. *Development* 109, 243 - 270.

Schofield, J. N., Rowe, A. and Brickell, P. M. (1992). Position-dependence of retinoic acid receptor-β gene expression in the chick limb bud. *Dev. Biol.* 152: 344-353.

Schwanzel-Fukuda, M. and Pfaff, D. W. (1990). The migration of Leuteinizing hormone-releasing hormone (LHRH) neurons from the medial nasal placode into the medial basal forebrain. *Experimentia* 46, 956-962.

Scott, M. and Weiner, A. J. (1984). Structural relationships among genes that control development: sequence homology between the *Antennapedia*, *Ultrabithorax*, and *fishi tarazu* loci of *Drosophila*. *Proc. Natl. Acad. Sci. USA* 81, 4115-4119.

Scott, M. P., Weiner, A. J., Hazelrigg, T. I., Polinsky, B. A., Pirrota, V., Scalenghe, F. and Kaufman, T. C. (1983). The molecular organization of the *Antennapedia* locus of *Drosophila. Cell* 35, 763-776.

Scotting, P., McDermott, H. and Mayer, R. J. (1991). Ubiquitin-protein conjugates and ∝B crystallin are selectively present in cells undergoing major cytomorphological organization in early chick embryos. *FEBS* 285: 75-79.

Sefton, A. J. (1968). The innervation of the lateral geniculate nucleus and anterior colliculus in the rat. *Vision Res.* 8, 867-881.

Sefton, A. J. and Dreher, B. (1985). Visual system. In: Paxinos, G. (ed.)*The Rat Nervous System.* Academic Press.

Sefton, A. J. and Martin, P. R. (1984). Relations of the parabigeminal nucleus to the superior colliculus and lateral geniculate nucleus in the hooded rat. *Exp. Brain Res.* 57, 107-117.

Sefton, A. J., Mackay-Sim, A., Baur, L.A. and Cottee, L. J (1981). Cortical projections to visual centres in the rat: An HRP study. *Brain Res.* 215, 1-13.

Sendtner, M., Schmalbruch, H., Stöckli, K. A., Carroll, P., Kreutzberg, G. W. and Thoenen, H. (1992). Ciliary neurotrophic factor prevents degeneration of motor neurons in mouse mutant progressive motor neuropathy. *Nature* 358, 502-504.

Serafini, T., Kennedy, T. E., Galko, M. J., Mirzayan, C., Jessel, T. M. and Tessier-Lavigne, M. (1994). The neurites define a family of axon-outgrowth promoting proteins homologous to *C. elegans* UNC-6. *Cell* 78, 409-424.

Serbedzija, G., Bronner-Fraser, M. and Fraser, S. E. (1992). Vital dye analysis of cranial neural crest cell migration in the mouse embryo. *Development* 116, 297-307.

Shapiro, D. N., Sublett, J. E., Li, B., Downing , J. R. and Naeve, C. W. (1993). Fusion of PAX3 to a member of the Forkhead family of transcription factors in human alveolar rhabdomyosarcoma. *Cancer Res.* 53, 5108-5112.

Shaw, M. W., Falls, H. F. and Neel, J. V. (1960). *Am. J. Hum. Genet.* 12, 389-415.

Shawlot, W. and Behringer, R. R. (1995). Requirement for *Lim1* in head-organizer function. *Nature* 347, 425-430.

Shipley, M. T. and Adamek, G. D. (1984). The connections of the mouse olfactory bulb: A study using orthograde and retrograde transport of wheatgerm agglutinin conjugated to horseradish peroxidase. *Brain Res. Bull.* 12, 669-688.

Shipley, M. T. and Geinisman, Y. (1984). Anatomical evidence for convergence of olfactory, gustatory, and visceral afferent pathways in mouse cerebral cortex. *Brain Res. Bull.* 8, 493-501.

Sidman, R. L. (1961). In *Structure of the Eye.* (ed. Smelser, G. K.) *pp.* 487-506. N.Y.:Academic Press.

Silver, J. and Robb, R. M. (1979). Studies of the development of the eye cup and optic nerve in normal mice and in mutants with congenital optic nerve aplasia. *Dev. Biol.* 68, 175-190.

Simenoe, A., Acampora, D., Arcioni, L., Andrews, P. W., Boncielli, E. and Mavilio, F. (1990). Sequential activation of *Hox2* homeobox genes by retinoic acid in human embryoal carcinoma cells. *Nature* 346, 763-766.

Simeone, A., Acamora, D., Nigro, V., Faiella, A., D'Esposito, M., Stornaiuolo, A., Mavilio, F. and Boncielli, E. (1991). Differential regulation by retinoic acid of the homeobox genes of the four *HOX* loci in human embryonal carcinoma cells. *Mech. Dev.* 33, 215-227.

Simon, H., Hornbruch, A. and Lumsden, A. (1995). Independent assignment of antero-posterior and dorso-ventral positional values in the developing chick hindbrain. *Current Biology* 5, 205-214.

Sive, H. L. and Cheng, P. F. (1991). Retinoic acid perturbs the expression of *Xhox.1ab* genes and alters mesodermal determination in *Xenopus* laevis. *Genes Dev.* 5, 1321-1332.

Sive, H. L., Drapper, B. W. and Weintraub, H. (1990). Identification of a retinoic acid-sensitive period during primary axis formation in *Xenopus laevis*. *Genes Dev.* 4, 932-942.

Skow, L. C., Donner, M. E., Huang, S.-M., Gardner, J. M. and Taylor, B. A. (1988). Mapping of the mouse gamma crystallin genes on chromosome 1. *Biochem. Genet* 26, 557-580.

Smith, S. M. and Eichele,G. (1991). Temporal and regional differences in the expression pattern of distinct retinoic acid receptor-β transcripts in the chick embryo. *Development* 111, 245-252.

Speman, H. (1938). *Embryonic Development and Induction.* Yale University Press, New Haven.

Sporn, M. B., Roberts, A. B. and Goodman, D. S. (1994). The retinoids, Second Edition, M. B. Sporn, A. B. Roberts, and G. S. Goodman eds. (Raven Press: New York), pp. 319 -350.

Spratt, N. T. Jr. (1946). Formation of the primitive streak in the explanted chick blastoderm marked with carbon particles. *J. Exp. Zool.* 103, 259-304.

Stapelton, P., Weith, A., Urbanek, P., Kozmik, Z. and Busslinger, M. (1993). Chromosomal localization of seven *PAX* genes and cloning of a novel family member, *PAX-9. Nature Genet.* 3, 292-298.

Stein, B. E. (1981). Organization of the rodent superior colliculus: Some comparisons with other mammals. *Behav. Brain Res.* 3, 175-188.

Steinbusch, H. W. M. (1981). Distribution of serotonin immunoreactivity in the central nervous system of the rat cell bodies and terminals. *Neurosci.* 6, 557-618.

Steindler, D. A., Cooper, N. G. F., Faissner, A. and Schachner, M. (1989). Boundaries defined be adhesion molecules during development of the cerebral cortex: The J1:tenasin glycoprotein in the mouse somatosensory cortical barrel field. *Dev. Biol.* 131, 243-260.

Stern, C. D. (1990). The marginal zone and its contribution to the hypoblast and primitive streak of the chick embryo. *Development* 109, 667-682.

Stevenson, J. A. and Lund, R. D. (1982a). A crossed parabigeminal-lateral geniculate projection in rats blinded at birth. *Exp. Brain Res.* 45, 95-100.

Stevenson, J. A. and Lund, R. D. (1982b). Alterations of the crossed parabihgeminal projection induced by neonatal eye removal in rats. *J. Comp. Neurol.* 207, 191-202.

Stone, J. (1983). *Parallel processing in the visual system: The classification of retinal ganglion cells and its impact on the neurobiology of vision.* Plenum, New York.

Storey, K. G., Crossley, J. M., De Robertis, E. M., Norris, W. E. and Stern, C. D. (1992). Neural induction and regionalization in the chick embryo. *Development* 114, 729-741.

Stoykova, A. S. and Gruss, P. (1994). Roles of *Pax* genes in developing and adult brain as suggested by expression patterns. *J. Neurosci.* 14, 1395-1412.

Stoykova, A., Fritsch, R., Walther, C. and Gruss, P. (1996). Forebrain patterning defects in *Small eye* mutant mice. *Development* 122, 3453-3465.

Stuart, E. T., Kioussi, C. and Gruss, P. (1994). Mammalian Pax genes. *Annu. Rev. Genet.* 28, 219-236.

Sulick, K. K. and Dehart, D. B. (1988). Retinoic acid -induced limb malformations resulting from apical ectodermal ridge cell death. *Teratology* 37, 527-523.

Sulick, K. K., Cook, C. S. and Webster, W. S. (1988). Teratogens and craniofacial malformations: relationships to cell death. *Development* 103 (*Suppl.*), 213-232.

Sumitomo, I., Sugitani, M., Fukuda, Y. and Iwama, K. (1979). Properties of cells responding to visual stimuli in the rat ventral lateral geniculate nucleus. *Exp. Neurol.* 66, 721-736.

Switzer R. C., De Olmos, J. and Heimer, L. (1985). Olfactory system. In: *The Rat Nervous System Vol 1* (**Paxinos, D. ed.**), Academic Press.

Takahashi, T. (1985). The organization of the lateral thalamus of the hooded rat. *J. Comp. Neurol.* 231, 281-309.

Tam, P. P. L. and Beddington, R. S. P. (1992). Establishment and organization of germ layers in the gastrulating mouse embryo. In: *Postimplantation Development in the Mouse. CIBA Symposium no. 165.*

Tamarin, A., Crawley, A., Lee, J. and Tickle, C. (1984). Analysis of upper beak defects in chicken embryos following with retinoic acid. *J. Embryol. Exp. Morphol.* 84, 105-123.

Tan, S. S. and Breen, S. (1993). Radial mosaicism and tangential cell dispersion both contribute to mouse neocortical development. *Nature* 362, 638-640.

Tan, S. S. and Morris-Kay, G. M. (1986). Analysis of cranial neural crest cell migration and early fates in postimplantation rat chimaeras. *J. Embryol. Exp. Morphol.* 98, 21-58.

Tassabehji, M., Read, A. P., Newton, V. E., Harris, R., Balling, R., Gruss, P. and Strachan, T. (1992). *Waardenburg's syndrome* patients have mutations in the human homologue of the *Pax-3* paired box gene. *Nature* 355, 635-636.

Tassabheji, M., Read, A. P., Newton, V. E., Patton, M., and Gruss, P. Mutations in the PAX-3 gene causing Waardenburgh syndrome type 1 and type 2. *Nature Genet.*3, 26-30.

Teillet, M. -A., Kalcheim, C. and Le Douarin, N. M. (1987). Formation of the dorsal root ganglia in the avian embryo: Segmental origin and migratory behaviour of neural crest progenitor cells. *Dev. Biol.* 120, 329-347.

Terasawa, K., Otani, K., and Yamada, J. (1979). Descending pathways of the nucleus of the optic tract in the rat. *Brain Res.* 173, 405- 417.

Tessier-Lavinge, M., Plazek, M., Dodd, J. and Jessel, T. M. (1988). Chemotropic guidance of developing axons in the mammalian central nervous system. *Nature* 336, 775-778.

Thaller, C. and Eichele, G. (1987). Identification and spatial distribution of retinoids in the developing chick limb bud. *Nature* 327, 625-628.

Thaller, C.and Eichele, G. (1990). Isolation of 3,4-didehydroretinoic acid, a novel morphogenetic signal in the chick wing bud. *Nature* 345: 815-819.

Theiler, K. and Varnum, D. S. (1981). Development of *Coloboma* (*Cm/+*), a mutation with anterior lens adhesion. *Anat Embryol* 162: 121-126.

Theiler, K., Varnum, D. S., Stevens, L. C. (1987). Development of *Dickie's Small eye*, a mutation in the house mouse. *Anat Embryol* 155, 81-86.

Thesleff, I., Vaahtokari, A. and Partanen, A. -M. (1995). Regulation of organogenesis. Common molecular mechanisms regulating the development of teeth and other organs. *Int. J. Dev. Biol.* 39, 35-50.

Thorogood, P., Smith, L., Nicol, R., McGinty, R. and Garrod, D. (1982). Effects of vitamin A on the behaviour of migratory neural crest cells in vitro. *J. Cell Sci.* 57, 331-350.

Tickle, C. (1991). Retinoic acid and chick limb bud development. *Development* (*Suppl.*) 1, 113-121.

Tickle, C., Alberts, B., Wolpert, L. and Lee, J. (1982). Local application of retinoic acid to the limb bond mimics the action of the polarizing region. *Nature* 296, 564-566.

Timmons, P. M., Wallin, J., Rigby, P. W. J. and Balling, R. (1994). Expression and function of Pax1 during development of the pectoral girdle. *Development* 120, 2773-2785.

Ton, C. C. T., Hiroshi, M. and Grady, F. S. (1992). *Small eye* (*Sey*): cloning and characterization of the murine homolog of the human aniridia gene. *Genomics* 13, 251-256.

Ton, C. C. T., Hirvonen, H., Miwa, H., Weil, M. W., Monaghan, P., Jordan, T., van Heyningen, V., Hastie, N. D., Meijers-Heijboer, H., Dreschler, M., Royer-Pokora, B., Collins, F., Swaroop, A., Strong, L. C. and Saunders, G. F. (1991). Positional cloning and characterization of a paired box-homeobox-containing gene from the aniridia region. *Cell* 67, 1059-1074.

Travis, J. (1994). Axon guidance: Wiring the nervous system. *Science* 266, 568-570.

Treisman, J., Gonczy, P., Vashishita, M., Harris, E. and Desplan, C. (1989). A single amino acid can determine the DNA binding specificity of homeodomain proteins. *Cell* 59, 553-562.

Treisman, J., Harris, E. and Desplan, C. (1991). The paired box encodes a second DNA-binding domain in the Paired homeo domain protein. *Genes Dev.* 5, 594-604.

Tripathi, B. J., Tripathi, R. C., Livingston, A. M. and Borisuth, N. S. C. (1991). The role of growth factors in the embryogenesis and differentiation of the eye. *Am. J. Anat.* 192, 442-471.

Trisler, D. (1991). Cell recognition molecules and pattern formation in the developing visual system. In *Vision and Visual Dysfunction vol 11*(ed. Cronly-Dillon, J. R.), Macmillam Press.

Tsukamoto, K, Nakamura, Y. and Niikawa, N. (1994). Isolation of two isoforms of the *PAX3* gene transcripts and their tissue-specific alternative expression in human adult tissues. *Hum. Genet.* 93, 270-274.

Tsukamoto, K., Tohma, T., Ohta, T., Yamakawa, K. and Fukushima, Y. (1992). Cloning and characterization of the inversion breakpoint at chromosome 2q35 in a patient with *Waardenburgh syndrome type I. Hum Genet* 91, 315-317.

Turner, D. L. and Cepko, C. L. (1987). A common progenitor for neurons and glia persists in rat retina late in development. *Nature* 328, 131-136.

Turque, N., Plaza, S., Radvanyi, F., Carriere, C. and Saule, S. (1994). *Pax-QNR/Pax-6,* a paired box- and homeobox-containing gene expressed in neurons, is also expressed in pancreatic endocrine cells. *Mol. Endo.* 8, 929-938.

Twal, W., Roze, L. and Zile, M. H. (1995). Anti-retinoic acid monoclonal antibody localizes All-trans-retinoic acid in target cells and blocks normal development in early quail embryo. *Dev. Biol.* 168, 225-234.

Underhill, T. M., Kotch, L. E. and Linney, E. (1995). Retinoids and mouse embryonic development. *Vitamin.. Hormon.* 51, 403-457.

Updyke, B. V. (1983). A reevaluation of the functional organization and cytoarchitecture of the feline lateral posterior complex, with observations on adjoining cell groups. *J. Comp. Neurol.* 219, 143-181.

Urbanek, P., Wang, Z.-Q, Fetka, I., Wagner, E.F. and Busslinger, M. (1994). Complete block of early B cell differentiation and altered patterning of the posterior midbrain in mice lacking Pax5/BSAP. *Cell* 79, 901-912.

Vaage, S. (1969). The segmentation of the primitive neural tube in chick embryos (*Gallus domestics*). *Adv. Anat. Embryol. Cell Biol.* 41, 1-88.

Vaahtokari, A., Aberg, T. and Thesleff, I. (1996). Apoptosis in the developing tooth: association with an embryonic signalling center and suppression by EGF and FGF-4. *Development* 122, 121-129.

Vaessen. M. -J., Carel Meijers, J. H., Bootsma, D. and Geurts, V. A. D. (1990). The cellular retinoic-acid-binding protein is exprressed in tissues associated with retinoic-acid-induced malformations. *Development* 110, 371-378.

Vainio, S., Karavanova, I., Jowett, A. and Thesleff, I. (1993). Identification of BMP-4 as a signal mediating secondary induction between epithelial and mesenchymal tissues during tooth development. *Cell* 75, 45-58.

Veening, J. G. (1978). Cortical afferents of the amygdaloid complex in the rat, an HRP study. *Neurosci. Lett.* 8, 191-195.

Vogan, K.L., Epstein, D. J., Trasler, D. G. and Gros, P. (1993). The *splotch -delayed* (Sp^d) mouse mutant carries a point mutation within the *paired* box of the *Pax-3* gene. *Genomics* 17, 364-9.

Waardenburg, P. (1951). A new syndrome combining developmental anomalies of the eyelids, eyebrows, and nose root with congenital deafness. *Am. J. Hum. Genet.* 3, 195-253.

Waddington, C. H. (1933). Induction by the primitive streak and its derivatives in the chick. *J. Exp. Biol.* 10, 38-46.

Wagner, M., Thaller, C.,Jessel, T. and Eichele, G. (1990). Polarizing activity and retinoid synthesis in the floor plate of the neural tube. *Nature* 345: 819-822.

Wakatsuki, Y. W., Neurath, M. F., Max E.E., and Strober, W. (1994). The B-cell specific transcription factor BSAP regulates B cell proliferation. *J. Exp. Med.* 179, 1099-1108.

Waldron, H. A. and Gwyn, D. G. (1969). Descending nerve tracts in the spinal cord of the rat. I. Fibers from the midbrain. *J. Comp. Neurol.* 60, 237-270.

Wallin, J., Wilting, J., Koseki, H., Fritsch, R., Christ, B., and Balling, R. (1994). The role of *Pax-1* in axial skeleton development. *Development* 120, 1109-1121.

Walsh, C. and Cepko, C. L. (1988). Clonally related cortical cells show several migration patterns. *Science* 241, 1342-1345.

Walsh, C. and Cepko, C. L. (1992). Wide-spread dispersion of neuronal clones across functional regions of the cerebral cortex. *Science* 255, 434-440.

Walsh, C. and Cepko, C. L. (1993). Clonal dispersion in proliferative layers of developing cerebral cortex. *Nature* 362, 632-635.

Walther, C. and Gruss, P. (1991). *Pax-6*, a murine paired box gene, is expressed in the developing CNS. *Development* 113, 1435-1449.

Walther, C., Guenet, J.-L. , Simon, D., Deutsch, U., Jostes, B., Goulding, M.D., Plachov, D., Balling, R. and Gruss, P. (1991). *Pax*: a murine multigene family of paired box containing genes. *Genomics* 11: 424-434.

Warren, N. and Price, D. J. (1997). Roles of *Pax-6* in murine diencephalic development. *Development* 124, 1573-1582.

Watanabe, K. and Kawana, E. (1979). Efferent projections of the parabigeminal nucleus in rats: A horseradish peroxidase (HRP) study. *Brain Res.* 168, 1-11.

Wedden, S. E. (1987). Epithelial-mesenchymal interactions in the development of chick facial primordia and the target of retinoid action. *Development* 99, 341-351.

White, L. E. Jr. (1965). Olfactory bulb projections of the rat. *Anat. Rec.* 152, 465-480.

Wilkinson, D., Bhatt, S., Chavrier, P., Bravo, R. and Charnay, P. (1989). Segmental expression of hox2 homeobox-containing genes in the developing mouse hindbrain. *Nature* 341, 405-409.

Williams, P. L. and Warwick, R. (1982). *Gray's Anatomy* (36th. ed.), Churchill Livingston.

Wistow, G. (1993). Lens crystallins: gene recruitment and evolutionary dynamism. *Trends Biochem. Sci.* 18: 301-306.

Wolpert, L. (1969). Positional information and the spatial pattern of cellular differentiation. *J. Theoret. Biol.* 25, 1-47.

Wright, A. F. (1992). New insights into genetic eye disease. *Trends Genet.*8, 85-91.

Wright, C. V. E. (1991). Vertebrate homeobox genes. *Curr. Opin. Cell Biol.* 3, 976-982.

Wright, M. E. (1947). *Undulated*: A new genetic factor in *Mus musculus* affecting the spine and tail. *Heredity* 1, 137-141.

Xu, P.-X., Woo, I., Her, H., Beier, D. R., and Maas, R. L. (1997). Mouse *Eya* homologues of the *Drosophila eyes absent* gene require *Pax6* for expression in lens and nasal placode. *Development* 124, 219-231.

Xu, W., Rould, M. A., Jun, S., Desplan, C., and Pabo, C. O. (1995). Crystal structure of a paired domain-DNA complex at 2.5 A resolution reveals structural basis for Pax developmental mutations. *Cell* 80, 639-650.

Yamada, G., Kioussi, C., Schubert, F. R., Eto., Y., Chowdhury, K., Pituello, F. and Gruss, P. (1994). Regulated expression of *Brachyury(T)*, *Nkx1.1* and *Pax* genes in embryoid bodies. *Biochem. Biophy. Res. Comm.* 199, 552-563.

Yamadori, T. (1981). An experimental anatomical study on the optic nerve fibers in the rat by using a new selective silver impregnation technique: Termination of the main optic tract. *Okajimas Fol. Jap.* 54, 229-246.

Young, W. D., Alheid, G. F. and Heimer, L. (1984). The ventral pallidal projection to the mediodorsal thalamus: A study with fluorescence retrograde tracers and immunohistofluorescence. *J. Neurosci.* 4, 1626-1638.

Zannini, M., Francis-Lang, H., Plachov, D. and Di Lauro, R. (1992). *Pax-8* , a paired domain-containing protein, binds to a sequence overlapping the recognition site of a homeodomain and activates transcription from two thyroid-specific promotors. *Mol. Cell Biol.* 12, 4230-4241.

Zavarzin, A. A. and Stroeva, O.G. (1964). In *A study of cell cycles and Metabolism of Nucleic Acid during Differentiation of the Cells.* eds. Zhinkhin, L.N. and Zavarzin, A.A. pp. 116-125. Moscow:Nauka.

Zhang, Y. and Emmons, S. E. (1995). Specification of sense-organ identity by a *Caenorhabditis elegans Pax-6* homologue. *Nature* 377, 55-59.

Zhang, Z. Y., Balmer, J. E., Lovlie, A., Fromm, S. H. and Blomhoff, R. (1996). Specific teratogenic effects of different retinoic acid isomers and analogs in the developing anterior central-nervous-system of zebrafish. *Developmental Dynamics* 206, 73-86.

Zilles, K.. and Wree, A. (1985). Cortex: areal and laminar structure. In: *The Rat Nervous System* (Paxinos, G. ed.), *pp.* 375-392.

Appendix

A. List of Abbreviations

ABC	avidin-biotinylated enzyme-complex
bp	base pair
BSA	bovine serum albumin
depc	diethyl pyrocarbonate
DIG	digoxgenin
DMSO	dimethyl sulfoxide
EDTA	ethylenediaminetetraacetic acid
FCS	fetal calf serum
IgG	immunoglobulin G
kb	kilobase
NBT	nitroblue tetrazolium
OD	optical density
PBS	phosphate-buffered saline
PBT	phosphate buffered saline with 0.1% Tween 20
PCR	polymerase chain reaction
rpm	revolutions per minute
SDS	sodium dodecyl sulphate
SSC	standard saline citrate
STE	sodium chloride-Tris.Cl-EDTA
TAE	tris-acetate-EDTA
TBS	tris-buffered saline
TE	tris-EDTA buffer
TEA	triethanolamine
TESPA	3-aminopropyltrimethoxy-silane
Tween 20	polyoxyethylenesorbitan monolaurate
BCIP	5-bromo-4-chloro-3-indolyl phosphate

B. Recipes and preparations:

1. LB (Luria-Bertani) medium (from Sambrook et al., 1989):

To 950 ml H_2O add:

10 g bacto-tryptone
5 g bacto-yeast extract
10 g NaCl

Adjust to pH 7.4 with 1 N NaOH
Add H_2O to 1 liter; autoclave to sterilized

2. Terrific Broth (from Tartof and Hobbs, 1987):

To 900 ml of deionized H_2O, add:

bacto-tryptone, 12 g
bacto-yeast extract, 24 g
glycerol, 4 ml

Shake until the solutes have dissolved and sterilize by autoclaving for 20 minutes at 15 lb/sq. in. on liquid cycle. Allow the solution to cool to 60° C or less, and then add 100 ml of 0.17 M KH_2PO_4, 0.72 M K_2HPO_4.

3. Ehrlich's haematoxylin (from Culling et al., 1985):

Haematoxylin	6 g
Absolute alcohol	300 ml
Distilled water	300 ml
Glycerol	300 ml
Glacial acetic acid	30 ml
Potassium alum- to saturation	10 - 14 g

The haematoxylin should be fully dissolved in the alcohol before the other ingredients are added.

4. Solutions for large-scale plasmid preparation (from Sambrook et al., 1989):

Solution I:

50 mM glucose
25 mM Tris.Cl (pH 8.0)
10mM EDTA (pH 8.0)

Prepared in batches of 100 ml, autoclaved for 15 minutes at 10 lb/sq. in. on liquid cycle, and stored at 4° C.

Solution II:

0.2 N NaOH (freshly diluted from a 10 N stock)
1% SDS

Solution III:

5 M potassium acetate	60 ml
glacial acetic acid	11.5 ml
H_2O	28.5 ml

The resulting solution is 3 M with respect to potassium and 5 M with respect to acetate.

5. TAE (tris-acetate buffer), 40 X:

To make 1 liter:

Tris base (1.6 M)	193.6 g
Na acetate.3 H_2O (0.8M)	108.9 g
EDTA-Na_2 .2 H_2O (40 mM)	15.2 g

pH to 7.2 with acetic acid; add water to make 1 liter

6. TE (Tris-EDTA) buffer:

To make 100 ml:

Tris, 10mM, pH 7.4 0.5 ml of 2 M stock
0.1 mM EDTA, pH 8.0 20 ul of 0.5 M stock
Add H_2O, 99.3 ml; store at room temperature

7. STE buffer:

To make 100 ml:

Tris 20 mM, pH 7.4 1.0 ml of 2 M stock

EDTA-Na_2 , 0.1mM	20 ul of 0.5 M stock
NaCl 10 mM	0.2 ml of 5 M stock

8. SSC buffer, 20 X:

To make 1 liter:

NaCl, 3 M	175.3 g
Na_3 Citrate. 2 H_2O, 0.3 M	88.2 g
water	800 ml

Adjust pH to 7.0 with 1 M HCl; add H_2O to 1 liter

9. SSPE buffer, 20 X:

To make 1 liter:

NaCl (3 M)	175.3 g
NaH_2PO_4 . H_2O (0.2 M)	27.6 g
EDTA-Na_2 (0.02 M)	40 ml of 0.5 M EDTA stock solution

Add 800 ml water; add 10 N NaOH to pH to 7.4 and add water to make 1 liter
Sterize by autoclaving; all components will dissolve into solution in autoclave.

10. Proteinase K buffer, 20 X:

To make 100 ml:

1 M Tris, pH 7.5	50 ml 2.0 M stock
0.1 M EDTA	20 ml 500 mM stock

Add distilled water to 100 ml.

11. 2.0 M TEA (Triethanolamine) :

To make 100 ml:

Add 26.6 ml TEA to 50 ml distilled water. pH to 8.0 by 10.0 M HCl and then top up to 100 ml.

12. *In situ* hybridization mix for sections:

To make 10 ml:

Deionized formamide (Sigma)	5 ml
20x SSPE	1 ml
Denhardt's solution, 100 x	0.5 ml
50% dextran sulphate (in depc-treated water)	2.0 ml
tRNA (yeast)	0.2 ml of 10 mg/ml stock
SDS	0.5 ml of 10% stock
depc-treated H_2O	0.8 ml

13. *In situ* hybridization mix for wholemounts:

To make 10 ml:

Deionized formamide (Sigma)	5.0 ml
SSC, 5 X (pH 4.5)	3.3 ml
tRNA (yeast)	50 ul of 10 mg/ml stock
SDS	1.0 ml of 10 % stock

Heparin 5 ul of 100 mg/ml stock

Mixed well and stored in -20° C; thawed and mixed well before use.

14. PBT (Phosphate Buffered Saline with 0.1% Tween 20):

To make 1 litre:

PBS, 10 X	100 ml
Distilled water	900 ml
Tween 20	1 ml

15. PBS (Phosphate Buffered Saline), 10 X:

To make 1 litre:

NaCl	74 g
Na_2HPO_4	9.94 g
NaH_2PO_4	4.14 g

Add water to make 1 litre; sterilize by autoclaving.

16. Denhardt's solution, 100 X:

To make 50 ml:

Polyvinylpyrolidone (PVP)	1.0 g
Bovine serum albumin (BSA)	1.0 g
Ficoll 400	1.0 g

Top up with distilled water to make 50 ml. Sterilize by filters; store at 4° C and mix well before use.

17. Ca++, Mg++ free Chick Ringer's solution:

To make 100 ml:

NaCl	0.9 g
KCl	0.42 g

Add distilled water to make 100 ml. Autoclave before use.

18. 4 % paraformaldehyde:

To make 1 litre:

Add 40 g of paraformaldehyde powder in 900 ml distilled water in a large flask. Heat the solution to 60 ° C with stirring on a hot plate. Add a few drops of 10 N NaOH to help dissolve the powder. Allow the solution to cool down and store in - 20° C. Thaw immediately before use.

19. depc-treated water:

To make 1 liter:

Add 0.75 ml depc to a litre distilled water under hood. Shake well and sit (preferably with stirring) the solution at room temperature under hood for at least 30 minutes. Sterilize by autoclaving.

20. NTMT:

Freshly made before use to avoid decrease of pH.

To make 60 ml:

NaCl	1.5 ml of 4 M stock
Tris, pH 9.5	3 ml of 2 M stock
$MgCl_2$	3 ml of 1 M stock
Tween 20	60 ul
Levamisol (Vector Laboratories, U.K.)	12 drops (optional)

Add distilled water to make up 60 ml.

21. Alkaline phosphatase buffer:

Same as NTMT.

22. Colour detection buffer:

For sections:

Add 34 µl of NBT (4-nitro blue tetrazolium chloride) and 27 µl of BCIP (5-bromo-4-chloro-3-indolyl-phosphate; also known as X-phosphate) in 75 ml of NTMT. Both NBT and BCIP are ready-to-use solutions that are commercially available from Boehringer-Mannhein.

For wholemounts:

Add 4.5 µl NBT and 3.5 µl BCIP per ml of NTMT.

23. TESPA coated slides:

As described in section 2.4.1.

24. Pannet-Compton saline (from Stern, 1993):

Solution A:

NaCl	121 g
K Cl	15.5 g
$CaCl_2.\ 2H_2O$	10.42 g
$MgCl_2.\ 6H_2O$	12.7 g

Add water to 1 liter.

Solution B:

$Na_2HPO_4.\ 2H_2O$	2.365 g
$NaH_2PO_4\ 2\ H_2O$	0.188 g

Add distilled water to 1 liter.

Before use, mix (in order): 40 ml Solution A, 900 ml H_2O, and 60 ml Solution B.

25. Embryo powder:

Step 1: Homogenize embryos (12.5 - 14.5 days post coitus in the mouse; Hamburger-Hamilton stages 15 - 20 in the chick) in minimum volume of 1x PBS and then add 4 volumes of ice-cold acetone, mix and incubate on ice for 30 minutes.

Step 2: Spin the solution at 3 - 4 K rpm for 10 minutes.

Step 3: Discard the supernatant. Wash the pellet with ice-cold acetone and spin again.

Step 4: Transfer the pellet out to a filter paper. Spread and grind the pellet into fine powder and allow it to be air-dried. The embryo powder can then be stored in an air-tight tube at 4° C.

26. TBS (Tris-Buffered Saline), 20 X:

To make 100 ml:

Tris.HCl, pH 7.4	5 ml of 1 M stock
NaCl	5 ml of 4 M stock

Add distilled water to make 50 ml.

27. Linder's silver stain solutions:

a. Buffer stock solution

2.4.6-Collidine	6.6 ml
Distilled water	450 ml

Adjust pH to 7.2 - 7.4 with 10 per cent nitric acid, and make up to 500 ml with distilled water.

b. Diluted buffer

Buffer stock	8 ml
Distilled water	92 ml

c. Silver cyanate impregnating solution

Distilled water	84 ml heated to 60° C
1% Silver nitrate	4 ml
0.38 % sodium cyanate	4 ml
0.38 % sodium cyanate	4 ml
Buffer stock solution	8 ml

d. Physical developer stock solution:

Sodium sulphite	20 g
Sodium tetraborate	4.75 g
Distilled water	450 ml

Heat the solution to about 50° C and add Gelatine 5.0 g (Belgium Gold label).

e. Physical developing working solution

Physical developer stock solution	95 ml
2 % hydroquinine	5 ml
1% silver nitrate	2 ml

Add the silver nitrate stirring constantly.